

MERCURY(II) THIOLATE AND SELENOLATE INTERACTIONS,  
AND CHELATION THERAPY

BY

ALAN PETER ARNOLD B.Sc. (Melb.), B.Sc. (Hons.), ARACI

A thesis submitted in fulfilment of the requirements for  
the degree of

Doctor of Philosophy

Chemistry Department  
University of Tasmania  
Hobart  
Tasmania  
Australia

1982

This thesis contains no material which has been accepted for the award of any other degree or diploma in any University, and to the best of my knowledge, contains no copy or paraphrase of material previously presented by another person, except where due reference is made in the text.

*Alan P. Arnold.*

Alan P. Arnold.

FOR MY PARENTS

### ACKNOWLEDGEMENTS

It is a pleasure to respectfully acknowledge the continuous patience and guidance given by Dr. A.J. Canty throughout this study.

I am grateful to Dr. G.B. Deacon and Mr. M. Hughes (Monash University) for their assistance with the measurement of far infrared spectra, to Dr. A.H. White and Dr. B.W. Skelton (University of Western Australia) for the X-ray crystallographic studies, and to Dr. R.N. Sylva (Australian Atomic Energy Commission) for supplying a listing of his new version of the program MINIQAD.

My sincere thanks are due to Mr. J.C. Bignall of the Central Science Laboratory (University of Tasmania) for his expert tuition and assistance with the intricacies of laser-Raman spectroscopy of intractable samples, his colleagues Mr. N.W. Davies and Mr. M. Power for the measurement of mass spectra and to Mr. R.R. Thomas for the  $^1\text{H}$  nmr spectra.

Mr. R. Ford of the Geology Department (University of Tasmania) is gratefully acknowledged for his assistance with the determination of the X-ray powder diffraction patterns of several malodorous mercury(II) selenolates.

I wholeheartedly thank Mrs. B. Dix and Mrs. M. Stafford for their immaculate typing and Mrs. H. Hen for several of the diagrams in this thesis. Any virtues in presentation are due to these ladies, all deficiencies to me.

To the academic and technical staff of this Department, I express my appreciation for their always cheerful assistance, and humbly



apologise to them for the indiscretions of an amateur organoselenium chemist.

Last, but by no means least, I thank my wife, Julie, for her understanding and encouragement during this work. Her patient assistance with many tedious potentiometric titrations and transcription of my writing into readable text has been invaluable.

Financial support from the National Health and Medical Research Council and the Commonwealth of Australia for a Postgraduate Research Award, is gratefully acknowledged.

## ABSTRACT

This thesis is an account of a study of some aspects of the biological chemistry of mercury. The interactions of mercury compounds with both simple and naturally occurring thiols, some selenols, and several antidotes for mercury poisoning have been investigated.

The dithiol antidotes 2,3-dimercaptosuccinic acid ( $\text{DMSH}_4$ ) and the sodium salt of 2,3-dimercaptopropane-1-sulfonate (Unithiol,  $\text{Na}[\text{UH}_2]$ ) form isolable complexes of stoichiometry  $(\text{MeHg})_2\text{DMSH}_2$  and  $\text{Na}[(\text{MeHg})_2\text{U}]$ . The mercury(II) complexes  $\text{Hg}(\text{DMSH}_2) \cdot 2\text{H}_2\text{O}$  and  $\text{Na}[\text{HgU}]$  have polymeric structures,  $(-\text{Hg}-\text{S}\sim\text{S}-)_n$ , similar to that reported for the  $\text{Hg}(\text{II})$  complex of the classic heavy metal antidote, British Anti-Lewisite ( $\text{BALH}_2$ ).

The stability constants for the interaction of  $\text{MeHg}(\text{II})$  with several monothiol in aqueous solution have been determined potentiometrically. High stability of complexes with  $\alpha$ -mercaptocarboxylic acids and  $\alpha$ -mercaptoamines ( $\log \beta_{110} \approx 15-17$ ) necessitated the use of a titration method involving iodide competition. 2,3-Dimercaptosuccinic acid forms a  $\text{MeHg}(\text{II})$  complex with  $\log \beta_{110} = 17.11(3)$ , similar to that expected for interaction of  $\text{MeHg}(\text{II})$  with a monothiol; but  $\text{BALH}_2$  and Unithiol form complexes with  $\log \beta_{110}$  2-3 orders of magnitude higher, suggesting the presence of chelation.

Implications of the results obtained from both synthetic and solution studies for the use of dithiols as antidotes for  $\text{MeHg}(\text{II})$  poisoning are discussed.

A computer program for the potentiometric evaluation of ligand hydrolysis constants has been written. The algorithm uses a rigorous

least-squares procedure and can be applied to mixtures of multiprotic acids or bases. Any titration parameter can be refined.

Complexes of Hg(II) with selenols have been prepared and the first structural studies of Hg(II) selenolates obtained. Comparison of vibrational spectra and X-ray powder diffraction patterns for these complexes and their thiol analogs allows assignment of structures for some complexes and suggests that, for  $\text{Hg}(\text{SeR})_2$ , polymeric structures may be more common than for  $\text{Hg}(\text{SR})_2$ . Thus,  $\text{Hg}(\text{SeR})_2$  ( $\text{R}=\text{Me}, \text{Et}, \text{Bu}^t$ ) are polymeric and  $\text{Hg}(\text{SeCH}_2\text{CO}_2\text{H})_2$  is linear, but for a large number of analogous thiolate complexes, only  $\text{Hg}(\text{SBu}^t)_2$  is known to be polymeric.

Single crystal X-ray diffraction studies show a polymeric structure for  $\text{Hg}(\text{SeMe})_2$  based on distorted tetrahedral geometry for mercury with bridging selenolate groups.

The structure of  $[\text{Bu}^t\text{SeHgCl}(\text{py})_{0.5}]_4$  is similar to those previously reported for the sulfur analogs with pyridine and 4-methylpyridine, and is isomorphous with the latter. The structure is based on an eight-membered ring of alternating Hg and Se atoms  $(-\text{Hg}-\text{SeBu}^t-)_4$  having a centre of symmetry and two mercury environments,  $'\text{Hg}(\mu-\text{SeBu}^t)_2(\mu-\text{Cl})_2'$  and  $'\text{Hg}(\mu-\text{SeBu}^t)_2\text{Cl}(\text{py})'$ , with a dichloro bridge linking the former mercury atoms. The complex  $[\text{EtSeHgCl}(\text{py})]_4$  has a similar structure but a dichloro bridge is absent and all mercury atoms have the environment  $'\text{Hg}(\mu-\text{SeEt})_2\text{Cl}(\text{py})'$ .

The first valid comparison between Hg-S and Hg-Se bond lengths for analogous thiolate and selenolate complexes of Hg(II) indicates that the Hg-Se bond lengths are slightly shorter than expected from comparisons of sulfur and selenium covalent radii.

Possible synthetic routes to selenium analogs of antidotal dithiols are discussed. Although selenium analogs of  $\text{BALH}_2$  and 1,3-dimercapto-2-propanol ( $\text{DMPH}_2$ ) could not be isolated, the new compounds selenetan-3-ol,

1,2-diselenan-4-ol and 1-bromo-3-selenocyanato-2-propanol were obtained from their attempted syntheses. The Hg(II) derivatives of the selenium analogs, Hg(SeBAL) and Hg(SeDMP), were isolated as intractable polymers. These polymers have tetrahedral geometry for Hg(II) in contrast to linear geometry for their thiol analogs, consistent with structural differences between simple complexes  $\text{Hg}(\text{XR})_2$  ( $\text{X}=\text{S}, \text{Se}$ ). The compounds 2-(benzylseleno)-fumaric acid and 2-(benzylseleno)succinic acid have been prepared as intermediates towards a projected synthesis of  $\text{SeDMSH}_4$ .

## INDEX

	<u>Page</u>
CHAPTER ONE : CHEMICAL ASPECTS OF MERCURY TOXICITY	
1.1 Introduction	1
1.2 Metabolism and toxicity of mercury(II) compounds	3
elemental mercury, $\text{Hg}^0$	3
mercurous mercury, $\text{Hg}_2^{2+}$	4
mercuric mercury, $\text{Hg}^{2+}$	4
alkylmercury(II) compounds	5
alkoxyalkyl and arylmercury compounds	7
1.3 Antidotes for mercury toxicity	8
1.3.1 complexing agents	8
(i) 2,3-dimercapto-1-propanol (British Anti-Lewisite, BALH <sub>2</sub> )	10
(ii) D-penicillamine (PenH <sub>2</sub> )	12
(iii) N-acetyl-DL-penicillamine (NAPH <sub>2</sub> )	13
(iv) 2,3-dimercapto-1-propanesulfonate, sodium salt [Unithiol, Na(UTH <sub>2</sub> )]	14
(v) meso-2,3-dimercaptosuccinic acid (DMSH <sub>4</sub> )	15
(vi) other thiols	16
(vii) synergistic and mixed complexing agents	17
1.3.2 Extracorporeal hemodialysis and hemoperfusion	17
1.3.3 Enterohepatic complexing agents	18
1.4 Mercury-selenium interactions	19
1.4.1 Selenium interactions with inorganic mercury	23
1.4.2 Selenium interactions with organic mercury compounds	27

## CHAPTER TWO : STRUCTURAL CHEMISTRY OF MERCURY(II) THIOLATES

2.1	Introduction	30
2.2	Structural features of MeHg(II) thiolates	32
2.3	Structural features of complexes of the type, $\text{Hg}(\text{SR})_2$	43
2.4	Structural features of Hg(II) dithiolate complexes	53
2.5	Structural features of $\text{RSHgX}$ species	55
2.6	Conclusions	59

## CHAPTER THREE : SOLUTION CHEMISTRY OF METHYLMERCURY(II) THIOLATES AND SELENOLATES

3.1	Introduction	61
3.2	The aqueous solution chemistry of methylmercury(II)	
3.2.1	Coordination of MeHg(II) in aqueous solution	62
3.2.2	NMR investigations and MeHg(II) interactions in solution	75
3.2.3	NMR evaluation of MeHg(II)-thiolate formation constants	77
3.3	Methylmercury(II) complexation with thiolate ligands	80
3.3.1	Methylmercury(II) monothiolate equilibria	80
3.3.2	Potentiometric determination of formation constants of MeHg(II) thiolates	87
	analysis of $\text{H}^+$ content	93
	analysis of MeHg content	94
	(i) 2-mercaptoethanol	97
	(ii) mercaptoacetic acid	103
	(iii) mercaptoacetic acid, O-methylester	105
	(iv) mercaptosuccinic acid	105
	(v) L-cysteine	108

(vi) DL-homocysteine	116
(vii) DL-penicillamine	117
(viii) N-acetyl-DL-penicillamine	120
(ix) glutathione	123
(x) thiocholine perchloate	126
(xi) 4-mercapto-N-methylpiperidine	129
3.3.3 Methylmercury(II) formation constants with vicinal dithiols	136
(i) 2,3-dimercapto-1-propanol, BALH <sub>2</sub>	136
(ii) 2,3-dimercapto-1-propanesulfonate(sodium salt), Unithiol	144
(iii) meso-2,3-dimercaptosuccinic acid, DMSH <sub>4</sub>	149
3.4 Interactions of antidotal thiols with MeHg(II) <i>in vivo</i>	155
3.4.1 Physiological pH	156
3.4.2 Competition of antidotal thiols with endogenous ligands <i>in vivo</i>	157
3.5 Methylmercury(II) interactions with selenium donors in aqueous solution	162
3.5.1 MeHg(II)-selenolate equilibria	162
3.5.2 MeHg(II)-diselenide interactions	169
3.6 Conclusions	171

## CHAPTER FOUR : SYNTHESIS, VIBRATIONAL SPECTROSCOPY AND STRUCTURE OF MERCURY(II) SELENOLATES

4.1 Preparation of Mercury(II) selenolates	173
4.1.1 Preparation of Hg(SeR) <sub>2</sub> complexes	173
4.1.2 Preparation of RSeHgX complexes	176
4.2 X-ray diffraction characterisation of mercury(II)- selenolates	178

4.2.1	Hg(SeR) <sub>2</sub>	178
4.2.2	RSeHgX	190
4.2.3	Comparison of Hg-S and Hg-Se bonding distances	213
4.3	Vibrational spectroscopy of mercury(II) selenolates	217
4.3.1	Bis(selenolato)mercury(II) complexes, Hg(SeR) <sub>2</sub>	217
4.3.2	Mercury(II) diselenolates	222
4.4	Conclusions	224

## CHAPTER FIVE : SELENIUM ANALOGS OF ANTIDOTAL DITHIOLS

5.1	Introduction	225
5.2	Possible routes for synthesis of dithiols and diselenols	227
5.2.1	Direct introduction to SeH	228
5.2.2	Use of protected thiols and selenols	229
5.2.3	Introduction of protected selenol groups	236
	(i) alkylation of selenolates	236
	(ii) addition of selenols to alkenes and alkynes	237
	(iii) lactone and epoxide ring opening	237
5.2.4	Choice of protective groups for SeBALH <sub>2</sub> and SeDMSH <sub>4</sub> syntheses	243
5.2.5	Selenols from selenocyanate hydrolysis	244
5.2.6	Other methods	246
	(i) reduction of trithiocarbonates and xanthates to dithiols	246
	(ii) conversion of alcohols to selenoethers	247
	(iii) reduction of episulfides	247
	(iv) addition of diselenides to alkenes and alkynes	248



5.3	Attempted syntheses of $\text{SeDMSH}_2$ and $\text{SeBALH}_2$	248
5.3.1	$\text{SeDMSH}_4$	248
	(i) benzoyl protection	249
	(ii) benzyl protection	250
5.3.2	$\text{SeBALH}_2$ and related $\text{SeDMPH}_2$	262
	(i) $\text{SeDMPH}_2$	262
	(ii) $\text{SeBALH}_2$	281
5.4	Conclusions	282

## CHAPTER SIX : POTENTIOMETRIC DETERMINATION OF AQUEOUS FORMATION CONSTANTS OF VERY STABLE COMPLEXES

6.1	Introduction	284
6.2	Evaluation of ligand hydrolysis equilibria	286
6.2.1	Definition of 'Equilibrium Constants' used in this work	286
6.2.2	Calibration of glass-electrodes as $[\text{H}^+]$ probes	291
6.2.3	Titration assembly	297
	titrant solutions	302
	titration procedure	302
	pH(s) buffers	305
6.2.4	Available computer programs for evaluation of ligand-hydrolysis equilibria	306
6.2.5	TITRAT and related programs for treatment of titrations of mixtures of multiprotic acids and bases	308
6.3	Evaluation of formation constants of stable complexes	317
6.3.1	$\text{H}^+$ - competition method for obtaining aqueous stability constants	317
6.3.2	Evaluation of high stability constants for $\text{MeHg}$ -thiolate complexes	323

6.3.3	Computer programs for the evaluation of metal-ligand stability constants	326
6.4	Display of titration data and species distributions	330
6.4.1	COMIX	331
6.4.2	COMIXH	332
6.5	Appendix: A simple device for monitoring attainment of pH equilibrium	333
CHAPTER SEVEN : EXPERIMENTAL		335
7.1	General reagents	336
7.2	General procedures used in organoselenium preparations	337
7.3	Preparation of complexes [MeHg(II) and Hg <sup>2+</sup> ] of dithiols and model thiols	340
7.4	Preparation of selenium compounds and complexes (and S-analogs)	347
REFERENCES		367
APPENDIX 1		401
APPENDIX 2		402
PUBLICATIONS		403

## CHAPTER ONE

### CHEMICAL ASPECTS OF MERCURY TOXICITY

#### 1.1 Introduction

Mercury and its compounds are not rare in nature, yet it has not been demonstrated that mercury has any essential role in any metabolic pathway of any known species. Today's concern with mercury is due to its environmental impact, and its deleterious effects on human health. Contamination of the natural environment by mercury compounds, particularly methylmercury(II), has become a serious problem in many parts of the world. Major outbreaks of human methylmercury(II) poisoning at Minamata Bay (1953) and Niigata (1965) in Japan have generated international awareness of Minamata Disease. The history and general background to these events and the clinical and pathological features of Minamata Disease, which include severe, irreversible central-nervous system damage and congenital abnormalities, have been recently reviewed.<sup>1,2</sup> Organo-mercurials have been responsible for further accidental poisoning episodes at Guatémala (1963),<sup>3</sup> Alamogordo, New Mexico (1969)<sup>4</sup> and in Iraq (1973),<sup>5,6</sup> due to grain treated with methyl- and phenylmercurial fungicides. Over 400 deaths resulted from the Iraqi poisonings alone.<sup>4</sup>

The Japanese outbreaks, directly attributed to industrial discharges,<sup>1,2</sup> were instrumental in promoting the sudden upsurge of interest in the biological and environmental behaviour of mercury (and of heavy metals in general) seen in the early 1960's. Although organomercurials had been known to be lethally toxic since 1865,<sup>7</sup> until the large-scale outbreaks most toxicological research concerned with mercury had been restricted to elemental mercury, particularly the vapour, inorganic mercury(II) compounds and mercurial diuretics. Biological methylation of inorganic

mercury by methylcorrinoid derivatives, e.g. methylcobalamin, is well established.<sup>8,9</sup>

Thus, potentially more dangerous methylmercury(II) results from inorganic mercury(II)-contaminated environments.

There is much evidence indicating the relevance of mercury(II) complexes with sulfhydryl ligands in the biotransport, metabolism, toxicity and microbiological transformations of mercury(II). For example, the toxic agent in the Minamata episodes seems to have been MeHgSMe, isolated from shellfish.<sup>1</sup> Biosynthesis of this compound may involve the complex of MeHg(II) with cysteine. Some cobalamin-independent organisms, e.g. *Neurospora Crassa* can methylate  $Hg^{2+}$ . Homocysteine and cysteine complexes are implicated in the mechanism.<sup>10</sup> Several antidotes for mercury toxicity will be discussed in this Introduction, all of which are thiols.

This thesis considers some of the chemical aspects in the solid state and in aqueous solution of mercury(II) coordination with thiolate ligands, including several with reported antidotal activity toward inorganic and methylmercury(II). Recent developments in the biological interactions between mercury and selenium are discussed, and some model mercury(II)-selenolates have been investigated in the solid state.

## 1.2 Metabolism and toxicity of mercury(II) compounds

The chemical features of the three oxidation states (0, 1+, 2+) of mercury differ markedly. For this reason it is convenient to consider them separately. The experimental toxicology and pharmacology of mercury has been extensively reviewed<sup>11-14</sup> and so only the salient features which distinguish the types of mercury compounds, are noted here. The mode of intoxication by mercury compounds is usually oral, or by inhalation in the case of mercury vapor.

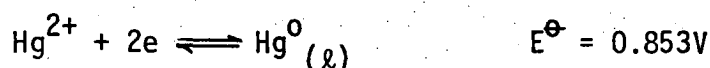
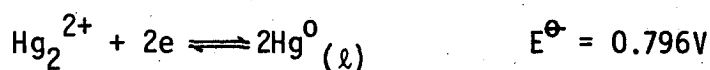
### Elemental mercury, $\text{Hg}^0$

In the liquid metallic form, mercury is not significantly toxic, passing through the gastrointestinal tract unabsorbed, and is fecally excreted.<sup>13</sup> The saturation vapor pressure of mercury under normal ambient conditions is sufficiently high (10-15 mg  $\text{Hg}/\text{m}^3$ ),<sup>13</sup> to pose a severe health threat in poorly ventilated areas. Due to its relatively high lipophilicity mercury vapor is efficiently (80%)<sup>14</sup> transferred from alveolar air into the bloodstream. In the bloodstream,  $\text{Hg}^0$  is rapidly oxidised to  $\text{Hg}^{2+}$  and although the half life of  $\text{Hg}^0$  is only 30s, this is sufficiently long to allow a significant proportion of  $\text{Hg}^0$  to traverse the blood-brain barrier (or the placental barrier) leading to a tenfold higher accumulation in the brain than for inorganic mercury poisoning.<sup>15,16</sup> Long-term exposure to low levels of mercury vapor is therefore of some concern.

Several minutes after inhalation, tissue distribution approaches that of  $\text{Hg}^{2+}$ , except for the significantly higher proportion retained in the brain, particularly in the cerebral and cerebellar cortex and certain brain nuclei.<sup>14</sup>

### Mercurous mercury, $\text{Hg}_2^{2+}$

Disproportionation of the (1+) oxidation state is rapid and reversible, with thermodynamic properties as shown.<sup>17</sup>



Because there are no commonly occurring oxidants with oxidation potentials between -0.796 and -0.853V, elemental mercury is always oxidised to  $\text{Hg}^{2+}$  with excess oxidant. In addition, mercury(I) salts, e.g. calomel,  $\text{Hg}_2\text{Cl}_2$ , generally have low aqueous and lipid solubility. Gastrointestinal absorption is so low that systemic intoxication is rare.<sup>14</sup>

For these reasons, the toxicology and environmental chemistry of inorganic mercury is primarily concerned with the (2+) oxidation state.

### Mercuric mercury, $\text{Hg}^{2+}$

Mercuric salts have played important pharmacological roles as ointments, antiseptics, diuretics and laxatives for centuries and they are widely used in agriculture, e.g. as rodenticides and in industry. Ingested mercuric salts are presumably absorbed as chloro-complexes formed in the high acidity and chloride content of the stomach, but gastrointestinal absorption is fairly low (~20%).<sup>14</sup> Mercuric salts, like mercury vapor and mercurous salts, are severely corrosive to mucosal membranes.<sup>18</sup>

After entering the bloodstream,  $\text{Hg}^{2+}$  is bound to sulfhydryl groups of proteins or other endogenous ligands in the plasma, and to the membrane and hemoglobin of erythrocytes. Nearly all (99%) of plasma

$\text{Hg}^{2+}$  is bound to non-filtrable protein thiols, e.g. albumin and globulin.<sup>13</sup> The concentrations of mercuric ion in the plasma and erythrocytes are approximately equal<sup>14</sup> and the target organs for  $\text{Hg}^{2+}$  are the kidneys.<sup>13</sup> Mercury is bound to 2 or 3 cysteinyl groups in kidney metallothionein.<sup>19</sup> Mercuric ion is gradually removed from the blood by passive glomerular filtration and active tubular transport in the kidneys, as well as by fecal excretion from gastrointestinal mucosa.<sup>14</sup> These two routes are of comparable importance and result in a half-life for  $\text{Hg}^{2+}$  of 1-2 months.<sup>14</sup>

#### Alkylmercury(II) compounds

Alkylmercurials are used widely as fungicides, and methylmercury(II) is the result of biomethylation of inorganic mercury residues in sediments.<sup>20</sup> Short chain monoalkyl mercurials, particularly  $\text{MeHg(II)}$ , are considerably more resistant to metabolic dealkylation (to form  $\text{Hg}^{2+}$ ) than long chain analogs, although significant biotransformation of  $\text{MeHg(II)}$  occurs in the kidneys and the liver.<sup>21-23</sup> The compounds of methyl- and ethylmercury(II) have been most closely studied. Because of its biological and environmental importance, only  $\text{MeHg(II)}$  will be discussed here.

The extremely high translational diffusion characteristics of  $\text{MeHgCl}$  seem to be responsible for its ready absorption from the stomach into the bloodstream, rather than lipid solubility.<sup>24</sup> The distribution ratio from water to lipid has been recently determined to be only  $\sim 2$ , thus,  $\text{MeHgCl}$  diffuses rapidly but does not partition well in lipids.<sup>24</sup>

Methylmercury(II) distribution in the body differs markedly from that of  $\text{Hg}^{2+}$ .<sup>25,26</sup> Preferential accumulation of  $\text{MeHg(II)}$  occurs in the erythrocytes, producing a characteristic erythrocyte:plasma mercury concentration ratio of 10:1.<sup>14</sup> Methylmercury(II) readily passes through

the blood-brain and placental barriers. Up to 10% of the whole-body burden of MeHg(II) may be found in the brain,<sup>13</sup> which is the target organ for methylmercury(II) poisoning. Congenital Minamata disease tragically results from foetal accumulation of acutely toxic doses of MeHg(II).<sup>1,2</sup> The neurotoxicity of MeHg(II) does not seem to be due solely to biotransformation to  $Hg^{2+}$  in brain tissue.<sup>27</sup>

There is little doubt that the toxic influence of MeHg(II) is due to inactivation of specific sulfhydryl sites of cysteinyl residues of proteins and enzymes.<sup>28</sup> Although the 1:1 MeHg(II)-sulfhydryl interaction serves as a selective biochemical probe for SH groups<sup>29</sup> the active cellular sites of MeHg(II) toxicity have not thus far been firmly established. Significant amounts of radioactively labelled MeHg(II) are found in mitochondria<sup>30</sup> and MeHg compounds directly affect rat liver mitochondria *in vitro*.<sup>31-33</sup> The ability of some thiols to reactivate MeHg(II)-inhibited enzymes of rat liver mitochondria *in vivo*<sup>34,35</sup> has recently been used to evaluate possible antidotal thiols.<sup>36</sup> MeHgCl also interacts with unsaturated phospholipids and disrupts lipid membrane permeability even at mercury concentrations of  $10^{-7}M$ ,<sup>37</sup> consequently, lipid biomembranes have been suggested to be the primary targets for MeHg(II).<sup>37-8</sup>

Several workers have characterised intracellular MeHg(II)-sulfhydryl species. A glutathione complex has been identified from rat liver cytosol, with 24% of mercury in the small molecular weight fraction,<sup>39</sup> and metallothionein-bound MeHg(II) has been reported to account for up to 40% of total protein-bound MeHg(II) in the liver cytosol of rainbow trout.<sup>40</sup> Attempts to relate these findings to the nature of MeHg(II) species *in vivo* must be limited by the rapid redistribution of mercurial among the mixture of sulfhydryl ligands resulting from cell-wall disruption.<sup>41</sup> Such ligand exchange is fast on the nmr timescale, and



is discussed later in this thesis (page 75 ). The methylmercury-thiolate species in the bile of rats has a molecular weight intermediate between that of the MeHg(II) complexes of cysteine and glutathione and is not the complex of N-acetylcysteine or homocysteine.<sup>42</sup>

The toxicology of methylmercury is dominated by its long biological half-life (~3 months) and hence, its propensity for accumulation with continued sub-acute exposure.<sup>13</sup> High concentrations of methylmercury(II) are found in the liver and kidneys but normal urinary excretion is low, accounting for only 10% of excreted mercury.<sup>14</sup> As a result, the predominant pathway for excretion is via MeHg(II) species in the bile. Unfortunately, the high rate of gastrointestinal reabsorption of biliary MeHg(II) species provides an efficient route for enterohepatic recirculation and contributes to the long half-life in the body.

Attempts to increase either urinary or fecal excretion of MeHg(II) form the basis of two possible courses for antidotal therapy for MeHg(II) intoxication and will be discussed in the next section.

Dialkylmercurials such as Me<sub>2</sub>Hg may pose higher health risks than monoalkylmercurials for acute exposure, as they are generally more volatile and lipophilic and hence, more easily absorbed. However, these compounds do not separately form a high environmental or biological hazard because they are readily degraded to monoalkylmercurials and/or mercuric ion.<sup>13</sup>

#### Alkoxyalkyl and Arylmercury(II) compounds

Alkoxyalkylmercurials are used in agriculture and industry as fungicides. These compounds are rapidly degraded to Hg<sup>2+</sup> which determines their toxicity and pharmacology.<sup>43</sup>

Arylmercurials, particularly phenylmercury(II), are widely used as fungicides and mould inhibitors in paints and as wood preservatives.

Large scale poisoning episodes e.g. in Pakistan<sup>44</sup> have occurred as a result of ingesting treated grain. Phenylmercury(II) is rapidly degraded to inorganic mercury(II), eventually showing the body distribution of  $\text{Hg}^{2+}$ .<sup>25</sup> Disproportionation of mercaptoamino acid and dithiolate complexes of  $\text{PhHg(II)}$  to diphenylmercury has been shown in this laboratory to occur *in vitro*.<sup>45</sup> Metabolic conversion of  $\text{PhHg(II)}$  to diphenylmercury<sup>46</sup> and to elemental mercury<sup>47,8</sup> has also been demonstrated in some microorganisms.

### 1.3 Antidotes for Mercury toxicity

The term antidote used throughout this thesis, defines a chemotherapeutic agent which aids the removal of toxic metal from the body after intoxication. Many forms of metal intoxication may be alleviated with therapeutic 'chelating' agents which enhance urinary excretion of metal. Alternatively, antidotes which enhance fecal excretion of metal released in the bile may be used.

These methods will be separately discussed below in relation to removal of inorganic  $\text{Hg}^{2+}$  and methylmercury(II).

#### 1.3.1 Complexing agents

The use of complexing agents for therapeutic manipulation of metals in the human body is now well established, and has been reviewed elsewhere.<sup>49</sup> The term 'chelating' agent seems to have been loosely used in the toxicological literature. In many situations there is little or no evidence that the reagent is bound entirely to one metal atom, in the chelating sense.<sup>17</sup> Evidence from this laboratory indicates that complexes formed between mercuric ion and several antidotal dithiols are not chelating (Section 2.4). Similarly, the methylmercury(I+) cation forms unidentate complexes particularly with thiolate ligands.

The term, complexing agent, will be used throughout this thesis, except in those situations where chelation can be established.

Because mercury will inevitably be bound to sulfhydryl groups of proteins, etc. after intoxication, an effective antidotal complexing agent must

(i) be of low toxicity,

(ii) be able to bind mercury strongly enough to compete with a multitude of biological ligands, e.g. chloride, nitrogenous bases, sulfhydryl-containing proteins, etc.,

(iii) discriminate against abundant endogenous metals such as zinc and calcium,

(iv) be sufficiently lipophilic to penetrate cell membranes to reach intracellular sites of metal deposition, and

(v) form a lipophilic complex in the body compartment where mercury is accumulated.

Highly charged species are inefficient in this regard e.g. polyamine carboxylic acids are largely retained in the extracellular space, and rely on endogenous ligands to remove metals from inside the cell.<sup>50</sup> If enhanced urinary excretion is desired, this complex should change to a new hydrophilic complex in the plasma, so that metal can be eliminated by the kidneys. While high mobility is required of the metal-antidote complex in this last step, redistribution into more susceptible organs, e.g. MeHg(II) into the brain, is undesirable.

Mercury(II) is a typical Class B<sup>51</sup> or 'soft'<sup>52</sup> metal and consequently has a high affinity for sulfur donor ligands and particularly for thiolates. Many compounds containing sulfhydryl groups have been evaluated as antidotes for various forms of mercury poisoning, and these will be discussed here.

(i) 2,3-dimercapto-1-propanol (British Anti-Lewisite, BALH<sub>2</sub>,\*  
Dimercaprol)

The efficacy of BALH<sub>2</sub> as a general heavy metal antidote was recognised during World War II. The historical development of its preparation and use has been recently reviewed.

Treatment for acute<sup>54-6</sup> and chronic<sup>57,8</sup> poisoning by metallic mercury has been reported but the therapeutic effect of BALH<sub>2</sub> is uncertain.<sup>26</sup> The life-saving effect of BALH<sub>2</sub> treatment for acute inorganic mercury(II) poisoning is well-established and has been reviewed.<sup>26</sup> There are conflicting reports as to the effect of BALH<sub>2</sub> on urinary excretion of mercury after inorganic mercury(II) poisoning, e.g. some workers report increased excretion,<sup>59-61</sup> in contrast to decreased excretion by others.<sup>62,3</sup> Fecal elimination of mercury is the major route for inorganic mercury poisoning, therefore, renal failure does not preclude metal decorporation.<sup>14</sup> Considerable redistribution of inorganic mercury between organs occurs with BALH<sub>2</sub> treatment, which may cause an increase in the amount of mercury in the brain.<sup>61-3</sup> This latter effect has been attributed to timing of BALH<sub>2</sub> treatment.<sup>61</sup>

Although BALH<sub>2</sub> increases biliary excretion of MeHg(II)<sup>64-5</sup> in rats, fecal elimination is not enhanced<sup>59,66</sup> due to a corresponding increase in gastrointestinal reabsorption.<sup>26</sup> Administration of BALH<sub>2</sub> increases the brain uptake rate of MeHg(II) in mice<sup>67</sup> and increases the level of MeHg(II) in the brain of rats.<sup>66</sup>

The use of BALH<sub>2</sub> is lethal in cases of methoxyethylmercury(II)

---

\*Throughout this work, antidotal thiols will be abbreviated to indicate loss of thiol protons on complex formation, e.g. BALH<sub>2</sub>, PenH<sub>2</sub>, DMSH<sub>4</sub>, etc. Although BALH<sub>2</sub> exists in stereoisomeric forms, only the racemic material has been used pharmacologically, although the optically active forms have been synthesised.<sup>68</sup>

poisoning,<sup>26</sup> but is the most effective antidote for phenylmercury(II) poisoned animals.<sup>26</sup>

The major disadvantages of  $\text{BALH}_2$  are related to its limited aqueous solubility<sup>15</sup> and relatively high nephrotoxicity<sup>69</sup> (Table 1.1). A typical course of  $\text{BALH}_2$  treatment for acute inorganic mercury(II) poisoning requires four-hourly deep intramuscular injections of BAL (3-5 mg/kg) for 2 days followed by six-hourly injections of a lower dose (2.5-3 mg/kg) for up to seven days.<sup>18</sup> Many patients suffer side effects from such treatment<sup>70</sup> and the mortality is ~2%, mainly from secondary infections.<sup>14</sup> Consequently, more water-soluble, less toxic thiol antidotes have been sought.

thiol	$\text{LD}_{50}$ (mg/kg)	ref.
$\text{BALH}_2$	90 (mice, im)	71
	80 (rabbit)	72
D-Penicillamine	3725 (mice)	73
	334 (mice)	74
	2289 (mice, iv)	75
N-Acetyl-D-penicillamine	>1000 (rats)	74
Unithiol	~2000 (rabbit)	76
$\text{DMSH}_4$	>2730 (human?)	77
	5000 (mice)	78

Table 1.1: Acute toxicity of antidotal thiols.

(ii) D-penicillamine<sup>†</sup> (PenH<sub>2</sub>)

In 1950 it was noted that treatment of inorganic mercury(II)-poisoned patients with penicillin produced increased urinary excretion of mercury.<sup>79</sup> The antidotal effect is due to the metabolite, D-penicillamine. However, this compound was not available commercially until its beneficial action in alleviating the symptoms of Wilson's disease (due to Cu accumulation) had been demonstrated.<sup>80</sup> PenH<sub>2</sub> is water-soluble and has low toxicity (Table 1.1). Although it is commonly administered nowadays (100 mg/kg orally)<sup>18</sup> subsequent to BALH<sub>2</sub> treatment of inorganic mercury poisoning, early reports of its efficacy in man were not encouraging<sup>81</sup> although marked reductions in mortality (better than BALH<sub>2</sub>) among HgCl<sub>2</sub> and HgNO<sub>3</sub>-intoxicated rats was observed,<sup>74</sup> but only at high doses (65 mg/kg).<sup>26</sup> PenH<sub>2</sub> is also used to treat sub-acute mercurialism.<sup>18</sup>

D-Penicillamine does not easily penetrate erythrocyte membranes *in vitro*,<sup>82</sup> however, Magos *et al.* have recently reported decreased levels of mercury in the brain following PenH<sub>2</sub> administration to MeHg(II) intoxicated rats.<sup>83</sup> Earlier contradictory reports by other workers<sup>26</sup> may have been due to low doses of antidote. High doses (220 mg/kg) removed MeHg(II) from all organs except the kidneys in rats but lower doses (80 mg/kg) were ineffective.<sup>84</sup> PenH<sub>2</sub> accelerates the urinary excretion of MeHg(II)<sup>5,85</sup> but unlike BALH<sub>2</sub>, does not redistribute MeHg(II) into the brain.<sup>84,86</sup> Biliary excretion of MeHg(II) is increased in rats treated with PenH<sub>2</sub><sup>65,83</sup> but fecal

---

<sup>†</sup>The nomenclature of this stereoisomer may be confused in the literature, being variously denoted D- and DL-penicillamine. The racemic isomer (DL-) is commercially available for therapeutic use as Metcaptase<sup>(R)</sup>. The Merck Index describes the D- isomer as naturally occurring.<sup>75</sup>

excretion is not, due to rapid reabsorption of the MeHg-pen complex from the gut.<sup>26</sup> High doses of PenH<sub>2</sub> (1 g/kg) to pregnant rats prevented fetal morphological changes caused by MeHgCl.<sup>87</sup>

In cases of rats poisoned by methoxyethylmercury, immediate injection of PenH<sub>2</sub> has a lifesaving effect, increasing urinary excretion of Hg, but is only marginally effective against phenylmercury.<sup>26,66</sup>

(iii) N-Acetyl-DL-penicillamine (NAPH<sub>2</sub>)

Acetylation of DL-penicillamine (or cysteine or homocysteine) increases the lipophilic character of the antidote. Thus NAPH<sub>2</sub> readily penetrates erythrocyte membranes, unlike PenH<sub>2</sub>.<sup>82</sup> NAPH<sub>2</sub> is even less toxic than PenH<sub>2</sub> (Table 1.1) and may be administered orally. N-acetylation of the amino group of PenH<sub>2</sub> and similar compounds, protects the molecule against the action of catabolic enzymes and reduces tubular reabsorption in the kidney glomeruli.<sup>88</sup> NAPH<sub>2</sub> is more effective than PenH<sub>2</sub> against acute HgCl<sub>2</sub> intoxication in mice and increases urinary Hg excretion.<sup>14</sup> Its use in sub-acute mercurialism has been recorded.<sup>18</sup> Failures of NAPH<sub>2</sub> to remove MeHg(II) from the brain in mice<sup>14</sup> and as an antidote for human MeHg(II) poisoning (Iraq)<sup>5</sup> were due to low doses of antidote.<sup>82</sup> Thus high doses (3-4 mmol/kg) remove up to 50% of mercury in the brain<sup>86,89</sup> and are therefore much more effective than PenH<sub>2</sub> in this regard, whereas lower doses (0.1-0.2 mmol/kg) have no effect.<sup>5,88-9</sup> Oral NAPH<sub>2</sub> treatment of MeHgCl intoxicated mice mobilised mercury from all organs and reduced fetal and maternal mercury levels.<sup>5</sup> Urinary and fecal Hg-excretion were increased.<sup>5</sup> NAPH<sub>2</sub> is more effective than PenH<sub>2</sub>, glutathione, cysteine, N-acetylcysteine or N-acetyl-homocysteine in the removal of MeHg(II) from an albumin complex *in vitro*.<sup>82</sup>

(iv) 2,3-dimercapto-1-propanesulfonate, sodium salt [Unithiol,<sup>†</sup> Na(UTH<sub>2</sub>)]

Because of the relatively high toxicity and low aqueous solubility of BALH<sub>2</sub>, its water-soluble sulfonate analog, Unithiol, was prepared in 1955.<sup>90,91</sup> The toxicity of Unithiol is very low (Table 1.1) and it may be administered orally with no long term effects. Chronic treatment (0.6 mmol/kg) produced transitory reductions in the copper concentration of some organs<sup>92</sup> and increased renal excretion of copper and zinc.<sup>93</sup> Although only recently available commercially in Western Europe and America, it has been used successfully in the U.S.S.R. to treat inorganic mercury(II) toxicity in man.<sup>94</sup> The high water solubility contributes to its relatively low gastrointestinal absorption rate (30%/24 hrs<sup>95</sup> in comparison with PenH<sub>2</sub> 60%<sup>96</sup>) and its rapid renal clearance (70-80%/24 hrs).<sup>97</sup> Thus Unithiol facilitates excretion of mercuric mercury via the kidneys.<sup>98</sup>

Despite its low lipophilicity and hence its low membrane permeability, high doses (180 mg/kg) of Unithiol seem to be more effective than PenH<sub>2</sub> (and N-acetyl-homocysteine thiolactone) in reducing the brain mercury level after MeHgCl intoxication.<sup>82</sup> This effect has been attributed to a reduced brain uptake rather than increased removal of mercury.<sup>99</sup> Treatment with lower doses (114 mg/kg) did not mobilise significant amounts of mercury from the brain in mice.<sup>100</sup> Urinary MeHg(II) excretion is substantially enhanced upon Unithiol treatment.<sup>99</sup> Fecal MeHg(II) excretion is also slightly enhanced,<sup>99</sup> although this may be due to the increased flow of bile and bile-salts caused by Unithiol.<sup>101</sup> Unithiol does not remove Cd from metallothionein

---

<sup>†</sup>Unithiol is marketed for therapeutic use under the name Dimaval (R) by Heyl & Co. Chem.-Pharm. Fabrik, Berlin. The stereoisomeric nature of Unithiol does not seem to have been reported. The commercial product is presumably a racemic form, like BALH<sub>2</sub>.



in the bile, but  $\text{BALH}_2$  does.<sup>102</sup>

(v) meso-2,3-dimercaptosuccinic acid ( $\text{DMSH}_4$ )<sup>†</sup>

Introduction of carboxylate groups into a dithiol molecule increases its aqueous solubility. Thus the disodium salt and the 1:1 mercury(II) complex of  $\text{DMSH}_4$  are water-soluble. The toxicity of  $\text{DMSH}_4$  is very low (Table 1.1) and like Unithiol, it may be administered orally with no long-term effects<sup>103</sup> although its metabolism is not well understood.<sup>100</sup>  $\text{DMSH}_4$  was first used therapeutically in 1954 as the trypanocidal antimony complex.<sup>104</sup> The arsenic complex has similar activity.<sup>105</sup>  $\text{DMSH}_2$  has been used as an antidote for lead<sup>106-7</sup> and arsenic<sup>103</sup> poisoning for which it is as effective as  $\text{BALH}_2$ , and is better than  $\text{PenH}_2$  at increasing urinary excretion of gold after Au-mercaptosuccinate(Myocrisin) treatment.<sup>108</sup>

$\text{DMSH}_4$  is an effective antidote to acute  $\text{HgCl}_2$  poisoning<sup>109</sup> and is more effective than  $\text{PenH}_2$  at removal of Hg from the kidneys, liver and brain of mice.<sup>78,107,110,111</sup>

$\text{DMSH}_4$  seems to be a most promising antidote for  $\text{MeHg(II)}$  toxicity. It is five times as effective as  $\text{PenH}_2$  for Hg excretion in mice after  $\text{MeHgBr}$  administration and decreases the Hg content of kidneys, liver and particularly the brain.<sup>78,110-1</sup> Doses of 90 mg/kg/day removed two thirds of mercury from the brain when given to  $\text{MeHgCl}$  intoxicated mice. For this purpose  $\text{DMSH}_4$  is better than  $\text{PenH}_2$ , mercaptosuccinic acid<sup>100</sup> and  $\text{BALH}_2$ .<sup>112</sup> Postexposure preventative treatment with  $\text{DMSH}_4$  to rats after  $\text{MeHgCl}$  injection prevents the increase of mercury levels in the

---

<sup>†</sup>Only this stereoisomer has been studied extensively, however the racemic form was reported to be better than the meso- form at accelerating urinary mercury elimination from rats after  $\text{HgCl}_2$  administration.<sup>112</sup>

brain.<sup>113</sup> The MeHg(II) level in the brains of neonatal rats is significantly lower than that of controls after administration of DMS to the dams.<sup>114</sup>

(vi) Other thiols

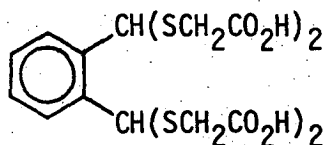
Several N-acetylated mercaptoamino acids (other than PenH<sub>2</sub>) have been tested as antidotes in animal experiments, particularly against MeHg(II) toxicity.

N-Acetylhomocysteine is nearly as effective as PenH<sub>2</sub> (and better than homocysteine) for decorporation of MeHg(II) from mice, and is less toxic.<sup>88</sup> The corresponding thiolactone produces larger increases in urinary excretion of mercury,<sup>88</sup> and mobilises more than MeHg(II) from the brain,<sup>115</sup> but very high doses are required. In contrast, the non-acetylated thiolactone does not mobilise mercury from the brain in mice or monkeys, and is toxic to monkeys.<sup>86</sup>

Diethyldithiocarbamate and disulfuran decrease urinary and biliary MeHg(II) excretion and increase the mercury content of the brain in mice.<sup>116</sup>

Oral doses of  $\beta$ -mercaptopropionylglycine (600 mg/day) produced 3- to 6-fold increases in urinary mercury excretion for Minamata patients, and was better than PenH<sub>2</sub> in this regard.<sup>117</sup>

The new tetrathioether, PTTA, was totally protective against high doses (30 mg/kg) of MeHgCl in mice, and is relatively non-toxic.<sup>118</sup>



Of several tested steroids containing thioacetyl groups (which are presumably hydrolysed *in vivo*), only thiocholesterol shows significant protective effects against MeHgCl intoxication in mice.<sup>119</sup> Pretreatment with the similar compound thiomestron (109 mg/kg) was as effective as BALH<sub>2</sub> treatment in decreasing the whole-body burden of MeHg(II) in mice, but unlike BALH<sub>2</sub>, did not redistribute mercury into the brain.<sup>120</sup> This thio steroid also decreases mercury retention after HgCH<sub>2</sub> administration.<sup>121</sup>

(vii) Synergistic and mixed complexing agents

Whereas treatment with one complexing agent may not significantly alter the rate of metal decorporation, simultaneous addition of a second agent may prove effective. The second agent may alter a metabolic process or function which enables the complex formed between the metal and first agent to be more efficiently excreted, e.g. phenobarbitone enhances biliary excretion<sup>11</sup> but is ineffective alone as a mercury antidote. Fecal elimination of mercury from MeHgCl intoxicated mice treated with a polythiol resin is thus enhanced by simultaneous treatment with phenobarbitone.<sup>122</sup>

The formation of ternary or mixed complexes between the metal and both complexing agents has been postulated to account for enhanced elimination of plutonium with salicylate and DTPA<sup>123†</sup> treatment, although some of the experimental evidence for the mixed species has been questioned.<sup>124</sup> Mixed ligand treatment (BAL/CaEDTA) has been used for lead<sup>125</sup> and copper<sup>126</sup> toxicity but mixed complexes have not been identified.

This form of treatment does not seem to have been widely used for treatment of mercury(II) toxicity.

1.3.2 Extracorporeal Hemodialysis and Hemoperfusion

Antidotal thiols such as penicillamine and N-acetylpenicillamine increase the fraction of non-protein bound MeHg(II) in the blood. *In vitro* studies have shown 55-60 fold increases in the low M.Wt. MeHg(II) fraction after  $10^{-2}$ M cysteine treatment, 44% of which is dialysable in a single pass.<sup>127</sup> *In vivo*, extracorporeal hemodialysis of blood from dogs intoxicated with MeHgCl, resulted in a 100 fold increase in MeHg removal rate after treatment with cysteine.<sup>128</sup> Significantly, mercury was removed from the brain. In contrast, clearance of  $Hg^{2+}$  was not

---

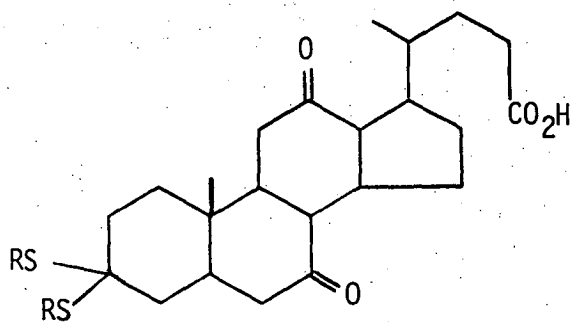
†diethylenetriaminepentacetic acid.

significantly increased after treatment with  $\text{BALH}_2$  and hemodialysis.<sup>129</sup>

The use of thiopolymers to remove mercury from the dialysate has been suggested.<sup>129</sup> Perfusion of human plasma through a bed of thiopolymer microspheres has recently been reported to decrease mercury levels, *in vitro*, and is cheaper than dialysis.<sup>130</sup>

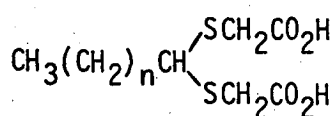
### 1.3.3 Enterohepatic complexing agents

Treatment of  $\text{MeHg(II)}$  toxicity with many thiol antidotes produces  $\text{MeHg(II)}$ -thiolate complexes which are excreted in the bile. However, the complexes are often reabsorbed in the small intestine from which they reenter the portal bloodstream to the liver. Antidotal agents may be designed to reduce the efficiency of this enterohepatic recirculation.<sup>11,131-2</sup> These agents may incorporate structural features similar to bile acids (e.g. mercaptal substituted cholic acids, I), or long chain fatty acids, but contain polar endgroups (II,III) resistant to metabolic breakdown.

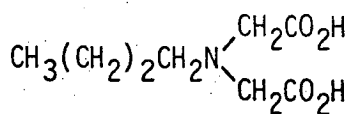


I.  $\text{R} = \text{CH}_3\text{CH}_2, \text{H}_2\text{OCCH}_2$ <sup>131</sup>

II



$n = 10, 16$ <sup>131</sup>



III

An alternative principle which disrupts enterohepatic recirculation employs insoluble polymers which contain many groups capable of  $\text{MeHg(II)}$  binding. The polymer is ingested and traps  $\text{MeHg(II)}$  in the gut from which it is fecally excreted without reabsorption. Powdered human hair treated with mercaptoacetate,<sup>133</sup> polystyrene polymers containing sulfhydryl groups,<sup>5,122,134</sup> polyterephthalate polymers containing thioether groups,<sup>118,135-6</sup> and mercaptostarch<sup>137</sup> have been used for this purpose. All of these agents increase the fecal elimination of mercury and several reduce brain mercury levels. Phenobarbitone has been used to increase bile flow and hence promote fecal  $\text{MeHg(II)}$  excretion from mice treated with polythiol resin.<sup>122,138</sup> Attempts to use the macromolecular polythiol, mercaptodextran, to disrupt enterohepatic recirculation have failed, presumably due to metabolic breakdown into its component, N-acetyl-homocysteine.<sup>115</sup>

#### 1.4 Mercury-Selenium interactions

Selenium was shown to be an essential trace element by Schwarz in 1957<sup>139</sup> and the biotransformations and metabolism of selenium are now fairly well established and have been summarised in Figure 1.1. The physical properties, chemistry and roles of selenium in trace-element metabolism have been elucidated in two recent comprehensive texts.<sup>40-1</sup> The most important process in the mammalian metabolism of selenite,  $\text{SeO}_3^{2-}$ , appears to be the formation of selenotrisulphides,  $\text{RSSeSR}$ <sup>142-6</sup> particularly with glutathione (Table 1.1). The major selenium-binding components in the blood plasma of rats appears to be albumin when  $\text{SeO}_3^{2-}$ , erythrocytes and plasma are incubated *in vitro*.<sup>147</sup> Selenium is concentrated in the albumin fraction of rat plasma after the administration of small doses of  $\text{SeO}_3^{2-}$ , primarily in association with proteins with a molecular weight of 77,000.<sup>148-9</sup> In mice, selenite is metabolised and

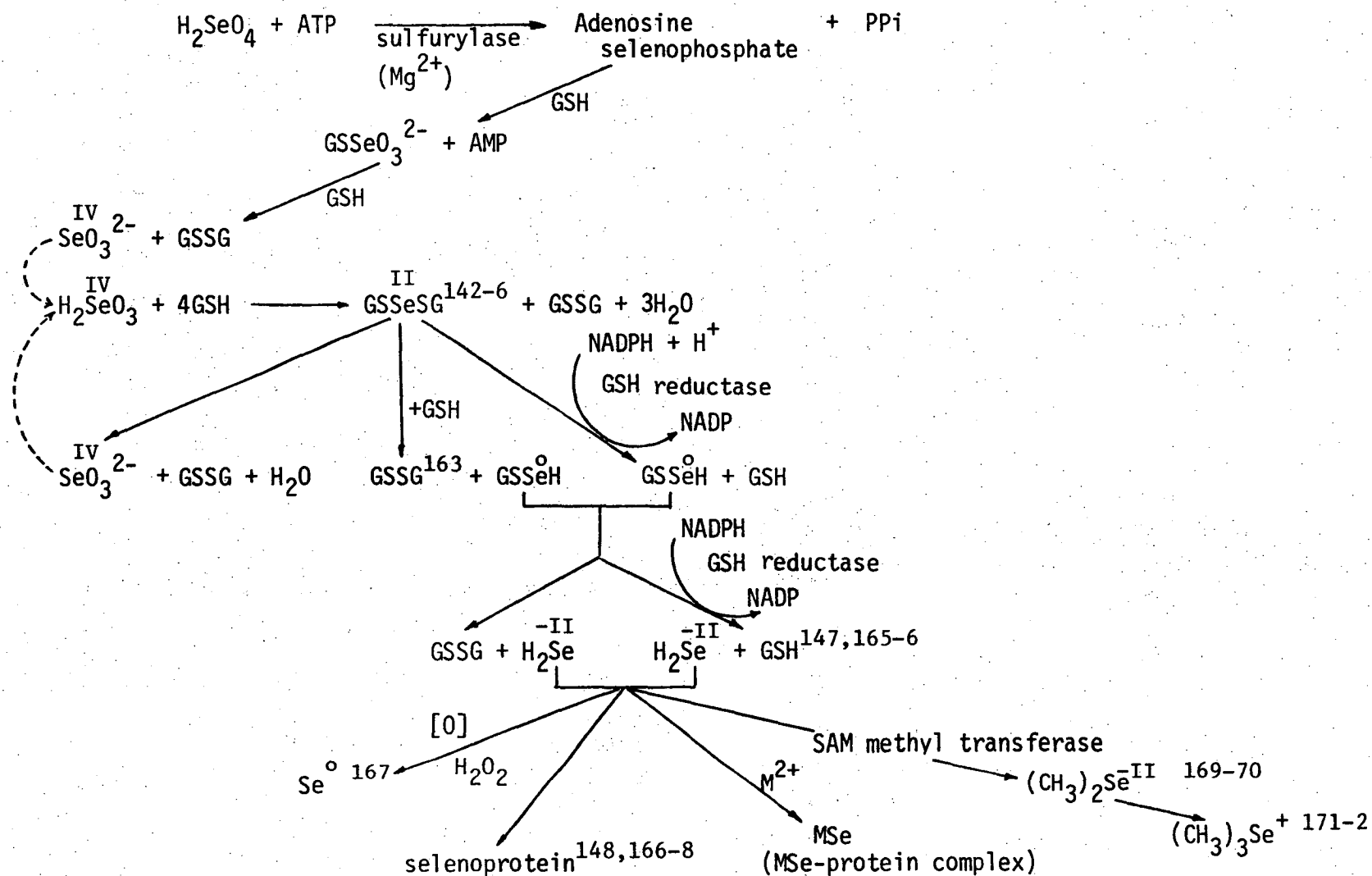
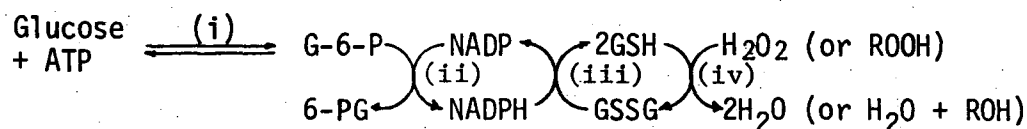


Figure 1.1: Mammalian metabolism of selenate and selenite (from ref. 160).

Glutathione  
Peroxidase <sup>173-4</sup>  
EC 1.11.1.9

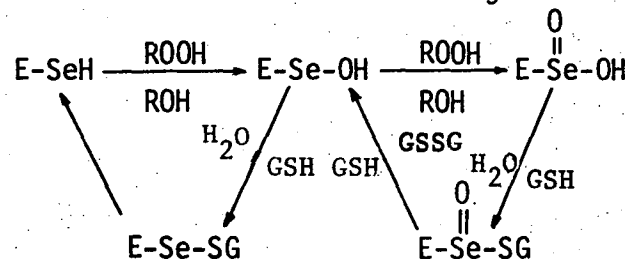
(MW 4 x 21,000)

Contains 4 selenium atoms <sup>175</sup> in reduced selenocysteine form. <sup>176</sup> Essential in the glucose-dependent reduction of peroxides.



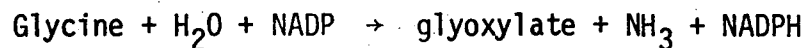
i, Hexokinase ii, G-6-P dehydrogenase  
iii, Glutathione reductase iv, Glutathione peroxidase

Selenium at the active site undergoes redox changes: <sup>177-8</sup>



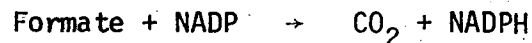
Glycine dehydrogenase  
(MW 12,000)  
EC 1.4.1.10

Contains 1 selenium atom in reduced selenocysteine form. <sup>179</sup> Catalyses the deamination of glycine in *Clostridium stricklandii*.



Formate Dehydrogenase  
(MW high) <sup>180</sup>  
EC 1.2.1.2.

Selenium content is unknown. Catalyses the oxidation of formate to CO<sub>2</sub>.



Present in several microorganisms, including *E. coli*.

Muscle Protein  
(MW 10,000)

Contains 1 selenium atom in an unknown form. Spectral properties are similar to CytC, amino-acid composition is similar to Cyt-b<sub>5</sub>. <sup>181</sup> Absence is associated with 'white-muscle' disease.

Table 1.1: Enzymes and proteins known to contain selenium.

and bound to albumin  $\beta_2$ -lipoprotein and an unidentified protein in the plasma.<sup>150</sup>

Since the initial observation (1960) that selenite is preventative against the injurious effects of cadmium salts on testes in rats,<sup>151</sup> and against renal and intestinal necrosis caused by inorganic mercury(II) salts<sup>152</sup> there has been much interest in the role of selenium as 'Nature's antidote to heavy metal toxicities'.<sup>153</sup> In an even earlier study with  $\text{BALH}_2$ , Tobias *et al.* noted that selenite protected mice against the otherwise lethal effects of inhaled  $\text{CdCl}_2$ ,<sup>154</sup> but twenty years elapsed until the pioneering work by Kar and co-workers.<sup>151</sup> There is evidence that selenium may be involved in the detoxification of  $\text{Tl}$ ,<sup>155-7</sup> and of  $\text{Ag}^+$ ,  $\text{Pb}$  (and perhaps  $\text{Cu}^{2+}$ ).<sup>158</sup> Particularly relevant to this work are the extensive reviews of the interactions of selenium with  $\text{Cd}^{2+}$  and  $\text{Hg}^{2+}$ ,<sup>152-3,8-9</sup> including two published very recently (1980).<sup>160-1</sup>

Despite much work in this area, the mechanisms of such trace element interactions are not yet well understood.<sup>162</sup> It is intriguing that none of the several enzymes and proteins (summarised in Table 1.1) which are known to contain selenium have been implicated in any mechanism for heavy-metal interaction. The confirmed existence of reduced selenohydryl groups in glutathione peroxidase and glycine dehydrogenase, and the scarcity of fundamental chemical information on mercury(II) compounds containing coordinated organoselenium ligands, led to those portions of the present study which are concerned with  $\text{Hg}^{2+}$ -selenohydryl (Chapter 4) and  $\text{MeHg(II)}$ -selenohydryl and diselenide (Chapter 3) interactions.

As an introduction to these Chapters, the salient features concerned with the preventative effects of selenium against inorganic mercury(II) and alkylmercury(II) toxicity, are discussed below.



#### 1.4.1 Selenium interactions with inorganic mercury

Interactions between selenium and inorganic mercury(II) compounds have recently been reviewed by several authors<sup>159,162,182-3</sup> but some of the more important findings are recorded here.

There do not appear to be many reports regarding the effects of selenium on intoxication by elemental mercury, other than that low levels of dietary selenite (0.1 mg Se/kg food) do not seem to increase the bodily retention of mercury in rats exposed to occupational levels of mercury vapor.<sup>184</sup>

Parizek has shown that dietary  $\text{SeO}_3^{2-}$  prevents growth depression due to oral administration of  $\text{HgCl}_2$  in rats.<sup>185</sup> Groth and co-workers report that long term dietary supplementation with selenate,  $\text{SeO}_4^{2-}$ , reduces chronic renal tubular damage in rats administered  $\text{HgCl}_2$ .<sup>186</sup> Selenate has a protective effect in rats on weight loss and histopathology due to  $\text{HgCl}_2$ .<sup>187</sup> Selenite and selenomethionine provide complete protection against kidney and intestinal necrosis in rats fed lethal doses of  $\text{HgCl}_2$ .<sup>152</sup> Remarkably, this effect is not due to improved elimination of mercury, on the contrary, the whole body elimination rate is decreased<sup>188</sup> as are urinary<sup>152,189</sup> and fecal<sup>190</sup> excretion rates in rats, although the effect is not marked in the latter case. Urinary excretion of selenium in mice is also depressed by administration of  $\text{HgCl}_2$  but the mercury excretion rate is dependent on the administered dose of selenite.<sup>191</sup> In lactating rats, selenite decreases the mercury content of fetuses, milk and sucklings, but increases the whole-body mercury content of the dams.<sup>159</sup>

Selenite<sup>152</sup> and selenate<sup>188</sup> increase the whole-body retention of mercury but dramatically change its organ distribution.<sup>192</sup> Single doses of selenite, selenate and selenomethionine all decrease mercury

levels in the kidney<sup>152,193</sup> and increase the content of the liver.<sup>194</sup> In contrast, repeated simultaneous administration of  $\text{Hg}^{2+}$  and selenite is reported to increase the mercury levels in kidneys of rats and mice.<sup>195</sup>

Selenite removes inorganic mercury from metallothionein *in vitro*.<sup>196-7</sup> but does not stimulate the biosynthesis of the apoprotein.<sup>198</sup> Chmielnicka and co-workers have shown that the selenite-induced translocation of inorganic mercury from the kidney (where it is bound presumably to metallothionein) to the liver,<sup>199</sup> is accompanied by an accumulation of mercury in the liver mitochondria.<sup>200</sup> In particular, combined and separate exposures of rats to  $\text{HgCl}_2$  (0.5 mg Hg/kg) and selenite (0.5 mg Se/kg) for 2 weeks decrease the content of mercury in intramitochondrial structures of the kidney and both Hg and Se accumulate in the inner and outer mitochondrial membranes.<sup>201</sup> Levander has also reported that  $\text{HgCl}_2$  inhibits the swelling of liver mitochondria, otherwise induced by selenite. Yamane *et al.* report nine-fold increases in mercury content of nuclei, microsomal and mitochondrial fractions of rat liver homogenates after concurrent administration of  $\text{HgCl}_2$  and  $\text{Na}_2\text{SeO}_4$ .<sup>194</sup> It is likely that these sites, where many important metabolic processes are catalysed, are the targets for damage by mercury<sup>11</sup> and may also be the sites relevant to molecular interactions between selenite and inorganic mercury.

Single injections of selenite cause a dramatic redistribution of inorganic mercury in the blood. Mercury is removed from the erythrocytes into the plasma<sup>149,189,203-5</sup> where it is bound to high molecular weight protein species containing equimolar amounts of mercury and selenium. The magnitude of the effect can be seen in rats where normally 50% of mercury is bound to low molecular weight protein

fractions in plasma, but after administration of selenite,<sup>205</sup> or selenate,<sup>194</sup> this proportion is less than 1%. Selenomethionine causes a similar redistribution, but higher doses are needed for the same response and liver enzymes are essential for the effect *in vitro*, presumably to metabolise selenomethionine to selenite.<sup>192</sup> Burk *et al.*,<sup>149</sup> have demonstrated that mercury and selenium appear together in rat plasma as a macromolecular protein complex of the type ProtSSeHgX. A very similar complex has been identified in hemosylates of rabbit blood.<sup>204</sup> The specific complex in these cases has not yet been identified, but appears to be similar to the 130,000 Dalton cadmium and selenium binding component found by Gasiewicz and Smith.<sup>148,165</sup> These authors have shown that  $H_2Se$  interacts with  $Hg^{2+}$  in plasma to yield a protein complex of molecular weight 330,000 containing equimolar amounts of mercury and selenium.<sup>147</sup> An analogous  $Cd^{2+}$  protein complex of molecular weight 130,000 formed under identical conditions is considered to be colloidal CdSe stabilised by association with specific but unidentified macromolecular proteins.<sup>147</sup> The formation of complexes of this type may explain changes in the biokinetics and toxicity of mercury but the biokinetics of  $Hg^{2+}$  salts are also altered in situations of selenium deficiency.<sup>206</sup>

The occurrence of an equimolar accumulation of selenium and mercury in the liver and brain of seals<sup>207</sup> and in the liver cells of Mediterranean cetaceans<sup>208</sup> has been reported. Ratios of Hg:Se of 1-3 have been reported in the liver and brain of whales.<sup>209</sup> The protective effects of selenate on  $HgCl_2$  toxicity has been associated with the formation of electron-dense particles in the kidney proximal tubule cells and the reticuloendothelial cell cytoplasm and the extracellular space of Disse in the liver.<sup>187</sup> Carmichael and Fowler have used energy-dispersive X-ray analysis to obtain a Hg:Se ratio of 1:2 in

these particles, which is in contrast to 1:1 ratio found by Groth *et al.*<sup>186</sup> This apparent discrepancy may be due to translocation of Hg or Se during sample processing or examination. The mercury in these particles has been shown to be thermally labile when a critical temperature under the X-ray beam is reached.<sup>157</sup> Interestingly, the administration of tellurite,  $\text{TeO}_3^{2-}$ , prevents the formation of these particles and is synergistic with  $\text{SeO}_3^{2-}$  in the prevention of renal necrosis caused by chronic exposure to  $\text{HgCl}_2$ .<sup>149</sup> In contrast to  $\text{SeO}_3^{2-}$ , administration of  $\text{TeO}_3^{2-}$  with  $\text{HgCl}_2$  does not affect the organ distribution of mercury, but it does protect against acute  $\text{HgCl}_2$  toxicity and increases the whole body retention of mercury.<sup>188</sup>

In man, elevated levels of mercury and selenium have been found in the brain, thyroid, pituitary and kidneys of mercury miners, 16 years after the cessation of exposure.<sup>210</sup> Although increased retention of selenium has also been reported elsewhere in persons occupationally exposed to inorganic mercury,<sup>211</sup> it is questionable whether selenite mitigated the effects of chronic mercury exposure in these cases.

Parizek has warned that not all the interactions between inorganic mercury and selenium are beneficial, and that the concomitant presence of mercury and certain selenium metabolites produces a lethal syndrome in rats, particularly if selenite is administered before  $\text{HgCl}_2$ .<sup>152</sup> These toxic effects have been shown to be similar to those caused by large doses of dimethylselenide.<sup>152</sup> Parenteral pretreatment with  $\text{HgCl}_2$  (10 mg/kg) decreases the excretion of volatile selenium compounds in female rats after administration of  $\text{Na}_2\text{SeO}_3$  (0.3 mg/kg ip).<sup>152,192</sup> The effect is more marked than identical pretreatment with  $\text{CdCl}_2$  or  $\text{ZnCl}_2$ , and selenomethionine acts similarly.<sup>212</sup> Curiously, male rats are much more susceptible to the toxic syndrome than females, but this sex-linked difference is not related to the sex-linked differences found

for dimethylselenide conversion to the excretion product, trimethylselenonium ion (see Figure 1.1). Parizek has postulated that the toxic effect may be due to a selenium metabolite such as  $\text{MeSe}^-$ , and that  $\text{HgCl}_2$  may either alter the metabolic pathways and/or distribution of this intermediate or sensitivity of the critical organs to  $\text{MeSe}^-$ , etc.

These unresolved toxic effects must, at the moment, restrict the use of selenium compounds in the prevention and/or therapy of mercury intoxication.

#### 1.4.2 Selenium interactions with organic mercury compounds

The interactions of selenium with organomercurials other than methylmercury(II), have not been well studied. Mengel and Karlog<sup>205</sup> report that selenite-induced translocation of mercury to macromolecular proteins in the plasma of rats treated with methoxyethylmercuric chloride is not observed, in contrast to previous reports.<sup>213</sup> Chmielnicka *et al.* report that selenite suppresses the induction of rat kidney metallothionein due to  $\text{EtHgCl}$  or to  $\text{PhHgCl}$ .<sup>214</sup>

The interactions of selenium with methylmercury(II) have been recently reviewed.<sup>162,215</sup> Concentrations of  $\text{MeHgCl}$  in excess of  $5 \times 10^{-5} \text{ M}$  completely inhibit the *in vitro* activity of the selenium-containing enzyme glutathione peroxidase (Table 1.1) in rat liver homogenates<sup>216</sup> and selenite suppresses the induction of metallothionein due to  $\text{MeHg-cyanoguanidine}$ .<sup>214</sup> Dietary selenite has been shown to be protective against the toxic effects of  $\text{MeHg(II)}$  in quail,<sup>217-9</sup> chicks,<sup>208,220</sup> rats<sup>190,221-4</sup> and pigs.<sup>225-6</sup> Contrariwise,  $\text{MeHg(II)}$  (10 mg Hg/kg) protected against selenite-induced weight loss in rats.<sup>185</sup> Selenium present in dietary fish may have a protective effect against  $\text{MeHg(II)}$ ,<sup>217,221</sup> but the fairly minor effects may be due to changes in

dietary protein, etc.

Fish meal containing selenium is reported to have delayed the growth retardation and reversed the neurological degeneration in weanling rats caused by dietary MeHgCl.<sup>221a</sup>

As in the case of inorganic mercury, the organ distribution of MeHg(II) is profoundly affected by selenite, but the changes differ markedly from those found with  $\text{Hg}^{2+}$ .

Single doses of  $\text{SeO}_3^{2-}$  to MeHgCl-treated rats, produce a BALH<sub>2</sub>-like effect which immediately increases the mercury level of the brain followed by a later decrease.<sup>222-3</sup> In rats administered both MeHgCl and  $\text{Na}_2\text{SeO}_3$ , seven-fold increases in the selenium content of the brain, liver and kidney have been reported.<sup>221,227</sup> Ohi *et al.*<sup>221</sup> report that the total mercury and inorganic mercury contents of the brain increase markedly when selenite is administered to MeHg(II) poisoned rats but in contrast, the MeHg(II) content in the brain and other organs is not significantly altered.

Closer relationships appear to exist between the Se and  $\text{Hg}^{2+}$  contents of various organs than with MeHg(II) content, which may reflect a selenium-induced change in the biotransformation of MeHg(II) to  $\text{Hg}^{2+}$ , however dietary selenium has no effect on the rate of C-Hg bond cleavage of MeHg(II) in rat liver homogenates *in vitro*.<sup>228</sup>

A direct interactive mechanism between selenium and MeHg(II) may also be possible. Half of the methylmercury(II) incubated in whole blood with an equivalent quantity of selenite, is benzene extractable without acidification.<sup>229</sup> Lipid soluble MeHg(II)-selenium complexes such as  $(\text{MeHg})_2\text{Se}$  (analogous to the active species in the Minamata episodes<sup>192</sup>) may be responsible for the redistribution of MeHg(II) into the brain after  $\text{SeO}_3^{2-}$  administration.

In summary, the interactions of selenium with mercury compounds (and heavy metals in general) appear to be affected by many variables such as age, sex and nutritional status of the experimental animals and much work needs to be done in these areas before clear mechanisms can be elucidated.

## CHAPTER TWO

### STRUCTURAL CHEMISTRY OF MERCURY(II) THIOLATES

#### 2.1 Introduction

Complex formation *in vivo* between mercury(II) compounds and endogenous thiols plays a major role in the biological chemistry of mercury (Chapter 1). All of the currently used antidotes for mercury toxicity take advantage of the higher thermodynamic affinity<sup>†</sup> of mercury for sulfhydryl donors than for other possible ligands such as nitrogen-containing bases, chloride, etc. The historically held rationale for the use of the dithiol BALH<sub>2</sub> as an antidote for mercury poisoning is based on the ability of this ligand to form stable chelate complexes with arsenic.<sup>54</sup> Curiously, despite the long and widespread use of BALH<sub>2</sub> as a heavy-metal antidote, no definitive evidence for chelation to any metal has been demonstrated; for example, no single-crystal X-ray structure of any BALH<sub>2</sub> complex (or of any closely related vicinal dithiol except the recent complex of MeHg(II) with trans-1,2-dimercaptocyclohexanedithiol<sup>230</sup>, page 42) has been reported. This situation is almost certainly due to the intractable nature of BALH<sub>2</sub> complexes which are often very poorly soluble in most solvents, making crystal growth very difficult. As will be discussed later, it has been shown by vibrational spectroscopy in this laboratory that the mercury(II) complex, HgBAL, is not a chelate, but rather has a polymeric structure, with linear 'SHgS' bonding.<sup>231</sup> Although chelating structures for HgBAL are chemically implausible considering the strong disposition of Hg(II) for linear sp or tetrahedral sp<sup>3</sup> coordination, such structures are

---

<sup>†</sup>Despite the unquestionable high stability of inorganic mercury(II) thiolates, the formation constants of Hg(SR)<sub>2</sub> complexes are very poorly established.<sup>232</sup>



still found in recent toxicological discussions.<sup>233</sup>

This study was derived from the reports that two water-soluble vicinal dithiols : meso-2,3-dimercaptosuccinic acid, DMSH<sub>4</sub> and the sodium salt of 2,3-dimercapto-1-propane sulfonic acid, Unithiol are promising antidotes for inorganic- and methylmercury(II) poisoning (Chapter 1, pages 14-15), yet the relevant Hg<sup>2+</sup> complexes such as HgDMSH<sub>2</sub> and Na[HgUT] had not previously been characterised. These complexes have been prepared in this work and shown here by vibrational spectroscopy to be polymeric, like HgBAL.

In addition to the formation of bithiolato complexes of the type Hg(SR)<sub>2</sub>, the ready availability of alternate donor ligands at the *in vivo* target site(s) for Hg binding has prompted much interest in the nature of monothiolato mercury(II) complexes of the type RSHgX where X is some neutral or anionic ligand such as chloride, acetate, etc.<sup>234,235</sup> Several model compounds of this type have been characterised in this laboratory and elsewhere and their structural chemistry will be briefly reviewed.

Although the use of thiol antidotes for MeHg(II) toxicity is widespread and the X-ray crystal structures of three important mercapto-aminoacid complexes with MeHg(II) have been reported,<sup>236,237</sup> the interactions with vicinal dithiol ligands is less well established. The complex (MeHg)<sub>2</sub>BAL has been previously investigated in this laboratory by vibrational spectroscopy and shown to have the expected linear 'SHgMe' geometry.<sup>238</sup> The previously unreported analogous compounds (MeHg)<sub>2</sub>DMSH<sub>2</sub> and Na[(MeHg)<sub>2</sub>UT] have been examined in this study, together with complexes of several monothiolates (including the new cationic complexes with thiocholine perchlorate and N-methyl-4-mercaptopiperidinium nitrate. The aqueous solution chemistry and MeHg(II) formation constants of these complexes will be elucidated in Chapter 3.

## 2.2 Structural features of MeHg(II) thiolates

The solid-state structural features of alkyl- and arylmercury(II) thiolates of the type  $\text{RHgSR}'$  are dominated by two-coordinate mercury in the strongly bound, linear 'C-Hg-S' moiety. Single-crystal X-ray crystallographic structures of six monothiolatomethylmercury(II) species,  $\text{MeHgSR}$ , and one dithiolatobis[methylmercury(II)] species, have been published to date. The important Hg-S and Hg-C bonding distances and C-Hg-S bonding angle of each of these complexes are recorded in Table 2.1.

The mercury-sulfur distances lie within the narrow range 2.32 - 2.39 Å as do those for the few other known thiolato-structures,  $\text{RHgSR}'$  ( $\text{R} \neq \text{Me}$ ):  $\text{PhHg}$  (dithizone) [2.372(2)],<sup>239</sup>  $\text{PhCH}_2\text{HgSC(Ph)}_3$  [2.363]<sup>240</sup> and  $\text{PhHgSC}_6\text{H}_4$ -2,6-diMe [2.33(1)].<sup>241</sup> The carbon-mercury bonding distances are also relatively constant: 2.04 - 2.12 Å. The structures of the complexes in Table 2.1 serve to characterise MeHg(II)-thiolate binding. The MeHg-S bond is always nearly linear, reflecting the predominantly sp character of the mercury atom, even in those situations where intramolecular bonding may be present, e.g. the cytosine derivatives, which all have Hg-N distances less than the sum of the van der Waal's radii of Hg and N (3.00 Å<sup>242-3</sup>). This demonstrates the very weak residual Lewis acidity of a sulfhydryl-bound MeHg(II) group.

In the dithiolato complex, direct evidence of chelation of one MeHg(II) group is reflected in the increased distortion of the MeHg-S bond angle (167.8°) from linearity, due to simultaneous weaker intramolecular binding to the alternate, already complexed, sulfhydryl group. The secondary, Hg-S', bonding distance, 2.857(3) Å is still considerably less than the sum of the van der Waal's radii (3.35 Å<sup>242-3</sup>), generating 'effective' three-coordination at one mercury atom.

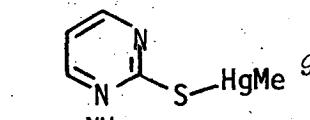
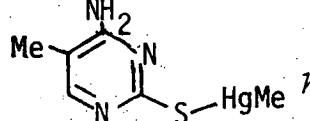
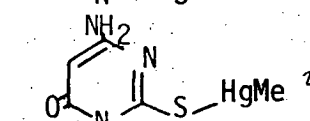
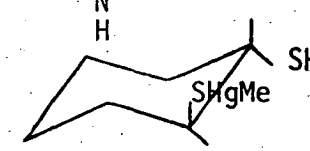
Complex	Hg-S/Å	C-Hg/Å	C-Hg-S/°	Ref
$[\text{MeHgSCH}_2\text{CH}(\text{NH}_3)\text{CO}_2^-] \cdot \text{H}_2\text{O}^b$	2.352(1)	2.10(4)	177.6(9)	236
$[\text{MeHgSC}(\text{Me})_2\text{CH}(\text{NH}_3)\text{CO}_2^-]_2 \cdot \text{H}_2\text{O}^c$	2.38(1), 2.36(1)	2.07(6), 2.09(5)	175(2), 175(2)	237 <sup>d</sup>
$[\text{MeHgSC}(\text{Me})_2\text{CH}(\text{NH}_2\text{HgMe})\text{CO}_2^-]^a$	2.35(1)	2.04(4), 2.07(4)	176(1)	237 <sup>f</sup>
 <sup>g</sup>	2.39(2)	2.13(6)	174	244
 <sup>h</sup>	2.393(4)	2.09(1)	178.6(4)	245
 <sup>i</sup>	2.390(6)	2.09(2)	178.6(9)	245
 <sup>j</sup>	2.363(4), 2.367(4)	2.08(2), 2.12(2)	167.8(5), 117.1(5)	230

Table 2.1: Mercury bonding distances and angles from the published crystal structures of MeHgSR complexes.<sup>a</sup>

## Footnotes to Table 2.1

- a* the mercaptoamino acid complexes have been reviewed by Carty<sup>246</sup>
- b* Figure 2.1
- c* Figure 2.2. Two independent molecules in the unit cell
- d* preliminary structure in ref. 247
- e* Figure 2.3. Bonding distance Hg-N 2.13(3)Å.
- f* preliminary structure in ref. 248
- g* weak bonding distance Hg...N 2.83(3)Å
- h* weak bonding distance Hg...N 2.80(2)Å
- i* weak bonding distance Hg...N 2.95(2)Å
- j* weak bonding distance Hg...S' 2.857(3)

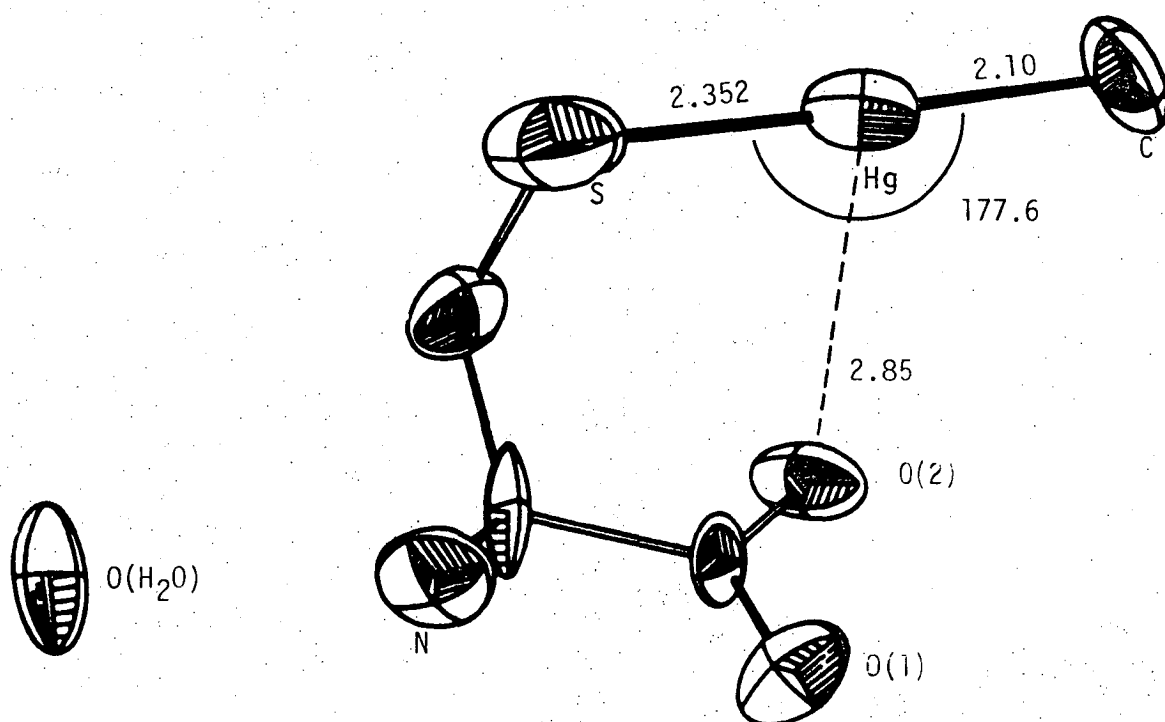


Figure 2.1: Molecular structure of Methyl-L-cysteinatomercury(II) from reference 236.

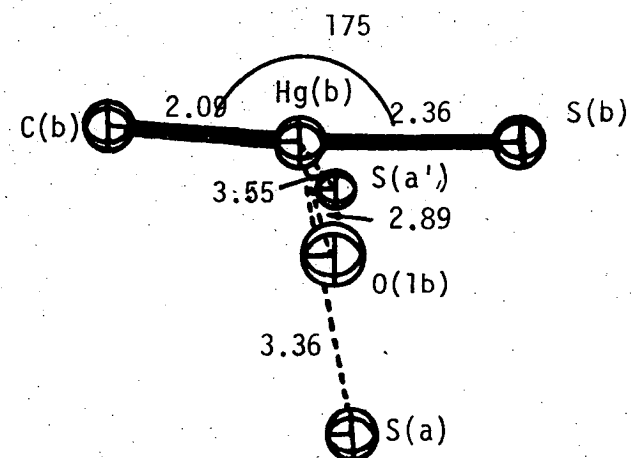
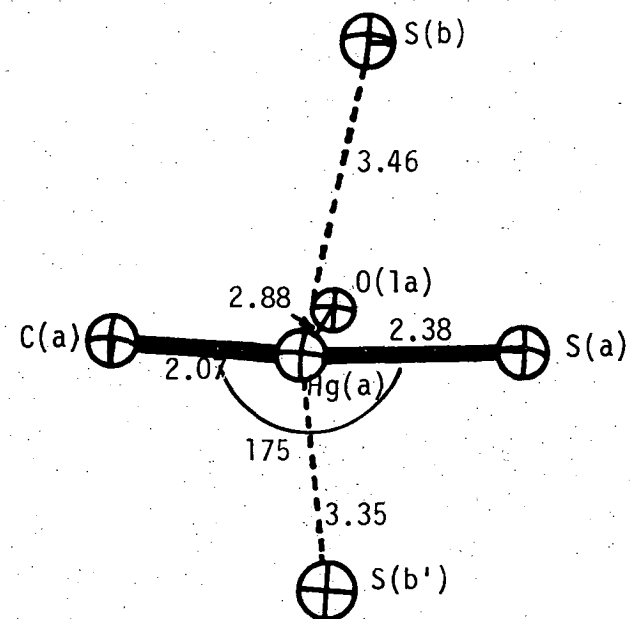
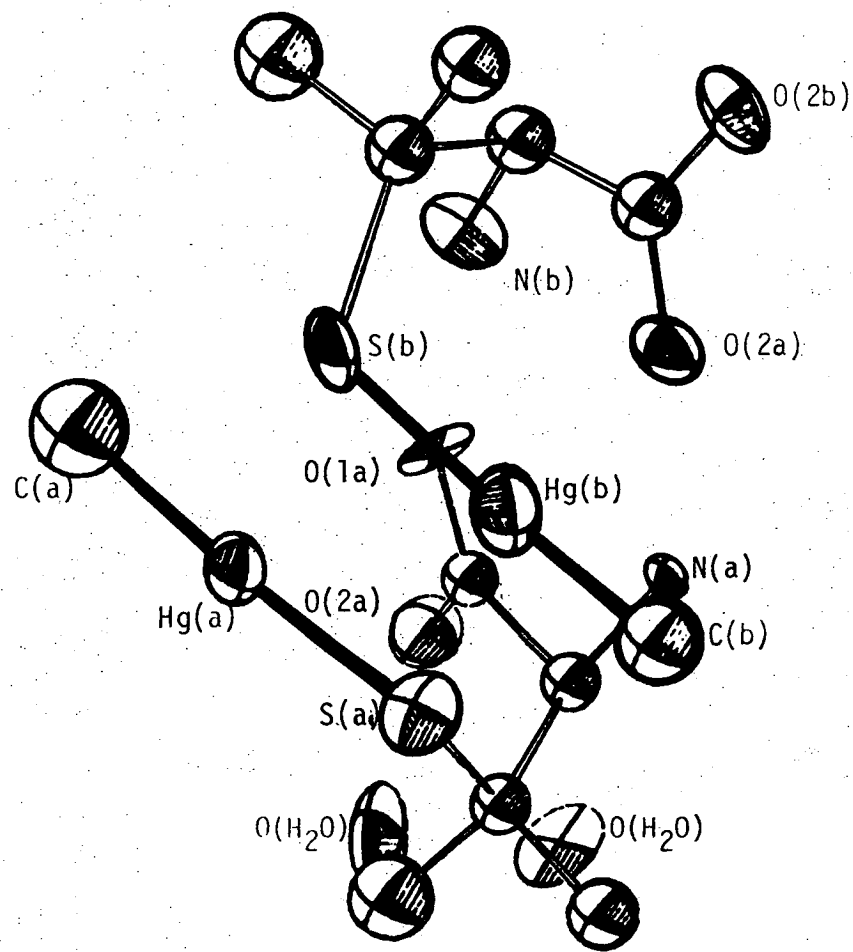


Figure 2.2: Molecular structure of methyl-DL-penicillaminatomercury(II) monohydrate from reference 237 showing weak interactions around Hg in the two crystallographically independent molecules in the unit cell.

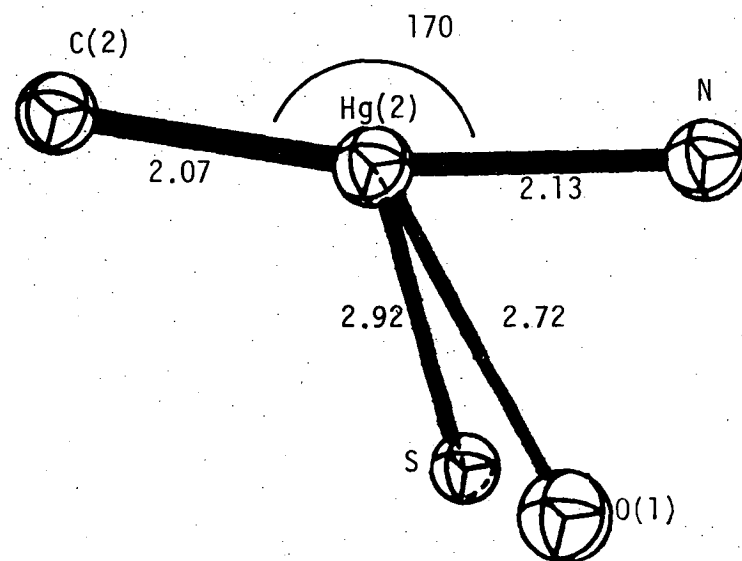
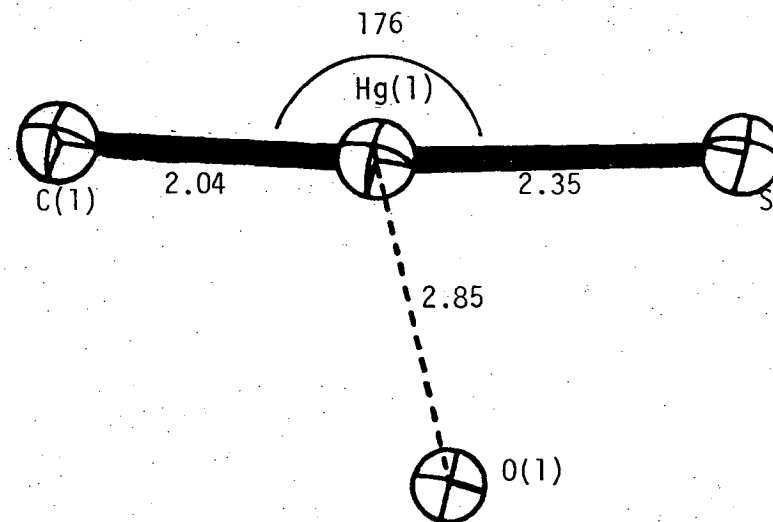
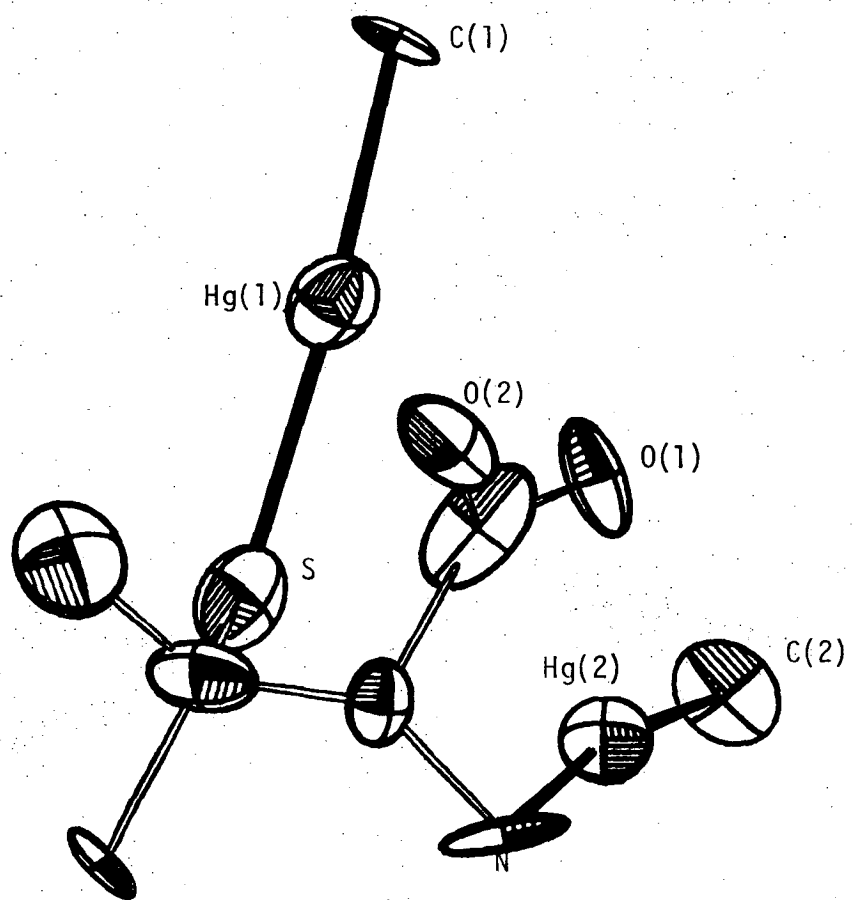
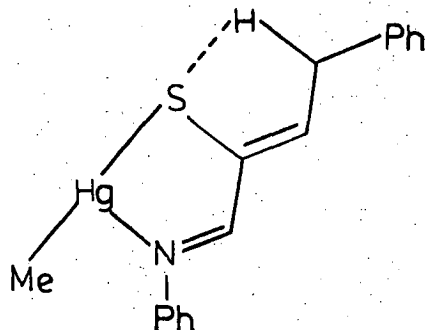


Figure 2.3: Molecular structure of D,L-penicillaminato-bis[methylmercury(II)] from reference 237 showing close contacts of the two Hg atoms.

Chelation of MeHg(II) by nitrogen donors is now well established in solution and in the solid-state (see reference 249 for a recent review). Three coordinate mercury involving a sulfur donor is also found in the solid-state structure of one isomer of the dithizone complex:<sup>239</sup>



One (or both) MeHg(II) groups of the 2:1 complexes with vicinal dithiols BALH<sub>2</sub>, DMSH<sub>4</sub> and Unithiol may be chelated in aqueous solution (Section 3.3.3, page 136).

Several MeHg(II) complexes of monothiolate and dithiolate ligands have been prepared in this study by the metathetic reaction of MeHgNO<sub>3</sub> (or MeHgOH) with the thiol or dithiol in aqueous solution. The non-polar complexes MeHgSBu<sup>t</sup> and MeHgSCH<sub>2</sub>Ph were extracted into hexane and recovered by evaporation of this solvent. These complexes have been isolated previously<sup>250</sup> and were not analysed. The other complexes were precipitated as crystalline solids, either immediately or upon slow evaporation of the aqueous solution to low volume. The microanalyses of these previously uncharacterised complexes are recorded in Table 2.2.

The vibrational spectra of the complexes were obtained in order to assist characterisation of the previously unstudied vicinal dithiol complexes of DMSH<sub>4</sub> and Unithiol. The pertinent Hg-S, Hg-C and C-S stretching frequencies for the new complexes are recorded in Table 2.3, together with previously assigned values for MeHgSR complexes reported elsewhere. These frequencies are coincident in the infrared and Raman

Complex	required %				found %			
	C	H	Hg	S	C	H	Hg	S
MeHgSCH <sub>2</sub> CO <sub>2</sub> H	11.8	1.97	65.4	10.5	11.6	2.01	65.1	10.1
[MeHgSCH <sub>2</sub> CH <sub>2</sub> NMe <sub>3</sub> ]ClO <sub>4</sub>	16.6	3.71	46.2	7.4	16.7	3.76	45.9	7.6
[MeHgSC <sub>5</sub> H <sub>10</sub> NHMe]NO <sub>3</sub> <sup>α</sup>	20.6	3.94	49.1	7.8	20.6	3.91	49.0	7.6
MeHgSCH(CO <sub>2</sub> H)CH <sub>2</sub> CO <sub>2</sub> H	16.5	2.21	55.0	8.8	16.8	2.43	55.1	8.7
MeHgSCHCO <sub>2</sub> H   MeHgSCHCO <sub>2</sub> H	11.8	1.65	65.6	10.5	12.0	1.74	65.5	10.2
MeHgSCH <sub>2</sub>   MeHgSCHCH <sub>2</sub> SO <sub>3</sub> Na	9.4	1.73	62.7	15.0	9.4	1.87	1.48	62.4

Table 2.2: Previously uncharacterised MeHg(II) thiolates and dithiolates

<sup>α</sup> monothiol is 4-mercapto-N-methylpiperidine

spectra, consistent with the absence of a centre-of-symmetry in these molecular solids. The most readily assigned vibrational band is due to  $\nu(\text{HgC})$  and is very sharp and intense in the Raman spectra, and almost invariant in frequency for these complexes ( $528\text{--}555\text{ cm}^{-1}$ ) and other methylmercury(II) complexes<sup>†</sup>, e.g. Me<sub>2</sub>Hg ( $\nu_s\ 515$ ,  $\nu_{as}\ 550$ )<sup>255</sup>; MeHgX, X=F ( $561\text{--}573$ )<sup>256</sup>, Cl( $539\text{--}558$ )<sup>257-63</sup>, Br( $538\text{--}545$ )<sup>257-8,262-4</sup>, I( $526\text{--}538$ )<sup>257-8,260-3</sup>; MeHgC(SiMe<sub>3</sub>)<sub>3</sub> ( $523\text{--}528$ )<sup>265</sup>; MeHgCN( $559\text{--}565$ )<sup>266</sup> and MeHgSCN( $543\text{--}562$ )<sup>267-8</sup>.

The expected mercury-sulfur coordination is confirmed by the absence of  $\nu\text{SH}$  near  $2500\text{ cm}^{-1}$ . This vibration is weak in the infrared spectra but very intense and characteristic in the Raman spectra of the thiol

<sup>†</sup>The values in parentheses represent the range reported by various authors in both i.r. and Raman spectra and are often solvent and phase dependent.



Complex	$\nu_{\text{HgS}}/\text{cm}^{-1}$	$\nu_{\text{HgC}}/\text{cm}^{-1}$	$\nu_{\text{CS}}/\text{cm}^{-1}$	Ref.
<u>monothiolate ligands</u>				
MeHgSMe	333m [329vs]	533 [537]	692 [700]	251
	329m [327w]	522 [533]	698 [697]	252
MeHgSBu <sup>t</sup>	383w [390m]	534m [536vs]	582m [586s]	
MeHgSPh	382m [382m]	536m [547vs]	692 [698]	253
MeHgSCH <sub>2</sub> Ph	346m [342s]	538m [540vs]	700s [702w] 680w [684m]	
MeHgSCH <sub>2</sub> CO <sub>2</sub> H <sup>e</sup>	334m (318msh [329s])	550vw,br (529w [538vs])	654m [676m] 627m	
[MeHgSCH <sub>2</sub> CH( $\overset{+}{\text{N}}\text{H}_3$ )CO <sub>2</sub> <sup>-</sup> ] <sub>2</sub> H <sub>2</sub> O	325m [326vs]	538m [538vs]	not reported	236
[MeHgSC(Me) <sub>2</sub> CH( $\overset{+}{\text{N}}\text{H}_3$ )CO <sub>2</sub> <sup>-</sup> ] <sub>2</sub> H <sub>2</sub> O	322vw,sh [322m]	555m [555m]	not reported	254
[MeHgSCH <sub>2</sub> CH <sub>2</sub> $\overset{+}{\text{N}}\text{Me}_3$ ]ClO <sub>4</sub> <sup>-</sup>	329s [331s]	542m [542s]	621vs [621w]	
MeHgSCH(CO <sub>2</sub> H)CH <sub>2</sub> CO <sub>2</sub> H <sup>f</sup>	361m [362m]	539m [550vs]	673m [677w]	
[MeHgSC <sub>5</sub> H <sub>10</sub> $\overset{+}{\text{N}}\text{HMe}$ ]NO <sub>3</sub> <sup>e</sup>	371 [373m] 348 [353m]	543w 533m [539s]	719w [718w] 748w [750s]	

(Table 2.3 continued over...)

dithiolate ligands

3,4-di(MeHgS)C <sub>6</sub> H <sub>3</sub> -Me <sup>b</sup>	354w [370&357m] <sup>g</sup> 335w [338m]	549w [553vw,sh] 528w [526vs]	685w [690m]	
MeHgSCH <sub>2</sub>   MeHgSCHCH <sub>2</sub> OH, (MeHg) <sub>2</sub> BAL	328m.br [328s,br]	530m [537vs]	662vw [656vw,sh]	238
MeHgSCHCO <sub>2</sub> H   MeHgSCH <sub>2</sub> CO <sub>2</sub> H, (MeHg) <sub>2</sub> DMSH <sub>2</sub>	352s [358m]	537m [535vw,sh] 550w,sh [550s]	686m [675m]	
MeHgSCH <sub>2</sub>   MeHgSCHCH <sub>2</sub> SO <sub>3</sub> Na , Na[(MeHg) <sub>2</sub> UT] <sup>h</sup>	333w,br [329m,br]	526m [531s]	660w [655vw] 586m [585vw]	
MeHgSCH <sub>2</sub> <sup>d</sup>   CH(OH)   MeHgS-CH <sub>2</sub> , (MeHg) <sub>2</sub> DMP	341s [342vs]	543s [537vs]	684m [687w]	238

Table 2.3: Hg-S, Hg-C and C-S stretching frequencies for MeHg(II) thiolates and dithiolates<sup>a</sup>

<sup>a</sup>this work unless otherwise stated. Raman values are shown in parentheses. <sup>b</sup>toluene-3,4-dithiol

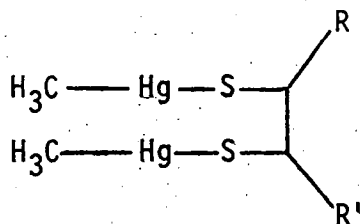
<sup>c</sup>N-methyl-4-mercaptopiperidine <sup>d</sup>1,3-dimercapto-2-propanol <sup>e</sup>in D<sub>2</sub>O (PD5.6)  $\nu_{\text{HgS}}$ [342m],  $\nu_{\text{CHg}}$ [546s]

<sup>f</sup>in D<sub>2</sub>O pD=5.6  $\nu_{\text{HgS}}$ [365m]  $\nu_{\text{HgC}}$ [547vs] <sup>g</sup>ligand has 364w <sup>h</sup>poor quality far infrared spectrum.

ligands. The mercury-sulfur stretching frequencies of the monothiolato complexes shown in Table 2.3 also fall within a fairly narrow range, 329-390  $\text{cm}^{-1}$ . The band due to this vibration is absent in the spectra of the thiol ligands but is usually of medium to strong intensity in both i.r. and Raman spectra of the complexes. The centrosymmetric sulfide complex  $(\text{MeHg})_2\text{S}$  also has  $\nu_{\text{HgS}}$  near this range [ $\nu_{\text{as}}$  344,  $\nu_{\text{s}}$  300].<sup>269</sup>

The carbon-sulfur stretching frequency is more difficult to assign in these complexes, as there are usually several weak to medium intensity ligand vibrations in the region 600-700  $\text{cm}^{-1}$ . The values of  $\nu_{\text{CS}}$  reported in Table 2.2 have been assigned by comparison with previously published values and are probably moderately coupled to other ligand vibrations, giving rise to variable intensities.

The vibrational features of the 2:1  $\text{MeHg(II)}$  complexes with dithiolate ligands are also shown in Table 2.3 and can be readily compared with those of monothiolato complexes. In the previously reported 2:1 complexes of vicinal  $\text{BALH}_2$  and its non-vicinal analog  $\text{DMPH}_2$ , values for  $\nu_{\text{HgC}}$ ,  $\nu_{\text{HgS}}$  and  $\nu_{\text{CS}}$  are all consistent with simple linear 'C-HgS' coordination.<sup>238</sup> The 2:1 complex with toluene-3,4-dithiol has been previously prepared<sup>230</sup> in conjunction with that of the chelating dithiol, trans-1,2-dimercaptocyclohexane (Figure 2.4), but no spectroscopic details are available. The vibrational features of the toluene-3,4-dithiol complex and those of the complexes with antidotal  $\text{DMSH}_4$  and Unithiol are also consistent with simple linear 'C-Hg-S' coordination to form structures of the type:



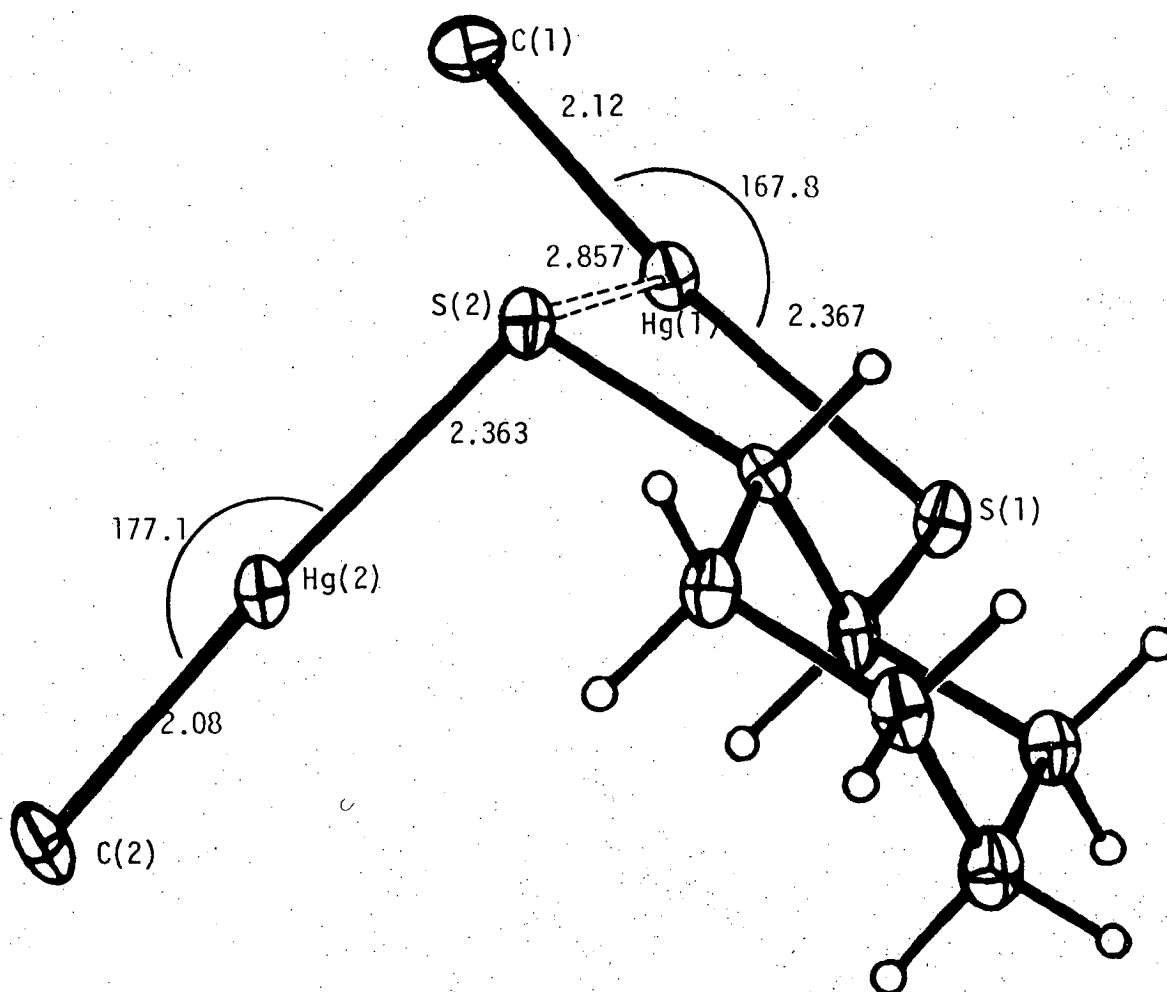


Figure 2.4: Molecular structure of trans-1,2-dimercaptocyclohexanebis [methylmercury(II)] from reference 230.

It is not possible to say whether the slight ( $15\text{--}20\text{ cm}^{-1}$ ) splitting seen in the C–Hg vibrational band of the toluene-3,4-dithiol and  $\text{DMSH}_4$  complexes, is due to two different C–Hg environments, *viz.* one chelated  $\text{MeHg}$ . Although such splitting is also seen in the mercaptoacetate and 4-mercapto-N-methylpiperidine monothiolate complexes, it is evident only in the i.r. spectra in these cases. The complex with confirmed chelated  $\text{MeHg(II)}$ <sup>230</sup> was not available for this study, but its vibrational spectra would seem to warrant some attention.

### 2.3 Structural features of complexes of the type, $\text{Hg}(\text{SR})_2$

The very high stability of the C-Hg and Hg-S bonds in  $\text{MeHgSR}$  species and the very low residual Lewis acidity of the  $\text{MeHgS-}$  group, always leads to dominant linear 2-coordination about mercury, with occasional weaker interactions with nearby donors to yield higher 'effective'<sup>243</sup> coordination numbers. In contrast, the mercury atom in a complex of the type  $\text{Hg}(\text{SR})_2$  has somewhat more freedom to assume alternate  $\text{sp}$  (linear) or  $\text{sp}^3$  (tetrahedral) coordination geometries, and in fact both situations arise in the few published single-crystal X-ray crystallographic studies of such complexes.

Preliminary crystallographic work carried out by Wells<sup>270</sup> in 1937, suggested that the complexes  $\text{Hg}[\text{S}(\text{CH}_2)_n\text{CH}_3]$   $n = 1, 2, 4, 5, 6$  were isomorphous, linear, molecular solids. The *n*-butyl ( $n=3$ ) and *n*-octyl ( $n=7$ ) members of this homologous series were apparently anomalous, e.g. crystals of these compounds were tetragonal and triclinic respectively, in contrast to monoclinic for the other members. Intriguingly, the anomalous *n*-butyl compound is also found in the trend for melting points and solid-state densities of this series (Figure 2.5).

The molecular structure of the methyl homolog (not studied by Wells) was unambiguously determined by Bradley and Kunchur<sup>271</sup>, and is shown in Figure 2.6. The structure clearly contains linear molecules,  $\text{Hg}(\text{SMe})_2$ , but secondary weak intramolecular Hg-S interactions produce a three-dimensional polymeric structure, consistent with the high melting point and density in the solid state (Figure 2.6). Figure 2.7 shows the structure of  $\text{Hg}(\text{SEt})_2$  subsequently determined by these workers<sup>274</sup>, in which intermolecular interactions between the linear molecules are essentially nonexistent (Hg-S 3.53 and 3.56 Å compared with the sum of the van der Waal's radii, 3.35 Å<sup>242-3</sup>).

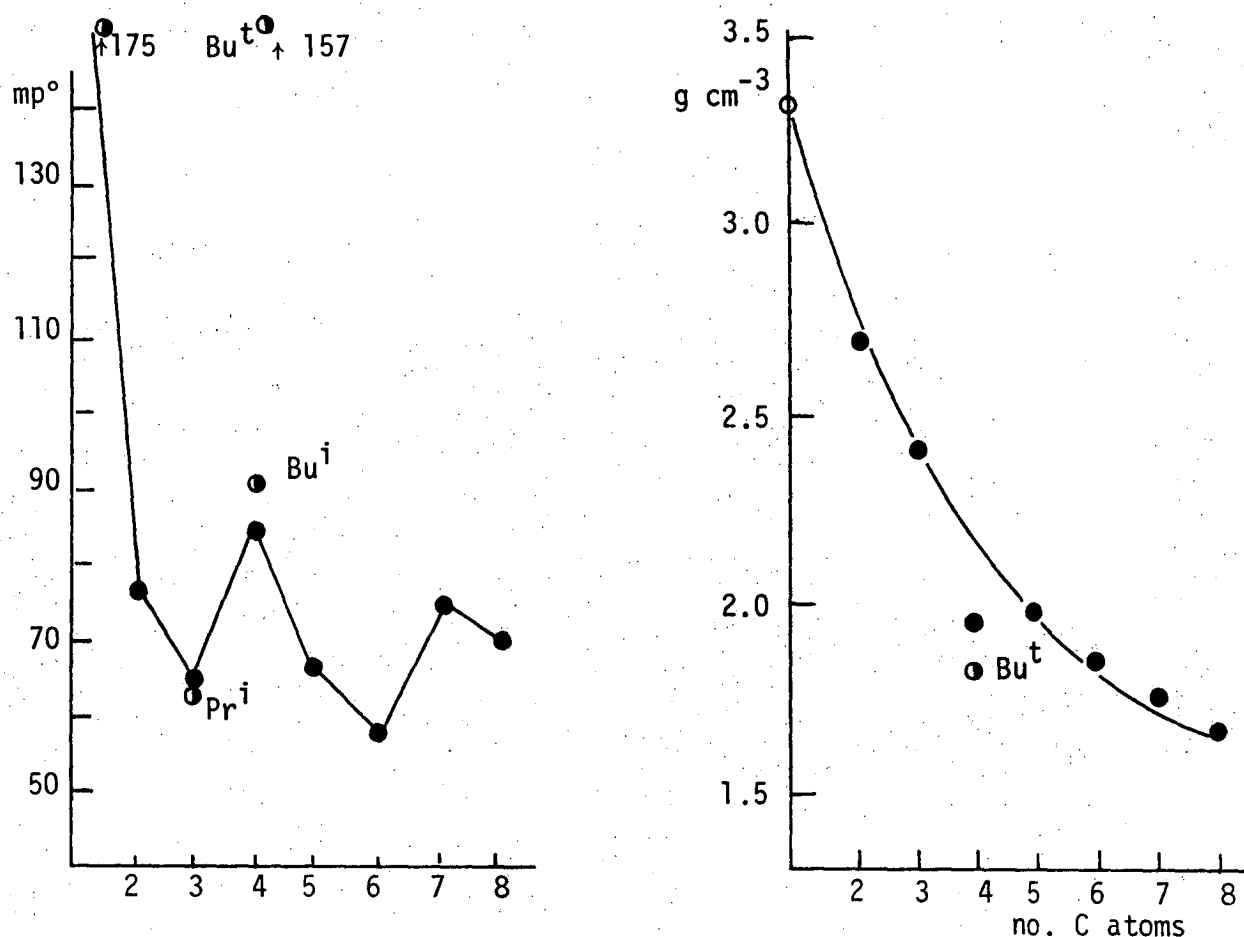


Figure 2.5: Comparison of melting point and solid-state density of bis(alkylthiolato)mercury(II) complexes.

- taken from reference 270 for the n-alkyl homologues    ○ ref. 271
- ref. 272 *tert*-butyl sublimes at 135° (ref. 273)

Particularly interesting in this series is the structure of the *tert*-butyl analog (not studied by Wells) which was also determined by Bradley.<sup>273</sup> Figure 2.8 shows the polymeric nature of Hg(SBu<sup>t</sup>)<sub>2</sub> (consistent with its high sublimation temperature and low density) in which the mercury atom is now clearly tetrahedrally coordinated to doubly-bridging sulfur atoms.

The transition from linear to tetrahedral geometry in the *tert*-butyl analog is probably a reflection of the relatively high Lewis basicity,

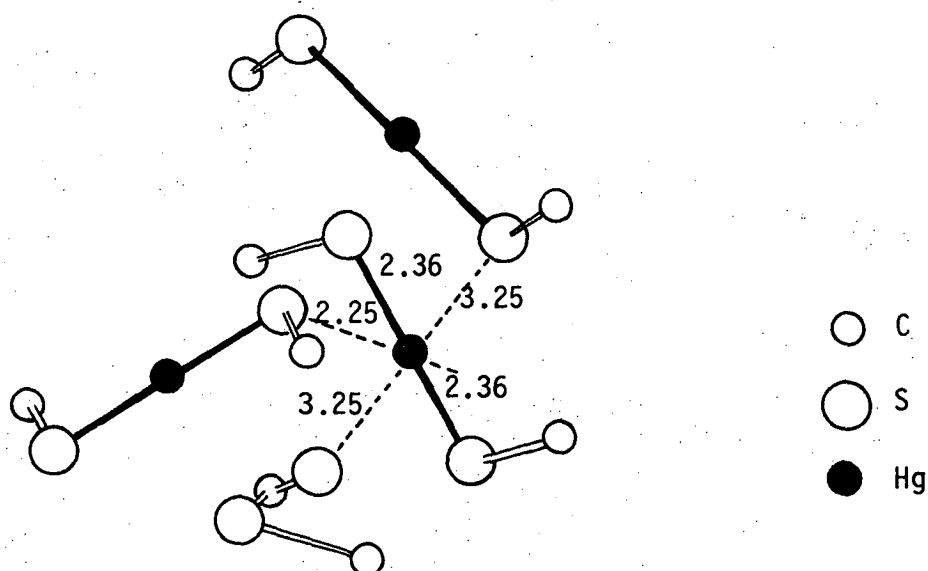


Figure 2.6: Molecular structure of  $\text{Hg}(\text{SMe})_2$  from reference 271

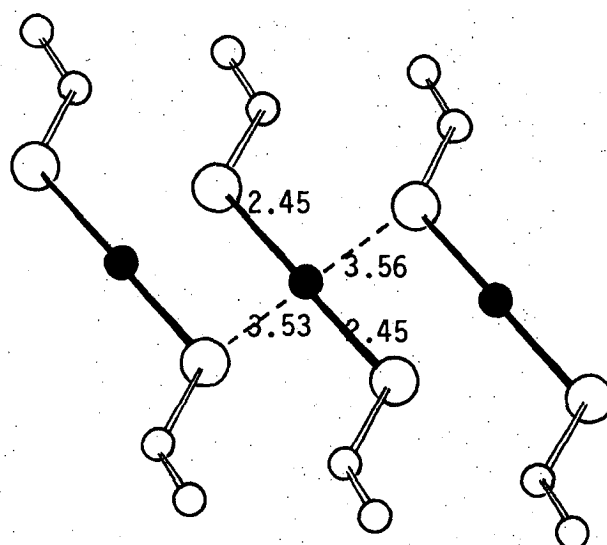


Figure 2.7: Molecular structure of  $\text{Hg}(\text{SEt})_2$  from reference 274

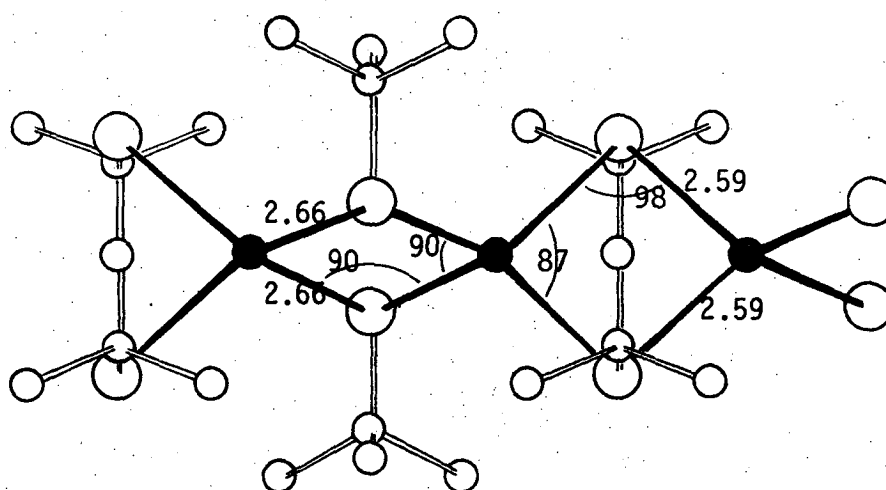
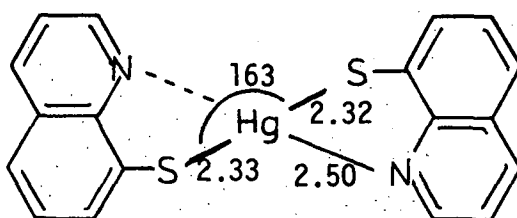


Figure 2.8: Molecular structure of  $\text{Hg}(\text{SBu}^t)_2$  from reference 273

hence high bridging ability, of the tert-butyl sulfur, but may also be influenced by steric effects. The complex of  $\text{Hg}^{2+}$  with 8-mercaptoquinoline (Figure 2.9) apparently has nearly linear ' $\text{HgS}_2$ ' geometry with strong Hg-N interactions.<sup>275</sup>

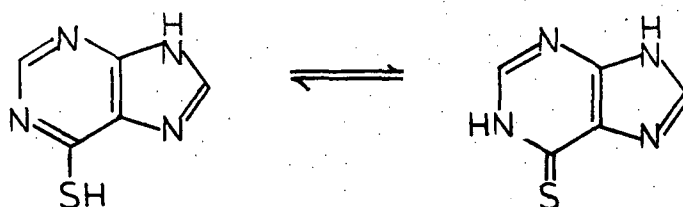


**Figure 2.9:** Molecular structure of bis(8-mercaptoquinolinato)mercury(II)

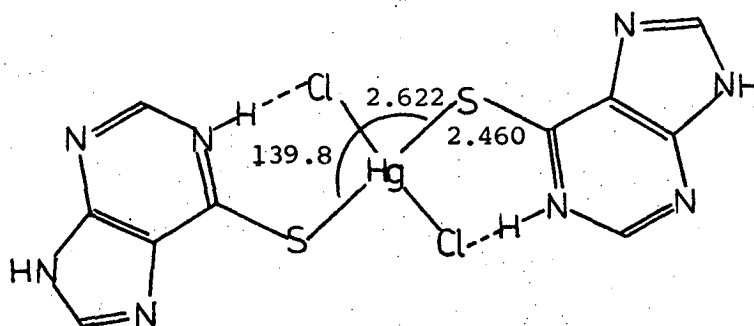
Details of the structure are unavailable in Tasmania and one abstracted distance,<sup>275</sup> Hg-N 1.36-1.50Å is surely incorrect (the covalent radii of digonal and tetrahedral Hg(II) are 1.30Å and 1.48Å. respectively<sup>243</sup>).

Dichlorobis(6-mercaptapurine)mercury(II) consists of discrete monomeric molecules with distorted tetrahedral ' $\text{HgS}_2\text{Cl}_2$ ' geometry about mercury<sup>276</sup> (Figure 2.10).

Interestingly, chelation of Hg by S and  $\text{N}_7$  is not observed due to the "preference (of Hg) for chlorine over nitrogen donors."<sup>276</sup> Although formally a thiol, the ligand has appreciable thione character which must assist in increasing the residual Lewis acidity of the ' $\text{HgS}_2$ ' moiety and thus favour tetrahedral over linear coordination.





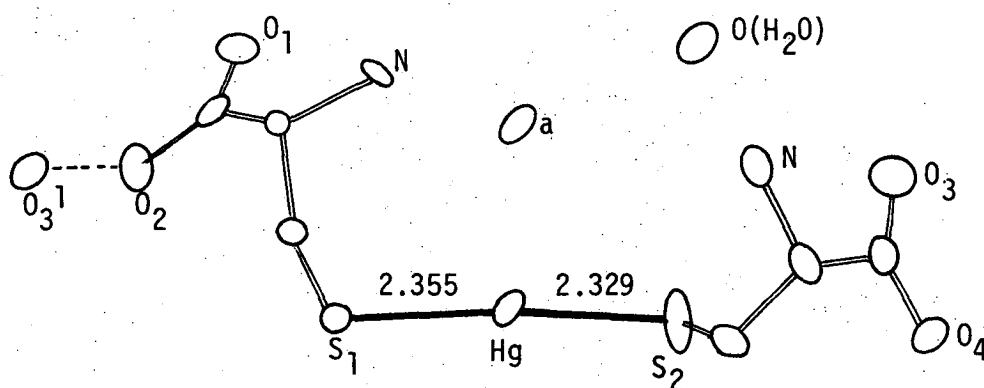


**Figure 2.10:** Molecular structure of dichlorobis(6-mercaptopurine)mercury(II), from reference 276.

The C-S bond retains an appreciable double-bond character in the complex but this is not directly reflected in the Hg-S bond distance (2.48Å), e.g.  $\text{Hg}(\text{SMe})_2$  has Hg-S 2.36Å but  $\text{Hg}(\text{SEt})_2$  has Hg-S 2.45Å.

The only other crystallographically studied bithiolato[mercury(II)] complexes, of which this author is aware, are those formed between  $\text{HgCl}_2$  and the biologically important thiols, L-cysteine<sup>277,246</sup> and DL-penicillamine<sup>278,246</sup>. The complex  $\text{Hg}[\text{SCH}_2\text{CH}(\text{NH}_3)\text{CO}_2][\text{SCH}_2\text{CH}(\text{NH}_3)\text{CO}_2\text{H}]\text{Cl} \cdot \frac{1}{2}\text{H}_2\text{O}$  has nearly linear 'HgS<sub>2</sub>' geometry and ionic chloride (Figure 2.11). As Carty points out,<sup>246</sup> this species has only one extra proton than "mercury cysteinate",  $\text{Hg}[\text{SCH}_2\text{CN}(\text{NH}_3)\text{CO}_2]_2$ , which is a metabolic product of certain mercurial diuretics.<sup>234</sup>

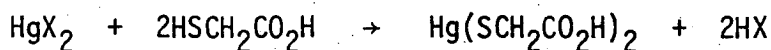
The closely related penicillamine complex  $\text{Hg}\{[\text{SC}(\text{Me})_2\text{CH}(\text{NH}_3)\text{CO}_2\text{H}]_2\text{Cl}\} \cdot \text{Cl} \cdot \text{H}_2\text{O}$  contains one additional proton (and hence one additional chloride for electroneutrality) and has a similar structure, but the linear molecules are



**Figure 2.11:** Molecular structure of  $\text{Hg}[\text{SCH}_2\text{CH}(\text{NH}_2)\text{CO}_2][\text{SCH}_2\text{CH}(\text{NH}_3)\text{CO}_2\text{H}] \text{Cl} \cdot \frac{1}{2}\text{H}_2\text{O}$ , from reference 277. The penicillamine complex is similar, but the chloride shown here bridges two molecules ( $\text{Hg}-\text{Cl}$  2.85Å)<sup>278</sup>

linked into spirals by the new (bridging) chloride.

The complex  $\text{Hg}(\text{SCH}_2\text{CO}_2\text{H})_2$ , I, was precipitated as glistening plates by the addition of  $\text{HgCl}_2$  or  $\text{Hg}(\text{CN})_2$  to two equivalents of mercaptoacetic acid (thioglycolic acid) in water.



Although this compound has been known for many years,<sup>279</sup> it does not seem to have been characterised in the solid state, and so its microanalysis is recorded below (Table 2.4). It is of interest in this study as a model for the complex with  $\text{DMSH}_4$ , and also for the bis(selenolato)mercury(II) analog ( page 186).

Dissolution of I in two equivalents of aqueous KOH and evaporation of the solution under nitrogen, produced  $\text{K}_2[\text{Hg}(\text{SCH}_2\text{CO}_2)_2]$  as a white powder.

This compound decomposes significantly (turning yellow) unless kept refrigerated in amber glass, but gives a satisfactory analysis under these conditions (Table 2.4).

Complex	required %				found %			
	C	H	Hg	S	C	H	Hg	S
$\text{Hg}(\text{SCH}_2\text{CO}_2\text{H})_2$	12.5	1.58	52.4	16.8	12.4	1.63	52.5	17.0
$\text{K}_2[\text{Hg}(\text{SCH}_2\text{CO}_2)_2]$	10.5	0.88	43.7	14.0	10.3	0.98	43.9	14.0
$\text{HgDMSH}_2 \cdot 2\text{H}_2\text{O}^a$	11.5	1.93	48.1	15.4	11.9	1.85	48.4	15.5

**Table 2.4:** Analysis of previously uncharacterised Hg(II) thiolates and dithiolates.<sup>b</sup>

<sup>a</sup>prepared elsewhere (Br. Pat. 716,647)<sup>280</sup>

<sup>b</sup>The complex with Unithiol was not obtained in sufficient purity to warrant microanalysis, but has been prepared elsewhere (page 53 )<sup>281</sup>

Two homologs of I,  $\text{Hg}(\text{SCH}_2\text{CH}_2\text{CO}_2\text{H})_2$ <sup>282</sup> and  $\text{Hg}[\text{SCH}(\text{Me})\text{CO}_2\text{H}]_2$ <sup>283</sup> have been prepared elsewhere, but only microanalysis and very little infrared data ( $\nu\text{C}=\text{O}$ ,  $\nu\text{C}-\text{O}$ ,  $\nu\text{C}-\text{S}$ ) were used to 'characterise' them.

It was expected that the monothiol analog of  $\text{DMSH}_4$ , 2-mercapto-succinic acid, would also form an  $\text{Hg}(\text{SR})_2$  complex, but it could not be isolated in this study (page 343). The 1:1 complex<sup>284</sup>

$\text{Hg}[\text{SCH}(\text{CO}_2\text{H})\text{CH}_2\text{CO}_2\text{H}]$  has been prepared elsewhere, but was only characterised on the basis of the infrared vibrations of the carboxylate group, and by differential thermal analysis.

Due to the varied coordination possibilities in  $\text{Hg}(\text{SR})_2$  complexes, interpretation of the solid-state vibrational spectra is considerably

more difficult than for MeHgSR species. The mercury-sulfur stretching frequency is the most characteristic for assignment of structure. It has been clearly demonstrated<sup>231</sup> that  $\nu(\text{Hg-S})$  decreases as coordination number increases for related model compounds. Thus two coordinate  $\text{Hg}(\text{SR})_2$   $\text{R}=\text{Me}, \text{Et}$ <sup>231</sup> have  $\nu_{\text{as}}(\text{SHgS})$  337, 407  $\text{cm}^{-1}$  and  $\nu_{\text{s}}(\text{SHgS})$  297, 268  $\text{cm}^{-1}$ , higher than four coordinate  $\text{Hg}(\text{SBU}^{\text{t}})_2$ <sup>231</sup> with  $\nu_{\text{as}}(\text{SHgS})$  172 and  $\nu_{\text{s}}(\text{SHgS})$  185  $\text{cm}^{-1}$ . Similar trends hold for chloromercury(II) complexes, e.g. two coordinate  $\text{PhHgCl}$ <sup>285</sup> has  $\nu(\text{HgCl})$  331  $\text{cm}^{-1}$  in contrast to four coordinate  $[\text{R}_4\text{N}]_2[\text{HgCl}_4]$ ,  $\text{R}=\text{Me}$ ,<sup>286</sup>  $\text{Et}$ <sup>287</sup> with  $\nu_{\text{as}}(\text{ClHgCl})$  225, 228  $\text{cm}^{-1}$  and  $\nu_{\text{s}}(\text{ClHgCl})$  264, 268  $\text{cm}^{-1}$ .

The assigned mercury-sulfur stretching frequencies of several bis(alkylthiolato)mercury(II) complexes, prepared in this work as models for dithiolate and selenolate complexation, are recorded in Table 2.5. Several previously prepared and spectroscopically characterised complexes have been included for comparison.

$\text{Hg}(\text{SMe})_2$ <sup>271</sup> and  $\text{Hg}(\text{SEt})_2$ <sup>274</sup> are known to have linear two-coordinate  $\text{HgS}_2$  geometry from crystallographic studies (page 45).

The complexes  $\text{Hg}(\text{SR})_2$   $\text{R}=\text{Pr}^{\text{n}}, \text{Ph}, \text{CH}_2\text{Ph}, \text{CH}_2\text{CO}_2\text{H}$  (and corresponding dipotassium salt) have therefore also been assigned two-coordinate ' $\text{HgS}_2$ ' geometry with  $\nu_{\text{as}}(\text{SHgS})$  in the range 330-410  $\text{cm}^{-1}$ , and  $\nu_{\text{s}}(\text{SHgS})$  in the range 290-390  $\text{cm}^{-1}$ . The symmetric Hg-S band is usually intense in the Raman spectrum and weak in the infrared spectrum of these complexes. The converse is true for  $\nu_{\text{as}}(\text{SHgS})$ . The linear structures in the solid-state are consistent with the monomeric behaviour of  $\text{Hg}(\text{SR})_2$  in pyridine ( $\text{R}=\text{Et}, \text{Pr}^{\text{n}}, \text{Pr}^{\text{i}}, \text{Bu}^{\text{n}}, \text{Bu}^{\text{i}}, \text{Bu}^{\text{t}}$ )<sup>272</sup> and chloroform ( $\text{R}=\text{Et}, \text{Bu}^{\text{t}}, \text{Ph}$ )<sup>238</sup> solutions.

The Raman spectrum of  $\text{K}_2[\text{Hg}(\text{SCH}_2\text{CO}_2)_2]$  in aqueous solution at  $\text{pH} \sim 7$  has an intense, strongly polarised, band at 347  $\text{cm}^{-1}$  which can be unambiguously assigned to  $\nu_{\text{s}}(\text{SHgS})$ . In the solid state, this complex has the same intense band at 328  $\text{cm}^{-1}$ . The spectra of this complex and of the

Complex	$\nu_{as}(\text{SHgS})$	$\nu_s(\text{SHgS})$	Ref. <sup>b</sup>
<u>monothiolates</u>			
Hg(SMe) <sub>2</sub> <sup>e</sup>	338vs [338w] 337vs [338vw]	298w [298m] 296m [297vs]	272 231
Hg(SEt) <sub>2</sub> <sup>d</sup>	405s,b	[394vs]	231
Hg(SPr <sup>n</sup> ) <sub>2</sub> <sup>e</sup>	408vs [412w]	392sh [395vs]	272
Hg(SPr <sup>i</sup> ) <sub>2</sub> <sup>f</sup>	assignment uncertain		272
Hg(SBu <sup>n</sup> ) <sub>2</sub> <sup>g</sup>	assignment uncertain		272
Hg(SBu <sup>i</sup> ) <sub>2</sub> <sup>h</sup>	assignment uncertain		272
Hg(SBu <sup>t</sup> ) <sub>2</sub> <sup>i</sup>	172vs,b <sup>j</sup>	[188vs]	231
Hg(SPh) <sub>2</sub>	365s,br	[344s]	238
Hg(SCH <sub>2</sub> Ph) <sub>2</sub>	381s [385vw,sh]	352w [356s]	
Hg(SCH <sub>2</sub> CO <sub>2</sub> H) <sub>2</sub>	379s [370w,sh]	351w [350s] <sup>k</sup>	
K <sub>2</sub> [Hg(SCH <sub>2</sub> CO <sub>2</sub> ) <sub>2</sub> ]	355s [360w.]	321w [328vs]	
<u>dithiolates</u>			
HgBAL	~348m,vbr	[298s,vb]	238
HgDMP	353m,b	[325vs]	238
HgDMSH <sub>2</sub> ·2H <sub>2</sub> O <sup>l</sup>	389m	306w	
Na[HgUT]	~360w,sh	[316s,b]	

Table 2.5: Mercury-sulfur stretching frequencies<sup>a</sup> for mercury(II) thiolate and dithiolate complexes.

Footnotes to Table 2.5

<sup>a</sup>Raman bands are shown in parentheses [ ].

Abbreviations: v, very; s, strong; m, medium; w, weak; b, broad; sh, shoulder; p, polarised.

<sup>b</sup>this work unless otherwise indicated. Assignments for R=Pr<sup>n</sup>, Pr<sup>i</sup>, Bu<sup>n</sup>, Bu<sup>i</sup> have been made from the spectral bands recorded in ref. 272 and often differ from those made by Biscarini *et al.*

<sup>c</sup>in pyridine<sup>272</sup>  $\nu_s$  355vs;  $\nu_{as}$  [318vs(p)]

<sup>d</sup>in pyridine<sup>272</sup>  $\nu_s$  330s;  $\nu_{as}$  [304vs(p)]

Biscarini assigns  $\nu_s$  268s;  $\nu_{as}$  246s in the solid state and the bands near  $400\text{ cm}^{-1}$  to  $\delta(\text{CCS})$  and notes the possibility of coexistence of rotational isomers.

<sup>e</sup>in pyridine<sup>272</sup>  $\nu_s$  359vs;  $\nu_{as}$  [329vs(p)]

<sup>f</sup>Biscarini assigns  $\nu_s$  256m;  $\nu_{as}$  [232vs] in the solid-state, however  $\nu_s$  388vs;  $\nu_{as}$  [380m] is also possible.

in pyridine:  $\nu_s$  352m, 260m;  $\nu_{as}$  [323m,p, 237vs,p]<sup>272</sup>

<sup>g</sup>Biscarini assigns  $\nu_s$  252vs;  $\nu_{as}$  [218vs] in the solid-state but  $\nu_s$  361vs,  $\nu_{as}$  (325vs,p) in pyridine<sup>272</sup>

<sup>h</sup>Biscarini assigns  $\nu_s$  277vs;  $\nu_{as}$  [250vs] in the solid-state but  $\nu_s$  366vs;  $\nu_{as}$  [323vs,p] in pyridine<sup>272</sup>

<sup>i</sup>Biscarini assigns  $\nu_s$  337vs but no  $\nu_{as}$  in the solid-state and  $\nu_s$  246s;  $\nu_{as}$  [233vs,p] in pyridine<sup>272</sup>

<sup>j</sup>this band not been by Biscarini ( $>180\text{ cm}^{-1}$ )

<sup>k</sup> $\nu_{as}$  [347s,p] in KOH solution, pH7.

<sup>l</sup>gives unusable Raman spectrum

<sup>m</sup>very poor quality for i.r. spectrum, see text.

protonated analog have been particularly valuable for the assignment of linear 'HgSe<sub>2</sub>' geometry to Hg(SeCH<sub>2</sub>CO<sub>2</sub>H)<sub>2</sub> (Chapter 4, page 220).

Mercury-sulfur vibrations due to the tetrahedral 'HgS<sub>4</sub>' moiety in Hg(SBu<sup>t</sup>)<sub>2</sub> lie at much lower wavenumbers,  $\nu_s$   $170\text{ cm}^{-1}$  and  $\nu_{as}$   $190\text{ cm}^{-1}$  and this complex is also of importance in the assignment of tetrahedral 'HgSe<sub>4</sub>' geometry to several Hg(SeR)<sub>2</sub> complexes (Chapter 4).

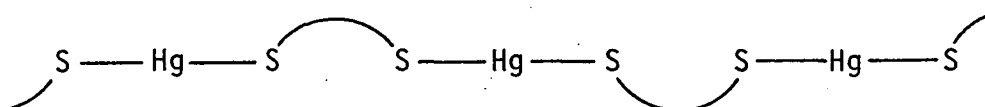
## 2.4 Structural features of Hg(II) dithiolate complexes

The 1:1 dithiolato complex of  $\text{DMSH}_4$  is a dihydrate and the infrared spectrum of this complex shows a broad absorption due to hydrogen bonded OH (3200-3600 m,br). The complex with Unithiol was isolated as the sodium salt from acidic solution. This product was consistently produced as a somewhat sticky solid which could not be dried (even by high vacuum pumping or storage over  $\text{P}_2\text{O}_5$ ) to an adequate state to warrant microanalysis. The near infrared spectrum of this product also showed broad OH absorption (3200-3600 w) and was generally of poorer quality than the other complexes studied. Both dithiolate complexes have very broad, low intensity, far infrared spectra (600-200  $\text{cm}^{-1}$ ). Only two bands are discernible in the far i.r. spectra of  $\text{HgDMSH}_2 \cdot 2\text{H}_2\text{O}$  : 389m, 306w and these absorptions do not appear in the spectrum of the ligand and have thus been assigned as  $\nu_{\text{as}}(\text{SHgS})$  and  $\nu_{\text{s}}(\text{SHgS})$  respectively.

All attempts to obtain a usable Raman spectrum from this solid were fruitless, even under conditions of low energy (red dye) laser excitation which did not seem to lead to sample decomposition.  $\text{HgBAL}$  has been shown to be amorphous and also gives relatively poor quality, diffuse spectra.<sup>231</sup>

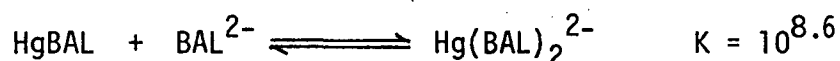
The Unithiol complex  $\text{Na}[\text{Hg}(\text{UT})] \cdot 2\text{H}_2\text{O}$  gives a poor quality far infrared spectrum, with a very broad medium intensity absorption [600-250  $\text{cm}^{-1}$ ] containing poorly resolved features at 580m, 540w, 360w,sh [ $\nu_{\text{as}}(\text{SHgS})$ ]. The Raman spectrum of this complex is featureless in the range 600-100  $\text{cm}^{-1}$  except for a strong, broad band at 316  $\text{cm}^{-1}$  assigned to  $\nu_{\text{s}}(\text{SHgS})$ .

The infrared spectrum of  $\text{HgDMSH}_2 \cdot 2\text{H}_2\text{O}$  and the infrared and Raman spectra of  $\text{Na}[\text{Hg}(\text{UT})]$  are consistent with the linear polymeric structure postulated for  $\text{HgBAL}$ .<sup>231</sup>



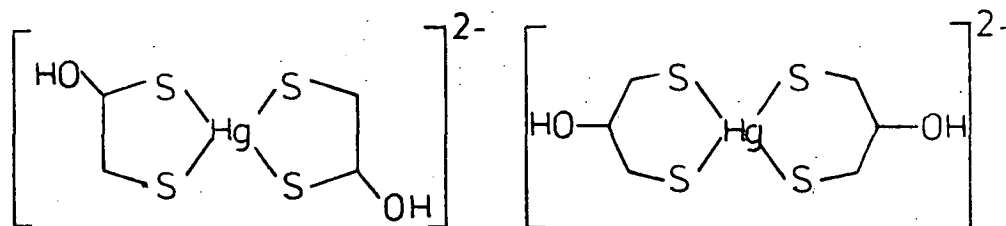
although the poor quality of the spectra cannot preclude regions of the polymer with higher coordination numbers for mercury.

It has been known for some time that intractable HgBAL will dissolve in excess dithiol ligand to give a conducting solution,<sup>288</sup> presumed to contain  $\text{Hg}(\text{BAL})_2^{2-}$  anions in which Hg is tetrahedrally coordinated. The equilibrium constant for this reaction has been established and is quite high:<sup>232</sup>

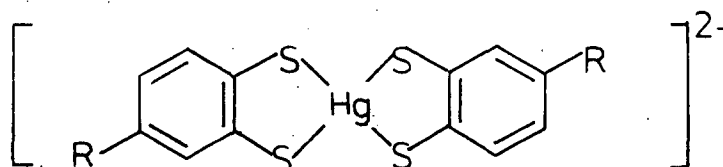


The conductivity of a solution containing two equivalents of  $\text{BAL}^{2-}$  per mercuric ion, is much higher than that of the analogous non-vicinal dithiolate,  $\text{DMP}^{2-}$ <sup>288</sup> which may reflect the preference for 5-membered over 6-membered chelate rings,

i.e.



Similar 1:2 bis(dithiolato)mercury(II) complexes have been isolated with toluene-3,4-dithiol and 1-chlorobenzene-3,4-dithiol, as the dipotassium and bis(quinine) salts respectively.

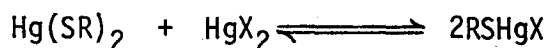


Interestingly, these compounds are molecularly dissymmetric, but have not been characterised in the solid state.



## 2.5 Structural features of RSHgX species

Many bis(alkylthiolato)mercury(II) complexes will dissolve in solutions of  $\text{HgX}_2$ ,  $\text{X}=\text{Cl}, \text{Br}, \text{I}$ , acetate to form complexes of the type  $\text{RSHgX}$  via the equilibria

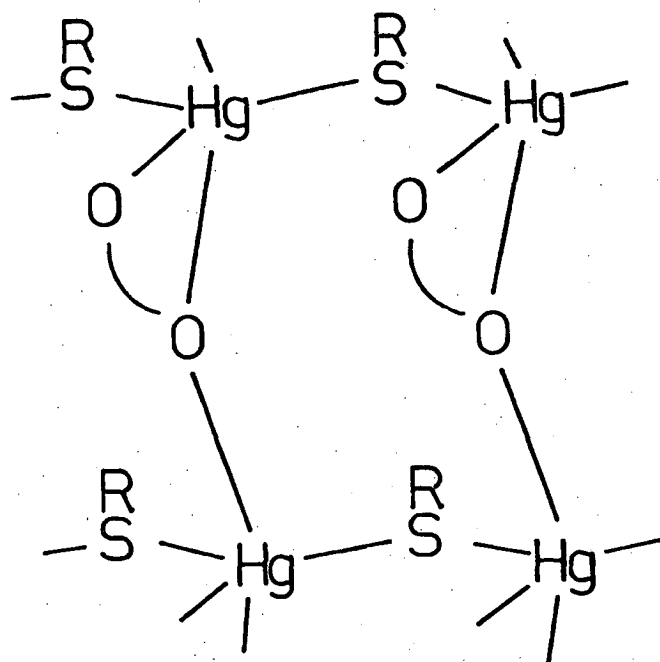


The equilibria for  $\text{R} = \text{CF}_3$ ;  $\text{X}=\text{Cl}, \text{Br}, \text{I}$ , have been followed by vibrational spectroscopy<sup>290</sup>. Such species may be of considerable importance in the biological context, since many endogenous ligands, e.g. nitrogen containing bases, chloride etc. will be present at the Hg-sulphydryl binding site(s) *in vivo*. Most 1:1  $\text{Hg}(\text{II})$  thiolates which could act as models for the biological interaction of  $\text{RSHg}(\text{II})$  with non-thiol ligands, are insoluble in water and common organic solvents, but several dissolve in coordinating solvents such as pyridine<sup>293,5</sup> or imidazole<sup>291</sup> to form adducts, some of which have also been crystallographically characterised.

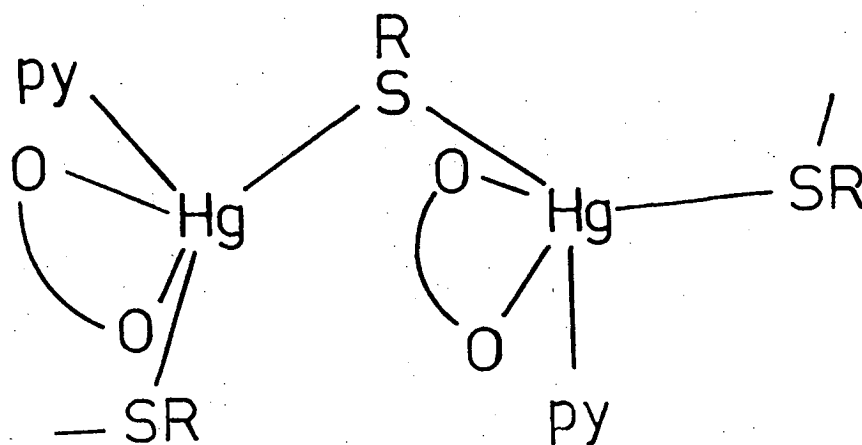
$\text{MeSHgO}_2\text{CMe}$  is uniquely water-soluble and has been shown by Raman spectroscopy to form a dimer in solution near  $\text{pH} 6$ <sup>292</sup>.

Although no new  $\text{RSHgX}$  species have been prepared in this study, the first  $\text{RSeHgX}$  analogs to be characterised by single-crystal X-ray diffraction are described in Chapter 4. For this reason, a brief review of the structural features of  $\text{RSHgX}$  complexes is included here.

All  $\text{RSHgO}_2\text{CMe}$  complexes studied crystallographically to date ( $\text{R}=\text{Me}$ ;<sup>293</sup>  $\text{Pr}^n$ ,  $\text{Bu}^n$ <sup>294</sup>) consist of polymeric  $(-\text{Hg}-\text{SR})_n$  parallel chains which are linked by acetate groups to form wrinkled sheets. The structure of the methyl analog is identical to that of isomorphous  $\text{MeSeHgO}_2\text{CMe}$  shown in Figure 2.12. In the N-base adducts  $\text{RSHgO}_2\text{CMe}(\text{py})$   $\text{R}=\text{Me}$ <sup>293</sup>,  $\text{Et}$ <sup>295</sup> and  $\text{MeSHgO}_2\text{CMe}(\text{4Mepy})$ <sup>295</sup>, coordination of pyridine or 4-methylpyridine results in displacement of bridging acetate groups to give isolated chains with



**Figure 2.12:** Schematic structure of polymeric  $\text{RSHgO}_2\text{CMe}$ ;  
 $\text{R}=\text{Me}^{293}$ ,  $\text{Pr}^n$  and  $\text{Bu}^n$  <sup>294</sup>.



**Figure 2.13:** Schematic structure of the pyridine adducts of  
 $\text{RSHgO}_2\text{CMe}$ ;  $\text{R}=\text{Me}^{293}$ ,  $\text{Et}^{295}$  and the 4-methylpyridine  
 adduct of  $\text{MeSHgO}_2\text{CMe}^{295}$ .

N-base and bidentate acetate coordination at each mercury atom.

The complexes  $\text{MeSHgX}$  ( $\text{X}=\text{Cl}$ ,  $^{296}\text{Br}^{295}$ ) are isostructural and are based on  $(\text{Hg-SMe})_n$  chains linked by triply bridging halogen atoms (coordinated to two mercury atoms in one chain and one mercury atom in an adjacent chain) to form wrinkled sheets.

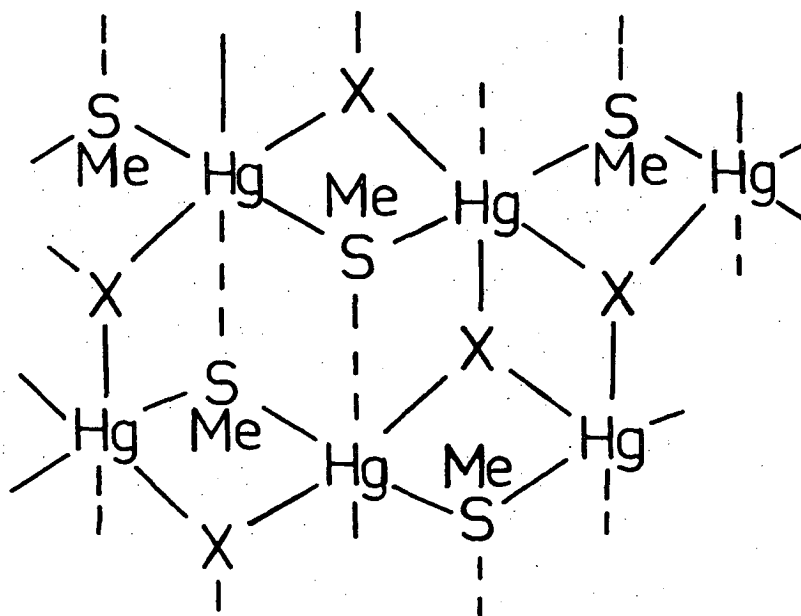


Figure 2.14: Schematic structure of  $\text{MeSHgX}$  ( $\text{X}=\text{Cl}$ ,  $^{296}\text{Br}^{295}$ ) taken from reference 297.

Other crystallographically characterised  $\text{RSHgX}$  ( $\text{X}=\text{halide}$ ) complexes which contain  $(-\text{Hg-SR})_n$  chains are those formed between  $\text{HgCl}_2$  and cysteine<sup>277</sup> or penicillamine;<sup>278</sup> and between  $\text{HgB}_2$  and the thiosteroid spiroxazone<sup>298</sup>.

The molecular structure of  $\text{HgCl}_2[\text{SCH}_2\text{CH}(\text{NH}_3)\text{CO}_2\text{H}]$  is shown in Figure 2.15a, and consists of chains of  $-(\text{Hg-SCys})_n$  groups in which the Hg atom is tetrahedrally coordinated with ' $\text{Hg}(\mu\text{-SCys})\text{Cl}_2$ ' geometry.

The penicillamine complex,  $(\text{HgCl}_2)_2[\text{SC}(\text{Me})_2\text{CH}(\text{NH}_3)\text{CO}_2\text{H}] \cdot 2\text{H}_2\text{O}$  has a more complex structure (Figure 2.15b) in which the sulphhydryl donor asymmetrically bridges two mercury atoms. The mercury atoms have distorted tetrahedral geometry of the types ' $\text{Hg}(\mu\text{-SPen})\text{Cl}_3$ ' and ' $\text{Hg}(\mu\text{-SPen})\text{Cl}(\text{Cl}')_2$ '. In the

latter case, two intermolecular Hg-Cl' contacts complete the coordination sphere.

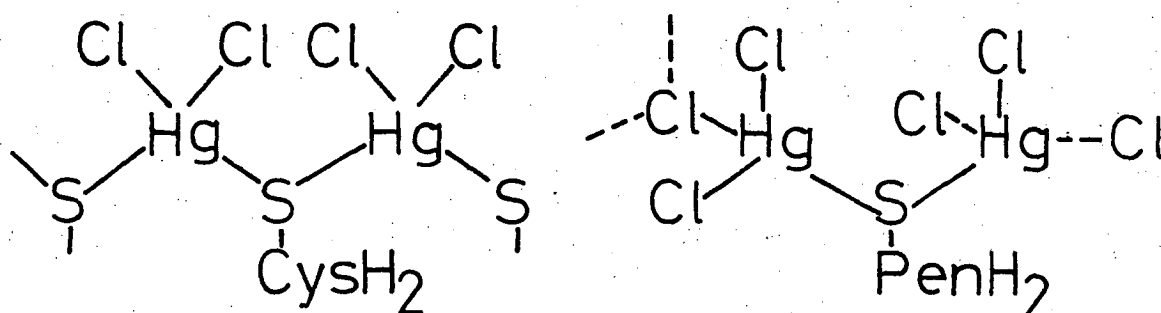


Figure 2.15: Schematic structures of a)  $\text{HgCl}_2(\mu\text{-SCysH}_2)$  and b)  $\text{HgCl}_2(\mu\text{-SPenH}_2) \cdot 2\text{H}_2\text{O}$ , from reference 246.

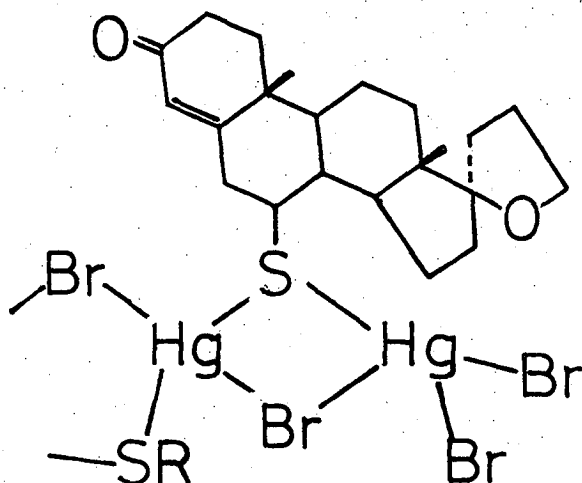


Figure 2.16: Schematic structure of the thioesteroid complex,  $(\text{SNX})\text{SHgBr}$  ( $\text{SNX-SH}$  = spiroxazone)<sup>298</sup>

The isostructural complexes  $[\text{Bu}^t\text{SHgCl}(\text{py})_{0.5}]_4$ <sup>293</sup> and  $[\text{Bu}^t\text{SHgCl}(4\text{-Mepy})_{0.5}]_4$ <sup>295</sup> differ from the other  $\text{RSHgX}$  complexes reported inasmuch as the tetrameric molecules are based on eight-membered  $(-\text{Hg-SBu}^t)_4$  rings, rather than infinite chains.<sup>293</sup> There are two mercury environments,  $'\text{Hg}(\mu\text{-SBu}^t)_2\text{ClN}'$  and  $'\text{Hg}(\mu\text{-SBu}^t)(\mu\text{-Cl})_2'$ . A new  $\text{RSeHgX}$  compound,  $[\text{Bu}^t\text{SeHgCl}(\text{py})_{0.5}]_4$  has been shown in this study to be isomorphous with the 4-Mepy adduct of the sulfur analog, and the crystal structures of these compounds are discussed in more detail in Chapter 4 of this thesis.

The vibrational spectra of polymeric  $\text{RSHgX}$  complexes are difficult to interpret. Canty has recently noted that assignment of structure based on simple point group approaches to the spectra of these molecules, may be misleading.<sup>297</sup> For example, the spectra of  $\text{MeSHgCl}$  were interpreted in terms of a monomeric, dimeric or polymeric structure based on  $'\text{Hg}(\mu\text{-SMe})_2\text{Hg}'$  or  $'\text{Hg}(\mu\text{-Cl})_2\text{Hg}'$  bridging units,<sup>299</sup> however the previously described single-crystal X-ray determination<sup>296</sup> (page 57) is not consistent with this interpretation.

Assignment of mercury-ligand vibrational frequencies is not straightforward for the  $\text{RSHg}(\text{halides})$  as mercury-sulfur and mercury-halogen vibrations occur at similar frequencies in related complexes, e.g.  $\text{HgCl}_2$ :  $\nu_{\text{as}}$  375<sup>285</sup>-368<sup>300</sup>,  $\nu_{\text{s}}$  330-310  $\text{cm}^{-1}$ ,<sup>300</sup> linear  $\text{Hg}(\text{SR})_2$ :  $\nu_{\text{as}}$  330-410,  $\nu_{\text{s}}$  290-390  $\text{cm}^{-1}$  (page 51), and  $\text{Bu}^t\text{SHgCl}$ : i.r. 359m, 273s, 236m; Raman 391m, 384m, 359m, 330m, 274vs, 223vs, 201vs  $\text{cm}^{-1}$ .<sup>301</sup>

## 2.6 Conclusions

The known crystallographic structures of  $\text{MeHg(II)}$ -thiolates have been reviewed and several  $\text{MeHgSR}$  complexes characterised by vibrational spectroscopy in the solid state. Coincident infrared and Raman bands in the range 320-390  $\text{cm}^{-1}$  have been assigned as Hg-S stretching modes,

and bands in the range  $520\text{--}560\text{ cm}^{-1}$  to Hg-C modes, consistent with the expected linear 'MeHgS' geometry. MeHg(II) dithiolates have similar vibrational spectroscopic and structural features.

Bis(thiolato)mercury(II) compounds,  $\text{Hg}(\text{SR})_2$  have vibrational spectra consistent with normally linear 'HgS<sub>2</sub>' geometry

$[\nu_{\text{as}}(\text{SHgS})\ 330\text{--}410\text{ cm}^{-1}\ \text{and}\ \nu_{\text{s}}(\text{SHgS})\ 290\text{--}390\text{ cm}^{-1}]$  ,

except for  $\text{Hg}(\text{SBut})_2$  which is known to have tetrahedrally coordinate mercury  $[\nu_{\text{s}}(\text{SHgS})\ \sim 170\text{ cm}^{-1}\ \text{and}\ \nu_{\text{as}}(\text{SHgS})\ \sim 190\text{ cm}^{-1}]$ .

All Hg(II)-dithiolates studied by vibrational spectroscopy to date seem to have polymeric, linear structures.

Monothiolatomercury(II) species,  $\text{MeSHgX}$ , have complex polymeric structures based on  $(\text{-Hg-SR})_n$  infinite chains or eight-membered rings. Interpretation of the vibrational spectra of these polymeric molecules cannot readily be achieved using simple point-group approaches.

### CHAPTER THREE

#### SOLUTION CHEMISTRY OF METHYLMERCURY(II) THIOLATES AND SELENOLATES

##### 3.1 Introduction

Methylmercury has a high affinity for 'soft' sulfhydryl ligands, consistent with the 'soft' acid nature of the metal and it is generally considered that many of the toxicological properties of MeHg(II) are due to bonding to sulfhydryl groups of peptides and proteins *in vivo*.<sup>12</sup> It is therefore somewhat surprising that only a small amount of detailed stability constant information for methylmercury thiolates is available, and that this includes some serious discrepancies in the magnitude of the formation constants for MeHg(II) with several monothiols. Since solution equilibrium constants may be of some significance in the understanding of the effectiveness of antidotal thiols for removal of MeHg(II) from body tissues, this study has involved redetermination of the MeHg(II) formation constants with the biologically important monothiols cysteine and glutathione, and the simple monothiols mercaptoethanol, mercaptoacetic acid, mercaptosuccinic acid, thiocholine and 4-mercapto-N-methylpiperidine. In addition, the complexation equilibria with antidotal thiols penicillamine and N-acetylpenicillamine and vicinal dithiols BALH<sub>2</sub>, Unithiol and DMSH<sub>4</sub> have been investigated.

When this work was near completion, Reid and Rabenstein published the results of their <sup>1</sup>H nmr evaluations of MeHg(II) formation constants with many of the monothiols mentioned above.<sup>302</sup> These workers have apparently determined the formation constants with glutathione, but the results were unpublished;<sup>303</sup> however, the formation constant of MeHg(II) with the biological monothiol homocysteine was reported. Attempts to investigate homocysteine in this study were unfortunately

frustrated by low purity of the commercially available product and rapid decomposition in solution.

A brief report of part of the work described in this Chapter of the thesis was presented at a conference prior to publication of the work by Reid and Rabenstein (Appendix 1). Publication of their work produced a unique opportunity to compare the results obtained from two widely different techniques and firmly establish stability constants for the MeHg(II) thiolate interaction.

The important features of the nmr technique, which has been used elsewhere for studies of MeHg(II) equilibria with many non-thiolate ligands, will be discussed below. The potentiometric method, used to evaluate the stability constants in this study, will be described in detail in Chapter 6 of this thesis, but the stability constants themselves will be discussed below.

The reported antagonistic effects of some selenium compounds against methylmercury toxicity and the existence of reduced selenohydryl groups in some selenoproteins (Chapter 1) has generated considerable interest in methylmercury selenolate interactions in solution. Several nmr studies have indicated that MeHg(II)-selenolate binding may be thermodynamically more favorable than analogous thiolate binding, but no stability constant data have been recorded. Attempts to study the methylmercury-selenoacetate system potentiometrically in this work have been frustrated by failure to obtain the free ligand in solution for accurate evaluation of its hydrolysis constants.

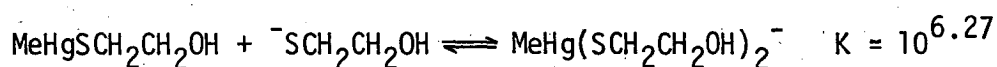
### 3.2 The Aqueous Solution Chemistry of Methylmercury(II)

#### 3.2.1 Coordination of MeHg(II) in aqueous solution

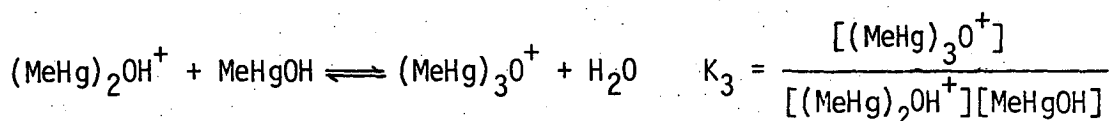
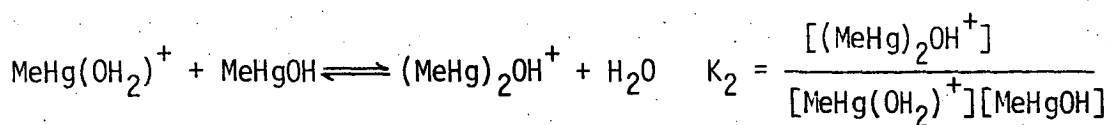
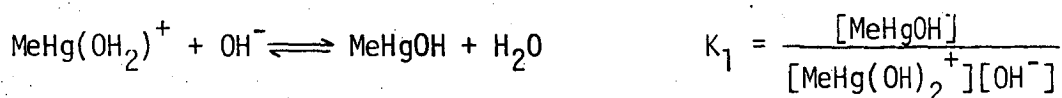
The solution chemistry of MeHg(II) has been recently reviewed,<sup>41</sup> and is dominated by the tendency of mercury toward linear two-coordination.



However, some residual Lewis acidity is evident from the formation of complexes with chelating ligands in which higher coordination numbers for MeHg(II) of three or four for mercury have been found. The chemistry of MeHg(II) with these ligands has been reviewed elsewhere.<sup>249,304</sup> In addition to polydentate ligands, some simple unidentate ligands also permit higher coordination, e.g. iodide,<sup>305</sup> cyanide<sup>305</sup> and thiocyanate.<sup>268</sup> The possibility of higher coordination with sulfur donors was considered for the interaction of MeHg(II) with thiols used in this study, particularly the antidotal vicinal dithiols BALH<sub>2</sub>, Unithiol, and DMSH<sub>4</sub>. Previous work in this laboratory has not indicated any definitive evidence for chelation in the complex (MeHg)<sub>2</sub>BAL in the solid state, but a recent simple crystal X-ray structure<sup>230</sup> of the complex trans-(1,2-cyclohexanedithiolato)bis[methylmercury(II)] shows S-chelated methylmercury (page 42). In solution, Schwarzenbach and Schellenberg<sup>305</sup> have shown that mercaptoethanol will interact with MeHg(II) to form a complex of the type MeHg(SR)<sub>2</sub><sup>-</sup>, as well as the highly stable monothiolate.



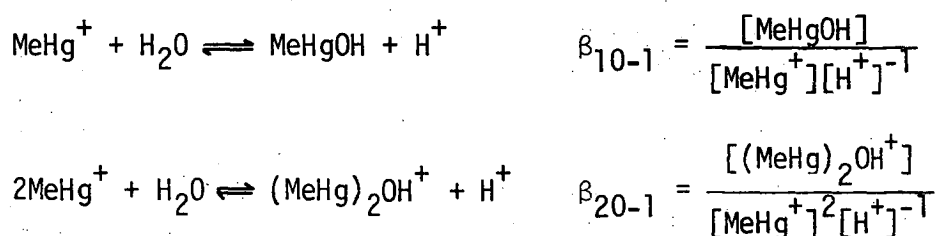
The aqueous solution chemistry of MeHg(II) is also dominated by the self-association and hydrolysis reactions:



The first two hydrolysis equilibria were proposed by Schwarzenbach and Schellenberg<sup>305</sup> from equilibrium constant measurements,<sup>305</sup> and have been

supported by Raman<sup>306-8</sup> and <sup>1</sup>H nmr<sup>306,309</sup> spectral data.

Equilibrium constants for these equilibria have been measured here under the conditions used for methylmercury-thiolate and thiol hydrolysis equilibria (0.1 M KNO<sub>3</sub>, 25°). Several acidic (HNO<sub>3</sub>) solutions of methylmercuric ion were titrated with 0.1 M KOH, and the composite data (186 titration points) treated by MINQUAD81 (page 326) to generate equilibrium constants  $\beta_{10-1}$  and  $\beta_{20-1}$  for the equilibria:<sup>†</sup>



The actual titration data are shown in Figure 3.1, fitted by curves calculated using these values of  $\beta_{10-1}$  and  $\beta_{20-1}$ . A comparison of these constants from this work, and those obtained elsewhere, is shown in Table 3.1. It should be noted that, unless values for  $K_w^C = [\text{H}^+][\text{OH}^-]$  are accurately known under actual experimental conditions used to determine  $\beta_{10-1}$  and  $\beta_{20-1}$ , these constants must be expressed in terms of  $[\text{H}^+]$  and *not*  $[\text{OH}^-]$ .

The trinuclear cation  $(\text{MeHg})_3\text{O}^+$  has been shown by <sup>1</sup>H nmr spectroscopy to be a very minor component in dilute solutions, since its equilibrium constant for formation is small,  $0.7 \pm 0.3$ .<sup>306</sup> The trinuclear cation has been isolated as perchlorate<sup>310</sup> or nitrate<sup>311</sup> salts from concentrated neutral aqueous solutions, and single crystal X-ray structures of these salts have been determined. In the dilute solutions used in this study,  $[\text{MeHg}] \sim 10^{-3}\text{M}$ ,  $(\text{MeHg})_3\text{O}^+$  constitutes, at most, 0.01% of the total MeHg(II) concentration, hence the corresponding equilibrium constant for its formation,  $\beta_{30-2}$ , was unobtainable.

<sup>†</sup>For brevity  $\text{MeHg}^+$  will be used subsequently to represent  $\text{MeHg}(\text{OH}_2)^+$ . The computer program MINQUAD81 will be discussed in Chapter 6.

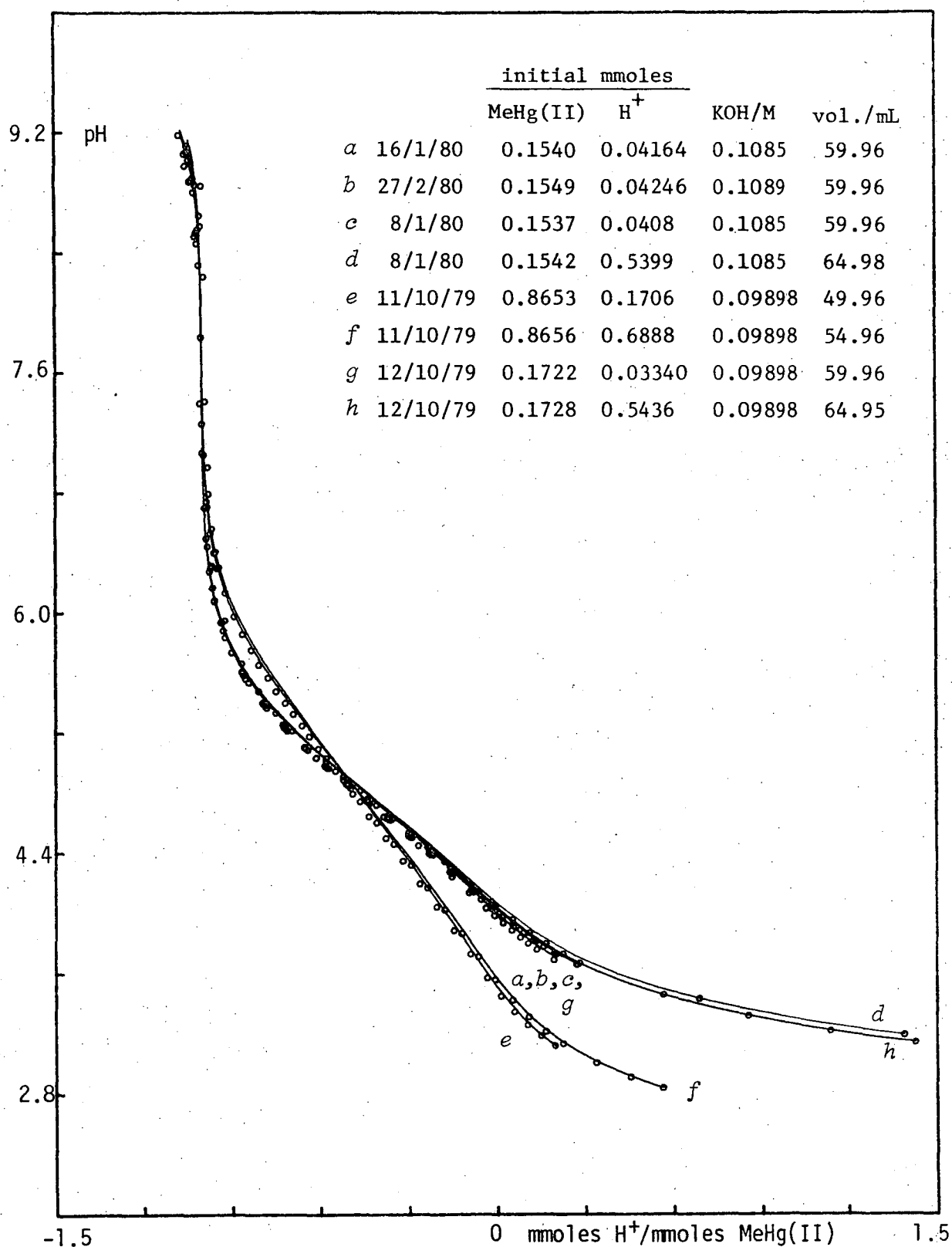


Figure 3.1: Methylmercury(II) hydrolysis data.

The solid curves were calculated by COMIXH for the experimental conditions shown, with  $\log \beta_{10-1} = -4.607$  and  $\log \beta_{20-1} = -2.234$ .

$\log \left( \frac{[\text{MeHgOH}]}{[\text{MeHg}^+][\text{H}^+]^{-1}} \right)$	$\log \left( \frac{[(\text{MeHg})_2\text{OH}^+]}{[\text{MeHg}^+]^2[\text{H}^+]^{-1}} \right)$	$\log \left( \frac{[\text{MeHgOH}]}{[\text{MeHg}^+][\text{OH}^-]} \right)$	$\log \left( \frac{[(\text{MeHg})_2\text{OH}^+]}{[\text{MeHgOH}][\text{MeHg}^+]} \right)$	method	conditions	ref.
-4.607(9) <sup>b</sup>	-2.234(18) <sup>b</sup>	9.25(3) <sup>d</sup>	2.37(4) <sup>d</sup>	gl. <sup>h</sup>	25°[0.1 KNO <sub>3</sub> ] pK <sub>W</sub> <sup>c</sup> =13.86(3)	this work
-4.59 <sup>e</sup>	{ -2.22 <sup>d</sup> -2.53 <sup>e</sup>	9.37 <sup>e</sup>	2.37 <sup>e</sup>	gl. <sup>j</sup>	20°[0.1 KNO <sub>3</sub> ] pK <sub>W</sub> <sup>c</sup> =13.96	305
-4.70 <sup>e</sup>	-2.33 <sup>e</sup>	{ 9.30 <sup>e</sup> 9.36(5) <sup>f</sup> 9.29 <sup>e</sup>	{ 2.37 <sup>e</sup> 2.87(7) <sup>f</sup> 2.31 <sup>e</sup>	nmr <sup>g,j</sup>	25°[0.19 MeHg(II)]	309
-4.56±0.05				nmr <sup>g,i</sup>	25°[0.3 MeHg(II)]	306
-4.686(15) <sup>e</sup>	-1.725(30) <sup>e</sup>	9.624(15) <sup>d</sup>	2.961(16) <sup>d</sup>	gl. <sup>h</sup>	25°[0.1 KNO <sub>3</sub> ]	312
-4.67(3) <sup>e,k</sup>				gl. <sup>h</sup>	25°[0.1 NaNO <sub>3</sub> ] pK <sub>W</sub> <sup>c</sup> =13.95	313
-4.50 <sup>e</sup>				gl.	25°[0.1 KNO <sub>3</sub> ]	314
-4.40(2) <sup>e</sup>		9.55(7) <sup>d</sup>		gl.	24-5°	315
		9.33±0.12 <sup>e</sup>	2.78±0.18 <sup>e</sup>	distr. <sup>h</sup>	25°[1.0 NaNO <sub>3</sub> /Cl/PO <sub>4</sub> ]	316
				nmr <sup>g,j</sup>	25°[0.1 NaNO <sub>3</sub> ]	317

Table 3.1: Methylmercury(II) hydrolysis constants.<sup>a</sup>

<sup>a</sup> estimated standard deviations of the last digit are recorded in parentheses.

<sup>b</sup> weighted geometric means of eight values calculated by MINQUAD81 from data shown in Figure 3.1.

<sup>c</sup> constant actually reported in original reference.

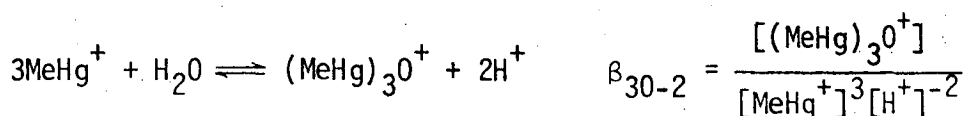
<sup>d</sup> formation constant (page 63) calculated using the values of K<sub>W</sub><sup>c</sup> recorded in the original reference.

<sup>e</sup> quoted in references 313,316

<sup>f</sup> recalculated in reference 317

<sup>g</sup> K<sub>W</sub><sup>c</sup> not given. electrodes calibrated in terms of [H<sup>+</sup>]. <sup>h</sup> electrodes calibrated by [H<sup>+</sup>]=10<sup>-pH</sup>.

<sup>i</sup> electrode calibration unspecified. <sup>j</sup> γ<sub>H<sup>+</sup></sub> calculated using the Davies equation<sup>318</sup> and used to correct mixed constants.



This species was neglected in subsequent evaluations of MeHg(II) equilibrium constants. A distribution diagram for the methylmercury(II) hydrolysis species is shown in Figure 3.2, calculated by COMIX for  $10^{-3}\text{M}$   $[\text{MeHg}]_{\text{total}}$  using the constants  $\beta_{10-1}$  and  $\beta_{20-1}$  obtained in this study. The constant  $\beta_{30-2}$  was calculated from the published values of  $K_3$  for formation of  $(\text{MeHg})_3\text{O}^+$  in concentrated solutions<sup>306</sup> (page 64) since

$$\begin{aligned} \beta_{30-2} &= \frac{[(\text{MeHg})_2\text{OH}^+]}{[\text{MeHg}^+]^2[\text{H}^+]^{-1}} \cdot \frac{[\text{MeHgOH}]}{[\text{MeHg}^+][\text{H}^+]^{-1}} \cdot \frac{[(\text{MeHg})_3\text{O}^+]}{[(\text{MeHg})_2\text{OH}^+][\text{MeHgOH}]} \\ &= \beta_{20-1} \cdot \beta_{10-1} \cdot K_3 = 10^{-7.0} \end{aligned}$$

From the logarithmic<sup>†</sup> concentration scale of Figure 3.2, it can clearly be seen that the trinuclear species is negligible.

A similar series of complexes,  $\text{MeHgS}^-$ ,  $(\text{MeHg})_2\text{S}$  and  $(\text{MeHg})_3\text{S}^+$  is formed from sulfide,  $\text{S}^{2-}$ , with formation constants several orders of magnitude higher than the hydroxo and oxo species.<sup>305</sup> The crystal structure of  $[(\text{MeHg})_3\text{S}]\text{ClO}_4$  has been reported.<sup>310</sup>

A comprehensive list of MeHg(II) formation constants with ligands containing various donor atoms (O, N, P, S, Se, C and halogens) is shown in Table 3.2, together with values for the protonation constants of the ligands and  $|^2\text{J}(^1\text{H}-^{199}\text{Hg})|$  (page 75) for the MeHg(II) complexes where available. The clear preference of MeHg(II), compared with  $\text{H}^+$ , for 'soft' donors (C, S, Se) can be seen from a comparison of stability constants in Table 3.2.

In a hypothetical system containing MeHg(II) and several competing ligands, some of which may participate in protolytic equilibria, the

---

<sup>†</sup>All other species distribution diagrams in this thesis have linear concentration scales.

ligand	$\log K_f^a$	$pK_a^d$	$ ^2J(^1H-^{199}Hg) ^e$
<u>O-donors</u>			
$O^{2-}$	$\sim 14$ <sup>319</sup>	$\sim 25$ <sup>320</sup>	
$CH_3HgO^-$	$\sim 12$ <sup>319</sup>	$\sim 20$ <sup>319</sup>	$158(C_6H_6)$ <sup>321</sup>
$OH^-$	9.25-9.5	15.7	$203.0,^{309} 204.0(C_6H_6), 214.2(pyr)^{322}$
$SeO_3^{2-}$	6.46 <sup>323</sup>	8.24	$223.5$ <sup>323</sup>
$(CH_3Hg)_2O$	$\sim 6$ <sup>319</sup>	$\sim 10$ <sup>319</sup>	
$CO_3^{2-}$	6.10 <sup>323</sup>	9.57	$221.4$ <sup>323</sup>
tropolonate	5.43 <sup>319,m</sup>	6.70 <sup>319,m</sup>	
phenolate	5.48, <sup>319</sup> $\sim 6.5$ <sup>324</sup>	9.62	$208.5(CDCl_3),^{325} 207(pyr)^{326-7}$ $206(CHCl_3)$ <sup>327</sup>
$HPO_4^{2-}$	5.03, <sup>305</sup> 4.74 <sup>316</sup>	6.79	
$HPO_3^{2-}$	4.67 <sup>305</sup>	6.3	
4- $NO_2$ -phenolate	3.80 <sup>319</sup>	7.15	
$(CH_3)_3C-CO_2^-$	3.50 <sup>309</sup>	4.95	$211.5(CDCl_3)$ <sup>325</sup>
$CH_3CH_2CO_2^-$	3.39 <sup>309</sup>	4.80	
$CH_3CO_2^-$	3.18, <sup>309</sup> $\sim 3.6$ , <sup>324</sup> 3.55, <sup>328</sup> 3.19 <sup>305</sup>	4.65	$214.3(C_6H_6), 220.8(pyr), 233.4(D_2O),^{322}$ $212.4(CDCl_3),^{329} 213.5(CDCl_3),^{325}$ $232, 220 (diox),^{330} 233.3^{309}$
$+NH_3(CH_2)_7CO_2^-$	3.15 <sup>331</sup>	4.56	
$+NH_3(CH_2)_5CO_2^-$	3.10 <sup>331</sup>	4.46	$230.4^{331}$
$+NH_3(CH_2)_4CO_2^-$	3.0 <sup>331</sup>	4.33	$230.2^{331}$
$+NH_3(CH_2)_3CO_2^-$	2.7 <sup>331</sup>	4.12	$230.0^{331}$
$SeO_3H^-$	2.70 <sup>323</sup>		
$(CH_3)_2CHCH(NH_3)CO_2^-$	2.7 <sup>331</sup>	2.29	
$CH_3CONHCH_2CO_2^-$ acetyl-glycine	2.68 <sup>309</sup>	3.40	$237.9^{309}$
$HCO_2^-$	2.67, <sup>309</sup> 2.68 <sup>313</sup>	3.55	
$+NH_3(CH_2)_2CO_2^-$ $\beta$ -alanine	2.52 <sup>331</sup>	3.61	$230.5^{331}$
$CH_3HgOH$	2.31-2.96 <sup>f</sup>	4.40-4.70 <sup>f</sup>	$232.5^{309}$
$ClCH_2CO_2^-$	2.19 <sup>309</sup>	2.75	$219.0(CDCl_3),^{325} 217.9(CHCl_3)^{329}$
$(CH_3)_3NCH_2CO_2^-$	1.71 <sup>309</sup>	1.87	
$Cl_2CHCO_2^-$	1.14 <sup>309</sup>	1.00	$233.0(CDCl_3),^{325} 222.8(CHCl_3),^{329}$ $245.8^{309}$
$SeO_4^{2-}$	1.12 <sup>323</sup>	1.8	$248.5^{323}$
$SO_4^{2-}$	0.94 <sup>323</sup>	1.36	$251.4^{323}$
$H_2O$	-1.7 <sup>g</sup>	-1.7 <sup>g</sup>	$260,^{330} 259.8(C_6H_6),^{322}$
$H_2PO_4^-$	-1.74		$251.8(CD_3OD)^{332}$
<u>N-donors</u>			
imidazolate	11.79 <sup>319</sup>	14.3 <sup>319</sup>	
$EDTA^{4-}$	9.263 <sup>333</sup>	10.0	
uridine(N-3)	9.0 <sup>334</sup>	9.2 <sup>334</sup>	
tryptophan	8.85 <sup>335</sup>	9.39 <sup>335</sup>	
8-hydroxyquinoline	8.8 <sup>312</sup>	9.63	
histidine(NH <sub>2</sub> )	8.8 <sup>324</sup>	9.1	
tryptamine	8.47 <sup>335</sup>	10.2 <sup>335</sup>	$213.1$ <sup>335</sup>
4-hydroxyquinoline-2- $CO_2H$	8.4 <sup>312</sup>	11.0	
8-hydroxyquinoline-5- $SO_3^-$	8.3 <sup>312</sup>	8.37	
$NH_2CH_2(CH_2C_6H_5)CO_2^-$ L-2-phenylalanine	8.29 <sup>331</sup>	9.16	$213.6$ <sup>336</sup>
$NH_2CH_2CH_2NH_2$	8.25	10.05	
$CH_3Hg$ -imidazole	8.18 <sup>319</sup>	9.65 <sup>319</sup>	
L-tyrosine(NH <sub>2</sub> )	8.12 <sup>337,z</sup>	9.11 <sup>337</sup>	$216.5$ <sup>336</sup>
guanosine(N-1)	$\sim 8.1$ <sup>334</sup>	9.2 <sup>334</sup>	
7-iodo-8-hydroxyquinoline-5- $SO_3^-$	8.1 <sup>312</sup>	7.10	

Table 3.2: Formation constants of  $MeHg(II)^a$  and  $Proton^{a,b}$  complexes of various ligands,<sup>c</sup> and  $^2J(^1H-^{199}Hg)$  for the  $MeHg(II)$  complexes.

$\text{NH}_2\text{CH}_2\text{CO}_2^-$ glycine	7.88, <sup>331</sup> 7.55 <sup>313</sup>	9.69	215.5, <sup>335</sup> 216.0 <sup>331</sup>
$\text{NH}_2(\text{CH}_2)_5\text{CO}_2^-$	7.83 <sup>331</sup>	10.84	211.8 <sup>331</sup>
$\text{NH}_2(\text{CH}_2)_4\text{CO}_2^-$	7.75 <sup>331</sup>	10.81	211.2 <sup>331</sup>
$\text{Fe}(\text{CN})_6^{4-}$	7.66 <sup>319m</sup>	4.17	
$\text{CH}_3\text{CH}_2\text{NH}_2$	7.64 <sup>331</sup>	10.82	211.0 <sup>331</sup>
$\text{NH}_2(\text{CH}_2)_7\text{CO}_2^-$	7.60 <sup>331</sup>	10.89	
$\text{NH}_3$	7.60, <sup>305</sup> 7.25, <sup>331</sup> 8.4 <sup>324</sup>	9.32	214.1 <sup>331</sup>
$\text{CH}_3\text{NH}_2$	7.57 <sup>331</sup>	10.81	211.5 <sup>331</sup>
$\text{NH}_2(\text{CH}_2)_2\text{CO}_2^-$ $\beta$ -alanine	7.56 <sup>331</sup>	10.25	213.9 <sup>331</sup>
$(\text{CH}_3)_2\text{CHNH}_2$	7.56 <sup>331</sup>	10.76	209.0 <sup>331</sup>
$\text{NH}_2(\text{CH}_2)_3\text{CO}_2^-$	7.54 <sup>331</sup>	10.48	211.9 <sup>331</sup>
$(\text{CH}_3)_3\text{CNH}_2$	7.52 <sup>331</sup>	10.81	210.2 <sup>331</sup>
$\text{NH}_2\text{CH}(\text{CO}_2^-)\text{CH}_3$ $\alpha$ -alanine	7.52 <sup>331</sup>	9.74	
$\text{CH}_3\text{SCHCH}_2(\text{CO}_2^-)\text{NH}_2$ methionine	7.5 <sup>338</sup>	-	
$(\text{CH}_3)_2\text{CHCH}(\text{CO}_2^-)\text{NH}_2$ valine	7.41 <sup>331</sup>	9.81	
1,10-phenanthroline	7.05, <sup>339</sup> 7.15 <sup>312</sup>	4.92	
imidazole	7.14, <sup>319</sup> 7.3 <sup>324</sup>	7.10	
$[\text{Fe}(\text{CN})_6-\text{HgCH}_3]^{3-}$	7.12, <sup>319</sup> m	-	
N-Me-imidazole	6.96 <sup>41</sup>	7.18	218.8, <sup>41</sup> 219.5( $\text{CD}_3\text{OD}$ ) <sup>249</sup>
$(\text{CH}_3)_2\text{NH}_2$	6.76 <sup>331</sup>	11.02	216.6 <sup>331</sup>
histidine(Im-N)	6.4 <sup>324</sup>	6.1	
2,2',2''-terpyridyl	6.35 <sup>339</sup>	4.69	243.0( $\text{CD}_3\text{OD}$ ) <sup>249</sup>
HEDTA <sup>3-</sup>	6.2 <sup>324</sup>		
L-tyrosine, Et ester	6.09 <sup>337L</sup>	7.33 <sup>337</sup>	
2,2'-bipyridyl	5.93, <sup>339</sup> 5.86 <sup>312</sup>	4.44	238.8( $\text{CD}_3\text{OD}$ ) <sup>332</sup>
quinoline-2- $\text{CO}_2\text{H}$	5.75 <sup>312</sup>	4.7	
pyridine-2-azo-p-dimethylaniline(2-pada)	5.75 <sup>339</sup>	4.50	
benzimidazole	5.27 <sup>335</sup>	4.34 <sup>335</sup>	218.4 <sup>335</sup>
4-Me-pyridine	5.03 <sup>319m</sup>	6.12	227.8( $\text{CD}_3\text{OD}$ ) <sup>332</sup>
$(\text{CH}_3)_3\text{N}$	~5.05 <sup>331</sup>	10.05	
pyridine-4-azo-p-dimethylaniline(4-pada)	4.76 <sup>339</sup>	5.60	
pyridine	4.72 <sup>324</sup>	5.29	229.6( $\text{CD}_3\text{OD}$ ) <sup>332</sup>
3-Me-pyridine	4.69 <sup>319m</sup>	5.80	228.2( $\text{CD}_3\text{OD}$ ) <sup>332</sup>
cytidine(N-3)	4.6 <sup>334</sup>	4.2 <sup>334</sup>	
2-Me-pyridine	4.35 <sup>319m</sup>	6.08	227.9( $\text{CD}_3\text{OD}$ ) <sup>332</sup>
$\text{Co}(\text{CN})_6^{3-}$	4.15 <sup>305</sup>	<0 <sup>305</sup>	
$\text{Fe}(\text{CN})_6^{3-}$	4.13 <sup>319m</sup>	<1	
quinoline	4.05 <sup>312</sup>	4.97	
$[\text{Fe}(\text{CN})_6-\text{HgCH}_3]^{2-}$	3.76 <sup>319m</sup>		
$[\text{Co}(\text{CN})_6-\text{HgCH}_3]^{2-}$	3.50 <sup>305</sup>	<0	
$[2,2',2''\text{-terpy}]\text{CH}_3\text{Hg}^+$	3.25 <sup>339</sup>		
$(\text{CH}_3)_3\text{N}(\text{CH}_2)_2\text{N}(\text{CH}_3)_2$	3.03 <sup>319m</sup>	6.07 <sup>319m</sup>	
adenosine(N-1)	~3 <sup>334</sup>	3.5 <sup>334</sup>	
4- $\text{NH}_2\text{C}_6\text{H}_4\text{SO}_3^-$	2.60 <sup>305</sup>	3.06 <sup>305</sup>	

#### Halogens

$\text{F}^-$	1.50 <sup>305</sup>	2.85	
$\text{Cl}^-$	4.90-5.64 <sup>h</sup>	~7	212(MeOH), <sup>340</sup> 215.2(pyr), <sup>322</sup> 211(diox), <sup>330</sup> 203.6( $\text{CDCl}_3$ ), <sup>341</sup> 221.5(DMSO) <sup>341</sup>
$\text{Br}^-$	6.62, <sup>305</sup> 6.37, <sup>342</sup> 5.98, <sup>314</sup> 6.70 <sup>315</sup>	~9	207(MeOH), <sup>340</sup> 212.0(pyr), <sup>322</sup> 221.5(DMSO), 214.5(pyr), <sup>343</sup> 207(diox), <sup>330</sup> 196.9( $\text{CDCl}_3$ ), <sup>341</sup> 217.7(DMSO- $d_6$ ) <sup>341</sup>
$\text{I}^-$	8.60, <sup>305</sup> 8.50 <sup>i</sup> , 8.7 <sup>315</sup>	~9.5	200.0(pyr), <sup>322</sup> 184( $\text{CDCl}_3$ ), <sup>341</sup> 208(DMSO- $d_6$ ) <sup>341</sup>

Table 3.2: Formation constants of  $\text{MeHg}(\text{II})^a$  and Proton<sup>a,b</sup> complexes of various ligands,<sup>c</sup> and  $^2\text{J}(^1\text{H}-^{199}\text{Hg})$  for the  $\text{MeHg}(\text{II})$  complexes.

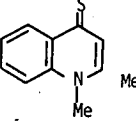
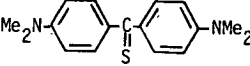
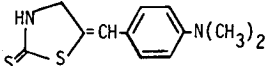
<u>P-donors</u>			
$P(CH_2CH_3)_3$	15 <sup>305 k</sup>	8.8 <sup>305</sup>	
$(CH_3CH_2)_2PCH_2CH_2OH$	14.6 <sup>305</sup>	8.12 <sup>305</sup>	
$(C_6H_5)_2PC_6H_4-3-SO_3^-$	9.15 <sup>305</sup>	~0 <sup>305</sup>	
<u>Se-donors</u>			
$SeCN^-$	6.79 <sup>323</sup>	<1	200.4 <sup>323</sup>
<u>S-donors<sup>j</sup></u>			
$S^{2-}$	21.2 <sup>305</sup>	~14	146 <sup>323</sup>
$CH_3HgS^-$	16.34 <sup>305</sup>	-	156.6(pyr) <sup>322</sup> 156(pyr) <sup>323</sup>
$S_2O_3^{2-}$	10.90 <sup>305</sup> 11.05	-	178(pyr) <sup>326</sup> 191.0 <sup>309</sup>
	1-methyl-quinaldine-thione	9.66 <sup>319</sup>	~1.1 <sup>319</sup>
	Michler's thioketone	8.28 <sup>305</sup>	~2 <sup>305</sup>
1-methylpyridine-2-thione	8.15 <sup>319</sup>	~1.6 <sup>344</sup>	
$SO_3^{2-}$	8.11 <sup>305</sup> 7.96 <sup>323</sup>	6.79	172.4 <sup>323</sup>
$(CH_3Hg)_2S$	~7 <sup>305</sup>	0	202 <sup>323</sup>
$(NH_2)_2C=S$	6.92 <sup>319</sup>	-1.2 <sup>319</sup>	
$HOCH_2CH_2SHgCH_3$	6.27 <sup>305</sup>	0	
$NCS^-$	6.05 <sup>305</sup> 6.1 <sup>324</sup>	<0 <sup>345</sup>	205.6(MeOH) <sup>268</sup> 208.0(pyr) <sup>322</sup>
$(HOCH_2CH_2S)_2(CH_2)_2$	4.27 <sup>319</sup>	<0 <sup>319</sup>	203 <sup>323</sup>
$S(CH_2CH_2CO_2^-)_2$	4.20 <sup>319</sup>	<0 <sup>319</sup>	
$(HOCH_2CH_2S)_2(CH_2)_5$	4.13 <sup>319</sup>	<0 <sup>319</sup>	
$(HOCH_2CH_2S)_2(CH_2)_3$	3.80 <sup>319</sup>	<0 <sup>319</sup>	
$(HOCH_2CH_2S)_2CH_2$	3.38 <sup>319</sup>	<0 <sup>319</sup>	
$(HOCH_2CH_2S)_2(CH_2)_5HgCH_3$	3.24 <sup>319</sup>	<0 <sup>319</sup>	
$Co(NH_3)_5NCS^+$	3.20 <sup>305</sup>	<0 <sup>305</sup>	
$HOCH_2SH_2SCH_2CH_2OH$	3.14 <sup>319</sup>	0 <sup>319</sup>	
		3.07 <sup>305k</sup>	0 <sup>305k</sup>
$(HOCH_2CH_2S)(CH_2)_3HgCH_3$	2.86 <sup>319</sup>	<0	
$(HOCH_2CH_2S)_2(CH_2)_2HgCH_3$	2.84 <sup>319</sup>	<0	
$CH_3SCH_2CH_2CH(CO_2^-)NH_3^+$ methionine	1.94 <sup>338</sup>		223 <sup>338</sup>
$S(CH_2CH_2SO_3^-)$	1.91 <sup>319</sup>	0 <sup>319</sup>	
$CH_3HgSCN$	1.65 <sup>305</sup>	0 <sup>305</sup>	239.9(MeOH) <sup>268</sup>
$CH_3SCH_3$	-1.4 <sup>346o</sup>		
<u>C-donors</u>			
$CH_3^-$	~37 <sup>n</sup>	~46	101(CHCl <sub>3</sub> ) <sup>341</sup> 101-109 (var.) <sup>347</sup> 105.1(DMSO) <sup>341</sup> 101(neat) <sup>325</sup> 104.3(pyr) <sup>322</sup> 100.6(C <sub>6</sub> H <sub>12</sub> ) <sup>322</sup> 101.5(neat) <sup>348</sup>
$C_6H_5^-$	~21 <sup>n</sup>	~30	109.0(CDCl <sub>3</sub> ) <sup>340</sup> 140(C <sub>6</sub> H <sub>6</sub> ) <sup>321</sup>
$CN^-$	14.0 <sup>305</sup> 14.2 <sup>324</sup>	9.14	177.6(pyr) <sup>343</sup> 178.0(pyr) <sup>322</sup> 176.0(C <sub>6</sub> H <sub>6</sub> ) <sup>322</sup> 175(diox) <sup>330</sup> 188(D <sub>2</sub> O) <sup>330</sup>
malononitrile	10.4 <sup>349</sup>	11.39	
diethylmalonate	<8.6 <sup>349</sup>	13.3	
$[Cu([13]dieneN_4)]^{2+}$	<6.5 <sup>349</sup>	9.95	
acetylacetone	5.9 <sup>349</sup>	9.0 <sup>350</sup>	

Table 3.2: Formation constants of  $MeHg(II)^a$  and Proton $^{a,b}$  complexes of various ligands,<sup>c</sup> and  $^2J(^{199}Hg)$  for the (cont.)  $MeHg(II)$  complexes.



$[\text{Ni}([\text{14}] \text{dieneN}_4)]^{2+}$	5.46 <sup>349</sup>	6.28
2-acetylcyclopentanone	<4.3 <sup>349</sup>	7.88
2-methyl-1,3-indandione	<4 <sup>349</sup>	6.18
Meldrum's Acid	3.72 <sup>349</sup>	4.83 <sup>351</sup>
dimedone	3.70 <sup>349</sup>	5.25 <sup>352</sup>
1,3-dimethylbarbituric acid	3.60 <sup>349</sup>	4.45
1,3-cyclopentenedione	2.1 <sup>349</sup>	4.25
$\text{CH}(\text{CN})_3$	<2 <sup>349</sup>	-5.1

Table 3.2: Formation constants of  $\text{MeHg(II)}^a$  and Proton<sup>a,b</sup> complexes of various ligands,<sup>c</sup> and  $^2\text{J}(^1\text{H}-^{199}\text{Hg})$  for the (cont.)  $\text{MeHg(II)}$  complexes.

<sup>a</sup>for the equilibrium  $\text{MeHg}^+ + \text{L}^- \rightleftharpoons \text{MeHgL}$ .

<sup>b</sup>experimental conditions are not included here, but equilibrium constants are in aqueous solution unless otherwise stated.

<sup>c</sup>this Table and Tables 3.1 (hydroxide), 3.3 (chloride), 3.4 (monothiolates - previous work), 3.6 (monothiolates - this work) and 3.11 (dithiolates - this work) form a comprehensive list of  $\text{MeHg(II)}$  stability constants to date (1981), and updates the unpublished compilation of Erni (1977).<sup>319</sup>

<sup>d</sup>for polyprotic ligands.  $\text{pK}_a$  refers to the  $\text{MeHg(II)}$ -coordinating group, reference 353, unless otherwise stated.

<sup>d</sup>for  $\text{MeHg(II)}$  complexes in aqueous solution unless otherwise indicated. This Table is not a comprehensive list of coupling constants. Only values of  $^2\text{J}$  of complexes for which the  $\text{MeHg(II)}$  formation constant is known, have been included.

<sup>f</sup>see Table 3.1, page .

<sup>g</sup>with  $[\text{H}_2\text{O}] = 55\text{M}$  by definition.

<sup>h</sup>see Table 3.3, page 81 .

<sup>i</sup>this work.

<sup>j</sup>not including monothiolates (Tables 3.4 and 3.6) and dithiolates (Table 3.11).

<sup>k</sup>20% EtOH.

<sup>l</sup>constants of the form  $\text{MeHgOH} + \text{HL} \rightleftharpoons \text{MeHgL} + \text{H}_2\text{O}$  have been converted using  $\log \beta (\text{MeHgOH}) = -4.60$  and  $\text{pK}_a (\text{HL})$  in the reference shown.

<sup>m</sup>theses by various authors (ETH Zürich) in reference 319.

<sup>n</sup>calculated from thermodynamic data in reference 319.

<sup>o</sup>with  $\text{MeHgO}_2\text{CMe}$  in  $\text{CH}_2\text{Cl}_2$ .

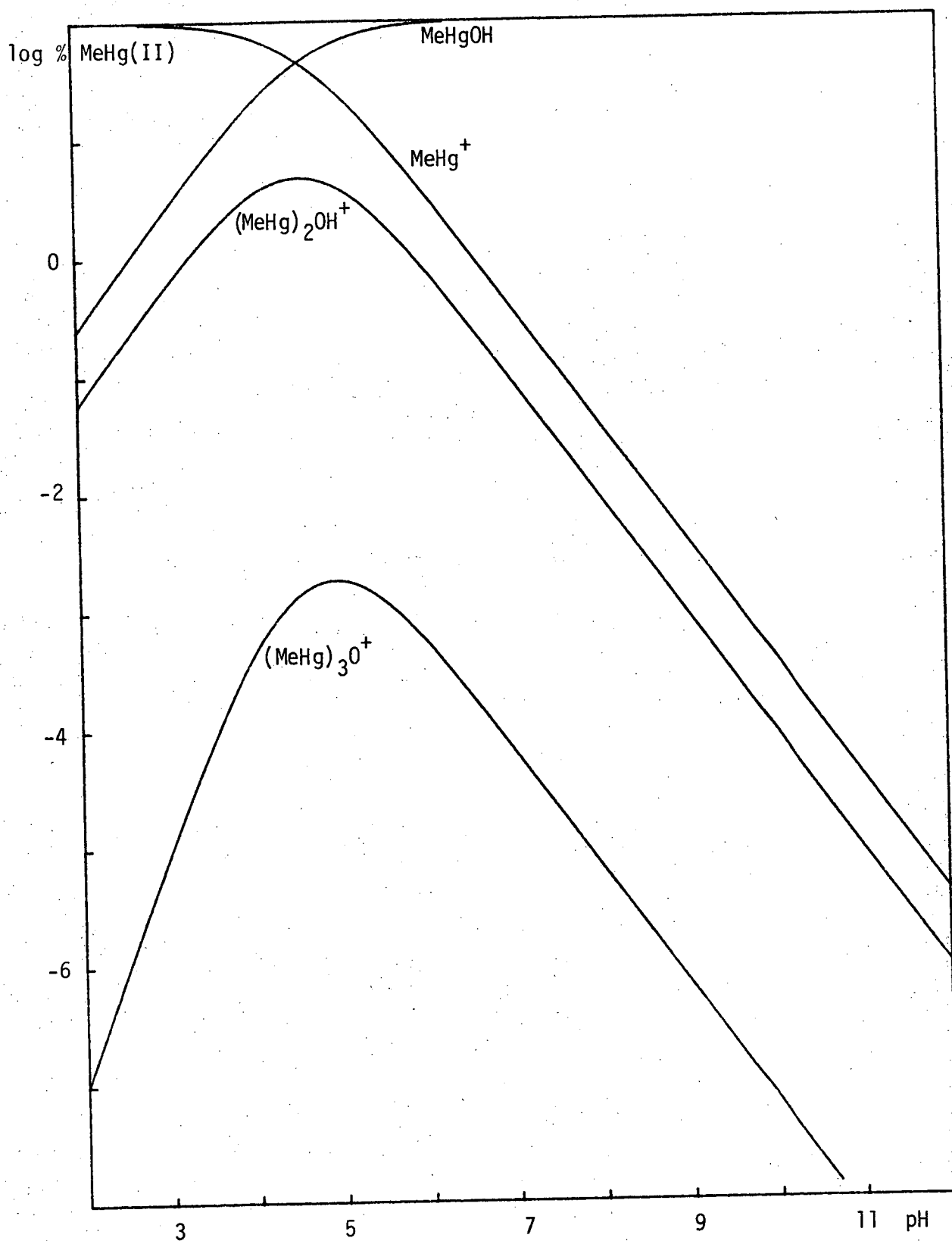


Figure 3.2: Species distribution calculated by COMIX for the hydrolysis of 0.001M MeHg(II), using the equilibrium constants:  $\log \beta_{10-1} = -4.607$  and  $\log \beta_{20-1} = -2.234$  (this work), and  $\log \beta_{30-2} = -7.0$  (page ).

nature of the dominant MeHg(II) complex(es) may frequently be postulated by comparison of the *conditional* stability constants of MeHg(II) with the various ligands. The conditional stability constant,  $K_{\text{cond}}$ , is defined generally by

$$K_{\text{cond}} = \frac{\sum \text{MeHgL}_{\text{all complexed species}}}{\left( \sum \text{MeHg(II)}_{\text{not bound to L}} \right) \left( \sum \text{L}_{\text{not bound to MeHg(II)}} \right)}$$

Even if the ligand is not involved in protolytic equilibria, since MeHg(II) is hydrolysable,  $K_{\text{cond}}$  is pH dependent. Figure 3.3 shows values of  $K_{\text{cond}}$  for MeHg(II) with a few of the ligands shown in Table 3.2. The conditional formation constant curves were calculated with COMIX for  $10^{-3}$  M solutions of MeHg(II) and ligand.<sup>†</sup> It can be seen that thiolate complexes predominate, except at either extreme of the pH scale. At low pH, protons compete more effectively than MeHg(II) for ligand, whereas at high pH, hydroxide competes more effectively than ligand for MeHg(II). The extremely stable MeHg(II) thiolate complexes require special techniques for determination of their formation constants since protons cannot compete effectively with MeHg(II) for thiolate (page 320). It is generally a simple matter to evaluate the dominant MeHg(II) species in a mixture of ligands, by comparison of the products,  $K_{\text{cond}}[L]$ .

If thiolates are involved in the equilibria and are present at more than trace amounts, they will usually dominate the MeHg(II) species distribution, but in one important biological situation this is not the case. If MeHg(II) is ingested orally, comparisons of  $K_{\text{cond}}$  indicate that significant concentrations of lipid-soluble MeHgCl occur at the low pH and chloride concentration of the stomach, facilitating absorption into the bloodstream.<sup>354</sup> In this work, use has been made of competitive equilibria between thiolate ligands and iodide, or between two thiolate ligands, to

<sup>†</sup>Programs COMIX, COMIXH and TITRAT are described in Chapter 6. A listing of COMIXH is given as Appendix 2.

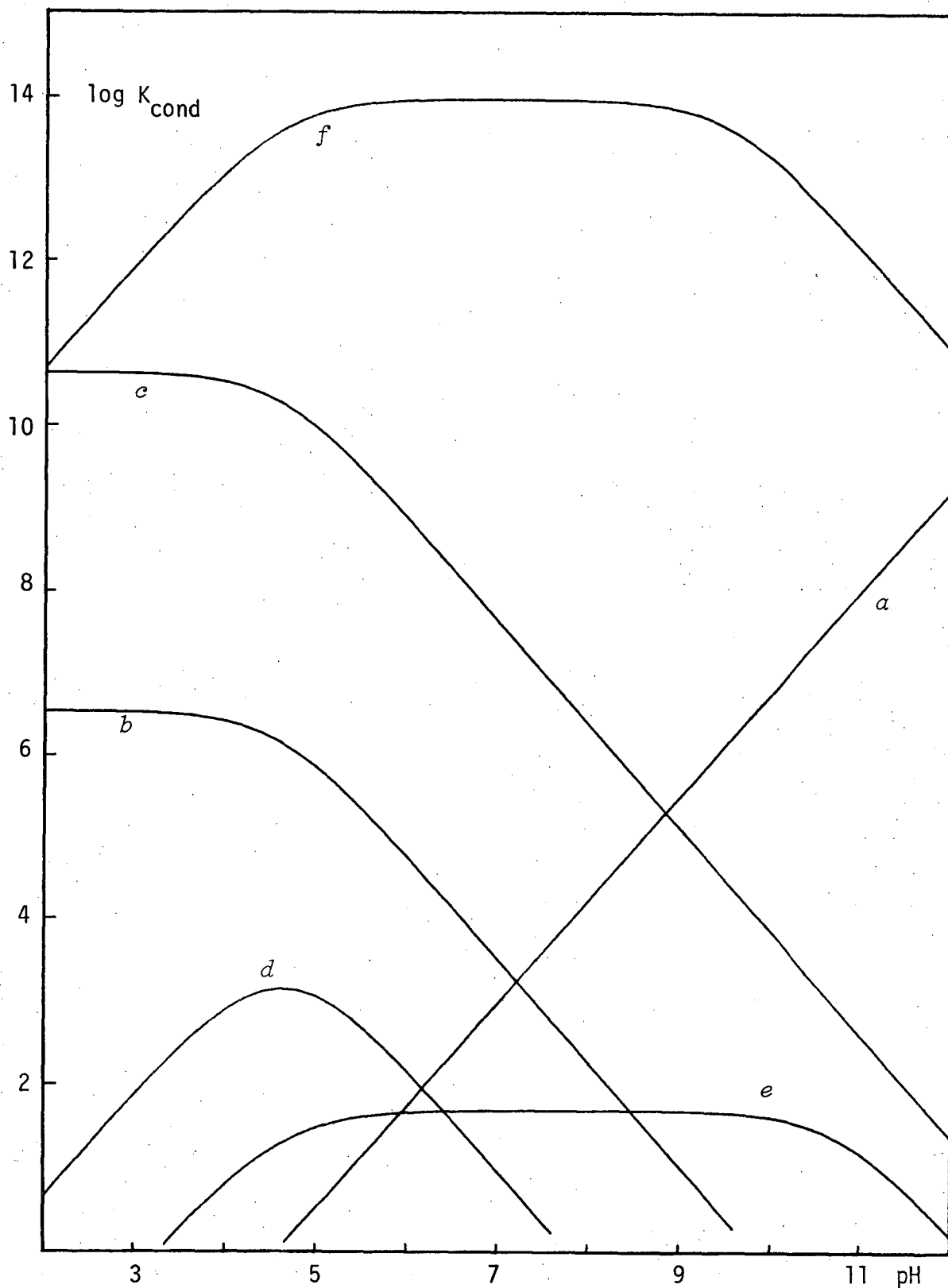


Figure 3.3: Conditional stability constants,  $\log K_{\text{cond}}$ , as a function of pH for MeHg(II) with several ligands. The donor atom is indicated.

*a* hydroxide (O), *b* chloride (Cl), *c* iodide (I), *d* acetic acid (O),  
*e* methylamine (N), *f* mercaptoethanol (S).

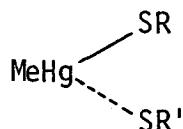
Calculated by COMIX for 0.001M MeHg(II) and 0.001M ligand.

obtain the stability constants for MeHg(II)-thiolate formation.

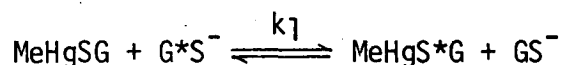
### 3.2.2 NMR investigations of MeHg(II) interactions in solution

Nuclear Magnetic Resonance techniques have produced much of the currently available information regarding MeHg(II) coordination in solution. The  $^1\text{H}$  nmr spectrum of the methyl group of MeHg(II) consists of a singlet accompanied by two less intense satellites due to protons of the methyl group bonded to the isotope  $^{199}\text{Hg}$  ( $I=\frac{1}{2}$ , 16.9% abundance), e.g. see Figure 3.34 page 168. The coupling is due to a Fermi contact mechanism and the magnitude of the coupling constant  $^2J(^1\text{H}-^{199}\text{Hg})$  is determined by the degree of s character of the Hg-C bond, and the s electron density at the nuclei of the coupled atoms.<sup>322,355</sup> Differences in the perturbation of the Hg 6s orbital electron density caused by bonding to donor atoms of different Lewis basicity, often allows the ligating atom to be identified in ambidentate ligands, by consideration of the magnitude of  $^2J(^1\text{H}-^{199}\text{Hg})$ , e.g. selenite,  $\text{SeO}_3^{2-}$ , has been shown to be bonded to MeHg(II) through oxygen<sup>323</sup> but sulfite, through sulfur.<sup>323</sup> Coordination of selenite through oxygen has been confirmed by Raman spectroscopy.<sup>323</sup> Since the donor Lewis basicity is often reflected in the Brønsted basicity,  $|^2J(^1\text{H}-^{199}\text{Hg})|$  decreases linearly as  $\text{pK}_a$  of the ligand donor increases, in series of structurally related compounds. Thus, linear correlations between  $|^2J(^1\text{H}-^{199}\text{Hg})|$  and ligand  $\text{pK}_a$  have been found for MeHg(II) complexes of unidentate pyridines, and N-substituted pyrazoles and imidazoles.<sup>304</sup>

Despite the high thermodynamic stability of MeHg(II)-thiolates, the Hg-S bond is extremely kinetically labile.<sup>356-8</sup> Thus, thiolate exchange in MeHgSR/SR' systems<sup>250</sup> is usually fast on the nmr time scale, taking place by an associative nucleophilic mechanism via intermediates of the type

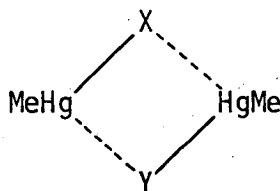


In the biological situation, the rapid exchange of glutathione, GSH, is of particular importance with regard to MeHg(II) transport.<sup>359</sup> The rate constant,  $k_1$ , for the attack of sulfhydryl deprotonated glutathione on the MeHgGSH complex is high,  $6 \times 10^8 \text{ M}^{-1} \text{ s}^{-1}$ .<sup>360</sup>

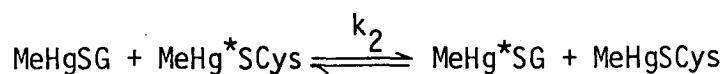


Although glutathione will be predominantly in the protonated form at physiological pH,  $k_1$  is sufficiently high that this pathway dominates the methylmercury exchange mechanism.<sup>359</sup> The analogous reaction, involving sulfhydryl-protonated glutathione, is slow ( $k_1 < 0.1 \text{ M}^{-1} \text{ s}^{-1}$ ).<sup>360</sup>

Direct exchange between MeHgX/MeHgY species is also rapid on the nmr timescale, except for the case where one of the complexes is MeHgCN.<sup>356</sup> The exchange mechanism proceeds via a four centre bridged intermediate of the type



The relative rates of bimolecular ligand exchange are proportional to the ligand bridging ability.<sup>250</sup> Thus, the reaction is fast for thiols, e.g. exchange between the MeHg(II) complexes of glutathione and cysteine has  $k_2 < 0.1 \text{ M}^{-1} \text{ s}^{-1}$ .<sup>360</sup>



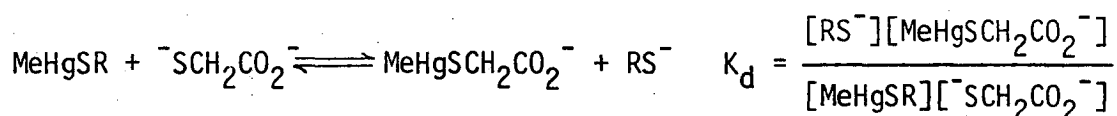
<sup>†</sup>Recent work by Bach *et al.* indicates that this may not be true for the interaction of  $\text{MeHgSCH}_2\text{CO}_2\text{H}$  with the  $\text{Fe}_2\text{S}_2(\text{SCys})_4$  cluster of adrenodoxin.<sup>361</sup>

The bimolecular exchange between  $\text{Bu}^t\text{HgSCH}_3$  and  $\text{Bu}^t\text{HgSCH}(\text{CH}_3)\text{C}_6\text{H}_5$  has  $k_2 \ 3 \times 10^7 \text{ M}^{-1} \text{ s}^{-1}$  in  $\text{HCF}_2\text{Cl}:\text{HCFCl}_2$  at  $25^\circ$ ,<sup>250</sup> which would be four orders of magnitude faster than diffusion controlled processes if the exchange mechanism was dependent on uncomplexed thiolate or organo-mercurial.<sup>250</sup>

When exchange is rapid on the nmr timescale, an exchange-averaged value for the chemical shift of methyl protons of  $\text{MeHg(II)}$ ,  $\delta\text{CH}_3$ , is observed. The pH-dependence of  $\delta\text{CH}_3$  has been used to evaluate  $\text{MeHg(II)}$  formation constants with a range of inorganic anions,<sup>323</sup> carboxylic acids,<sup>309</sup> amines and aminocarboxylic acids,<sup>331</sup> methionine,<sup>338</sup> and recently, of several monothiol.<sup>302</sup>

### 3.2.3 NMR evaluation of $\text{MeHg(II)}$ -thiolate formation constants

Reid and Rabenstein<sup>302</sup> have measured the displacement constants,  $K_d$  in their terminology, for the exchange equilibria:



The monothiols,  $\text{RSH}$  = mercaptoethanol, penicillamine, N-acetylpenicillamine, cysteine, homocysteine and mercaptosuccinic acid, are among the several whose formation constants with  $\text{MeHg(II)}$  were evaluated in this study using the potentiometric titration method.

By monitoring the chemical shift of the methylene protons of mercaptoacetate,  $(\text{MA}^{2-})$ , as the pH of the equilibrium mixture is altered,  $K_d$  can be determined because the relative affinities of  $\text{RSH}$  and  $\text{MAH}_2$  for  $\text{MeHg(II)}$  are pH-dependent. Since  $K_d$  is the quotient of the individual formation constants of the two thiols for  $\text{MeHg(II)}$ :

$$K_d = \frac{[\text{MeHgSR}]}{[\text{MeHg}^+][\text{RS}^-]} \bigg/ \frac{[\text{MeHgSCHCO}_2^-]}{[\text{MeHg}^+][^-\text{SCH}_2\text{CO}_2^-]} \\ = K_f(\text{MeHgSR}) \bigg/ K_f(\text{MeHgMA}^-)$$

knowledge of  $K_f(\text{MeHgMA}^-)$  and  $K_d$  gives  $K_f(\text{MeHgSR})$ . The value of  $K_d$  is near unity for the thiols studied, and can therefore be precisely evaluated, despite the extremely high individual  $\text{MeHg(II)}$ -thiolate formation constants (Table 3.8, pages 98-100).

$K_d$  can be expressed in terms of the fraction  $P_f$  of  $\text{MAH}_2$  in the free, uncomplexed ( $\text{MA}^{2-}$ ) form:

$$K_d = \left( \frac{P_f}{1-P_f} \right) \frac{\alpha_1 \alpha_3}{\alpha_2 \alpha_4}$$

where  $\alpha_1$  is the fraction of  $\text{MAH}_2$  in the fully protonated ( $\text{MAH}_2$ ) form,  $\alpha_2$  is the fraction of  $\text{MeHgMA}^-$ ,  $\alpha_3$  is the fraction of thiol in the  $\text{MeHgSR}$  form and  $\alpha_4$  is the fraction of  $\text{RS}^-$ . All these fractions can be expressed in terms of only the relevant ligand or complex protonation constants, and measured pH (for mixed constants) or  $[\text{H}^+]$  (for concentration constants).

The fraction  $P_f$  was evaluated by Reid and Rabenstein from the exchange-averaged proton chemical shifts of the free and complexed  $\text{MA}^{2-}$  forms,

$$P_f = (\delta_{\text{obs}} - \delta_c) / (\delta_f - \delta_c)$$

since thiolate exchange is fast on the nmr timescale. Collected values of  $\delta$  as a function of pH were fitted by non-linear least-squares to yield values of  $K_d$  at 25° (0.3M ionic strength).

The formation constant of the  $\text{MeHgMA}^-$  complex was evaluated in an analogous manner, using mercaptoethanol (MEH) competition and the value  $K_f(\text{MeHgME})$  reported by Schwarzenbach and Schellenberg.<sup>305</sup> The reliability of  $K_f(\text{MeHgME})$  is crucial to the reliability of the derived constants,  $K_f(\text{MeHgMA}^-)$  and hence  $K_f(\text{MeHgSR})$ . The value of



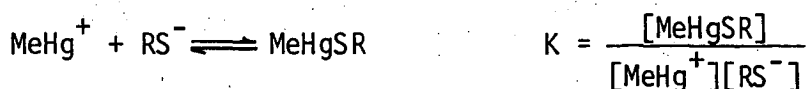
$\log K_f(\text{MeHgME})$  found in this study (page 98) [16.135(4), 0.1M ionic strength, 25°] is in excellent agreement with that reported by Schwarzenbach and Schellenberg [16.12, 0.1M ionic strength, 20°].<sup>305</sup> Therefore, values of  $\log K_f(\text{MeHgSR})$  found by Reid and Rabenstein should be directly comparable to those found here, except for a minor correction due to  $\log \gamma_{\text{H}^+}$  to convert mixed constants into concentration constants.

The formation constants  $\log K_f(\text{MeHgSR})$  and proton dissociation constants of the MeHgSR complexes, found by Reid and Rabenstein, have been included in Table 3.8 with those found during this study and will be discussed later in this Chapter.

### 3.3 Methylmercury(II) Complexation with Thiolate Ligands

#### 3.3.1 Methylmercury(II) monothiolate equilibria

The thermodynamic stability of complexes formed between MeHg(II) and monothiolate ligands has not been extensively studied. Until the commencement of this study, and the publication of the work by Reid and Rabenstein,<sup>302</sup> few reports had been published containing formation constants of MeHg(II)-thiolate complexes. Some of the earlier work, by Simpson,<sup>324</sup> with cysteine and glutathione and by Schwarzenbach and Schellenberg<sup>305</sup> with mercaptoethanol recorded formation constants for the equilibria:



in the range  $15.2 < \log K < 16.2$ , indicating the high stability of these complexes. A series of substituted thiophenols has been studied by Schwarzenbach<sup>362</sup> indicating that the MeHg(II)-thiolate formation constants are linearly related to the thiophenolic acid dissociation constants,  $\text{pK}_a$ . For 17 substituted thiophenols, the linear relationship is found to be

$$\log K = 0.798 \text{ pK}_a + 8.77$$

(which also reproduces  $\log K$  for cysteine, glutathione and mercaptoethanol within 0.5 log units).

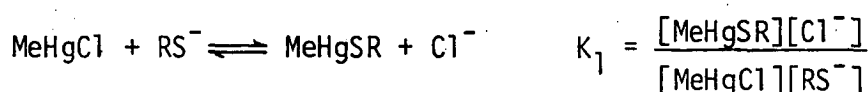
It was therefore of some concern that Hojo *et al.*<sup>363</sup> have more recently reported equilibrium constants for the interaction of MeHg(II) with some previously unstudied monothiols which were several orders of magnitude lower than expected by consideration of the aliphatic thiol acidity in the above correlation. Thus,  $\text{pK}_a$  values in the range 8.0 to 10.4 would indicate  $\log K$  values in the range 15 to 17, but values of 6.7 to 9.0 were recorded by these workers. In addition, reported values

of log K for cysteine, glutathione and mercaptoethanol (7.19, 8.11, 8.76 respectively) were 8 or 9 orders of magnitude lower than reported by Simpson<sup>324</sup> and Schwarzenbach and Schellenberg<sup>305</sup> for these thiols (Table 3.2).

Equilibrium constants given by Hojo *et al.* are, in their terminology, of the form

$$K_1 = [M] / [L][M]$$

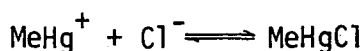
where [L] represents deprotonated ligand. Unfortunately, [M] was undefined by these workers but presumably represents [MeHgCl] since methylmercury(II) was obtained commercially as the chloride. The quoted  $K_1$  is therefore assumed to correspond to the equilibrium constant for the exchange reaction



Using a mean value for the formation constant of MeHgCl  $\log K_{\text{MeHgCl}} = 5.3$ , taken from several literature sources shown in Table 3.3, Hojo's values for log  $K_1$  have been corrected to give the MeHg(II)-thiolate formation constants defined previously (page 80 ).

log K	medium	ref.
5.25	20°, 0.1 M KNO <sub>3</sub>	305
5.45	25°, ~0	315
4.90	20°, 0.1 M KNO <sub>3</sub>	314
5.32(9)	25°, 1M NaClO <sub>4</sub>	366
5.64(1)	25°, 2.5 M NaNO <sub>3</sub>	342
5.22(1)	25°, 0.1 M KNO <sub>3</sub>	this work

Table 3.3: Equilibrium Constants for the equilibrium



RSH	$\log K_{(\text{MeHgSR})}^{a,b}$	medium	ref.
cysteine	15.7 7.19 (12.5) <sup>c</sup>	~25°, ~0 22°, ~0	324 363
glutathione	15.9 8.11 (13.4) <sup>c</sup>	~25°, ~0 22°, ~0	324 363
2-mercaptoethanol	16.2 8.76 (14.1) <sup>c</sup>	20°, 0.1M KI 22°, ~0	305 363
penicillamine	6.72 (12.0) <sup>c</sup>	22°, ~0	363
N-acetylpenicillamine	8.87 (14.2) <sup>c</sup>	22°, ~0	363
2-mercaptopropionic acid	9.03 (14.3) <sup>c</sup>	22°, ~0	363
2-mercaptosuccinic acid	8.16 (13.5) <sup>c</sup>	22°, ~0	363
thiophenol	14.67	20°, 0.1M KI in 1:1 MeOH/H <sub>2</sub> O	362
2-MeO	15.60	"	"
3-MeO	14.48	"	"
4-MeO	14.94	"	"
4-OH	14.88	"	"
2,4-diMe	14.82	"	"
2-Me	14.71	"	"
3-Me	14.62	"	"
4-Me	14.69	"	"
4-F	14.13	"	"
2-Cl	13.89	"	"
3-Cl	13.85	"	"
4-Cl	14.09	"	"
2-Br	13.77	"	"
3-Br	13.82	"	"
4-Br	13.86	"	"
3-I	13.70	"	"
2-SO <sub>3</sub> <sup>-</sup> , 4-NO <sub>2</sub>	12.72	20°, 0.1 KNO <sub>3</sub>	364
2,4-diNO <sub>2</sub>	10.48	"	364
4-NO <sub>2</sub>	12.3	20°, 0.1 NaClO <sub>4</sub>	365

**Table 3.4:** Previously reported<sup>d</sup> formation constants of methylmercury(II)-monothiolate complexes.

<sup>a</sup> for the equilibrium  $\text{MeHg}^+ + ^-\text{SR} \rightleftharpoons \text{MeHgSR}$

<sup>b</sup> the thiolate is considered to be completely deprotonated.

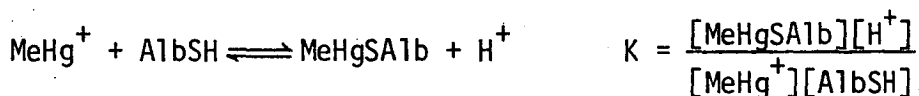
<sup>c</sup> corrected for MeHgCl equilibria, using  $\log K(\text{MeHgCl}) = 5.3$ .

<sup>d</sup> not including nmr studies by Reid and Rabenstein,<sup>302</sup> discussed on page 77 and recorded in Table 38 (page 98).

Even with this correction, if appropriate, the data in Table 3.4 show that serious discrepancies remain in the accepted values for methylmercury-thiolate formation constants. For this reason, the equilibrium constants for MeHg(II) complexation with 2-mercaptoethanol, mercaptoacetic acid and its O-methylester, mercaptosuccinic acid, cysteine, homocysteine, penicillamine, N-acetylpenicillamine, glutathione, thiocholine and N-mercapto-piperidine (shown in Figure 3.4) were investigated by the potentiometric method involving iodide competition, described in detail in Chapter 6 of this thesis. Formation constants of MeHg(II) with cationic thiolates such as thiocholine have not previously been reported.

Perhaps surprisingly, the earliest reported MeHg(II)-thiolate stability constants, determined by Hughes, involved the most complex thiols studied to date. Equilibrium constants for MeHgI exchange with human and bovine serum albumin, bovine oxyhemoglobin and bovine carbonyl-hemoglobin were determined by distribution of MeHgI between toluene and aqueous phases of the thiols.<sup>367-8</sup>

The equilibrium constant of MeHg(II) with the sulfhydryl protonated form of human mercaptoalbumin



has been calculated by Simpson<sup>324</sup> to be  $10^{6.9}$  using values of the distribution constant for MeHgI between toluene and water,  $D = 500$  and for MeHgI formation,  $10^{8.7}$  determined by him; and Hughes<sup>368</sup> value for MeHgI/AlbSH exchange in toluene,  $10^{-4.5}$ .

$$\begin{aligned} \text{Thus } K &= \frac{[\text{MeHgSR}][\text{H}^+][\text{I}^-]}{[\text{MeHgI}(\text{toluene})][\text{AlbSH}]} \cdot \frac{[\text{MeHgI}(\text{toluene})]}{[\text{MeHgI}]} \cdot \frac{[\text{MeHgI}]}{[\text{MeHg}^+][\text{I}^-]} \\ &= 10^{-4.5} \cdot 500 \cdot 10^{8.7} = 10^{6.9} \end{aligned}$$

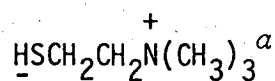
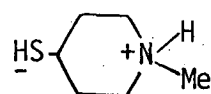
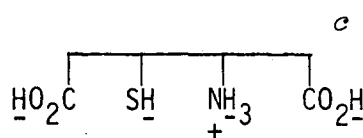
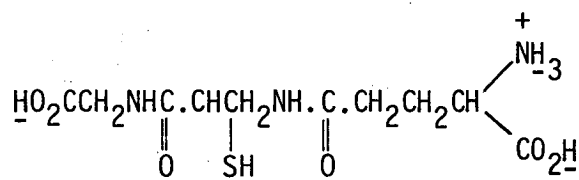
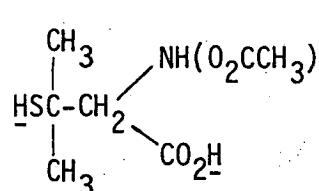
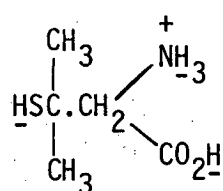
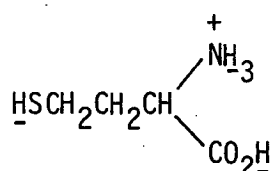
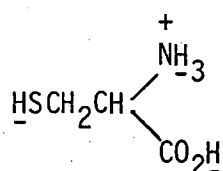
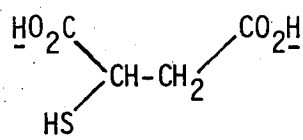
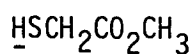
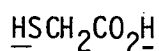
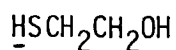


Figure 3.4: Fully protonated forms<sup>b,d</sup> of monothiolate ligands used for complexation of MeHg(II) in this work.

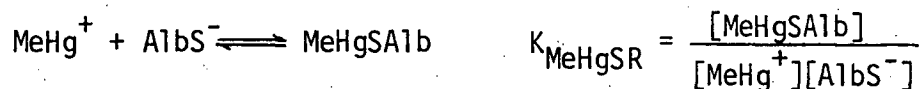
<sup>a</sup>used as the perchlorate salt.

<sup>b</sup>all thiols were used as neutral ligands, except for thiocholine

<sup>c</sup>this shorthand structure is used by Rabenstein,<sup>369</sup> and will be used here for brevity.

<sup>d</sup>dissociable protons are underlined.

An approximation for the average sulfhydryl dissociation constant  $K_a \sim 10^{10}$  for mercaptoalbumin<sup>367-8</sup> gives the formation constant of MeHg(II) with deprotonated albumin



$$\begin{aligned} \text{since } K_{\text{MeHgSR}} &= \frac{[\text{MeHgSA1b}][\text{H}^+]}{[\text{MeHg}^+][\text{AlbSH}]} \cdot \frac{[\text{AlbS}^-]}{[\text{AlbS}^-][\text{H}^+]} \\ &= 10^{6.9} \cdot 10^{10} = 10^{16.9} \end{aligned}$$

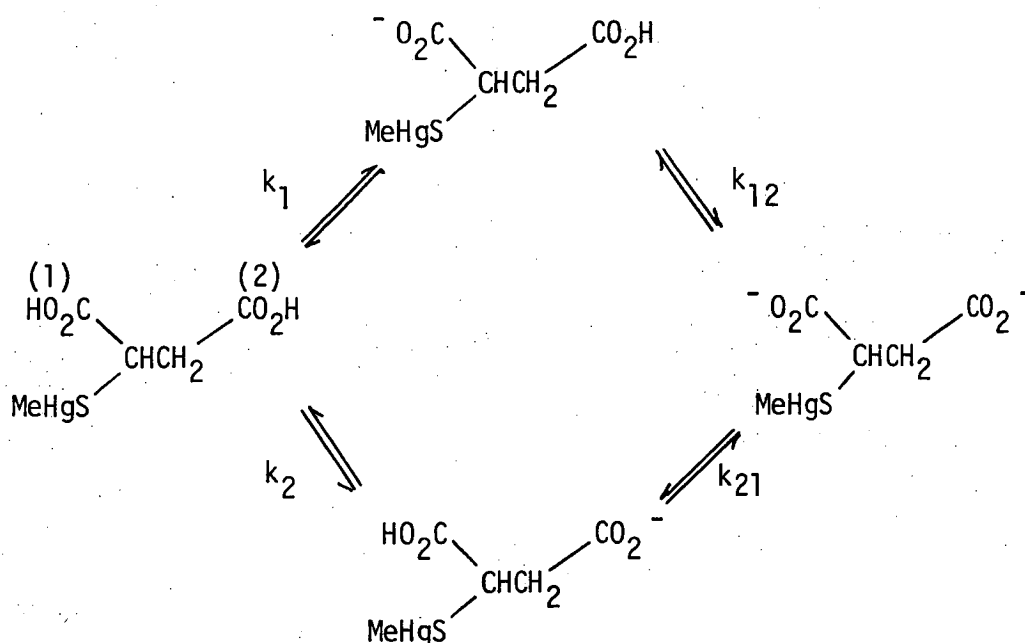
This constant is directly comparable with the MeHg(II)-thiolate formation constants determined in this work and will be recalled later (page 158).

The value,  $10^{22}$ , recorded by Rabenstein<sup>41</sup> and Carty,<sup>246</sup> would seem to be too high.

It can be seen from Figure 3.4 that the thiol ligands investigated, except for 2-mercaptoethanol and thiocholine, have functional groups other than sulfhydryl which can be involved in protolytic equilibria. As a result, attempts to determine the equilibrium constant for complexation of MeHg(II) by fully deprotonated ligands must also consider the coexistence of MeHg-thiolate species which are protonated at sites other than sulfur. The residual Lewis acidity of the coordinated sulfhydryl group is so low that protonation at this site is usually considered to be negligible. (A possible exception to this condition, occurring at low pH, will be discussed on page 111).

For two of the monothiolate ligands used in this work, mercaptosuccinic acid and glutathione, sulfhydryl complexation of MeHg(II) leaves two carboxylic acid groups of comparable acidity which will protonate simultaneously in the range  $3 < \text{pH} < 5$ . Under these conditions *microscopic* equilibrium constants can be defined, e.g. for the

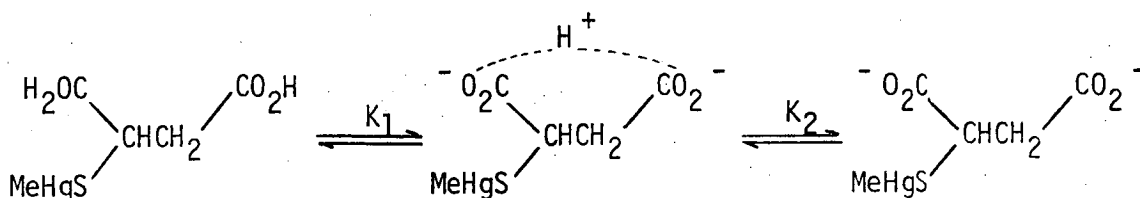
MeHg(II) mercaptosuccinic acid complex, shown in Figure 3.5.



**Figure 3.5:** Microscopic proton dissociation scheme<sup>a</sup> for the 1:1 MeHg(II) complex of mercaptosuccinic acid (page

<sup>a</sup>The equilibrium constant nomenclature is Rabenstein's.<sup>369</sup> The last subscript digit denotes the group being deprotonated in the equilibrium under consideration. The previous digit indicates an already deprotonated site.

Unlike the nmr method in which non-labile protons near each carboxylate group can be monitored simultaneously,<sup>369</sup> the potentiometric titration method cannot give any information regarding these *microscopic* constants. Instead, *macroscopic* equilibrium constants,  $K_1, K_2$ , referring to deprotonation of an 'average' carboxylate group, were determined:





It can be shown<sup>369</sup> that the microscopic and macroscopic equilibrium constants are related by the equations

$$K_1 = k_1 + k_2 \quad \text{and} \quad K_2 = \frac{k_{12}k_{21}}{k_{12} + k_{21}}$$

Completely analogous microscopic equilibria have been described elsewhere for the MeHg-glutathione complex.<sup>369</sup>

### 3.3.2 Potentiometric determination of formation constants of MeHg(II) thiolates

By alkalimetric titration of equilibrium mixtures containing 1:1 ratios of MeHg(II) and monothiolate in acid solution, and in the presence of 0.1 M KI to maintain constant ionic strength, the exchange equilibria



were investigated. The pH-titration data from several such titrations were evaluated by MINQUAD81 (page 326) for the thiol ligands shown in Figure 3.4. The titrations were performed in the following manner: After standardisation of the electrode assembly in the pH(S) 4.008, 6.865 and 10.012 buffers (page 305), a solution of weighed thiol in 0.1 M KI was titrated with 0.1 M KOH, and the titration data treated to evaluate the ligand acid-dissociation constants, analytical thiol concentration, and electrode calibration constants  $\text{pH}_{\text{cal}}$  and  $K_w^{\text{C}}$  (page 295). An aliquot of  $\text{MeHg(II)/H}^+/\text{NO}_3^-$  solution<sup>†</sup> was added to the iodide/thiolate solution in order to obtain nearly 1:1 MeHg(II)-thiolate stoichiometry and at such a rate to prevent local precipitation of MeHgI. If the resultant solution (usually at pH 3 to 4) was cloudy, KOH was immediately added with vigorous nitrogen purging and magnetic stirring to dissolve MeHgI. The dissolution of precipitated MeHgI is

---

<sup>†</sup>the preparation and standardisation of this solution is described on pages 92-6

often slow, taking several hours if the precipitate is allowed to coagulate. On the few occasions the solution remained cloudy above pH 5, they were discarded, and the process repeated with more dilute solutions of thiolate and MeHg(II), or additional KOH was added to the KOH-titrated thiolate, prior to addition of MeHg(II) so that the final pH was not less than 4 to 5.

In the discussion below of the MINQUAD81 treatment of MeHg(II)-thiolate formation constants, reference will be made to a 'sum-of-squares' value,  $U$ , generated by the program. Values of  $U < 10^{-9}$  generally indicate that all titration points are, on average, fitted to better than 0.005 pH units. Values  $U < 10^{-10}$  indicate fits to better than 0.002 pH units. This degree of agreement is difficult to depict on figures showing calculated and experimental titration curves over the range  $3 < \text{pH} < 10$ . For such figures the experimental data points are circled, with circle radii equivalent to 0.02 pH units for clarity. This does not represent the reliability of pH or volume measurements, which for individual titrations were considered to be 0.002 pH units and 0.001 mL respectively. Typical agreement between calculated and experimental titrations is shown in Table 3.5 for the MeHg(II)-mercaptoacetate-iodide system (page 103), calculated by COMIXH using values of equilibrium constants used by MINQUAD81. All MINQUAD81 treatments were performed using fixed values of the equilibrium constants for MeHg(II) hydrolysis, e.g.  $\log \beta_{10-1} = -4.607$ . The binuclear species  $(\text{MeHg})_2\text{OH}^+$ , with  $\log \beta_{20-1} = -2.234$ , needed only to be considered in acidic solutions containing excess MeHg(II) in the absence of iodide. Inclusion of this species otherwise increased the program running time with no decrease in  $U$  or improvement in parameter standard deviations. Constants for ligand protonation were fixed at the weighted geometric means of values obtained from preliminary titrations (using TITRAT) and are shown in Table 3.6.

volume 0.09947M KOH/mL	pH	
	measured	calculated
0.000	3.030	3.022
0.070	3.068	3.063
0.130	3.104	3.100
0.190	3.141	3.139
0.250	3.180	3.179
0.310	3.221	3.221
0.370	3.264	3.265
0.430	3.309	3.311
0.480	3.348	3.350
0.530	3.388	3.391
0.580	3.429	3.433
0.630	3.473	3.477
0.680	3.518	3.522
0.730	3.565	3.568
0.780	3.613	3.616
0.820	3.653	3.655
0.860	3.693	3.696
0.9-0	3.736	3.738
0.940	3.779	3.781
0.980	3.825	3.825
1.020	3.871	3.871
1.060	3.919	3.919
1.100	3.969	3.968
1.140	4.022	4.020
1.180	4.076	4.074
1.220	4.134	4.131
1.260	4.195	4.191
1.300	4.259	4.255
1.340	4.328	4.324
1.380	4.402	4.398
1.420	4.482	4.479
1.450	4.548	4.545
1.480	4.620	4.617
1.510	4.696	4.697
1.540	4.783	4.785
1.570	4.880	4.886
1.600	4.990	5.002
	mean deviation	0.003

**Table 3.5:** Calculated<sup>a</sup> and measured pH values for the Methylmercury(II)-Iodide-Mercaptoacetic acid and titration data treated by MINQUAD81.<sup>b</sup>

<sup>a</sup>calculated by COMIXH (Appendix 2) using the equilibrium constants refined by MINQUAD81 and shown in Tables 3.6 and 3.8 and the experimental conditions shown on Figure 3.8.

<sup>b</sup>sum-of-squares,  $U = 5.1 \times 10^{-10}$ .

	this work [0.1 KNO <sub>3</sub> or KI]			previous values <sup>b</sup>			Ref.	
1. Mercaptoacetic Acid	3.553(8)	10.157(7)		3.35(1)	9.93(2)	[0.3 KNO <sub>3</sub> ]	302	
				3.58	9.78	[0.15 KNO <sub>3</sub> ]	370	
				3.48	9.92	[0.58 NaNO <sub>3</sub> ]	371	
				3.60	10.55	[ ~0 ]	372	
				3.42	10.20	[0.1 KCl]	373	
2. O-Methylmercaptoacetate	7.944(3)			7.95(2)			374	
3. 2-Mercaptosuccinic Acid	3.119(5)	4.588(2)	10.386(3)	3.64	4.64	10.37	[0.1 KNO <sub>3</sub> ]	375
				3.30	4.94	10.64		376
				3.06(1)	4.56(1)	10.39(1)		377
4. 2-Mercaptoethanol	9.583(2)			9.47		[0.3 NaClO <sub>4</sub> ]	378	
				9.444		[ ~0 ]	379	
				9.72		[ ~0 ]	380	

Table 3.6: Proton dissociation constants<sup>a</sup> of monothiol ligands used for MeHg(II) solution studies.

<sup>a</sup>Macroscopic concentration constants obtained with TITRAT. Recorded values are weighted geometric means with estimated standard deviations of the last digit in parentheses.

<sup>b</sup>Literature values at 25°. Mixed constants have been converted to concentration constants by calculation of log<sub>H</sub><sup>+</sup> according to the Davies equation.<sup>318</sup>

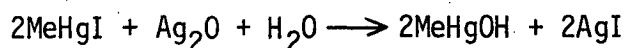
5. L-cysteine	1.98(1)	8.226(3)	10.367(6)	1.896(6)	8.178(2)	10.361(1)	[0.1KCl]	381		
				1.97(1)	8.20(1)	10.87(1)	[0.1 KNO <sub>3</sub> ]	382		
					8.48	10.55	[0.15 KNO <sub>3</sub> ]	370		
					8.13	10.11	[0.1 KNO <sub>3</sub> ]	383		
6. DL-Homocysteine	2.54(2)	8.94(1)	10.48(4)	2.27(2)			[0.3 KNO <sub>3</sub> ]	302		
					8.66	10.55		384		
7. DL-Penicillamine	2.43(8)	7.998(12)	10.591(15)	1.90(2)	7.932(4)	10.658(3)	[0.1 KCl]	381		
				2.44	7.97	10.46	[0.15 KNO <sub>3</sub> ]	385		
				1.94	7.93	10.39		386		
				2.02(2)	7.92(1)	10.75(1)	[0.1 KNO <sub>3</sub> ]	382		
				1.95(1)	7.99(1)	10.56(1)	[0.1 KNO <sub>3</sub> ]	387		
					7.88	10.43		383		
8. N-Acetyl-DL-penicillamine	3.303(8)		10.137(13)	3.18		10.04		388		
				3.69(5)		10.01(10)	[0.1 NaClO <sub>4</sub> ]	232		
9. Glutathione	1.98(2)	3.488(5)	8.754(3)	9.691(9)	2.05	3.40	8.72	9.49	[0.2-0.5]	369
							8.74	9.62	[0.16 KNO <sub>3</sub> ]	389
						3.59	8.75	9.65	[0.15 KNO <sub>3</sub> ]	390
					2.09(2)	3.48(1)	8.67(1)	9.54(1)	[0.1 KNO <sub>3</sub> ]	382
10. Thiocholine		7.883(4)				7.80		[ ~0 ]	391	
						7.7			392	
11. 4-Mercapto-N-methylpiperidine		8.330(6)	10.345(8)		not previously determined					

Table 3.6: Proton dissociation constants<sup>a</sup> of monothiol ligands used for MeHg(II) solution studies.  
(cont.)

Each ligand was titrated with 0.1M KOH and the titration equivalence point treated as a TITRAT parameter together with ligand  $pK_a$ 's and electrode calibration constants,  $pH_{cal}$  and  $K_W^C$  (page 295). The 'proton purity' of the ligands was thereby established for each titration by comparing the refined equivalence point with that calculated from the weighed amount of thiol. The value of  $K_W^C$  was always refined by MINQUAD 81 in titrations involving data above pH 9. For example, titrations used to determine MeHg(II) hydrolysis constants (Figure 3.1) gave  $K_W^C$  values in the range 13.79(2) - 13.96(13) in agreement with values found by TITRAT during evaluations of thiol dissociation constants.

Two stock solutions containing MeHgNO<sub>3</sub> (~0.02M) in dilute HNO<sub>3</sub> were prepared for potentiometric studies. Care was taken to minimise contamination by mercuric ion, often present in commercial MeHg(II) salts. Methylmercury iodide was prepared, free of inorganic mercury, by Erni's method.<sup>319,339</sup> Commercial MeHgI (10.0 g, 30 mmole) was dissolved in 400 mL 2.5M NaOH. The grey, slightly cloudy solution was filtered through slow paper (Whatman No. 5) and acidified with conc. HNO<sub>3</sub> to reprecipitate MeHgI. This precipitate was stirred with excess KI to convert inorganic mercury to soluble iodide complexes (some MeHgI will be converted to MeHgI<sub>2</sub><sup>-</sup> by this process). The purified MeHgI was refiltered on a sinter, washed with water and dried *in vacuo* over P<sub>2</sub>O<sub>5</sub> (yield 9.5 g, 95%).

A portion of this product (20 mmole) was converted to methylmercuric hydroxide by stirring overnight under nitrogen with freshly prepared silver oxide (~20 mmole) in 50 mL freshly boiled water:



The resultant brown mixture was filtered in a nitrogen-flushed glovebox through fast paper (Whatman No. 54) directly into a one litre volumetric

flask containing a slight excess of nitric acid (20 mmole).

After dilution to 1000 mL with freshly deionised water, the  $\text{MeHg}^+/\text{H}^+/\text{NO}_3^-$  solution was nominally 0.02M  $[\text{MeHg}^+]$  and 0.005M  $[\text{H}^+]$ . When required, aliquots were withdrawn under nitrogen. This solution and another prepared similarly, were stored in the dark and the concentrations of  $\text{MeHg(II)}$  and  $\text{H}^+$  determined periodically by the methods described below.

#### Analysis of $\text{H}^+$ content

Unless the  $\text{MeHg(II)}$  content is known, alkimetric titrations of  $\text{MeHg}^+/\text{H}^+/\text{NO}_3^-$  solutions cannot be used to determine the  $\text{H}^+$  content because  $\text{MeHgOH}$  species are readily formed (page 63 ). The equivalence point, which corresponds to the composite  $\text{MeHg}^+ + \text{H}^+$  content, of a titration of 0.005M ( $\text{MeHg}^+/\text{H}^+/\text{NO}_3^-$ ) with 0.1M KOH can be located potentiometrically with a glass/double junction calomel (1M  $\text{KNO}_3$ , sat. KCl) electrode pair. Although the equivalence point is not very sharp (e.g. Figure 3.1) it can be reliably located with a precision of 1-2 parts-per-thousand (ppt), by employing Gran Type-I<sup>393</sup> or Type-II<sup>394</sup> calculation procedures.

In mixtures of 0.005M  $\text{MeHg(II)}$  and 0.01M chloride (or iodide),  $\text{MeHg(II)}$  hydrolysis is suppressed to the extent that  $\text{MeHgOH}$  comprises less than 1% of the total  $\text{MeHg(II)}$  content below pH 7.0 (or 10.3) due to formation of  $\text{MeHgCl}$  (or  $\text{MeHgI}$ ).

To determine only the  $\text{H}^+$  content of  $\text{MeHg}^+/\text{H}^+/\text{NO}_3^-$  solutions, aliquots were titrated with standardised KOH in the presence of 0.1M KI. The resultant strong acid-strong base titrations were monitored potentiometrically and the sharp equivalence points located by Gran methods<sup>395</sup> with a precision limited by the content of weakly acidic impurities in the titration vessel e.g. carbonate, silicates etc.

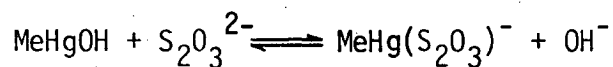
For example, 0.1M KOH titration of 10 mL aliquots of  $\text{MeHg}^+/\text{H}^+/\text{NO}_3^-$

$\text{NO}_3^-$  solution, diluted to 50 mL with freshly deionised water, gave Gran plots which were curved near the equivalence point<sup>395</sup> indicating the presence of  $\sim 0.2 \mu\text{mole}$  of weakly acid impurities. This amount corresponds to a titre of  $<0.002 \text{ mL}$  or  $<4 \text{ ppt}$  of the equivalence point. Similar levels of weakly acidic impurities were found in subsequent titrations of  $\text{MeHg(II)}$ -thiolate systems in either  $0.1\text{M KI}$  or  $\text{KNO}_3$  media. These titrations have equivalence points  $\sim 0.002 \text{ mL}$  higher than expected from consideration of analytical concentrations of the component solutions. The impurities presumably arise from the 50 mL water,  $0.5\text{-}0.8 \text{ g KI}$  or  $\text{KNO}_3$ , titration-cell walls etc. (page 304).

The  $\text{H}^+$  content of the  $0.02\text{M MeHg}^+ / 0.005\text{M H}^+ / \text{NO}_3^-$  solution was monitored periodically by this method over a period of 16 months and showed an increase from  $0.003\text{M}$  to  $0.005\text{M}$  during this time.

#### Analysis for $\text{MeHg(II)}$ content

Various methods have been reported previously for the analysis of methylmercury(II) stock solutions. Libich and Rabenstein<sup>309,331</sup> used an nmr titrimetric method, based on thiosulfate complexation of  $\text{MeHg(II)}$ , to analyse  $0.19\text{M MeHgOH}$  solutions.



The endpoint of this reaction was determined by  $^1\text{H}$  nmr with a standard deviation of  $4\text{-}5 \text{ ppt}$ . These workers confirmed the accuracy of the nmr method by atomic absorption spectrophotometric analysis of mercury, but with somewhat lower precision ( $10 \text{ ppt}$ ). Jawaid<sup>333,342</sup> and co-workers have used an atomic absorption method<sup>396</sup> for analysis of  $\text{MeHg}^+ / \text{H}^+ / \text{NO}_3^-$  solutions. Instrumentation for atomic absorption and nmr methods was unavailable for this study.

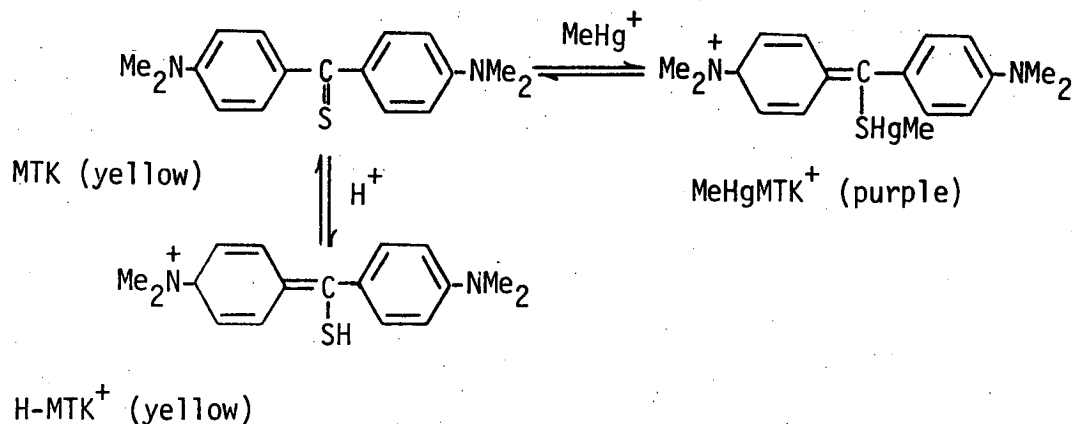
Rabenstein and co-workers have subsequently determined the methyl-



mercury(II) content of stock MeHgOH solutions by chloride titration at pH 2 in 80% EtOH, with potentiometric endpoint detection.<sup>306,360</sup> Preliminary results indicated that the potentiometric chloride method could not be used to analyse the dilute (0.02M)  $\text{MeHg}^+/\text{H}^+/\text{NO}_3^-$  solutions used in this work due to a significant chloride leak from the calomel reference electrode. A double-junction reference electrode was unavailable at that time. Ingman<sup>366,397</sup> has used a spectrophotometric titration based on dithizone to determine MeHg(II) with a precision better than 10 ppt. Simpson and co-workers<sup>324,398</sup> and Hughes<sup>367-8</sup> have used dithizone titrimetric methods, with visual endpoints.

The most convenient method was found to be that described by Erni<sup>319,339</sup> in which MeHg(II) is titrated with thiosulfate in 50% aqueous methanol, using Michler's thioketone\* (MTK) as an indicator.

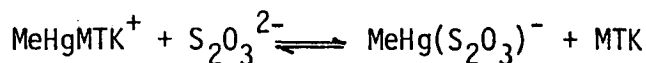
Schwarzenbach and Schellenberg<sup>305</sup> have determined the formation constant,  $\log K = 8.27$ , of the 1:1 MeHg(II) - MTK complex:



and report that protonation of MTK occurs with  $\text{pK}_a \sim 2$ . At pH 4, in the presence of MeHg(II), all the indicator is in the MeHg-MTK<sup>+</sup> form. Titration with thiosulfate displaces MeHg(II), giving a sharp colour change

\* Michler's thioketone, bis[4-(dimethylamino)phenyl]methanethione, was obtained from ICN Pharmaceuticals Inc. as bis(dimethylamino)benzophenone and stored at -20°C.

from purple to yellow at the equivalence point due to the equilibrium:



Ten mL aliquots of  $\text{MeHg}^+/\text{H}^+/\text{NO}_3^-$  solution were diluted with 10 mL 1M pH 4 acetate buffer and 20 mL methanol then titrated in triplicate with 0.2M  $\text{Na}_2\text{S}_2\text{O}_3$  using MTK indicator (3 drops 0.1% MTK in acetone). An alternative but less convenient procedure was also used to determine the  $\text{MeHg}(\text{II})$  content of the  $\text{MeHg}^+/\text{H}^+/\text{NO}_3^-$  solutions. The total  $\text{MeHg}(\text{II}) + \text{H}^+$  content was evaluated by alkalimetric titration with Gran<sup>393-5</sup> equivalence point evaluation and corrected for  $\text{H}^+$  content which had been previously determined in the presence of iodide (page 93).

A comparison of the results from both methods is found in Table 3.7.

	$[\text{MeHg}(\text{II})]_1$		$[\text{MeHg}(\text{II})]_2$
8.1.80	0.015386(19) <sup>b</sup>	11.10.79	0.017330(25) <sup>b</sup>
16.1.80	0.015381(21) <sup>b</sup>	12.10.79	0.017242(25) <sup>b</sup>
27.2.80	0.015364(20) <sup>b</sup>	8.5.80	0.017186(23) <sup>c</sup>
8.5.80	0.015324(27) <sup>c</sup>	18.12.80	0.017201(26) <sup>b</sup>
28.4.81	0.015396(25) <sup>c</sup>		

Table 3.7:  $\text{MeHg}(\text{II})$  content<sup>a</sup> of two  $\text{MeHg}^+/\text{H}^+/\text{NO}_3^-$  stock solutions.

<sup>a</sup> values in parentheses are standard deviations of triplicate determinations.

<sup>b</sup>  $[\text{MeHg}(\text{II})]$  determined alkalimetrically as  $[\text{MeHg}(\text{II}) + \text{H}^+] - [\text{H}^+]$

<sup>c</sup>  $[\text{MeHg}(\text{II})]$  determined by thiosulfate titration with MTK indicator. Thiosulfate titrant (0.2M) was standardised against primary standard  $\text{KIO}_3$ .<sup>399</sup>

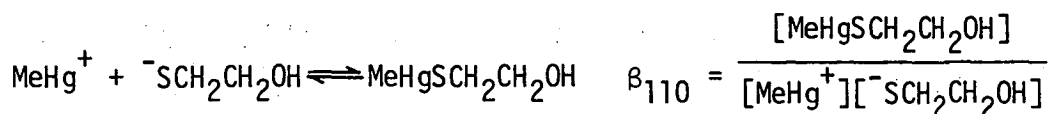
It can be seen from the above table that the  $\text{MeHg}(\text{II})$  content of

both solutions remained unchanged, within experimental uncertainty, over a period of 15 months.

Formation constants of MeHg(II) with the monothiols are discussed below and are recorded in Table 3.8.

(i) 2-Mercaptoethanol was fractionally distilled *in vacuo*, bp 63.3-63.5°/18 mm (lit.<sup>75</sup> 157-8° (dec.)/742 mm) and stored under nitrogen at -20°. Titrations with KOH indicated a proton purity of 99.9(2)%. Values for the proton dissociation constant of mercaptoethanol were identical in 0.1M KNO<sub>3</sub> and 0.1M KI solutions, indicating no iodide-thiolate interaction. The proton dissociation constant is in good agreement with that determined elsewhere (Table 3.6). In the presence of MeHg(II) and 0.1M KI, four sets of titration data were fitted satisfactorily with MINQUAD 81 by considering the complex MeHgSCH<sub>2</sub>CH<sub>2</sub>OH as the only MeHg(II)-thiolate species present. No evidence of ternary MeHg(II)-iodide-thiolate species was indicated. In the presence of 0.1M KI, species such as (MeHg)<sub>2</sub><sup>+</sup>SCH<sub>2</sub>CH<sub>2</sub>OH can be neglected.

The value found for log β<sub>110</sub> [16.135(4), Table 3.8], agrees with that found by Schwarzenbach and Schellenberg (16.12)<sup>305</sup> but is in disagreement with the value found by Hojo *et al.*<sup>363</sup>



Calculated and experimental titration curves are shown in Figure 3.6, and the species distribution in the presence of 0.1M KI, in Figure 3.7.

Because Schwarzenbach and Schellenberg<sup>305</sup> have reported the existence of a complex MeHg(SCH<sub>2</sub>CH<sub>2</sub>OH)<sub>2</sub><sup>-</sup>, a titration of MeHg(II) and a ten-fold excess of mercaptoethanol in the presence of iodide was performed. Treatment of these data by MINQUAD 81, using fixed values of the equilibrium constants for MeHg(II) hydrolysis, ligand protonation and

Thiol ligand	Equilibrium constants <sup>a, b</sup> of MeHg(II) complexes				
	equilibrium constant	this work			Rabenstein <i>et al.</i>
		with iodide competition	with no competing ligand		
1. Mercaptoacetic acid	log $\beta_{110}$ $\beta_{111}$	16.932(12) 20.689(11)	3.757(6) 3.730(2), 3.78(2) <sup>c</sup>		16.92(1) <sup>g</sup> 20.57(2) } 3.65(1)
2. O-Methylmercapto- acetic acid	log $\beta_{110}$	14.98(2)			
3. 2-Mercaptosuccinic acid	log $\beta_{110}$ $\beta_{111}$ $\beta_{112}$	17.142(7) 21.983(5) 25.110(11)	4.841(2) 3.127(7)		17.31(6) <sup>g</sup> 22.01(8) } 4.70(2) 25.39(11) } 3.38(3)
4. 2-Mercaptoethanol	log $\beta_{110}$	16.135(4)	16.12 <sup>h</sup>		
5. L-cysteine	log $\beta_{110}$ $\beta_{111}$ $\beta_{112}$	16.464(14) 25.476(9) rejected	9.012(6) 8.936(6) 25.40(1) } 2.66(2) 11.60(2) 28.06(3)		16.67(1) <sup>g</sup> 25.32(3) } 8.65(2) 27.61(11) } 2.29(8)
	$\beta_{210}$ $\beta_{211}$ $\beta_{212}$		25.26(2) 8.800(7) = log $K_{2f}$ 29.69(3) 13.221(13) 32.13(13) 15.67(12) <sup>d</sup>		4.42(2) 2.45(10) <sup>d</sup>
	$\beta_{310}$		29.02(3) 12.56(2) <sup>d</sup> = log $K_{3f}$		

Table 3.8: Methylmercury(II)-monothiolate equilibrium constants refined by MINIQAD81.

6. DL-Homocysteine	log $\beta_{110}$	<i>e</i>			16.45(1) <sup>g</sup>	8.97(2)
	$\beta_{111}$				25.42(3)	2.11(6)
	$\beta_{112}$				27.53(9)	
7. DL-Penicillamine	log $\beta_{110}$	16.596(15)	} 8.743(7)		16.94(2) <sup>g</sup>	7.99(1)
	$\beta_{110}$	25.339(10)			24.93(3)	2.18(5)
	$\beta_{112}$	rejected			27.11(8)	
8. N-Acetyl-DL-Penicillamine	log $\beta_{110}$	16.505(6)	} 3.29(3)			
	$\beta_{111}$	19.80(4)				
9. Glutathione	log $\beta_{110}$	15.994(15)	} 9.263(7)			9.11(2) <sup>i</sup>
	$\beta_{111}$	25.257(9)				3.41(12)
	$\beta_{112}$	28.68(2)				3.27(5)
	$\beta_{113}$	rejected				
10. Thiocholine <sup>f</sup>	log $\beta_{110}$	14.603(12)				
11. 4-Mercapto-N-methyl piperidine	log $\beta_{110}$	16.06(3)	} 9.268(7)			
	$\beta_{111}$	25.33(3)				

Table 3.8: Methylmercury(II)-monothiolate equilibrium constants refined by MINIQAD81.

(cont.)

<sup>a</sup>the equilibria corresponding to the macroscopic constants are described in the text. Constants which have been derived (e.g. pK<sub>a</sub>'s) rather than measured, are italicised.

<sup>b</sup> values in parentheses are estimated standard deviations of the last digit from the least-squares refinement. Standard deviations of constants derived from two overall constants were calculated using correlation coefficients from the least-squares refinement (footnote, page 329).

<sup>c</sup> obtained by TITRAT treatment of titration data from the solid MeHg(II) complex.

<sup>d</sup> these constants are highly correlated and should be regarded as tentative.

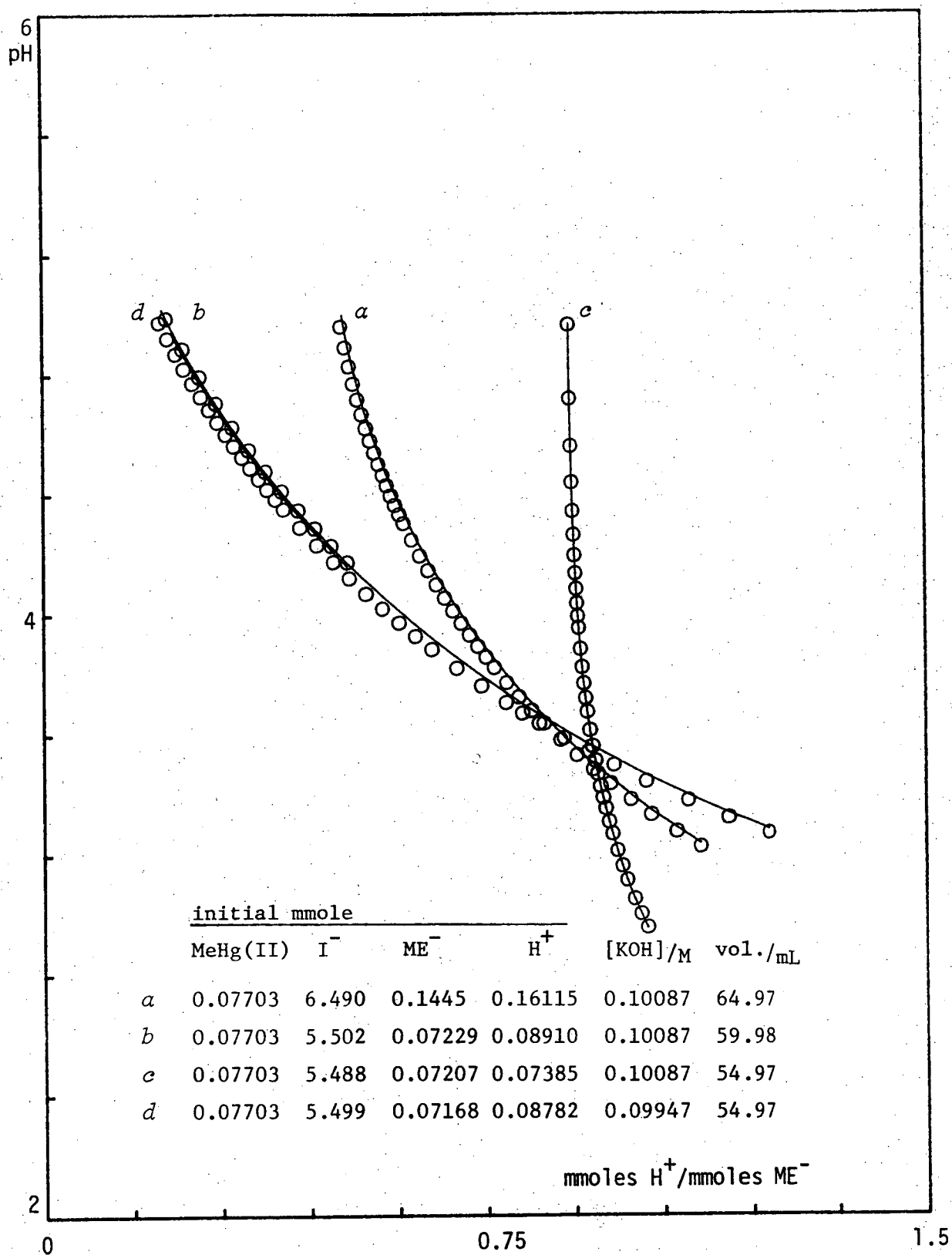
<sup>e</sup> not studied because of low ligand purity.

<sup>f</sup> as the perchlorate.

<sup>g</sup> ref. 302, 25° and 0.3M ionic strength. Mixed constants involving protons have been converted to concentration constants using  $-\log \gamma_{H^+} = 0.15$  from the Davies equation.

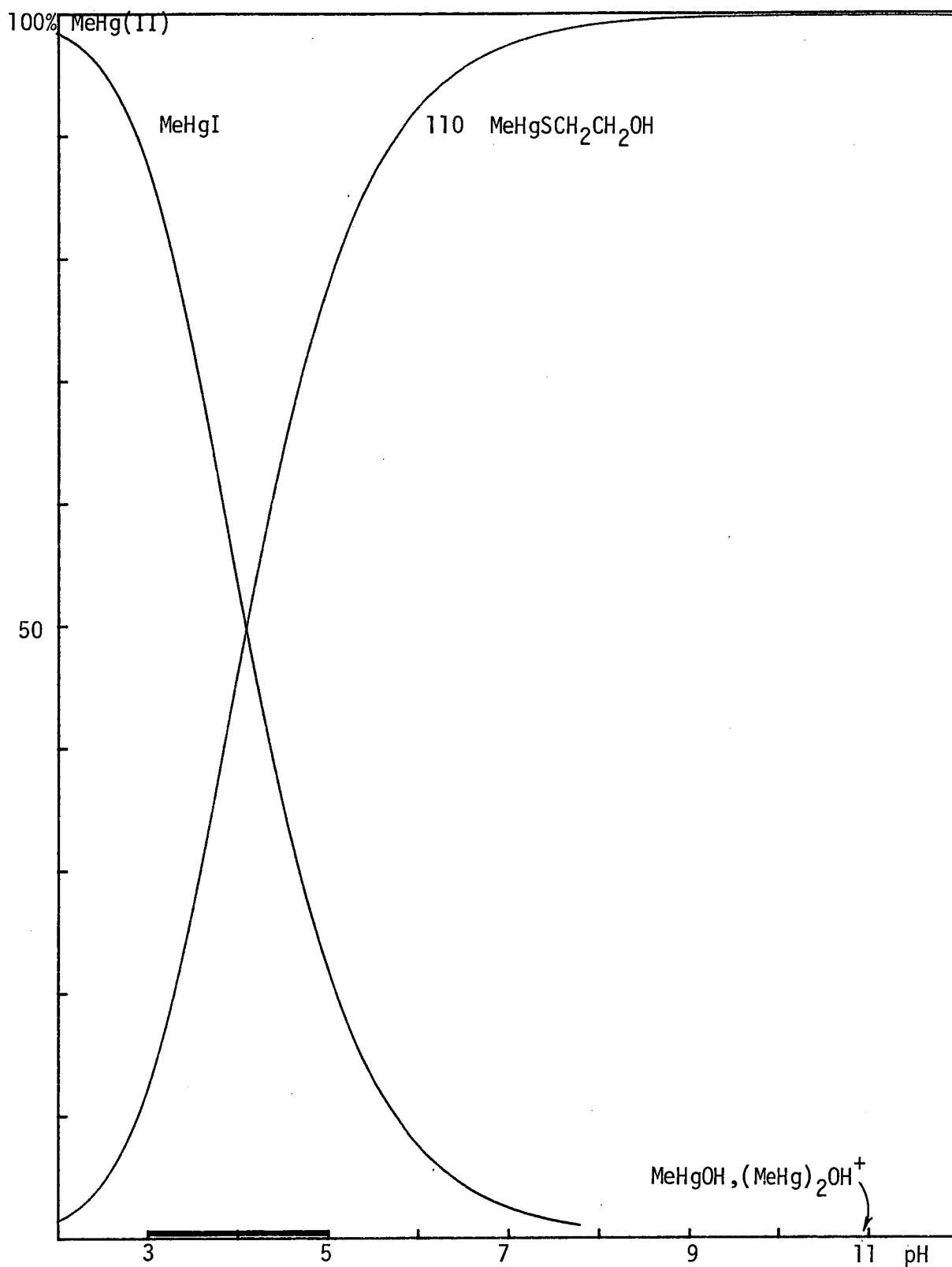
<sup>h</sup> ref. 305, 20° and 0.1M ionic strength.

<sup>i</sup> ref. 309, 25° and 0.3-0.4M ionic strength.



**Figure 3.6:** Methylmercury(II)-Mercaptoethanol (MEH) titration data with iodide competition.

The fitted curves were calculated by COMIXH, using  $\log \beta(\text{MeHgI}) = 8.500$  and the equilibrium constants in Tables 3.6 and 3.8.



**Figure 3.7:** Species distribution calculated by COMIX for 0.0014M MeHg(II) and 0.0014M 2-Mercaptoethanol in 0.1M KI, using the equilibrium constants in Tables 3.6 and 3.8.

The heavy line indicates the pH-range of MINIQUAD81 data.

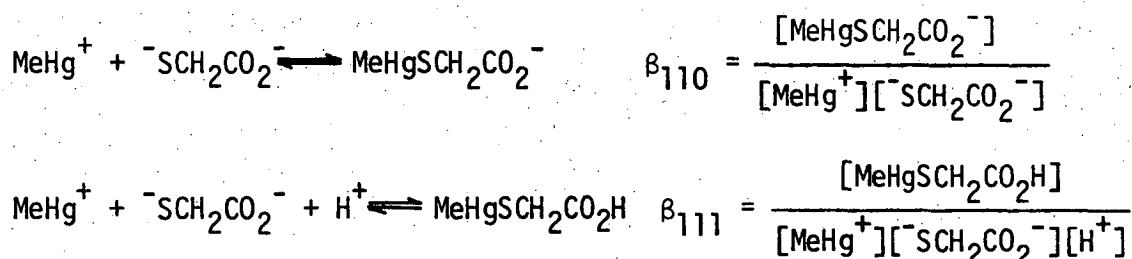


MeHgSCH<sub>2</sub>CH<sub>2</sub>OH formation, could not refine a formation constant for the 1:2 complex. Similar 1:2 formation constants were not sought for the other thiol ligands described below.

(ii) Mercaptoacetic acid was fractionally distilled under reduced nitrogen pressure following azeotropic removal of water with benzene, <sup>400</sup> bp. 58.5-60.5°/0.5 mm (lit.<sup>401</sup> 95-6°/8 mm). The thiol was stored under nitrogen as a solid at -20°. Titrations with KOH indicated a proton purity of 98.0(5)%.

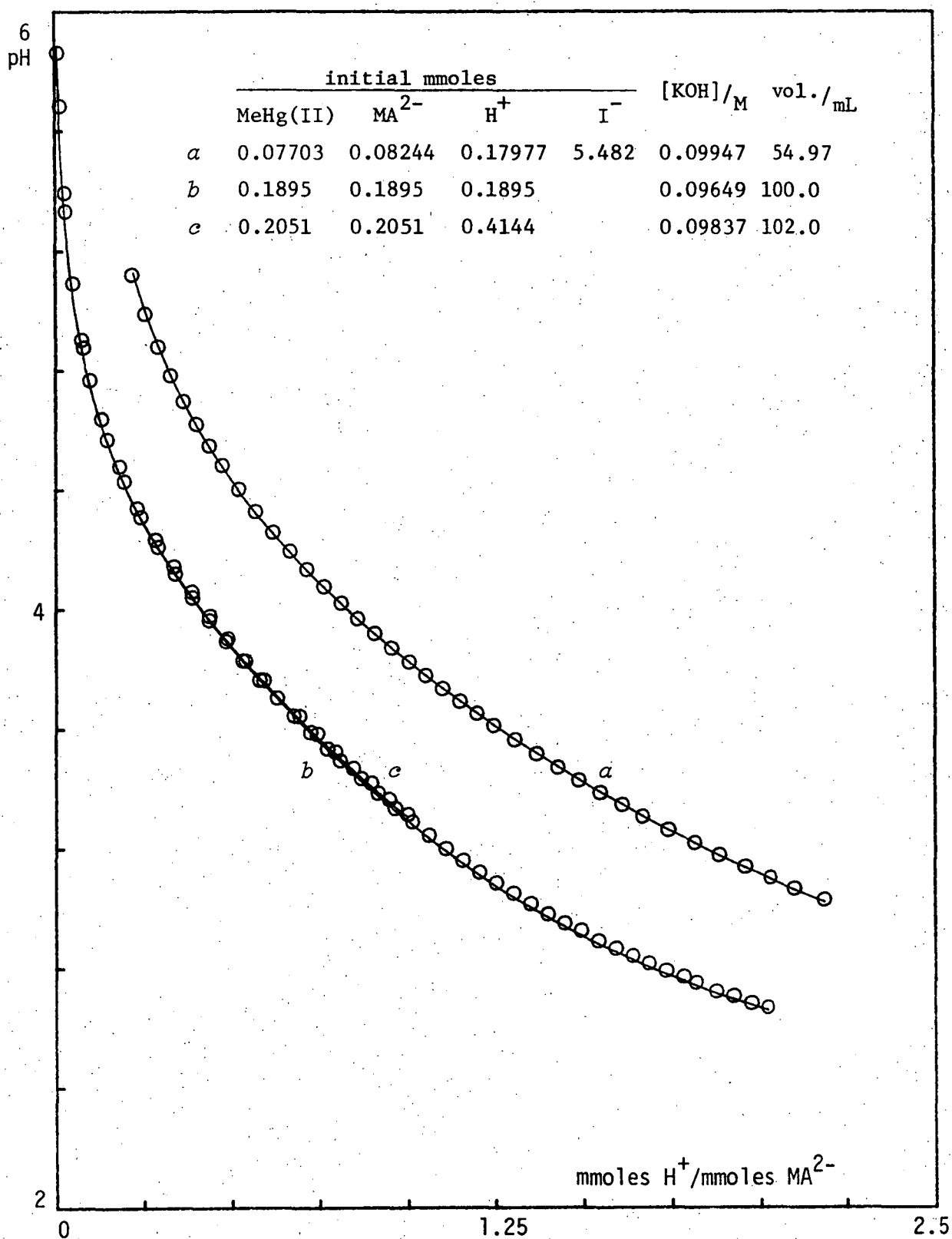
Values for the proton dissociation constants of the ligand are shown in Table 3.6 and fall within the range of previously reported values.

In the presence of 0.1M KI and MeHg(II), KOH titrations could be fitted satisfactorily by consideration of the species MeHgSCH<sub>2</sub>CO<sub>2</sub><sup>-</sup> and MeHgSCH<sub>2</sub>CO<sub>2</sub>H with coexist with MeHgI below pH 5.



The constant  $\beta_{110}$  agrees with that found by Reid and Rabenstein in 0.3M KNO<sub>3</sub>.<sup>302</sup> Their value for the proton dissociation constant,  $\text{pK}'_{\text{a}}[3.65(1)]$  of the MeHg(II) complex is close to that found here as  $\log \beta_{111} - \log \beta_{110} [3.76(1)]$ .<sup>†</sup> In the absence of iodide, the solid complex (page 38) titrates as a monoprotic acid with  $\text{pK}'_{\text{a}} 3.74(1)$  in good agreement with the above values. Calculated and experimental titration curves are shown in Figure 3.8 and the species distribution in the presence of 0.1M KI, in Figure 3.9.

<sup>†</sup> Mixed constants reported by these workers have been converted to concentration constants in 0.3M ionic strength, using  $\log \gamma_{\text{H}^+} = 0.15$  from the Davies equation.



**Figure 3.8:** Methylmercury(II)-Mercaptoacetic acid (MAH<sub>2</sub>) titration data. *a* with iodide competition; *b, c* with no competing ligand.

The fitted curves were calculated by COMIXH, using  $\log \beta(\text{MeHgI}) = 8.500$  and equilibrium constants in Tables 3.6 and 3.8.

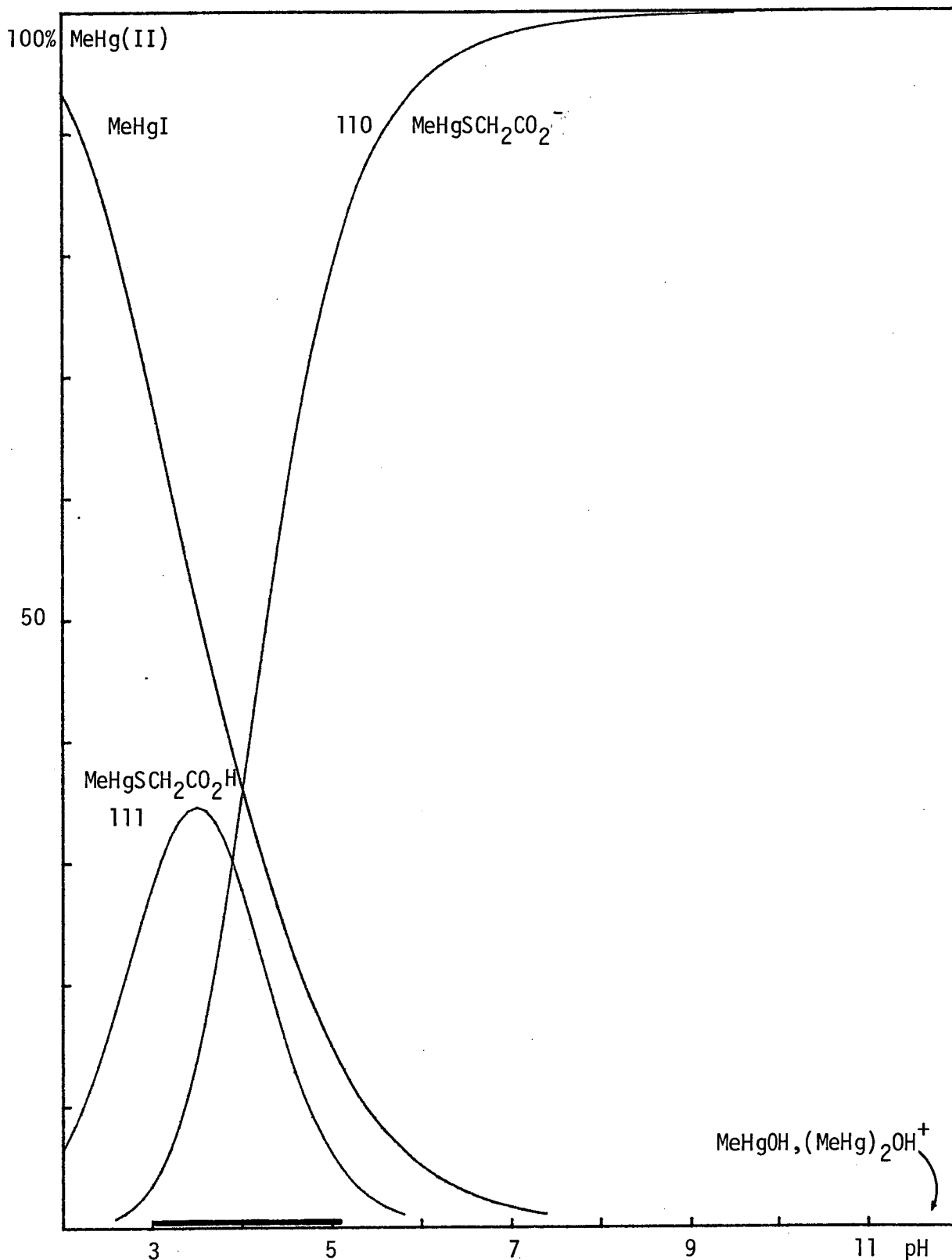
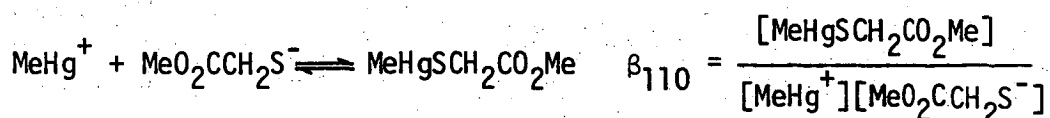


Figure 3.9: Species distribution calculated by COMIX for 0.0014M MeHg(II) and 0.0014M Mercaptoacetic acid in 0.1M KI, using the equilibrium constants in Tables 3.6 and 3.8.

The heavy line indicates the pH-range of MINIQAD81 data.

(iii) Mercaptoacetic acid, O-methyl ester was prepared by acid catalysed O-alkylation of mercaptoacetic acid in refluxing methanol. Fractional vacuum distillation gave a colourless oil bp. 46-7.5°/4 mm (lit.<sup>378</sup> 42-3°/10 mm). Data from alkalimetric titrations of this thiol could not be fitted adequately by TITRAT without assuming the presence of a moderately acidic impurity, presumably mercaptoacetic acid. Treatment by TITRAT of this ligand as a mixture of mercaptoacetic acid and the O-methyl ester gave the relatively imprecise value of acid dissociation constant for the ester, shown in Table 3.6. The concentrations of both compounds were treated as parameters with fixed values for mercaptoacetic acid dissociation constants, indicating ~1.4% of this impurity. An approximate value for the previously unreported MeHg(II) formation constant of the O-methyl ester was obtained by titration of the (impure) ligand with MeHg(II) in 0.1M KI and is shown in Table 3.8. The MeHg(II) complexes of the mercaptoacetic acid impurity were included in the MINQUAD 81 treatment, using values for their formation constants recorded previously (page 98)



(iv) Mercaptosuccinic acid was purified by extraction of an alkaline aqueous solution with ether, followed by acidification of the aqueous layer.<sup>400</sup> The white crystalline thiol was dried over P<sub>2</sub>O<sub>5</sub> under nitrogen, mp. 147-50° (lit. 153-4°,<sup>400</sup> 149-50°<sup>75</sup>). Titrations with KOH gave a proton purity of 98.5(4)%. Values for the two carboxylate and thiol proton dissociation constants obtained by TITRAT are shown in Table 3.6, and are in agreement with previously published literature values. In the presence of MeHg(II) and 0.1M KI the titrations could be fitted satisfactorily with the three equilibria shown below:

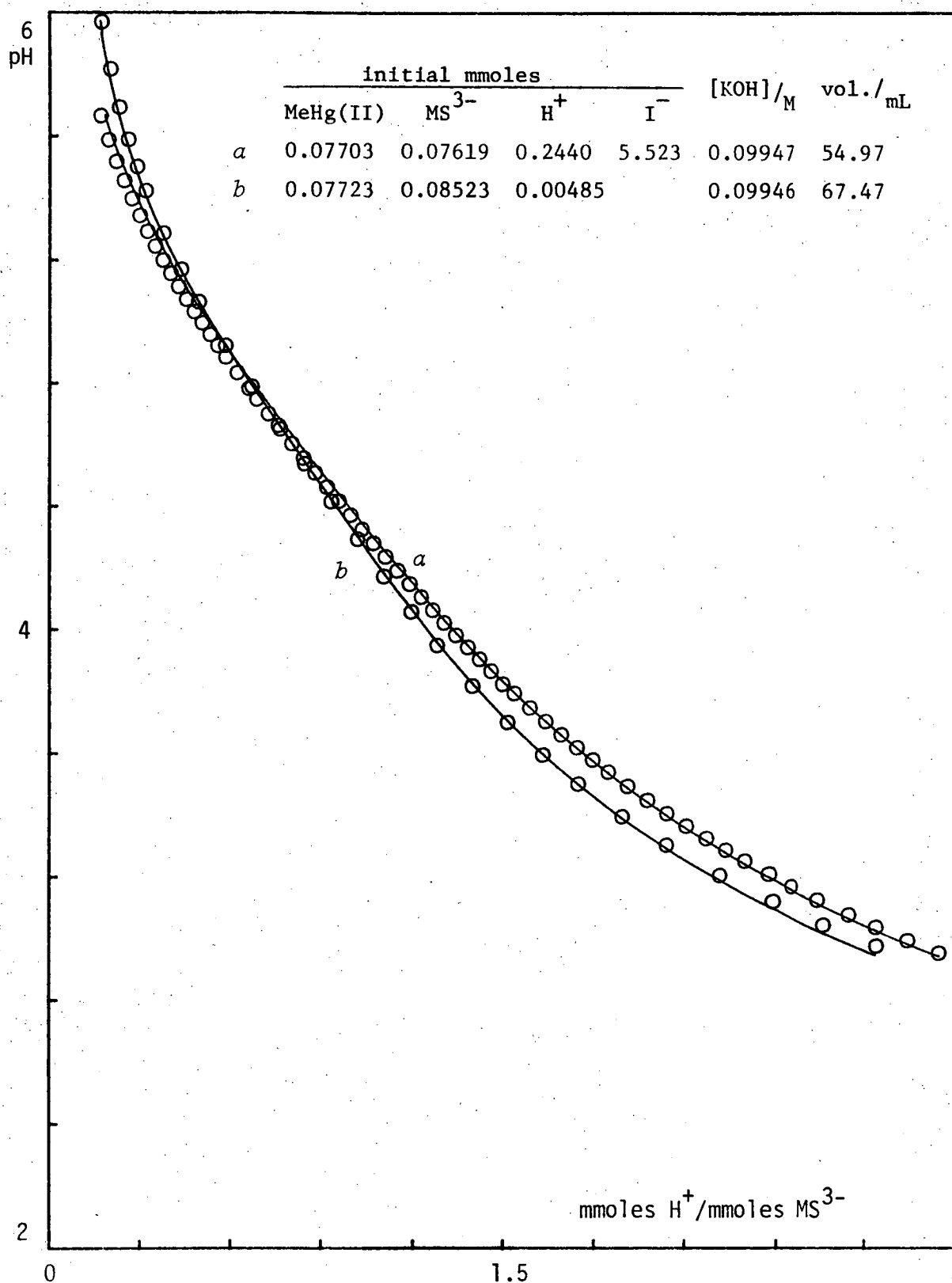
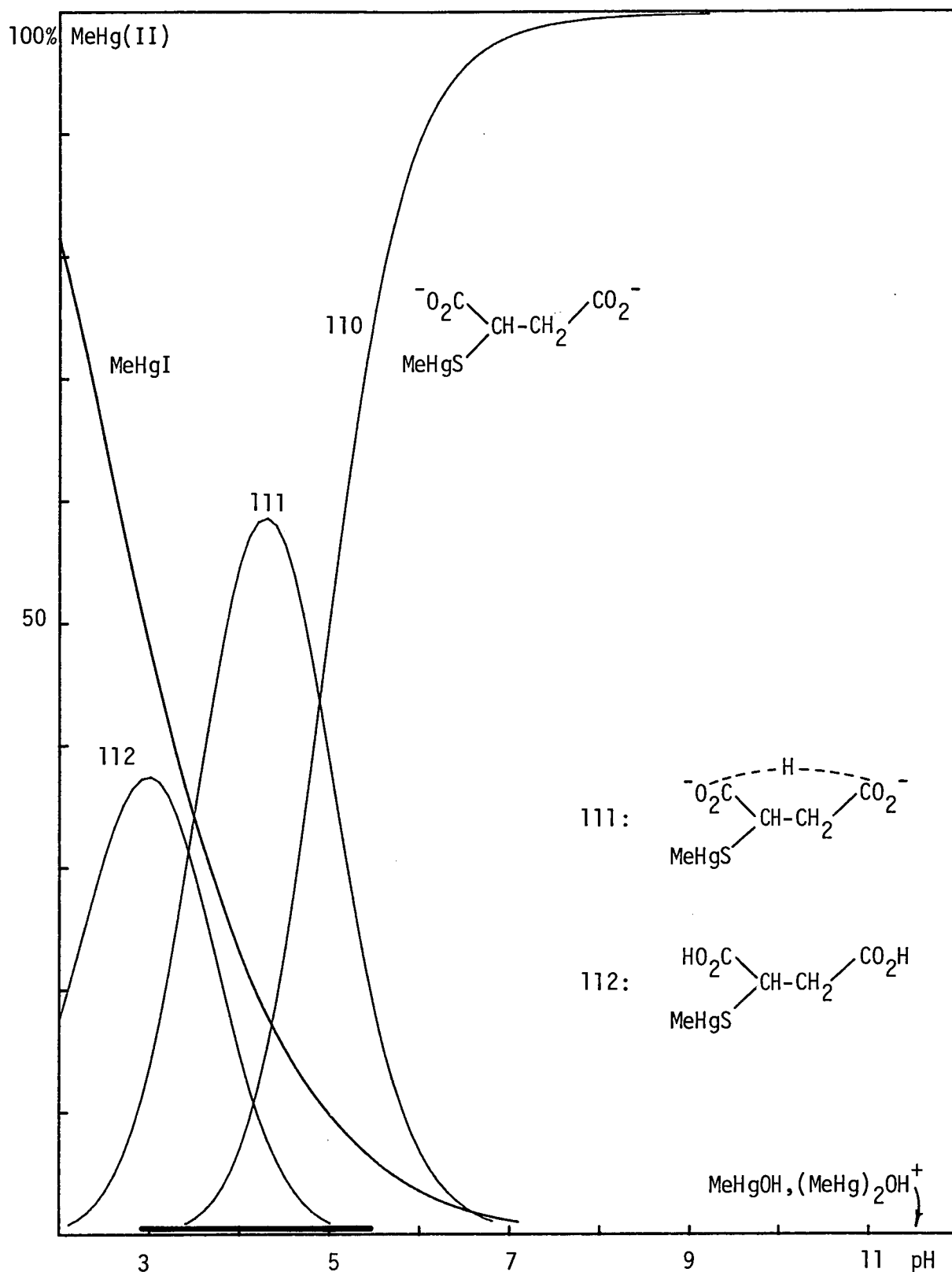


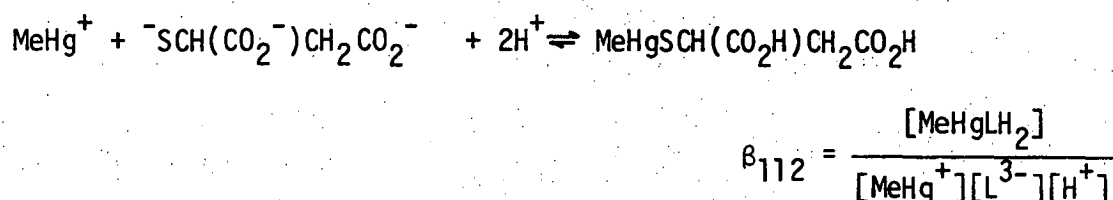
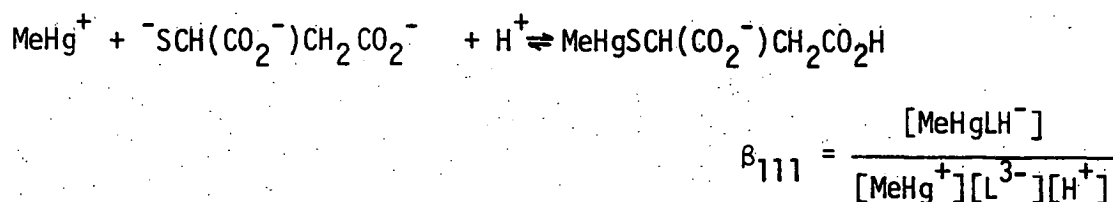
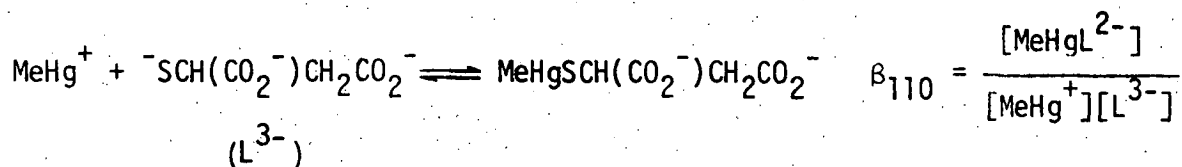
Figure 3.10: Methylmercury(II)-2-Mercaptosuccinic acid ( $MSH_3$ ) titration data. *a* with iodide competition; *b* with no competing ligand.

The fitted curves were calculated by COMIXH, using  $\log \beta(\text{MeHgI}) = 8.500$  and the equilibrium constants in Tables 3.6 and 3.8.

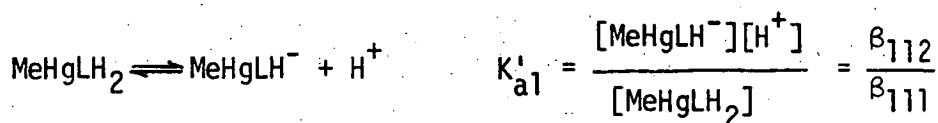


**Figure 3.11:** Species distribution calculated by COMIX for 0.0014M MeHg(II) and 0.0014M 2-Mercaptosuccinic acid in 0.1M KI, using the equilibrium constants shown in Tables 3.6 and 3.8.

The heavy line indicates the pH-range of MINIQVAD81 data.

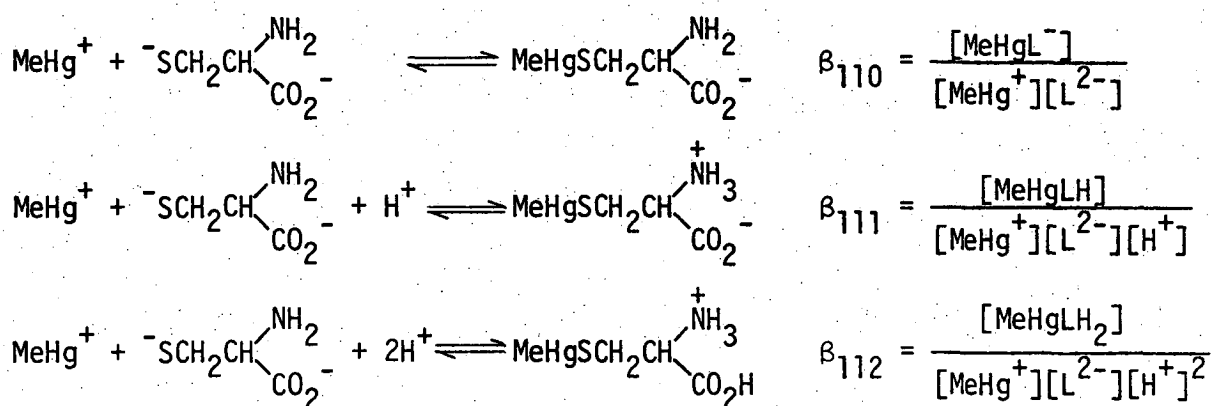


Calculated and experimental titration curves are shown in Figure 3.10 and the species distribution in Figure 3.11. Values of  $\beta_{110}$ ,  $\beta_{111}$  and  $\beta_{112}$  were highly correlated (page 328). The overall constants yielded values of the proton dissociation constants  $\text{pK}'_{a1}$  [3.13(2)] and  $\text{pK}'_{a2}$  [4.84(1)] for the carboxylate groups of the MeHg(II)-thiolate complex which are close to those found by Reid and Rabenstein in 0.3M  $\text{KNO}_3$ ,  $\text{pK}'_{a1}$  [3.38(3)] and  $\text{pK}'_{a2}$  [4.70(2)].<sup>302</sup>



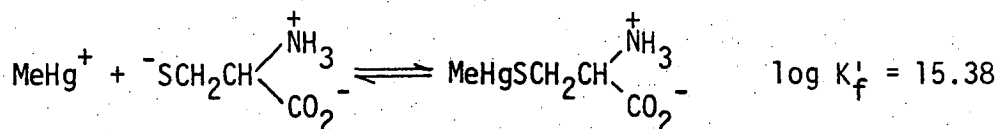
(v) L-cysteine was used as received and stored over  $\text{P}_2\text{O}_5$  under nitrogen, mp. 205 (dec.) [lit.<sup>402</sup> 220 (dec)]. Titrations with KOH, after addition of  $\text{HNO}_3$  to fully protonate the zwitterion, gave a proton purity of 99.0(6)%. Macroscopic acid dissociation constants are shown in Table 3.6, and are in agreement with previously published values. In the

presence of MeHg(II) and 0.1M KI, the titration curve,  $\alpha$ , shown in Figure 12, was fitted satisfactorily ( $U = 8 \times 10^{-10}$ ) by assuming the presence of the complex species shown below. The  $pK'_a$  value of the mono-protonated species [9.01(1)] was obtained from the appropriate overall formation constants. The constant,  $\beta_{112}$ , could not be refined precisely from these data, and could be evaluated more readily from data in the absence of iodide, described later.



The equilibrium constants are recorded in Table 3.8.

Expected sulfhydryl binding is supported by the crystal structure of the 1:1 complex (page 34 ).<sup>236</sup> Reid and Rabenstein<sup>302</sup> report microscopic constants in 0.3M KNO<sub>3</sub> for the equilibrium with deprotonated ligand ( $\log K_f = 16.69$  in their terminology, in close agreement with  $\beta_{110}$  above), and with amino-protonated ligand:



Addition of cationic MeHg<sup>+</sup> to the sulfhydryl group of the amino-protonated ligand is seen to be less favorable than to the deprotonated form. Microscopic proton dissociation constants of the ligand show a similar trend for addition of a proton (instead of MeHg<sup>+</sup>) to the sulfhydryl site.



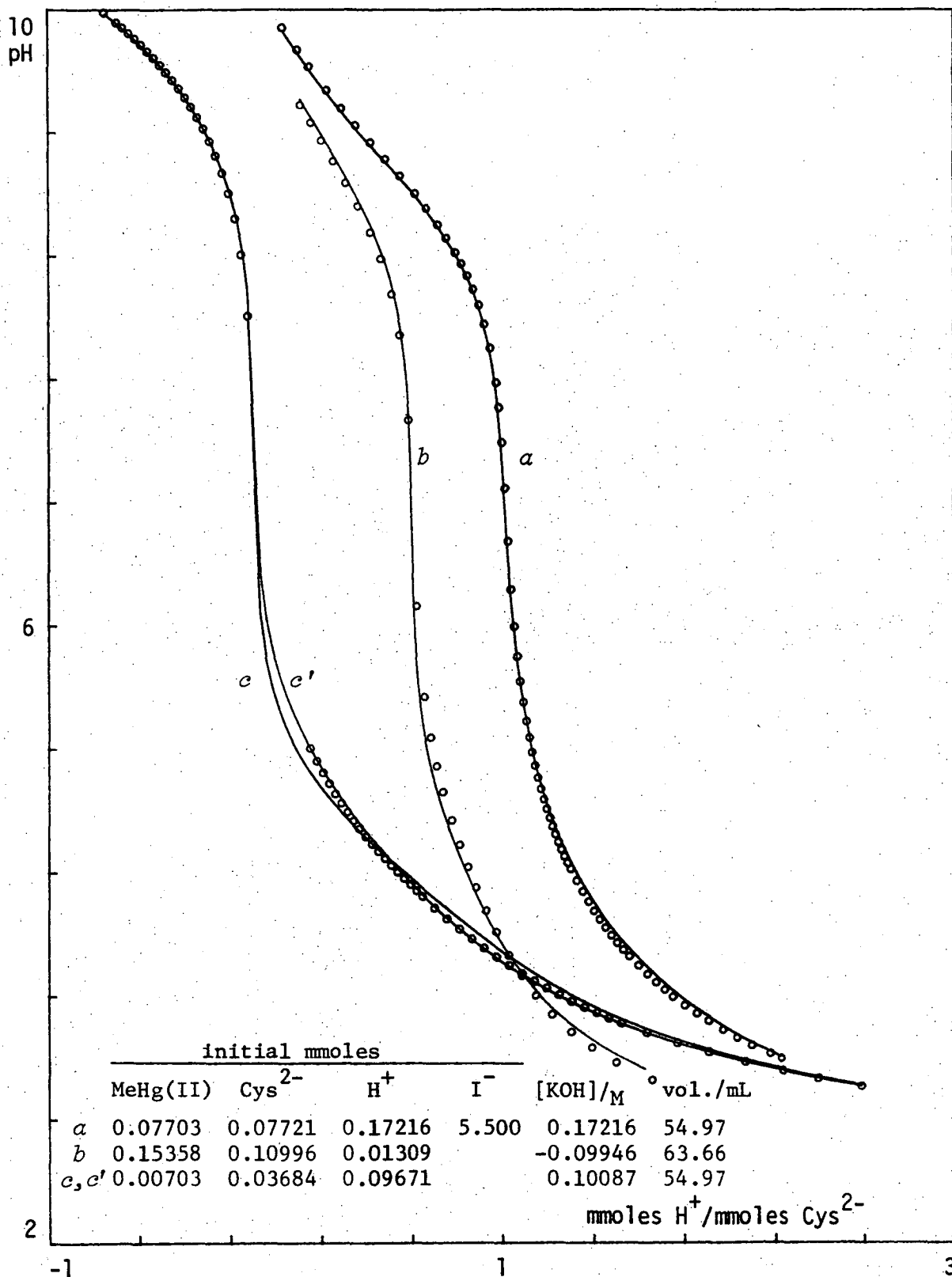


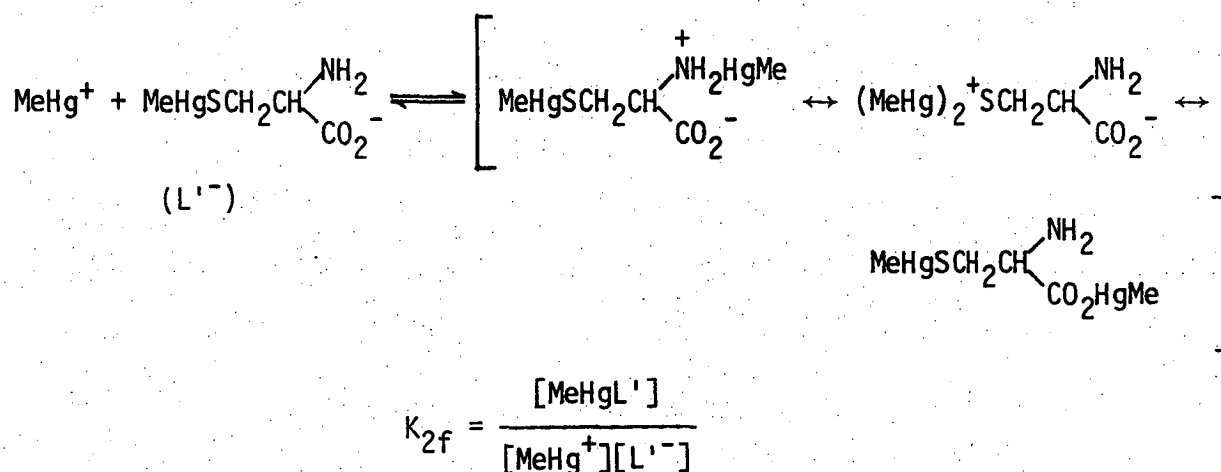
Figure 3.12: Methylmercury(II)-L-cysteine (CysH<sub>2</sub>) titration data.

The fitted curves *a, b, c* were calculated by COMIXH using  $\log \beta(\text{MeHgI}) = 8.500$  and the equilibrium constants in Tables 3.6 and 3.8. The 310 species was neglected. Curve *c* includes the 310 species.

Rabenstein and Fairhurst have nmr evidence that the MeHg(II)-complexed sulfhydryl group of the 1:1 glutathione and penicillamine complexes, may be protonated below pH2.<sup>360</sup> This study did not involve such acidic conditions and this type of species was therefore not considered for cysteine of the other mercaptoamino acids described subsequently.

The equilibrium distribution diagram for the 1:1 system in the presence of iodide is shown in Figure 3.13a.

In addition to the 1:1 MeHg(II)-cysteine complex, a 2:1 complex of closely related DL-penicillamine has been isolated by Carty *et al.* which has been shown to have deprotonated-amino-bound MeHg(II) as well as the expected MeHg(II)-sulfhydryl binding (page 36 ).<sup>248</sup> The 2:1 MeHg(II)=cysteine system has been investigated here by the titration of cysteine solutions containing more than one equivalent of MeHg(II) in the *absence* of iodide. Under these conditions, the sulfhydryl group is always coordinated, therefore the equilibria were treated by MINIQAD81 assuming a 'ligand' of the form  $\text{MeHgSCH}_2\text{CH}(\text{NH}_2)\text{CO}_2^-$ , which may form complexes with MeHg(II) as follows:



The second stepwise constant,  $\log K_{2f}$ , for formation of the 2:1 complex was found to be 8.81(2). This is similar to that for amine complexes

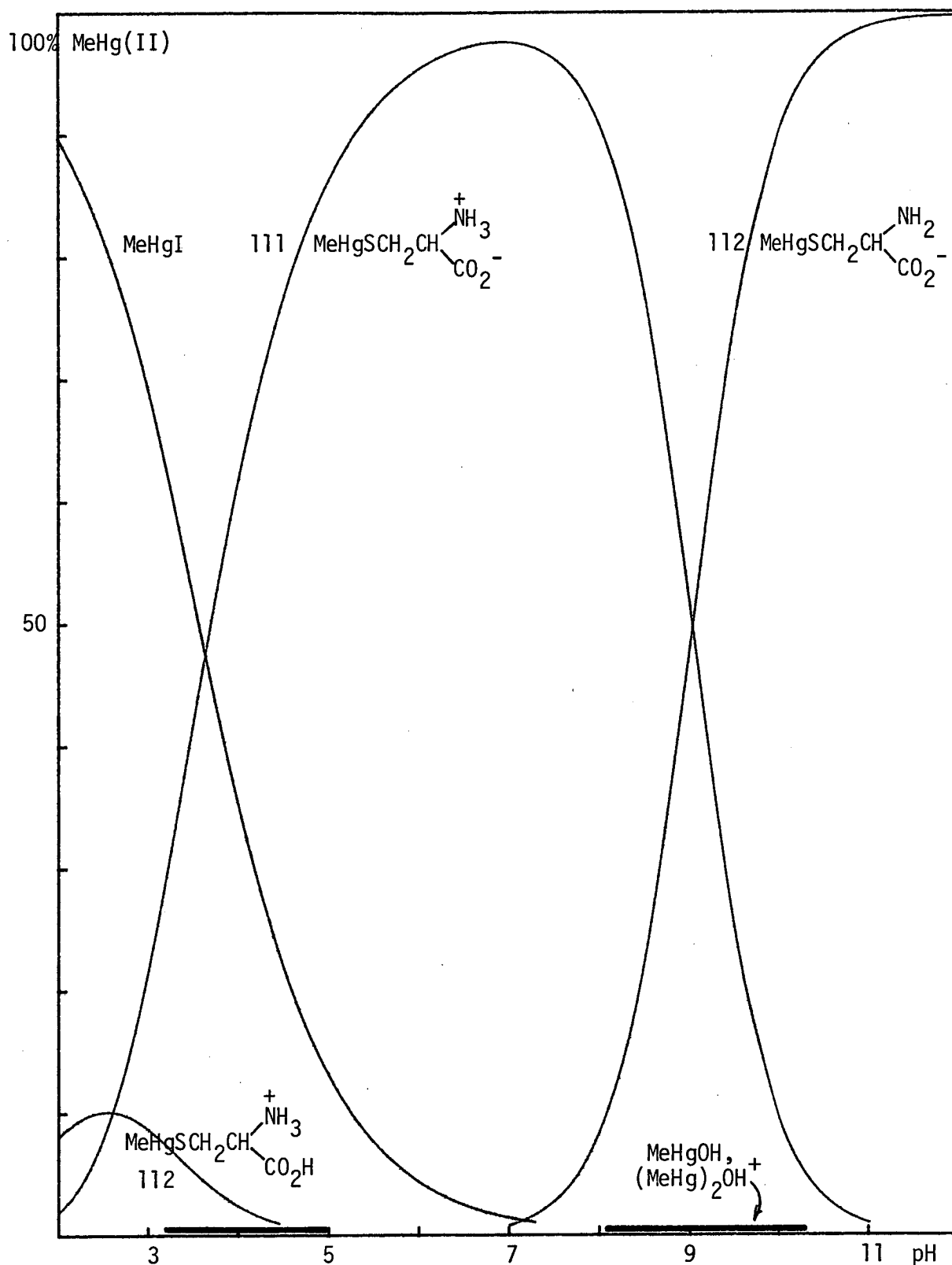
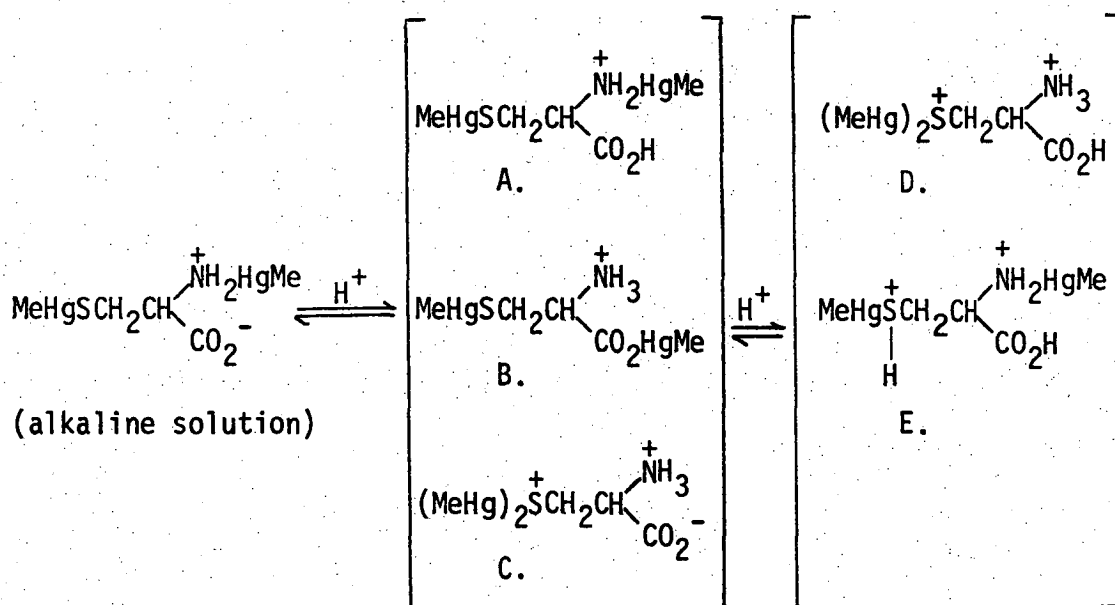


Figure 3.13a: Species distribution calculated by COMIX for 0.0014M  $\text{MeHg(II)}$  and 0.0014M L-cysteine in 0.1M KI, using the equilibrium constants in Tables 3.6 and 3.8.

The heavy line indicates the pH-range of MINIQUAD81 data.

but much higher than that for carboxylate and thioether complexes shown in Table 3.2, and is consistent with amino coordination such as that found in the 2:1 solid-state complex of penicillamine.<sup>248</sup>

Successive protonation of the 2:1 complex could occur at either the uncomplexed carboxylate group (A), or at the MeHg-complexed amino group with a concomitant shift of MeHg(II) to the carboxylate group (B).

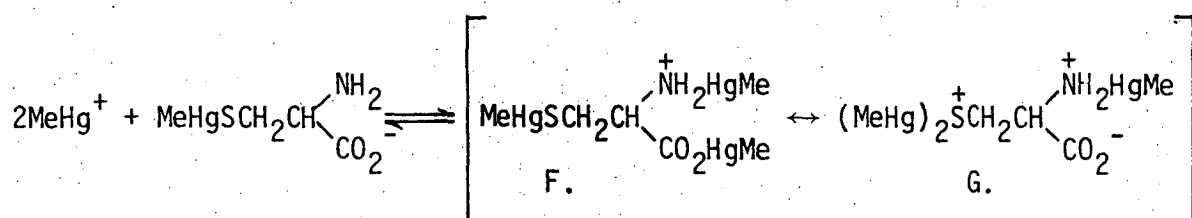


A second MeHg(II) group has been shown to bind to the MeHg-complexed group of glutathione in the range  $0 < \text{pH} < 4$ , but to the amino group at higher pH,<sup>360</sup> so conceivably, a third species (c) is also possible. Binding of two MeHg(II) groups in solution to the sulfhydryl site of N-acetyl-L-cysteine has also been described,<sup>403</sup> whereas a crystal structure of the 2:1 penicillamine complex isolated from *alkaline* solution, shows coordination to both amino and sulfhydryl sites.<sup>248</sup> By analogy, the species A (with carboxylate  $\text{pK}_a$  equal to  $\log \beta_{211} - \log \beta_{210}$  [4.42(2)]) is probably formed with cysteine.

The experimental data obtained in the absence of iodide are shown in

Figure 3.12. The fitted curves shown in Figure 3.12 were calculated using fixed values of the formation constants for unprotonated and mono-protonated 1:1 species (page 109) and 2:1 species, together with refined values shown in Table 3.8 for the diprotonated 1:1 and 2:1 (D or E) species. The distribution diagram for 0.002M MeHg(II) and 0.001M L-cysteine is shown in Figure 3.13b.

The titration curves obtained in absence of iodide cannot be fitted well ( $U = 7 \times 10^{-9}$  for the two sets of data) in the range  $4 < \text{pH} < 5$ , using the abovementioned set of constants. The MeHg(II):cysteine ratios used in these titrations were 1.04 and 2.10. Refinement of the formation constant of 3:1 species significantly improved the fit to these data, which was most marked ( $U = 5.5 \times 10^{-9} \rightarrow 4 \times 10^{-11}$ ) for the titration with  $\text{MeHg(II)} = \text{cysteine} > 2$ .



$$K_{3f} = \frac{[(\text{MeHg})_2\text{L}^+]}{[\text{MeHg}^+]^2[\text{L}^+]}$$

However, the 3:1 formation constant shown in Table 3.8 was very highly correlated with that for the twice protonated 2:1 species and both of these constants should be regarded as tentative. The magnitude of the third stepwise constant for addition of  $\text{MeHg}^+$  [3.76(1)] may be consistent with weak carboxylate binding near to the cationic complexed-amino group (F) or to a thioether type of binding (G), similar to that found with methionine (Table 3.2) and glutathione at low pH.<sup>360</sup> Under these ~2:1

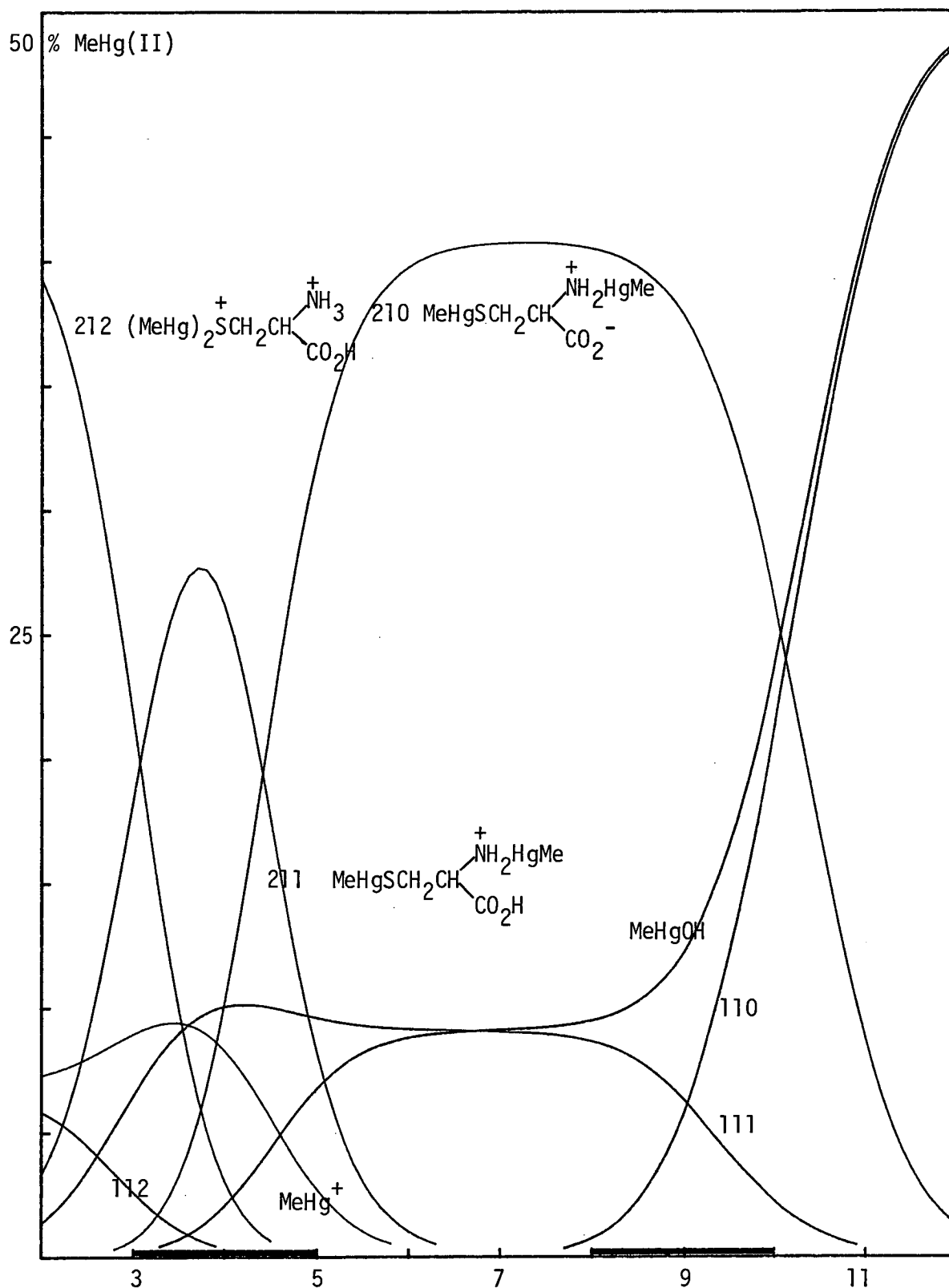


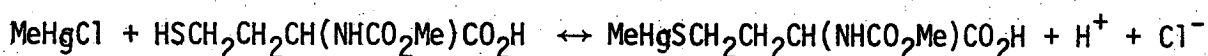
Figure 3.13b: Species distribution calculated by COMIX for 0.002M MeHg(II) and 0.001M L-cysteine, using the equilibrium constants in Tables 3.6 and 3.8.

The heavy line indicates the pH range of MINIQUAD 81 data.

The 1:1 species (red) are depicted on Figure 3.12. Note that MeHgOH (blue) and free MeHg<sup>+</sup> (black) account for significant proportions of MeHg(II).

conditions, only a small proportion of the 3:1 species is formed in the range  $4 < \text{pH} < 6$ , at the expense of the 2:1 species.

In their nmr study of MeHg(II) complexation with N-Acetyl-L-homocysteine, Simpson *et al.*<sup>403</sup> do not preclude the formation of  $(\text{MeHg})_3\overset{2+}{\text{S}}\text{CH}_2\text{CH}_2\text{CH}(\text{NHCO}_2\text{CMe})\text{CO}_2\text{H}$  at high MeHg(II): thiol ratios. Such a species is unlikely because of the high positive charge on the sulfur donor. In that study, the nmr solutions would have been appreciably acidic ( $\text{pH} < 4$ ) due to the release of the sulfhydryl proton upon MeHg(II) coordination:



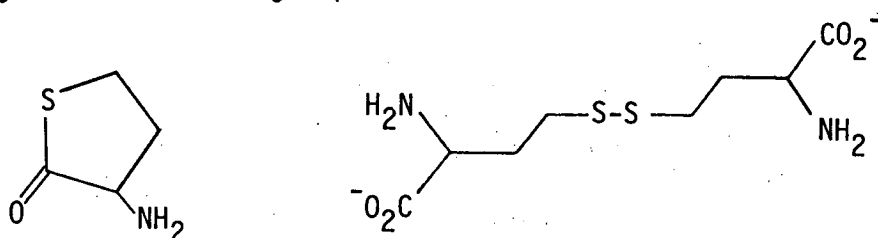
Formation of a 2:1 species with protonated carboxylate is likely to be favored over that of the 3:1 species under these conditions. In this work however, the amino group of cysteine is available for coordination to form the 3:1 species, F and G above, in which the doubly-positive charge is delocalised by analogy with the 2:1 protonated species, D and E.

The refinement problems associated with 2:1 and 3:1 species (high correlation, large numbers of refinable constants, etc.) were avoided with the thiols described below by the use of MeHg(II) : RSH ratios close to unity.

(vi) DL-homocysteine was used as received but stored over  $\text{P}_2\text{O}_5$  under nitrogen, mp. 225 (dec.) (lit.<sup>400</sup> 232-3°). Titrations with KOH, after addition of  $\text{HNO}_3$  to fully protonate the zwitterion, were evaluated with

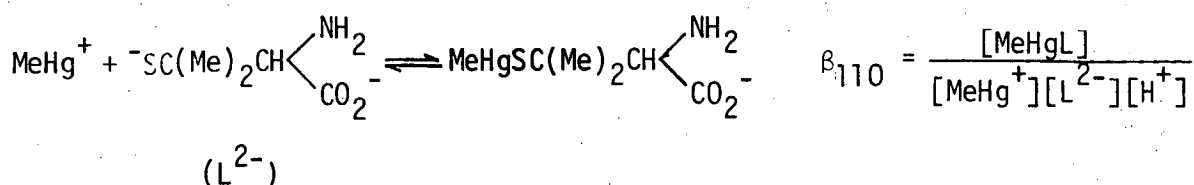
TITRAT to give the acid dissociation constants shown in Table 3.6. The relatively imprecise values of these constants reflect the proton purity, 85.5(1.4)%, of the thiol.

Titration data obtained in the presence of MeHg(II) and 0.1M KI, could not be fitted using MINQUAD 81. This was ascribed to further decomposition of the already impure ligand, which may have been catalysed by MeHg(II). The likely decomposition products homocysteine thiolactone or deprotonated homocysteine shown below may also complex MeHg(II) to some extent, e.g. via the amino groups.



The formation constant shown in Table 3.8 is that obtained by Rabenstein and Reid who added small amounts ( $2 \times 10^{-5}$ M) of Na<sub>2</sub>H<sub>2</sub>EDTA to their homocysteine solutions to minimise metal-catalysed decomposition.<sup>302</sup>

(vii) DL-Penicillamine was used as received, but stored over P<sub>2</sub>O<sub>5</sub> under nitrogen, mp. 190° (dec.) [lit.<sup>75</sup> 201° (dec.)]. Titrations with KOH, after addition of HNO<sub>3</sub> to fully protonate the zwitterion, were evaluated with TITRAT to give the acid dissociation constants shown in Table 3.6 in good agreement with previously published values, and proton purity of 101.1(1)%. Titration data obtained in the presence of one equivalent of MeHg(II) and 0.1M KI were fitted with MINQUAD 81 by simultaneously refining the overall formation constants  $\beta_{110}$  and  $\beta_{111}$  in a fashion identical to the cysteine system.





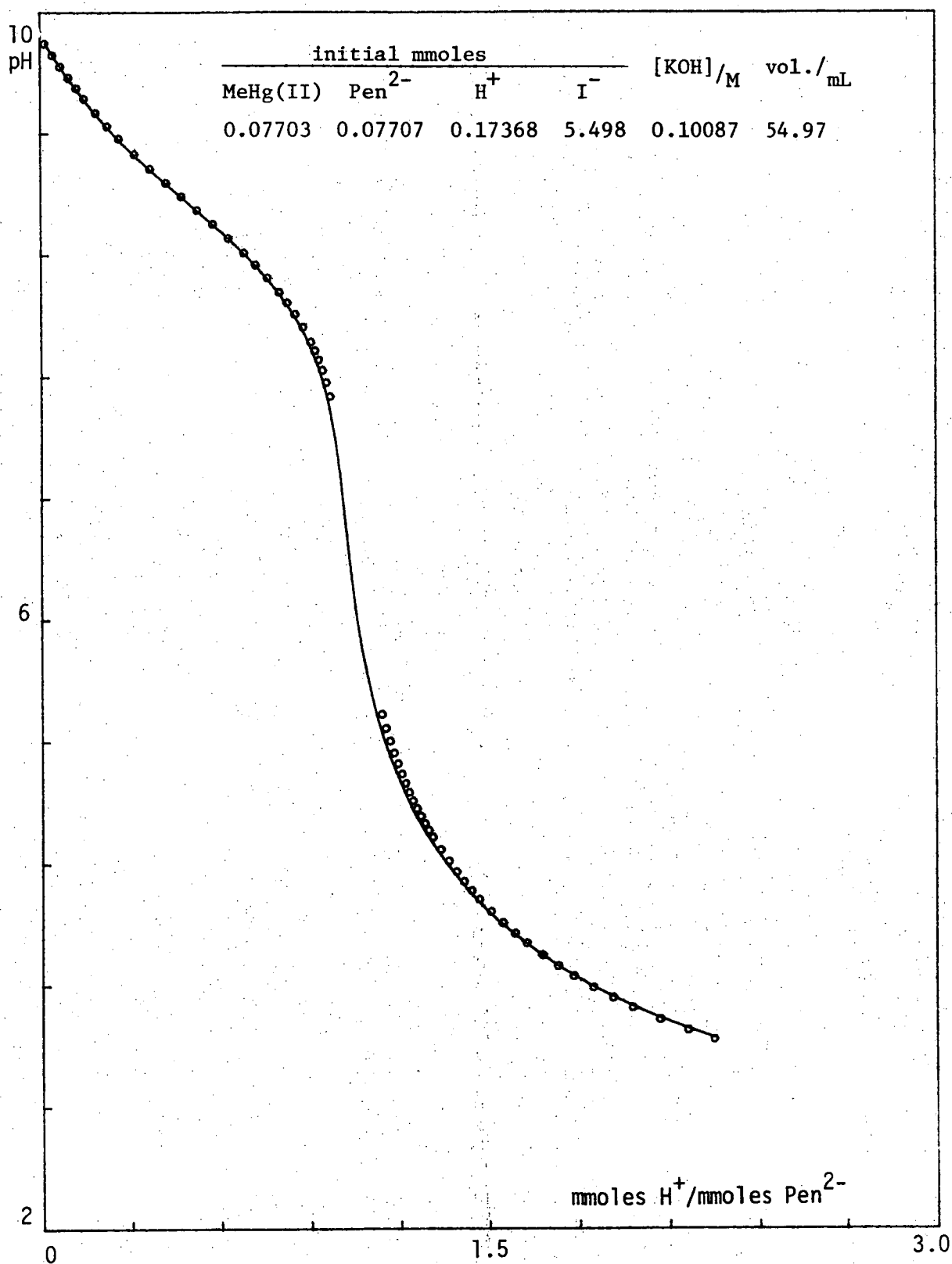


Figure 3.14: Methylmercury(II)-DL-Penicillamine(PenH<sub>2</sub>) titration data with iodide competition.

The fitted curve was calculated by COMIXH, using  $\log \beta(\text{MeHgI}) = 8.500$  and the equilibrium constants in Tables 3.6 and 3.8.

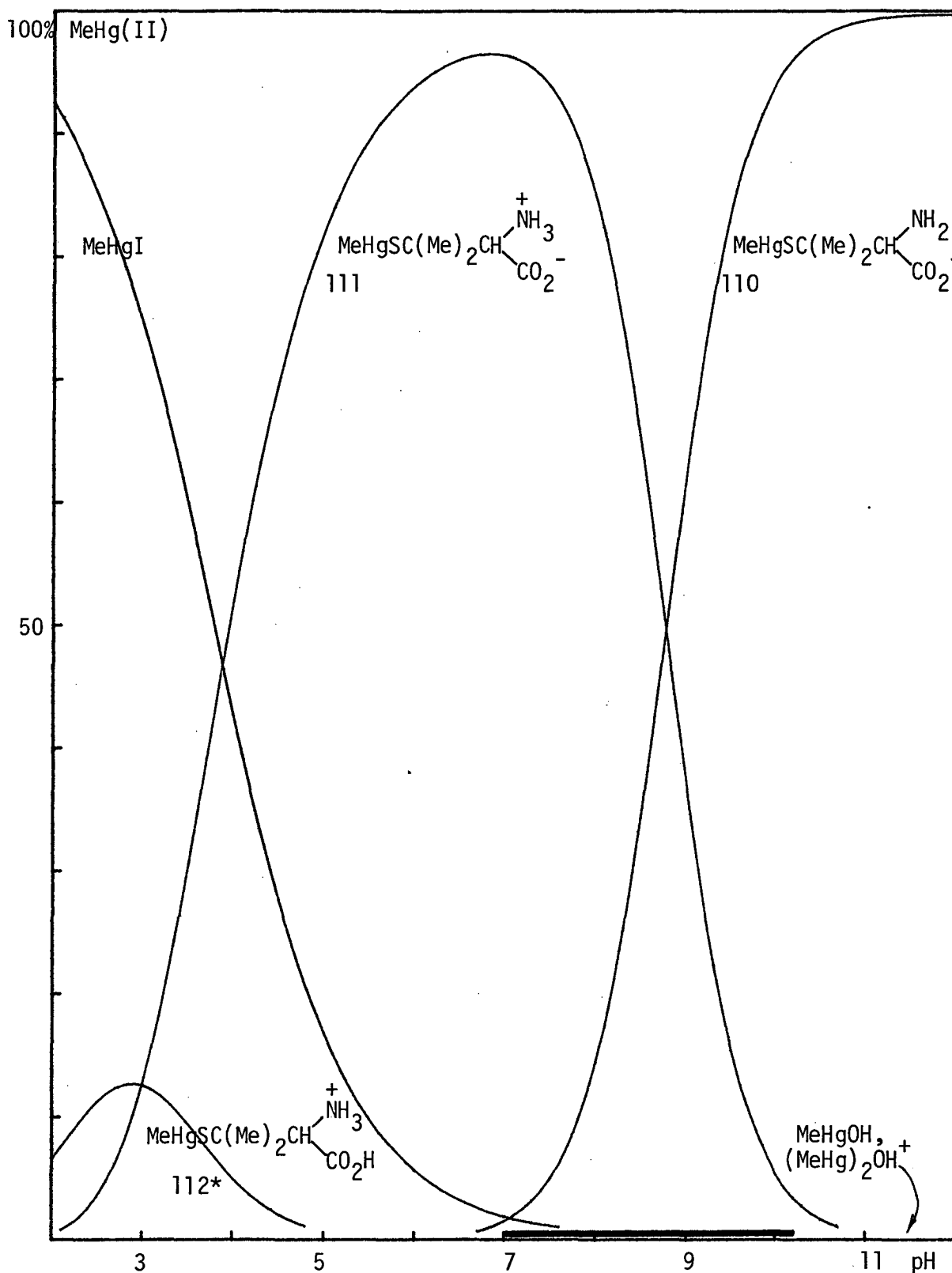
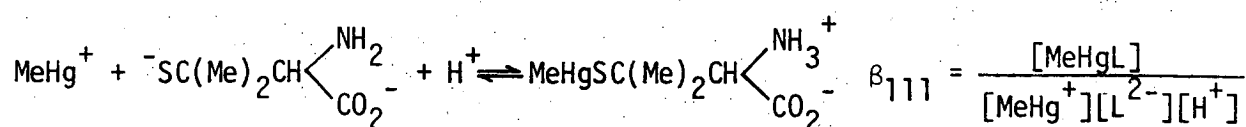


Figure 3.15: Species distribution calculated by COMIX for 0.0014M MeHg(II) and 0.0014M DL-penicillamine in 0.1M KI, using the equilibrium constants in Tables 3.6 and 3.8.

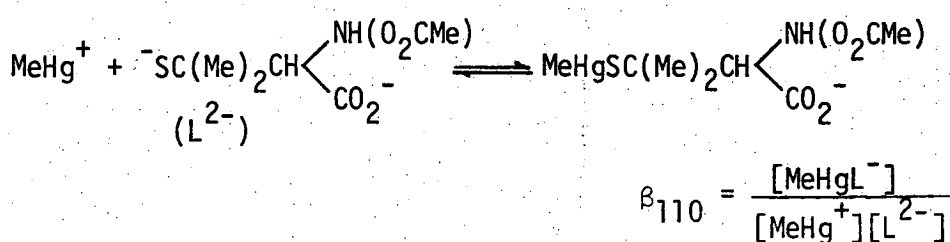
The heavy line indicates the pH-range of MINIQAD81 data.

(\* $\beta_{112}$  estimated from the L-cysteine system).



These are recorded in Table 3.8 and are in good agreement with the microscopic constants found by Reid and Rabenstein for complexation with amino deprotonated ligand.<sup>302</sup> Expected sulfhydryl binding is supported by the crystal structure of the 1:1 complex.<sup>247</sup> Addition of more than one equivalent of MeHg(II) to penicillamine was expected to produce an equilibrium mixture of protonated and deprotonated 2:1 complexes with pH-dependent MeHg(II) binding sites similar to cysteine (page 111) and was therefore not studied here. A 2:1 complex with sulfhydryl-bound and amino-bound MeHg(II) groups has been isolated from alkaline solution.<sup>248</sup> Calculated and experimental titration curves are shown in Figure 3.14 and the 1:1 distribution diagram in presence of 0.1M KI, in Figure 3.15. The  $\text{pK}'_a$  of the doubly protonated complex could not be evaluated in the pH range used here ( $\text{pH} > 4$ ) but was estimated to be  $\sim 3$ , similar to that for the 1:1 cysteine complex.

(viii) N-Acetyl-DL-Penicillamine was used as received but stored over  $\text{P}_2\text{O}_5$  under nitrogen, mp.  $180-1^\circ$  (lit.<sup>75</sup>  $183^\circ$ ). Titration with KOH and treatment of the data with TITRAT gave the acid dissociation constants recorded in Table 3.6, in good agreement with previously recorded values, and indicated a proton purity of 94.4(1)%. Since the amide group is not protonated in aqueous solution the 1:1 equilibrium system with MeHg(II) in the presence of 0.1M KI was treated by MINQUAD 81 by considering only the two equilibria shown:



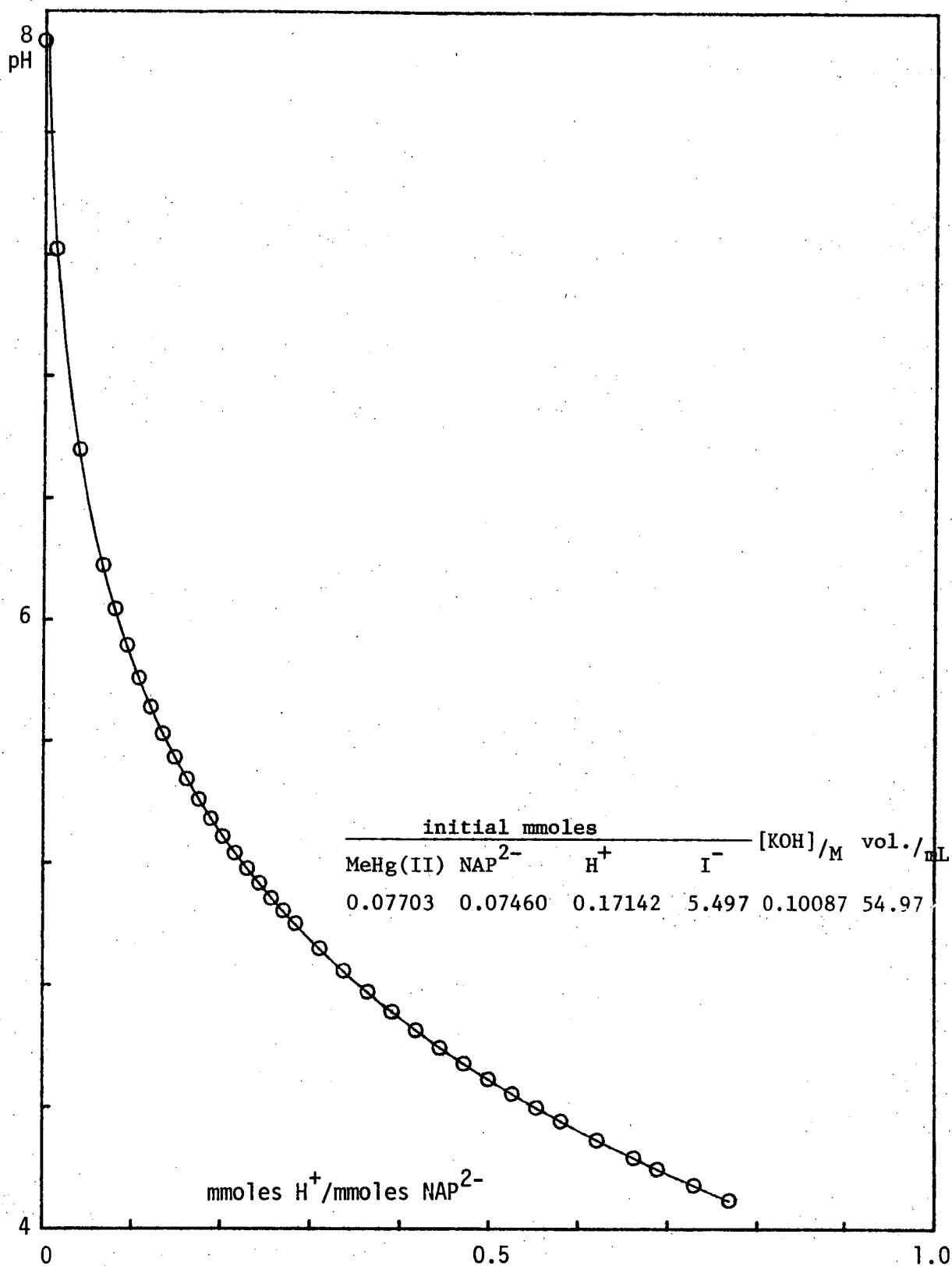


Figure 3.16: Methylmercury(II)-N-Acetyl-DL-penicillamine (NAPH<sub>2</sub>) titration data with iodide competition.

The fitted curve was calculated by COMIXH using  $\log \beta(\text{MeHgI}) = 8.500$  and the equilibrium constants in Tables 3.6 and 3.8.

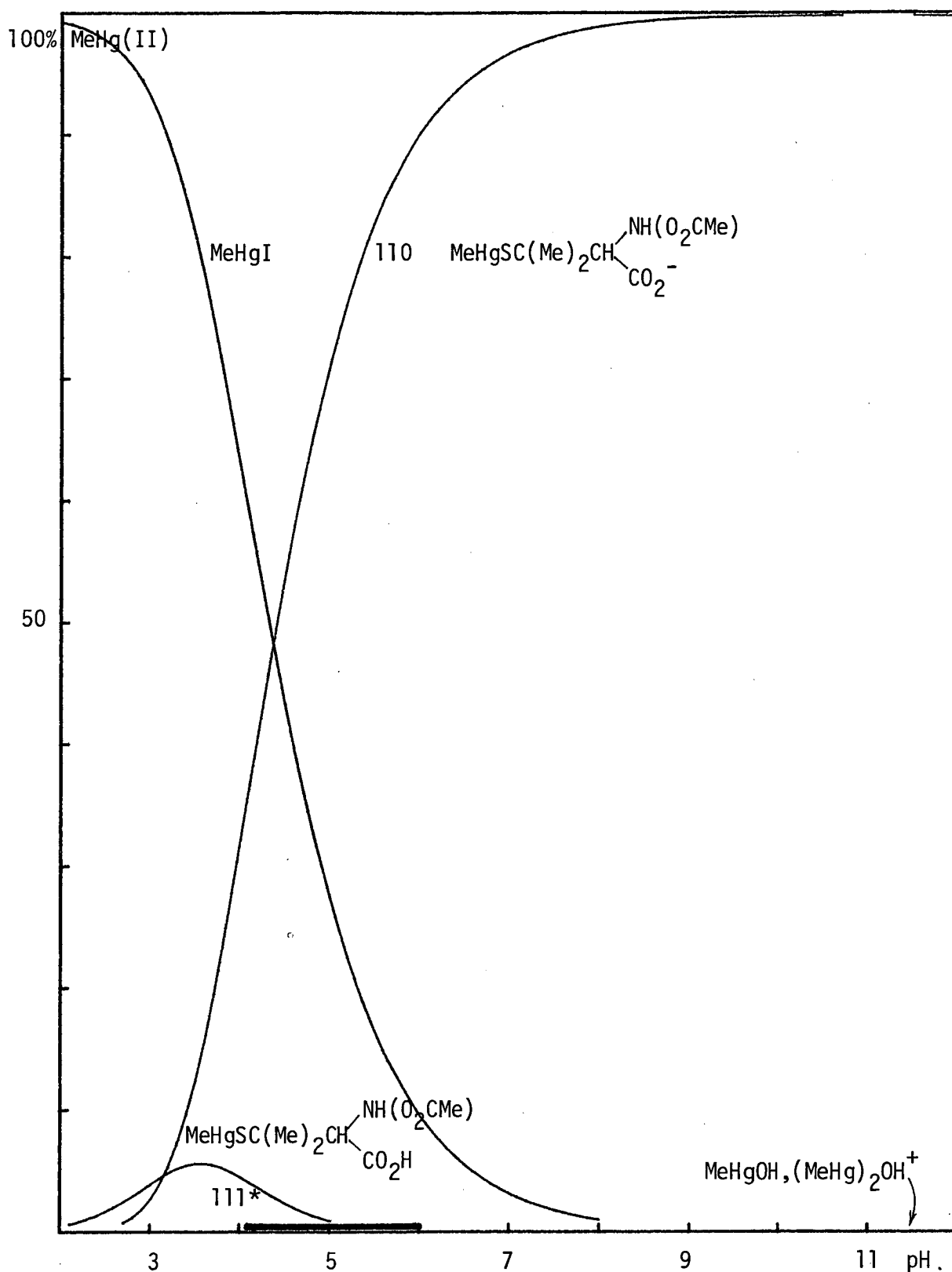
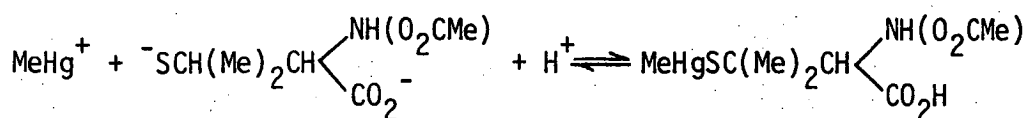


Figure 3.17: Species distribution calculated by COMIX for 0.0014M  $\text{MeHg(II)}$  and 0.0014M N-Acetyl-DL-Penicillamine in 0.1M KI, using the equilibrium constants in Tables 3.6 and 3.8.

The heavy line indicates the pH-range of MINIQVAD81 data.

(\* $\beta_{111}$  estimated from the L-cysteine system).



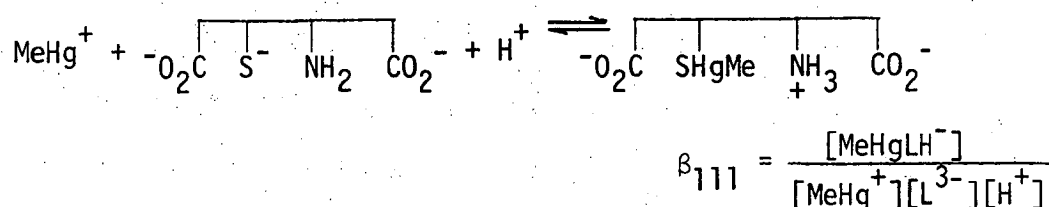
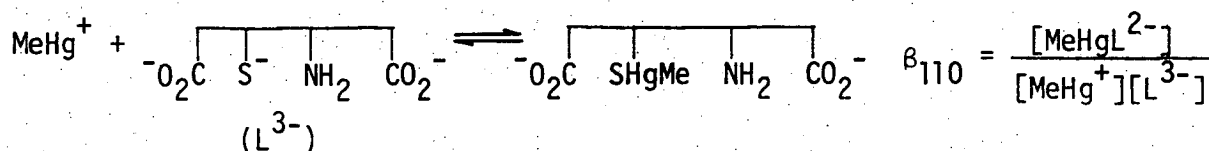
$$\beta_{111} = \frac{[\text{MeHgLH}]}{[\text{MeHg}^+][\text{L}^{2-}][\text{H}^+]}$$

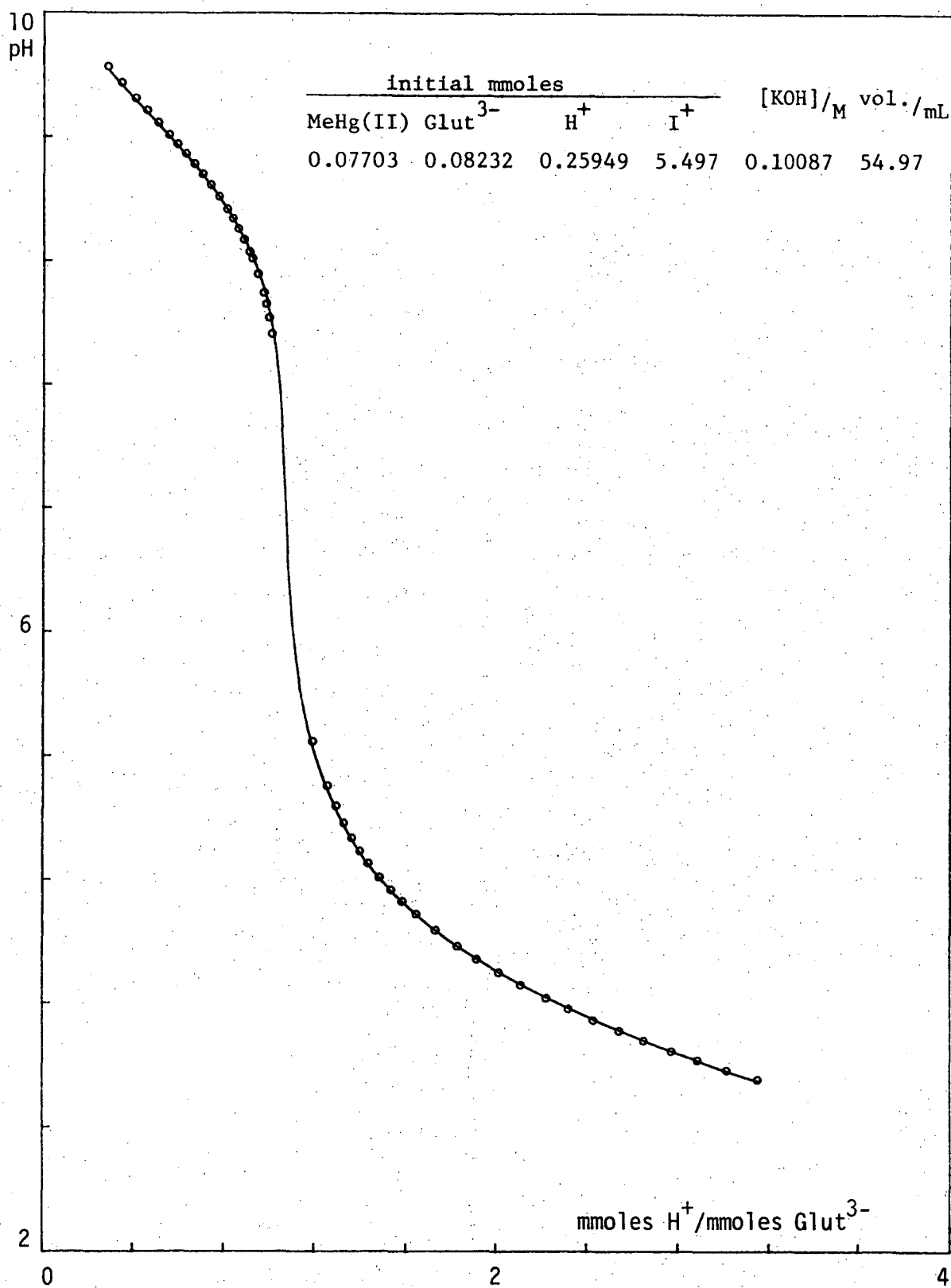
The 1:1 formation constants are recorded in Table 3.8. The value of  $\beta_{110}$  is in good agreement with that found by Reid and Rabenstein in 0.3M  $\text{KNO}_3$ .<sup>302</sup> The protonated complex is not very soluble below pH 5 and so the value of  $\beta_{111}$  is not precise, being calculated from few data points. The proton dissociation constant,  $\text{pK}'_a$  [3.29(5)], of the complex is close to that found by the abovementioned workers [2.95(7)].

Calculated and experimental titration curves are shown in Figure 3.16, and the species distribution with 0.1M KI, in Figure 3.17. The 2:1 system was not studied.

(ix) Glutathione was used as received but stored over  $\text{P}_2\text{O}_5$  under nitrogen, mp.  $190^\circ$  (dec.) (lit.<sup>75</sup>  $195^\circ$ ). Protonation constants of the tripeptide were obtained by KOH titration of acidified solutions. Treatment of the data with TITRAT gave the results shown in Table 3.6, in good agreement with those previously reported. The proton purity was found to be 104.0(2)%.

In the presence of one equivalent of  $\text{MeHg(II)}$  and 0.1M KI, titration data over the range  $4 < \text{pH} < 10$  were evaluated with MINQUAD 81 for the equilibria below:





**Figure 3.18:** Methylmercury(II)-Glutathione (GlutH<sub>3</sub>) titration data with iodide competition.

The fitted curve was calculated by COMIXH using  $\log \beta(\text{MeHgI}) = 8.500$  and the equilibrium constants in Tables 3.6 and 3.8.

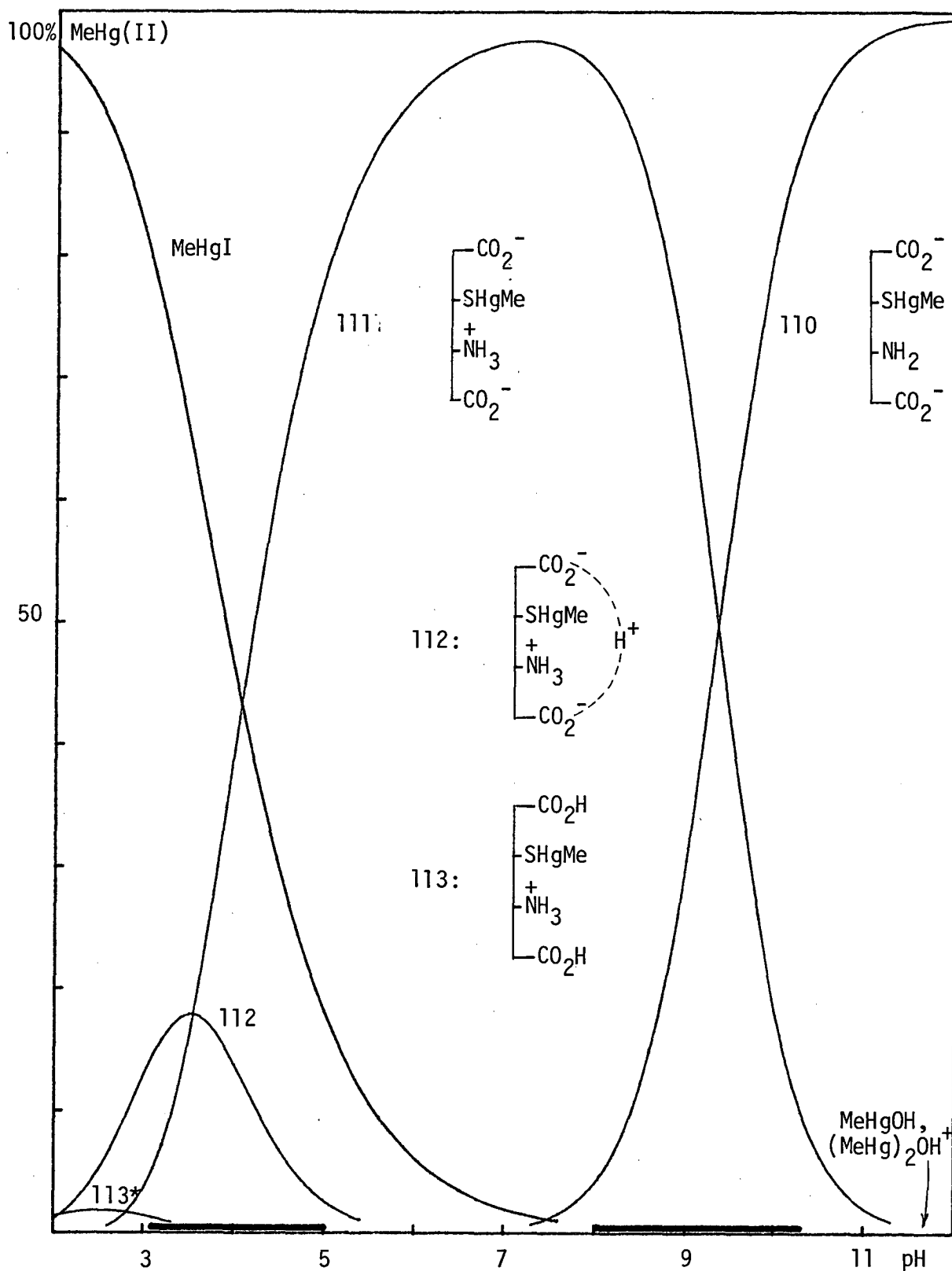
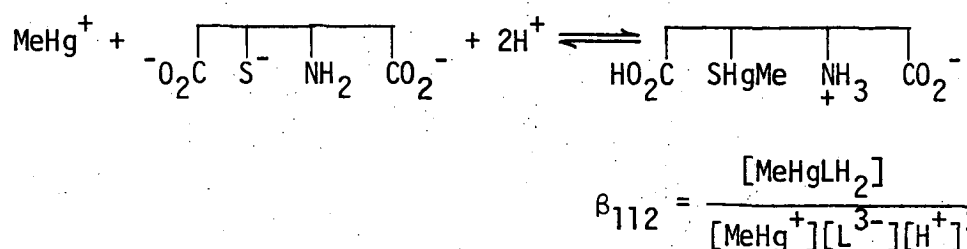


Figure 3.19: Species distribution calculated by COMIX for 0.0014M MeHg(II) and 0.0014M Glutathione in 0.1M KI, using the equilibrium constants in Tables 3.6 and 3.8.

The heavy lines indicates the pH-range of MINIQAD81 data.

(\* $\beta_{113}$  estimated from the microscopic constants in ref. 309)





The formation constants are recorded in Table 3.8. Inclusion of a thrice protonated complex ( $\beta_{113}$ ) did not improve the fit to the data. The value of  $\beta_{110}$  agrees with the previously reported values of Schwarzenbach and Schellenberg<sup>305</sup> and Simpson.<sup>324</sup> Reid and Rabenstein have not published a value of this constant. Proton dissociation constants of the 1:1 complex, corresponding to  $\log \beta_{112} - \log \beta_{111}$  [ $\text{pK}'_{a1} = 3.42(1)$ ] and  $\log \beta_{111} - \log \beta_{110}$  [ $\text{pK}'_{a2} = 9.26(1)$ ] are in agreement with the macroscopic constants calculated from microscopic constants reported by Rabenstein<sup>309</sup> [3.31(12) and 9.11(2) respectively]. The calculated and experimental titration curves for the 1:1 MeHg(II)-glutathione system are shown in Figure 3.18. The species distribution over the range  $2 < \text{pH} < 12$  is shown in Figure 3.19, using values  $\beta_{110}$ ,  $\beta_{111}$ ,  $\beta_{112}$  evaluated in this work, and an estimate of  $\log \beta_{113} \sim 3.5$  from the microscopic constants reported by Rabenstein.<sup>309</sup> The 2:1 system has been previously studied<sup>360</sup> and was not considered here.

(x) Thiocholine perchlorate was kindly provided by Philip Guerney (University of New South Wales), and stored at  $-20^\circ$  under nitrogen, mp.  $137-9^\circ$

Although the MeHg(II) complex of cysteamine has been isolated,<sup>405</sup> the formation constants of MeHg(II) with cationic thiolates such as thiocholine have not been reported. Titration of the perchlorate salt of the ligand with KOH, and treatment of the data with TITRAT, gave the acid dissociation constant in agreement with the previously reported value, shown in Table 3.6, and proton purity 96.1(2)%.

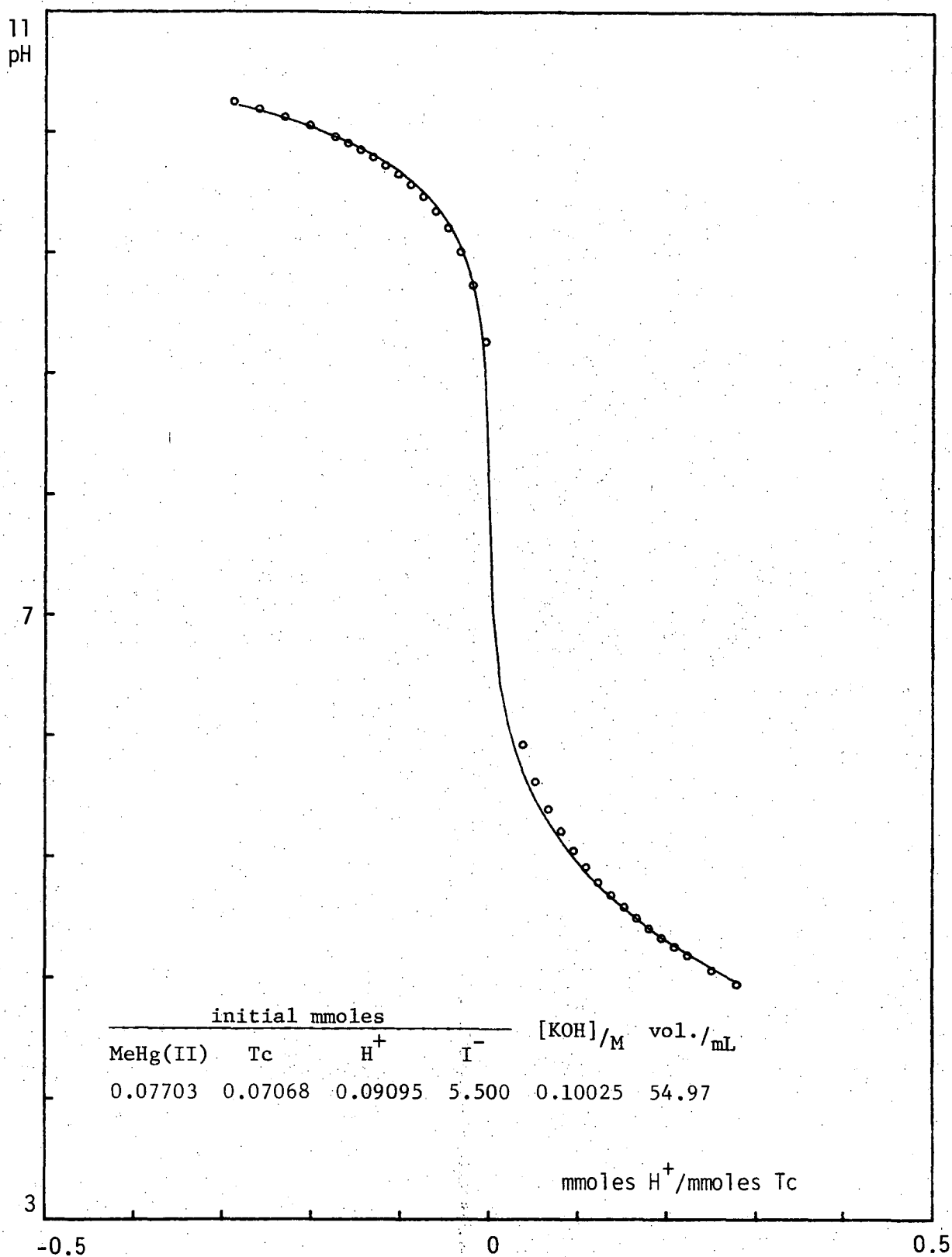


Figure 3.20: Methylmercury(II)-Thiocholine perchlorate ( $\text{TcH}^+$ ) titration data with iodide competition.

The fitted curve was calculated by COMIXH using  $\log \beta(\text{MeHgI}) = 8.500$  and the equilibrium constants in Tables 3.6 and 3.8.

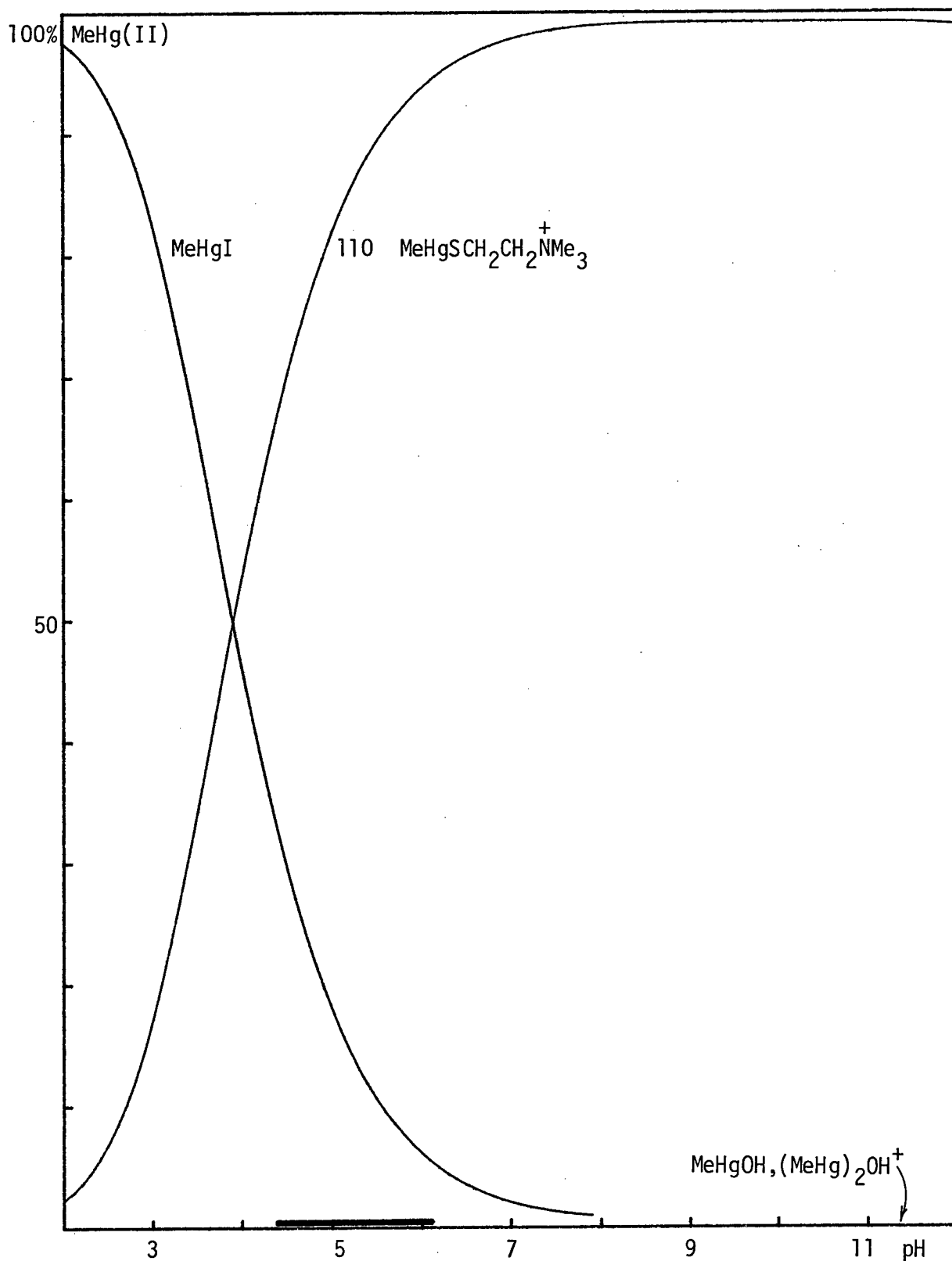
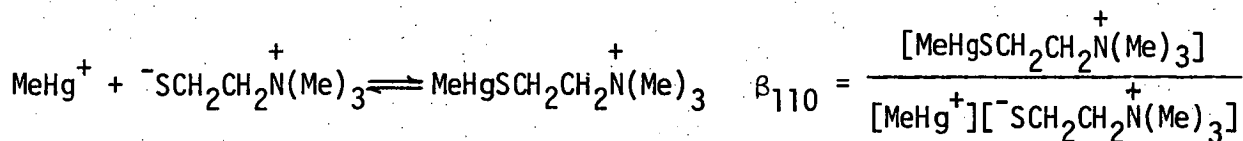


Figure 3.21: Species distribution calculated by COMIX for 0.0014M MeHg(II) and 0.0014M Thiocholine perchlorate in 0.1M KI, using the equilibrium constants in Tables 3.6 and 3.8.

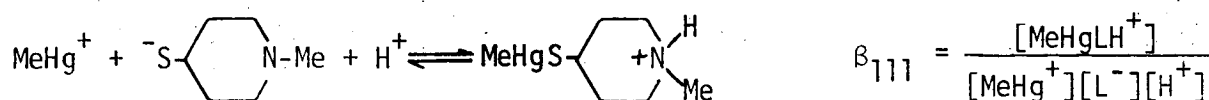
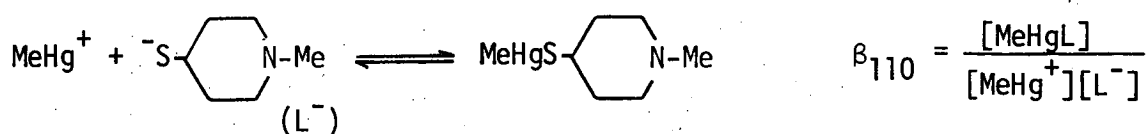
The heavy line indicates the pH-range of MINIQUAD81 data.

Titration of the solid 1:1 MeHg(II) complex with KOH in the presence of 0.1M KI yielded the value of  $\beta_{110}$  (Table 3.8), using MINIQUAD 81 on data in the range  $4 < \text{pH} < 10$ .



This constant is the smallest stability constant of MeHg(II) with the thiols studied here, reflecting the relatively high acidity of the thiocholine sulphydryl group. Calculated and experimental titration curves are shown in Figure 3.20 and the distribution diagram in the presence of 0.1M KI, in Figure 3.21.

(xi) 4-Mercapto-N-methylpiperidine was prepared by the method of Barrera and Lyle<sup>406</sup> from N-methylpiperidine via 4,4'-dimercapto-N-methylpiperidine hydrate (page 344) to give a colourless oil, which was fractionally distilled under reduced nitrogen pressure, bp.  $31-2^\circ/1 \text{ mm}$  (lit.<sup>406</sup>  $62^\circ/0.8 \text{ mm}$ ) and stored under nitrogen at  $-20^\circ$ , mp.  $7-9^\circ$ . Titration of the thiol with KOH after protonation with  $\text{HNO}_3$ , and treatment of the data with TITRAT, gave acid dissociation constants shown in Table 3.6, and proton purity 92.9(2)%. Titration of the solid 1:1 MeHg(II) complex (page 38) with KOH in the presence of 0.1M KI, yielded the values  $\beta_{110}$  and  $\beta_{111}$  (Table 3.8) by treatment with MINIQUAD 81.



Ligand hydrolysis and complexation with MeHg(II) have not previously been reported. Calculated and experimental titration curves are shown in

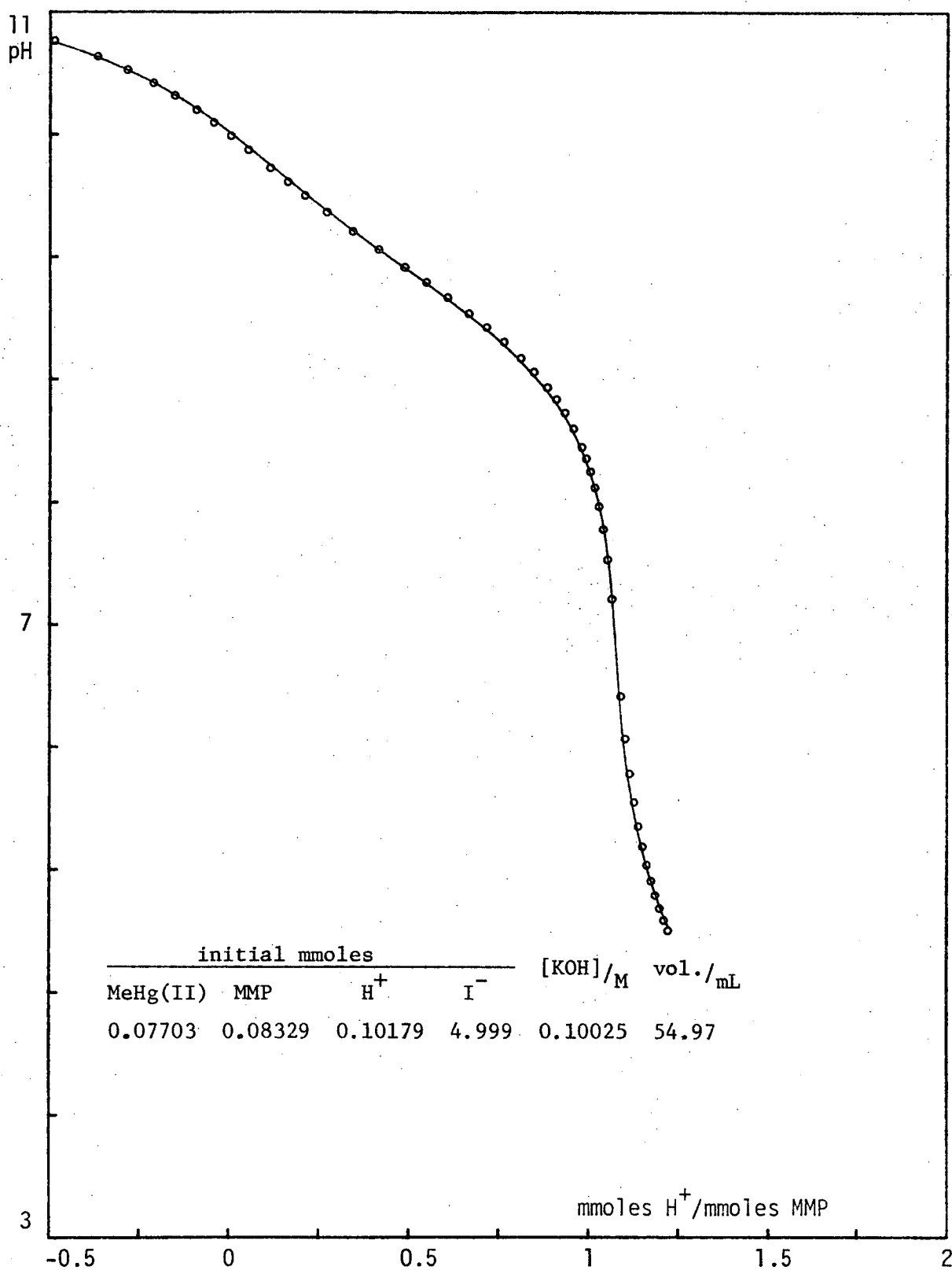


Figure 3.22: Methylmercury(II)-4-Mercapto-N-methylpiperidine (MMP) titration data with iodide competition.

The fitted curve was calculated by COMIXH using  $\log \beta(\text{MeHgI}) = 8.500$  and the equilibrium constants in Tables 3.6 and 3.8.

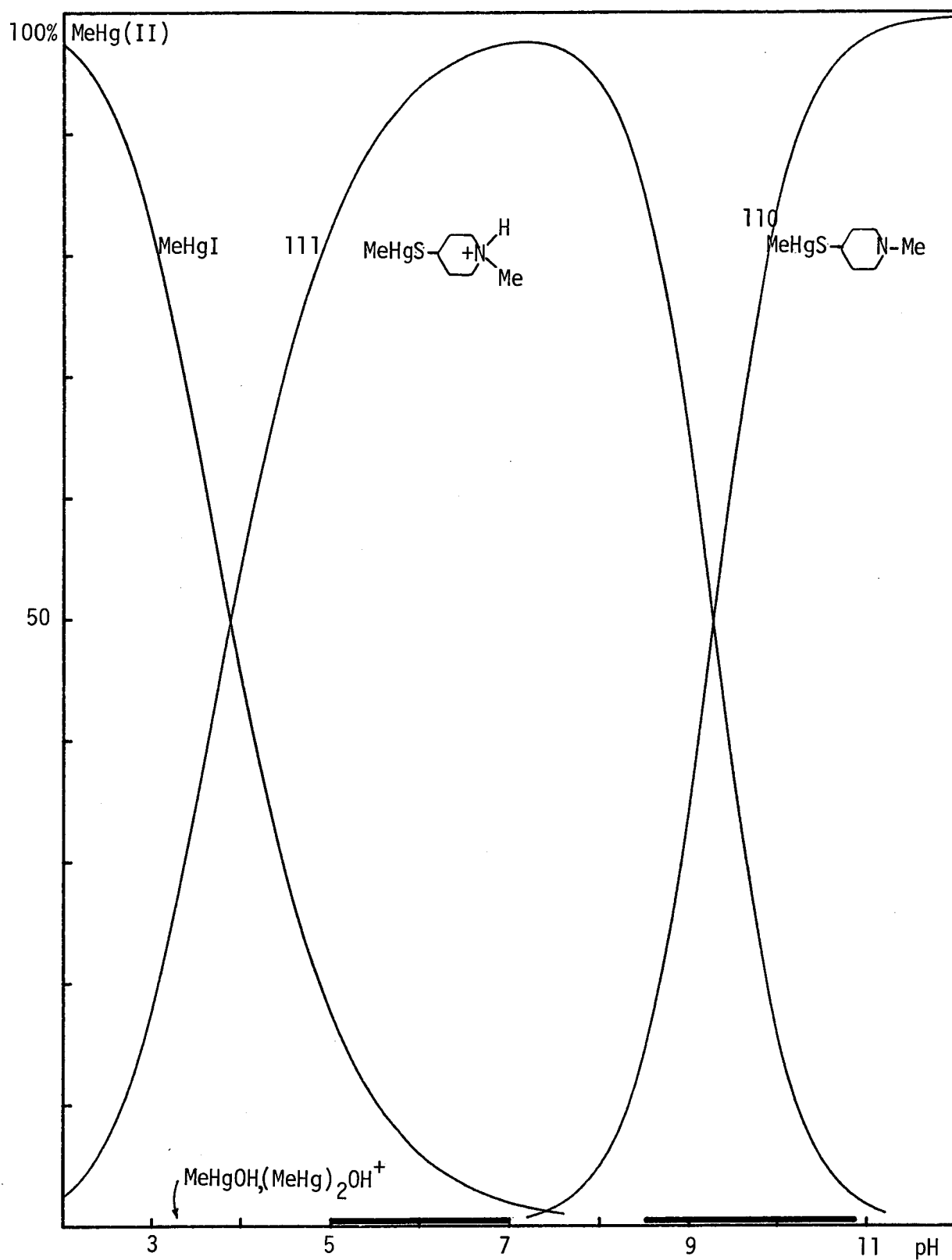


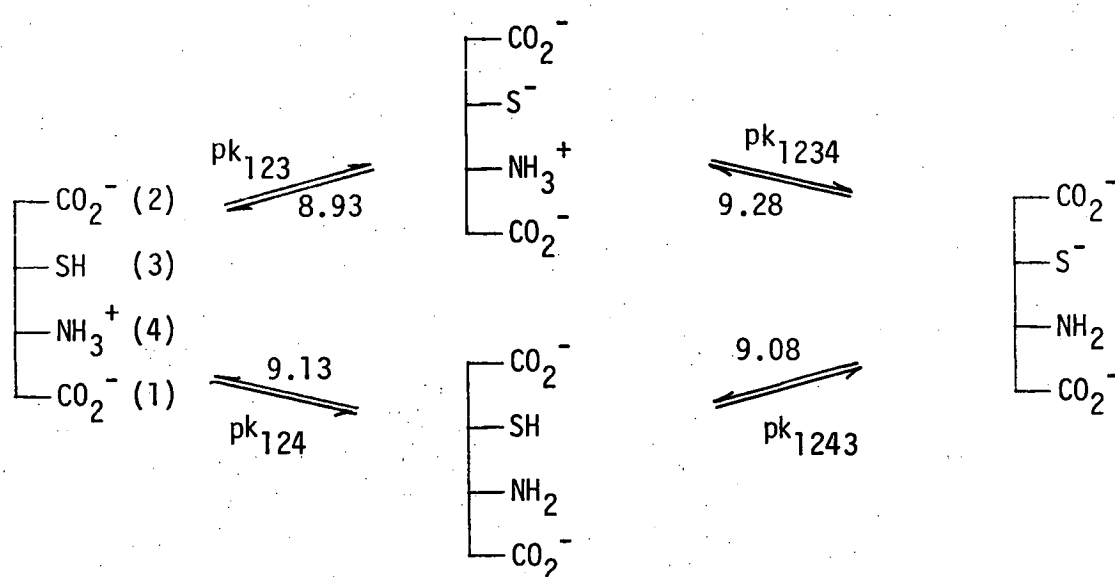
Figure 3.23: Species distribution calculated by COMIX for 0.0014M MeHg(II) and 0.0014M 4-mercapto-N-methylpiperidine in 0.1M KI, using the equilibrium constants in Tables 3.6 and 3.8.

The heavy line indicates the pH-range of MINIQUAD81 data.

Figure 3.22 and the species distribution in the presence of 0.1M KI, in Figure 3.23.

The equilibrium constants for MeHg(II)-monothiolate interaction found in this study, and elsewhere, lie in the range 14.64 to 17.60 and are highly correlated with the Brønsted basicity of the sulfhydryl donor groups. This can clearly be seen from the plot of  $\log \beta_{110}$  versus  $pK_a(\text{SH})$  in Figure 3.24 which includes values for all monothiols studied in this work and by Reid and Rabenstein.<sup>302</sup> The values found by Hojo *et al.*<sup>363</sup> are in disagreement.

The intrinsic Brønsted basicity of the sulfhydryl group in the  $\alpha$ -mercaptoamine ligands studied here, cannot adequately be represented by macroscopic proton dissociation constants because the amine and thiolate groups protonate simultaneously. Microscopic sulfhydryl protonation constants for these ligands were estimated by assuming the same relationships between macroscopic and microscopic constants as were found in glutathione by Rabenstein.<sup>369</sup> For glutathione, the following microscopic constants were determined<sup>369</sup>



The amino group is apparently 0.2 log units more basic than the thiolate group, independent of whether these groups are protonated or deprotonated.

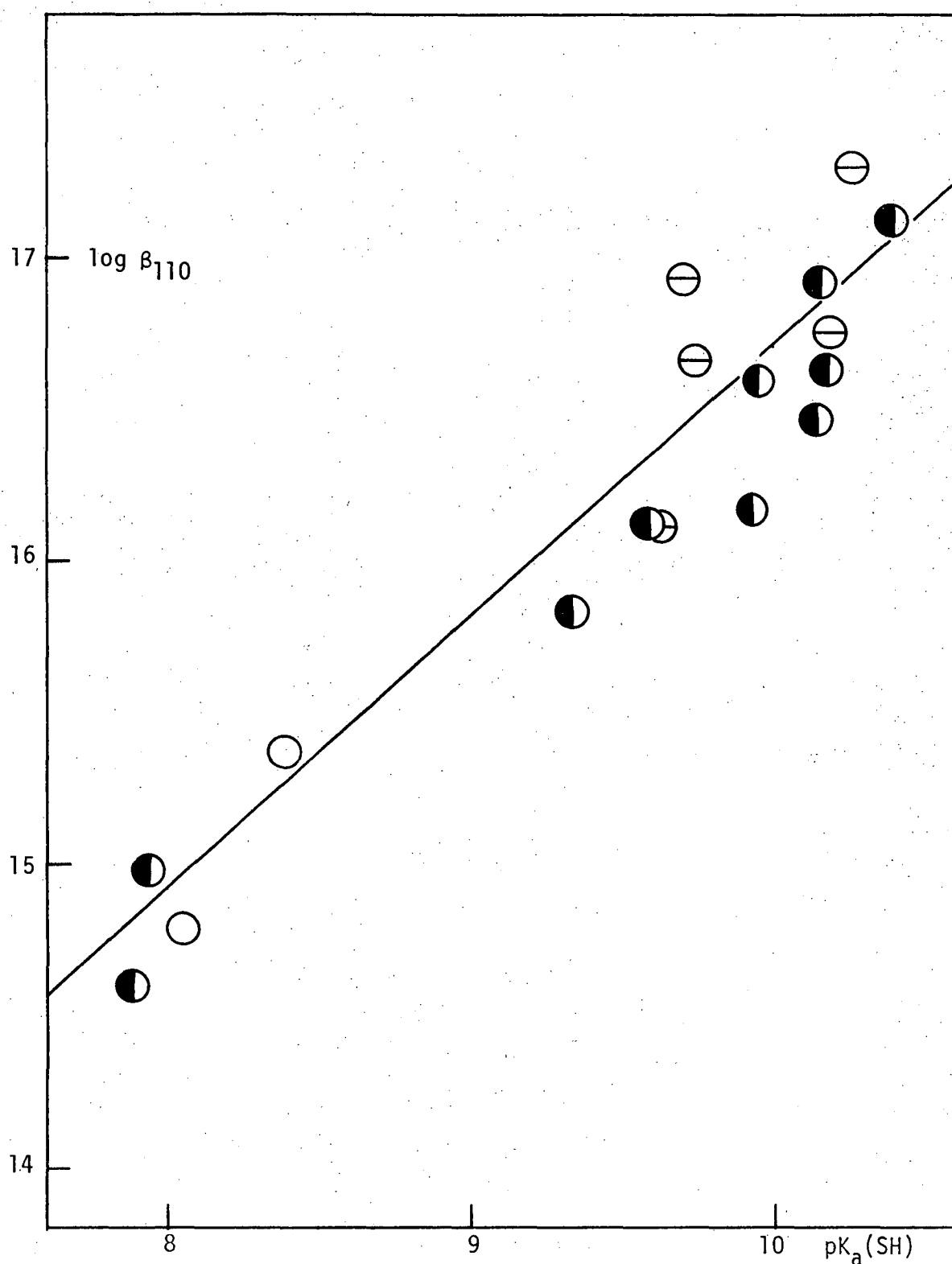


Figure 3.24: Correlation between the MeHg(II)-thiolate formation constant,  $\log \beta_{110}$ , and Brønsted basicity of the sulfhydryl donor,  $pK_a(SH)$ . The monothiol ligand numbering follows that of Tables 3.6 and 3.8.

$\log \beta_{110}$  from this work, ●, using estimates of microscopic  $pK_a(SH)$  for mercaptoamines (page 134) and microscopic constants reported by Reid and Rabenstein<sup>302</sup> for ligands in which the amino group is protonated, ○, and unprotonated, ⊖.



Similar relationships have been found for the microscopic constants of cysteine.<sup>407</sup>

Macroscopic constants for composite  $\text{SH} + \text{NH}_3^+$  deprotonation,  $K_{a1}$  and  $K_{a2}$ , are related to the microscopic constants by the relationships

$$K_{a1} = K_{123} + k_{123}$$

$$K_{a2} = \frac{k_{1234} \cdot k_{1243}}{k_{1234} + k_{1243}}$$

Use of the approximations  $\text{pk}_{1234} = \text{pk}_{1243} + 0.2$  and  $\text{pk}_{124} = \text{pk}_{123} + 0.2$  enables the microscopic protonation constants of the sulfhydryl ( $k_{1243}$ ) amine ( $k_{1234}$ ) groups of the mercaptoamines to be separately evaluated from the macroscopic constants and these are recorded in Table 3.9.

	$\text{pk}_a(\text{NH}_3^+)$	$\text{pk}_a(\text{SH})$
L-cysteine	10.15 (10.09)	9.95 (9.74) <sup>302</sup>
DL-penicillamine	10.38 (10.29)	10.18 (9.70) <sup>302</sup>
glutathione	9.53	9.33 (9.20) <sup>407</sup>
4-mercapto-N-methylpiperidine	10.13	9.93

**Table 3.9:** Estimated<sup>a</sup> microscopic proton dissociation constants of amine and sulfhydryl groups of fully deprotonated  $\alpha$ -mercaptoamines.

<sup>a</sup>Using the approximation  $\text{pk}_a(\text{NH}_3^+) = \text{pk}_a(\text{SH}) + 0.2$  described in the text and using macroscopic constants recorded in Table 3.6.

The relationship between  $\beta_{110}$  for  $\log K_{\text{MeHgSR}}$  and  $\text{pK}_a(\text{SH})$  from this combined data is found to be

$$\log K_{\text{MeHgSR}} = 0.893 \text{ pK}_a(\text{SH}) + 7.77$$

The relevance of these formation constants to the interaction of antidotal thiols *in vivo* will be discussed in the next Section, after the formation constants with some vicinal dithiols have been established.

### 3.3.3 Methylmercury(II) Formation Constants with Vicinal Dithiols

The only formation constants in the literature of methylmercury(II) with a dithiolate ligand seem to be those reported by Hojo *et al.* for the interaction with  $\text{BALH}_2$ .<sup>363</sup> Some serious discrepancies with values obtained by these workers for the formation constants of  $\text{MeHg(II)}$ -monothiolate complexes have previously been discussed (page 80 ). As several important antidotes for methylmercury(II) toxicity are vicinal dithiols ( $\text{BALH}_2$ , Unithiol and  $\text{DMSH}_4$ ) it was of interest to determine the equilibrium constants for the formation of  $\text{MeHg(II)}$  complexes with these ligands.

To completely describe the solution chemistry of  $\text{MeHg(II)}$  complexes with dithiols, both 1:1 and 2:1 species (protonated and unprotonated) need to be considered, which renders evaluation of individual equilibrium constants much more difficult than for monothiols.

Attempts to purify the non-vicinal dithiol, 1,3-dimercapto-2-propanol,  $\text{DMPH}_2$ , by fractional distillation under reduced nitrogen pressure, bp.  $61.5\text{--}3.5^\circ/0.2\text{ mm}$  (lit.<sup>400</sup>  $82^\circ/1.5\text{ mm}$ ) apparently caused decomposition, indicated by low proton-purity of the product (<85% by alkalimetric titration). Consequently, comparison of  $\text{MeHg(II)}$  stability constants with  $\text{DMPH}_2$  and its vicinal dithiol analog,  $\text{BALH}_2$ , was not possible.

(i) 2,3-dimercapto-1-propanol,  $\text{BALH}_2$ , was fractionally distilled under reduced nitrogen pressure, bp.  $74\text{--}5^\circ/0.5\text{ mm}$  (lit.<sup>408</sup>  $74\text{--}6^\circ/1\text{ mm}$ ), and stored under nitrogen at  $-20^\circ$ . Titration of the dithiol with KOH, and treatment of the data with TITRAT, gave the two macroscopic proton dissociation constants recorded in Table 3.10, and indicated a proton purity of 97.5(6)%. It should be noted that, since the two sulfhydryl groups are of comparable basicity, they are simultaneously protonated

	this work [25°, 0.1 KNO <sub>3</sub> or KI]	previous values <sup>b</sup>	ref.
2,3-dimercapto-1-propanol, BALH <sub>2</sub>	8.654(2) 10.620(4)	8.69 10.79 [25°, 0.1 NaCl]	409
		8.618 10.567 [25°, ~0 ]	379
meso-2,3-dimercaptosuccinic acid, DMSH <sub>4</sub>	2.24(1) 3.429(3) 9.648(3) 11.50(2)	2.71 3.48 8.89 10.79 [25°, 0.1 KNO <sub>3</sub> ]	375
		2.31 3.69 9.68 11.14 [20°, 0.1 KCl]	410
		2.40 3.46 9.44 11.82 [20°, 0.1 KCl]	411
2,3-dimercapto-1-propanesulfonate (sodium salt), Unithiol	8.691(1) 11.379(16)	8.84 11.20	412
		8.65(2) 11.91(4) [25°, 0.1 KCl]	413
		8.74(10) 11.17(1)	414

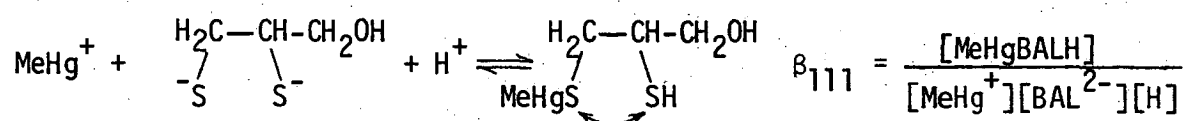
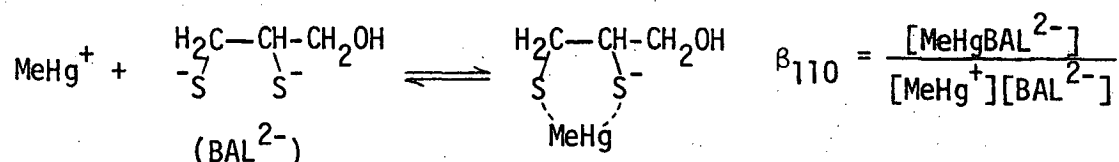
Table 3.10: Proton dissociation constants<sup>a</sup> of dithiol ligands used for MeHg(II) solution studies.

<sup>a</sup> Macroscopic concentration constants obtained with TITRAT. Recorded values are weighted geometric means with estimated standard deviations of the last digit, in parentheses.

<sup>b</sup> Mixed constants have been converted to concentration constants by calculation of  $\log \gamma_{H^+}$  according to the Davies equation.<sup>318</sup>

above pH 9 in a similar fashion to the  $\alpha$ -mercaptoamines described previously. Microscopic proton dissociation constants of vicinal dithiols do not seem to have been previously recorded.

Addition of one equivalent of MeHg(II) to BALH<sub>2</sub> is expected to establish the following equilibria:<sup>†</sup>



Proton and MeHg(II) exchange in the 111 species is likely to be rapid. An order-of-magnitude estimate for the equilibrium constant for the addition of one MeHg(II) group to the deprotonated dithiol ligand was made using the correlation between sulfhydryl basicity,  $\text{pK}_a(\text{SH})$ , and  $\log K_{\text{MeHgSR}}$  for monothiolates (page 135). If the *microscopic*  $\text{pK}_a$ 's of the sulfhydryl donors are assumed to be between the macroscopic proton dissociation constants,  $\log \beta_{110}$  should be in the range 15 to 17, and therefore be amenable to evaluation by iodide competition. However, when equivalent quantities of MeHg(II) and BALH<sub>2</sub> were titrated with KOH in the presence of 0.1M KI, it became apparent that MeHg(II) was not dissociated from sulfur in the range  $4 < \text{pH} < 10$ , indicating  $\log \beta_{110} > 17$  to 18. Only the proton dissociation constant ( $K'_a = \beta_{111}/\beta_{110}$ ) of the 1:1 protonated species could be obtained from these data. More

<sup>†</sup>Dotted lines indicate that MeHg<sup>+</sup> may be bound to either donor, possibly to both, and the curved arrow indicates rapid exchange in subsequent diagrams in this chapter.

efficient competition for MeHg(II) was achieved by using mercaptoethanol instead of iodide. A similar approach was coincidentally taken by Reid and Rabenstein in their nmr studies of monothiolates, using mercaptoacetate competition.<sup>309</sup> This monothiol has only a single proton nmr resonance but mercaptoethanol has the advantage in this work of contributing only two extra equilibria to the overall equilibrium scheme, i.e. ligand hydrolysis and MeHg(II) complexation.

Titration of a solution containing equivalent quantities of mercaptoethanol,  $\text{BALH}_2$ , and MeHg(II) over the range  $5 < \text{pH} < 10$ , yielded data which were treated with MINIQUAD81 to give  $\log \beta_{110} = 19.56(10)$  for the 1:1 MeHg(II) complexation of  $\text{BALH}_2$  and  $\text{pK}'_a = 7.60(1)$  for the protonation of the 1:1 complex (Table 3.11). The calculated and experimental titration curve for this titration is shown in Figure 3.25 and the distribution diagram for the 1:1:1 system is shown in Figure 3.26A.

The magnitude of  $\beta_{110}$  is approximately 100 times higher than expected for a simple monothiolate interaction, even considering the availability of two sulfhydryl groups, which is expected to statistically advantage MeHg(II)-sulfhydryl coordination.

In contrast to the very high stability of the 1:1 complex, addition of a second MeHg(II) group is less favorable. Addition of a second equivalent of MeHg(II) to the 1:1 system, in the presence of mercaptoethanol gave titration data which could be fitted adequately assuming only the 1:1 complex and  $\text{MeHgSCH}_2\text{CH}_2\text{OH}$ . Similarly, with 0.1M iodide competition, suitable for MeHg(II)-thiolate interactions with  $\log \beta$  in the range 13 to 17, the second MeHg(II) group preferentially formed insoluble MeHgI. Thus both mercaptoethanol and iodide compete more effectively for the second MeHg(II) group, than does the remaining sulfhydryl donor of the 1:1 complex.

Dithiol ligand	Equilibrium constants <sup>a</sup> of MeHg(II) complexes				
	with competition			with no competing ligand	
2,3-dimercapto-1-propanol (BALH <sub>2</sub> )	log	110	19.56(9) <sup>b</sup>	} 7.60(1)	30.02(11) 10.46(10) =log K <sub>2f</sub>
		111	21.155(6)		
		112			
2,3-dimercapto-1-propanesulfonate, sodium salt (Na[UTH <sub>2</sub> ])	log	110	21.01(8) <sup>b</sup>	} 7.559(4)	10.26(8) 1.90(8) <sup>d</sup>
		111	28.57(8)		
		112	30.82(8)	} 2.250(7) <sup>d</sup>	
		210			
		211			
meso-2,3-dimercaptosuccinic acid (DMSH <sub>4</sub> )	log	110	17.11(3) <sup>c</sup>	} 8.50(15)	} 4.565(8) <sup>f</sup> } ~4 <sup>e</sup>
		111	25.61(16)		
		112	30.42(18)	} 4.81(8)	
		113	34.2	} 3.8(3)	
		210		3.1.1	
		211		35.6	
		212		39.6	

Figure 3.11: Methylmercury(II)-dithiolate equilibrium constants refined by MINQUAD81

a values in parentheses are estimated standard deviations of the last digit, from the least-squares refinement. Standard deviations of derived constants (italicised) were calculated using correlation coefficients from the least-squares refinement (footnote, page 329).

bmercaptoethanol competition. ciodide competition. dassuming pK<sub>a</sub>(SO<sub>3</sub>H)=2.0. eestimated from behaviour of several titrations. Complete MINQUAD81 refinement non-convergent. ftitration of (MeHg)<sub>2</sub>DMSH<sub>2</sub>, no competition.

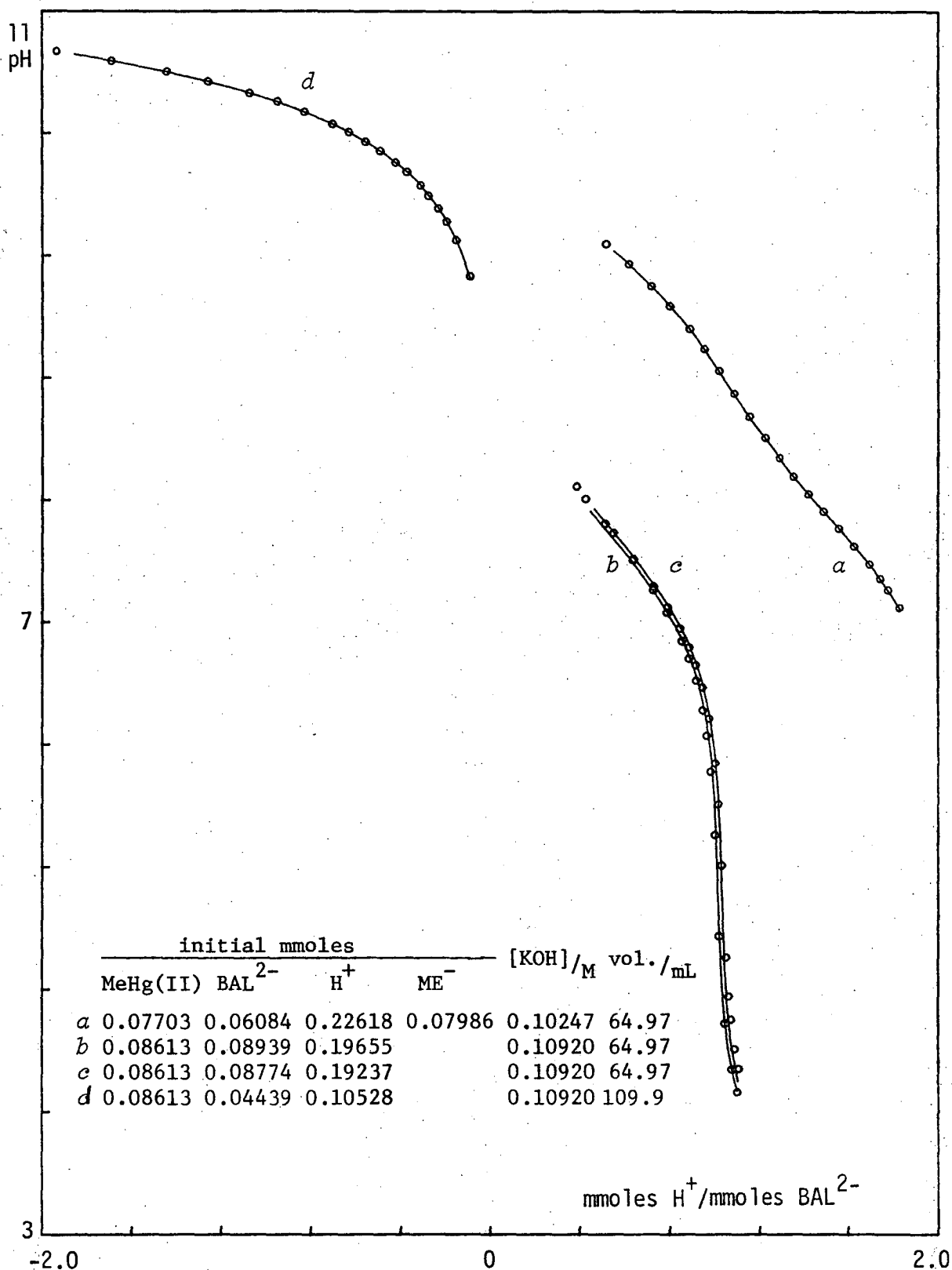


Figure 3.25: Methylmercury(II)-BALH<sub>2</sub> titration data.

*a* with mercaptoethanol (MEH) competition; *b-d* with no competing ligand.

The fitted curves were calculated by COMIXH, using the equilibrium constants in Tables 3.6, 3.8, 3.10 and 3.11.



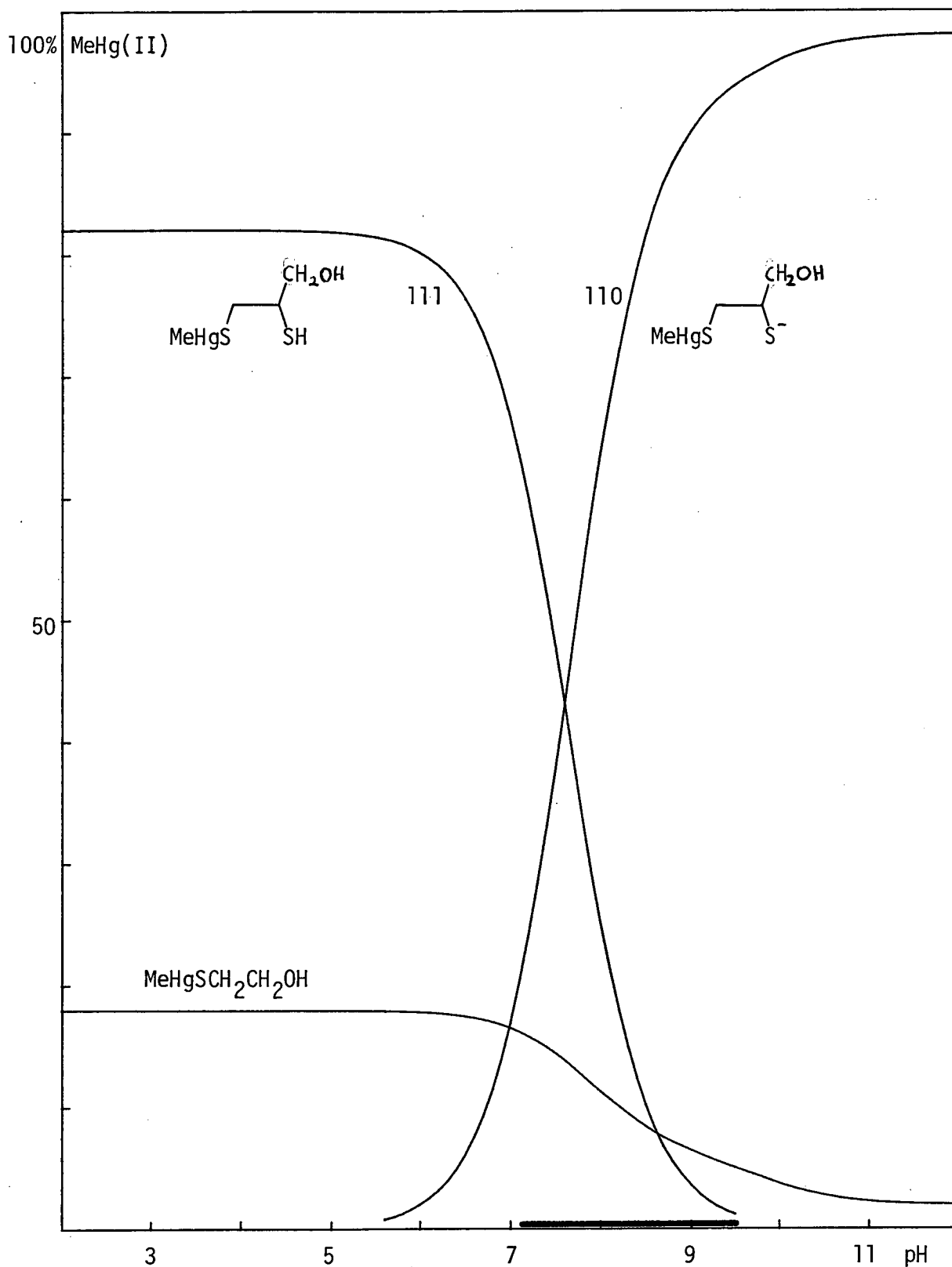


Figure 3.26A: Species distribution calculated by COMIX for 0.0014M MeHg(II), 0.0014M BALH<sub>2</sub> and 0.0014M Mercaptoethanol, using the equilibrium constants in Tables 3.6, 3.8, 3.10 and 3.11. The heavy line indicates the pH-range of MINIQUAD81 data.

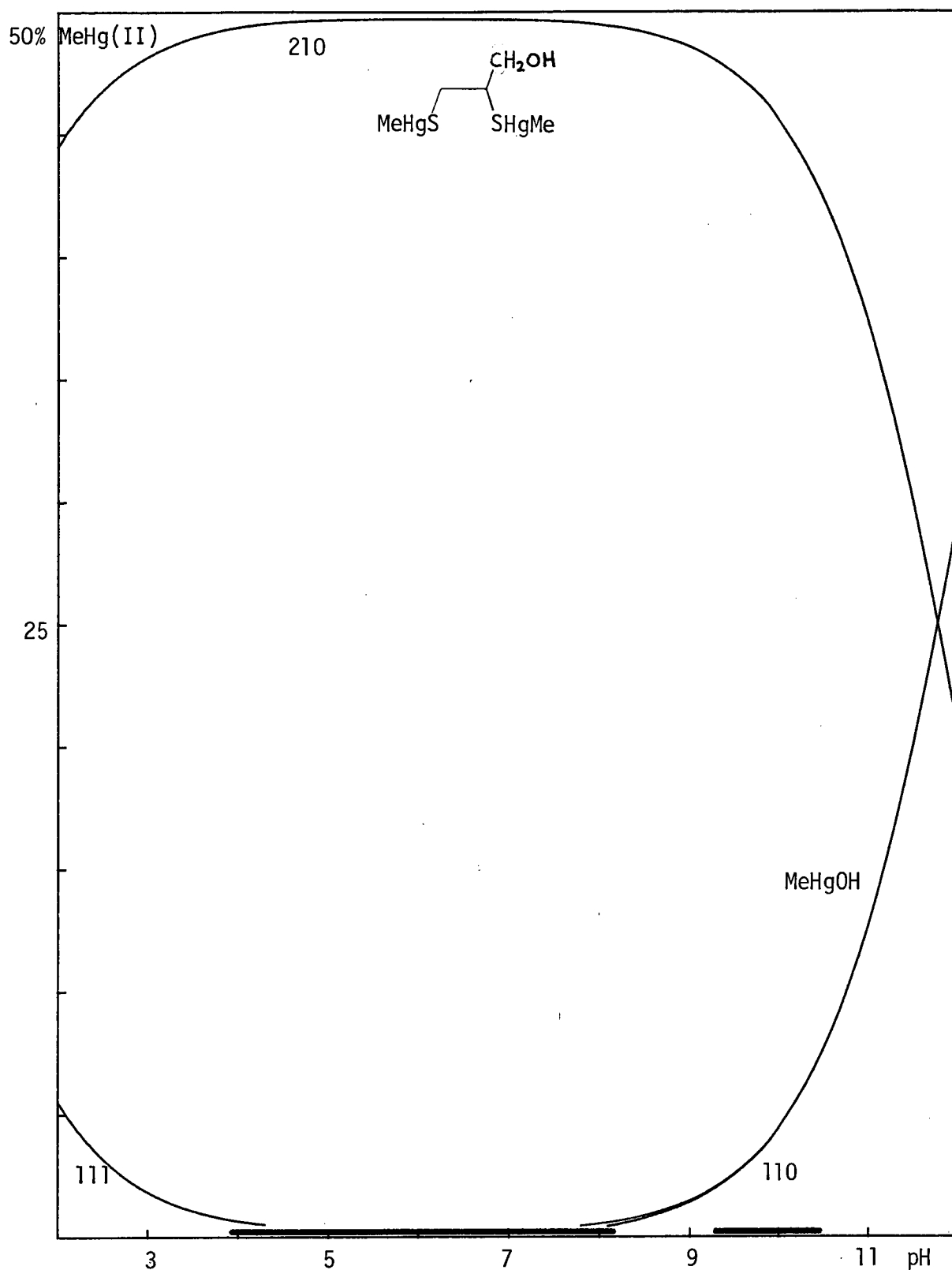
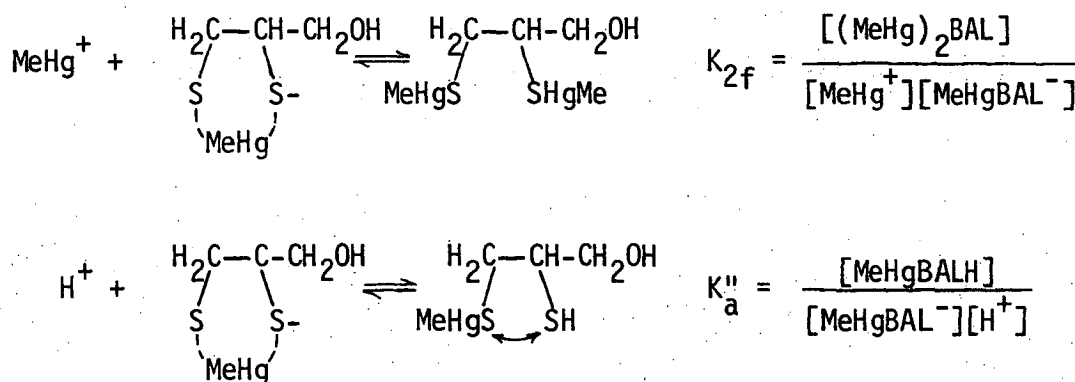


Figure 3.26B: Species distribution calculated by COMIX for 0.002M MeHg(II) and 0.001M BALH<sub>2</sub>, using the equilibrium constants in Tables 3.10 and 3.11.

The heavy line indicates the pH-range of MINIQUAD81 data.

The 1:1 species are depicted on Figure 3.26A.

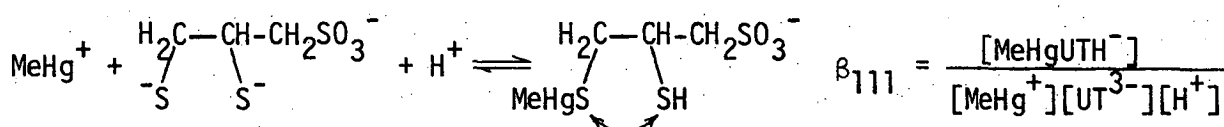
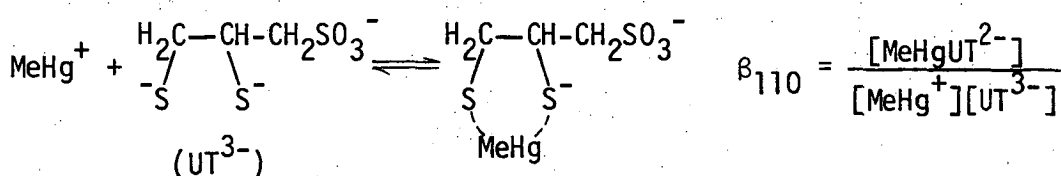
By titration of the 2:1 system in the absence of competing ligands (as for the 2:1 cysteine and penicillamine systems) MINIQUAD81 was able to treat titration data over the range  $5 < \text{pH} < 10$  by assuming that the 1:1 complex,  $\text{MeHgBAL}^-$ , is never dissociated and treating it as a 'ligand'. Calculated and experimental 2:1 titration curves are also shown in Figure 3.25. Equilibrium constants for the following reactions were determined under these conditions and are also recorded in Table 3.11.



The 2:1 species distribution for 0.002M  $\text{MeHg(II)}$  and 0.001M  $\text{BALH}_2$  in the absence of competing ligand is shown in Figure 3.26B.

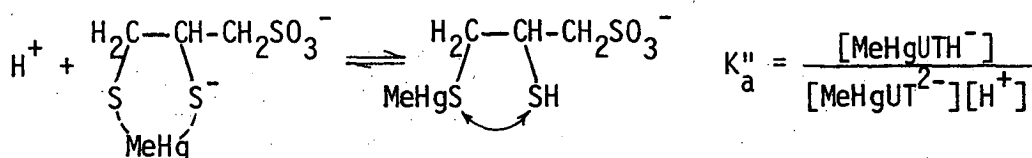
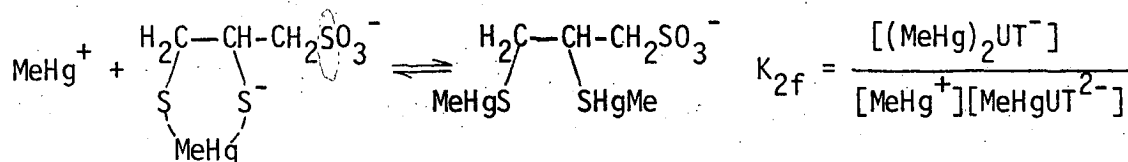
(ii) 2,3-dimercapto-propanesulfonate (sodium salt), Unithiol, was used as received and stored under nitrogen at  $-20^\circ\text{C}$ . The compound is a monohydrate of the sodium salt,<sup>91</sup> mp.  $210^\circ(\text{dec.})$  [lit.<sup>402</sup>  $229(\text{dec.})$ ], and is dehydrated by storage over  $\text{P}_2\text{O}_5$ .<sup>90</sup> However, it was more convenient to weigh the hydrate, as the anhydrous salt was found to be quite hygroscopic. Titration of the hydrate with KOH, and treatment of the data with TITRAT, gave values for the acid dissociation constants shown in Table 3.10, and proton purity of 97.0(7)%. No evidence was found for protonation of the sulfonate group above pH 2. Consequently,  $\text{MeHg(II)}$  species with protonated or complexed sulfonate were not considered in MINIQUAD81 treatments.

Titration of equivalent quantities of Unithiol and MeHg(II) in the presence of iodide indicated that iodide competition is inappropriate as a method of evaluating  $\log \beta_{110}$ , as was the case for BALH<sub>2</sub>. Titration of equivalent quantities of mercaptoethanol, Unithiol and MeHg(II) over the range  $4 < \text{pH} < 11$  and treatment with MINQUAD81, gave values of the constants,  $\log \beta_{110}$  [21.01(8)] and  $\text{pK}'_a$  [7.56(1)] for the species in the equilibria below:



The calculated and experimental 1:1:1 titration curve is shown in Figure 3.27 and the species distribution in Figure 3.28A.

Formation of the 2:1 MeHg(II)-Unithiol complex was evaluated in the absence of competing thiol or iodide, in an identical fashion to that for BALH<sub>2</sub>, to give the constants (Table 3.11) corresponding to the equilibria:



The calculated and experimental titration curve for the 2:1 system is also shown in Figure 3.27, and the distribution diagram for 0.002M MeHg(II) with 0.001M Unithiol, in the absence of competing ligand, in

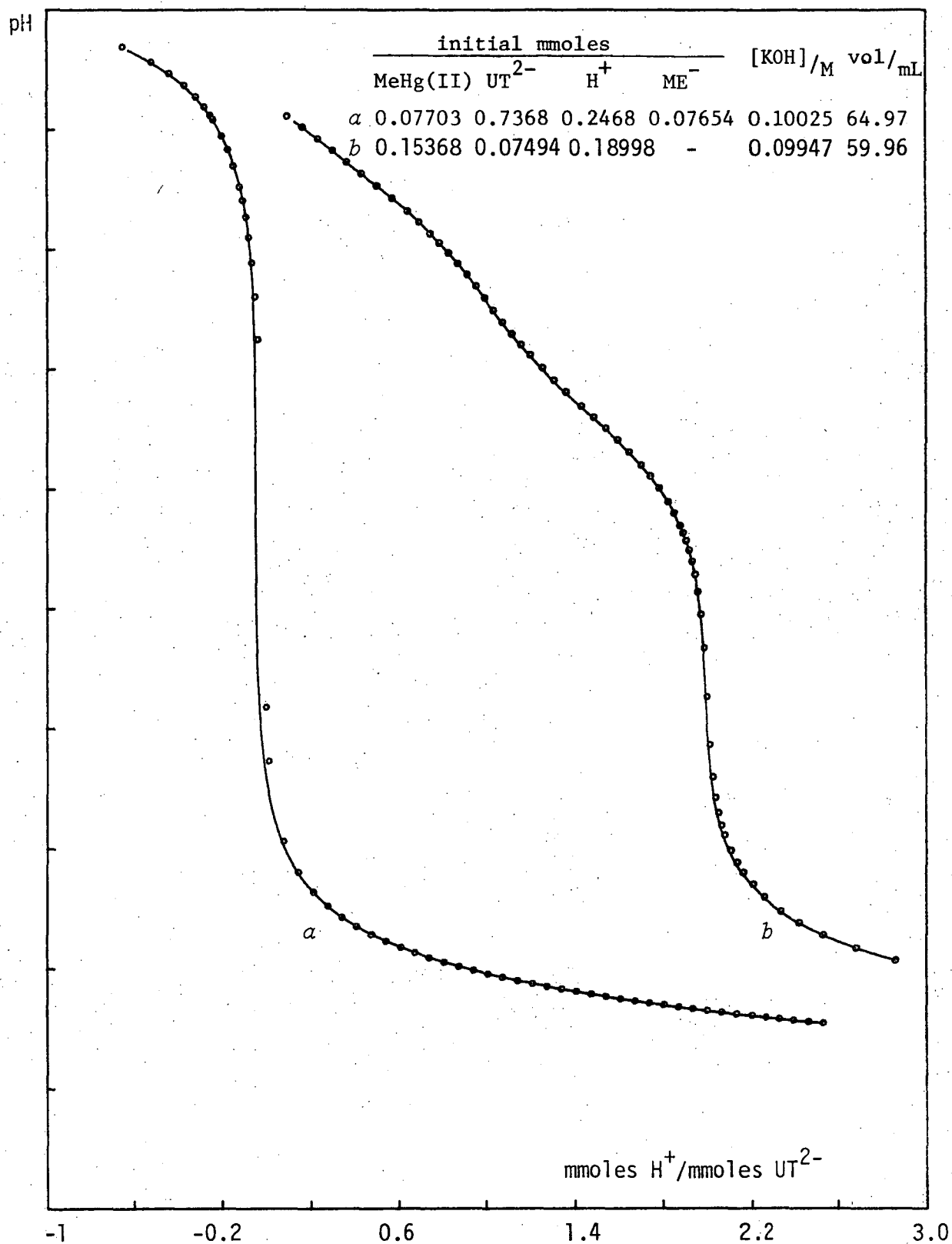
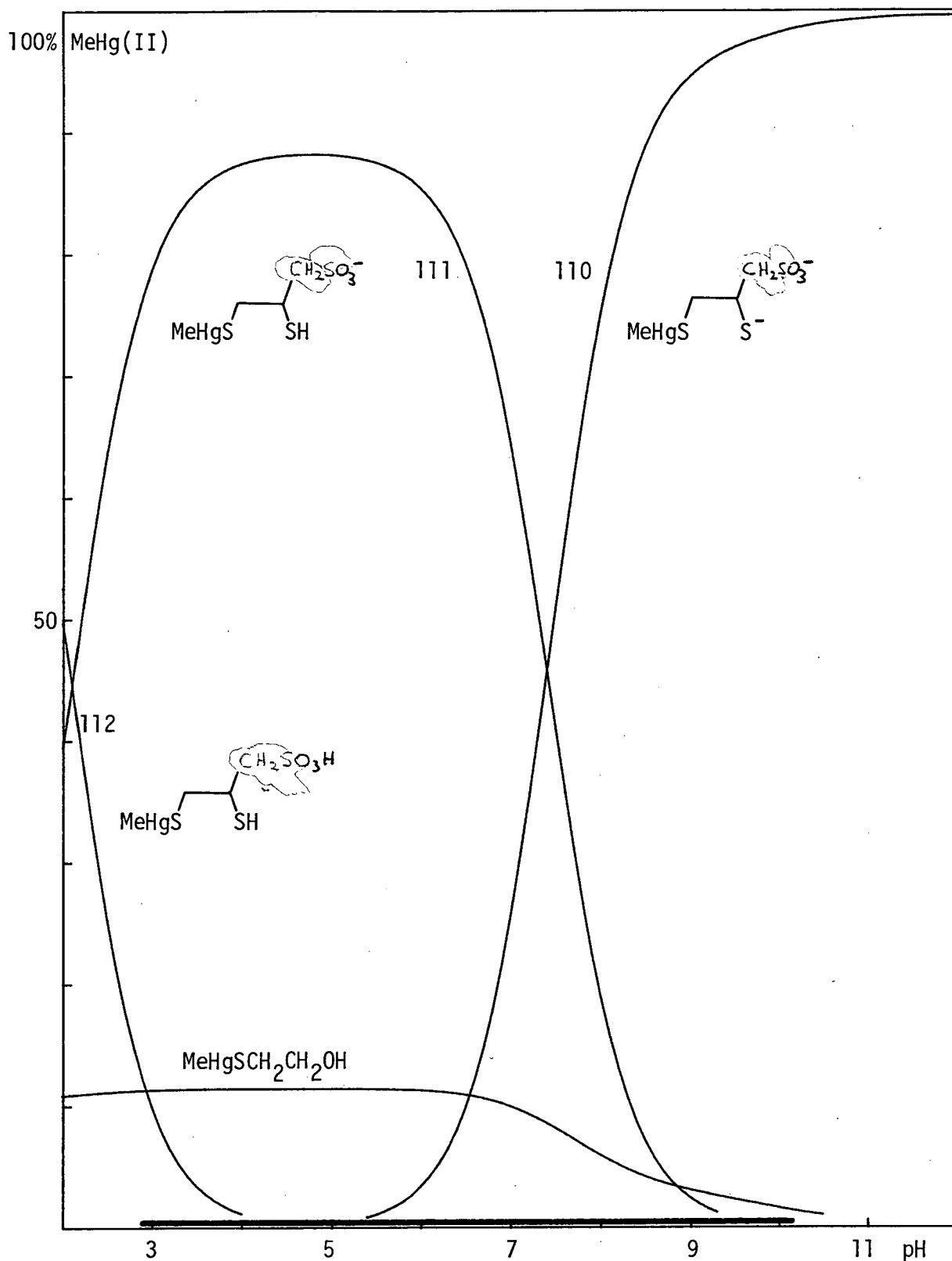


Figure 3.27: Methylmercury(II)-Unithiol (Na[UTH<sub>2</sub>]) titration data.  
*a* with Mercaptoethanol (MEH) competition; *b* with no competing ligand.

The fitted curves were calculated by COMIX, using the equilibrium constants in Tables 3.6, 3.8, 3.10 and 3.11.



**Figure 3.28A:** Species distribution calculated by COMIX for 0.0014M MeHg(II), 0.0014M Unithiol and 0.0014M Mercaptoethanol, using the equilibrium constants in Tables 3.6, 3.8, 3.10 and 3.11. The heavy line indicates the pH-range of MINIQUAD81 data.

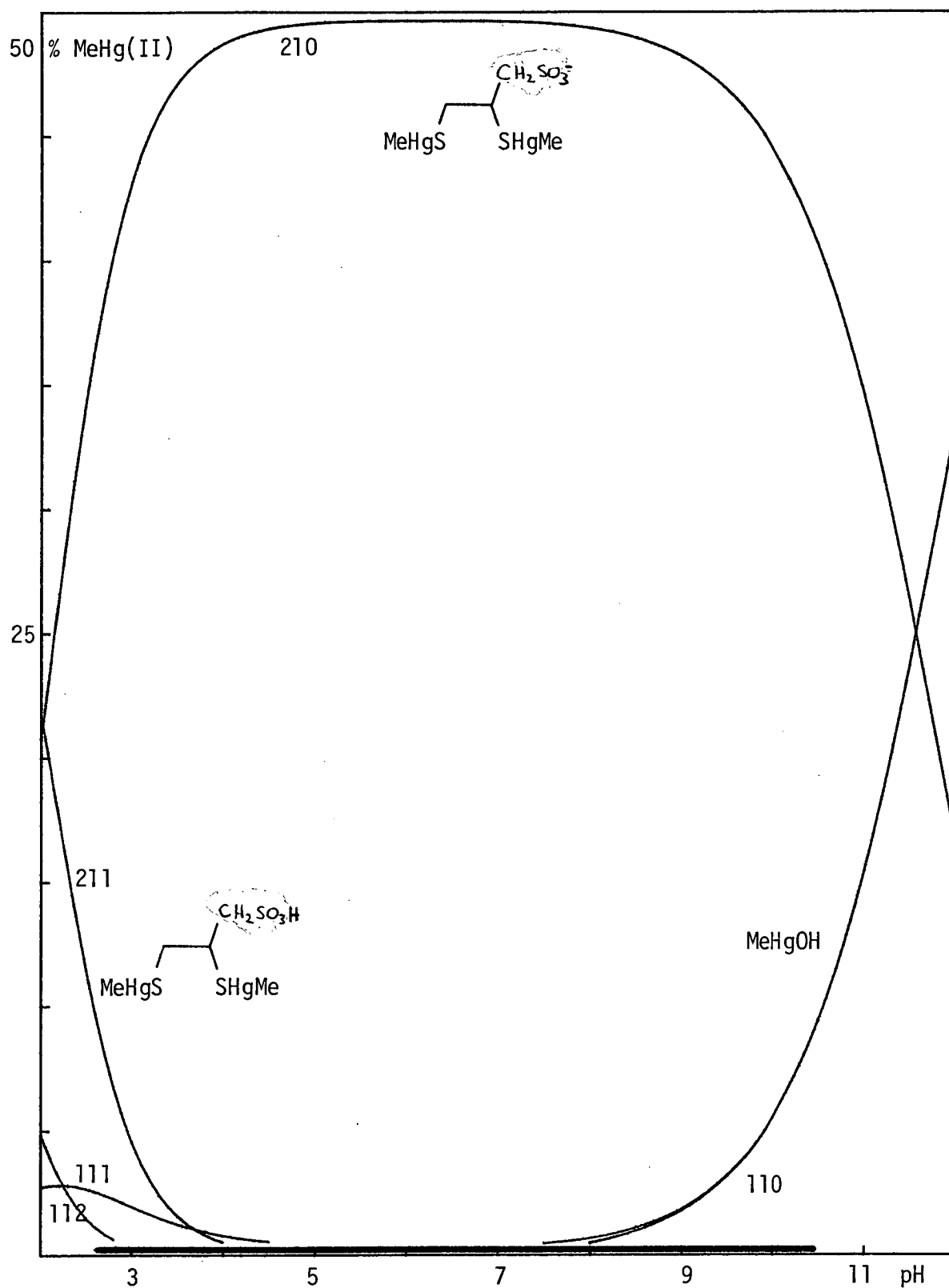


Figure 3.28B: Species distribution calculated by COMIX for 0.002M MeHg(II) and 0.001M Unithiol, using the equilibrium constants in Tables 3.10 and 3.11.

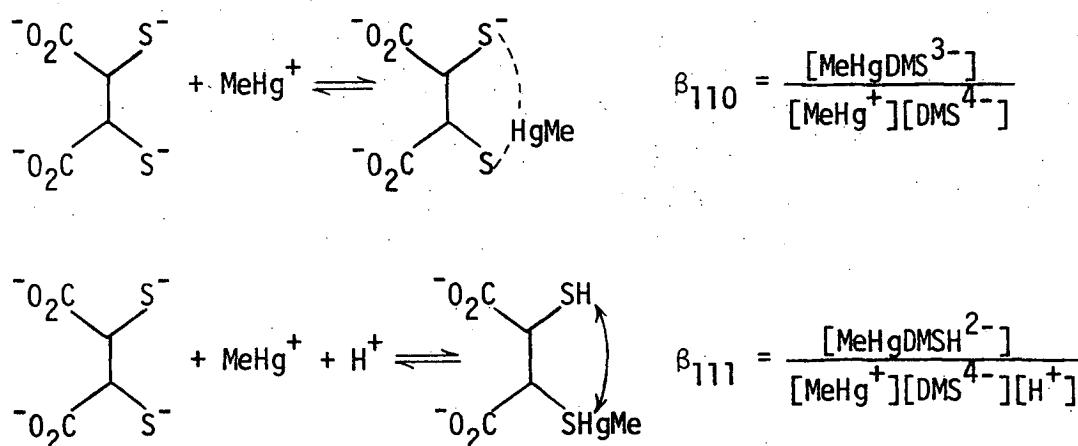
The heavy line indicates the pH-range of MINIQUAD81 data.

The 1:1 species are depicted on Figure 3.28A.

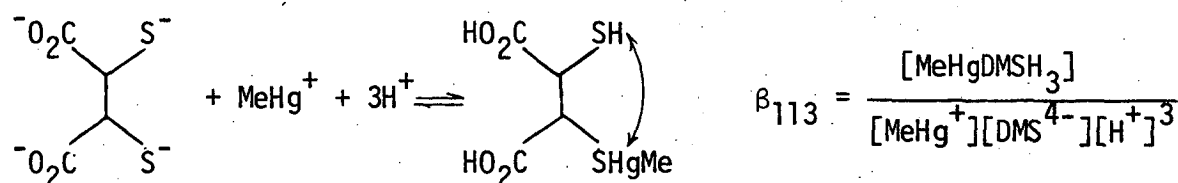
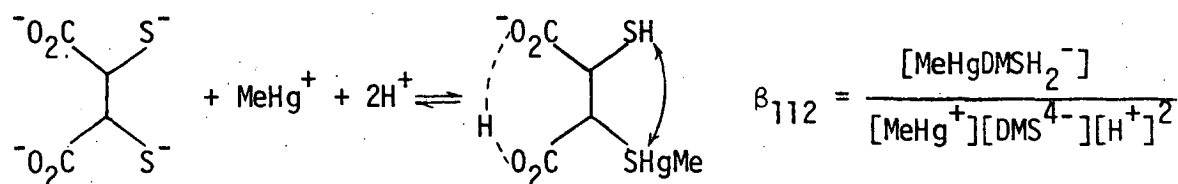
Figure 3.28B.

(iii) meso-2,3-dimercaptosuccinic acid was used as received but stored over  $P_2O_5$  under nitrogen, mp.  $185^\circ$  (dec.) [lit.  $182-5^\circ$ ,<sup>415</sup>  $210-11^\circ$ ,<sup>416</sup> (dec.) ]. Titration with 0.1M KOH, after addition of  $HNO_3$  to pH 2.8 to 3.0, and treatment of the data with TITRAT provided values of the two carboxylic acid and two thiol proton dissociation constants recorded in Table 3.10 and proton purity 97.6(3)%. The value for  $pK_{a4}$  is in least agreement with previously recorded values. The determination of  $pK_a$ 's  $> 10.5$  has been found in this study to be extremely sensitive to the value used for  $K_W^C$ .  $K_W^C$  was treated as a parameter by TITRAT and hence contributes to some of the imprecision of  $pK_{a4}$ . The refined values of  $K_W^C$  for DMSH<sub>4</sub> titrations are entirely consistent with those values found during refinement of acidity constants for all the other thiols used in this study, whereas the value for  $K_W^C$  is often not recorded by other workers or has been taken from previously reported literature values. It is particularly noticeable (Tables 3.8 and 3.10) that large disparities exist in previously recorded  $pK_a$ 's above 10.

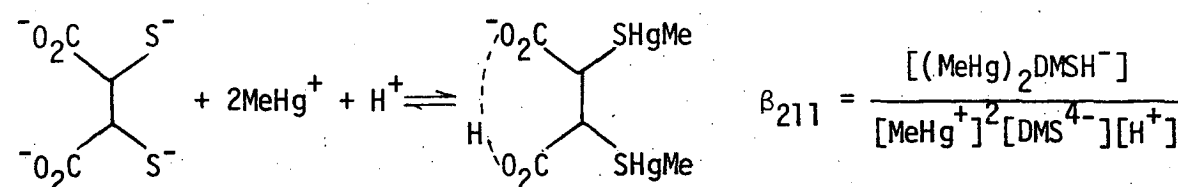
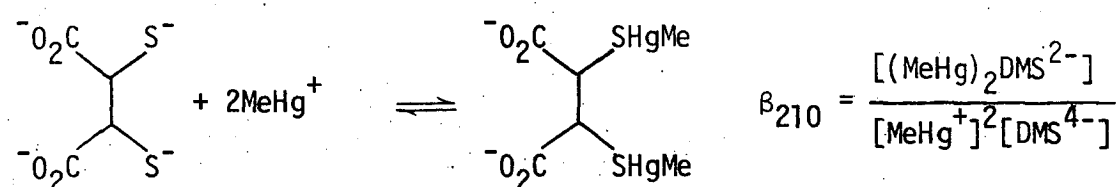
In an equilibrium mixture of DMSH<sub>4</sub> and one equivalent of MeHg(II), the following equilibria involving 1:1 MeHg(II)-DMSH<sub>4</sub> complexes are expected:

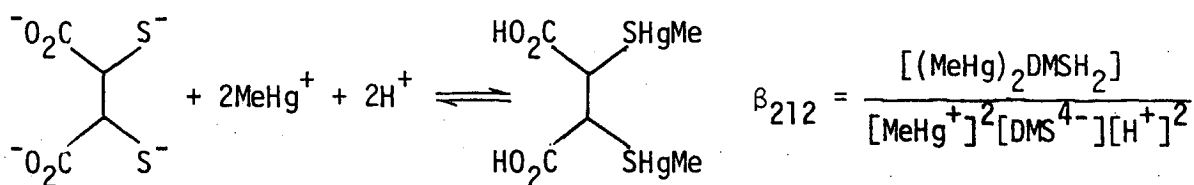






Unlike the 1:1 systems of MeHg(II)-BALH<sub>2</sub> and MeHg(II)-Unithiol, titration of MeHg(II) and DMSH<sub>4</sub> in the presence of mercaptoethanol gave a formation constant for the 1:1 complex,  $\beta_{110}$ , of approximately  $10^{16}$ , accompanied by three successive protonation equilibria as shown. And in contrast to the BALH<sub>2</sub> and Unithiol 1:1 systems, in order to satisfactorily fit the titration data with MINIQUAD81, a series of 2:1 species needed to be simultaneously included. Unsatisfactory results were obtained by simultaneous refinement of all 1:1 and 2:1 constants, since these were highly correlated, but the 2:1 constant  $\beta_{210}$  was indicated to be in the range  $10^{14}$ - $10^{16}$ . Iodide competition was therefore necessary to obtain the 2:1 formation constants for the equilibria shown:





Titrations of  $\text{DMSH}_4$  solutions containing more than two equivalents of  $\text{MeHg(II)}$  in the presence of iodide where the 1:1 species can be neglected, gave values for the overall formation constant for the 2:1 mono-protonated complex,  $\beta_{211}$  but not for the diprotonated complex,  $\beta_{212}$ . The twice protonated 2:1 complex has been isolated and characterised in the solid state (page 38). The formation constant of the unprotonated 2:1 complex,  $\beta_{210}$ , could not be refined precisely since the system is highly correlated, however MINQUAD81 consistently indicated a value  $\log \beta_{210} \sim 14$ . The value for  $\beta_{210}$  of  $10^{14}$  was fixed in a subsequent MINQUAD81 refinement of the formation constants corresponding to the unprotonated, once and twice protonated 1:1 species and once protonated 2:1 species over the range  $4 < \text{pH} < 10$  in the presence of 0.1M KI, to give the refined values shown in Table 3.11. The calculated and experimental titration curves are shown in Figure 3.29.

Using the formation constants for the 2:1 and 1:1 complexes shown in Table 3.11, the distribution diagram was calculated for a 1:1 ratio of  $\text{MeHg(II)}:\text{DMSH}_4$  in the presence of 0.1M iodide. Figure 3.30 indicates the complexity of the system, which involves six  $\text{MeHg(II)}$  species at significant concentrations in the range  $2 < \text{pH} < 12$ .

A comparison of the 1:1 and stepwise 2:1 formation constants for  $\text{MeHg(II)}$  complexation with Unithiol,  $\text{BALH}_2$  and  $\text{DMSH}_4$  is of interest (Table 3.12). It can be seen that Unithiol and  $\text{BALH}_2$  form 1:1 species with enhanced stability compared to  $\text{DMSH}_4$  and monothiolates. The high stability of these 1:1 complexes is not solely due to high sulphydryl basicity, since the sulphydryl groups of  $\text{DMSH}_4$  are more basic than those

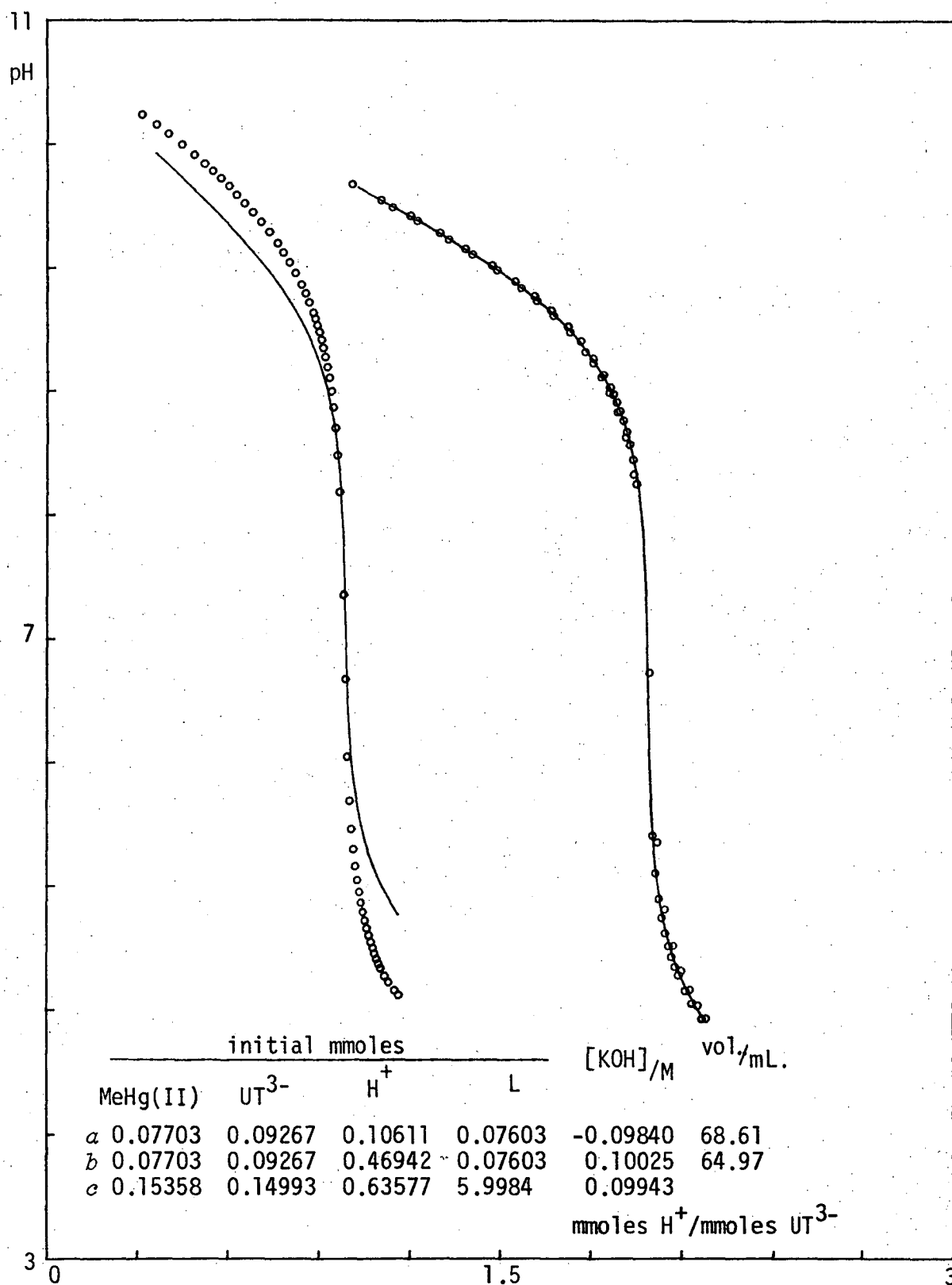
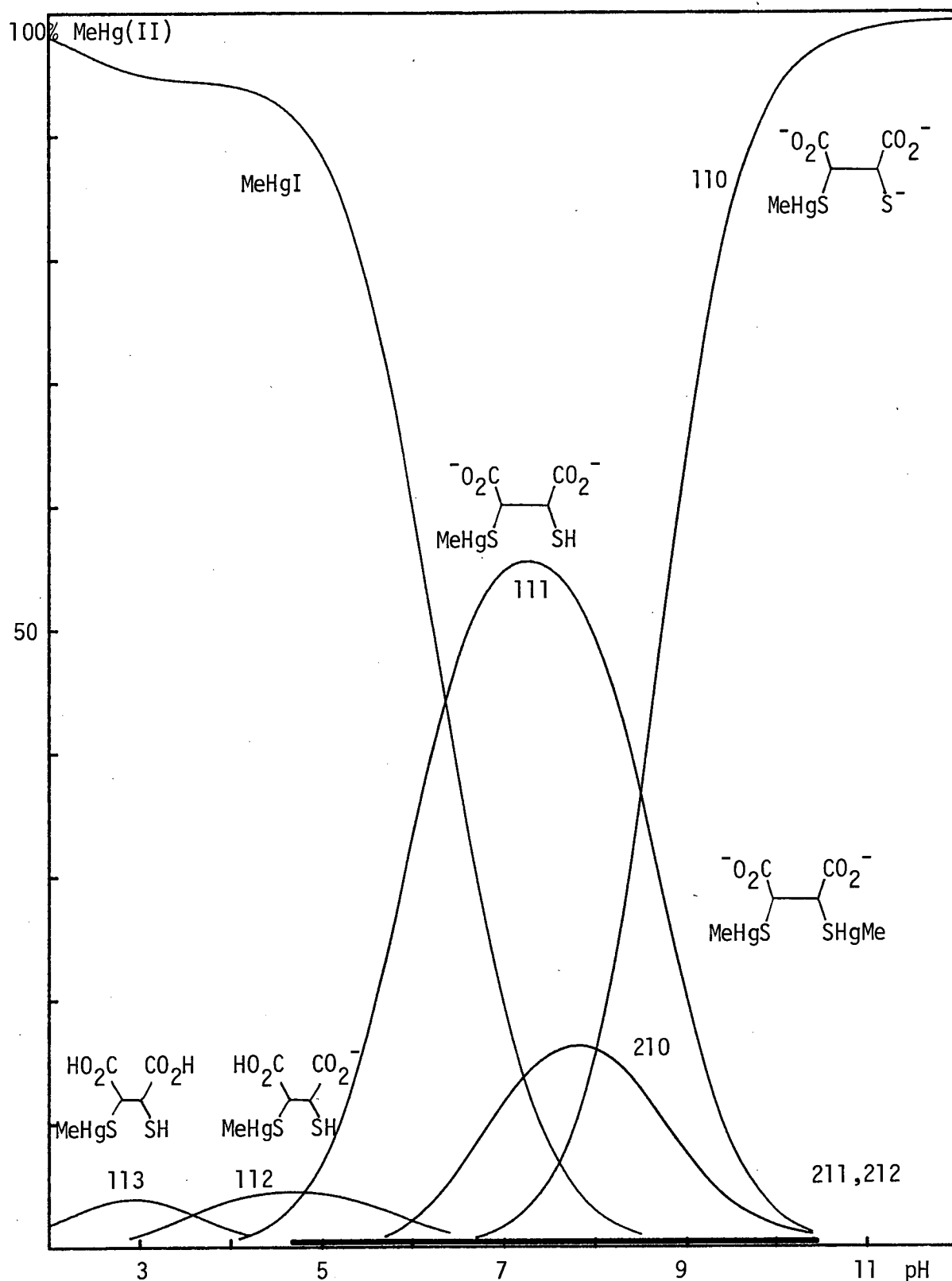


Figure 3.29: Methylmercury-Unithiol (Na[UTH<sub>2</sub>]) titration data.

a,b with mercaptoethanol (L=ME<sup>-</sup>) competition

c with iodide competition (L=I<sup>-</sup>)

The fitted curves were calculated by COMIXH, using the equilibrium constants in Tables 3.6, 3.8, 3.10 and 3.11 with  $\log \beta(\text{MeHgI}) = 8.500$ .



**Figure 3.30:** Species distribution calculated by COMIX for 0.0014M MeHg(II) and 0.0014M DMSH<sub>4</sub> in 0.1 KI, using the equilibrium constants in Tables 3.10 and 3.11.

Note the existence of a 2:1 species (green) at these concentrations. The heavy line indicates the pH-range of MINIQAD81 data.

of  $\text{BALH}_2$  and Unithiol. The carboxylate groups of  $\text{DMSH}_2^{2-}$  do not appear to reduce the Brønsted basicity of the sulfhydryl donors and it is unlikely that an electronic effect could produce the marked reduction in  $\text{MeHg(II)}$  affinity.

ligand	$\log \beta_{110}^a$	$\log \beta_{210} - \log \beta_{110}^b$	$\text{pK}_{a1}(\text{SH})$	$\text{pK}_2(\text{SH})$
Unithiol	21.01(8)	10.26(7)	11.38(2)	8.69(1)
$\text{BALH}_2$	19.56(9)	10.47(10)	10.62(1)	8.65(1)
$\text{DMSH}_4$	17.11(3)	$\sim 14$	11.50(1)	9.65(1)
mercaptoacetic acid <sup>c</sup>	17.10(1)		10.16(1)	

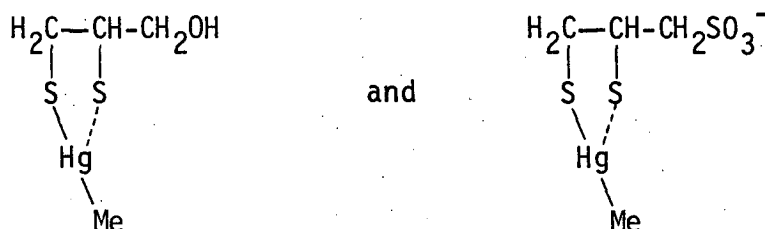
**Table 3.12:** Methylmercury(II)-sulfhydryl association constants for the dithiolate antidotes.

<sup>a</sup>indicates the magnitude of binding of one  $\text{MeHg(II)}$  group to the dithiolate.

<sup>b</sup>indicates the magnitude of binding of  $\text{MeHg(II)}$  to the remaining sulfhydryl group of the 1:1 complex.

<sup>c</sup>typical monothiol included for comparison. Data taken from Tables 3.6 and 3.8.

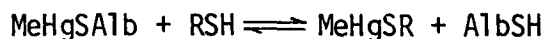
The enhanced stability is attributed to a chelate effect due to bridging  $\text{MeHg(II)}$  in the 1:1 complexes of Unithiol and  $\text{BALH}_2$  as shown



The absence of such bridging in the 1:1 MeHg(II)-DMSH<sub>4</sub> complex may be due to an unfavorable conformation of the meso-dicarboxylic acid, possibly caused by steric or electrostatic effects of the two bulky negatively charged carboxylate groups. The 2:1 complexes for the three vicinal dithiols all have overall formation constants in the range 10<sup>30</sup> to 10<sup>31</sup>. Thus it would appear that the structures of the 2:1 complexes may be similar, and may all involve either simple monodentate MeHg-S bonding, or chelated structures similar to that found by Moore *et al.* for the 2:1 MeHg(II) complex of *trans*-1,2-cyclohexane-dithiol<sup>230</sup> (Figure 2.4, page 42). Such chelating behaviour may also be present in solution in the 1:1 complexes of Unithiol and BALH<sub>2</sub>. There does not appear to be definitive vibrational spectroscopic evidence for MeHg(II) chelation in the solid-state of these 2:1 antidotal dithiol complexes (Chapter 2).

### 3.4 Interactions of antidotal thiols with MeHg(II) *in vivo*

The mechanisms of MeHg(II) toxicity will not be discussed here but it is assumed that interactions with endogenous sulphydryl groups are of primary importance (Chapter 1). The modes of action of several monothiols and vicinal dithiols for which stability constant data have been obtained in this study, will be discussed in terms of their competition with biological sulphydryl groups for MeHg(II). It is further assumed that the antidotal thiols (RSH) which will be protonated at physiological pH act by removing MeHg(II) from binding sites of a model protein, mercaptalbumin, AlbSH, according to the rapidly established equilibrium:



The physicochemical properties of the complex MeHgSR are assumed to be primarily responsible for the subsequent pattern of methylmercury redistribution and, hopefully, excretion. Polar and/or charged complexes are expected to be amenable to rapid renal clearance. In contrast, relatively non-polar, uncharged species are expected to have enhanced lipid solubility, thus facilitating possible redistribution through lipid membranes, in particular, the blood-brain barrier.

### 3.4.1 Physiological pH

In order to predict the metal-ligand species distribution in a simple biological model, some estimate must be made of the 'pH' at or near the site of metal interaction, e.g. in blood plasma, inside erythrocytes or at the surface of cell membranes, etc. The pH of many biological environments has been measured by both intrusive methods, e.g. micro pH-electrodes<sup>417</sup> or indirect methods, e.g. monitoring phosphate equilibria *in vivo* by <sup>31</sup>P nmr.<sup>418</sup>

In this study, no attempt has been made to examine actual sites of MeHg(II) binding *in vivo*. In discussing the possible existence of methylmercury(II) thiolate species in extremely simplistic models of biological systems, it has been assumed that the pH of the interactive site is near 7.4.<sup>†</sup> Since no effort has been made to propose a complex system of competing ligands, e.g. a plasma model such as that used for Ca<sup>2+</sup>, Mg<sup>2+</sup>, Mn<sup>2+</sup>, Fe<sup>3+</sup>, Cu<sup>2+</sup>, Zn<sup>2+</sup>, Pb<sup>2+</sup> speciation,<sup>419</sup> it was felt that this pH represents a reasonable value for the sake of chemical rather than toxicological discussion. Further, it will be seen that

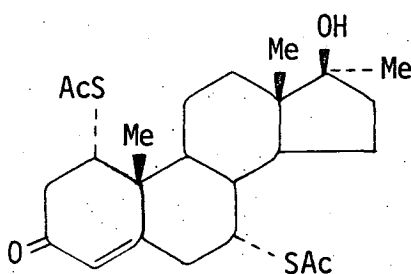
---

<sup>†</sup> pH 7.40 is the generally accepted value for plasma pH under conditions of pCO<sub>2</sub> = 5.33 kPa and constant saturation-fraction of O<sub>2</sub> in arterial blood at 37°. <sup>420</sup>

in most cases discussed here, variations in pH in the range 6.0 to 8.0 have little effect on conclusions drawn at pH 7.4. In addition, it should be realised that the site of interaction may not even be in an environment of constant pH, since many of the multitudinous reactions in cell metabolism involve protolytic equilibria and which may be dependent on the partial pressures of oxygen and  $\text{CO}_2$ .<sup>417</sup>

### 3.4.2 Competition of antidotal thiols with endogenous ligands *in vivo*

For an antidotal thiol to remove intracellularly bound  $\text{MeHg(II)}$  from protein binding sites, it must firstly be capable of reaching the target cell without undergoing appreciable metabolic breakdown. Cysteine and glutathione are unsuitable as antidotes since they are readily incorporated into normal metabolic pathways,<sup>354</sup> and in fact, glutathione has been shown to increase the  $\text{MeHg(II)}$  content of the brain after administration to mice.<sup>82</sup> The metabolic product of some antidotes may be more active than the administered form, e.g. the substituted steroid thiomestron (below) has some antidotal activity towards  $\text{HgCl}_2$  and  $\text{MeHgCl}$  which may be due to the deacetylated (sulfhydryl form).<sup>120</sup>



Once transported to the  $\text{MeHg(II)}$  binding area, the thiolate must be suited to passage through the cell membrane to the presumed intracellular binding site. Here it must compete effectively with endogenous ligands to form a  $\text{MeHg(II)}$  complex having the required properties to pass out of the cell, and which may be sufficiently water soluble to be renally excreted. Lipophilic  $\text{MeHg(II)}$  complexes may be excreted with the



bile into the gut, where they may be localised by thiol-containing polymers (page 18).

Both methods of treatment require that the antidote compete effectively for MeHg(II) in comparison with endogenous ligands. Since many of these ligands will contain sulfhydryl groups, thiol antidotes are generally used (Chapter 1). Effective competition need not imply that the MeHg(II)-antidote complex predominate at the site of interaction. If the antidotal thiol-complex is highly mobile, even a relatively low concentration of the complex may serve to remove MeHg(II) from protein bound sites. For this reason, low molecular weight, highly polar thiols are usually effective at mobilising MeHg(II). A high negative correlation between molecular weight and the ability of thiol to mobilise inorganic mercury from bovine hemoglobin *in vitro* has been demonstrated.<sup>421</sup> The distribution of the antidotal-thiol complex between lipid and aqueous phases is crucial in determining the redistribution of MeHg(II). In this context, BALH<sub>2</sub> is a poor antidote for MeHg(II) intoxication, since it is found to redistribute the metal into the brain.<sup>66-7</sup>

In discussing postulated equilibria involving MeHg(II), antidotal thiols and endogenous ligands *in vivo*, it will be assumed that MeHg(II) is initially complexed to protein with a stability constant of  $10^{17}$ , similar to that calculated by Simpson<sup>324</sup> from Hughes' data for human mercaptalbumin<sup>368</sup> (page 85 ). Further, it has been assumed that the effective 'concentration' of protein sulfhydryl groups is 10 mM at the binding site, which is the total sulfhydryl content of human erythrocyte proteins.<sup>354</sup> A 5,000-fold excess of sulfhydryl groups over MeHg(II)<sup>359</sup> ( $2 \times 10^{-7}$  M) has been considered. This is typical at the MeHg(II) levels at which toxic symptoms first appear.<sup>422</sup>

Although MeHg(II) has been found to be predominantly in the form

of a hemoglobin complex in erythrocytes, formation constants with hemoglobin are unknown.

It is more difficult to estimate the antidote concentration at the active site. Under conditions used for animal studies, typically the antidote is given at a level more than 100 times greater than the MeHg(II) burden. If 1 g of antidotal monothiol with M.Wt. 200 was equally dispersed throughout 5 L of body fluids, its concentration would be 1 mM. As a comparison, the cellular glutathione concentration is 0.1-10 mM.<sup>423</sup> A preliminary *in vitro* distribution of MeHg(II)-DMSH<sub>4</sub> species using this antidote:metal ratio was presented at a conference in 1981 and is included as Appendix 1 of this thesis. Figure 3.31 shows conditional stability constants calculated under the above conditions for the antidotal thiols penicillamine and N-acetylpenicillamine, and the dithiols BALH<sub>2</sub>, DMSH<sub>4</sub> and Unithiol obtained in this work. Human mercaptalbumin, described above, is included for comparison. The MeHg(II) species distribution diagrams for each of these antidotal thiols in the presence of human mercaptalbumin, are shown in Figure 3.32. Although a chloride concentration of 0.1M was included in the COMIX calculation to simulate the plasma chloride content,<sup>424</sup> MeHgCl is negligible on the scale shown.

The relative proportions of protein-bound and antidote-bound MeHg(II) species will vary considerably due to errors in the postulated concentrations of MeHg(II), antidotal, and protein thiols, but the pH-dependence of the species distribution will not. Therefore to assess antidotal activity, we may consider the nature of the major predicted antidotal-thiol MeHg(II) species at pH 7.4, irrespective of whether it predominates over protein-bound MeHg(II).

For the antidotal thiols shown, except BALH<sub>2</sub>, it can be seen that all the major MeHg(II) thiolate species are anionic at pH 7.4. It is

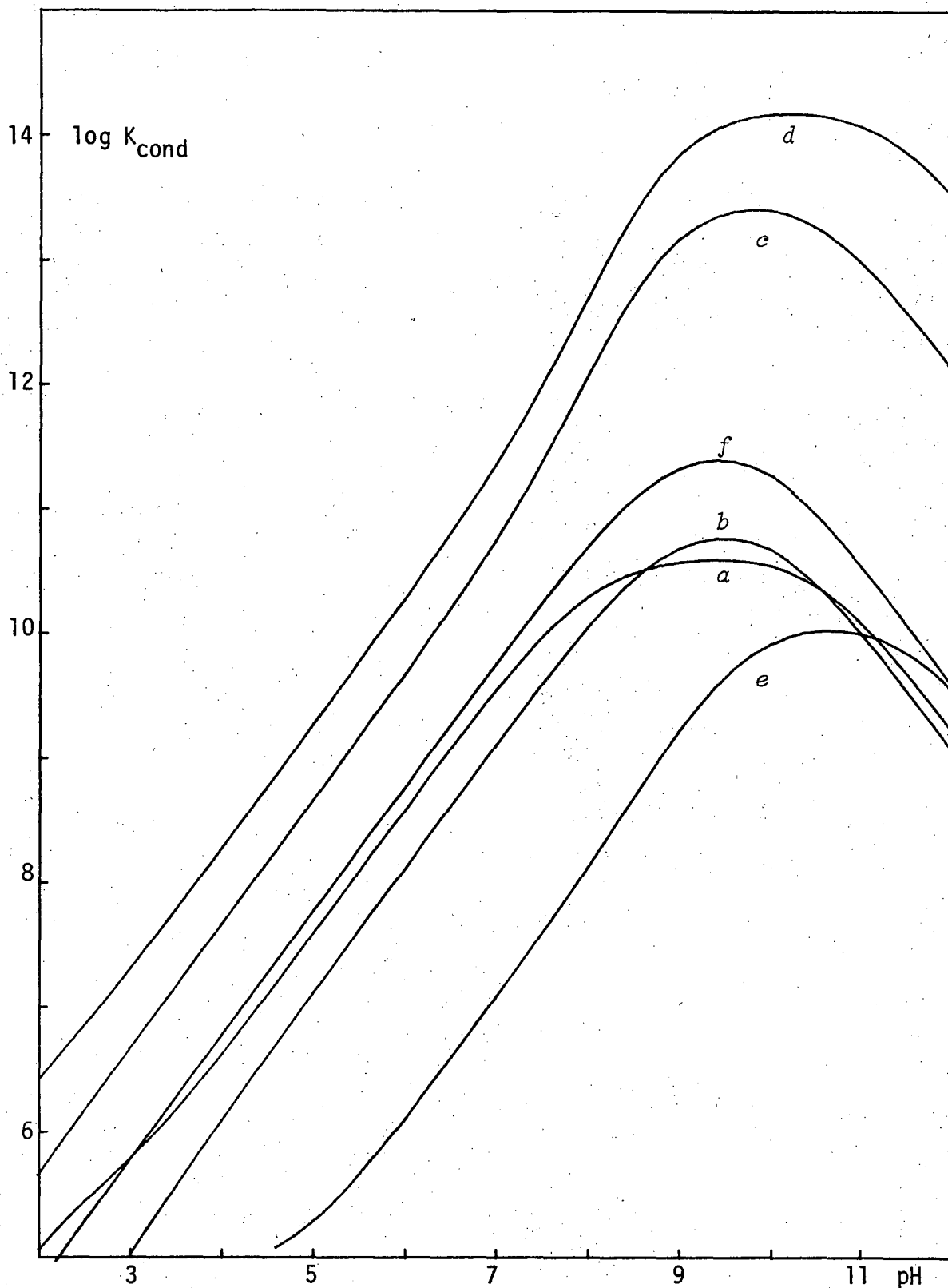


Figure 3.31: Conditional stability constants of antidotal thiols and dithiols with MeHg(II).

Calculated using the equilibrium constants in Tables 3.6, 3.8, 3.10 and 3.11 for  $2 \times 10^{-7}$  M MeHg(II) and 0.1 M chloride with 0.001 M thiols:

*a* DL-penicillamine, *b* N-acetyl-DL-penicillamine, *c* BALH<sub>2</sub>,  
*d* Unithiol and *e* DMSH<sub>4</sub>.

*f* mercaptalbumin (0.010 M) is included for comparison.

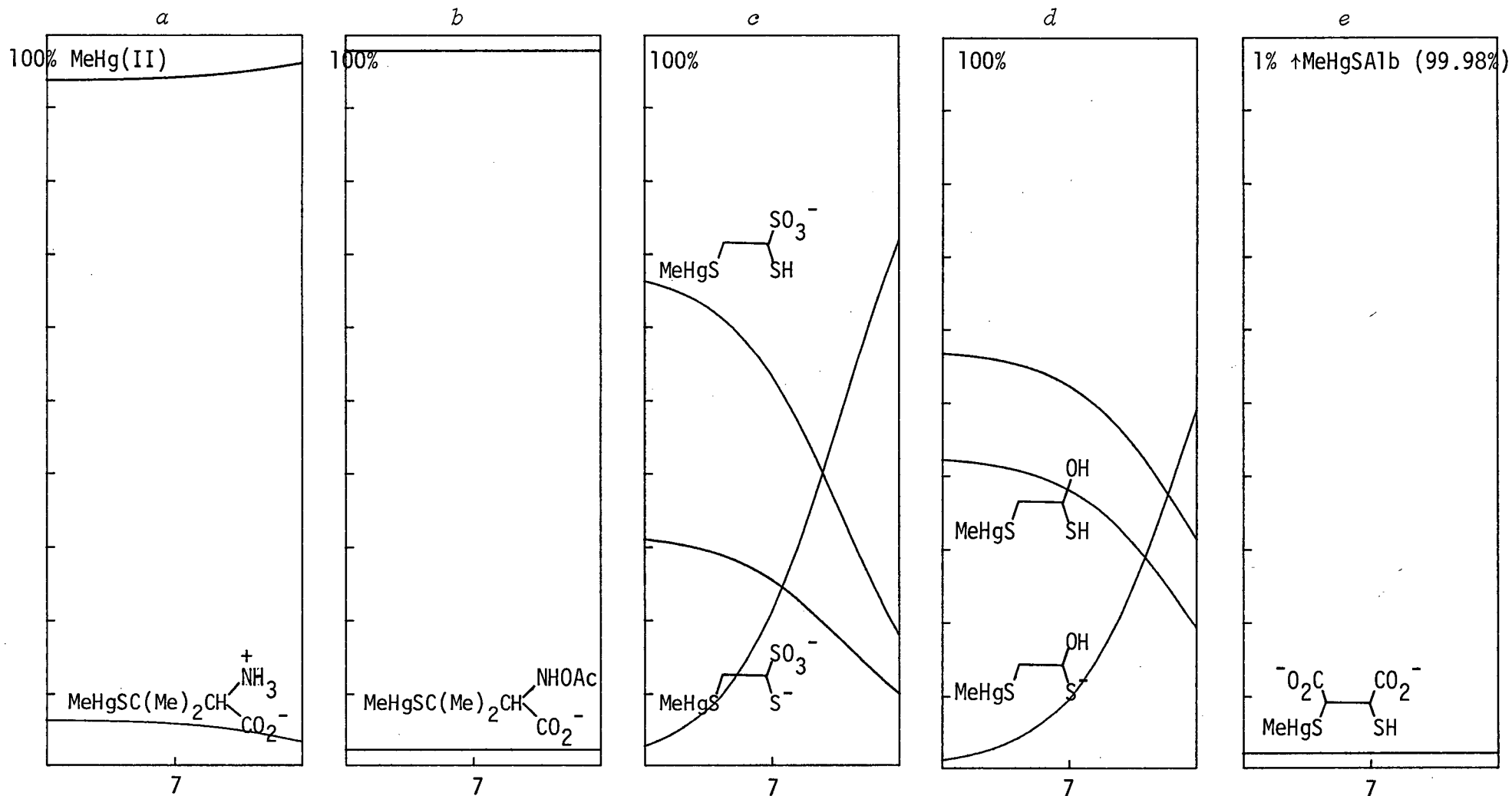


Figure 3.32: Species distribution in the range  $6 < \text{pH} < 8$  calculated by COMIX for  $2 \times 10^{-7} \text{ M}$  MeHg(II);  $0.10 \text{ M}$  Chloride,  $10 \times 10^{-3} \text{ M}$  Mercaptoalbumin (AlbSH) and  $1 \times 10^{-3} \text{ M}$  antidotal thiols: a) DL-Penicillamine, b) N-Acetyl-DL-Penicillamine, c) Unithiol, d) BALH<sub>2</sub> and e) DMSH<sub>4</sub>. Equilibrium constants are taken from Tables 3.6, 3.8, 3.10 and 3.11. MeHg(II)-antidote species are shown in red, MeHgSA1b in green. Note the different scale for DMSH<sub>4</sub>.

expected that these species would have high aqueous and relatively low lipid solubility. All are 1:1 species, consistent with the low MeHg:thiolate ratio at the active site.

The situation with  $\text{BALH}_2$  is unique in this series of thiols in that a large proportion of the  $\text{MeHg(II)-BAL}$  complex is uncharged at pH 7.4 and probably relatively lipophilic. This presumably is responsible for the ready passage of BAL-complexed  $\text{MeHg(II)}$  through the blood/brain barrier. The species  $(\text{MeHg})_2\text{BAL}$  is present at a concentration of  $10^{-17}\text{ M}$  under these conditions, too low to affect  $\text{MeHg(II)}$  redistribution. The low formation constants of  $\text{DMSH}_4$  result in a very small fraction of antidote-bound  $\text{MeHg(II)}$  compared with the other thiols shown. This antidote has been shown to effectively increase urinary  $\text{MeHg(II)}$  excretion however (page 15 ), supporting the hypothesis that only small concentrations of mobile low molecular weight species are necessary for efficient  $\text{MeHg(II)}$  transport.

### 3.5 Methylmercury(II) interactions with selenium donors in aqueous solution

#### 3.5.1 MeHg(II)-selenolate equilibria

There is indirect evidence from  $^1\text{H}$  nmr studies that selenium in selenoamino acids<sup>404</sup> and selenocyanate<sup>323</sup> has a higher affinity for  $\text{MeHg(II)}$  than sulfur in corresponding mercaptoamino acids and thiocyanate. The pH-dependence of chemical shift data for  $\text{MeHgSeCN}$  has been used to show that the formation constant of this complex (Table 3.2) is 0.72 log units higher than for  $\text{MeHgSCN}$ .<sup>323</sup> For several selenoamino acids, the evidence relies on the observation that  $|^2\text{J}(^1\text{H}-^{199}\text{Hg})|$  is smaller than for analogous mercaptoamino acids. Similarly  $|^2\text{J}(^1\text{H}-^{199}\text{Hg})|$  is smaller for selenocyanate than for thiocyanate<sup>323</sup> and selenide than for sulfide.<sup>323</sup>

Formation constants for MeHg(II) with selenohydryl-containing ligands are of some interest, considering the presence of reduced selenol groups in glutathione peroxidase<sup>176</sup> and glycine reductase,<sup>179</sup> and the uncertain method by which selenium reduces the toxicity of MeHg(II) (page 27). Furthermore, selenols are stronger Brønsted acids than are thiols, e.g. selenocholine has a selenohydryl  $pK_a = 4.68(5)$ ,<sup>425</sup> while thiocholine has  $pK_a = 7.883(4)$  (Table 3.6), yet <sup>1</sup>H nmr evidence indicates the possibility of higher MeHg(II) stability constants with selenols than for thiols. Because no MeHg(II)-selenohydryl formation constants have been reported to date, some consideration was given in this work to the potentiometric study of these systems.

Most of the monothiols investigated in this work have previously reported selenium analogs. The ease of oxidation of the selenohydryl group renders these ligands difficult to prepare and maintain in a pure state, e.g. Zdansky doubts whether selenocysteine and selenohomocysteine have been obtained in pure forms.<sup>426</sup> The fairly lengthy published synthetic routes to selenocysteine,<sup>427-8</sup> selenopenicillamine<sup>429</sup> and selenocholine<sup>425</sup> were not attempted. 2-Selenoethanol was prepared in low yield by reduction of the diselenide,<sup>430</sup> but the oily compound was difficult to handle and decomposed when stored over molecular sieves (page 360). Selenoglutathione does not seem to have been isolated in an unprotected form (Table 5.1).<sup>431</sup> 2-Selenosuccinic acid is unknown (but see page 241 for a possible synthesis).

Because the complex MeHgSeCH<sub>2</sub>CO<sub>2</sub>H had been prepared for solid-state characterisation of MeHg(II)-selenolates (page 220), attempts were made to study the MeHg-selenoacetate system in solution. The proton nmr spectrum of this complex (Figure 3.33) has  $|^2J(^1H-^{199}Hg)|$  166.5 Hz, which is smaller than that for the analogous thiolato complex (170.0 Hz, page 359), but the difference is less than that for the seleno-amino acids reported by Sugiura<sup>404</sup>

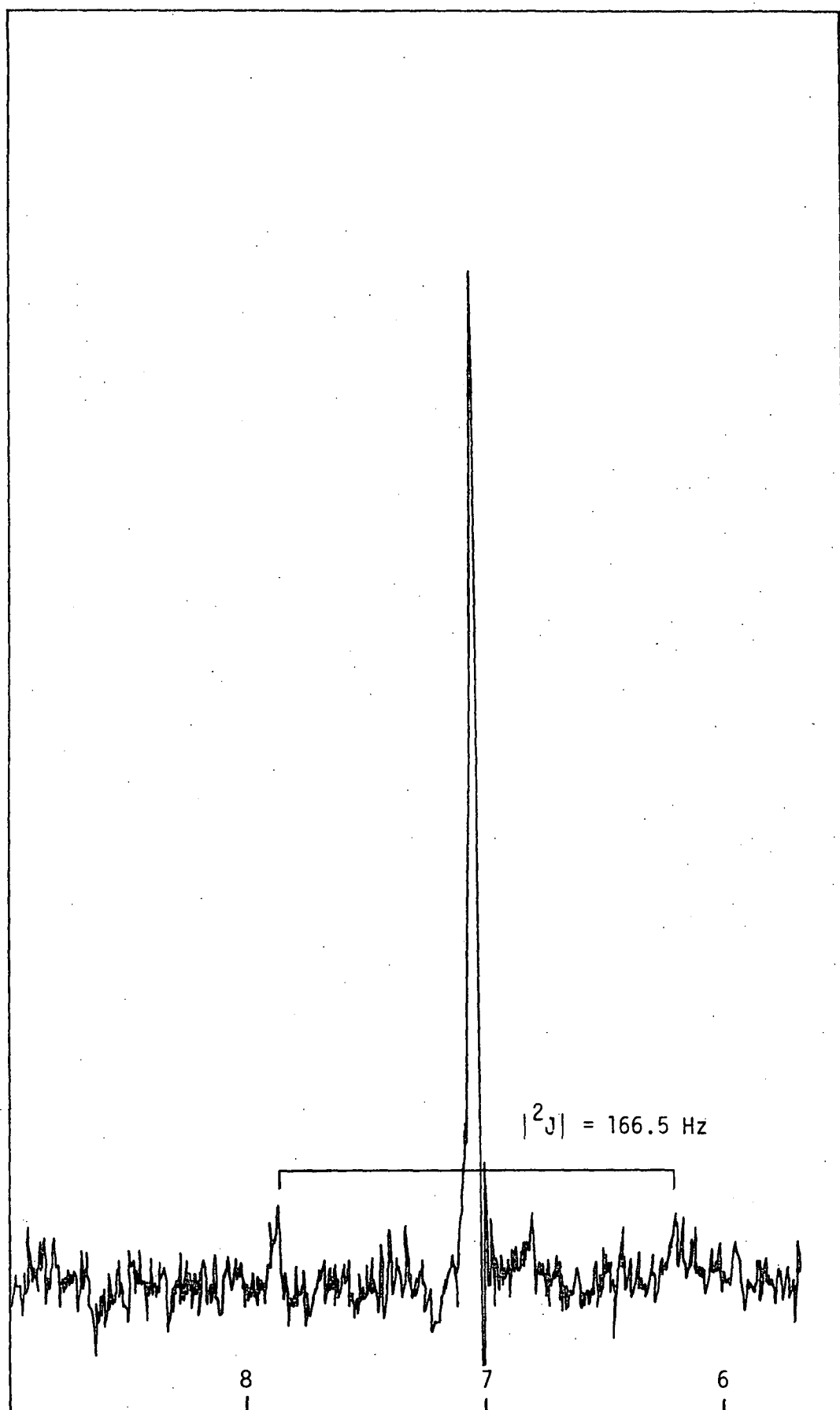


Figure 3.33: Proton nmr spectrum of  $\text{MeHgSeCH}_2\text{CO}_2\text{H}$  in  $\text{D}_2\text{O}$  (pD = 5.4) showing  $^1\text{H}$ - $^{199}\text{Hg}$  coupling. The methylene proton resonance ( $\delta = 7.06$ ) is measured relative to dioxane ( $\delta=10.00$ ) internal

and shown in Table 3.13. In order to determine the MeHg-selenoacetate formation constant, the proton dissociation constant of the free ligand is required.

Attempts to isolate the ligand by borohydride reduction of diselenodiacetic acid were unsuccessful. Since the MeHg(II)-selenoacetate formation constant will be very sensitive to the dissociation constant used for selenohydryl dissociation, any preparative procedure for the ligand must ensure the absence of acidic or basic impurities. This situation is difficult to achieve using commonly used reductants sodium borohydride, hypophosphorus acid, etc. Although electrochemical reduction of various diselenides has been reported,<sup>432</sup> this technique does not seem to have been used for the preparation of selenols for proton dissociation studies, but may be suitable in this regard.

Microscopic hydrolysis constants of selenoacetic acid have been previously determined spectrophotometrically.<sup>374</sup> The selenol was prepared by borohydride reduction of the diselenide and extraction into chloroform. From the small difference in  $|^2J(^1H-^{199}Hg)|$  between selenolate- and thiolate-complexes, it was expected that selenohydryl binding to MeHg(II) would probably be less than one log unit (at most) stronger than thiol binding. It was considered that the use of macroscopic ligand hydrolysis constants derived from the microscopic constants determined elsewhere, under different conditions, may have produced a misleading comparison between selenoacetate and mercaptoacetate binding.

A valid comparison between MeHg(II) selenolate- and thiolate-formation constants awaits future accurate determination of selenohydryl dissociation constants. The MeHg(II) complex of  $Bu^tSH$  has the lowest mercury-sulfur coupling constant of MeHg(II)-thiolates studied to date.<sup>250</sup> In fact, only the complexes with sulfide and the carbanions  $CH_3^-$  and  $C_6H_5^-$  (Table 3.2) have lower values of  $^2J$ , reflecting the high basicity



complex	$ ^2J(^1H-^{199}Hg) ^a$			
	X=S	ref.	X=Se	ref.
$MeHgXCH_2CH(CO_2^-)NH_3^+$	174.0	360,433	166.5 (pH=4) 164.3	433 404
$MeHg[XCH_2CH(CO_2^-)NH_3^+]_2$			185.4	404
$MeHgXCH_2CH_2NH_3^+$	185.7	404-5	162.0	404-5
$MeHg[XCH_2CH_2NH_3^+]_2$	216.6	404	187.0	404
$MeHgXCH_2CH_2NH_3^+$			159 <sup>b</sup>	404
$MeHg[CH_3XCH_2CH_2CH(CO_2^-)NH_3^+]$	217.4 (pD=0.8)	404	217.0 (pH=0.5) 214.6, 216.0 <sup>c</sup> (pH=1)	404 433
$MeHg[NH_2CH(CO_2^-)CH_2CH_2XCH_3]$	209.2 (pD=10.8) 223 (pH=7)	404 338	210.5 (pD=10.5) 215.2, 225.8 <sup>c</sup> (pH=7)	404 433
$[MeHgXC(NH_2)_2]^+$	199.6±0.4 <sup>d</sup>	434	191.0±0.4 <sup>d</sup>	434
$[MeHgXC(NH_2)(NMe_2)]^+$			191.2 <sup>e</sup>	434
$MeHgX^-$	146.2	323	143.1	323
$MeHgXHgMe$	156.6 <sup>f</sup>	250	146 <sup>g</sup>	435
$MeHgXCN$	203.0 <sup>h</sup>	323	200.4	323
$MeHgXMe$	157.1, <sup>f</sup> 158.2 <sup>i</sup>	250 433	155.3, <sup>i</sup> 158.7 <sup>j,c</sup>	433
$MeHgXBu^t$	150.2 <sup>f</sup> 150.1 <sup>k</sup>	250 this work	146.8 <sup>k</sup>	this work
$MeHgXCH_2CO_2^-$	170.5 (pH=5.6)	this work	166.5 (pH=5.8)	this work
$MeHgXC_6H_5$	161.5 <sup>f</sup> 168.4 <sup>i</sup>	250 433	154.0, <sup>j,k</sup> 164.8 <sup>j,c,k</sup>	433
$MeHg[C_6H_5XXC_6H_5]$			193.9 <sup>j</sup>	433

**Table 3.13:** Mercury-Proton coupling constants of Methylmercury(II) Complexes with selenium-containing ligands and their sulfur analogs.

a) measured from  $^1H$  spectra in aqueous solution unless otherwise stated. b) taken from Figure 2, ref. 404 c) from  $^{199}Hg$  spectra. d) as  $Br^-$ ,  $Cl^-$ ,  $NO_3^-$  or  $ClO_4^-$  salts. e) as  $Br^-$  salt f) in  $CH_2Cl_2$ . g) in  $CS_2$ . h) see also Table 3.2 for additional values of  $^2J$ . i) in DMF. j) in DMSO. k) in  $CDCl_3$ .

of the *tert*-butyl group. Since  $\text{Bu}^t\text{SeH}$  had been prepared in order to synthesise the new bis mercury(II) selenolate  $\text{Hg}(\text{SeBu}^t)_2$  (page 186) it was of interest to prepare  $\text{MeHgSeBu}^t$  and compare  $|^2J(^1\text{H}-^{199}\text{Hg})|$  for this complex with that of the sulfur analog.

Addition of an ethereal solution of  $\text{Bu}^t\text{SeH}$  (prepared by the Grignard route, page 349) to an ice-cold solution of  $\text{MeHgOH}$  (3.3 mmole) in 1:2 aqueous methanol (50 ml) and careful evaporation of the combined hexane extracts (5 x 25 ml) at  $0^\circ\text{C}$  under low vacuum (25 mm Hg), produced crude  $\text{MeHgSeBu}^t$ . The white solid was purified by sublimation ( $50-60^\circ/15$  mm), mp.  $57-8.5^\circ$ , and analysed satisfactorily for carbon, hydrogen and mercury (page 351). The analogous thiolate was prepared similarly using  $\text{Bu}^t\text{SH}$ . The proton nmr spectrum of  $\text{MeHgSeBu}^t$  in  $\text{CDCl}_3$  is shown in Figure 3.34. The mercury-proton coupling constant (measured from an expanded spectrum) was found to be 146.8 Hz, lower than that for the sulfur analog under the same conditions. The  $^1\text{H}$  nmr resonances of the methyl and *tert*-butyl protons are shifted downfield in  $\text{MeHgSeBu}^t$  ( $\delta = 0.85, 1.65$  relative to TMS) compared with those in  $\text{MeHgSBu}^t$  ( $\delta = 0.78, 1.51$ ). Similar small downfield shifts have been found in several selenium-substituted dicarboxylic acids discussed in Chapter 5.

Due to the correlation between  $^2J$  and donor basicity,  $\text{MeHgSeBu}^t$  presumably has the highest  $\text{MeHg(II)}$ -selenohydryl formation constant of the selenols in Table 3.13.

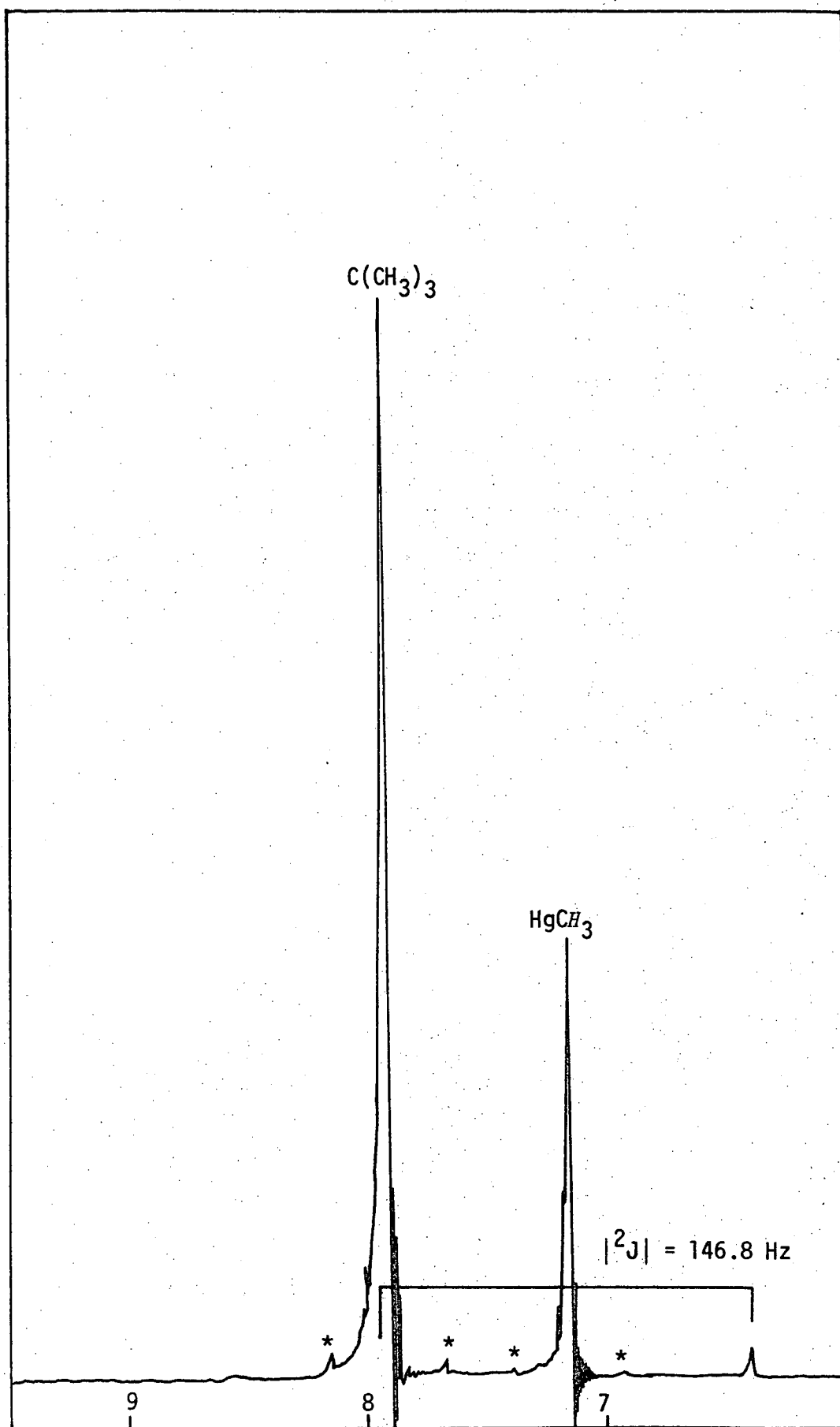


Figure 3.34: Proton nmr spectrum of  $\text{MeHgSeBu}^t$  in  $\text{CDCl}_3$  showing  $^1\text{H}$ - $^{199}\text{Hg}$  coupling. Spinning sidebands are indicated by asterisks. (Dioxane = 10.0 $\delta$ ).

### 3.5.2 MeHg(II)-Diselenide interactions

Sugiura *et al.* have reported that values of  $|^2J(^1H-^{199}Hg)|$  in mixtures of MeHg(II) and the diselenides, selenocystamine and selenocystine (Table 3.13), are similar to those with sulfhydryl donors, implying that these diselenides have an affinity for MeHg(II) comparable to that of thiols.<sup>404</sup> As the interactions of MeHg(II) with disulfides are weak, the possibility of strong interaction in solution between MeHg(II) and diselenodiacetic acid was investigated potentiometrically.

Attempts to obtain solid complexes from mixture of diselenodiacetic acid and MeHgNO<sub>3</sub> in acetone were unsuccessful, always resulting in recovery of diselenide. A similar situation resulted with dibenzyl-diselenide which was unsuited to potentiometric studies here since it is aprotic and insoluble in water. Elsewhere, attempts to prepare a MeHg(II) complex with selenocystamine dihydrochloride have failed, and no cleavage product was obtained.<sup>433</sup>

Titrations of MeHg(II) and diselenodiacetic acid in the presence of competing ligand in the range  $2.7 < pH < 10.4$ , show that MeHg(II) hydrolysis is suppressed, indicating complexation. These titrations, shown in Figure 3.34, were treated with MINQUAD81 but only poor fits ( $U > 10^{-8}$ ) were obtained above pH 5. Below this pH, the data can be fitted as a simple diprotic acid with  $pK_{a1} = 3.04(3)$  and  $pK_{a2} = 4.00(4)$  which are similar to values for the diselenide ligand,  $pK_{a1} = 3.196(1)$ ,  $pK_{a2} = 4.058(2)$ . This is consistent with very weak interaction (if any) with the carboxylate groups. It appears that the MeHg(II)-diselenide complex is stable, with  $\log \beta \geq 10$ , since the titrations can be fitted reasonably by assuming that MeHg(II) is never dissociated from the complex below pH 5.

In the presence of 0.1M KI, insoluble MeHgI is formed below pH 10.5 with  $[MeHg(II)] = 1.5 \times 10^{-3}M$  and  $[RSeSeR] = 3 \times 10^{-3}$ . The same MeHg(II)

concentration was used in the monothiolate systems described previously, but MeHgI was absent above pH 4, thus it appears that the diselenide is not as efficient at competing with iodide for MeHg(II) as the monothiols described previously. Therefore the MeHg(II)-diselenide formation constant is probably less than  $10^{16}$ . With more dilute solutions, ( $0.05\text{M I}^-$ ,  $0.7 \times 10^{-3}\text{M MeHg(II)}$ ,  $1.5 \times 10^{-3}\text{M RSeSeR}$ ), no precipitation of MeHgI was observed in the range  $3 < \text{pH} < 11$ . This titration was treated with MINQUAD81, using several hypothetical systems of equilibria involving 1:1 and 1:2 MeHg(II)-RSeSeR complexes and their protonated analogs but the data could not be fitted adequately ( $U > 10^{-8}$ ) over this pH-range with any combination of these species.

## Conclusions

Equilibrium constants which describe the aqueous solution behaviour of equivalent quantities of MeHg(II) and various monothiols over the pH-range  $3 < \text{pH} < 10$ , have been determined potentiometrically using iodide competition. The values obtained here agree well with those found elsewhere by an nmr method<sup>302</sup> for the monothiol ligands 2-mercaptoethanol, mercaptoacetic acid, mercaptosuccinic acid, L-cysteine, DL-penicillamine, N-acetyl-DL-penicillamine and glutathione. In addition, new formation constants are reported for the thiocholine cation and 4-mercapto-N-methylpiperidine. Monothiolate-MeHg(II) formation constants are now firmly established and may be estimated from the correlation with  $\text{pK}_a$  of the sulfhydryl donor:

$$\log K (\text{MeHgSR}) = 0.893 \text{ pK}_a(\text{SH}) + 7.77$$

Previously unreported equilibrium constants with the vicinal dithiol antidotes BALH<sub>2</sub> and Unithiol indicate that significantly more stable 1:1 complexation occurs for BALH<sub>2</sub> and Unithiol than is expected from estimates of the basicity of the sulfhydryl donors in these ligands. Chelation of MeHg(II) by the vicinal  $\delta$ -donor atoms is suggested as an explanation for this phenomenon. In contrast, DMSH<sub>4</sub> behaves like a monothiol in the 1:1 interaction.

Equilibrium constants for the competition of human mercaptalbumin with the antidotal thiols DL-penicillamine, N-Acetyl-DL-penicillamine, Unithiol and DMSH<sub>4</sub> for MeHg(II), indicate that polar, electrically charged MeHg(II)-antidote species are formed at physiological pH. In contrast, a large proportion of the complex formed with BALH<sub>2</sub> is neutral and non-polar, which may explain the observed redistribution of MeHg(II) into the brain upon administration of BALH<sub>2</sub>.<sup>66,67</sup>

## CHAPTER FOUR

### SYNTHESIS, VIBRATIONAL SPECTROSCOPY AND STRUCTURE OF MERCURY(II) SELENOLATES

Direct chemical interactions between mercury and selenium have been recognised for many years. The first characterised organoselenium compound, 'selenomercaptan', EtSeH, produced the first example of Hg-Se bonding in 1847 as yellow crystalline  $\text{Hg}(\text{SeEt})_2$ <sup>436</sup>. Despite the preparation of many such 'selenomercaptides' as derivatives for the qualitative identification of selenols, the structural chemistry of these bis(selenolato)mercury(II) compounds has not been studied.

It has already been shown (Chapter 1) that interactions between selenium and mercury(II) may be of some importance in the mechanisms of the protective effect of Se against inorganic (and perhaps organic) mercury(II) toxicity. In this light, it is therefore somewhat surprising that no complexes, formed between mercury(II) and selenohydryl-containing ligands, have been investigated although Ganther<sup>224</sup> has reported that the important selenite metabolite, selenodiglutathione (Figure 1.1, page 20) interacts with  $\text{Hg}^{2+}$  *in vitro*.

In this study, several complexes of the type  $\text{Hg}(\text{SeR})_2$  formed between  $\text{Hg}^{2+}$  and simple monoselenols RSeH (R=Me, Et, Bu<sup>t</sup>, CH<sub>2</sub>Ph) and CH<sub>2</sub>CO<sub>2</sub>H) have been prepared and structurally characterised in the solid state by X-ray diffraction and vibrational spectroscopic methods. It will be demonstrated that several of these complexes are not isostructural with their sulfur analogs. In addition, 1:1 complexes of the type RSeHgX have been prepared and characterised either directly (HgX=Me, O<sub>2</sub>CMe) or as pyridine adducts (R, X=Et, Cl; Bu<sup>t</sup>, Cl)

by crystallography.

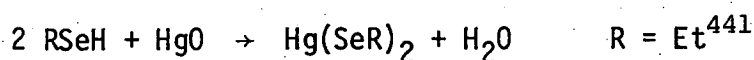
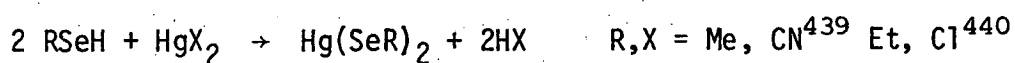
It is hoped that some of these simple model compounds may be of use for future characterisation of Hg-Se complexes of biological significance.

#### 4.1 Preparation of mercury(II) selenolates

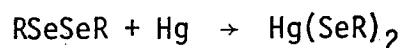
##### 4.1.1 Preparation of $\text{Hg}(\text{SeR})_2$ complexes

Several complexes  $\text{Hg}(\text{SeR})_2$  have previously been prepared as derivatives for selenol identification, generally by two methods:

(i) reaction of the selenol with a mercuric salt or oxide following the analogous mercaptide procedure of Wertheim<sup>437</sup> or Claesson<sup>438</sup>



and (ii) reductive cleavage of diselenides by metallic mercury.



( $\text{R} = \text{CH}_3^{443}$ ;  $\text{CH}_2\text{CO}_2\text{H}^{444}$  (and other alkyl carboxylic acids)<sup>440</sup>;  $\text{C}_6\text{H}_5^{445-6}$ ;  $(\text{CH}_3)_2\text{CH}$ ,  $(\text{CH}_3)_2\text{CH}_2^\downarrow$ ,  $\text{C}_6\text{H}_5\text{CH}_2\text{CH}_2^{442}$ ;  $\text{CF}_3^{447-8}$ ,  $\text{C}_3\text{F}_7$ ,  $\text{C}_6\text{F}_5^{449-50}$ , and the mixed complex  $\text{C}_6\text{F}_5\text{SHgSeC}_6\text{F}_5^{450}$ ).

Trifluoromethylselenyl chloride,  $\text{CF}_3\text{SeCl}$ , reacts with metallic mercury to form  $\text{Hg}(\text{SeCF}_3)_2^{447}$ . Bis(n-butylselenolato)mercury(II) has been prepared by the reaction of diethylmercury with n-butylselenol.<sup>451</sup>

The compounds  $\text{Hg}(\text{SeR})_2$ ,  $\text{R} = \text{Me, Et, CH}_2\text{CO}_2\text{H}$  have been obtained in this work by the reductive cleavage of the appropriate diselenide with excess metallic mercury. The compounds with  $\text{R} = \text{Bu}^t$  and  $\text{CH}_2\text{Ph}$  were obtained from the appropriate selenols and mercuric cyanide. All complexes have been isolated in analytical purity (Table 4.1).

The complexes, except for the selenoacetate complex, are very poorly soluble in common solvents.



Hg(SeR) <sub>2</sub>	calc %			found %			mpt.		Method of preparation
	C	H	Hg	C	H	Hg	this work <sup>a</sup>	Hg(SR) <sub>2</sub>	
R = Me	6.2	1.6	51.6	6.3	1.5	51.8	119(dec)	175 <sup>437</sup>	MeSeSeMe + Hg $\xrightarrow{\text{pyr}}$ Hg(SeMe) <sub>2</sub>
Et	11.5	2.4	48.2	11.2	2.3	47.7	72(dec)	76 <sup>437</sup>	EtSeSeEt + Hg $\xrightarrow{\text{CHCl}_3}$ Hg(SeEt) <sub>2</sub>
Bu <sup>t</sup>	20.3	3.8	42.2	20.3	3.9	42.7	145(dec) <sup>b</sup>	159-60 <sup>452</sup>	2Bu <sup>t</sup> SeH + Hg(CN) <sub>2</sub> $\xrightarrow{\text{Et}_2\text{O}}$ Hg(SeBu <sup>t</sup> ) <sub>2</sub>
CH <sub>2</sub> Ph	31.1	2.6	37.1	30.9	2.6	36.9	111(dec)	117-8 <sup>d</sup>	2PhCH <sub>2</sub> SeH + Hg(CN) <sub>2</sub> $\xrightarrow{\text{MeOH}}$ Hg(SeCH <sub>2</sub> Ph) <sub>2</sub>
CH <sub>2</sub> CO <sub>2</sub> H	10.1	1.3	42.1	10.3	1.4	42.1	80(dec) <sup>e</sup>	>190(dec) <sup>d</sup>	(HO <sub>2</sub> CCH <sub>2</sub> Se) <sub>2</sub> + Hg $\xrightarrow[2.\text{H}_2\text{SO}_4]{1.\text{NaHCO}_3}$ Hg(SeCH <sub>2</sub> CO <sub>2</sub> H) <sub>2</sub>

Table 4.1: Methods of preparation and analytical data for bis(alkylselenolato)mercury(II) complexes.

<sup>a</sup>all compounds blacken without melting. <sup>b</sup>sublimes 165°/0.1 mm. <sup>c</sup>this compound is photosensitive.

<sup>d</sup>this work.

The complex  $\text{Hg}(\text{SeMe})_2$  can be crystallised as yellow, diamond-shaped plates from a large volume of hot pyridine. These were sufficiently well-formed to permit single crystal X-ray diffraction studies on the complex - the first mercury(II) selenolate structure reported.

The complex  $\text{Hg}(\text{SeEt})_2$  was obtained as a yellow crystalline product by very slow evaporation (several months) of a pyridine solution. However, the crystals were not of sufficient quality for X-ray structure determination and give a very poor quality X-ray powder diffraction pattern - perhaps indicating a highly polymeric structure.

The complex  $\text{Hg}(\text{SeBu}^t)_2$  seems to be previously unreported and could be recrystallised from benzene or chloroform as fine, hairlike, colourless needles, very similar to the sulfur analog, but were unsuitable for X-ray analysis. The reported single crystal X-ray structure of  $\text{Hg}(\text{SBu}^t)_2$  used crystals obtained by vacuum sublimation of the complex. The selenium analog could be sublimed but the resulting crystals were extensively twinned and unsuitable for single crystal analysis.

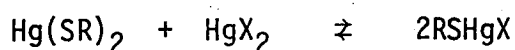
The complex  $\text{Hg}(\text{SeCH}_2\text{Ph})_2$ , previously reported by Antweiler,<sup>449b</sup> was crystallised from benzene or chloroform as a yellow microcrystalline product unsuitable for single crystal analysis. The sulfur analog was obtained similarly as a white product.

The complex  $\text{Hg}(\text{SeCH}_2\text{CO}_2\text{H})_2$  was obtained as a fine yellow powder on acidification of an aqueous alkaline (bicarbonate) solution. It can be recrystallised from methanol, but this does not produce high quality crystals. Fredga has reported that this compound gives large crystals (1 cm) when crystallised in large quantity from water,<sup>440</sup> but insufficient material was obtained here for this approach. The sulfur analog was obtained as small, shining, colourless plates by the reaction of two equivalents of mercaptoacetic acid with mercuric cyanide in ethanol.

Although most of these  $\text{Hg}(\text{SeR})_2$  compounds have been reported previously, they have not previously been structurally characterised in any way. The complexes prepared here are generally yellow (except for  $\text{Hg}(\text{SeBu}^t)_2$ , which is colourless) and light sensitive, particularly water-soluble  $\text{Hg}(\text{SeCH}_2\text{CO}_2\text{H})_2$ . An abstract of Fredga's early work with this compound, records it as grey,<sup>444</sup> which may have been due to contamination by metallic mercury in his preparation. All of the compounds appear to be stable when refrigerated in amber glass at  $-20^\circ$ .

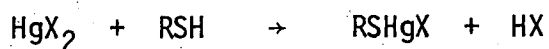
#### 4.1.2 Preparation of $\text{RSeHgX}$ complexes

Thiolatomercury(II) complexes,  $\text{RSHgX}$ , can be prepared by the reaction of equimolar amounts of  $\text{Hg}(\text{SR})_2$  with mercuric salts,  $\text{HgX}_2$ :



This reaction is an equilibrium (in MeOH) for  $\text{CF}_3\text{SHgX}$  ( $\text{X} = \text{Cl}, \text{Br}, \text{I}$ ), with equilibrium constants  $K = 2.3 \pm 0.3$  for  $\text{CF}_3\text{SHgBr}$  and  $20 \pm 10$  for  $\text{CF}_3\text{SHgCl}$  formation.<sup>290</sup>

Alternatively, reaction of  $\text{HgX}_2$  with  $\text{RSH}$  also produces  $\text{RSHgX}$  products:



Many of these compounds form adducts with pyridine bases, some of which have been crystallographically studied (Chapter 2, page 55).

The only analogous selenolatomercury(II) derivatives reported to date have been  $\text{CF}_3\text{SeHgX}$  ( $\text{X} = \text{Cl}, \text{Br}, \text{I}, \text{CN}, \text{SCN}, \text{O}_2\text{CMe}$ ).<sup>448</sup> [Dr. A.J. Carty (University of Waterloo) has kindly described the formation of  $\text{PhSeHgCl}$  from  $\text{Hg}(\text{SePh})_2$  and  $\text{HgCl}_2$ ,<sup>433</sup> but this work has not yet been published.]

Of particular interest in this study was the preparation of  $\text{MeSeHgO}_2\text{CMe}$ ,

whose sulfur analog has been shown by Raman spectroscopy to be dimeric in aqueous solution at pH 6.<sup>292</sup> Yellow, otherwise insoluble  $\text{Hg}(\text{SeMe})_2$  dissolves in an aqueous ethanolic solution of  $\text{Hg}(\text{O}_2\text{CMe})_2$  to precipitate white, crystalline  $\text{MeSeHgO}_2\text{CMe}^+$  which has been shown by X-ray powder diffraction (page 190) to be isomorphous with  $\text{MeSHgO}_2\text{CMe}$ . Unfortunately, the selenium analog is not sufficiently water-soluble to allow Raman spectroscopic investigation of its structure in solution. Preliminary experiments with other  $\text{Hg}(\text{SeR})_2$  complexes suggest that preparation of  $\text{RSeHgO}_2\text{CMe}$  complexes with  $\text{Hg}(\text{O}_2\text{CMe})_2$  may be a general phenomenon.

In contrast to the water-soluble  $\text{MeSHgO}_2\text{CMe}$ , monothiolatomercury(II) halides are insoluble (Chapter 2, page 55) and so no new  $\text{RSeHgX}$  ( $\text{X}$  = halide) complexes were characterised here, although preliminary experiments showed that they are readily formed, as expected. However, reaction of  $\text{Hg}(\text{SeR})_2$  ( $\text{R} = \text{Et}, \text{Bu}^t$ ) with  $\text{HgCl}_2$  in pyridine produced colourless crystalline adducts which were recrystallised from ethanolic pyridine to produce relatively large good-quality crystals. The single-crystal X-ray diffraction structures of  $[\text{EtSeHgCl}(\text{py})]_4$  and  $[\text{Bu}^t\text{SeHgCl}(\text{py})_{0.5}]_4$  will be described later in this Chapter.

---

<sup>†</sup> $\text{MeSeHgO}_2\text{CMe}$  ( $\text{C}_3\text{H}_6\text{O}_2\text{SeHg}$ ) requires: C 10.2, H 1.71, Hg 56.7%; found: C 10.2, H 1.75, Hg 56.5%.

## 4.2 X-ray Diffraction Characterisation of Mercury(II)-Selenolates

### 4.2.1 Hg(SeR)<sub>2</sub>

As a preliminary investigation into the structure of the complexes Hg(SeR)<sub>2</sub> (R=Me, Et, Bu<sup>t</sup>, CH<sub>2</sub>Ph, CH<sub>2</sub>CO<sub>2</sub>H), X-ray powder diffraction patterns were obtained and compared with those of the sulfur analogs. The complexes Hg(SR)<sub>2</sub> (R=Me, Et, Bu<sup>t</sup>,<sup>231,453</sup> CH<sub>2</sub>Ph, CH<sub>2</sub>CO<sub>2</sub>H) were obtained as white crystalline products. The methanethiolato complex can occur in two crystalline modifications.<sup>291</sup> The X-ray powder diffraction pattern of Hg(SMe)<sub>2</sub> prepared by Wertheim's method<sup>437</sup> in this laboratory and re-crystallised from ethanol can be indexed with unit-cell dimensions reported by Bradley and Kunchur.<sup>271</sup> Samples prepared by addition of imidazole to aqueous solutions of MeHgSO<sub>2</sub>CMe<sup>291</sup> gave a different powder diffraction pattern. In historical context, these will be referred to as the 'old' and 'new' forms respectively. Infrared spectra of the two forms are similar, indicating linear S-Hg-S geometry in the new form. The structures of the compounds with R=Me, (old form),<sup>271</sup> Et,<sup>274</sup> Bu<sup>t</sup><sup>273</sup> have been determined by single crystal X-ray diffraction (Section 2.3, page 43 ).

Because the compounds Hg(SeMe)<sub>2</sub>, Hg(SeEt)<sub>2</sub>, and Hg(SeBu<sup>t</sup>)<sub>2</sub> have unpleasant odours, Debye-Scherrer powder diffraction patterns were recorded photographically from ground samples contained in sealed Lindemann glass capillaries.<sup>†</sup> The analogous sulfur compounds were treated identically (though they are odourless) facilitating comparison of the patterns. The seleno- and mercaptoacetate complexes are odourless and although photographic powder patterns were obtained from samples in Lindemann capillaries, better results were obtained from automatic chart-recordings using larger (planar) specimens in a powder diffractometer.

For the qualitative comparison of the powder diffraction-patterns

---

<sup>†</sup>The assistance of Mr. R. Ford (Geology Department) in this task is gratefully acknowledged.

of analogous sulfur- and selenium compounds, due care must be taken of the different scattering powers of S and Se. Differences in atomic radii of sulfur and selenium were expected to produce relatively small changes in unit-cell parameters for isomorphous compounds. In compounds containing large quantities of both selenium and mercury, the intensity of the diffracted X-rays might be expected to differ considerably from the sulfur analog, where the Hg-atom scattering dominates more than for selenolates.

If the powder diffraction patterns of a known isomorphous pair of Hg-S and Hg-Se compounds could be obtained, the magnitude of this sulfur *versus* selenium 'phase' problem could be assessed qualitatively. Such a pair of compounds was unavailable prior to this work.

It will be shown subsequently (see Figure 4.5), that the compounds  $[\text{Bu}^t\text{SeHgCl}(\text{py})_{0.5}]_4$  and  $[\text{Bu}^t\text{SHgCl}(4\text{-Mepy})_{0.5}]_4$  are isomorphous and that the powder diffraction intensities and positions of both compounds are very similar, and are particularly characteristic at low ( $2\theta < 20^\circ$ ) scattering angles. Powder diffraction patterns of pairs of compounds  $\text{Hg}(\text{XR})_2$  ( $\text{X}=\text{S}, \text{Se}$ ) ( $\text{R}=\text{Me}, \text{Et}, \text{Bu}^t, \text{CH}_2\text{CO}_2\text{H}, \text{CH}_2\text{Ph}$ ) were examined qualitatively in view of this finding.

#### $\text{Hg}(\text{XMe})_2$ ( $\text{X}=\text{S}, \text{Se}$ )

X-ray powder pattern data obtained for bis(methaneselenolato)mercury(II) were measured from a photographic recording and are shown in Table 4.2, together with powder diffraction data for both forms of the sulfur analog.

The complex  $\text{Hg}(\text{SeMe})_2$  does not seem to be isomorphous with either crystalline modification of its sulfur analog. Fortunately, crystals of the selenolate grown from pyridine were available and a single-crystal X-ray diffraction study was undertaken by Drs. A.H. White and B.W. Skelton

$\text{Hg(SMe)}_2$ $d_{\text{meas}}/\text{\AA}$		$\text{Hg(SeMe)}_2$ $d_{\text{meas}}/\text{\AA}$
'old' form <sup>b</sup>	'new' form <sup>c</sup>	
9.86 s	10.05, 9.61, s,db 8.91, 8.41, s,db	8.3 s,br 6.63 vw 5.61 w 4.16 m 3.90 w 3.63 m 3.31 w 3.17 vw 3.07 m 2.90 w 2.70 w 2.66 w 2.56 m 2.46 w 2.42 vw 2.27 m 2.22 vw 2.05 w 1.96 vw 1.91 m 1.87 w 1.78 vw
3.005 w	3.02, 2.99 w,db 2.87 w	
2.457 m	2.66 w 2.59 w 2.45 w 2.37 w 2.23 w 2.08, 2.05, w,db 1.99 w	
1.966 w	1.96 w	
1.903 vw		
1.602 w		

**Table 4.2:** X-ray powder diffraction data for  $\text{Hg(XMe)}_2$  ( $\text{X}=\text{S},\text{Se}$ )<sup>a</sup>

<sup>a</sup>the finely ground samples were contained in 0.3 mm diameter Lindemann capillaries.

<sup>b</sup>prepared by Wertheims method in ref. 291

<sup>c</sup>Ni-filtered  $\text{CuK}_\alpha$  (12 hrs). <sup>d</sup>Mn-filtered  $\text{FeK}_\alpha$  (6.5 hrs.)

(University of Western Australia). The powder diffraction pattern could be satisfactorily indexed using cell dimensions obtained from the single crystal used for data collection.

### Crystal and molecular structure of $\text{Hg}(\text{SeMe})_2$

A crystal of this complex was mounted in Tasmania and preliminary Weissenberg and oscillation photographs taken to ensure its suitability for single crystal structure refinement. Subsequently, a yellow prismatic crystal  $0.10 \times 0.16 \times 0.16$  mm was used for the crystallographic work at the University of Western Australia. A unique data set was gathered at 295 K using a Syntex P2<sub>1</sub> four-circle diffractometer in the conventional  $2\theta/\theta$  mode, within the limits  $2\theta < 50^\circ$ . 1058 reflections were obtained, 818 of these with  $I > 3\sigma(I)$  were considered 'observed' and used in the least-squares refinement after absorption correction. The crystal did not deteriorate appreciably during data collection.

### Crystal data for $\text{Hg}(\text{SeMe})_2$

$\text{C}_2\text{H}_6\text{HgSe}_2$ ,  $M = 388.6$ , Monoclinic, space group  $P2_1/c$  ( $C_{2h}^5$ , No. 14).

$a = 8.440(4)$ ,  $b = 10.732(3)$ ,  $c = 6.681(3)$  Å

$\beta = 96.14(4)^\circ$

$U = 601.7(4)$  Å<sup>3</sup>,  $D_c$  ( $Z=4$ ) =  $4.29$  g cm<sup>-3</sup>

$F(000) = 664$

Monochromatic Mo  $K\alpha$  radiation,  $\lambda = 0.71069$  Å,  $\mu = 339$  cm<sup>-1</sup>.

The structure was solved by the heavy atom method and refined by full matrix least squares with anisotropic thermal parameters for the non-hydrogen atoms. Hydrogen atoms were included with ( $x$ ,  $y$ ,  $z$ ,  $U$ ) as invariant estimates. Neutral atom scattering factors were used, those for non-hydrogen atoms being corrected for anomalous dispersion ( $f'$ ,  $f''$ ).<sup>454-6</sup> All computations were performed using the X-RAY 76 system<sup>457</sup> implemented by S.R. Hall on a Perkin-Elmer 32/40 computer.



(University of Western Australia).

The structure was refined to residuals  $R, R' = 0.044, 0.057$ , with reflection weights  $(\sigma^2(F_o) + 0.0005(F_o)^2)^{-1}$ .

The complex  $\text{Hg}(\text{SeMe})_2$  is polymeric, with infinite one-dimensional chains along  $b$ . The mercury atoms are pseudo-tetrahedrally coordinated to pairs of bridging methane-selenolato ligands. The chain is generated by a succession of inversion centres and twofold (screw) rotations. The pseudo-tetrahedral mercury geometry is similar to that in  $\text{Hg}(\text{SBu}^t)_2$  although the thiolate has an inversion centre between each mercury atom. An ORTEP diagram of the unit-cell contents, projected down  $c$ , is shown in Figure 4.1.

The spacings between successive mercury atoms are different and alternating, being  $3.538(1) \text{ \AA}$  for a pair of mercury atoms bridged by a pair of  $\text{Se}(2)$  ligands (related by an inversion centre), and  $4.070(2) \text{ \AA}$  for a pair separated by two  $\text{Se}(1)$  ligands (related by a 2-fold axis). Mercury-selenium(1) distances are similar,  $2.625(2), 2.659(2) \text{ \AA}$ , and are comparable to one of the  $\text{Hg-Se}(2)$  distances,  $2.614(2) \text{ \AA}$ . The other  $\text{Hg-Se}(2)$  distance is appreciably longer,  $2.764(2) \text{ \AA}$ , reflecting the distorted mercury geometry. Moreover, whereas the three angles, about  $\text{Se}(1)$ , are nearly equal,  $98.6(7)$ - $100.77(7)^\circ$ , those about  $\text{Se}(2)$  are more irregular,  $82.61(6)$ - $100.7(6)^\circ$ . The smallest angle,  $82.61(6)^\circ$ , is contained between two mercury atoms and  $\text{Se}(2)$ . This geometrical distortion about  $\text{Se}(2)$  may be a consequence of methyl-methyl interactions within the chain about its twofold (screw) axis.

The distances  $\text{C}(2)\text{-C}(2)$  and  $\text{C}(1)\text{-C}(1)$  are  $4.21(3) \text{ \AA}$  and  $3.80(4) \text{ \AA}$  respectively.

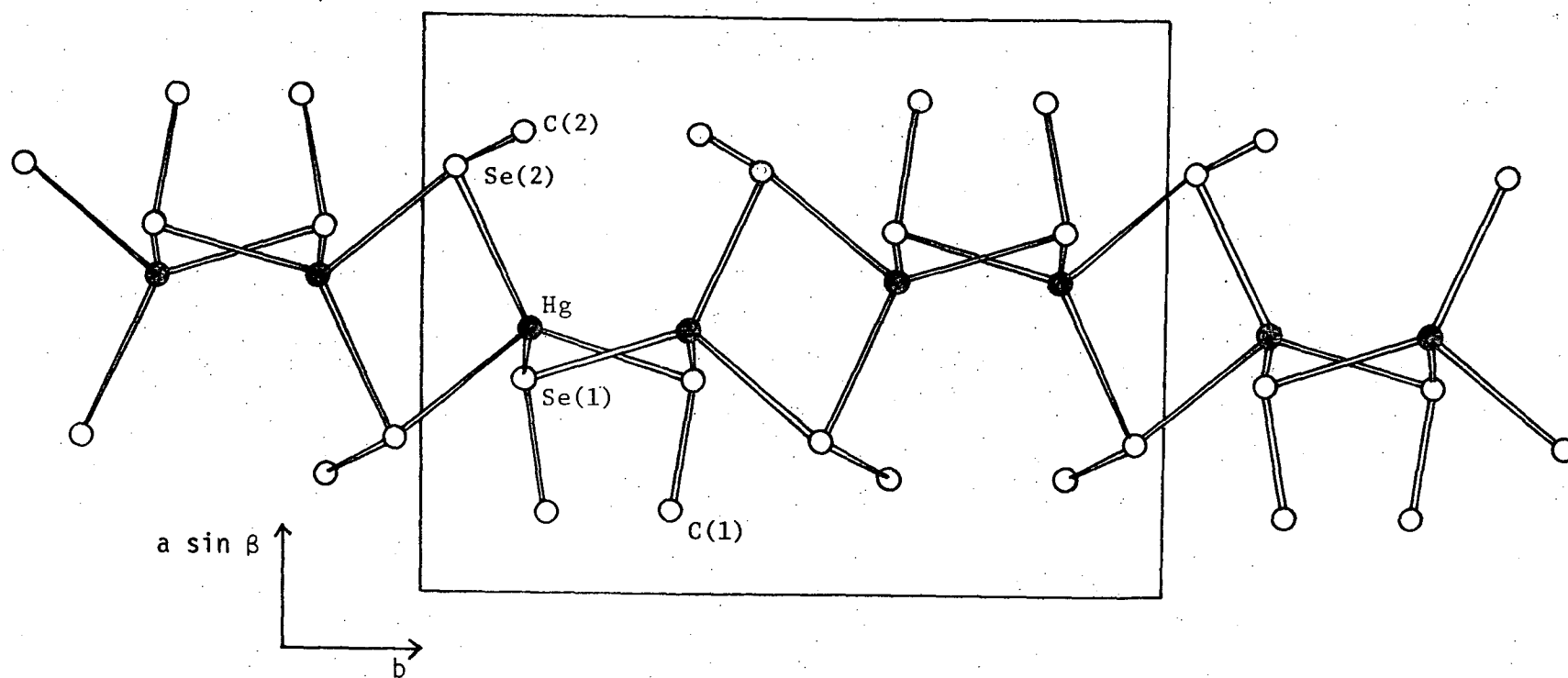


Figure 4.1: Unit-cell contents of  $\text{Hg}(\text{SeMe})_2$  projected down  $c$ .

Atoms	Parameters
Distances/Å <sup>°*</sup>	
Hg-Se(1)	2.625(2)
Hg-Se(2)	2.614(2)
Hg-Se(2 <sup>i</sup> )	2.764(2)
Hg-Se(1 <sup>ii</sup> )	2.659(2)
Se(1)-C(1)	1.96(2)
Se(2)-C(2)	1.97(3)
Angles/deg.	
Se(1)-Hg-Se(2)	124.63(8)
Se(1)-Hg-Se(2 <sup>i</sup> )	111.01(6)
Se(1)-Hg-Se(1 <sup>ii</sup> )	103.70(7)
Se(2)-Hg-Se(2 <sup>i</sup> )	97.79(7)
Se(2)-Hg-Se(1 <sup>ii</sup> )	115.02(7)
Se(2 <sup>i</sup> )-Hg-Se(1 <sup>ii</sup> )	102.64(6)
Hg-Se(1)-C(1)	98.6(7)
Hg-Se(1)-Hg <sup>iii</sup>	100.77(7)
C(1)-Se(1)-Hg <sup>iii</sup>	99.3(8)
Hg-Se(2)-C(2)	100.7(6)
Hg-Se(2)-Hg <sup>i</sup>	82.21(6)
C(2)-Se(2)-Hg <sup>i</sup>	99.3(7)

Atom transformations: i (1-x,  $\bar{y}$ ,  $\bar{z}$ )

ii (x,  $\frac{1}{2}$ -y,  $\frac{1}{2}$ +z)

iii (x,  $\frac{1}{2}$ -y, z- $\frac{1}{2}$ )

\*Hg...Hg<sup>i</sup>, 3.538(1) Å, Hg...Hg<sup>ii</sup>, 4.070(2) Å

**Table 4.3:** Interatomic bonding distances and angles (non-hydrogen atoms) for Hg(SeMe)<sub>2</sub>.

Least-squares estimated standard deviations of the last digit are given in parentheses.

Atom	x	y	z	$U_{11}$	$U_{22}$	$U_{33}$	$U_{12}$	$U_{13}$	$U_{23}$
Hg	0.45780(9)	0.14166(7)	0.11886(12)	38.2(5)	31.7(5)	41.6(6)	1.2(4)	13.3(3)	-3.3(3)
Se(1)	0.3715(2)	0.3651(2)	-0.0100(3)	36.7(11)	28.5(10)	32.2(10)	-4.6(8)	7.3(8)	-2.0(8)
C(1)	0.143(3)	0.335(2)	-0.072(4)	38(12)	59(15)	71(16)	6(11)	21(11)	5(13)
H(1A)	0.120(-)	0.272(-)	-0.176(-)	84(-)					
H(1B)	0.092(-)	0.310(-)	0.042(-)	84(-)					
H(1C)	0.110(-)	0.414(-)	-0.121(-)	84(-)					
Se(2)	0.7335(2)	0.0392(2)	0.0774(3)	26.1(10)	31.1(10)	44.0(11)	-5(8)	2.8(8)	-3.3(9)
C(2)	0.794(3)	0.131(2)	-0.158(4)	44(13)	30(11)	81(17)	-14(9)	19(12)	4(11)
H(2A)	0.721(-)	0.118(-)	-0.276(-)	78(-)					
H(2B)	0.805(-)	0.218(-)	-0.135(-)	78(-)					
H(2C)	0.895(-)	0.094(-)	-0.176(-)	78(-)					

Table 4.4: Atomic coordinates (x,y,z), and anisotropic thermal parameters ( $10^3 U_{ij}$  Å<sup>2</sup>) for Hg(SeMe)<sub>2</sub>.  
Least-squares estimated standard deviations of the last digit are given in parentheses.  
Anisotropic thermal parameters are of the form:  $\exp(-2\pi^2(U_{11}h^2a^{*2}+...2U_{23}klb^*c^*))$ .

Hg(XEt)<sub>2</sub>, (X=S,Se)

The complex Hg(SeEt)<sub>2</sub>, contained in a 0.3 mm diameter Lindemann capillary, gave a very diffuse X-ray powder pattern on exposure to Ni-filtered CuK<sub>α</sub> (6 hours) or Fe-filtered CoK<sub>α</sub> (22 hours) radiation. The sulfur analog, in contrast, diffracts well under the same conditions.

The selenolate is hard and brittle and may be a glass.

Hg(XBu<sup>t</sup>)<sub>2</sub>, (X=S,Se)

The complex Hg(SBu<sup>t</sup>)<sub>2</sub> is of interest as it is the only simple 1:2 complex to show pseudo-tetrahedral 'HgS<sub>4</sub>' geometry.<sup>273</sup> It is therefore the model compound for vibrational spectroscopic characterisation of thiolate-mercury(II) compounds with tetrahedral coordination.<sup>231</sup>

Bis(tert-butaneseelenolato)mercury(II) was isolated as fine, long, colorless hairlike needles, identical in nature to the thiol analog. These crystals were unsuitable for single crystal X-ray studies.

The powder diffraction data for Hg(XBu<sup>t</sup>)<sub>2</sub> (X=S,Se) were obtained photographically and are recorded in Table 4.5, and are very similar to that obtained for the sulfur analog under identical conditions. The selenolate data can be indexed satisfactorily using the published<sup>273</sup> orthorhombic unit-cell parameters of the sulfur analog.

The compounds Hg(XBu<sup>t</sup>)<sub>2</sub> (X=S,Se) are therefore considered to be isomorphous. The vibrational spectra are discussed in Section 4.3.1 in terms of tetrahedral 'HgSe<sub>4</sub>' geometry.

Hg(XCH<sub>2</sub>CO<sub>2</sub>H)<sub>2</sub> (X=S,Se)

The complex Hg(SCH<sub>2</sub>CO<sub>2</sub>H)<sub>2</sub> can be dissolved in aqueous solution by deprotonation, and vibrational studies in both solid state and in solution indicate that it has the expected linear 'HgS<sub>2</sub>' coordination

$\text{Hg}(\text{SBu}^t)_2^b$		$\text{Hg}(\text{SeBu}^t)_2^c$	
$d_{\text{meas}}$		$d_{\text{meas}}$	$d_{\text{calc}} (\text{hkl})^d$
9.0 s,br		9.3 vs,br	9.18(200)
6.58 m,br		6.45 m,br	6.49(210) <sup>e</sup>
4.54 m		4.58 w	4.59(020,400)
4.15 m		4.10 m	4.11(220), 4.22(311)
3.97 m		3.89 w	3.92(021,401)
3.03 m		3.06 w	3.03(312)
2.71 w		2.74 m	2.74(330)
2.32 w		2.30 w	2.30(040)

Table 4.5: X-ray powder diffraction data<sup>a</sup> for  $\text{Hg}(\text{XBu}^t)_2$  (X=S,Se)

<sup>a</sup>The finely ground samples were contained in 0.3 mm diameter Lindemann capillaries. <sup>b</sup>Mn-filtered  $\text{FeK}_\alpha$ , 24 hrs. <sup>c</sup>Mn-filtered  $\text{FeK}_\alpha$ , 16 hrs. <sup>d</sup>Using  $h,k,l < 4$  and orthorhombic unit cell parameters for  $\text{Hg}(\text{SBu}^t)_2$ .<sup>273</sup>

<sup>e</sup>However, the (210) reflection is not allowed for space group C222.

geometry (Section 2.3). The analogous selenolate was obtained as small shiny plates, similar to the sulfur compound, and is similarly soluble in aqueous alkaline solution. As this compound is odourless, powder diffraction patterns could be obtained from a large powdered sample using a Philips diffractometer, although significant darkening was evident after 3 hours exposure to 40 kV  $\text{CuK}_\alpha$  radiation.

The powder diffraction patterns of the selenolate and analogous thiolate are shown in Figure 4.2. Peak splitting at low angle, in the selenolate case, results from presence of an inadequate amount of sample in the sample holder. Photographically recorded Lindemann capillary samples do not show this splitting.

The two compounds are apparently not isomorphous, although it will

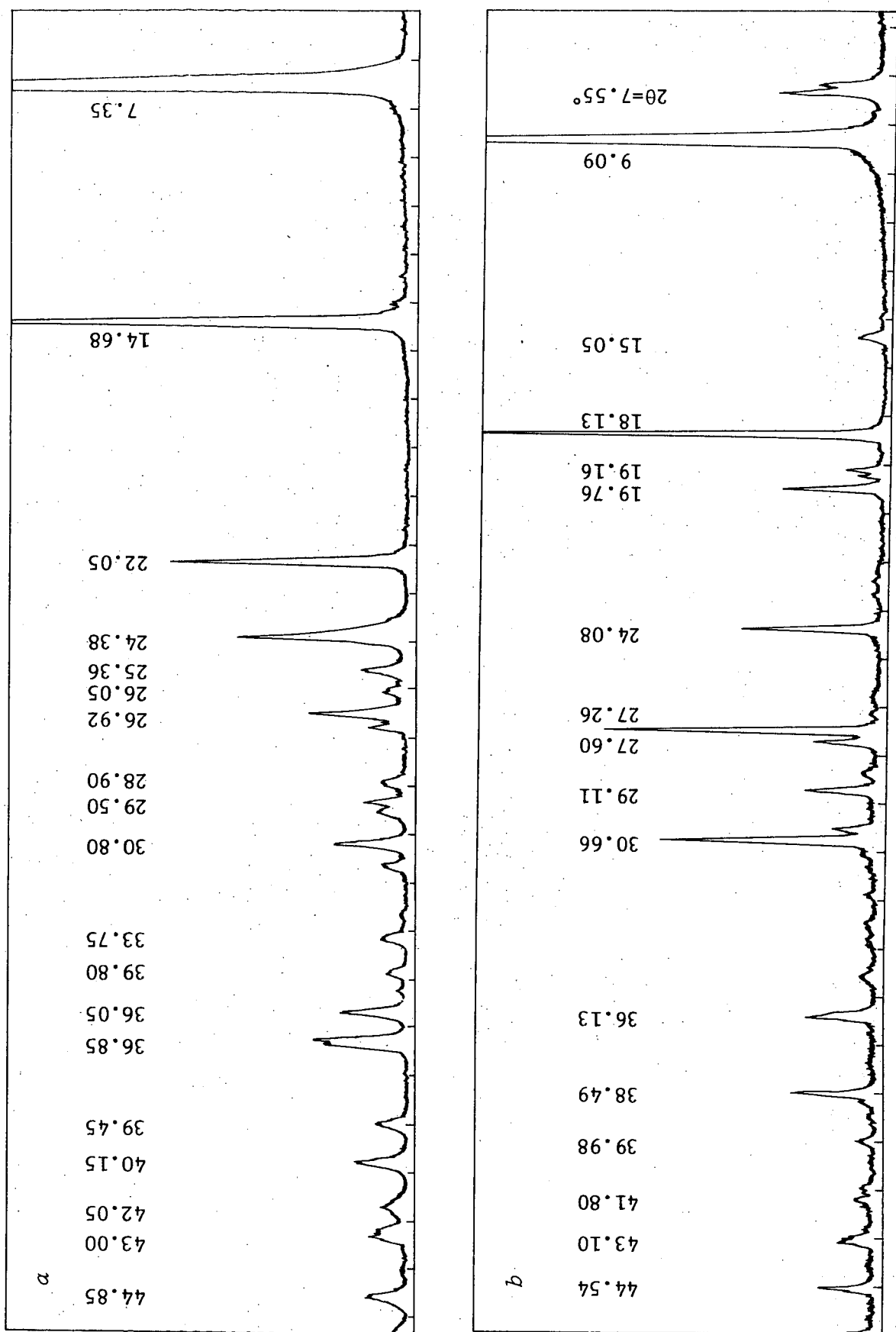


Figure 4.2:  $\text{CuK}\alpha$  X-ray powder diffraction patterns of  $\alpha$   $\text{Hg}(\text{SCH}_2\text{CO}_2\text{H})_2$  and  $\beta$   $\text{Hg}(\text{SeCH}_2\text{CO}_2\text{H})_2$ .

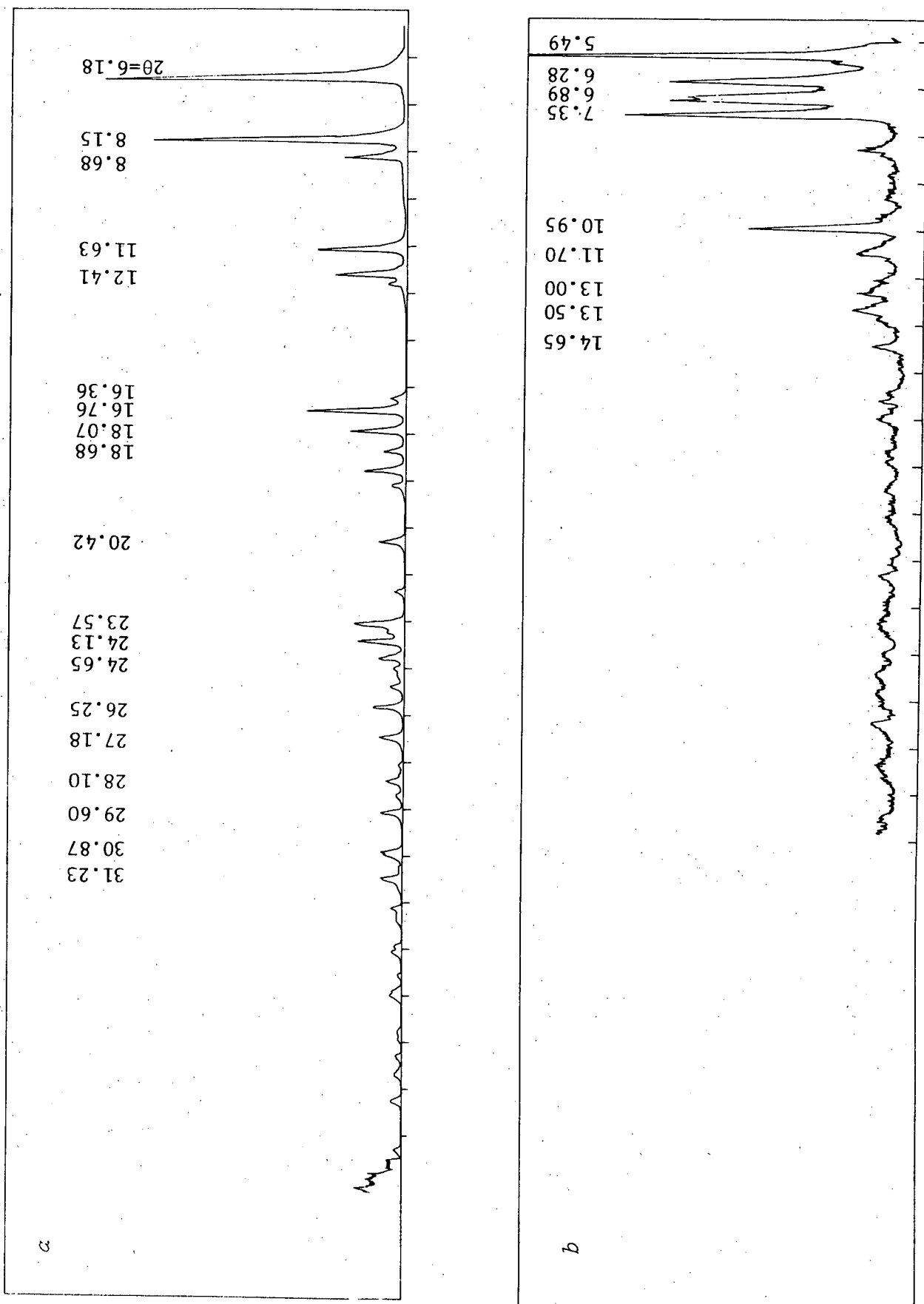


Figure 4.3:  $\text{CuK}\alpha$  X-ray powder diffraction patterns of  $\alpha$   $\text{Hg}(\text{SCH}_2\text{Ph})_2$  and  $\beta$   $\text{Hg}(\text{SeCH}_2\text{Ph})_2$ .



be shown from vibrational spectral studies (Section 4.3) that  $\text{Hg}(\text{SeCH}_2\text{CO}_2\text{H})_2$  has linear ' $\text{HgSe}_2$ ' in the solid state.

#### $\text{Hg}(\text{XCH}_2\text{Ph})_2$ (X=S,Se)

X-ray powder diffraction patterns obtained from these compounds, as flat specimens in a diffractometer, show significant differences in the low-angle scattering region (Figure 4.3). Subsequent vibrational studies (page 220) have shown that, like  $\text{Hg}(\text{XMe})_2$ , the sulfur compound has linear ' $\text{HgS}_2$ ', but the selenium compound has tetrahedral ' $\text{HgSe}_4$ ' geometry.

#### 4.2.2 X-ray diffraction studies of $\text{RSeHgX}$

In a similar manner to  $\text{Hg}(\text{SeR})_2$  compounds, X-ray powder diffraction patterns were obtained from analogous pairs of compounds  $\text{MeXHgO}_2\text{CMe}$  (X=S,Se) and the pyridine adducts of  $\text{Bu}^t\text{XHgCl}$  (X=S,Se).

#### $\text{MeXHgO}_2\text{CMe}$ (X=S,Se)

The sulfur compound of the analogous pair has previously been characterised by single crystal X-ray diffraction.<sup>293</sup> The X-ray powder diffraction pattern of  $\text{MeSeHgO}_2\text{CMe}$ , obtained photographically, is identical to that obtained from  $\text{MeSHgO}_2\text{CMe}$  under similar conditions (Table 4.6). The pattern can be adequately indexed using monoclinic unit cell parameters obtained from the single-crystal study of  $\text{MeSHgO}_2\text{CMe}$ .<sup>293</sup>

The selenium compound was therefore considered to be isomorphous with  $\text{MeSHgO}_2\text{CMe}$ , and thus has a polymeric structure of  $(-\text{Hg}-\text{SeMe}-)_n$  chains linked into sheets by bridging acetate groups (Figure 4.4). The small amount of  $\text{MeSeHgO}_2\text{CMe}$  available could not be crystallised sufficiently well for a single crystal X-ray diffraction confirmation of its isomorphism with  $\text{MeSHgO}_2\text{CMe}$ .

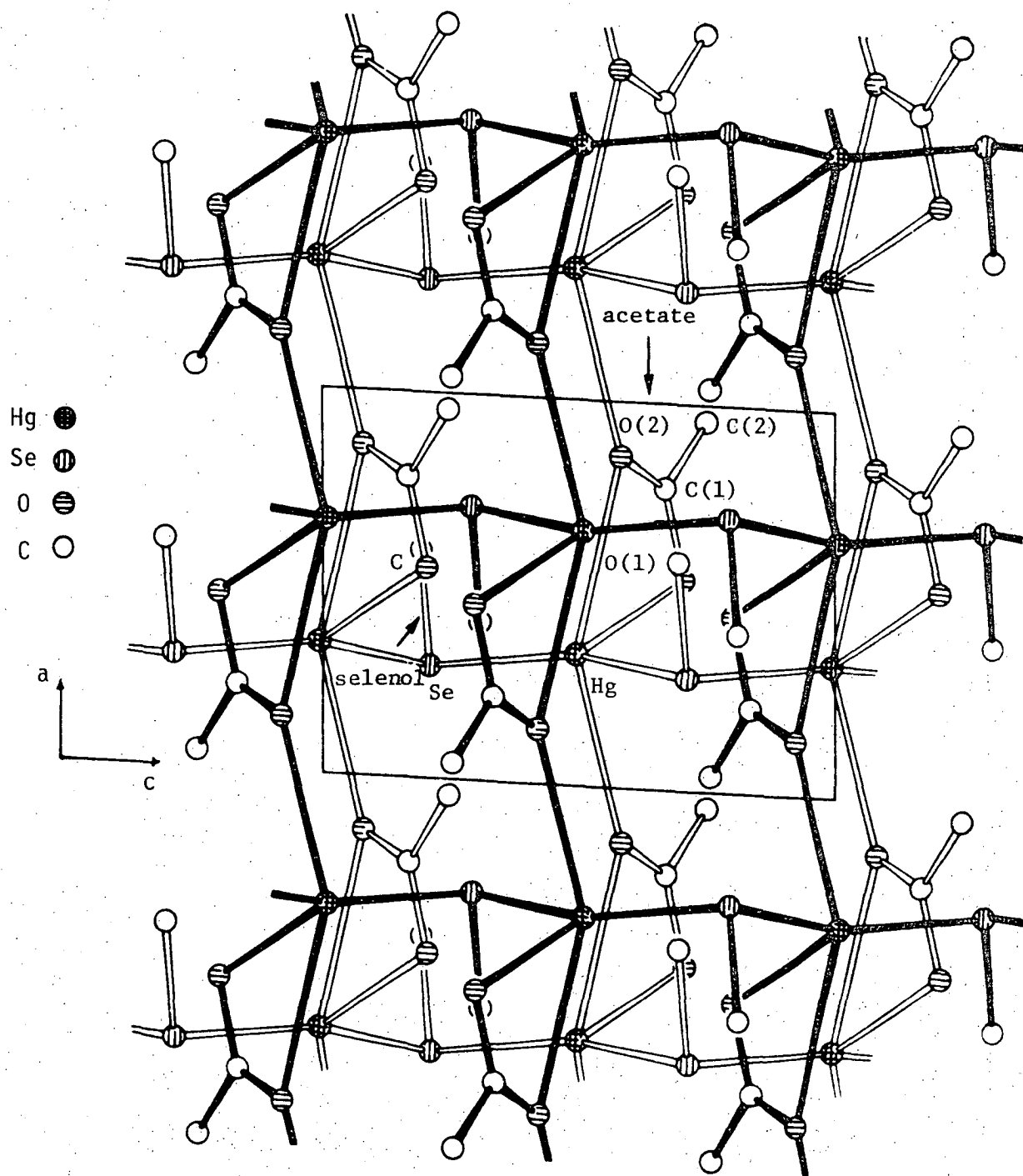


Figure 4.4: The structure of  $\text{MeSeHgO}_2\text{CMe}$  projected along  $b$ .

$\text{MeSHgO}_2\text{CMe}$	$\text{MeSeHgO}_2\text{CMe}$	
$d_{\text{meas}}$	$d_{\text{meas}}$	$d_{\text{calc}} (hkl)^a$
8.2 s,br	8.15 br	8.0(020)
4.98 m	4.86 w	5.02(110)
4.02 w	3.99 w	3.98(040) 4.00(111)
3.73 m		3.73(130)
3.23 x	3.21 m	$\begin{cases} 3.26(131) & 3.23(022) \\ 3.18(140) \end{cases}$
2.64 w	2.65 m,br	2.64(042,200)

**Table 4.6:** X-ray powder diffraction data for  $\text{MeXHgO}_2\text{CMe}$  ( $X=\text{S},\text{Se}$ )<sup>a</sup> using  $h, k, l \leq 4$  and monoclinic unit cell parameters for  $\text{MeSHgO}_2\text{CMe}$ .<sup>293</sup>

$[\text{Bu}^t\text{XHgCl}(\text{py})_{0.5}]_4$  and  $[\text{Bu}^t\text{XHgCl}(4\text{-Mepy})_{0.5}]_4$  ( $X=\text{S},\text{Se}$ )

The complexes  $[\text{Bu}^t\text{SHgCl}(\text{py})_{0.5}]_4$ <sup>293</sup> and  $[\text{Bu}^t\text{SHgCl}(4\text{-Mepy})_{0.5}]_4$ <sup>295</sup> have been examined by single-crystal X-ray diffraction and have been found to be isostructural but not isomorphous. The eight-membered ring structures,  $(-\text{Hg}-\text{SBu}^t)_4$ , have been described in Chapter 2. Insufficient of the 4-Mepy adduct was available for powder diffraction studies, but the low angle X-ray powder diffraction pattern of the pyridine adduct is shown in Figure 4.5 and should be compared with those obtained from the sulfur compounds described above. Close coincidence of peaks can be seen for  $[\text{Bu}^t\text{SeHgCl}(\text{py})_{0.5}]_4$  and with  $[\text{Bu}^t\text{SHgCl}(4\text{-Mepy})_{0.5}]_4$  but not with  $[\text{Bu}^t\text{SHgCl}(\text{py})_{0.5}]_4$  (Figure 4.6), suggesting that the former two compounds are isomorphous.

Crystals of  $[\text{Bu}^t\text{SeHgCl}(\text{py})_{0.5}]_4$  grown from ethanolic pyridine were

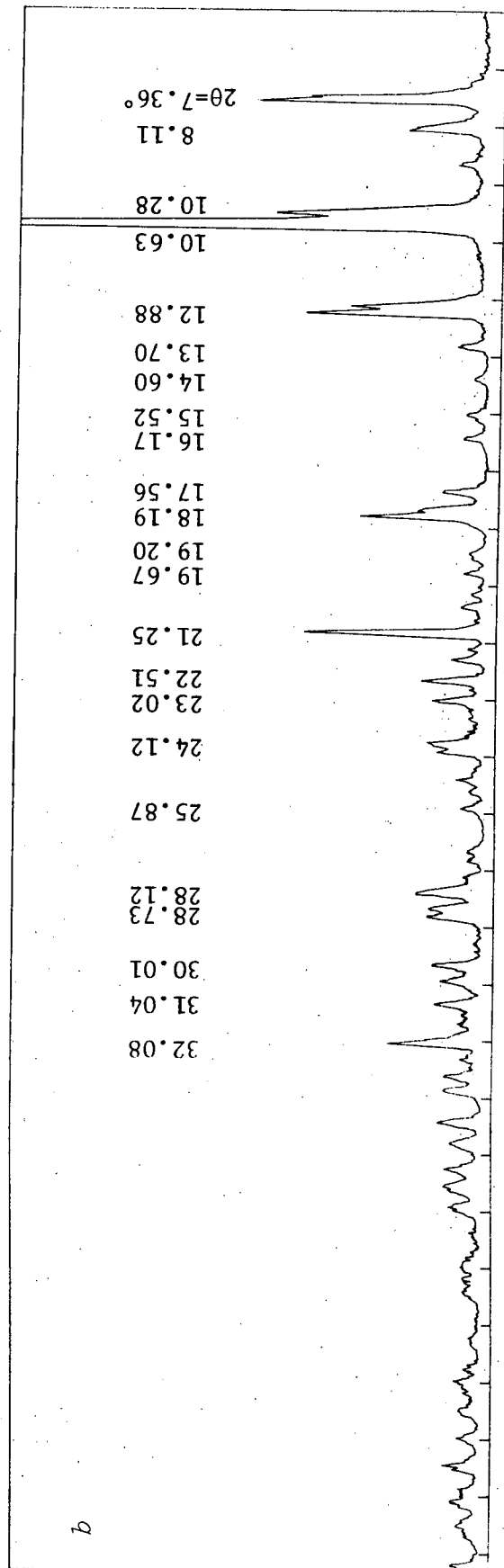
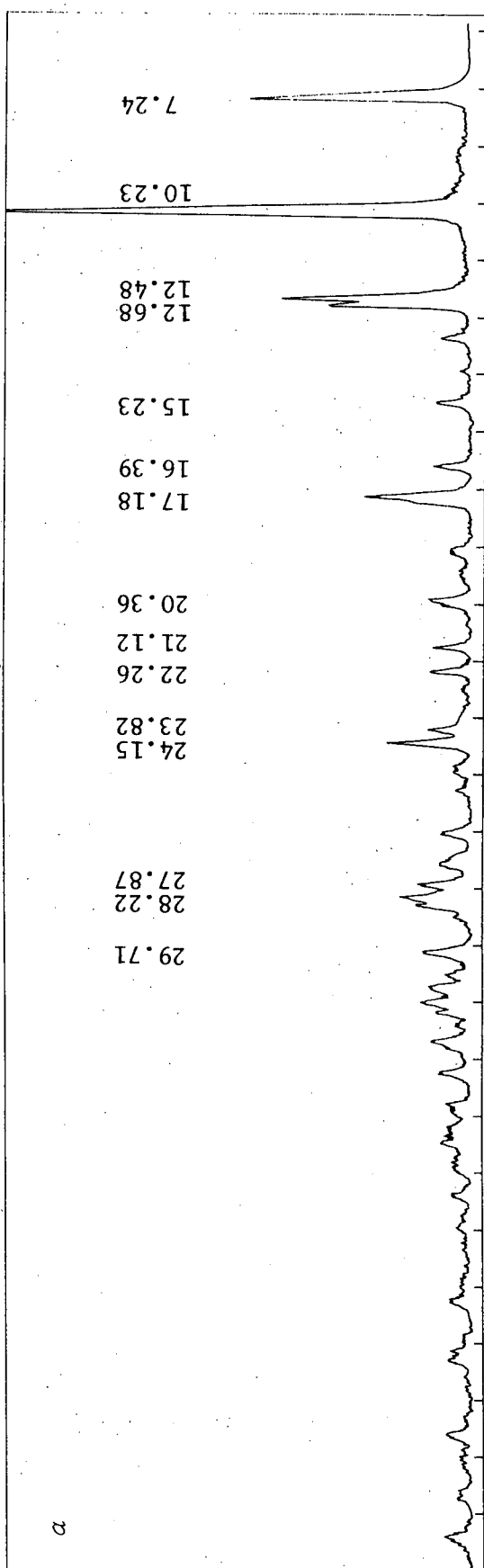


Figure 4.5a:  $\text{CuK}_\alpha$  X-ray powder diffraction patterns of *a*  $[\text{Bu}^t\text{SHgCl}(4\text{-Mepy})_{0.54}]$  and *b*  $[\text{Bu}^t\text{SeHgCl}(\text{py})_{0.5}]_4$ .

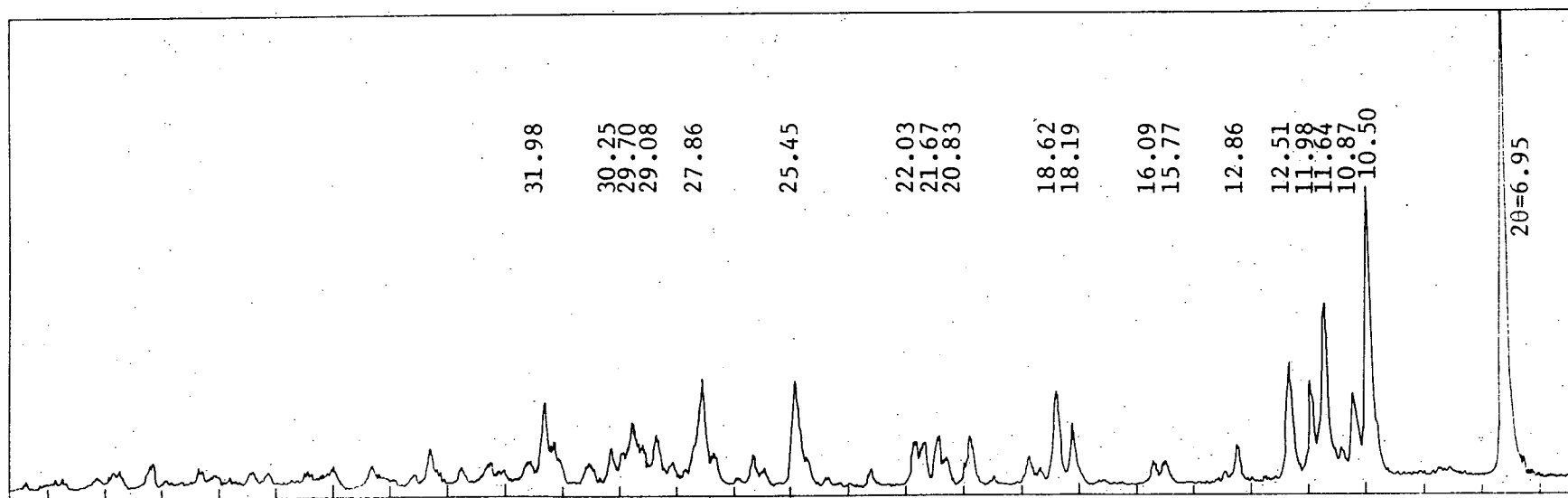


Figure 4.5b:  $\text{CuK}_{\alpha}$  X-ray powder diffraction pattern of  $[\text{Bu}^t\text{SHgCl}(\text{py})_{0.5}]_4$  (cf. Fig. 4.5a)

examined in Tasmania for single-crystal diffraction suitability.

Preliminary oscillation and Weissenberg photographs of one such crystal mounted about the c-axis gave estimates of unit cell parameters  $c = 9.95 \text{ \AA}$  and  $\xi(a) = 0.127$ ,  $\xi(b) = 0.09121$  (giving  $a = 12.14 \text{ \AA}$ ,  $b = 16.91 \text{ \AA}$  assuming  $\alpha = \beta = \gamma \approx 90^\circ$ ). The 0-level Weissenberg photograph required reflections  $0k0$ ,  $k=2n$ , consistent with species group  $P2_1/c$ , and also appeared to have all reflections  $h10$  absent.

A single crystal X-ray diffraction study of this crystal was undertaken by Drs. A.H. White and B.W. Skelton (University of Western Australia).

#### Crystal and Molecular structure of $[\text{Bu}^t\text{SeHgCl}(\text{py})_{0.5}]_4$

A unique data set was gathered at 295 K from a crystal  $0.26 \times 0.1 \times 0.55 \text{ mm}$  mounted in a capillary containing some pyridine, using a Syntex P/2<sub>1</sub> four-cycle diffractometer in the conventional  $2\theta/\theta$  mode within the limits of  $2\theta < 50^\circ$ . 3209 reflections were obtained, 2016 with  $I > 3\sigma(I)$  were considered to be 'observed'. The crystal blackened badly during data collection, necessitating appropriate scaling of the reflection intensities.

#### Crystal data for $[\text{Bu}^t\text{SeHgCl}(\text{py})_{0.5}]_4$

$\text{C}_{28}\text{H}_{50}\text{Cl}_4\text{Hg}_2\text{N}_2\text{Se}_4$ ,  $M = 836.4$ , Monoclinic, space group  $P2_1/c$ .

$a = 12.151(5)$ ,  $b = 16.738(7)$ ,  $c = 10.138(6) \text{ \AA}$ ,  $\beta = 90.93(4)^\circ$

$U = 2062(2) \text{ \AA}^3$ ,  $D_c (Z=2) = 2.69 \text{ g cm}^{-3}$

$F(000) = 1512$

Monochromatic  $\text{MoK}_\alpha$  radiation,  $\lambda = 0.71069 \text{ \AA}$ ,  $\mu_{\text{Mo}} = 180 \text{ cm}^{-1}$

The structure was refined in an identical manner to that for  $\text{Hg}(\text{SeMe})_2$  (page 181) to residuals  $R, R' = 0.058, 0.066$ .

The tetranuclear complex  $[\text{Bu}^t\text{SeHgCl}(\text{py})_{0.5}]_4$  is isomorphous with the 4-methylpyridine complex  $[\text{Bu}^t\text{SHgCl}(4\text{-Mepy})_{0.5}]_4$  ( $a = 12.334(7)$ ),

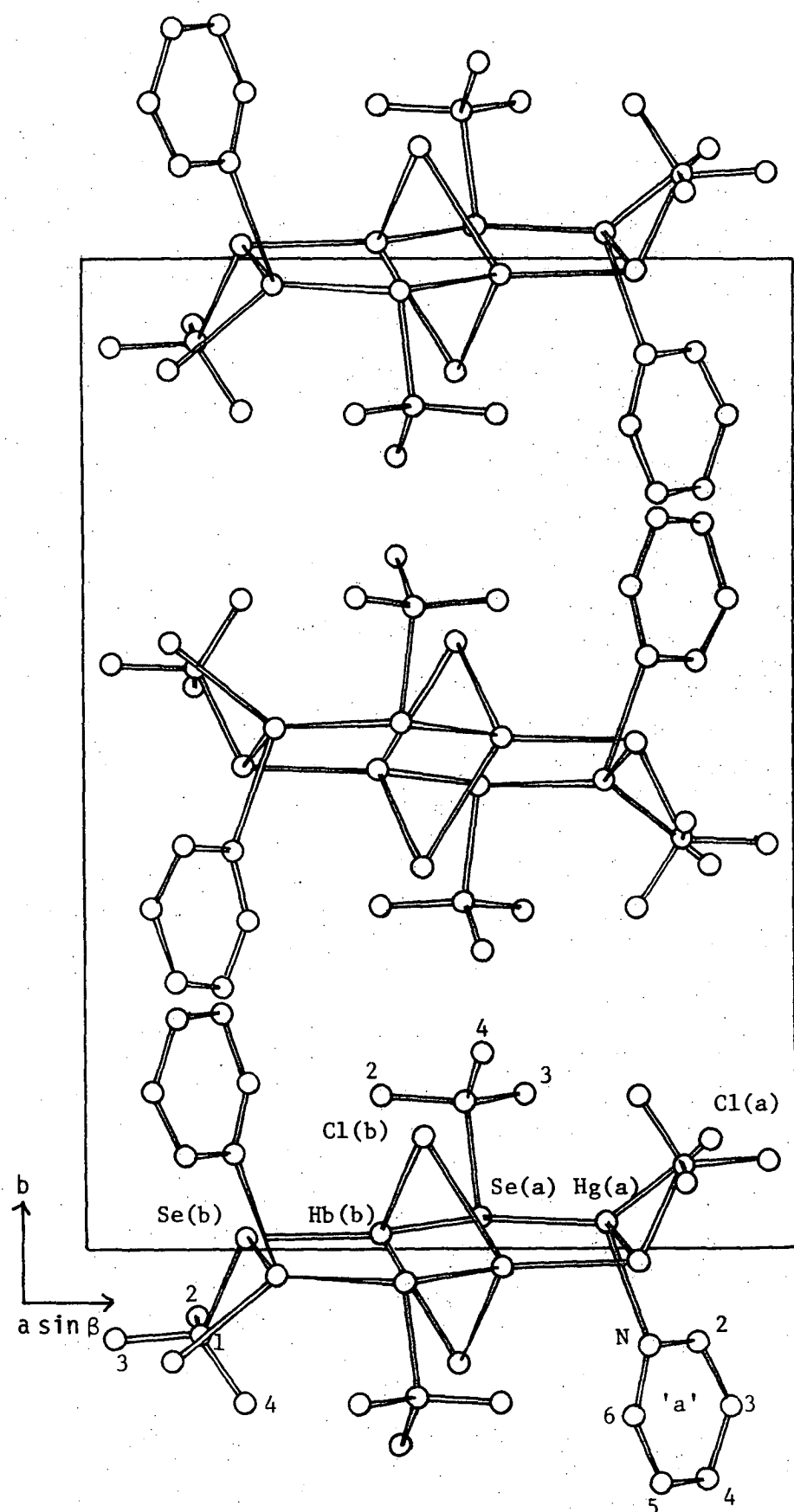


Figure 4.6: Unit-cell contents of  $[\text{Bu}^t\text{SeHgCl}(\text{py})_{0.5}]_4$  projected down  $c$ .

Atom	Distance	Atoms	Angle	Atoms	Angle
Mercury a					
Hg(a)-Cl(a)	2.478(9)	Cl(a)-Hg(a)-Se(a)	112.9(2)	Se(a)-Hg(a)-Se(b <sup>i</sup> )	133.7(1)
Hg(a)-Se(a)	2.579(3)	Cl(a)-Hg(a)-N	95.6(5)	N-Hg(a)-Se(b <sup>i</sup> )	99.1(5)
Hg(a)-N	2.49(2)	Cl(a)-Hg(a)-Se(b <sup>i</sup> )	110.6(2)	Hg(b)...Hg(a)...Hg(b <sup>i</sup> )	
Hg(a)-Se(b <sup>i</sup> )	2.589(3)	Se(a)-Hg(a)-N	91.7(5)		
Mercury b					
Hg(b)-Cl(b)	2.723(6)	Cl(b)-Hg(b)-Se(b)	89.4(1)	Hg(a)...Hg(b)...Hg(a <sup>i</sup> )	123.85(3)
Hg(b)-Se(b)	2.501(3)	Cl(b)-Hg(b)-Se(a)	107.1(1)	Hg(b <sup>i</sup> )...Hg(b)...Hg(a <sup>i</sup> )	62.10(2)
Hg(b)-Se(a)	2.503(3)	Cl(b)-Hg(b)-Cl(b <sup>i</sup> )	95.2(2)		
Hg(b)-Cl(b <sup>i</sup> )	2.720(6)	Se(b)-Hg(b)-Se(a)	155.0(1)		
Hg(b)...Hg(a)	3.905(2)	Se(b)-Hg(b)-Cl(b <sup>i</sup> )	108.2(1)		
Hg(b)...Hg(b <sup>i</sup> )	3.670(2)	Se(a)-Hg(b)-Cl(b <sup>i</sup> )	89.3(1)		
Hg(b)...Hg(a <sup>i</sup> )	3.892(2)	Hg(a)...Hg(b)...Hg(b <sup>i</sup> )			
Chlorine b					
		Hg(b)-Cl(b)-Hg(b <sup>i</sup> )	84.8(2)		
Selenium a					
Se(a)-C(1a)	2.03(2)	Hg(b)-Se(a)-Hg(a)	100.4(1)	Se(a)-C(1a)-C(4a)	111(17)
C(1a)-C(2a)	1.51(3)	Hg(b)-Se(a)-C(1a)	102.0(6)	C(2a)-C(1a)-C(3a)	111(2)
C(1a)-C(3a)	1.56(3)	Hg(a)-Se(a)-C(1a)	105.3(7)	C(2a)-C(1a)-C(4a)	114(2)

cont...

Table 4.7: Interatomic distances (Å) and angles (degrees) for  $[\text{Bu}^t\text{SeHgCl}(\text{py})_{0.5}]_4$ .

Transformation of the asymmetric unit:  $i$  (1-x,  $\bar{y}$ , 1-z)

Least-squares estimated standard deviations of the last digit are given in parentheses.



C(1a)-C(4a)	1.42(4)	Se(a)-C(1a)-C(2a)	105(2)	C(3a)-C(1a)-C(4a)	113(2)
		Se(a)-C(1a)-C(3a)	102(2)		
Selenol b					
Se(b)-C(1b)	2.02(3)	Hg(b)-Se(b)-C(1b)	102.3(7)	Se(b)-C(1b)-C(4b)	111(2)
C(1b)-C(2b)	1.50(4)	Hg(a <sup>i</sup> )-Se(b)-C(1b)	106.3(8)	C(2b)-C(1b)-C(2b)	106(2)
C(1b)-C(3b)	1.54(4)	Hg(b)-Se(b)-Hg(a <sup>i</sup> )	99.7(1)	C(2b)-C(1b)-C(4b)	115(3)
C(1b)-C(4b)	1.44(4)	Se(b)-C(1b)-C(2b)	106(3)	C(3b)-C(1b)-C(4b)	113(3)
		Se(b)-C(1b)-C(3b)	106(2)		
Pyridine					
N-C(2)	1.37(3)	Hg(a)-N-C(2)	120(2)	C(4)-C(5)-C(6)	117(3)
N-C(6)	1.27(5)	Hg(a)-N-C(6)	126(2)	C(5)-C(6)-N	129(3)
C(2)-C(3)	1.33(5)	C(2)-N-C(6)	113(3)		
C(3)-C(4)	1.38(6)	N-C(2)-C(3)	124(3)		
C(4)-C(5)	1.35(6)	C(2)-C(3)-C(4)	118(3)		
C(5)-C(6)	1.33(5)	C(3)-C(4)-C(5)	118(3)		

**Table 4.7:** Interatomic distances (Å) and angles (degrees) for  $[\text{Bu}^t\text{SeHgCl}(\text{py})_{0.5}]_4$ .

(cont.) Transformation of the asymmetric unit:  $i(1-x, \bar{y}, 1-z)$

Least-squares estimated standard deviations of the last digit are given in parentheses.

Atom	Section a			Section b		
	x	y	z	x	y	z
Hg	0.73230(8)	0.02706(7)	0.31574(9)	0.41321(8)	0.01682(6)	0.35281(9)
Cl	0.8800(6)	0.1126(6)	0.2266(8)	0.4758(5)	0.1137(4)	0.5563(6)
Selenol						
Se	0.5531(2)	0.0326(1)	0.1762(2)	0.2228(2)	0.0129(2)	0.4426(2)
C(1)	0.534(2)	0.149(1)	0.126(2)	0.159(2)	-0.085(2)	0.355(2)
C(2)	0.417(2)	0.156(2)	0.075(3)	0.154(3)	-0.067(3)	0.210(3)
C(3)	0.618(2)	0.158(2)	0.011(2)	0.039(2)	-0.090(2)	0.399(3)
C(4)	0.560(3)	0.200(2)	0.235(3)	0.222(2)	-0.155(2)	0.390(4)
Pyridine						
N	0.792(2)	-0.097(1)	0.204(2)			
C(2)	0.861(2)	-0.094(2)	0.099(3)			
C(3)	0.905(3)	-0.157(3)	0.041(3)			
C(4)	0.872(4)	-0.232(2)	0.083(4)			
C(5)	0.807(3)	-0.237(2)	0.189(4)			
C(6)	0.770(2)	-0.168(2)	0.238(3)			

Table 4.8: Non-hydrogen atom atomic coordinates of  $[\text{Bu}^t\text{SeHgCl}(\text{py})_{0.5}]_4$ .  
Least-squares estimated standard deviations of the last digit are given in parentheses.

Atom	$U_{11}$	$U_{22}$	$U_{33}$	$U_{12}$	$U_{13}$	$U_{23}$
Section a						
Hg	29.8(6)	47.6(7)	48.6(6)	-1.0(5)	-0.1(4)	5.3(5)
Cl	42(5)	94(7)	91(6)	-19(5)	6(4)	32(5)
Selenol a						
Se	32(1)	28(1)	37(1)	-1(1)	-2(1)	0(1)
C(1)	53(17)	15(12)	31(12)	-2(11)	11(10)	-1(10)
C(2)	34(17)	46(17)	72(18)	13(13)	5(13)	16(15)
C(3)	54(18)	59(19)	39(14)	-21(15)	1(12)	2(13)
C(4)	96(26)	51(20)	56(18)	4(18)	-17(16)	17(15)
Pyridine						
N	45(15)	47(15)	45(12)	11(12)	-6(10)	-1(11)
C(2)	56(20)	60(21)	54(17)	11(16)	-1(13)	-15(15)
C(3)	63(24)	137(41)	64(21)	0(26)	12(16)	-21(24)
C(4)	103(31)	55(24)	104(29)	-3(23)	9(22)	-32(22)
C(5)	111(33)	46(21)	106(28)	7(21)	45(24)	-8(21)
C(6)	57(21)	86(28)	58(18)	-1(20)	23(14)	-19(19)
Section b						
Hg	27.4(6)	40.2(6)	43.9(5)	-5.1(5)	1.5(4)	2.8(5)
Cl	45(4)	25(3)	50(3)	-1(3)	-1(3)	-5(3)
Selenol b						
Se	26(1)	47(2)	42(1)	2(1)	1(9)	0(1)
C(1)	22(15)	94(26)	55(16)	-20(16)	7(11)	-29(16)
C(2)	77(27)	227(59)	73(24)	-62(33)	6(18)	-24(29)
C(3)	23(16)	89(25)	76(19)	-11(16)	14(12)	-23(13)
C(4)	31(21)	71(25)	222(44)	13(18)	-35(23)	-86(28)

Table 4.9: Anisotropic thermal parameters for  $[\text{Bu}^t\text{SeHgCl}(\text{py})_{0.5}]_4$ .  
Form:  $\exp(-2\pi^2(U_{11}h^2a^{*2} + \dots + 2U_{23}klb^*c^*))$

Atom	x	y	z	$10^3 U \text{ \AA}^2$	$r_{C-H} \text{ \AA}$	$\theta^\circ$	$\phi^\circ$
Selenol a							
H(2a)	0.404(-)	0.123(-)	-0.002(-)	78(-)	0.96(-)	111(-)	109(-)
H(2b)	0.365(-)	0.142(-)	0.140(-)	78(-)	0.95(-)	113(-)	110(-)
H(2c)	0.407(-)	0.211(-)	0.050(-)	78(-)	0.96(-)	106(-)	108(-)
H(3a)	0.691(-)	0.147(-)	0.036(-)	72(-)	0.94(-)	114(-)	109(-)
H(3b)	0.598(-)	0.124(-)	-0.063(-)	72(-)	0.96(-)	112(-)	109(-)
H(3c)	0.610(-)	0.213(-)	-0.015(-)	72(-)	0.97(-)	103(-)	110(-)
H(4a)	0.514(-)	0.189(-)	0.307(-)	93(-)	0.95(-)	112(-)	108(-)
H(4b)	0.636(-)	0.192(-)	0.264(-)	93(-)	0.98(-)	111(-)	105(-)
H(4c)	0.553(-)	0.256(-)	0.213(-)	93(-)	0.97(-)	113(-)	108(-)
Selenol b							
H(2a)	0.105(-)	-0.021(-)	0.191(-)	160(-)	1.00(-)	111(-)	106(-)
H(2b)	0.223(-)	-0.055(-)	0.173(-)	160(-)	0.94(-)	115(-)	110(-)
H(2c)	0.122(-)	-0.122(-)	0.164(-)	160(-)	0.96(-)	109(-)	106(-)
H(3a)	0.034(-)	-0.095(-)	0.490(-)	81(-)	0.93(-)	112(-)	110(-)
H(3b)	-0.002(-)	-0.044(-)	0.370(-)	81(-)	0.96(-)	111(-)	108(-)
H(3c)	0.007(-)	-0.136(-)	0.356(-)	81(-)	0.97(-)	106(-)	110(-)
H(4a)	0.296(-)	-0.151(-)	0.368(-)	133(-)	0.92(-)	113(-)	108(-)
H(4b)	0.218(-)	-0.163(-)	0.486(-)	133(-)	0.99(-)	108(-)	105(-)
H(4c)	0.191(-)	-0.203(-)	0.352(-)	133(-)	0.96(-)	112(-)	110(-)

**Table 4.10:** Methyl hydrogen atom parameters for  $[\text{Bu}^t\text{SeHgCl}(\text{py})_{0.5}]_4$ .  
 $\sigma = \text{C-C-H}$ ,  $\phi = \text{H}(n)\text{-C-H}(n+1)$ ,  $n = \text{a,b,c}$ .

$b = 17.468(9)$ ,  $c = 9.999(5)$  Å,  $\beta = 91.18(4)^\circ$ , space group  $P2_1/c$ ) but not with the analogous pyridinate  $[\text{Bu}^t\text{SHgCl}(\text{py})_{0.5}]_4$  ( $a = 14.399(6)$ ,  $b = 9.893(6)$ ,  $c = 9.597(5)$  Å,  $\alpha = 121.82(1)$ ,  $\beta = 102.52(4)$ ,  $\gamma = 102.94(4)^\circ$ , space group  $P\bar{1}$ ). These findings are consistent with X-ray powder diffraction patterns. Consistent with the presence of pyridine rather than 4-Mepy, the complex has an asymmetric unit volume of  $515.5(5)$  Å<sup>3</sup>, very similar to  $517.8(4)$  Å<sup>3</sup> for  $[\text{Bu}^t\text{SHgCl}(\text{py})_{0.5}]_4$ , but not the 4-Mepy analog,  $538.5(5)$  Å<sup>3</sup>.

Finally, no peaks in the Fourier difference map could be attributed to presence of a methyl carbon of 4-Mepy, indicating that a mistake in sample labelling or preparation had not occurred. In addition, a freshly prepared sample of  $[\text{Bu}^t\text{SHgCl}(\text{py})_{0.5}]_4$  had all unit cell parameters in agreement with those previously published. Molecules of tetrameric  $[\text{Bu}^t\text{SeHgCl}(\text{py})_{0.5}]_4$  are based on an eight-membered ring of alternating mercury and selenium atoms  $(-\text{Hg}-\text{SeBu}^t)_4$ . The rings have a centre of symmetry and two mercury environments,  $[\text{Hg}(\mu\text{-Se})_2(\mu\text{-Cl})_2]$  and  $[\text{Hg}(\mu\text{-Se})_2\text{Cl}(\text{py})]$  with a dichloro bridge linking the former mercury atoms (Figure 4.6). The close relationships between the eight membered ring structures for  $[\text{Bu}^t\text{SeHgCl}(\text{py})_{0.5}]_4$  and the sulfur analogs  $[\text{Bu}^t\text{SHgCl}(4\text{-Mepy})_{0.5}]_4$  (isomorphous) and  $[\text{Bu}^t\text{SHgCl}(\text{py})_{0.5}]_4$  can be clearly seen as projections of these structures normal to planes containing the four Se or S atoms (Figure 4.7). All of these compounds have distorted tetrahedral geometry for mercury, with the largest angles formed by dominant Se-Hg-Se and S-Hg-S moieties.

#### $[\text{EtSeHgCl}(\text{py})]_4$

Reaction of equimolar quantities of  $\text{Hg}(\text{SeEt})_2$  and  $\text{HgCl}_2$  in pyridine

produces a colorless crystalline complex which does not readily lose pyridine and analyses as  $\text{EtSeHgCl(py)}$ . The analogous sulfur compound is unknown. High quality prismatic crystals were deposited when the complex was dissolved in pyridine, and ethanol added, to produce a 1:1 EtOH/pyridine ratio.

A single crystal X-ray diffraction study was performed by Drs. A.H. White and B.W. Skelton (University of Western Australia) on a crystal of this complex.

#### Crystal and molecular structure of $[\text{EtSeHgCl(py)}]_4$

A unique data set was gathered at 295 K from a crystal 0.11 x 0.07 x 0.06 mm mounted in a sealed capillary to minimise pyridine loss. A Syntex P2<sub>1</sub> four-circle diffractometer was used in the conventional  $2\theta/\theta$  mode with  $2\theta < 60^\circ$  to give 3794 reflections, 1678 with  $I > 3\sigma(I)$  were considered to be 'observed'. The crystal blackened during data collection, but no data scaling was necessary.

#### Crystal data for $[\text{EtSeHgCl(py)}]_4$

$\text{C}_{28}\text{H}_{40}\text{Cl}_4\text{Hg}_4\text{N}_4\text{Se}_4$ ,  $M = 1692.7$ , Monoclinic, space group  $\text{P2}_1/\text{c}$   
 $a = 8.044(5)$ ,  $b = 17.387(14)$ ,  $c = 15.585(21)$  Å,  $\beta = 101.75(2)^\circ$   
 $U = 2134(3)$  Å<sup>3</sup>,  $D_c$  ( $Z=2$ ) =  $2.63 \text{ g cm}^{-3}$   
 $F(000) = 1520$

Monochromatic  $\text{MoK}_\alpha$  radiation,  $\lambda = 0.71069$  Å,  $\mu_{\text{Mo}} = 174 \text{ cm}^{-1}$

The structure was refined in an identical manner to  $\text{Hg}(\text{SeMe})_2$  (page 181) to residuals  $R, R' = 0.046, 0.049$ .

Molecules of tetrameric  $[\text{EtSeHgCl(py)}]_4$  are based on the same eight-membered ring found in tert-butylthiolato and tert-butylselenolato hemi-base adducts described previously. The  $(-\text{Hg-SeEt}-)_4$  rings contain mercury atoms bridged by ethaneselenolate groups, but contain only one mercury environment ' $\text{Hg}(\mu\text{-SeEt})_2\text{Cl(py)}$ ' in contrast to the *t*-butyl

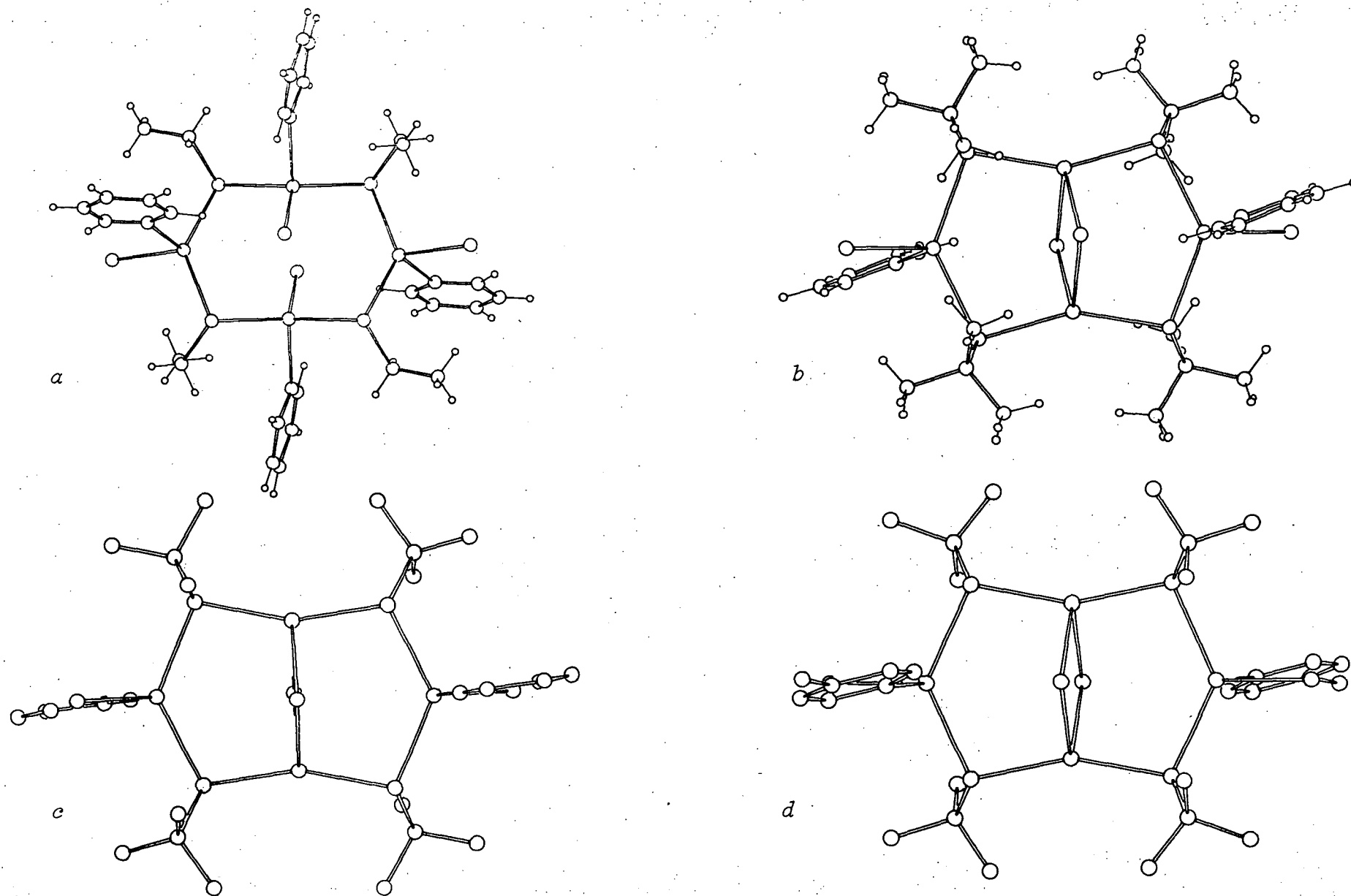


Figure 4.7: Single molecules of *a*  $[\text{EtSeHgCl(py)}]_4$ , *b*  $[\text{Bu}^t\text{SeHgCl(py)}_{0.5}]_4$ , *c*  $[\text{Bu}^t\text{SeHgCl(py)}_{0.5}]_4$  and *d*  $[\text{Bu}^t\text{SHgCl(4-Mepy)}_{0.5}]_4$  projected normal to the plane of the four chalcogen atoms.

Atoms	Parameters
Distances/Å	
HgCl	2.543(7), 2.546(6)
Hg-N	2.42(2), 2.48(2)
Hg-Se(A)	2.542(3), 2.541(4)
Hg-Se(B)	<i>2.543(3)</i> , 2.551(3)
Angles/degrees	
Cl-Hg-N	92.8(5), 95.0(5)
Cl-Hg-Se(A)	111.9(2), 113.6(2)
Cl-Hg-Se(B)	<i>103.7(2)</i> , 106.7(2)
N-Hg-Se(A)	99.3(5), 101.3(6)
N-Hg-Se(B)	<i>106.5(5)</i> , 99.7(5)
Se(A)-Hg-Se(B)	<i>134.7(1)</i> , 132.2(1)
Hg-Se-C(11)	103.6(8), 101.3(8)

Also: Hg(A), C(1B)-Se(B)-Hg(A)( $\bar{x}$ ,1-y,1-z), 99.20(8), 100.7(9)°.

**Table 4.11:** Mercury/selenium geometries for [EtSeHgCl(py)]<sub>4</sub>.

The two entries in each column are for Hg, Se, A,B respectively. Italicized entries involve Se(B) ( $\bar{x}$ ,1-y,1-z).

Least-squares estimated standard deviations of the last digit are given in parentheses.



	Ligand a	Ligand b
(a) ethaneselenolate ligand		
Distances/Å		
Se-C(11)	1.92(3)	1.99(3)
C(11)-C(10)	1.35(5)	1.47(5)
Angles/degrees		
Se-C(11)-C(12)	120(3)	113(2)
(b) pyridine rings		
Distances/Å		
N(1)-C(2)	1.33(4)	1.36(4)
N(1)-C(6)	1.31(3)	1.32(4)
C(2)-C(3)	1.36(5)	1.38(4)
C(3)-C(4)	1.34(5)	1.40(4)
C(4)-C(5)	1.33(4)	1.37(5)
C(5)-C(6)	1.34(4)	1.36(5)
Angles/degrees		
C(2)-N(1)-C(6)	118(2)	120(2)
N(1)-C(2)-C(3)	120(3)	120(2)
C(2)-C(3)-C(4)	121(3)	120(3)
C(3)-C(4)-C(5)	118(3)	118(3)
C(4)-C(5)-C(6)	119(3)	121(3)
C(5)-C(6)-N(1)	123(2)	122(3)
Hg-N(1)-C(2)	120(2)	114(2)
Hg-N(1)-C(6)	122(2)	125(2)

Table 4.12: Ligand geometries for  $[\text{EtSeHgCl}(\text{py})]_4$ .

Least-squares estimated standard deviations of the last digit are given in parentheses.

Atom	Section a			Section b		
	x	y	z	x	y	z
Hg	0.00980(13)	0.47808(6)	0.29104(7)	0.21525(13)	0.43468(6)	0.53369(6)
Cl	-0.0344(9)	0.3927(4)	0.1559(4)	-0.0868(8)	0.3846(4)	0.5182(4)
Se	0.3016(3)	0.4589(1)	0.3880(2)	0.2883(3)	0.5038(1)	0.6809(2)
C(11)	0.373(4)	0.361(2)	0.351(2)	0.370(4)	0.417(2)	0.762(2)
C(12)	0.266(6)	0.301(2)	0.342(2)	0.421(5)	0.440(3)	0.854(3)
N(1)	0.068(3)	0.590(1)	0.290(1)	0.353(3)	0.309(1)	0.576(1)
C(2)	0.109(3)	0.657(2)	0.252(2)	0.519(4)	0.306(1)	0.571(2)
C(3)	0.153(4)	0.718(2)	0.207(2)	0.605(3)	0.237(2)	0.581(2)
C(4)	0.155(4)	0.713(2)	0.121(2)	0.518(4)	0.169(2)	0.592(2)
C(5)	0.115(4)	0.647(2)	0.081(2)	0.349(4)	0.175(2)	0.595(2)
C(6)	0.077(4)	0.586(1)	0.127(1)	0.270(4)	0.244(2)	0.585(2)

Table 4.13: Non-hydrogen atom coordinates for [EtSeHgCl(py)]<sub>4</sub>.

Least-squares estimated standard deviations of the last digit are given in parentheses.

Atom	$U_{11}$	$U_{22}$	$U_{33}$	$U_{12}$	$U_{13}$	$U_{23}$
Section a						
Hg	50.4(6)	56.6(7)	53.2(6)	-4.4(6)	19.9(5)	-4.2(6)
Cl	77(5)	76(5)	68(5)	- 4(4)	20(4)	-26(4)
Se	50(1)	63(2)	63(2)	7(1)	28(1)	4(1)
C(11)	134(29)	61(21)	62(19)	58(21)	19(19)	- 8(17)
C(12)	293(56)	32(18)	107(30)	-26(28)	-13(32)	-35(20)
N(1)	71(14)	67(16)	37(12)	1(12)	21(11)	- 8(11)
C(2)	68(19)	81(22)	53(18)	- 9(17)	21(15)	16(17)
C(3)	126(29)	103(28)	54(20)	-27(22)	15(20)	- 6(20)
C(4)	133(28)	40(18)	103(26)	- 3(19)	49(23)	53(19)
C(5)	184(33)	60(20)	27(15)	23(21)	51(18)	4(15)
C(6)	135(27)	52(18)	48(17)	-13(17)	37(18)	11(14)
Section b						
Hg	54.6(6)	58.6(7)	53.3(6)	9.4(6)	22.5(5)	-0.6(6)
Cl	55(4)	61(4)	71(5)	- 5(3)	27(4)	- 5(4)
Se	47(2)	64(2)	67(2)	- 8(1)	20(1)	-11(1)
C(11)	113(26)	77(23)	64(19)	51(19)	0(18)	41(17)
C(12)	171(41)	184(42)	101(30)	12(34)	- 5(28)	-44(31)
N(1)	62(17)	69(18)	91(19)	30(14)	28(14)	1(14)
C(2)	82(20)	32(14)	50(16)	10(15)	20(15)	1(12)
C(3)	52(17)	102(25)	64(18)	40(18)	19(15)	23(18)
C(4)	100(26)	51(20)	116(27)	25(18)	49(22)	13(18)
C(5)	67(22)	70(23)	143(31)	- 1(18)	44(21)	- 2(21)
C(6)	73(22)	86(25)	127(29)	-14(21)	53(21)	- 8(23)

Table 4.14: Non-hydrogen atom thermal parameters,  $10^3 U_{ij} \text{ \AA}^2$  for  $[\text{EtSeHgCl}(\text{py})]_4$ .

Anisotropic thermal parameters are of the form:

$$\exp(-2\pi^2(U_{11}h^2a^{*2} + \dots + 2U_{23}klb^*c^*))$$

Least-squares estimated standard deviations of the last digit are given in parentheses.

Atom	x	y	z	$10^3 u \text{ \AA}^2$	$r \text{ \AA}$	$\theta^\circ$	$\phi^\circ$	$\chi^\circ$
Aromatic hydrogens $\theta, \phi = N, C(n+1)-C(n)-H(n)$								
Section a								
H(2)	0.114(-)	0.661(-)	0.315(-)	81(-)	0.98(-)	120(-)	120(-)	
H(3)	0.180(-)	0.768(-)	0.238(-)	115(-)	1.00(-)	120(-)	119(-)	
H(4)	0.181(-)	0.758(-)	0.088(-)	97(-)	0.97(-)	122(-)	120(-)	
H(5)	0.117(-)	0.641(-)	0.021(-)	104(-)	0.95(-)	122(-)	119(-)	
H(6)	0.055(-)	0.536(-)	0.098(-)	97(-)	0.99(-)	120(-)	117(-)	
Section b								
H(2)	0.578(-)	0.354(-)	0.560(-)	63(-)	0.99(-)	120(-)	120(-)	
H(3)	0.728(-)	0.235(-)	0.582(-)	84(-)	0.99(-)	120(-)	120(-)	
H(4)	0.579(-)	0.120(-)	0.597(-)	92(-)	0.98(-)	120(-)	122(-)	
H(5)	0.287(-)	0.128(-)	0.607(-)	104(-)	1.00(-)	119(-)	120(-)	
H(6)	0.148(-)	0.248(-)	0.583(-)	106(-)	0.97(1)	120(-)	118(-)	
Methyl hydrogens $\theta = C-C-H$ , $\phi = H(n)-C-H(n+1)$ , $n = A, B, C$								
Section a								
H(12A)	0.229(-)	0.294(-)	0.398(-)	165(-)	0.98(-)	108(-)	105(-)	
H(12B)	0.164(-)	0.317(-)	0.301(-)	165(-)	0.98(-)	106(-)	109(-)	
H(12C)	0.300(-)	0.254(-)	0.325(-)	165(-)	0.91(-)	120(-)	108(-)	

cont...

Table 4.15: Hydrogen atom parameters for  $[(EtSeHgCl)py]_4$ .

Least-squares estimated standard deviations of the last digit are given in parentheses.

Section b

H(12A)	0.511(-)	0.476(-)	0.860(-)	155(-)	0.94(-)	110(-)	110(-)
H(12B)	0.327(-)	0.464(-)	0.873(-)	155(-)	0.96(-)	110(-)	107(-)
H(12C)	0.458(-)	0.397(-)	0.893(-)	155(-)	0.97(-)	113(-)	109(-)

Methyl hydrogens  $\theta, \phi = \text{Se}, \text{C-C-H}, \chi = \text{H-C-H}$

Section a

H(11A)	0.412(-)	0.369(-)	0.297(-)	104(-)	0.97(-)	108(-)	109(-)	104(-)
H(11B)	0.478(-)	0.347(-)	0.394(-)	104(-)	1.00(-)	107(-)	108(-)	

Section b

H(11A)	0.277(-)	0.377(-)	0.757(-)	98(-)	1.00(-)	109(-)	109(-)	104(-)
H(11B)	0.461(-)	0.389(-)	0.743(-)	98(-)	0.97(-)	111(-)	110(-)	

Table 4.15: Hydrogen atom parameters for  $[(\text{EtSeHgCl})\text{py}]_4$ .  
(cont.)

	[EtSeHgCl(py)] <sub>4</sub>		[Bu <sup>t</sup> SeHgCl(py) <sub>0.5</sub> ] <sub>4</sub>
	Plane a (2)	Plane b (2)	(3)
10 <sup>4</sup> p	9332	0351	7733
10 <sup>4</sup> q	-2750	1264	0103
10 <sup>4</sup> r	2315	9914	6340
s	-2.174	9.410	8.710
σ	0.01	0.01	0.02
δN(1)	-0.02	0.02	0.00
δC(2)	0.00	-0.02	-0.01
δC(3)	0.01	0.01	0.03
δC(4)	-0.01	0.00	-0.03
δC(5)	-0.01	0.00	0.02
δC(6)	0.02	-0.01	0.00
δHg	0.13	-0.38	0.16

**Table 4.16:** Pyridine ring planes for [EtSeHgCl(py)] and [Bu<sup>t</sup>SeHgCl(py)<sub>0.5</sub>]<sub>4</sub>.

Least-squares planes are given in the form  $pX + qY + rZ = s$ , where the R.H. orthogonal Å frame (X,Y,Z) is defined with X parallel to a, Z in the ac plane. σ(defining atoms) and atom deviations, δ, are in Å. Planes are defined by the C<sub>5</sub>N skeleton.

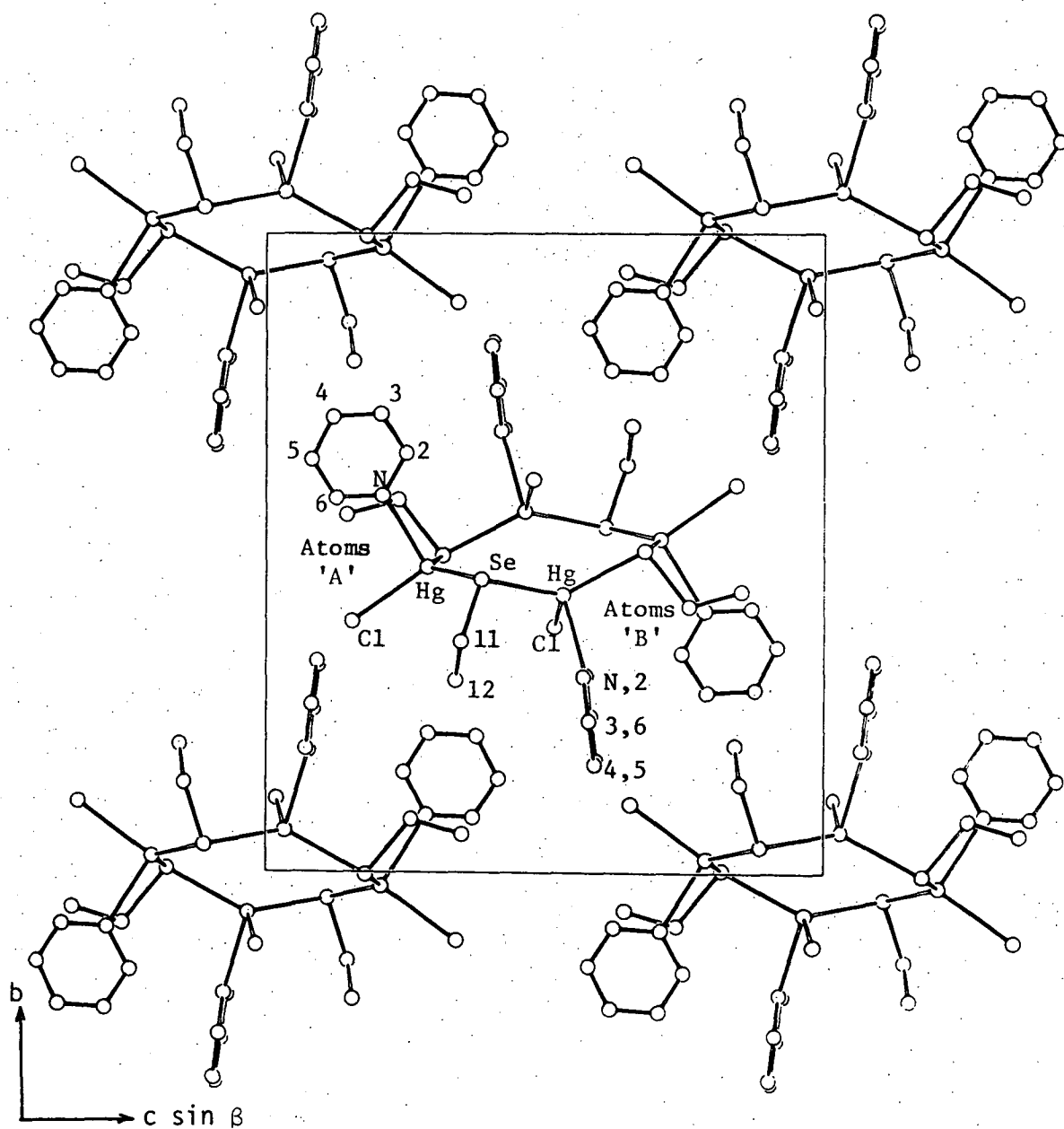


Figure 4.8: Unit-cell contents of  $[\text{EtSeHgCl}(\text{py})]_4$  projected down  $a$ .

derivatives. A projection of the unit cell contents along  $c$  is shown in Figure 4.8. The molecule is centrosymmetric about a crystallographic symmetry element, and the two independent mercury atoms have very similar geometries with bond distances within  $2\sigma$  and bond angles within  $3^\circ$  (except for angles N-Hg-Se(b) which differ by  $6.8^\circ$ ). The structure lacks a dichloro bridge between Hg atoms found in the *t*-butyl substituted derivatives, but instead has an extra pyridine molecule coordinated to these mercury atoms.

A view of a single molecule of  $[\text{EtSeHgCl(py)}]_4$  projected normal to the plane containing the four selenium atoms is shown in Figure 4.7. In the *t*-butyl derivatives, steric hindrance permits coordination of only two pyridine bases per tetrameric unit, in contrast to four for the ethyl derivative, with concomitant dichloro bridging to maintain tetrahedral mercury coordination. The disposition of *t*-butyl methyl groups in  $[\text{tBuSeHgCl(py)}_{0.5}]_4$  is consistent with this observation, being such as to allow coordination of pyridine bases to two of the centrosymmetrically related mercury atoms when the ring is chlorine bridged, but not at the other pair.

The pyridine rings in  $[\text{EtSeHgCl(py)}]$  and  $[\text{Bu}^t\text{SeHgCl(py)}_{0.5}]_4$  are planar as expected. The maximum deviation from least squares planes, defined by the  $\text{C}_5\text{N}$  skeletons, being  $-0.03 \text{ \AA}$  in the *t*-butyl derivative. Table 4.16 shows that mercury atoms coordinated to pyridine lie close to the pyridine plane.

#### 4.2.3 Comparison of Hg-S and Hg-Se bonding distances

This work has produced the first report of Mercury(II)-selenolate bond distances. It is of interest to compare Hg-S and Hg-Se bond distances in closely related complexes because it has been noted earlier


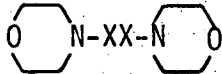
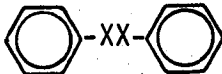
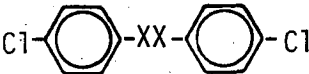
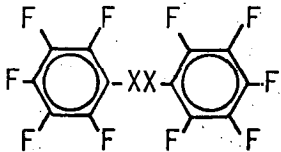


that Hg-Se bond lengths in  $[\text{HgCl}_2(\text{Ph}_3\text{PSe})]_2$ <sup>458</sup> (2.53 Å) and the selenourea complex of MeHg(II),  $[\text{MeHgSeC}(\text{NH}_2)_2]\text{NO}_3$ <sup>434</sup> (2.477(3) Å) are shorter than expected, even though for these complexes suitable sulfur analogs are not available for a direct comparison.

The covalent radii of sulfur and selenium differ by 0.13 Å (Pauling)<sup>242</sup>, although recent determinations of the structures of elemental sulfur and selenium, and of  $\text{R}_2\text{X}_2$  (X=S,Se) result in distances  $\{\frac{1}{2}[(\text{Se-Se})-(\text{S-S})]\}$  covering the range 0.13(2) - 0.182(4) Å (Table 4.17).

Values of Hg-S and Hg-Se bond distances in closely related complexes are given in Table 4.18 for ' $\text{Hg}(\mu\text{-SR})_4$ '; the difference between average values is 0.04 Å. For  $[\text{Bu}^t\text{SeHgCl}(\text{py})_{0.5}]_4$  which has bond angles at mercury within 5° of those for the sulfur analogs, the differences are 0.12 Å for ' $\text{Hg}(\mu\text{-XBu}^t)_2(\mu\text{-Cl})_2$ ' and 0.08 Å for ' $\text{Hg}(\mu\text{-XBu}^t)_2\text{ClN}$ '.

In general it can be concluded that Hg-Se bond distances are slightly shorter than expected from a consideration of sulfur and selenium covalent radii. In the MeHg(II)-selenourea complex, this has been considered to be a reflection of 'strong' Hg-Se bonding.<sup>434</sup> Sugiura has suggested that this may be due to the enhanced ability of selenium to participate in metal-ligand backbonding.<sup>404</sup>

Structure	S-S/Å	Se-Se/Å	$\frac{1}{2}[(\text{Se-Se})-(\text{S-S})]/\text{Å}$
monoclinic- $\text{X}_8$	2.046(4) <sup>459</sup>	2.334(6) <sup>460</sup>	0.144(5)
$\text{K}_2\text{X}_3$	2.083(1) <sup>461</sup> 2.076(5) <sup>462</sup>	2.383(2) <sup>461</sup> 2.40(5) <sup>462</sup>	0.150(2) 0.16(3)
	2.069(15) <sup>463</sup>	2.321(15) <sup>463</sup>	0.126(15)
	2.068(8) <sup>464</sup>	2.346(1) <sup>465</sup>	0.139(5)
	2.030(5) <sup>466</sup> 2.023(1) <sup>467</sup>	2.290(10) <sup>466</sup>	0.134(6)
	2.039 <sup>468</sup>	2.333(15) <sup>469</sup>	0.147
	2.059(4) <sup>466</sup>	2.319(4) <sup>466</sup>	0.130(4)
$[(\text{H}_2\text{N})_2\text{C}-\text{XX}-\text{C}(\text{NH}_2)_2]\text{Cl}_2$	2.017(2) <sup>470</sup>	2.380(6) <sup>470</sup>	0.182(4)
<hr/>			
X-X distances	1.009(1)-1.042(1) <sup>a</sup>	1.145(5)-1.190(3) <sup>b</sup>	

**Table 4.17:** Differences between covalent radii in isomorphous sulfur and selenium structures.

<sup>a,b</sup>The X-X distances are in good agreement with the Pauling covalent radii of 1.16 Å (Se) and 1.02 Å (S).<sup>242</sup>

	Hg-Se/Å	Hg-S/Å	[(Hg-Se)-(Hg-S)]/Å
'Hg( $\mu$ -XR) <sub>2</sub> (-Cl) <sub>2</sub> '	2.501(3), 2.503(3) <sup>a</sup>	$\left( \begin{array}{l} 2.38(1), 2.39(1)^{293^b} \\ 2.379(8), 2.395(8)^{295^c} \end{array} \right)$	0.12
'Hg( $\mu$ -XR) <sub>2</sub> ClN'	2.579(3), 2.589(3) <sup>a</sup>	$\left( \begin{array}{l} 2.488(7), 2.509(9)^{293^b} \\ 2.501(8), 2.505(8)^{295^c} \end{array} \right)$	0.08
	2.541(4)-2.511(3) <sup>d</sup>		
'Hg( $\mu$ -XR) <sub>4</sub> '	2.624(2)-2.764(2) <sup>e</sup>	2.59, 2.68 <sup>273^f</sup>	0.04
'MeHgXCH <sub>2</sub> CH(NH <sub>3</sub> )(CO <sub>2</sub> ).H <sub>2</sub> O'	2.466(5) <sup>433</sup>	2.352(12) <sup>236</sup>	0.06

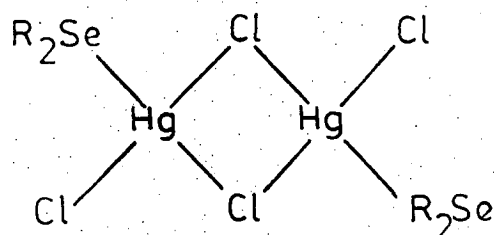
Table 4.18: Comparisons of Hg-S and Hg-Se bond lengths in closely related structures.

<sup>a</sup>[Bu<sup>t</sup>SeHgCl(py)<sub>0.5</sub>]<sub>4</sub>, <sup>b</sup>[Bu<sup>t</sup>SHgCl(py)<sub>0.5</sub>]<sub>4</sub>, <sup>c</sup>[Bu<sup>t</sup>SHgCl(4-Mepy)<sub>0.5</sub>]<sub>4</sub>, <sup>d</sup>[EtSeHgCl(py)]<sub>4</sub>,  
<sup>e</sup>Hg(SeMe)<sub>2</sub>, <sup>f</sup>Hg(SBu<sup>t</sup>)<sub>2</sub>.

### 4.3 Vibrational spectroscopy of mercury(II) selenolates

#### 4.3.1 Bis(selenolato)mercury(II) complexes, $\text{Hg}(\text{SeR})_2$

No vibrational spectroscopy has been reported to date for bis(alkylseleno)mercury(II) compounds. During this work Dr. A.J. Carty (University of Waterloo) kindly informed us of work in his laboratory<sup>433</sup> which involved structural and vibrational characterisation of mercury(II),  $\text{CH}_3\text{Hg}(\text{II})$  and  $\text{CF}_3\text{Hg}(\text{II})$  complexes with the selenoamino acids seleno-D,L-methionine and seleno-D,L-cysteine, but is as yet unpublished. Infrared and Raman spectroscopic data have been reported for the perfluoroalkyl-seleno complex  $(\text{CF}_3\text{Se})_2\text{Hg}$ , which was ascribed an approximately linear structure<sup>448</sup> with  $\nu_{\text{as}}(\text{SeHgSe}) 233$  and  $\nu_{\text{s}}(178 \text{ vs cm}^{-1})$  polarised in Raman by comparison with the spectra of  $(\text{CF}_3\text{S})_2\text{Hg}$ .<sup>490</sup> Some infrared spectroscopic data is available from the dimeric complexes formed between mercuric halides and selenoethers.<sup>471</sup> Detailed vibrational studies have not been reported, but it is claimed that infrared absorptions at  $190, 202 \text{ cm}^{-1}$ <sup>471</sup> attributed to Hg-Se stretching are consistent with the expected centrosymmetric dimeric structure containing bridging halides, by analogy with 1:1 mercuric halide complexes with tertiary phosphines and arsines.<sup>458</sup>



Similarly, a centrosymmetric chlorine bridged structure has been determined for  $[\text{HgCl}_2(\text{Ph}_3\text{PSe})]_2$ <sup>458</sup> by single crystal X-ray diffraction.

Vibrational spectra of  $\text{Hg}(\text{SR})_2$  have mercury-sulfur stretching modes which show the expected<sup>472</sup> decrease in frequency with increasing

coordination number, e.g.  $\text{Hg}(\text{SMe})_2$  which has linear ' $\text{HgS}_2$ ' geometry<sup>271</sup> (Figure 2.6, page 45) has  $\nu_s(\text{SHgS})$   $297\text{ cm}^{-1}$  and  $\nu_{as}(\text{SHgS})$   $337\text{ cm}^{-1}$  whereas tetrahedral<sup>273</sup>  $\text{Hg}(\text{SBut})_2$  (Figure 2.8, page 45) has  $\nu_s(\text{SHgS})$   $188\text{ cm}^{-1}$  and  $\nu_{as}(\text{SHgS})$   $172\text{ cm}^{-1}$ .<sup>231</sup> Substitution of sulfur by selenium in *isostructural* compounds would be expected<sup>473</sup> to lead to a decrease in the mercury-chalcogen stretching frequencies, according to the ratio of Hg-S and Hg-Se reduced-masses, as follows:

$$\nu_{\text{HgSe}} \approx \nu_{\text{HgS}} \left[ \frac{m_{\text{S}}/m_{\text{S}}+m_{\text{Hg}}}{m_{\text{Se}}/m_{\text{Se}}+m_{\text{Hg}}} \right]^{1/2} = 0.7 \nu_{\text{HgS}}$$

This calculation can only be considered an approximation which assumes that vibrational force-constants remained unchanged on substitution of S by Se. Since there is some evidence that Hg-Se bonds may be somewhat stronger than Hg-S bonds (page 214), calculated values of  $\nu_{\text{HgSe}}$  will be, to a first approximation, too low.

Linear ' $\text{HgSe}$ ' coordination is therefore expected to give rise to  $\nu_{as}(\text{SeHgSe})$   $\sim 235\text{ cm}^{-1}$  and  $\nu_s(\text{SeHgSe})$   $\sim 210\text{ cm}^{-1}$  by comparison with  $\text{Hg}(\text{SMe})_2$ . The perfluorinated complex  $\text{Hg}(\text{SeCF}_3)_2$ <sup>448</sup> has  $\nu_{as}$   $233\text{ cm}^{-1}$  (solid mull), and  $\nu_s$   $178\text{ cm}^{-1}$  (MeOH solution) which is in good agreement with the calculated value  $\nu_s$   $170\text{ cm}^{-1}$  (from  $\nu_s$   $243\text{ cm}^{-1}$  for  $\text{Hg}(\text{SCF}_3)_2$  in MeOH solution<sup>290</sup>). Similarly  $\text{Se}(\text{HgMe})_2$ <sup>435</sup> has  $\nu_{as}$   $231$ ,  $\nu_s$   $201\text{ cm}^{-1}$ , compared with  $\nu_{as}$   $344$ ,  $\nu_s$   $300\text{ cm}^{-1}$  for the linear sulfur analog.<sup>269</sup>

Tetrahedral ' $\text{HgSe}_4$ ' coordination can similarly be expected to give both  $\nu_{as}$  and  $\nu_s$  near  $140\text{ cm}^{-1}$ , by consideration of  $\text{Hg}(\text{SBut})_2$  which has  $\nu_s$   $172$  (IR) and  $\nu_{as}$   $188$  (Raman)  $\text{cm}^{-1}$ .<sup>219</sup> Tetrahedral  $[\text{Ph}_4\text{P}]_2[\text{Hg}(\text{SePh})_4]$  has  $\nu_s$   $150\text{ cm}^{-1}$ .<sup>474</sup>

Vibrational spectra of the  $\text{Hg}(\text{SeR})_2$  complexes prepared in this work are recorded in Table 4.19 together with the spectra of their sulfur

Hg(SMe) <sub>2</sub> <sup>b</sup>	Hg(SeMe) <sub>2</sub>	Hg(SET) <sub>2</sub>	Hg(SeEt) <sub>2</sub>	Hg(SBu <sup>t</sup> ) <sub>2</sub>	Hg(SeBu <sup>t</sup> ) <sub>2</sub>	Hg(SCH <sub>2</sub> Ph) <sub>2</sub>	Hg(SeCH <sub>2</sub> Ph) <sub>2</sub> <sup>i</sup>	Hg(SCH <sub>2</sub> CO <sub>2</sub> H) <sub>2</sub>	Hg(SCH <sub>2</sub> CO <sub>2</sub> <sup>-</sup> ) <sub>2</sub>	Hg(SeCH <sub>2</sub> CO <sub>2</sub> H) <sub>2</sub> <sup>i,j</sup>
	578w,sh[576w,sh] 570w [572m]		570w,sh 555m [550m]	573m [579m]		565m[566w]	598s [605s] 549m [550w]			
				514m [519s]		472m[476vw]		464w,sh 446s,b	431s[437w] [417w]	446m 433w,sh
		405s,br <sup>a,e</sup> [394vs]		416vw[410m] 397m						
				377m [382vs]		381s[385vw,sh] <sup>c</sup> 352w[356vs] <sup>d</sup>		379s[370w,sh] <sup>c</sup> 351w[347s] <sup>d</sup>	355s[360w] <sup>c</sup>	
337vs[338w] <sup>a</sup>		332w [335w]		336s [336m] 322m [322vs]		325vw[327w,sh]	328vw[335vw]		321w[328vs] <sup>d</sup>	[313m] [284s]
296m [297vs] <sup>d</sup>		268s <sup>d,f</sup> [245vs]	291w [298w]	292vs[293w] 270w[272w]	296w[299m]					
204m [178m]			198w 175vs,vb	[188vs] <sup>d</sup> 172vs,b <sup>c</sup>		246w [244s]	236w [237w]		235w[241w]	241s <sup>g</sup> 222m[224m] [192s] <sup>h</sup> [172m]
	161vs,b[158m] 151vs,b 134vs,b[131vs] <sup>g</sup>	161m [151s]	150vs,vb 130vs[131vs] <sup>g,h</sup>			<sup>k</sup> 135vs[139vs,b] <sup>g,h</sup>	158s,vb[149vs,b] <sup>g,h</sup>	155m [142vw]	<sup>k</sup>	
110s,vb	103m[112w]		110vs,b	119m		[107vs]				

Table 4.19: Vibrational spectra (600-100 cm<sup>-1</sup>) for Hg(XR)<sub>2</sub> (X=S,Se).<sup>a</sup>

<sup>a</sup>Raman values in parentheses [ ]. Abbreviations: v, very; s, strong; m, medium; w, weak; b, broad; s, shoulder.

<sup>b</sup>'old' phase structure determined by X-ray crystallography.<sup>271</sup>

<sup>c</sup> $\nu_{as}$ (SHgS). <sup>d</sup> $\nu_s$ (SHgS). <sup>e</sup> $\nu_{as}$ (SHgS) may be 268 cm<sup>-1</sup>.<sup>231</sup>  
<sup>f</sup> $\nu_s$ (SHgS) may be 245 cm<sup>-1</sup>.<sup>231</sup> <sup>g</sup> $\nu_{as}$ (SeHgSe). <sup>h</sup> $\nu_s$ (SeHgSe). <sup>i</sup>very weak Raman spectrum obtained with orange-red

excitation. <sup>j</sup>Raman spectrum obtained at 10 K. <sup>k</sup>region not examined. <sup>l</sup>Hg(SePh)<sub>2</sub> has been assigned  $\nu_{as}$ (SeHgSe) 218s,  $\nu_s$ (SeHgSe) [202s] (ref. 205) and is probably linear.

analog. The single-crystal X-ray structure of  $\text{Hg}(\text{SeMe})_2$  indicates polymeric ' $\text{HgSe}_4$ ' geometry (Figure 4.1, page 183) and powder diffraction patterns confirm that  $\text{Hg}(\text{SeBu}^t)_2$  is isomorphous with the tetrahedral sulfur analog.

The spectra of  $\text{Hg}(\text{SeMe})_2$  and  $\text{Hg}(\text{SeBu}^t)_2$  have intense bands at  $130\text{--}140\text{ cm}^{-1}$  which have been assigned as Hg-Se stretching modes by analogy with  $\text{Hg}(\text{SBu}^t)_2$ . The features 158s,vb [149vs,b] in the spectrum of  $\text{Hg}(\text{SeCH}_2\text{Ph})_2$  have also been assigned as Hg-Se modes due to the tetrahedral ' $\text{HgSe}_4$ ' moiety. X-ray powder diffraction indicates that this complex is not isomorphous with its sulfur analog (Figure 4.3, page 189).

In contrast to these tetrahedral complexes,  $\text{Hg}(\text{SeCH}_2\text{CO}_2\text{H})_2$  appears to be linear, although X-ray powder diffraction (Figure 4.2, page 188) indicates that it is not isomorphous with its sulfur analog.

The selenium compound is photosensitive,<sup>444</sup> and very readily decomposes in the Raman laser-beam. By using low energy (red) excitation and cooling the sample to 10K, a weak, but informative Raman spectrum was obtained which has a strong band at  $192\text{ cm}^{-1}$  (absent in the infrared) which has been assigned  $\nu_s(\text{SeHgSe})$ , and no significant bands in the range  $170\text{--}100\text{ cm}^{-1}$ . The strong infrared band at  $241\text{ cm}^{-1}$  is probably  $\nu_{as}(\text{SeHgSe})$ . These values compare well with  $\nu_s$  178(MeOH) and  $\nu_{as}$   $233\text{ cm}^{-1}$  for  $\text{Hg}(\text{SeCF}_3)_2$ <sup>448</sup> and  $\nu_s$  201,  $\nu_{as}$   $231\text{ cm}^{-1}$  for  $\text{Se}(\text{HgMe})_2$ <sup>435</sup> which are assumed to be linear.

The methylmercury(II) complex  $\text{MeHgSeCH}_2\text{CO}_2\text{H}$ , which is almost certainly linear, is also somewhat photosensitive, but a Raman spectrum was obtained from a solution which had been used to measure the proton nmr spectrum (Figure 3.34, page 164). Although rather noisy, the Raman spectrum shown in Figure 4.9 has moderate intensity bands which are

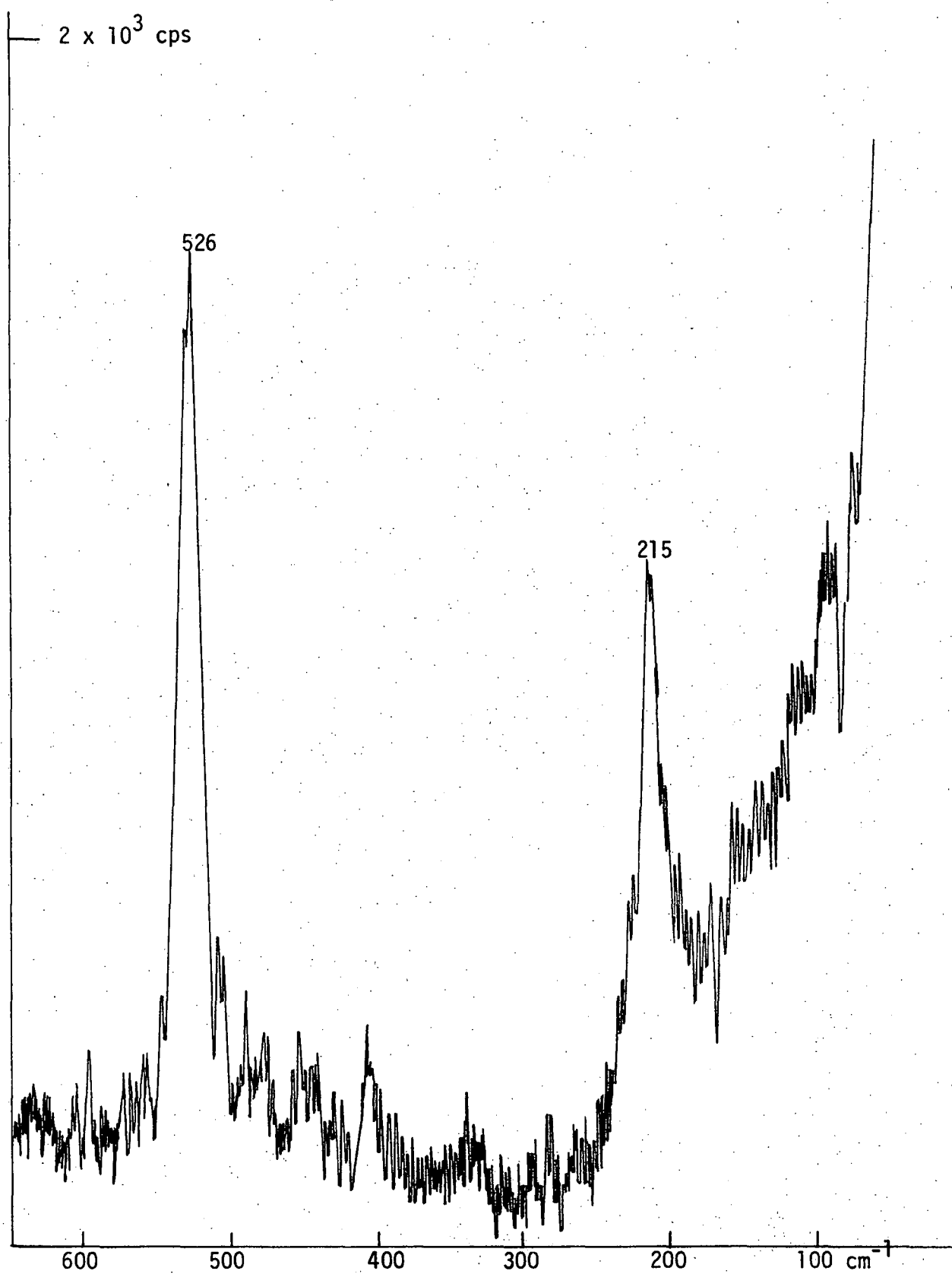


Figure 4.9: Raman spectrum<sup>a</sup> of MeHgSeCH<sub>2</sub>CO<sub>2</sub>H in D<sub>2</sub>O ( $\sim 0.2\text{M}$ , pH=5.6)

<sup>a</sup> 100 mW Ar<sup>+</sup> (514.5nm) excitation at the sample.



coincident in the infrared:  $\nu(\text{HgC})$  526s[526s] and  $\nu(\text{HgSe})$  210s,b[215m]. The spectra of  $\text{MeHgSeBu}^t$  confirm these assignments:  $\nu(\text{HgC})$  521m [526m] and  $\nu(\text{HgSe})$  194s [200s]. The unpublished spectra of a selenocysteine complex,<sup>433</sup>  $\text{MeHg}[\text{SeCH}_2\text{CH}(\text{NH}_3)\text{CO}_2]\cdot\text{H}_2\text{O}$ , also has  $\nu(\text{HgC})$  536s [530s] and  $\nu(\text{HgSe})$  228m [220s] and is apparently isomorphous<sup>433</sup> with the (linear) sulfur analog (Figure 2.1, page 34).

#### 4.3.2 Mercury(II) diselenolates

During the attempted preparation of 1,3-diseleno-2-propanol (the selenium analog of the non-vicinal isomer of  $\text{BALH}_2$ ,  $\text{DMPH}_2$ ), an intractable pale-yellow mercury(II) complex was obtained by the addition of  $\text{Hg}(\text{CN})_2$  to a solution containing the diselenolate (Chapter 5, page 274). The product has an analysis consistent with 1:1 stoichiometry<sup>†</sup> and is the selenium analog of  $\text{HgDMP}$ , previously characterised in this laboratory.<sup>238</sup>  $\text{HgDMP}$  has the interesting property that it can be obtained as a crystalline adduct,  $\text{HgDMP}(\text{py})_{1.5}$ , from pyridine, and is dimeric in this solvent.<sup>238</sup> Unfortunately,  $\text{HgSeDMP}$  is insoluble (<100 mg/100 ml) in pyridine and appears to be insoluble in all common solvents, like  $\text{HgBAL}$ . Like the dithiolates studied in this laboratory (Chapter 2, page 53),  $\text{HgSeDMP}$  has very broad, diffuse vibrational spectra, consistent with a polymeric structure.

The far infrared spectrum of  $\text{HgSeDMP}$  shows only two weak, extremely broad features at  $400\text{--}500\text{ cm}^{-1}$  and  $100\text{--}220\text{ cm}^{-1}$  and is thus unusable. In contrast, the Raman spectrum shows an intense band at  $167\text{ cm}^{-1}$  as the only feature below  $600\text{ cm}^{-1}$ . This is probably  $\nu_s(\text{SeHgSe})$ , due to tetrahedral ' $\text{HgSe}_4$ ' centres in the polymer, and this distinguishes

---

<sup>†</sup> $\text{HgDMP}$  ( $\text{HgC}_3\text{H}_6\text{OSe}_2$ ) requires C 8.65, H 1.45, Hg 48.2%; found C 8.88, H 1.56, Hg 48.2%.

HgSeDMP from its sulfur analog which has a linear, polymeric structure with  $\nu(\text{HgS})$  333m,b [325vs].<sup>238</sup>

A similar attempted preparation of the vicinal diselenol analog of  $\text{BALH}_2$ , 2,3-diseleno-1-propanol, failed, but a very small quantity of yellow powder was obtained by the addition of  $\text{Hg}(\text{CN})_2$  to the solution suspected to contain the diselenolate. Like HgSeDMP, this powder was insoluble in all common solvents. Some of this product was stored under pyridine for three months (in an attempt to induce some dissolution and/or crystallisation), but only an insignificant amount had dissolved in this time.

The near infrared ( $3000\text{--}300\text{ cm}^{-1}$ ) spectrum of the pyridine-insoluble residue shows several bands which appear to be due to coordinated pyridine, e.g. 1607, 1590m, 615m, and 413, 406w (free pyridine has these bands at 1518, 601 and  $403\text{ cm}^{-1}$ <sup>475</sup>), despite prolonged (24 hrs/ 0.1 mm) high vacuum pumping and subsequent storage over concentrated  $\text{H}_2\text{SO}_4$ . The Raman spectrum of this product is superimposed on a high intensity background which gradually decays over several hours to reveal two sharp bands at 1036s,  $1004\text{ m cm}^{-1}$  due to the totally symmetric ring mode of coordinated pyridine (free pyridine has  $990\text{ cm}^{-1}$ <sup>476</sup>) and a strong band at  $179\text{ cm}^{-1}$  (HgSeDMP has  $168\text{ cm}^{-1}$ ) due to  $\nu(\text{HgSe})$ . Unfortunately, insufficient sample was available for microanalysis or far infrared spectrum, but it would appear that this product may also have a polymeric, tetrahedral structure like HgSeDMP, and unlike HgBAL,<sup>231</sup> consistent with the general tendency toward tetrahedral ' $\text{HgSe}_4$ ' geometry in mercury(II) selenolates.

#### 4.4 Conclusions

Evaluation of vibrational spectra for many complexes of the type  $\text{Hg}(\text{SR})_2$  shows a predominance of linear (S-Hg-S) geometry. In contrast, single-crystal X-ray diffraction studies of  $\text{Hg}(\text{SeMe})_2$  and vibrational studies of  $\text{Hg}(\text{SeR})_2$  suggest that polymeric structures with tetrahedral 'HgSe<sub>4</sub>' geometry may be more common for Hg(II) selenolates.

All 1:1 thiolates  $\text{RSHgX}$  examined crystallographically, are polymeric and form complexes with pyridine bases which are polymeric or tetrameric. Analogous 1:1 selenolates  $\text{RSeHgX}$  behave similarly, e.g.  $\text{MeXHgO}_2\text{CMe}$  (X = S, Se) are isomorphous,  $[\text{Bu}^t\text{SeHgCl}(\text{py})_{0.5}]_4$  is isomorphous with  $[\text{Bu}^t\text{SHgCl}(4\text{-Mepy})_{0.5}]_4$ , and  $[\text{EtSeHgCl}(\text{py})]_4$  has a similar eight-membered  $(\text{-Hg-SeR-})_4$  structure, but lacks a dichloro bridge found in the *tert*-butyl complexes.

The intractable complexes  $\text{HgSeBAL}$  and  $\text{HgSeDMP}$  are probably polymeric with tetrahedral 'HgSe<sub>4</sub>' geometry, in contrast to the linear sulfur analogs  $\text{HgBAL}$  and  $\text{HgDMP}$ .

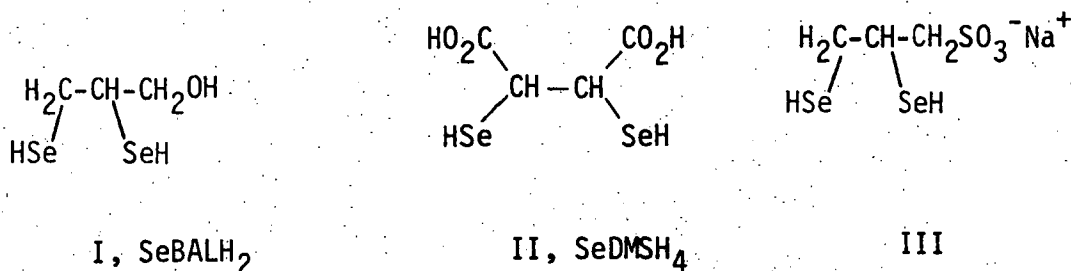
## CHAPTER FIVE

### SELENIUM ANALOGS OF ANTIDOTAL DITHIOLS

#### 5.1 Introduction

Selenium analogs of dithiol antidotes have not been reported. Attempts to synthesise analogs for studies of their interactions with Hg(II) and MeHg(II) were commenced for several reasons. Of particular interest are structural differences between  $\text{Hg}(\text{SR})_2$  and  $\text{Hg}(\text{SeR})_2$  favouring higher co-ordination numbers for mercury in the selenolates (Chapter 4), and solution results suggesting that some dithiols act as bidentate ligands toward MeHg(II) (Chapter 3).

It was hoped that free diselenol ligands could be obtained so that MeHg-diselenol stability constants could be determined and compared with those for the analogous dithiols. In view of possible direct *in vivo* interactions between mercuric ion and selenium, synthetic routes to analogs of antidotal dithiols  $\text{BALH}_2$  and  $\text{DMSH}_4$  were investigated.\* It was expected that a diselenol analog of Unithiol, III, would probably form intramolecular mixed S-Se species (e.g. organo-Bunte salts  $\text{RSSeO}_3$ ),<sup>477</sup> and its synthesis was not considered.

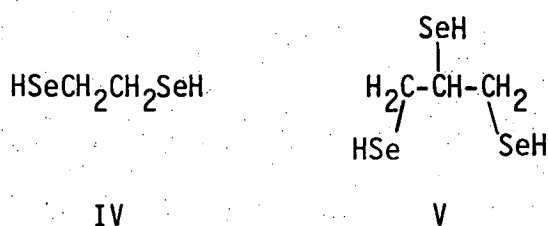



---

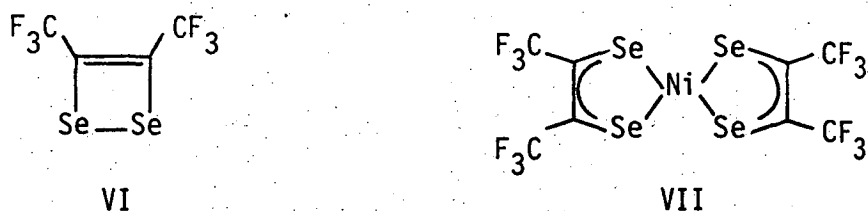
\*For convenience, these will be abbreviated as  $\text{SeBALH}_2$ , I, and  $\text{SeDMSH}_4$ , II.

Two general strategies can be applied to the determination of viable synthetic routes to diselenols, namely (i) extensions of those methods used to prepare thiols, using selenium analogs of organosulfur reagents and (ii) methods using particular properties of organoselenium reagents.

Additionally, consideration was given to the fact that the dithiols of interest contain *vicinal* thiol groups. Few synthetic routes have been applied to the synthesis of vicinal dithiols and only two vicinal diselenols, ethane-1,2-diselenol, IV,<sup>478</sup> and 1,2,3-triselenopropane, V,<sup>479</sup> have been described. Another report claims that IV is inherently unstable and eliminates  $\text{H}_2\text{Se}$  and selenium.<sup>480</sup>



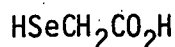
Several metal complexes of vicinal diselenols have been reported, but the diselenols have not been isolated, e.g. the novel unsaturated heterocycle bis(trifluoromethyl)-1,2-diseleneten, VI, reacts with  $\text{Ni}(\text{CO})_4$  to produce crystalline *cis*-[1,2-di(trifluoromethyl)ethylene-1,2-diselenolato] nickel(II) complex,<sup>481</sup> VII, but the free diselenol ligand is unknown.



It should also be noted that  $\text{SeDMSH}_4$ , in addition to being a vicinal diselenol, would have carboxylic acid groups geminal to the selenohydril groups. Only one example of such  $\alpha$ -selenocarboxylic acids has previously been isolated. Selenoacetic acid, VIII, has been prepared in variable

yield in aqueous alkaline solution by removal of mercury from  $\text{Hg}(\text{SeCH}_2\text{CO}_2\text{H})_2$  with  $\text{Na}_2\text{S}$ ,<sup>482</sup> or by electrolytic reduction of the diselenide, IX, under a hydrogen atmosphere in 50% yield.<sup>432,482</sup>

A spectrophotometric determination of the acidity constants of VIII was achieved by reduction of IX with sodium borohydride, careful acidification with deaerated  $\text{HCl}$  and extraction into  $\text{CHCl}_3$ .<sup>374</sup>



VIII

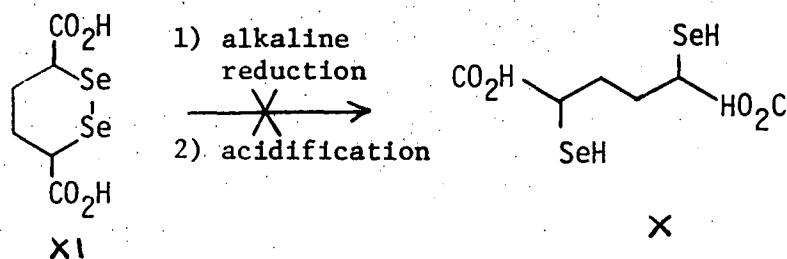


IX

The difficulties involved in obtaining compounds with geminal carboxylic acid and selenohydril groups have been noted elsewhere.<sup>483</sup>

Fredga has attempted to produce the diselenol, X, by reduction of 1,2-diselenane-3,6-dicarboxylic acid, XI,<sup>484</sup> in alkaline solution.

Acidification leads to rapid decomposition and formation of red selenium.



Similarly, in this work, it has not been possible to isolate  $\text{SeBALH}_2$  and  $\text{SeDMSH}_4$  despite several attempts using various synthetic routes, but the  $\text{Hg}(\text{II})$  complex of  $\text{SeBALH}_2$  and of the isomeric non-vicinal diselenol have been prepared.

## 5.2 Possible routes for synthesis of dithiols and diselenols

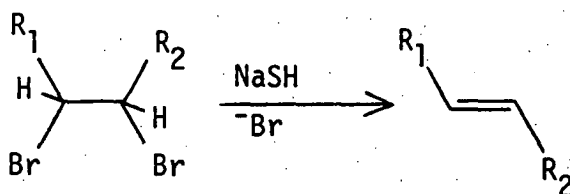
Free selenols are very easily oxidised e.g. by atmospheric oxygen to form diselenides. This is of paramount importance in all reported selenol syntheses described below.

### 5.2.1 Direct introduction of SeH

Alkylation of NaHSe to form alkaneselenols has often been reported.<sup>485-6</sup>



Common alkylating agents used are alkyl halides and potassium alkyl sulfates. The sodium hydrogen selenide reagent can be prepared by dissolving gaseous  $\text{H}_2\text{Se}$  in NaOH, by dissolving Se in methanolic NaOMe or, more recently by reducing Se with sodium borohydride in aqueous or ethanolic solution.<sup>487</sup> Many thiols, including several non-vicinal dithiols, have been prepared in this fashion, using  $\text{H}_2\text{S}$ , or metal sulphides etc.<sup>488-9</sup> Vicinal dithiols, e.g.  $\text{BALH}_2$ ,<sup>490-1</sup> Unithiol<sup>91</sup> are formed under these conditions but in lower yields. If both halide groups are secondary, extensive dehalogenation occurs to produce a trans-olefin.<sup>492-5</sup>



Owen has commented that halide replacement, to produce dithiols, is most favorable when both groups are primary and less favorable when one is secondary,<sup>496</sup> e.g. 2,3-dimercapto-1-butanol and 2,3-dibromo-2-methyl-1-propanol could not be prepared by this method.<sup>497</sup>

Although  $\text{HSeCH}_2\text{CH}_2\text{SeH}$  cannot be prepared in this way,<sup>480</sup> the non-vicinal diselenols  $\text{HSe}-(\text{CH}_2)_3-\text{SeH}$ <sup>480</sup> and  $\text{HSeCH}_2\text{CH}(\text{OH})\text{CH}_2\text{SeH}$ <sup>479</sup> have been prepared using this method, but they are often contaminated with cyclic diselenides formed by oxidation.

Interestingly, the only reported triselenol, propane-1,2,3-triselenol, V, the selenium analog of glycerine, was reputedly formed<sup>479</sup>

from alkylation of an alkaline solution of sodium hydrogen selenide by 1,2,3-tribromopropane. Although the preparation of the related compounds 1-seleno-2,3-propanediol and 1,3-diseleno-2-propanol has been reported by Baroni,<sup>479</sup> the compound of interest here, 2,3-diseleno-1-propanol,  $\text{SeBALH}_2$ , was not prepared. It should be noted that the parent vicinal dibromide in this case contains one primary and one secondary bromide group.

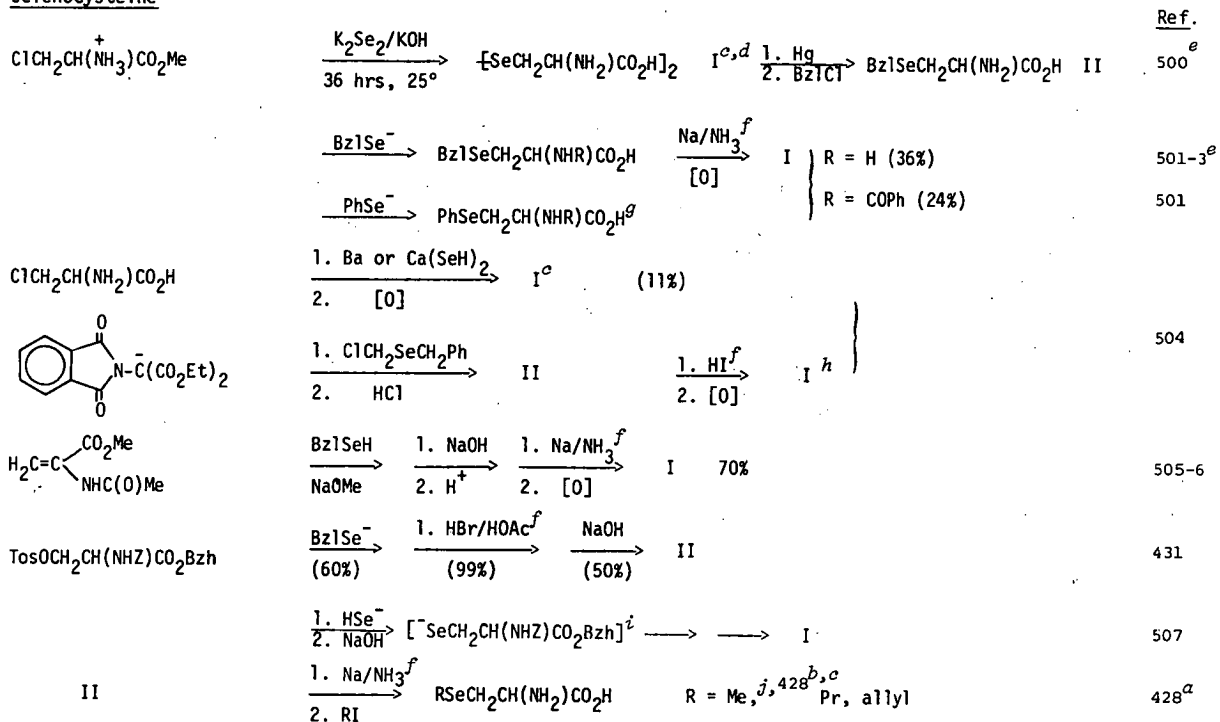
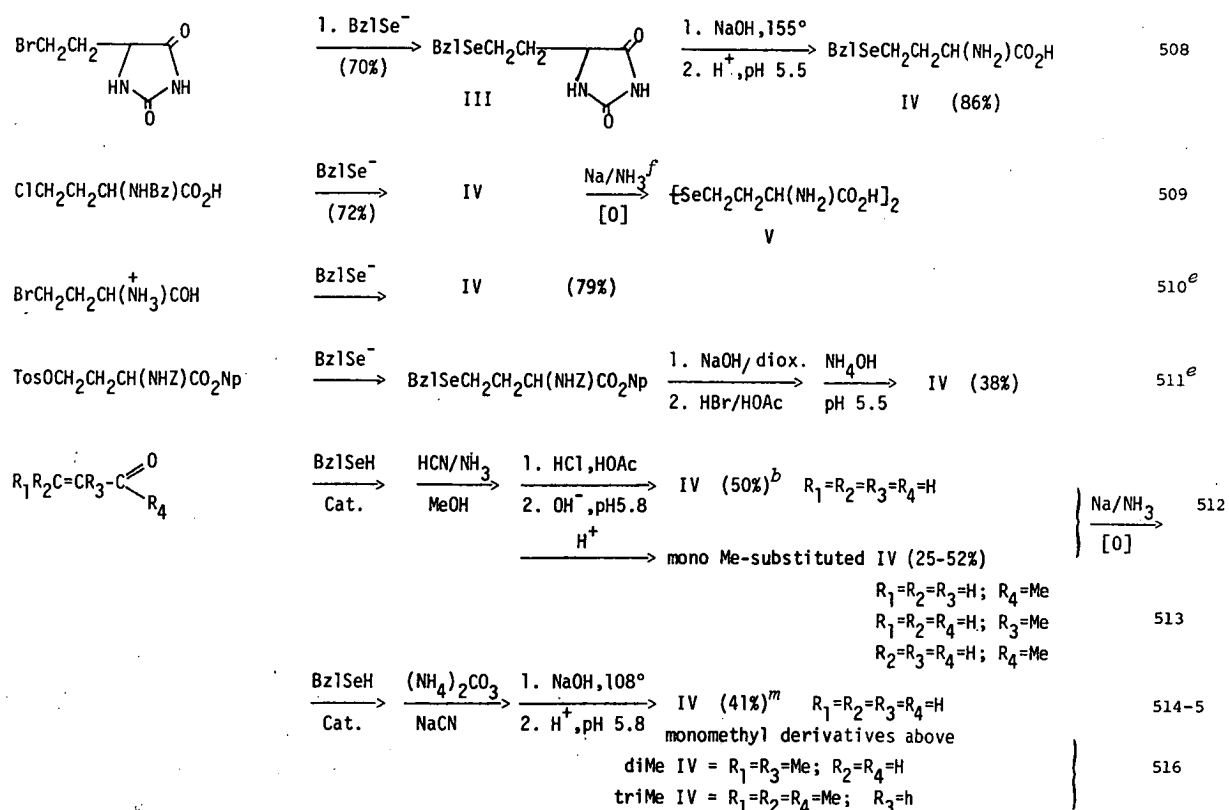
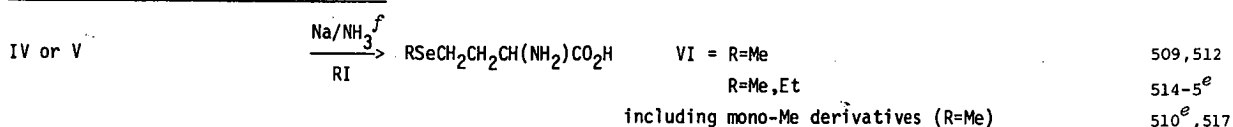
Considering the ease of oxidation of the selenohydryl group, it is more usual to introduce selenium as a protected selenoether during monoselenol syntheses, especially if subsequent modifications are to be made to other functional groups. The last stage in a multi-step synthesis of such compounds is cleavage of the Se- protecting group (deprotection).

#### 5.2.2 Use of protected Thiols and Selenols

In the multi-step synthesis of complex molecules containing the -XH ( $\text{X}=\text{S}, \text{Se}$ ) function, it is generally necessary to introduce X as the thio- or selenoether group in order to protect against oxidation. Much of the literature concerning sulfur and selenium protecting groups is concerned with the preparation of peptides containing cysteinyl- or selenocysteinyl residues. The literature of thiol protecting groups has been well reviewed.<sup>498-9</sup> Protecting groups which have been used for selenoamino acid and selenopeptide syntheses are summarised in Table 5.1.

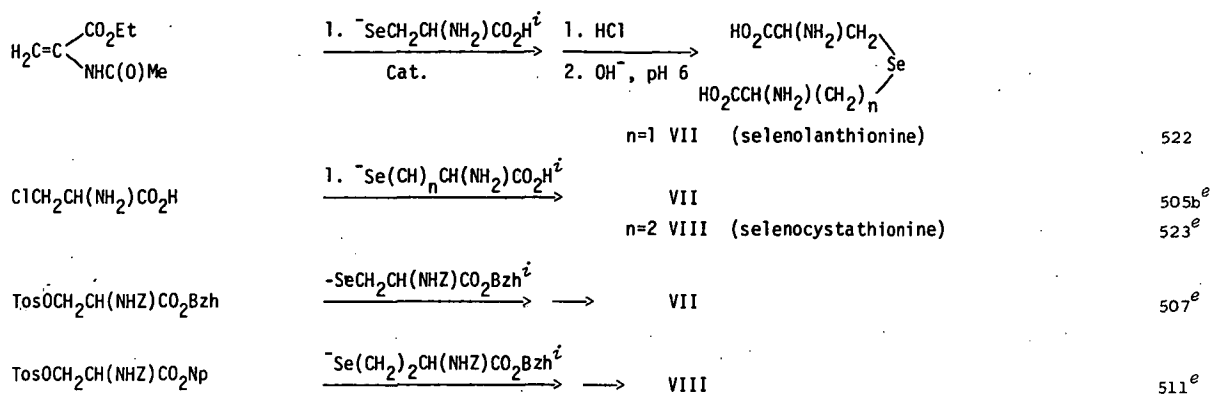
About seventy thiol protecting groups have been described.<sup>499</sup> Many have been used to protect an already existing -SH function, so that subsequent reactions may be carried out elsewhere in the molecule. For the current purpose, these are therefore not useful. However, if the protective reaction involves generation of a thiol group *in situ* by reduction of a disulfide, it was considered for inclusion in this work.



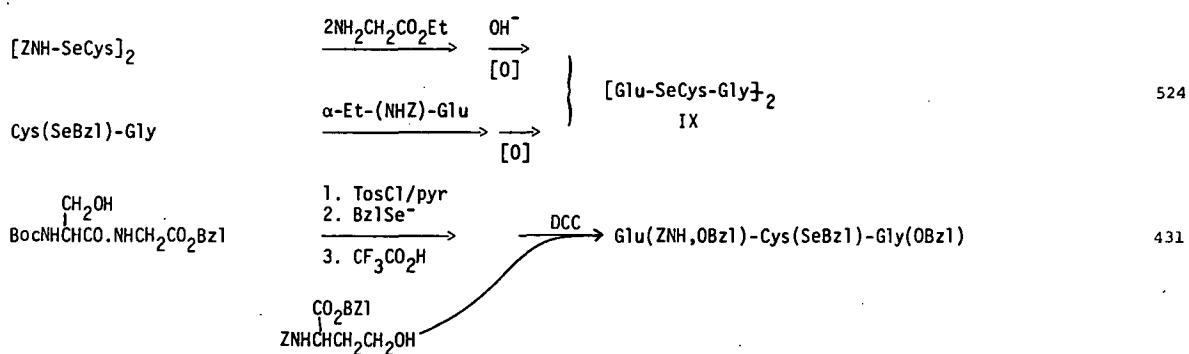
selenocysteine<sup>b</sup>selenohomocysteine<sup>b</sup>selenomethionine and selenoethionine<sup>z</sup>Table 5.1: Synthesis of selenoamino acids and selenopeptides.<sup>a</sup>



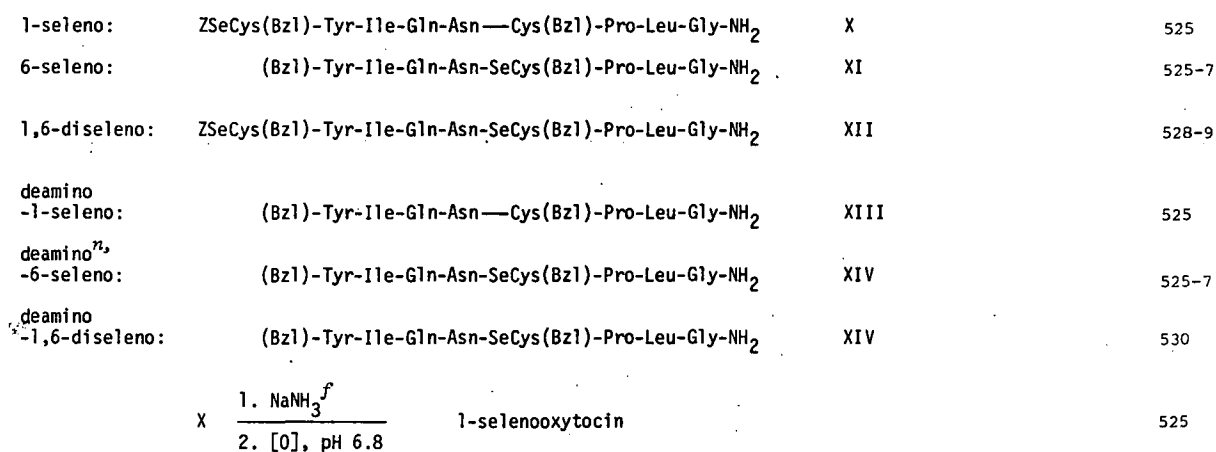
selenolanthionine and selenocystathionine<sup>1, j</sup> 519-21



selenoglutathione (Glu-SeCys-Gly)<sup>b</sup>



selenooxytocins (and uncyclised nonapeptides)



selenocoenzyme-A, and isoselenocoenzyme-A

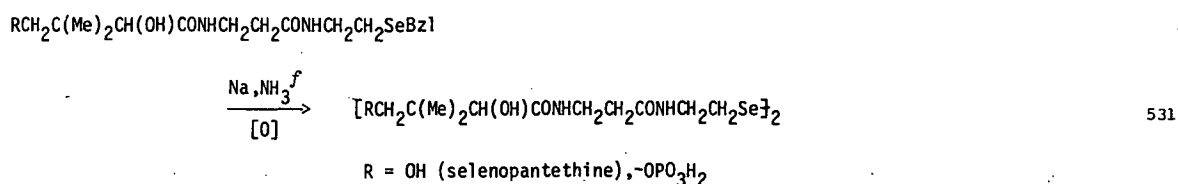
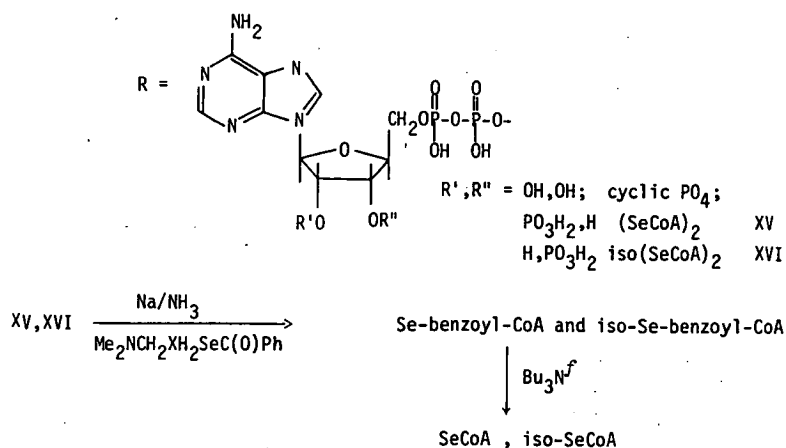


Table 5.1: Synthesis of selenoamino acids and selenopeptides.  
(cont.)



**Table 5.1:** Synthesis of selenoamino acids and selenopeptides.  
(cont.)

<sup>a</sup> or substituted derivatives, usually DL- or meso- as shown (except see *e*).

The following abbreviations are used: Bzl = benzyl, BZ = benzoyl, Bzh = diphenylmethyl, Boc = *tert*-butoxycarbonyl, Z = benzyloxycarbonyl, Tos = *p*-toluene sulfonyl, Mpr =  $\beta$ -mercaptopropionyl, Np = *p*-nitrophenyl, DCC = N,N'-dicyclohexylcarbodiimide.

<sup>b</sup> the selenohydril amino acid has not been isolated in a pure state.

<sup>c</sup> no protective group was used.

<sup>d</sup> Fischer-Raske cystine synthesis. Inconsistent yield.

<sup>e</sup> applied to preparation of optically active products.

<sup>f</sup> reagent for removal of the selenohydril-protecting group.

<sup>g</sup> the protective group could not be removed without decomposition to PhSeSePh.

<sup>h</sup> Gabriel-Sørensen phthalimidomalonate synthesis. Low yields.

<sup>i</sup> selenolate not isolated but used *in situ*.

<sup>j</sup> naturally occurring selenoamino acid.

<sup>k</sup> Strecker synthesis.

<sup>l</sup> selenoethers.

<sup>m</sup> Bucherer-Bergs hydantoin synthesis.

<sup>n</sup> crystallographic data are available.

In addition, many routes use organosulfur reagents for which the organoselenium derivatives are either unknown, or hypothetically would require reagents which would be difficult to manipulate ( $\text{H}_2\text{Se}$  or  $\text{CSe}_2$ ).

The common protecting groups meeting these requirements are described below. In addition to the preparation of the protected selenol, the means of deprotection or cleavage of the protected group was considered (e.g. methods which required anhydrous HF were rejected).

The benzyl (Bzl) group is the earliest widely used protective group for cysteinyl residues, and remains the most widely used for Se-containing peptides, etc. (Table 5.1). The benzyl group could be introduced using either benzylselenol (a foul smelling colourless oil, but readily handled under non-oxidising conditions) or its sodium salt (formed *in situ* by reduction of the diselenide under alkaline conditions, e.g. using sodium borohydride or Rongalite). Benzylselenol can also be formed from the diselenide by *in situ* reduction with hypophosphorus acid. Removal of the benzyl group from benzyl protected selenium peptides for example, is usually accomplished by sodium reduction in liquid ammonia, followed by acidification of the ammonium salt of the selenol. Alternatively, benzyl-protected thiols have been deprotected with strong acids e.g. HF/anisole<sup>498</sup> or  $\text{CF}_3\text{SO}_3\text{H}$ .<sup>533</sup>

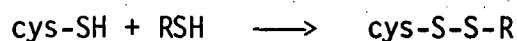
Substituted benzyl groups, notably 4-MeOBzl or 4- $\text{NO}_2$ -Bzl, generally offer little advantage over the unsubstituted groups for thiol protection, except that milder deprotective conditions have been used. The selenols<sup>534-7</sup> and diselenides are known.<sup>538-9</sup>

The S-triphenylmethyl (trityl) protecting group has been used in several thiol-peptide syntheses. The trityl group can be removed by formation of the mercury(II)-thio-peptide complex. Mercury is subsequently removed as the sulfide<sup>540-1</sup> or by electrolytic reduction at a mercury cathode.<sup>542</sup> Triphenylmethaneselenol and diselenide do not seem to have

been prepared to date.

The  $\text{Bu}^t$ - protecting group is usually added to a pre-existing thiol group in thio-peptide syntheses, using  $\text{Bu}^t\text{OH}$ . It has been cleaved by anhydrous HF, but a recent report indicates that it can be cleaved under milder conditions by conversion to the S-(2-nitrophenyl)sulfonyl derivative or by  $\text{NaBH}_4$  reduction.<sup>543</sup> Since we have used  $\text{Bu}^t\text{SeH}$  in the preparation of  $\text{Hg}(\text{SeBu}^t)_2$  and  $\text{MeHgSeBu}^t$  (see pages 350-1 ), the formation of  $\text{Bu}^t$ -selenoethers was considered as a means of selenol protection, although this has not been previously reported.

Several thiols have been used to convert the cysteinyl moiety into asymmetric disulfides<sup>544-7</sup> as a means of protection of RSH:

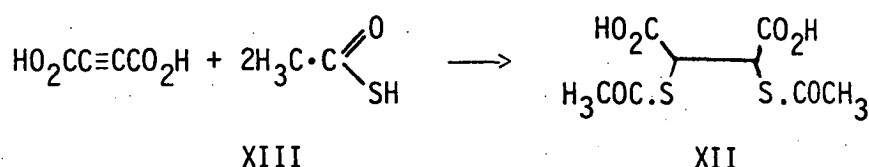


It should be noted that under these conditions, it is an entire cys-S-group which is the protecting group, i.e. the disulfide bond is cleaved on deprotection. Although selenol and diselenide reagents (for generation of selenol *in situ*) are available for use as protecting groups in this way, this technique does not seem to have been used for selenol protection.

The Acetamidomethyl group has apparently become preferred to the Bzl group for thiol protection in peptide synthesis,<sup>548</sup> but it does not appear to have been used as a selenium protecting group. The selenol and diselenide are unknown.

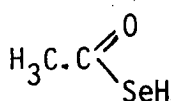
Schotte<sup>549</sup> has indicated that, despite several synthetic routes to non-vicinal dimercaptodicarboxylic acids, "special methods" need to be applied in the case of dimercaptosuccinic acid ( $\text{DMSH}_4$ ). The only reported preparations of  $\text{DMSH}_4$  have utilised the mild hydrolysis of S-acetyl protecting groups of 2,3-bis(acetylthio)succinic acid, XII.<sup>416,550</sup> The bis(S-acetyl) compound was prepared by addition of thiolacetic acid,

XIII, to acetylenedicarboxylic acid.

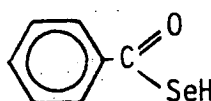


By careful control of reaction temperatures, a predominance of racemic- or meso-XII could be obtained.<sup>415-6</sup> Removal of the acetyl groups can be accomplished in one minute using 3N NaOH at 40°.<sup>416</sup> The acetylthio group has been widely used by Owen in the synthesis of vicinal dimercapto alcohols, e.g.  $\text{CH}_2\text{SH}\cdot\text{CHSH}(\text{CHOH})_n\text{CH}_2\text{OH}$  [ $n=0$  (BALH<sub>2</sub>)],<sup>551</sup> 1,<sup>492,2,492</sup> 3<sup>552</sup>],  $\text{CH}_2\text{SH}\cdot\text{CHSH}(\text{CH}_2)_n\text{CH}_2\text{OH}$  [ $n=1$ ,<sup>553</sup> 2,<sup>554</sup> ] and propane-1,2,3-trithiol.<sup>555</sup>

Direct utilisation of this technique for SeDMSH<sub>4</sub> synthesis would require the use of selenolacetic acid, XIV. This compound has been mentioned in the early organoselenium literature. Addition of the Grignard reagent HSeMgBr (from H<sub>2</sub>Se with EtMgBr) to acetylchloride in ether is reported to form XIV, which decomposed to red selenium on attempted isolation.<sup>556</sup> An earlier report showed that XIV could not be obtained by acetylation of NaSeH.<sup>557</sup> More recently, attempts to prepare acetyl, propionyl and isobutyryl selenols by the reaction of the acyl chlorides with H<sub>2</sub>Se in pyridine were unsuccessful.<sup>558</sup> (A report of XIV as an oil, bp. 135°, from the reaction of diacetyl-yohimbine with Se at 300°<sup>559</sup> is almost certainly incorrect given the extreme oxidation sensitivity of acyl selenols<sup>558</sup>).

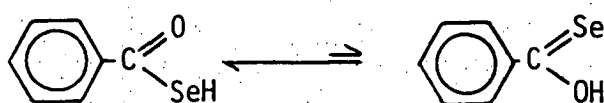


XIV



XV

The use of acyl-protecting groups other than acetyl is minimal, benzoyl (Bz) being the only common alternative reported for selenopeptide synthesis (Table 5.1). Benzoyl-protected DMSH<sub>4</sub> has not been prepared. Dibenzoyldiselenide is a stable, odourless, crystalline material which can be reduced to form an oily selenol, XV, *in situ*.<sup>558</sup> The Bz group is usually removed by mild hydrolysis or methanolysis.<sup>488-9</sup> Benzoyl selenol has been shown to exist primarily as the selenohydril tautomer the OH form being negligible.<sup>558</sup>



### 5.2.3 Introduction of protected Selenol groups

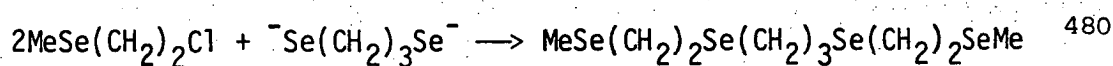
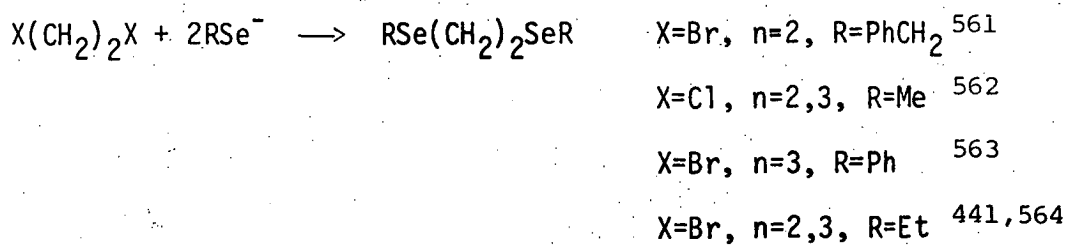
The actual introduction of protected selenol groups into substrate molecules can be achieved in several ways:

#### (i) Alkylation of selenolates

The most common method for the preparation of mono-selenoethers (protected selenols) involves alkylation of a selenolate nucleophile with an alkyl halide, sulfate etc.



Numerous examples of this type have been reported, and have been reviewed elsewhere.<sup>485-6,560</sup> In a few instances, alkylation has been performed with non-vicinal dihalides, to produce non-vicinal bis(alkylseleno)ethers.



Vicinal bis(alkylthio)ethers can be prepared using this route e.g.  $n=1$  above, but usually only when the halide groups are not both secondary, e.g. 1,4-diacetoxy-2,3-dibromobutane eliminates bromide when treated with thiolacetic acid/pyridine to form 1,4-diacetoxybut-2-ene<sup>492</sup> (but 10,11-bis(acetylthio)hendecanoic acid is formed from the corresponding vicinal secondary dibromide under the same conditions<sup>565</sup>).

Attempts to alkylate selenolates, using reagents with vicinal leaving groups, do not seem to have been reported, perhaps because of problems faced in the analogous dithiol syntheses (see page 228 for preparations of non vicinal diselenols, using NaSeH).

#### (ii) Addition of Selenols to alkenes and alkynes

The addition of thiols to activated alkenes and alkynes is well established and may proceed via either radical<sup>566</sup> or base-catalysed<sup>567</sup> pathways e.g. the base-catalysed reaction has been used to prepare crystalline derivatives of olefins<sup>568</sup> and several new dithioethers which may be potential heavy-metal antidotes have similarly been prepared from acetylenedicarboxylic acid.<sup>569</sup> Analogous addition of selenols (mainly aryl) has also received much attention, almost solely from Russian workers. Reported addition reactions of selenols to alkenes and alkynes have been summarised in Tables 5.2 and 5.3 respectively.

#### (iii) Lactone and epoxide ring opening

The preparation of selenium-containing carboxylic acids is often carried out by lactone ring opening, and epoxides are similarly opened to produce alcohols. These reactions have been summarised in Table 5.4. Phenyl selenide has recently been reviewed as an effective reagent for  $S_N2$ -type cleavages of lactones and esters.<sup>585</sup> To prepare protected  $SeDMSH_4$  using this method, two selenoether groups would need to be introduced. A possible route is shown below:



alkene	product	ref.
<u>ionic additions (base catalysed)</u>		
<u>BzISeH:</u>		
$\text{Me}_2\text{C}=\begin{array}{l} \text{CO}_2\text{H} \\ \text{CO}_2\text{H} \end{array} \xrightarrow[\text{Et}_2\text{NH}]{\text{Et}_3\text{N}} \xrightarrow[\text{-CO}_2]{\Delta} \xrightarrow[2. \text{O}_2]{1. \text{Na/NH}_3(\ell)^b} \left[ \text{SeC}(\text{CH}_3)_2\text{CH}_2\text{CO}_2\text{H} \right]_2$		570
$\text{BzISeCH}_2\text{CH}(\text{CO}_2\text{H})\text{CH}=\text{CH}_2$	$\text{BzISeCH}_2\text{CH}(\text{CO}_2\text{H})\text{CH}_2\text{CH}_2\text{SeBzI}$	571
$\begin{array}{l} \text{R}_1 \\ \text{R}_2 \end{array} \text{C}=\text{C} \begin{array}{l} \text{R}_3 \\ \text{C(=O)R}_4 \end{array} \xrightarrow[0^\circ]{\text{Et}_3\text{N}}$	$\text{BzISeC}(\text{R}_1)\text{CR}_2\text{CH}(\text{R}_3)\text{C(=O)R}_4$	572
$\text{R}_1, \text{R}_2, \text{R}_3, \text{R}_4 = \text{H, H, H, Me; Me, H, H, H; H, H, Me, H; Me, Me, H, Me}$		516
$\text{H}_2\text{C}=\text{C} \begin{array}{l} \text{CO}_2\text{Me} \\ \text{NHC(=O)Me} \end{array} \xrightarrow{\text{NaOMe}} \xrightarrow[2. \text{Fe}^{3+}, \text{O}_2]{1. \text{Na/NH}_3(\ell)^b} \xrightarrow{\text{H}^+} \left[ \text{SeCH}_2\text{CH}(\text{CO}_2^-)\text{NH}_3^+ \right]_2$		506
$\text{H}_2\text{C}=\text{C} \begin{array}{l} \text{H} \\ \text{CO}_2\text{H} \end{array} \xrightarrow[25^\circ, 12 \text{ hr.}]{\text{piperidine}}$	$\text{BzISeCH}_2\text{CHCO}_2\text{H}$	573
<u>PhSeH:</u>		
$\begin{array}{l} \text{R}_1 \\ \text{H} \end{array} \text{C}=\text{C} \begin{array}{l} \text{R}_2 \\ \text{CO}_2\text{R}_3 \end{array} \xrightarrow{\text{NaOMe(Et)}}$	$\text{PhSeCH}(\text{R}_1)\text{CH}(\text{R}_2)\text{CO}_2\text{R}_3$	574
$\text{R}_1, \text{R}_2, \text{R}_3 = \text{H, H, H; H, Me, H; H, Me, Me}$		
$\text{CO}_2\text{H, H, H; CO}_2\text{Et, H, Et}$		

Table 5.2: Addition of selenols<sup>a</sup> to alkenes.<sup>a</sup>under ionic conditions the selenol is deprotonated.<sup>b</sup>to cleave the benzyl group.

alkyne	products <sup>b</sup>	ref.
<u>ionic additions (base catalysed)</u>		
PhSeH	$R_1C\equiv CR_2 \xrightarrow[\text{piperidine}]{Et_2O} \begin{array}{c} R_1 \\ \diagdown \\ \text{PhSe}-C=CHR_2 \end{array}$ <p>trans <math>R_1, R_2 = H, CO_2Me; Ph, CO_2H; H, CH_2OCOMe; CO_2Me, CO_2Me</math></p> $R_1C\equiv CCOR_2 \xrightarrow{EtOH} \begin{array}{c} R_1 \\ \diagdown \\ \text{PhSe}-C=CH-COR_2 \\   \\ H \end{array}$ <p><math>R_1, R_2 = PhPh; CO_2H, Ph; C(OH)Me_2, Ph</math> (also 4-NO<sub>2</sub>-PhSeH) <math>H, H</math></p>	575
	$HC\equiv C\begin{array}{c} R \\   \\ OH \\   \\ Me \end{array} \xrightarrow[MeOH, 70^\circ, 3hrs.]{sat. NaOMe} \begin{array}{c} H \\ \diagdown \\ \text{PhSe}-C=CH-C(OH)Me \end{array}$ <p>trans: <math>R=Me</math> cis <math>R=Et, Pr^n</math>; cis &amp; trans: <math>R=Me</math></p>	578 579
$Bu^nC\equiv CH$	$\xrightarrow[EtOH, 120^\circ, 20hr]{sat. NaOEt} \begin{array}{c} Bu^n \\ \diagdown \\ \text{PhSe}-C=CH_2^c \end{array} + PhSeCH=CHBu^n$	
$R_1C\equiv CR_2$	$\begin{array}{c} R_1 \\ \diagdown \\ \text{PhSe}-C=CHR_2 \end{array}$ <p>cis <math>R_1, R_2 = H, Ph</math> trans <math>R_1, R_2 = Ph, Ph</math>; (also <math>H, 5-(2-Me\text{-pyridyl})^d</math>)</p>	580
$EtO_2CC\equiv CAr$	$\xrightarrow[MeOH]{NaOMe} \begin{array}{c} Ar \\ \diagdown \\ \text{PhSe}-C=CH-CO_2Et \\   \\ H \end{array}$ <p><math>Ar=Ph; 4-MeOPh; 2,5-diMeO-Ph; 2-MeO-C_{10}H_6</math></p>	581
<u>radical additions</u>		
PhSeH	$EtO_2C\equiv CAr \xrightarrow{neat} \begin{array}{c} CO_2Et \\ \diagup \\ ArCH=C \\ \diagdown \\ SePh \end{array}$ <p><math>Ar=Ph; 4-MeOPh; 2,5-diMeOPh; 2-MeO-C_{10}H_6</math> <math>Ar=Ph^e</math></p>	581 582
PhSeH	$HC\equiv CR \xrightarrow{CCl_4} \begin{array}{c} R \\ \diagdown \\ H_2C=C-SePh \end{array}$ <p><math>R=Ph, COPh, CO_2Et, OEt</math> (mainly cis)</p>	583
	$HC\equiv CR \xrightarrow{neat} PhSeCH=CHR$ <p>cis and trans <math>R=Ph</math> (also <math>R=5-(2-Me\text{-pyridyl})^d</math>)</p>	580
EtSeH	$HC\equiv CXEt \xrightarrow[3\text{ hr.}]{Et_2O} \begin{array}{c} H & H \\ \diagdown & / \\ EtSe & -C= \\ &   \\ & XEt \end{array}$ <p><math>(X=O, S)</math></p>	584

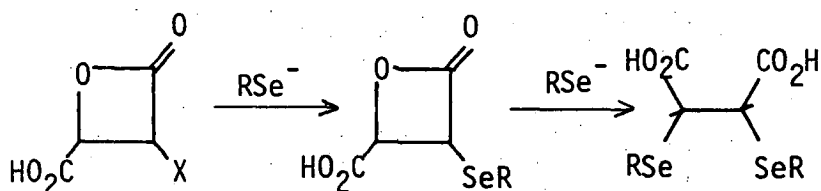
Table 5.3: Addition of selenols<sup>a</sup> to alkynes.

Table 5.3: Addition of selenols<sup>a</sup> to alkynes.  
(cont.)

<sup>a</sup>under ionic addition conditions the selenol is deprotonated.

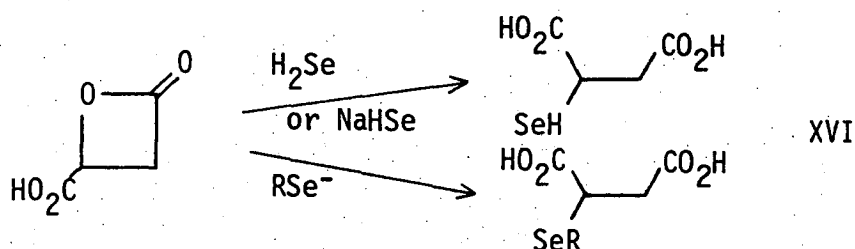
<sup>b</sup>stereochemistry is that indicated in the original reference and appears to be solvent dependent.

<sup>c</sup>appears to be an exception to 1,2-addition. <sup>d</sup>stereochemistry not given under base-catalysed conditions. <sup>e</sup>stereochemistry incorrectly assigned<sup>581</sup> in ref.<sup>582</sup>

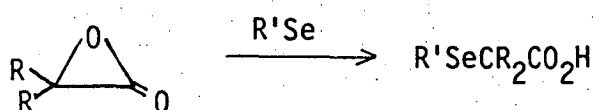


The starting  $\beta$ -lactones of  $\alpha$ -halomalic acids are unknown (although an  $\alpha,\beta$ -dimethyl substituted analog has been prepared<sup>586</sup>) and are probably unstable with respect to the isomers of 2-halobutenedioic acids.

The related selenol of interest, 2-selenosuccinic acid, XVI, may possibly be obtained using this technique.

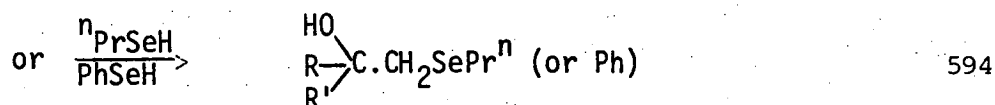
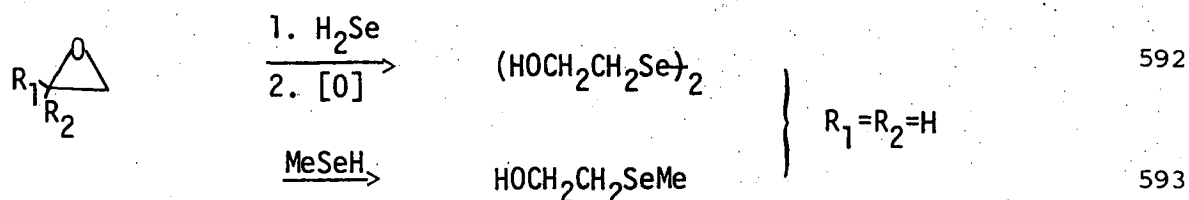


In this case, the starting  $\beta$ -lactone of malic acid is known<sup>587</sup>. It may be noted in passing that this route has not been attempted with  $\alpha$ -lactones, which could be expected to generate protected, substituted  $\alpha$ -selenocarboxylic acids.



$\alpha$ -Lactones ( $R = \text{CH}_3$ ,  $^n\text{Bu}$ ,  $-(\text{CH}_2)_n-$ ,  $n = 2, 3, 4$ ,<sup>588</sup>  $\text{Bu}^t$ ,<sup>589</sup>  $\text{CF}_3$ <sup>590</sup>) can be prepared in high yield photochemically at 77 K, but most polymerise above this temperature.<sup>588</sup> Their stability can be enhanced electronically e.g.  $R = \text{CF}_3$  has a half life of 8 hours at 24°C,<sup>590</sup> or sterically, e.g.  $R = \text{Bu}^t$  which is stable below -20°C.<sup>589</sup> The usual route to these  $\alpha$ -selenocarboxylic acids would be alkylation of the selenolate  $\text{HO}_2\text{CCR}_2\text{Se}^-$  formed by *in situ* reduction of the corresponding diselenides. However, in most of the cases above (except  $R = \text{Me}$ <sup>591</sup>) the highly substituted diselenides are unknown.

ref.



$Pr^n$ :  $R_1, R_2 = Me, Me; Me, H; ClCH_2, H; CH$   
 $CH_2=CH, Me; CH_2=CH; H;$   
 $CH_2=CCl, H$

$Ph$ :  $R_1, R_2 = Me, Me; Me, H; ClCH_2, H$

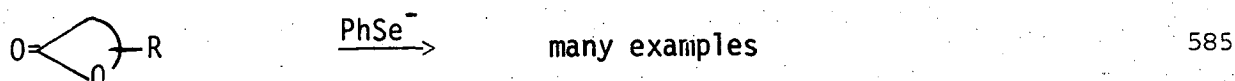
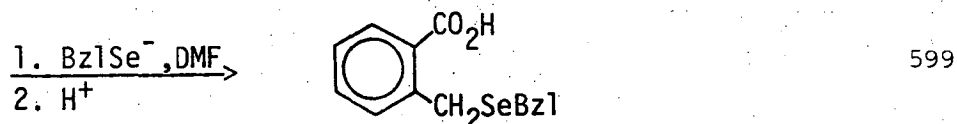
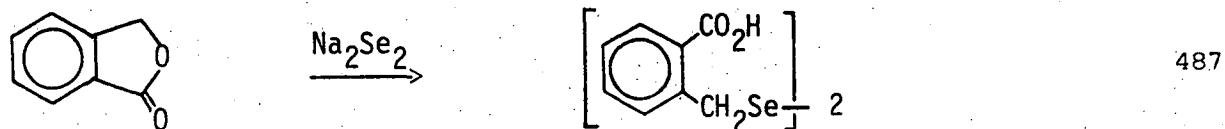
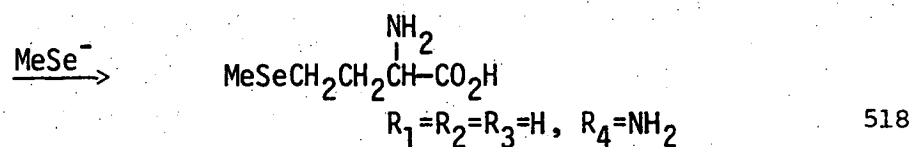
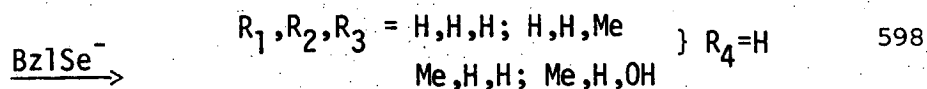
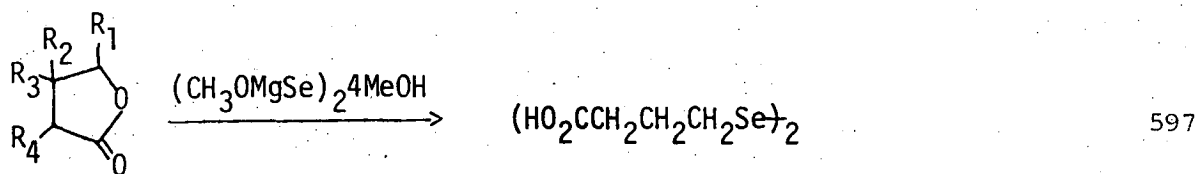
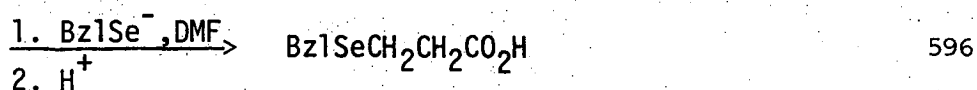
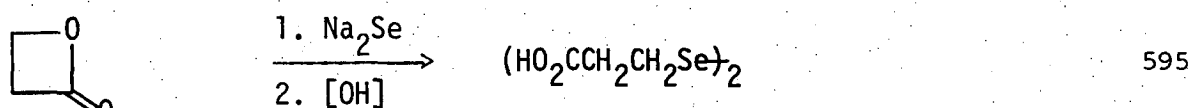
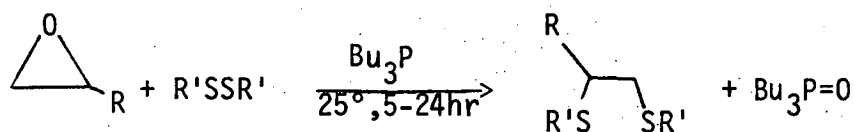


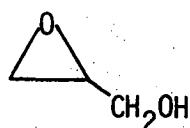
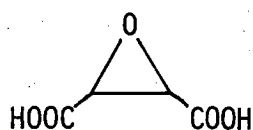
Table 5.4: Opening of lactones and epoxides by organoselenium reagents.

Epoxides can be opened with disulfides to yield protected vicinal dithiols,<sup>600</sup> but epoxide ring opening with diselenides is unreported.



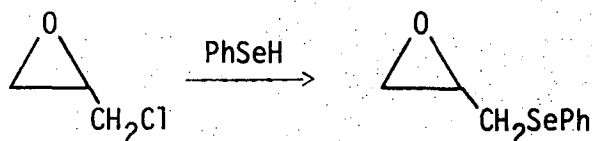
(R,R'=MePh; Ph,Me; Ph,Ph; cyclohexyl,Ph)

The epoxides of succinic acid<sup>601</sup> and 1-propanol<sup>602</sup>

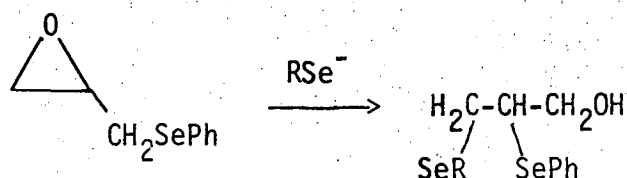


may be suitable starting materials for synthesis of protected SeDMSH<sub>4</sub> and SeBALH<sub>2</sub> using this method.

Kataev has selectively added selenophenol to epichlorohydrin, without epoxide ring cleavage,<sup>603</sup> and this may be a route to a protected



form of SeBALH<sub>2</sub> if the product can be subsequently ring opened with a second selenol.

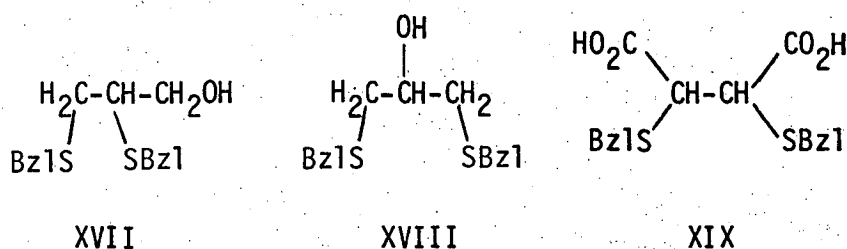


#### 5.2.4 Choice of Protective groups for SeBALH<sub>2</sub> and SeDMSH<sub>4</sub> Syntheses

Choice of protecting groups was based on the review presented above, in particular on the widespread use of the benzyl protecting group in selenopeptide synthesis and reports of successful syntheses of analogous dithiols. Acetyl-protection as a potential route to SeDMSH<sub>4</sub>

synthesis was rejected since selenolacetic acid is not available, but the benzoyl group was considered as a possible alternative although 2,3-bis(benzoylthio)succinic acid is unknown.

The benzyl group has been successfully used for protection in the synthesis of  $\text{BALH}_2$ .<sup>604</sup> Bis-benzylthiolation can be achieved using vicinal dibromides in which the bromide groups are not both primary, e.g. 2,3-dibromo-2-methyl-1-propanol (cf. page 23).<sup>497</sup> However, alkylation of benzylthiolate with 2,3-dibromo-1-propanol produces the 1,3-bis(benzylthio)-2-propanol as the almost exclusive product, due to rearrangement via an epoxide.<sup>604-5</sup> Removal of benzyl groups from 2,3-bis(benzylthio)-1-propanol, XVII, and the isomeric 1,3-bis(benzylthio)-2-propanol, XVIII, can be achieved by hydrogenolysis<sup>605</sup> or by sodium reduction in liquid ammonia.<sup>490,604</sup> 2,3-Bis(benzylthio)succinic acid, XIX, has been prepared<sup>606</sup> by Larsson, by addition of benzylthiol to acetylenedicarboxylic acid, suggesting the similar use of benzylselenol for synthesis of  $\text{SeDMSH}_4$ .



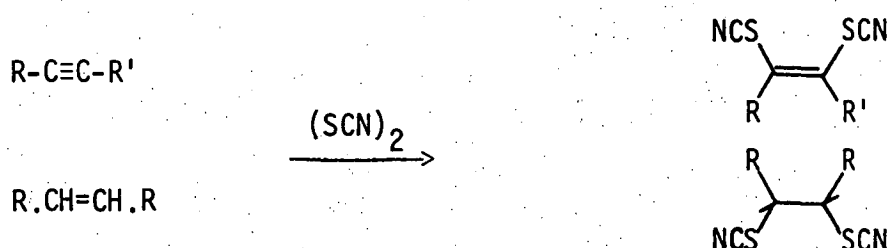
#### 5.2.5 Selenols from Selenocyanate Hydrolysis

The hydrolysis of selenocyanates is a well established route to monoselenols. Hydrolysis may be achieved in alkaline media (e.g.  $\text{Zn}/\text{NaOH}$ <sup>607</sup> or  $\text{KOH}/\text{ROH}$ <sup>608</sup>), usually producing diselenides during the workup. Advantage may be taken of the higher stability of selenols in acidic solution by reduction with other reagents, e.g.  $\text{Zn}$ <sup>609</sup> or  $\text{H}_3\text{PO}_2$ .<sup>478,610</sup> Alkylselenocyanates are conveniently prepared by displacement of bromide from alkyl bromides using  $\text{KSeCN}$  in acetone, and many non-

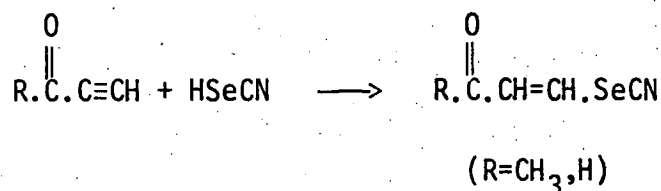
vicinal diselenocyanates have been prepared using this method.<sup>611-14</sup>

Addition of KSeCN to vicinal dibromides leads to the elimination of selenium and bromide to produce an olefin,<sup>615</sup> except in the case of 1,2-dibromoethane, where 1,2-diselenocyanatoethane can be isolated as a stable crystalline material.<sup>613-4</sup>

A recent report of the addition of thiocyanogen to alkenes (under hetero-<sup>616</sup> and homolytic <sup>617</sup> conditions) and alkynes <sup>618</sup> (homolytic conditions only) shows that vicinal dithiocyanates are formed

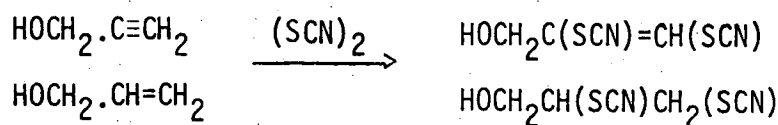


Selenocyanogen would be required to extend this reaction to selenium analogs. Although reported to be isolable as a very unstable solid,<sup>619</sup> it can readily be produced in good yield at  $-60^\circ\text{C}$  by the action of bromine on KSeCN.<sup>608</sup> It has been used as a selenocyanating agent for N-heterocycles,<sup>608</sup> but addition of  $(\text{SeCN})_2$  to alkenes and alkynes does not seem to have been reported. Wille has briefly reported on the addition of HSeCN to propynal and 3-butyne,<sup>620</sup> e.g.



These additions are usually prevented by electron withdrawing groups, e.g.  $\text{R}=\text{Cl}$ ,  $\text{CO}_2\text{H}$ ,  $\text{CO}_2\text{Et}$ ,  $\text{Bu}^t$ , and thus the reaction would not seem to be appropriate for  $\text{SeDMSH}_4$  synthesis. Addition of  $(\text{SCN})_2$  to propargyl or vinyl alcohols has not been attempted and these may be possible routes to  $\text{SeBALH}_2$  as shown:



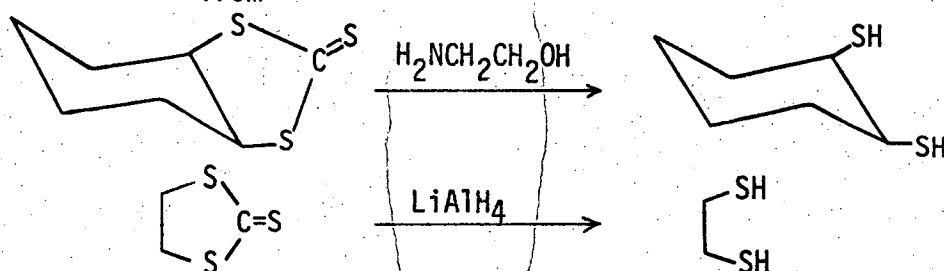


KSeCN will also open lactones to quantitatively produce seleno-cyanato-carboxylic acids,<sup>596</sup> but epoxides are opened without Se inclusion.<sup>621</sup>

### 5.2.6 Other Methods

#### (i) Reduction of Trithiocarbonates and Xanthates to Dithiols

1,2-Dithiols can be obtained by  $\text{LiAlH}_4$  reduction of trithiocarbonates<sup>622</sup> or xanthates (O-alkyldithiocarbonates) or by distillation of trithiocarbonates from aminoethanol<sup>623</sup>

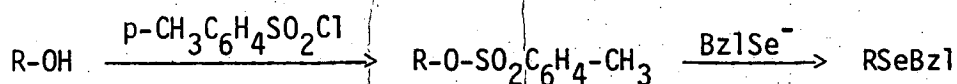


Few organo-triselenocarbonates are known, although the ion has been obtained as Ba and K salts,<sup>624-5</sup> and these require  $\text{CSe}_2$  for their preparation e.g. ethylene and methylene triselenocarbonates.<sup>626</sup>

Like their sulfur analogs, O-alkyldiselenocarbonates  $\text{RO-CSe}_2$  ( $\text{R}=(\text{CH}_2)_n\text{CH}_3$ ,<sup>627</sup>  $n=1,2,3,4,5,7,8,9,11$ ;  $\text{Et}$ <sup>628</sup>) can be prepared similarly from  $\text{CSe}_2$  and  $\text{ROH}$  but reduction of these compounds does not seem to have been reported.

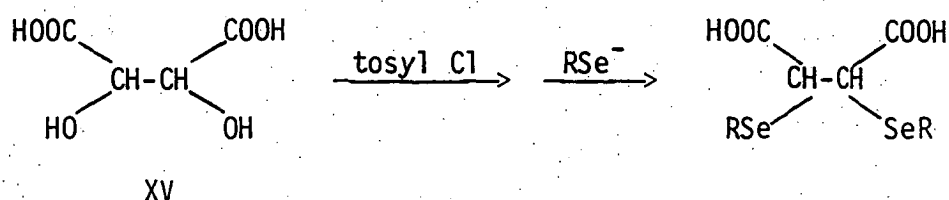
#### (ii) Conversion of Alcohols to Selenoethers

Displacement of p-toluenesulfonate (tosyl) by benzylselenolate, can be used to convert alcohols into protected selenoethers.



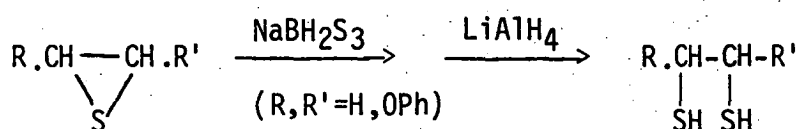
This route has been used for protection of serine and homoserine in peptide syntheses,<sup>431,511</sup> with the carboxyl group in serine protected by benzyl or 4-NO<sub>2</sub> benzyl before tosylation. Several vicinal dithiols have been prepared from vicinal primary diols, but secondary alcoholic groups react less favorably.<sup>629</sup>

The tosyl derivative of tartaric acid may provide a route to SeDMSH<sub>4</sub>, but does not appear to have been reported.

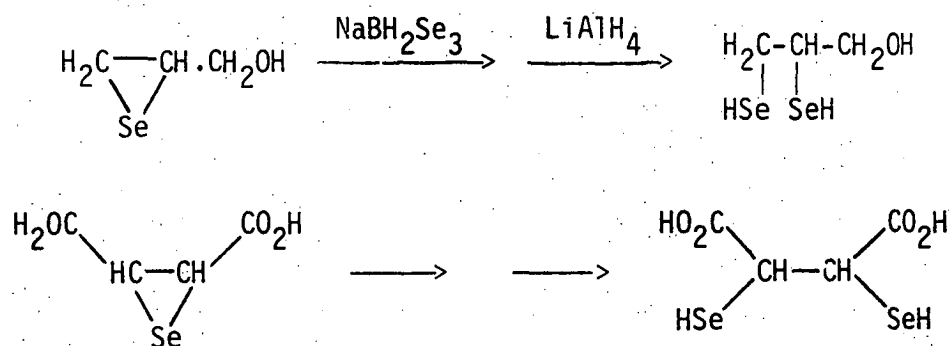


### (iii) Reduction of Episulfides

The recent use of 'sulfurated' sodium borohydride, NaBH<sub>2</sub>S<sub>3</sub>, to convert episulfides to vicinal dithiols has been reported.<sup>630</sup>



Selenium reacts with sodium borohydride to form a product suggested to be NaBH<sub>2</sub>Se<sub>3</sub>,<sup>631</sup> and thus the reactions below may be possible routes to SeBALH<sub>2</sub> and SeDMSH<sub>4</sub> respectively,



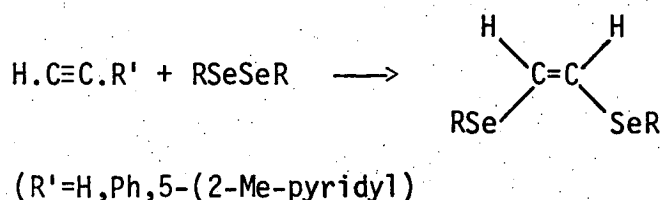
Although the existence of a few seleniranes has been reported, e.g. episelenides of cyclohexane, 1-octene and stilbene,<sup>632</sup> they are unstable

and cannot be isolated.

The reaction of selenourea with epoxides, following the procedure for the preparation of thiiranes,<sup>633</sup> does not seem to have been attempted.

#### (iv) Addition of diselenides to alkenes and alkynes

Kataeva<sup>634</sup> has briefly reported that diselenides (R=Me,Et,Ph) will add to substituted acetylenes under alkaline conditions.



Addition to alkenes does not seem to have been reported. Hydrogenation of disubstituted alkenes to the alkanes required for SeDMSH<sub>2</sub> and SeBALH<sub>2</sub> synthesis is likely to be difficult, and would probably result in hydrogenolysis of the RSe-protecting groups.<sup>635</sup> Hydrogenation of bis(alkylthio)alkenes is not a convenient route to dithiols.<sup>496</sup>

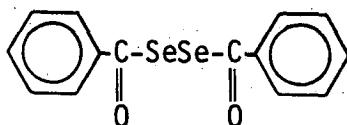
### 5.3 Attempted Syntheses of SeDMSH<sub>4</sub> and SeBALH<sub>2</sub>

#### 5.3.1 SeDMSH<sub>4</sub>

Reported below are attempts to produce SeDMSH<sub>4</sub> via precursors containing benzoyl or benzyl protecting groups, following the general procedure of Owen's DMSH<sub>4</sub> synthesis<sup>550</sup> (addition of thiolacetic acid to acetylenedicarboxylic acid). All reactions were performed in a nitrogen atmosphere. Addition of benzoylselenol to alkenes or alkynes has not been reported previously. Benzoyl protection of thiol-containing peptides has previously been carried out by alkylation of the existing thiol into benzoyl chloride.

(i) Benzoyl Protection

Dibenzoyldiselenide, XXI, was prepared by alkylation of ethanolic NaSeH (from Se in  $\text{NaBH}_4$ ) and oxidation of the resulting yellow solution with air



XXI

The odourless, yellow crystalline material is a convenient source of benzoyl selenol. Addition of excess sodium borohydride to an ethanolic suspension of XXI under nitrogen caused the solid to dissolve, yielding a deep yellow solution. (Reduction of diselenides to selenols usually causes the disappearance of the yellow colour due to the diselenide chromophore. However, Jensen reports that oily benzoyl selenol is yellow in sodium hydroxide solution<sup>558</sup>). Filtration of this solution under nitrogen into a stoichiometric quantity of acetylenedicarboxylic acid in ethylacetate yielded a deep red solution. Dibenzoyldiselenide and grey selenium were obtained as the only components of a grey precipitate which formed overnight. Dilution of the filtrate with water and extraction with ether produced a small amount of diselenide from the yellow ether layer. The components of the aqueous phase could not be separated; red selenium was produced on acidification and evaporation to low volume.

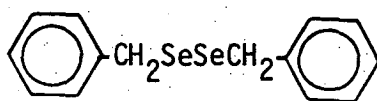
The expected highly polar dicarboxylic acid product is likely to be very difficult to separate, without decomposition, from boric acid formed from borohydride oxidation. The acidity of the carboxylic acid groups, e.g.  $\text{DMSH}_4$  has  $\text{pK}_1$  2.24(1) and  $\text{pK}_2$  3.43(1), requires low pH to ensure solvent extraction from aqueous systems. The products were too polar for alumina or silica column chromatographic separation. Reduction

of dibenzoyldiselenide with 50% hypophosphorus acid ( $\text{H}_3\text{PO}_2$ ) was complete in 5 minutes at  $90^\circ$ . Addition of aqueous acetylenedicarboxylic acid (1:1 mole ratio) produced a pink solution (and some  $\text{H}_2\text{Se}$  evolution) which was filtered from a small amount of unreduced diselenide.

Addition of water produced a pink precipitate identified as benzoic acid (ir, mass spec. identical with authentic benzoic acid) contaminated with selenium.

### (ii) Benzyl Protection

Dibenzyl diselenide, XXII, was produced as a yellow crystalline material by the reaction of benzaldehyde and ethanolic  $\text{NaSeH}$  in the presence of morpholine hydrochloride<sup>636</sup>



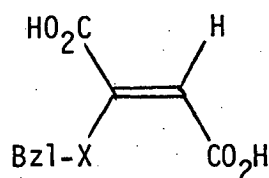
XXII

A preliminary attempt to alkylate meso-2,3-dibromosuccinic acid with benzylselenolate in ethanol (from reduction of the diselenide with sodium borohydride) produced the diselenide and fumaric acid (by comparison with ir spectra of the authentic compound). The compounds 2-(benzylseleno)fumaric acid, XXIIb, and 2-(benzylseleno)succinic acid, XXIVb, (also produced in this work) were not detected as products. (These compounds have several distinctive strong infrared absorptions:  $\nu \text{ C=O}$  at 1705, 1688 and  $1696 \text{ cm}^{-1}$  respectively. The former also has strong  $\nu \text{ C=C}$   $1670 \text{ cm}^{-1}$ ).

Addition of  $\text{NaSH}$  to 2,3-dibromosuccinic acid,<sup>493</sup> and addition of thiols to 2,3-dihalogenosuccinic acids and esters,<sup>550</sup> is reported to produce fumaric acid by trans-elimination of bromide.

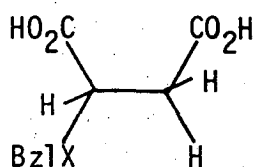
The 1:1 base-catalysed addition of benzylthiol to acetylene-

dicarboxylic acid, ADCA, has been reported to result in the formation of 2-(benzylthio)fumaric acid, XXIIIa.<sup>637</sup>



XXIII a, X=S

b, X=Se



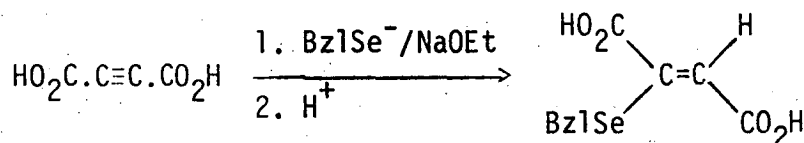
XXIV a, X=S

b, X=Se

Addition of two benzylthio groups to ADCA was also achieved, to produce the previously mentioned protected DMSH<sub>4</sub> derivative meso-2,3-bis(benzylthio)succinic acid, XIX. Reaction conditions can be varied to give predominantly the racemic or meso product.<sup>606</sup> The meso-2:1 adduct also results from addition of benzylthio to the trans-1:1 adduct, XXIIIa.<sup>638</sup>

Following this approach it was found that the base-catalysed addition of benzylselenol to ADCA produced only the new unsaturated 1:1 adduct, XXIIIb. Benzylselenol was obtained as a foul smelling, colourless oil (bp. 61.0-61.5°/8mm) by Painter's Grignard-reagent method.<sup>501</sup>

Using Larsson's procedure, neat benzylselenol was added to one equivalent of ADCA dissolved in sodium bicarbonate solution. The colourless solution was stirred for 36 hours under nitrogen, then extracted with ether to remove any unreacted diselenide. Upon acidification with HCl (Congo red), the yellow product XXIIIb (55%) was obtained. Recrystallisation from aqueous ethanol gave XXIIIb as bright yellow needles, m.p. 180-3°(dec.).



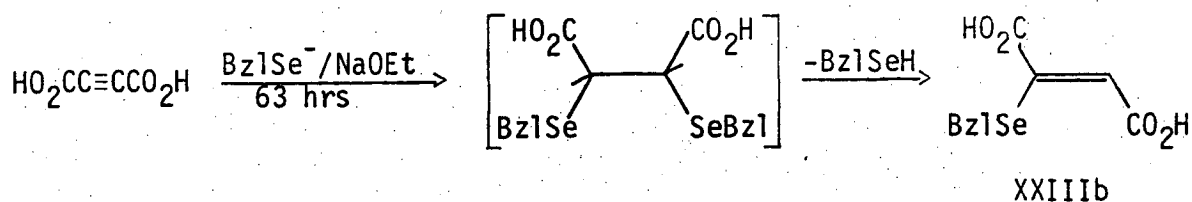
An alternative preparative procedure, used by Kataev<sup>580</sup> for selenophenol addition reactions, was more rapid and produced the same product. The reactants were dissolved in a saturated ethanolic solution of sodium ethoxide cooled in ice. After 15 minutes, the thick white suspension was diluted with water and worked up as previously to give XXIIIb.

The previously reported sulfur analog, XXIIa, was prepared under identical conditions.

Attempts to obtain the required 2:1 addition product using either of these methods (Larsson, Kataev) failed, even with prolonged reaction times (1 week). The 1:1 adduct and dibenzyl diselenide were always obtained with the usual workup. Similarly, the selenol (or benzyl thiol) could not be added to the 1:1 adduct. In contrast, reaction of benzylthiol with ADCA in 2:1 mole ratio, produced white meso-2,3-bis(benzylthio)succinic acid, XIX, which was also synthesised from  $\text{DMSH}_4$  and benzylchloride.

Kataev has reported the failure to add a second molecule of selenophenol to 2-(phenylseleno)fumaric acid,<sup>580</sup> which he claims is due to "both the low polarisation of the double bond, and the fact that it is shielded." The use of benzylselenol in place of selenophenol might have been expected to reduce these inhibitory effects.

It was found, however, that NaOEt catalysed addition of benzylselenol to ADCA produced a pale-yellow precipitate after 63 hours. On filtration and rapid washing with ethylacetate, to remove yellow XXIIIb, the product was nearly white, but rapidly became bright yellow with the evolution of foul-smelling benzylselenol.



The white product may have been the required 2:1 benzyl protected  $\text{SeDMSH}_4$ , but its instability precludes its use to conveniently obtain a deprotected product.

The  $^1\text{H}$  nmr spectra (in acetone- $\text{d}_6$ ) of XXIIIa and XXIIIb are summarised in Table 5.5.

<u>2-(benzylX)fumaric acid</u>	<u><math>\text{C}_6\text{H}_5</math></u>	<u><math>\text{CH}_2</math></u>	<u><math>\text{CH}=\text{C}</math></u>	<u><math>\text{CO}_2\text{H}^\alpha</math></u>
X=S (this work)	7.38	4.25	6.45	5.1(br)
(ref. 637)	-	4.23	6.50	-
X=Se (this work)	7.39	4.21	6.69	5.3(br)

Table 5.5: Proton chemical shifts for the acids  $\text{trans-HO}_2\text{CC}(\text{XCH}_2\text{C}_6\text{H}_5)=\text{CHCO}_2\text{H}$  in acetone- $\text{d}_6$  ( $\delta \pm 0.02$ )  $^\alpha$ resonances due to carboxylate protons and  $\text{H}_2\text{O}$  impurity in solvent.

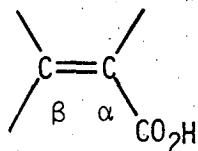
The benzylic protons in these compounds are essentially unaffected by substitution of sulfur by selenium. This result is somewhat unexpected, and may reflect a balance between differences in inductive and mesomeric effects of the chalcogens in these conjugated systems. In contrast, the benzylic protons in dibenzyl diselenide (3.83 $\delta$  in  $\text{CDCl}_3$ , this work) are deshielded with respect to dibenzyl disulfide (3.51 $\delta$  in  $\text{CCl}_4$ )<sup>639</sup> and shielded with respect to dibenzyl ditelluride (4.25 $\delta$  in  $\text{CDCl}_3$ , this work). The methyl protons of dimethyl polysulfides and polyselenides show analogous behaviour.<sup>639</sup> In addition, the olefinic proton of the selenium analog (6.45 $\delta$ ) is deshielded with respect to the sulfur derivative (6.69 $\delta$ ). This deshielding effect has also been noted in several compounds where selenium is part of a conjugated system,<sup>640</sup> indicating that mesomeric influences may be dominant.



Larsson has compared the olefinic proton chemical shifts in  $D_2O$  of the disodium salts of 2-(benzylthio)fumaric acid (6.24 $\delta$ ) and 2-(benzylthio)maleic acid (5.68 $\delta$ ).<sup>637</sup> From Table 5.5 it can be seen that the proton chemical shifts of XXIIIb are close to those of the trans- sulfur analog, supporting the assignment of trans- stereochemistry for XXIIIb. No coupling between selenium and the benzylic protons of XXIIIb could be observed. Although one-, two- and three-bond  $^1H$ - $^{77}Se$  couplings have been observed elsewhere,<sup>641</sup> the  $^{77}Se$  satellites are of low intensity (7.5% natural abundance) and were not detected in any  $^1H$  nmr spectra recorded in this work.

The selenium compound, XXIIIb, is bright yellow and the analogous sulfur compound, XXIIIa, also synthesised in this study, is light yellow. Aqueous alkaline solutions of these compounds are colourless. The near ultraviolet absorption spectra of XXIIIa and XXIIIb are shown in Figure 5.1. It can be seen that the yellow colours of these compounds are due to tailing of and intense absorption near 300 nm into the visible region.

The expected position of  $\lambda_{max}$  for the  $n \rightarrow \pi^*$  transition of the  $\alpha, \beta$ -unsaturated carboxylic acid chromophore of the sulfur compound can be calculated. The position of  $\lambda_{max}$  for simple  $\beta$ -substituted  $\alpha, \beta$ -unsaturated carboxylic acids is given as  $208 \pm 5$  nm by Nielsen.<sup>642</sup>



It has been reported that carboxylate substitution in the  $\beta$ -position of simple enone chromophores has no effect on the position of  $\lambda_{max}$ .<sup>643</sup> Similarly, addition of  $CO_2H$  to  $\alpha, \beta$ -unsaturated carboxylic acids does not alter the position of  $\lambda_{max}$  of the chromophore, e.g. the  $\alpha, \beta$ -unsaturated

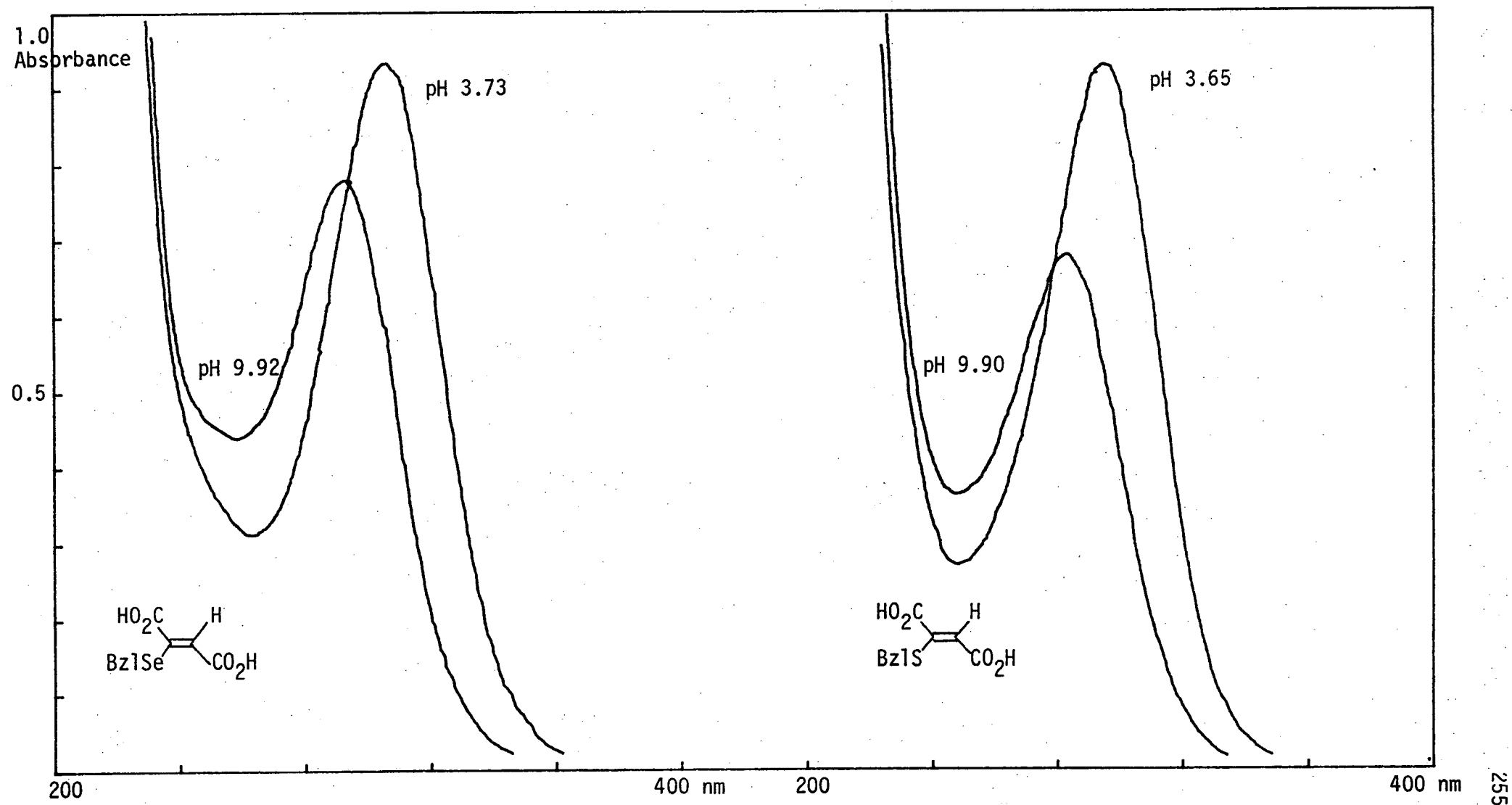


Figure 5.1: Ultraviolet absorption<sup>a</sup> of 2-(benzylseleno)fumaric acid and 2-(benzylthio)fumaric acid.

<sup>a</sup>  $1.0 \times 10^{-4}$  M solutions at the pH shown, in 1 cm cells.

dicarboxylic acids, maleic and fumaric acids, have  $\lambda_{\max}$  ( $\epsilon$  in water) of 210( $1.3 \times 10^4$ ) and 208( $1.4 \times 10^4$ ), respectively.<sup>644</sup>

The degree of bathochromic shift caused by an S-alkyl substituent can be deduced from the change in  $\lambda_{\max}$  for enones<sup>643</sup> to be  $\pm 85$  nm.

The sulfur analog XXIIIa is thus expected to have  $\lambda_{\max}$  (in water) at 293 nm ( $208 + 85$ ). The position of  $\lambda_{\max}$  is found to be 294 nm at pH 3.7, where the compound is 92% protonated (the hydrolysis constants  $pK_{a1}$ ,  $pK_{a2}$  have been measured to be 2.03(1), 4.49(1) for XXIIIa and 2.01(1), 4.46(1) for XXIIIb at 25° in 0.1M  $KNO_3$ ).

By comparing the spectra for protonated forms of XXIIIa and XXIIIb it is clear that substitution of selenium for sulfur causes a bathochromic shift in the  $n \rightarrow \pi^*$  transition of +12 nm.

Thus, the contribution to the position of  $\lambda_{\max}$  due to  $\beta$ -Se-alkyl substitution would appear to be +98 nm.

Bathochromic shifts are often found to be in the order  $O < S < Se$  for analogous compounds. This may be explained by a hyperconjugative mechanism. Thus, in compounds XXIIIa and XXIIIb the lower energy for  $n \rightarrow \pi^*$  transition in the selenium analog may be due to stabilisation of a charge-separated excited state (in extended conjugation with the  $\alpha, \beta$ -unsaturated system) due to the increased ability of Se to accept a delocalised negative charge.

This possibility has been postulated by Mautner and co-workers to explain the bathochromic trends in compounds containing the selenoamide moiety.<sup>645-7</sup>

Deprotonation of XXIIIa and XXIIIb causes the  $n \rightarrow \pi^*$  transition to move to higher energy (hypsochromic shift) (Table 5.6).

	<u><math>n \rightarrow \pi^*</math> transition energy/kJ mol<sup>-1</sup></u>	
	XXIIIa X=S	XXIIIb X=Se
2(Bz1X)C(CO <sub>2</sub> H)=CH(CO <sub>2</sub> H)	422	407
2(Bz1X)C(CO <sub>2</sub> <sup>-</sup> )=CH(CO <sub>2</sub> <sup>-</sup> )	405	389

Table 5.6:  $\alpha,\beta$ -unsaturated carbonyl transition energy shifts of XXIIIa,b on deprotonation of the carboxylate groups.

The new saturated analog of XXIIIb, 2-(benzylseleno)-succinic acid, XXIVb, was also prepared. Base-catalysed (NaOEt) addition of benzylselenol to maleic acid, and the usual workup to remove dibenzyldiselenide, produced a white product on acidification. Recrystallisation from aqueous ethanol produced XXIVb as fine white needles, mp. 185-7°. The sulfur analog XXIVa has been previously prepared by Larsson, and was<sup>648</sup> synthesised in this work using the NaOEt catalysed method.

Microanalyses for the new compounds XXIIIb and XXIVb are shown below.

	<u>found %</u>			<u>calc. %</u>		
	C	H	Se	C	H	Se
2-(benzylseleno)fumaric acid	46.6	3.6	27.8	46.7	3.5	27.7
2-(benzylseleno)succinic acid	46.0	4.4	27.2	46.0	4.2	27.5

The 100 MHz proton nmr spectra (in acetone-d<sub>6</sub>) of XXIVa and XXIVb are shown in Figures 5.2 and 5.3 respectively. Substitution of Se for S has caused the expected small downfield shift (see page 253) in the singlet resonance of the benzylic protons (4.03δ for XXIVa compared with 4.09δ for XXIVb). These values are close to those previously recorded

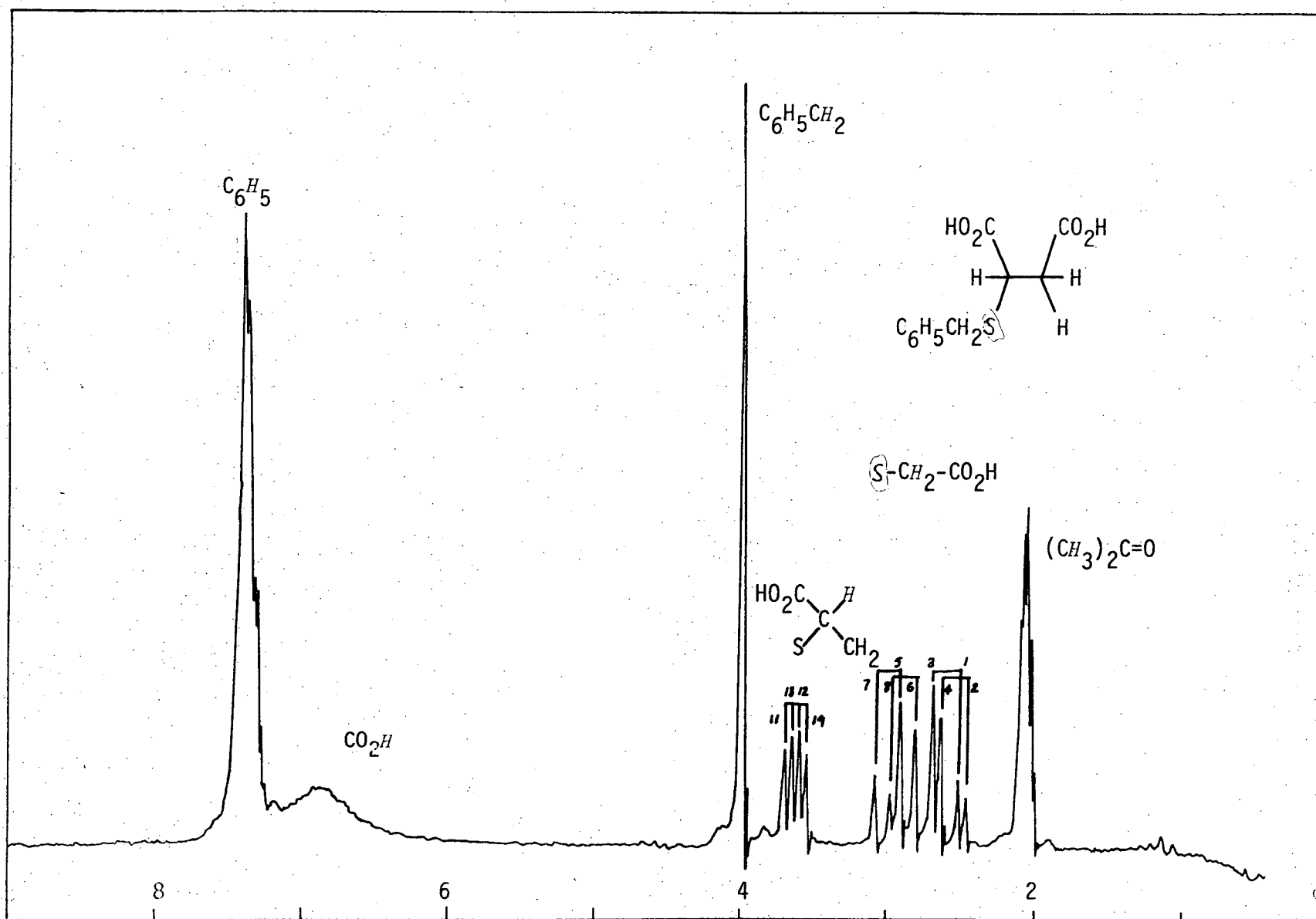


Figure 5.2: 100 MHz proton nmr spectrum of 2-(benzylthio)succinic acid in acetone- $d_6$ .

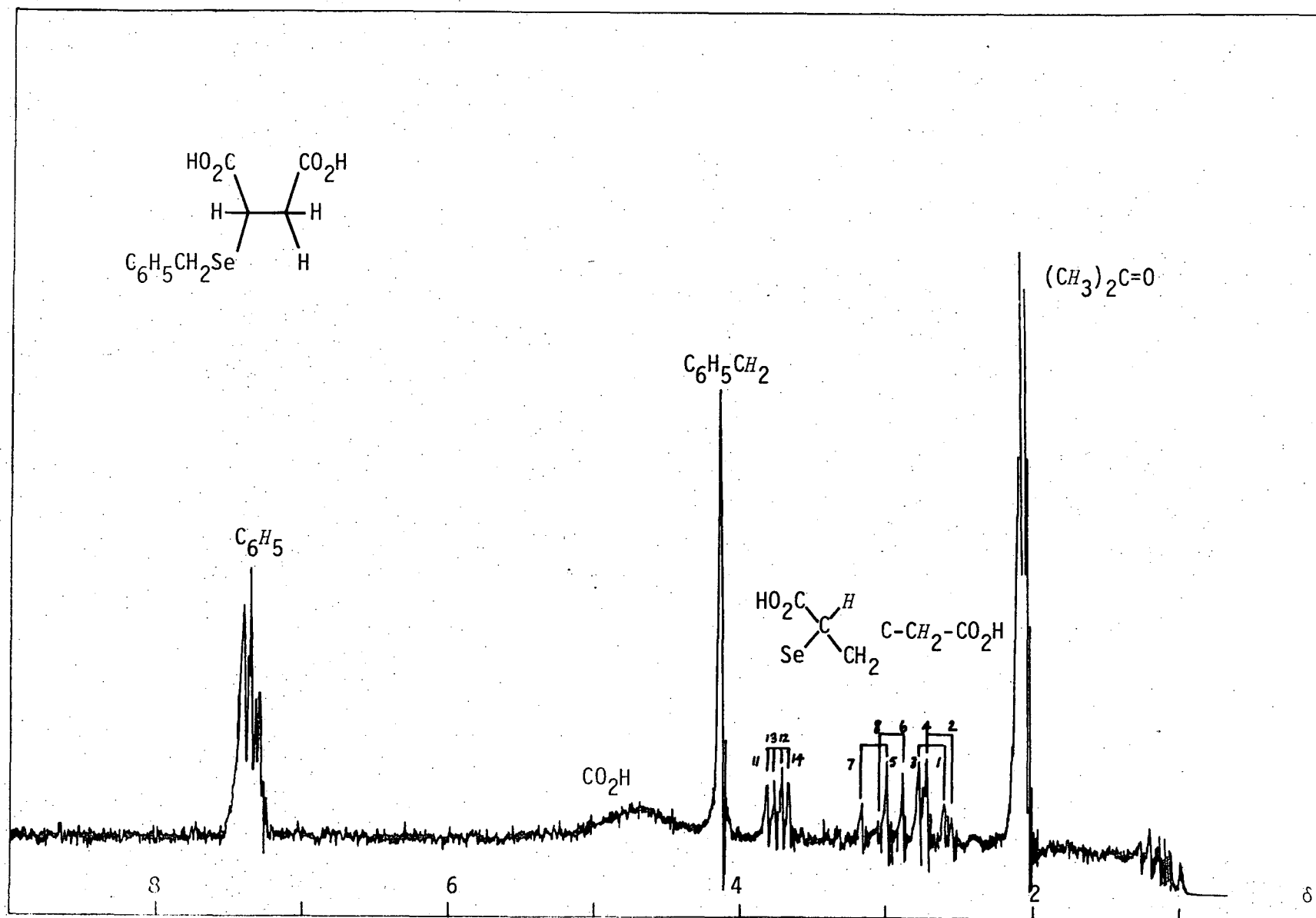
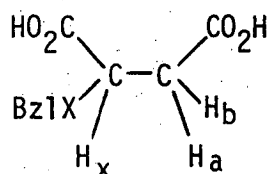


Figure 5.3: 100 MHz proton nmr spectrum of 2-(benzylseleno)succinic acid in acetone- $\text{d}_6$ .

for the unsaturated analogs XXIIIa and XXIIIb (page 253). In the nmr spectrum of XXIVb,  $^1\text{H}$ - $^{77}\text{Se}$  coupling was not observed.

A feature of interest in these spectra is the well-resolved 12 line-ABX system of methylene (A,B) and methine (X) protons.



The spectra were treated by the method of Garbisch<sup>649</sup> to obtain the coupling constants  $J_{ax}$ ,  $J_{bx}$  and  $J_{ab}$ . The geminal coupling,  $J_{ab}$ , was considered to be negative.<sup>650</sup> The numbering of the ABX transitions shown in Figures 5.2 and 5.3 is the only combination which satisfies the intensity and coupling constant relationships required by Garbisch, with  $J_{ab} < 0$ .<sup>649</sup> The values for  $J_{ax}$  and  $J_{bx}$  derived from second-order treatment of the spectra are summarised in Table 5.7.

Both compounds are expected to be in conformational (rotational) equilibrium in acetone- $d_6$  which is rapid on the nmr timescale. The three possible staggered conformations are shown in Figure 5.4.

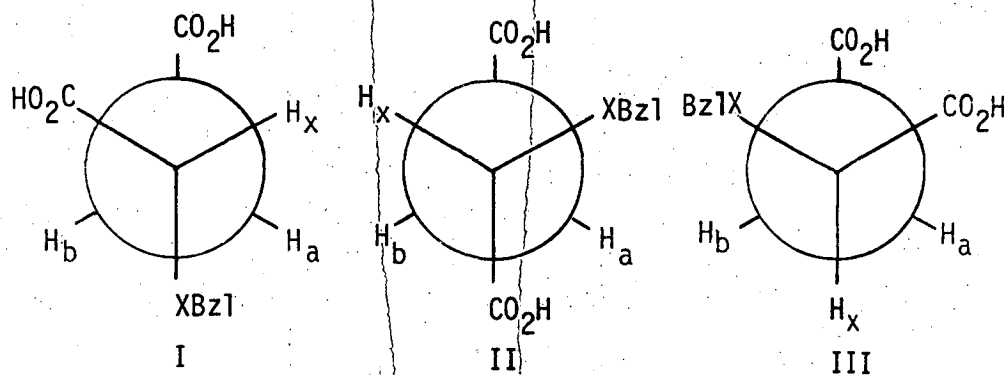


Figure 5.4: Staggered conformations of XXIVa and XXIVb.

Conformer III is expected to be the least energetically favorable due to the interactions of three gauche bulky groups. The magnitude of  $J_{ax}$  (10 Hz) requires the exchange-averaged  $H_a-H_b$  dihedral angle to be near  $180^\circ$ ,<sup>650</sup> which mitigates against a significant population of rotamer III. An estimate of the relative populations of rotamers I and II can be made using  $J_{ax}$  and  $J_{bx}$ <sup>651</sup>

$$n_I/n_{II} = \frac{(J_{bx}/J_{ax}) - 0.180}{1 - 0.180(J_{bx}/J_{ax})}$$

(This relationship assumes  $H_a-H_x$  and  $H_b-H_x$  dihedral angles of  $65^\circ$  and  $185^\circ$  respectively, which seem to be relatively invariant in a range of trisubstituted ethanes<sup>651</sup>).

	$J_{ab}$	$J_{ax}^a$	$J_{bx}$	$n_I/n_{II}$
XXIVa	-17.1	10.9	5.0	0.3
XXIVb	-17.1	10.7	4.5	0.3

**Table 5.7:** Coupling constants<sup>b</sup> obtained from the ABX subspectra of XXIVa, XXIVb.

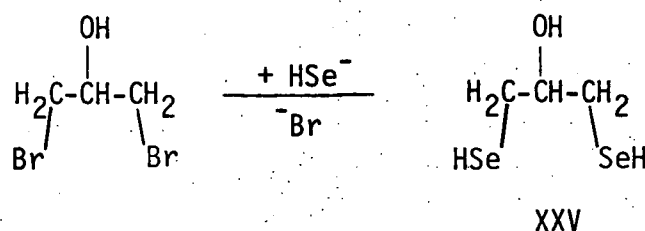
<sup>a</sup>assumed to be  $<0$ ; <sup>650</sup> <sup>b</sup> transition frequencies were measured with a sweep width of 90 Hz, errors in peak positions of  $\pm 0.2$  Hz generate errors of approx.  $\pm 0.5$  Hz in the coupling constants.

From Table 5.7 it can be seen that conformation II appears to be preferred for both compounds, which may reflect a hydrogen bonding interaction between gauche carboxyl and X-benzyl groups.



### 5.3.2 $\text{SeBALH}_2$ and related $\text{SeDMPH}_2$

Baroni <sup>479</sup> has reported that  $\text{HSe}^-$  will displace bromide from 1,3-dibromo-2-propanol to form the non-vicinal diselenol 1,3-diseleno-2-propanol, XXV, ( $\text{SeDMPH}_2$ , bp.  $114^\circ/20$  mm) which was isolated as the  $\text{Hg(II)}$  complex. It was reported that the free selenol could be regenerated by removal of mercury with  $\text{H}_2\text{Se}$ . Baroni did not report the preparation of isomeric  $\text{SeBALH}_2$ , of interest in this work.



The non-vicinal dithiol analog, 1,3-dimercapto-2-propanol,  $\text{DMPH}_2$ , has no antidotal activity towards mercury intoxication. In fact, the high toxicity of early preparations of  $\text{BALH}_2$  have been ascribed to  $\text{DMPH}_2$  impurities.<sup>605</sup> The interest in  $\text{SeDMPH}_2$  in this work derives from the fact that the  $\text{Hg(II)}$  complex of its dithiol analog forms a crystalline adduct with pyridine,  $\text{HgDMP(py)}_{1.5}$ .<sup>238</sup> In contrast,  $\text{HgBAL}$  is insoluble in common solvents and can only be obtained as an amorphous polymer (page 53). A similar alkylation using 1,3-dibromopropane is reported to form the disodium salt of 1,3-diselenopropane, which was not isolated but used *in situ*.<sup>652</sup>

Attempted syntheses of  $\text{SeDMPH}_2$  and of protected  $\text{SeBALH}_2$  are reported below.

#### (i) $\text{SeDMPH}_2$

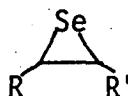
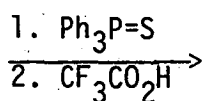
Following the principle of Baroni's synthesis, alkylation of alkaline ethanolic  $\text{NaSeH}$  with 1,3-dibromo-2-propanol gave a colourless solution containing the disodium salt of  $\text{SeDMPH}_2$ . ( $\text{NaSeH}$  was conveniently

prepared by the action of sodium borohydride on selenium, in contrast to Baroni's use of  $\text{H}_2\text{Se}$ ). Acidification of this solution to pH 4-5 resulted in the evolution of  $\text{H}_2\text{Se}$  (from  $\text{Se}^{2-}$  impurities) which was removed by purging with nitrogen (under slight vacuum) until the effluent gas did not darken lead acetate paper (2 hours). Evaporation under nitrogen and ether extraction gave an orange oil which could be distilled under reduced pressure. The light orange distillate (bp.  $79-85^\circ/3.5$  mm) solidifies at  $-20^\circ$ . The Raman spectrum of this oil showed no bands in the region  $2000-2700\text{ cm}^{-1}$ . Free selenols have an intense polarised Raman band due to  $\nu\text{SeH}$  at  $2280-2300\text{ cm}^{-1}$  which is weak in infrared spectra. Additionally, a weak absorption at  $286\text{ cm}^{-1}$  in the Raman spectrum indicated that diselenide was only a minor component. Aliphatic diselenides,  $\text{RSeSeR}$ , give an intense polarised Raman band at  $233-293\text{ cm}^{-1}$  ( $\text{R}=\text{Me}$ ,  $^{653}\text{ Bu}^n$ ,  $^{654}\text{ Bu}^t$ ,  $^{655}$ ) which is weak in infrared spectra. No values of  $\nu\text{SeSe}$  have been reported for spectra of 1,2-diselenocycloalkenes.

Mass spectrometry (Figure 5.5a) indicated that the product is predominantly a compound with the formula  $\text{C}_3\text{H}_6\text{OSe}$  ( $M^+$  137.9603, calc. 137.9603) with a minor proportion of a less volatile diselenide  $\text{C}_3\text{H}_6\text{OSe}_2$  (Figure 5.5b).

The mixture could not be separated by fractional distillation under reduced pressure, or chromatographically on alumina, but could be partially separated by fractional distillation under high vacuum to give two selenium containing fractions, enriched in the first and second compounds respectively.

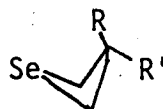
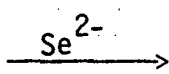
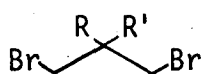
Cyclic selenides have previously been prepared as major products from non-vicinal dibromides (Table 5.8). The proton nmr spectrum (Figure 5.6) of the mixture, is consistent with the major component being selenetan-3-ol, XXVI. The minor component is most likely 1,2-

seleniranes

R = H, R' = Ph, octyl

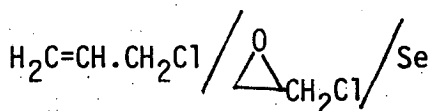
Ref

632

selenetanes

R=R'=H, Me

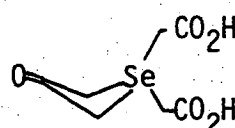
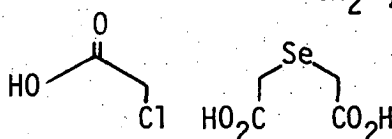
656-7



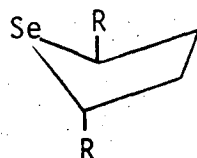
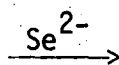
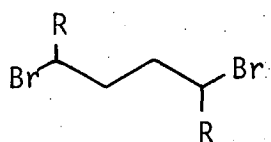
electrolysis

R=H, R'=OH

658



591

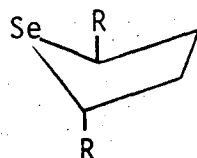
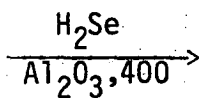
selenolanes

R=H

659-60

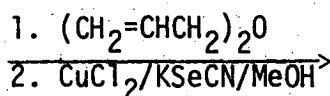
CO2H

661



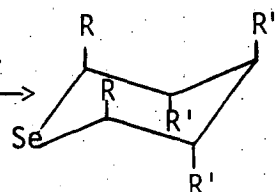
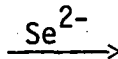
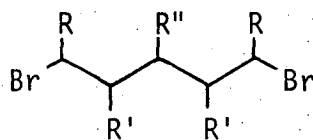
H

662

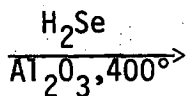


CH2OMe

663

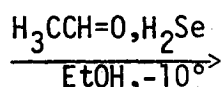
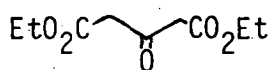
selenanesR=R'=R''=H  
(and others)

660, 664



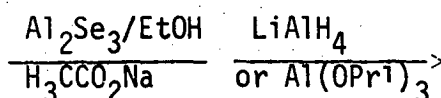
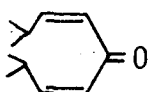
R=R'=R''=H

662

R=Me, R'=CO2tt, R''=O  
CO2H H2 H

665

666



R=Ph, R'=H, R''=O

667

R, R' various, R''=OH, H

668-9

Table 5.8: Previously reported monoselenoalkanes.<sup>a</sup>

<sup>a</sup> many of these compounds undergo addition reactions with halogens to produce 1,1'-dihalogeno- and ring-substituted products but these are not considered here. Similarly, many 1,1-dioxides are known.

ref.

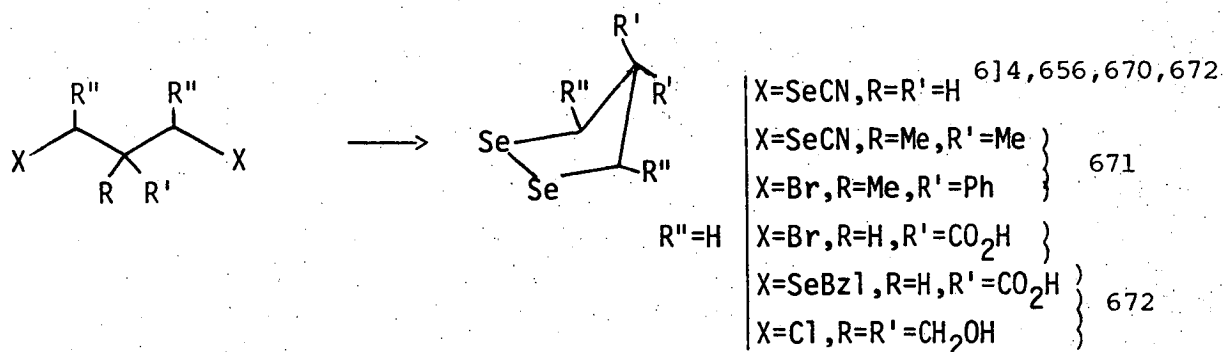
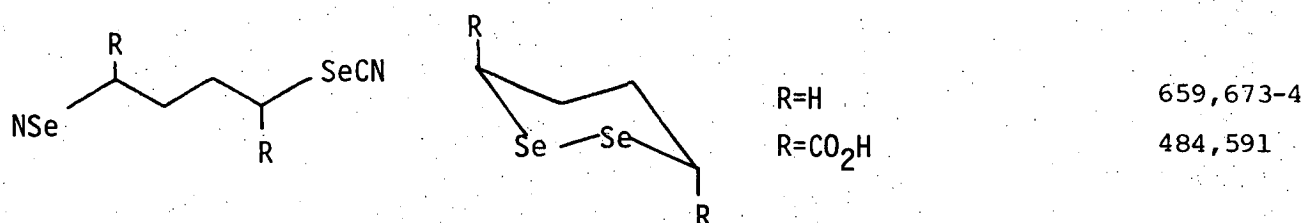
diselenolanesdiselenanes

Table 5.9: Previously reported 1,2-diselenocycloalkenes.

diselenolan-4-ol, XXVII. It is to be expected that these compounds would have very similar physical properties, which is consistent with difficulties experienced with their attempted separation.

The selenetane seems to be unusual in that the four-membered ring is only mono-substituted, all others reported to date being at least disubstituted. The carboxylic acid analog of the 1,2-diselenolane has been prepared by Fredga<sup>484</sup> (Table 5.9).

In the 70 eV mass spectrum of XXVI (Figure 5.5a), the molecular ion ( $m/e$  138) is not the base peak, but is in fact the second most intense peak. This is indicative of fairly high thermal stability of the compound, since thermally labile organoselenium compounds rarely show an intense molecular ion. In addition, no peaks due to polyselenide fragments are observed, consistent with high thermal stability.<sup>675</sup> The mass spectrum of selenetane has not been reported, but that of thietan-3-ol has recently been recorded<sup>676</sup> and has the most intense peaks all containing sulfur at  $m/e$  46 [ $\text{CH}_2\text{S}^+$ ], 61 [ $\text{C}_2\text{H}_5\text{S}^+$ ] and 90 ( $\text{M}^+$ ) [ $\text{C}_3\text{H}_6\text{OS}^+$ ]. Similar fragmentations are shown in the mass spectrum of XXVI at  $m/e$  94 (base peak) [ $\text{CH}_2\text{Se}^+$ ], 109 [ $\text{C}_2\text{H}_5\text{Se}^+$ ] and 138 ( $\text{M}^+$ ) [ $\text{C}_3\text{H}_6\text{OS}^+$ ].

The mass spectrum of less volatile XXVII (Figure 5.5b) shows the parent peak at  $m/e$  58 ( $\text{M}-\text{C}_3\text{H}_6\text{O}^+$ ) and the expected  $\text{Se}_2$  fragments at  $m/e$  218 ( $\text{M}^+$ ) and 160 [ $\text{Se}_2^+$ ]. Mass spectra of substituted 1,2-diselenolanes have not been previously reported for comparison.

After the completion of this work, the first reported preparation of selenetan-3-ol appeared.<sup>658</sup> The product was made in 50% yield by electrolysis of an electrolyte containing allyl chloride, epichlorohydrin and selenium metal. The diselenolane XXVII has not previously been reported.

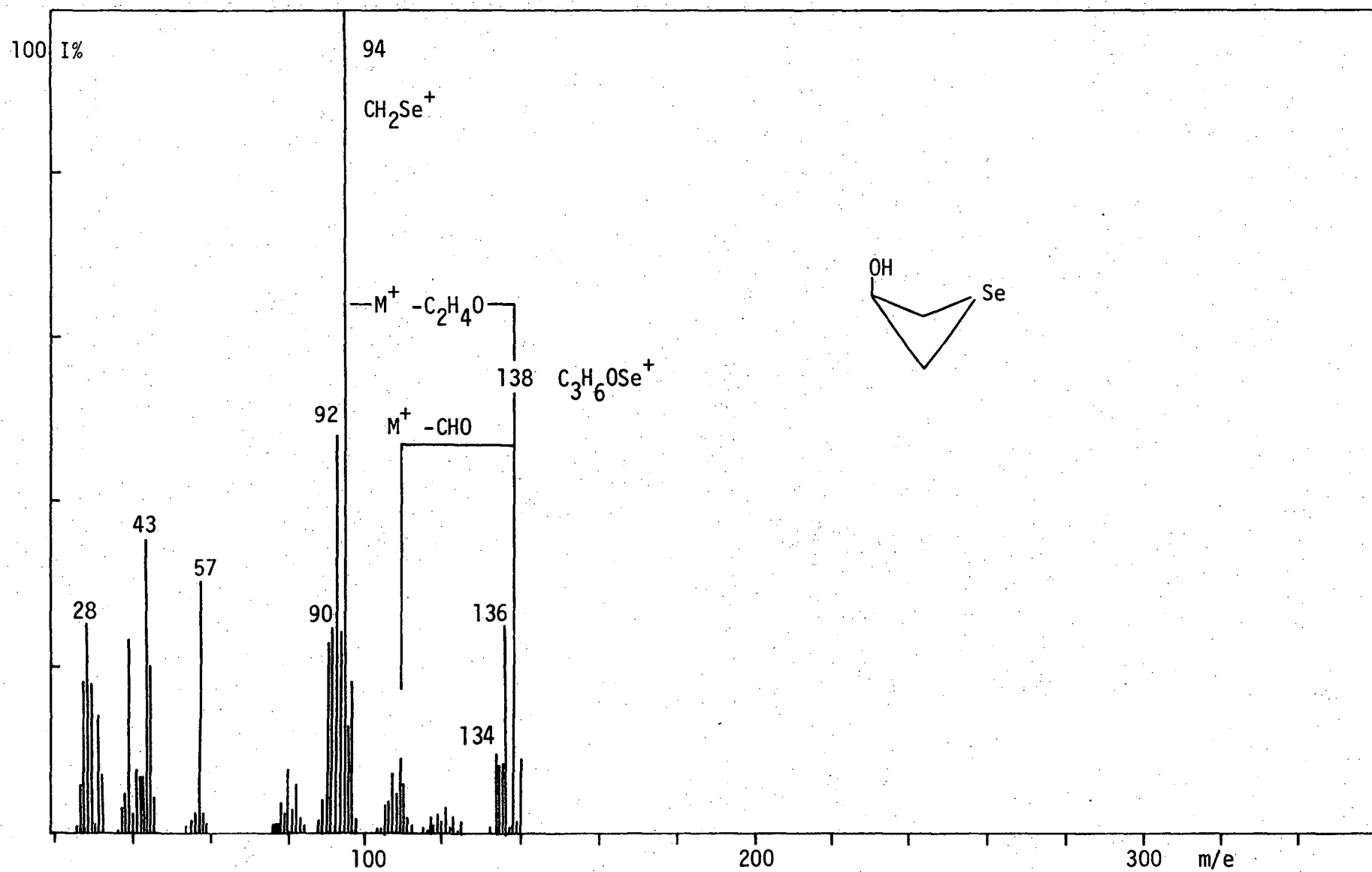


Figure 5.5a: Low resolution 70 eV mass spectrum of XXVI.

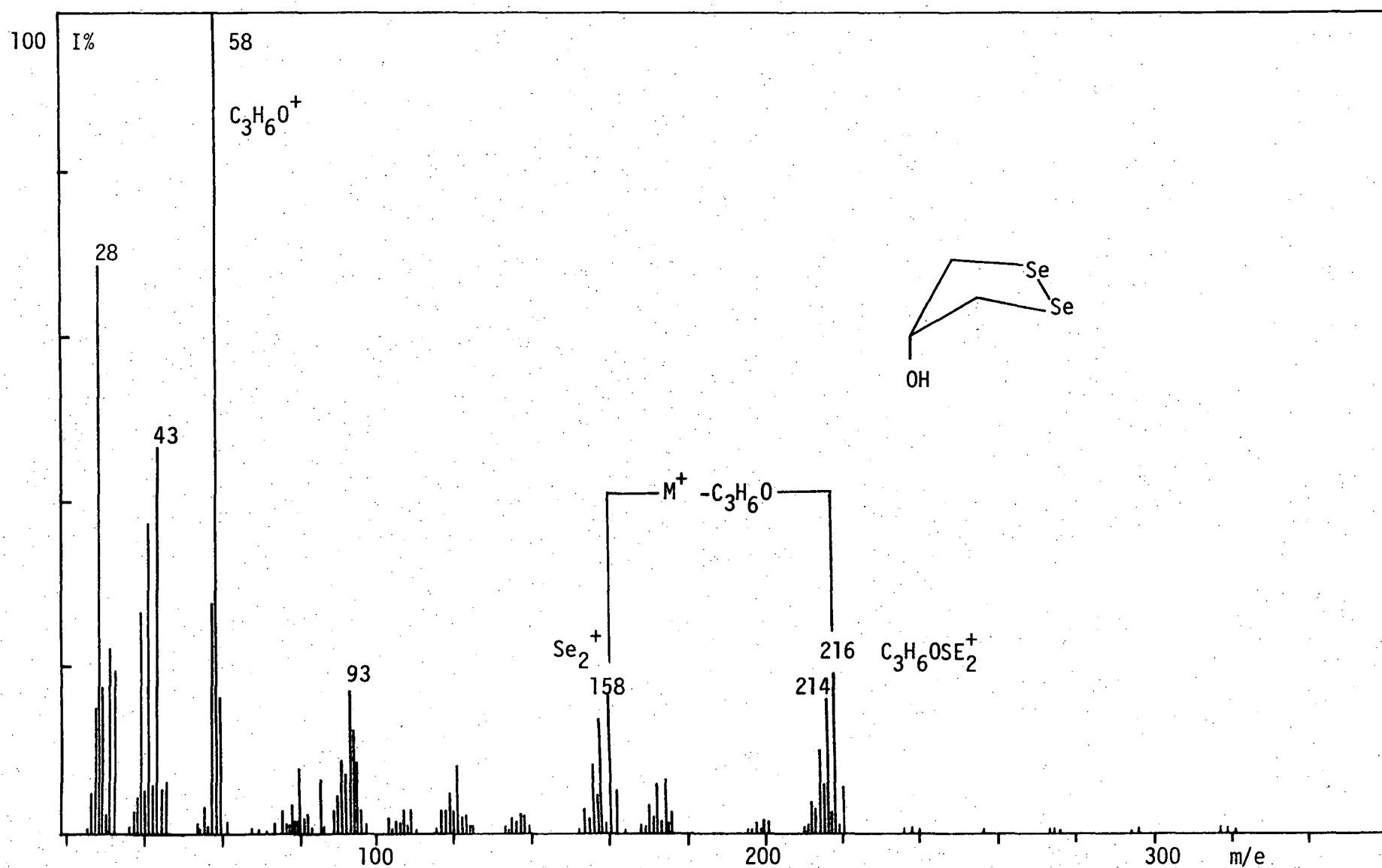


Figure 5.5b: Low resolution 700 eV, mass spectrum of XXVII.

The proton nmr spectrum of XXVI in  $\text{CDCl}_3$  is shown in Figure 5.6. Apart from a minor impurity at 1.33 $\delta$  (m, 0.4H), the spectrum can be interpreted in a first-order fashion as two triplets centred at 3.12 $\delta$  (2H) and 3.37 $\delta$  (2H) respectively, corresponding to two sets of axial and equatorial protons, each of which is coupled to the proton geminal to the hydroxyl group, giving rise to a quintet (1H) centred at 4.85 $\delta$ . Selenetane has a similar methylene proton multiplet at 3.2 $\delta$ .<sup>677</sup> The  $\text{D}_2\text{O}$  exchangeable OH proton appears as a broad signal centred at 1.45 $\delta$  (1H). Satellites due to  $^2J(^1\text{H}-^{77}\text{Se})$  cannot be observed. The proton nmr spectrum of the sulfur analog, thietan-3-ol, has recently been interpreted,<sup>678</sup> and is apparently consistent with the expected saddle-conformation of the four-membered ring having an equilibrium saddle angle of 140-150°. Details of the nmr spectrum of this compound are not available, as the original Russian paper is unavailable in Tasmania.

The closely related compound 3-acetylthietane has been mentioned in an nmr study of thietene-1,1-dioxides.<sup>679</sup> The axial and equatorial methylene protons are reported as a multiplet 333 Hz downfield from TMS in  $\text{CCl}_4$  (5.55 $\delta$  on the 60 MHz instrument) which differs somewhat from the value of 4.35 $\delta$  found here for selenetan-3-ol. The positions of  $\alpha$ -methylene proton resonances were not recorded in the abovementioned study.<sup>679</sup>

A complete description of the proton nmr spectrum of selenetan-3-ol involves treatment of an  $\text{A}_2\text{B}_2\text{X}$  spin system. The two pairs of axial and equatorial protons are magnetically non-equivalent due to long range spin coupling and the occurrence of conformational equilibria shown below:



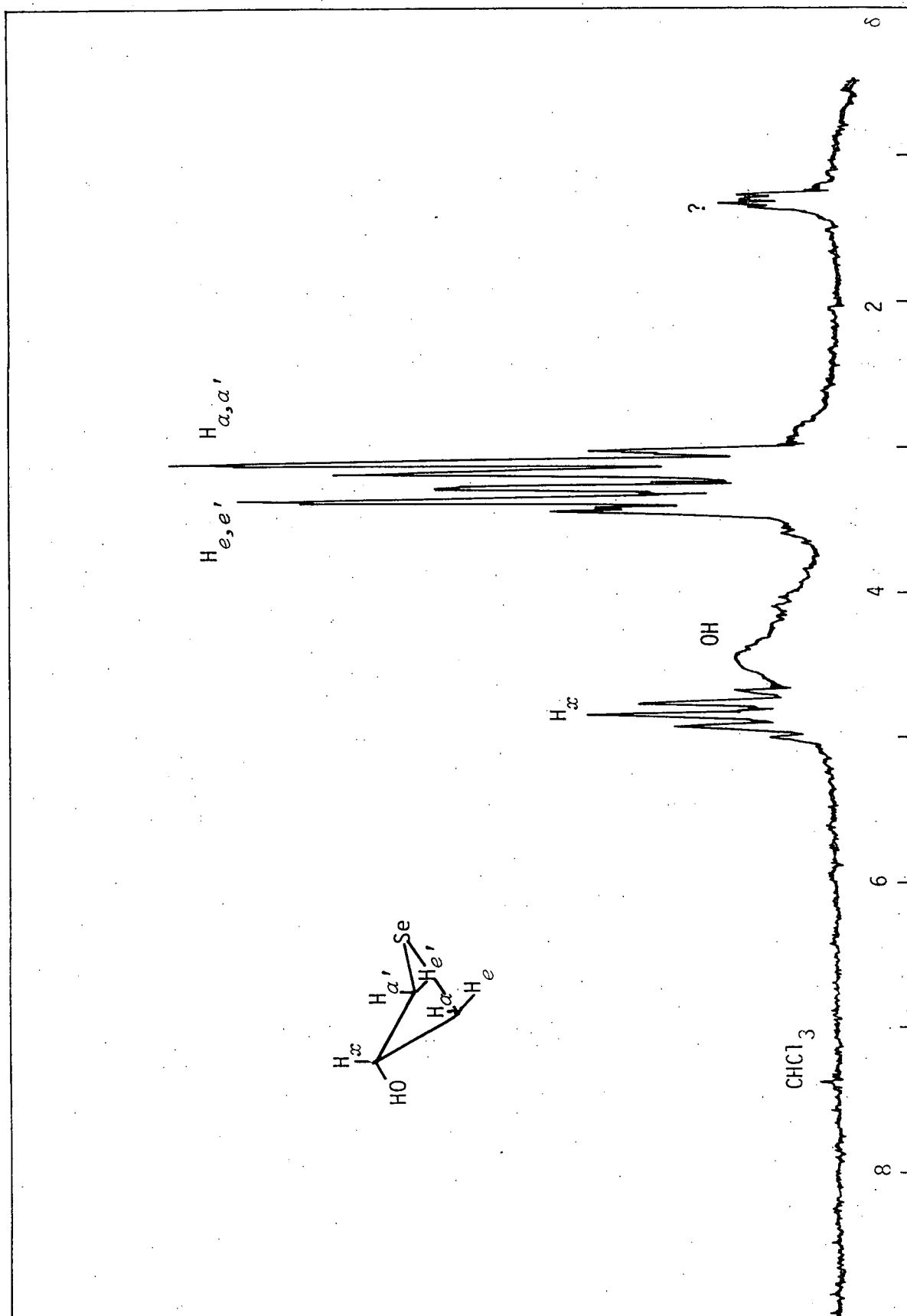


Figure 5.6: Proton nmr spectrum of selenetan-3-ol in  $\text{CDCl}_3$ .

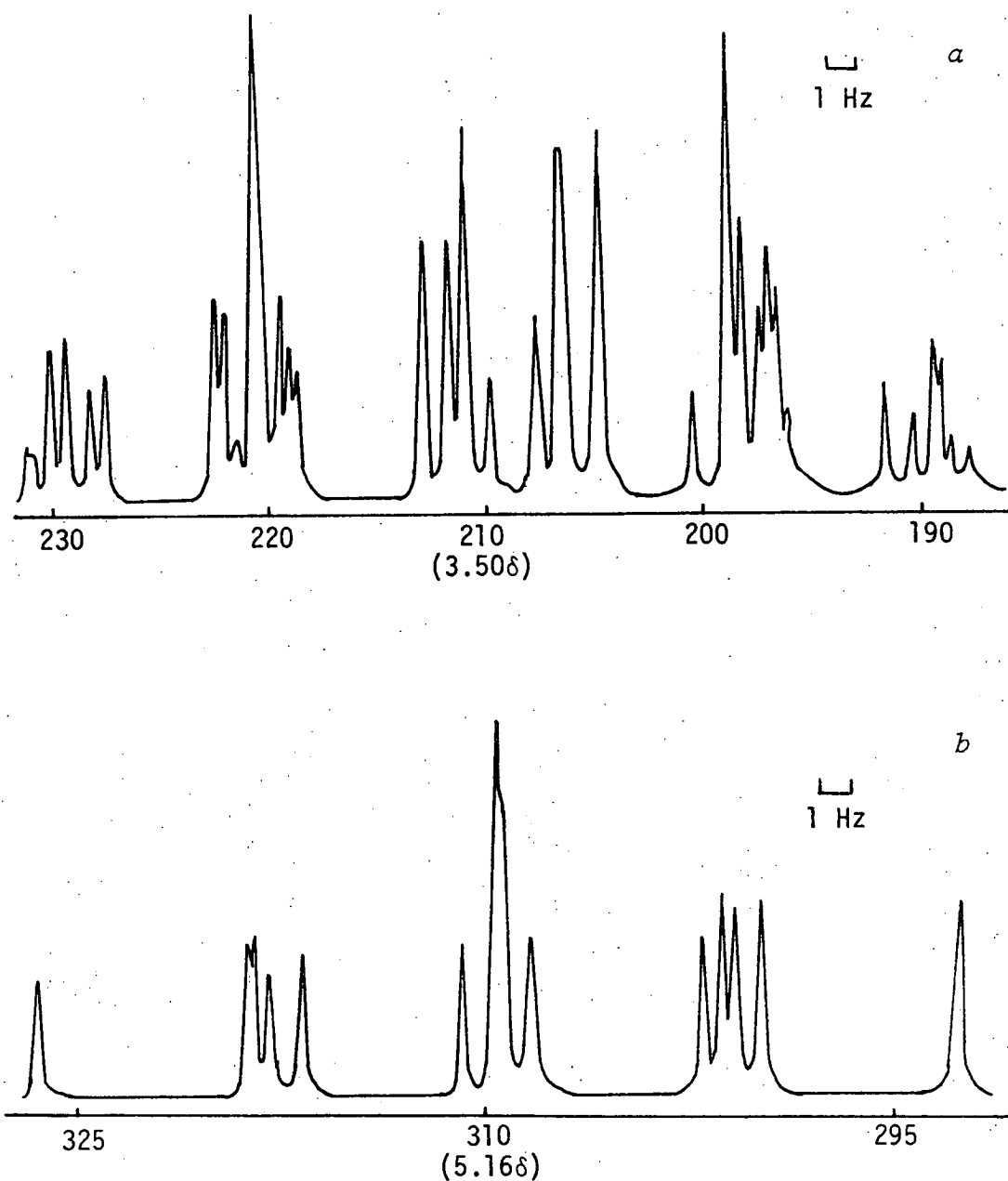
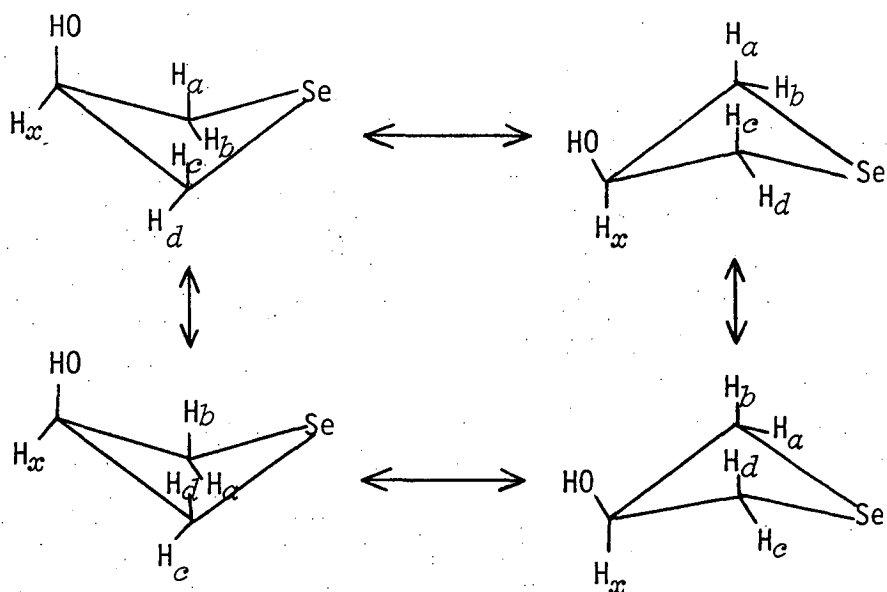


Figure 5.7: High resolution (60 MHz) proton nmr spectrum of 3-chlorothietane, taken from reference <sup>679</sup>.

*a*)  $A_2B_2$ (methylene), and *b*) X(methine) subspectra.

Chemical shifts ( $\delta$ ) were calculated from the frequencies (Hz) downfield from TMS, as shown.



Such a treatment has been carried out for 3-chlorothietane,<sup>680</sup> and sixty-four lines of the  $A_2B_2X$  system identified (Figure 5.7). At lower resolution, such as that under which the spectra were recorded in this work, the  $A_2B_2$  sub-spectrum can be considered as two asymmetric closely coupled triplets. The  $X$  sub-spectrum is a quintet. These features appear in the spectrum of selenetan-3-ol (Figure 5.6).

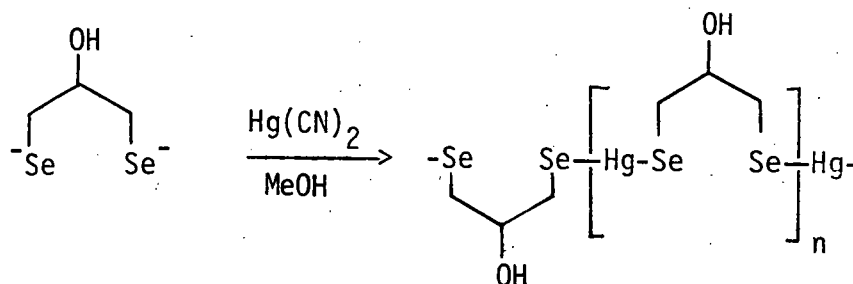
Details of vibrational assignments of spectra of 3-substituted thietanes do not seem to have been published, although a small diagram of the infrared spectrum of thietan-3-ol is available,<sup>681</sup> which is similar to that of XXVI. The vibrational spectra of thietane<sup>682-5</sup> and of selenetane<sup>685</sup> have been assigned. The infrared spectrum of XXVI can be tentatively assigned by comparison with those of 1,3-disubstituted 2-propanols and selenetane<sup>686</sup> and is shown in Table 5.10 below.

XXVI <sup>a</sup>	selenetane <sup>686</sup>	assignment
3150-3550s, vbr		H-bonded $\nu$ OH
2995m	3008	sym $\nu$ CH $\alpha$
2960vs, sh	2967, 2963	asym $\nu$ CH $\beta$
2935m and 2900vs, sh	2939, 2908	sym $\nu$ CH $\beta$
2830w, sh	2850	
1700vw		
1625w		
1436s	1486	$\delta$ CH $\alpha$
1410s	1457, 144	$\delta$ CH $\beta$
1320m	1291	CH $\beta$ wag
1270w	1228, 1197	CH $\alpha$ wag
1160s	1172	$\tau$ CH $\beta$
1120s	1133	$\tau$ CH $\alpha$
1000vs	993	$\delta$ OH and $\tau$ CH $\alpha$
976vw, sh	980	$\rho$ CH $\alpha$
928m	939	in plane ring 'breathing'
891m	902	$\rho$ CH $\alpha$
868m	833	$\rho$ CH $\beta$
810w	792	$\nu$ CC
650w	645	$\nu$ CC
570w	570	asym $\nu$ CSe
402w	418	sym $\nu$ CSe

Table 5.10: Tentative infrared band assignment of selenetan-3-ol XXVI by comparison with the spectrum of selenetane (ref. <sup>686</sup>, neat liquid sample).

<sup>a</sup>neat liquid sample.

Because 1,3-diseleno-2-propanol could not be isolated directly from the alkylation of NaSeH with 1,3-dibromo-2-propanol, Baroni's method of isolation, as an insoluble mercury(II) complex,<sup>479</sup> was attempted. Addition of methanolic  $\text{Hg}(\text{CN})_2$  to the ethanolic solution containing the disodium salt of SeDMPH<sub>2</sub> (see page 262) produces a light-yellow powder, HgSeDMP, in quantitative yield (based on selenium used). X-ray powder diffraction showed this compound to be amorphous, similar to its sulfur analog<sup>238</sup> (Chapter 4), but unlike its sulfur analog, it is insoluble in pyridine.

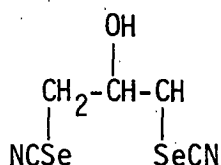


Passage of hydrogen sulfide through a methanolic suspension of HgSeDMP produced no darkening due to the formation of mercuric sulfide. Addition of solid sodium sulfide to this  $\text{H}_2\text{S}$ -saturated suspension produced immediate darkening. During precipitation of  $\text{HgS}$ , small samples of the supernatant solution were tested under nitrogen with aqueous ferric chloride. Selenols, like thiols, give deep blue colours with this test.<sup>598</sup> No free selenol was detected. After stirring for 12 hours, black  $\text{HgS}$  was removed by filtration through acid-washed sand, under nitrogen. The orange filtrate was evaporated under reduced nitrogen pressure to give an orange oil, found to be mainly selenetan-3-ol, XXVI, containing some 1,2-diselenolan-4-ol, XXVII.

Although Baroni precipitated  $\text{HgSe}$  with hydrogen selenide it is likely that the product he obtained was seleneten-3-ol and not the desired vicinal diselenol. Baroni's 'yellow' oil has bp.  $114^\circ/20 \text{ mm}$ <sup>479</sup> which would correspond to approximately  $80^\circ/3.5 \text{ mm}$ , close to the bp. of

XXVI (79-85°/3.5 mm) using the usual bp.-pressure nomograms.<sup>687</sup>

An alternative synthetic route to SeDMP was attempted. A small scale attempt to prepare 1,3-diselenocyanato-2-propanol by refluxing the dibromide with two equivalents of KSeCN in methanol, produced an orange oil after evaporation and ether extraction under nitrogen. High vacuum fractional distillation afforded two fractions. The first, minor, fraction (bp. 50-53°/0.01 mm) showed no infrared absorption in the region expected for  $\nu\text{C}\equiv\text{N}$  of selenocyanates e.g.  $2150\text{ cm}^{-1}$  for several  $\alpha,\beta$ -alkoxyselenocyanates,<sup>688</sup> and was discarded.



XXVIII

The second major fraction (bp. 60-75°/0.01 mm) showed intense infrared absorption at  $2135\text{ cm}^{-1}$  consistent with the presence of selenocyanate. In addition, the remainder of the infrared spectrum was very similar to that of 1,3-dibromopropanol. Extensive hydroxyl hydrogen bonding was indicated by a strong, broad absorption at  $3100\text{-}3600\text{ cm}^{-1}$ . Mass spectrometry (Figure 5.8) indicated a parent ion containing one atom of both bromine and selenium in its parent ion  $m/e$  243, consistent with the formula  $\text{C}_4\text{H}_6\text{BrNOSe}(\text{M}^+ \cdot 242.8814, \text{calc. } 242.8796)$ . The expected patterns of isotopic peaks in fragments containing  $\text{Br}_2$ ,  $\text{BrSe}$  and  $\text{Se}_2$  are shown in Figure 5.9. The parent ion in Figure 5.8 clearly contains the  $\text{BrSe}$  fragment. The product is probably 1-bromo-3-selenocyanato-2-propanol, XXIX.

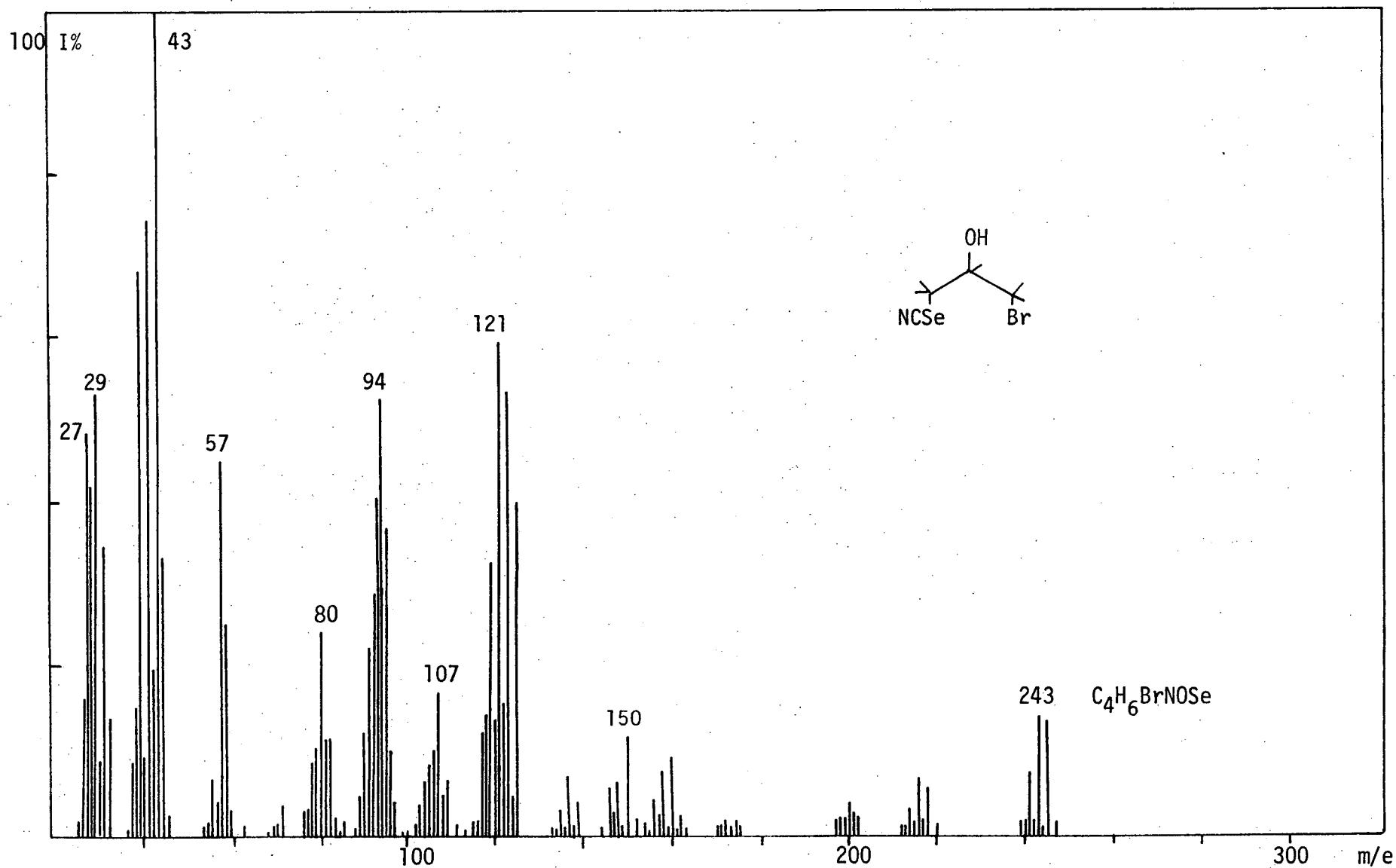
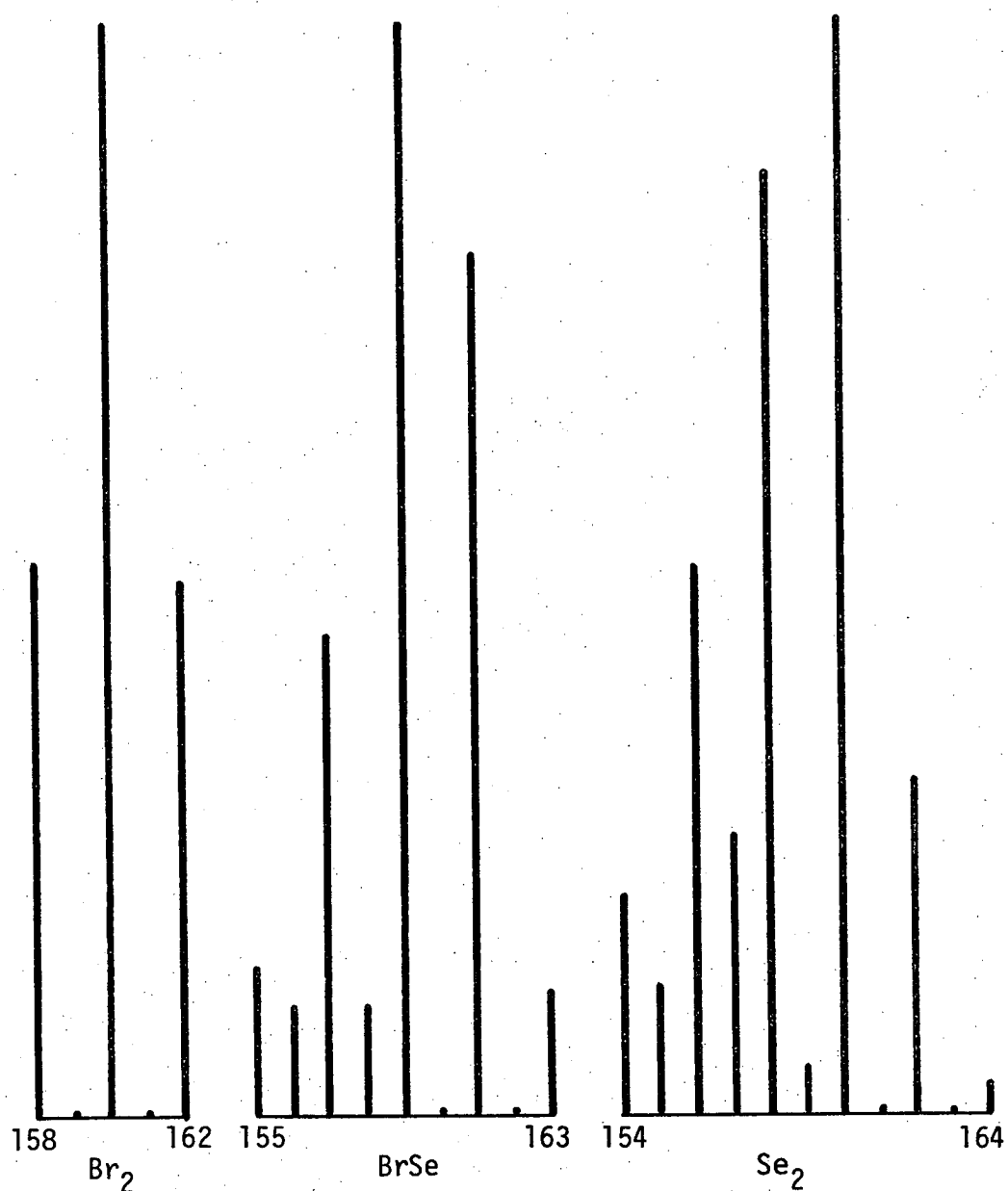


Figure 5.8: Low resolution 70 eV mass spectrum of 1-bromo-3-selenocyanato-2-propanol, XXIX.



**Figure 5.9:** Isotopic patterns for Br<sub>2</sub>, BrSe and Se<sub>2</sub> isotopic fragments.

The presence of a minor component of diselenide was indicated by a very weak isotopic cluster at  $m/e$  444, containing the Se<sub>2</sub> fragment, in the chemical ionisation mass-spectrum.

The structure, XXIX, was confirmed by the <sup>1</sup>H nmr spectrum in CDCl<sub>3</sub> (Figure 5.10). The main features of the spectrum are:

(i) broad hydroxyl proton resonance at 2.9δ(H), which disappears with D<sub>2</sub>O exchange. This type of broad resonance is observed in nmr



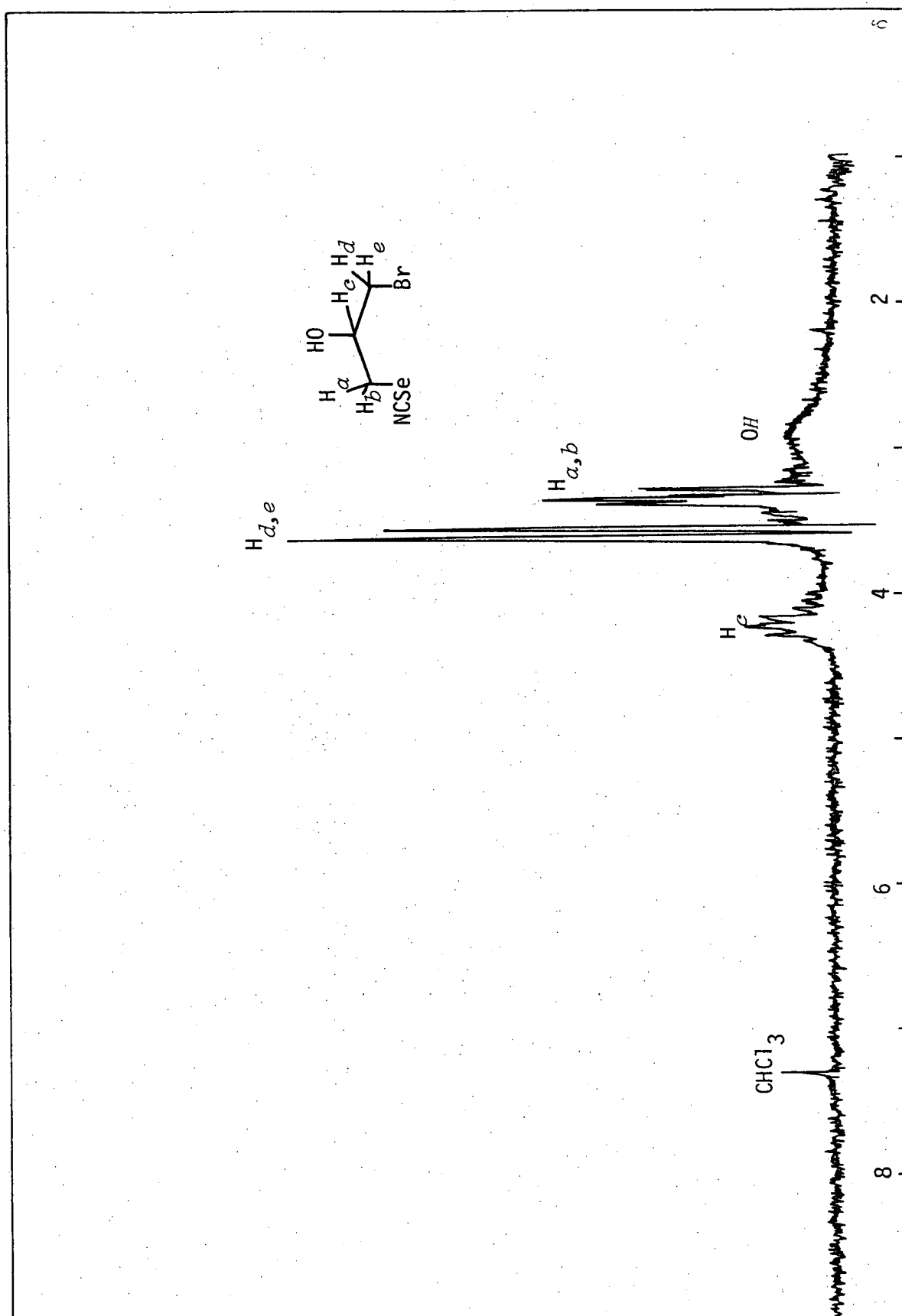


Figure 5.10: Proton nmr spectrum of XXIX in CDCl<sub>3</sub>.

spectra of  $\text{DMPH}_2$ ,  $\text{BALH}_2$  and other disubstituted propanols used in this work, but the position of resonance is quite variable.

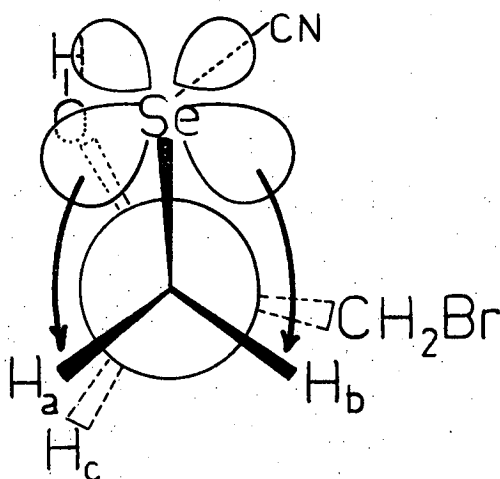
(ii) a multiplet centred at 4.23 $\delta$ (1H), similar to the multiplet (quintet, 1H) appearing at 4.03 $\delta$  in the spectrum of 1,3-dibromo-2-propanol which is due to  $\text{H}_c$ , geminal to the hydroxyl group.

(iii) an asymmetric doublet 3.56, 3.62 $\delta$ (2H), identical to that in the spectrum of 1,3-dibromo-2-propanol, due to the protons geminal to the bromine,  $\text{H}_{d,e}$ , which appear to be magnetically equivalent. The coupling  $J_{cd}=J_{ce}$  is 6 Hz.

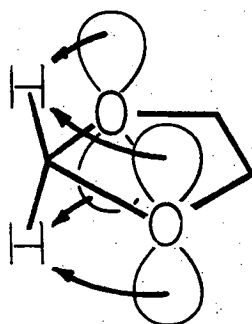
(iv) three singlet resonances at 3.28, 3.35, 3.38 $\delta$ (2H) which must be associated with protons  $\text{H}_{a,b}$  geminal to the selenocyanate. This pattern can be rationalised by assigning the central (most intense) singlet resonance arbitrarily to  $\text{H}_a$ , which requires  $J_{ad} \approx 0$ . The outer pair of resonances form an asymmetric doublet which is similar to (iii) due to  $\text{H}_b$ , with  $J_{bd}=10$  Hz. Satellites due to  $^2J(^1\text{H}-^{77}\text{Se})$  could not be observed.

Two points arise, namely, the lack of coupling of  $\text{H}_a$  with  $\text{H}_d$ , yet  $J_{bd}=10$  Hz and the lack of geminal coupling between  $\text{H}_a$  and  $\text{H}_b$ .

The lack of coupling between  $\text{H}_a$  and  $\text{H}_d$  suggests that the dihedral angle between these protons must be near to  $90^\circ$ , from consideration of the Karplus equation.<sup>650</sup> A conformation of XXIX consistent with this requirement is shown in the diagram below, which is a Newman projection of the molecule, viewed along the  $\text{C}(\text{SeCN})-\text{C}(\text{OH})$  bond. This conformation also accounts for hydrogen bonding between the hydroxyl and one selenium lone pair forming a five-membered ring. Evidence of extensive hydrogen bonding is found in the infrared spectrum (page 365) and is also consistent with  $J_{ad} \approx 6$  Hz since the dihedral angle between  $\text{H}_a$  and  $\text{H}_d$  is approximately  $30^\circ$ .<sup>650</sup> Additionally, the geometry of the two selenium lone pairs is suited to donation of electron density into

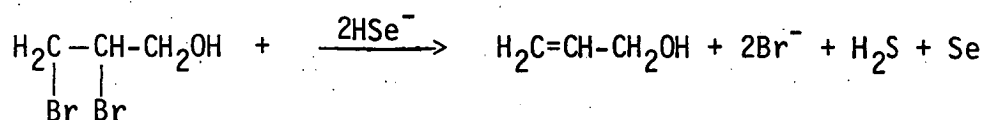


adjacent  $H_a$  and  $H_b$   $\sigma$ -bonds. Such hyperconjugative donation will make the geminal coupling constant,  $J_{ab}$ , more positive.<sup>650</sup> Since unperturbed geminal coupling constants are usually negative<sup>650</sup> this accounts for  $J_{ab} \sim 0$  in this case. An identical situation, depicted below, is found in 1,3-dioxolane producing  $J_{ab} \sim 0$ .<sup>650</sup>



(ii) SeBALH<sub>2</sub>

The failure to obtain non-vicinal SeDMPH<sub>2</sub> did not encourage the preparation of vicinal SeBALH<sub>2</sub> by similar routes. Attempted alkylation of ethanolic NaSeH by 2,3-dibromo-1-propanol produced a deep red-brown solution from which allyl alcohol (detected by gc. retention time comparison with an authentic sample) could be extracted.



Nucleophilic substitution of vicinal dibromides with thiols has often been reported to cause elimination to form an olefin.

Addition of ethanolic mercuric acetate to the red-brown solution precipitated a small quantity of pale-yellow powder, which was insoluble in hot pyridine and other common solvents. This complex was not identical to HgSeDMP as might have been expected if 2,3-dibromo-1-propanol was contaminated with a small quantity of the non-vicinal isomer.

Selenocyanation of 2,3-dibromo-1-propanol was not attempted in view of the failure to obtain a diselenocyanate of SeDMPH<sub>2</sub>.

Addition of two equivalents of benzylselenol to propargyl alcohol dissolved in ethanolic sodium ethoxide solution produced a crystalline product after 2½ hours. This product (probably a 1:1 adduct similar to those found during additions to acetylenedicarboxylic acid) was not isolated but redissolved to give a red solution overnight. Extraction into petroleum ether removed dibenzyldiselenide to leave a red oil which decomposed to produce selenium on standing. The products were not examined further in view of difficulties experienced with product.

separation from attempted  $\text{SeDMSH}_4$  synthesis. Addition of excess thiolacetic acid to pent-3-yn-1-ol is reported to produce only a mono-adduct,<sup>554</sup> due to an inactivating effect of the hydroxyl group e.g. hex-1-yne produces both mono- and di- adducts under these conditions.<sup>689</sup>

No attempt was made to alkylate sodium benzylselenolate with 2,3-dibromo-1-propanol because the analogous thiolate reaction produces the rearranged product 1,3-bis(benzylthio)-2-propanol, exclusively<sup>604-5</sup> (page 244).

#### 5.4 Conclusions

Possible methods for the preparation of Se-protected diselenols have been reviewed, and several routes to synthesis of protected selenium analogs of  $\text{DMSH}_4$  and  $\text{BALH}_2$  and its isomer  $\text{DMPH}_2$  have been investigated. The protected  $\text{SeDMSH}_4$  compound, 2,3-bis(benzylseleno) succinic acid could not be obtained in this study.

Addition of two equivalents of benzylselenolate to acetylenedicarboxylic acid gives only the new 1:1 addition product XXIIb, in contrast to the addition of benzylthiolate where a 2:1 adduct can be obtained. Similarly, the new saturated analog of XXIIb, XXIVb was obtained by addition of benzylselenolate to maleic acid. Benzylthiolate reacts identically.

Perturbations of the  $n \rightarrow \pi^*$  electronic transition of an  $\alpha, \beta$ -unsaturated carbonyl chromophore by the benzylselenolate group produces a large bathochromic shift which causes XXIVb to appear bright yellow. The analogous thioether is pale yellow, consistent with the similar but smaller effect of the benzylthiolate group.

Second-order analysis of the ABX  $^1\text{H}$  nmr spectra of XXIVb and its sulfur analog shows a preference for a conformation in which one carboxyl group is gauche to the chalcogen.

Attempted preparation of  $\text{SeDMPH}_2$  from 1,3-dibromo-2-propanol leads to the cyclic product selenetan-3-ol, only recently reported in the literature. The 100 MHz proton nmr spectrum can be interpreted as an incompletely resolved five spin  $A_2B_2X$  coupled system. Reaction of 1,3-dibromo-2-propanol with two equivalents of  $\text{KSeCN}$ , resulted in the addition of only one selenocyanate group. The new product 1-bromo-3-selenocyanato-2-propanol has been characterised by  $^1\text{H}$  nmr, ms and ir spectroscopy and shows considerable hydrogen bonding between the hydroxyl and selenocyanate groups.

Attempted preparations of  $\text{SeBALH}_2$  by alkylation of  $\text{NaSeH}$  with 2,3-dibromo-1-propanol, lead to the expected formation of allyl alcohol by elimination of bromide. No characterisable products other than Se and dibenzyldiselenide could be isolated from reaction of benzylselenolate with propargyl alcohol.

## CHAPTER SIX

### POTENTIOMETRIC DETERMINATION OF AQUEOUS FORMATION

#### CONSTANTS OF VERY STABLE COMPLEXES

##### 6.1 Introduction

The aqueous formation constants of MeHg(II)-thiolate complexes had not been extensively studied until this work, and the work of Reid and Rabenstein<sup>302</sup> (Chapter 3). Apparent discrepancies in previously reported values for the formation constants of MeHg(II) monothiolates, and the need to evaluate the stability of MeHg(II) complexes with antidotal vicinal dithiols led to the determination of the constants which have been discussed in Chapter 3.

In order to compare the formation constants for MeHg(II) with a range of monothiol and vicinal dithiol (containing sulfhydryl groups with acid dissociation constants in the range  $9.0 < \text{pK}_a < 11.5$ ), a method which is able to determine these constants with some precision is required. The methods currently available for this requirement are based on potentiometric, spectrophotometric and nuclear magnetic resonance techniques. (Other methods, e.g. polarography, solvent extraction, ion exchange, etc. are generally less precise and of more limited applicability<sup>690</sup>). All of these methods depend on the ability to monitor the concentration(s) of one or more equilibrium components as the equilibrium position is altered. Each of these techniques has been reviewed and extensively used to study solution equilibria.<sup>690-1</sup>

The most widely used and the most precise is the potentiometric method, which was considered to be best suited to investigation of equilibria between MeHg(II) and thiolate ligands in this study. The spectrophotometric method, although it offers a unique advantage of

sometimes determining the number of significant equilibrium species, was unsuitable because the thiolate ligands and methylmercury(II) ion do not have chromophores which are sensitive to equilibrium conditions, e.g. pH, and which are readily accessible in the near UV/visible spectral regions. NMR Methods (e.g.  $^{13}\text{C}$ ,  $^{360}\text{ }^{199}\text{Hg}$ ,  $^{317}$  and  $^{1}\text{H}$   $^{309,360,369}$ ) have been used extensively to study MeHg(II) and offer the advantage of being able to determine the concentrations of species involved in microscopic equilibria, e.g. the protonation or complexation of sulfhydryl and amino groups of biologically important mercaptoamines can be monitored individually. (The technique has been discussed in some detail in Chapter 3 of this thesis).

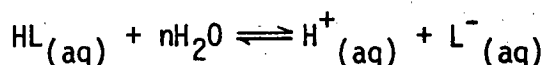


## 6.2 Evaluation of ligand hydrolysis equilibria

### 6.2.1 Definition of 'Equilibrium Constants' used in this work

The term 'equilibrium constant', used in this work, warrants some clarification.

Consider a simple monoprotic Brønsted acid dissociation in aqueous solution, the equilibrium for which can be written



Although all species,  $\text{HL}_{(\text{aq})}$ ,  $\text{L}^-_{(\text{aq})}$ ,  $\text{H}^+_{(\text{aq})}$ , are probably extensively solvated, few methods of investigation can distinguish between degrees of hydration, and solvent molecules will not be included in subsequent equilibria although it should not be forgotten that they may be involved in primary coordination. In particular, the methylmercury(II) cation will be represented by  $\text{MeHg}^+$  for brevity, instead of  $\text{MeHg}(\text{OH}_2)^+$ , and the proton will be considered as  $\text{H}^+$ . In addition, the concentration or activity of water is considered to be constant, at least for dilute solutions. The thermodynamic acid dissociation constant for the above equilibrium, which can be related directly to free energy changes, is written as  $K^\ominus$

$$K^\ominus = \frac{\{\text{H}^+\}\{\text{L}^-\}}{\{\text{HL}\}}$$

where the parentheses {} indicate activities of the relevant species.

To determine  $K^\ominus$ , the activities, or at least the activity coefficients,  $\gamma$  (which relate activity to concentration, e.g.  $\{\text{L}^-\} = \gamma_{\text{L}^-}[\text{L}^-]$ ), of all species must be determined. Although  $\gamma_{\text{H}^+}$  has been extensively studied, e.g. for the determination of pH standards, this has only been achieved for a limited range of electrolyte conditions. Estimates of mean activity coefficients,  $\gamma_{\pm}$ , for electrolyte species other than protons

are usually made using empirical relationships between  $\gamma_{\pm}$  and solution ionic strength. Table 6.1 shows that these relationships may give widely different values for mean molar activity coefficients, especially for electrolytes which are not of the 1:1 type, even at the moderate ionic strength (0.1M) used in many equilibrium constant studies.<sup>692</sup> For highly charged ions, e.g. the anion  $\text{DMS}^{4-}$ , such calculations of activity coefficients are highly tenuous. It is more usual to ignore activities of species other than protons by defining 'mixed' or operational equilibrium constants.

$$K^m = \frac{\{H^+\}[L]}{[HL]}$$

Proton activities are determined directly from the relationship  $\text{pH} = -\log\{H^+\}$  after calibration of a glass indicator electrode in solutions of known proton activity. The concentrations of other species can be determined directly, e.g. spectrophotometrically using the Beer-Lambert-Bouger relationship between absorbance and concentration, or with other potentiometric electrodes calibrated in terms of concentration (very rarely available), but are more usually calculated. The mathematical evaluation of species concentrations assumes the validity of the equilibrium expression, electroneutrality, and mass-balance equations, and in this case requires two independent measurements of pH from different equilibrium solutions. The abovementioned equations can be solved for  $[L^-]$  and  $[HL]$ . It is usual to over-determine these equations, i.e. obtain many more experimental observations than there are unknowns, and use least-squares or other multiparametric curve-fitting procedures to obtain  $[L^-]$  and  $[HL]$  (page 306). It should be noted that  $[H^+]$  is required in the mass-balance and electroneutrality expressions, still necessitating an empirical estimate for  $\gamma_{H^+}$ . It has been

Model	$z_+z_- = 1$	2	3	4	6	8	9	12	16	Comments
Debye-Hückel	0.6890	0.4747	0.3271	0.2254	0.1070	0.0508	0.0350	0.0114	0.0026	$\log \gamma_{\pm} = -z_+z_-A\sqrt{I}$ may be extended to take into account ionic 'size' $\log \gamma_{\pm} = -z_+z_-A\sqrt{I}/(1+Ba\sqrt{I})$
Guntelberg	0.7535	0.5678	0.4278	0.3224	0.1830	0.1039	0.0783	0.0335	0.0108	$\log \gamma_{\pm} = -z_+z_-A\sqrt{I}/(1+\sqrt{I})$ may be extended by considering a constant ionic size of $3A^\circ$ . $\log \gamma_{\pm} = -z_+z_-A\sqrt{I}/(1+3B\sqrt{I})$
Davies	0.7715	0.5952	0.4592	0.3542	0.2108	0.1255	0.0968	0.0444	0.0157	$\log \gamma_{\pm} = -z_+z_-A\sqrt{I}/(1+\sqrt{I})$ $+0.2Az_+z_-I$
Scatchard	0.7767	0.6033	0.4686	0.3460	0.2196	0.1325	0.1029	0.0482	0.0176	$\log \gamma_{\pm} = -z_+z_-A\sqrt{I}/(1+1.5\sqrt{I})$ may be extended by considering a temperature dependent demoninator $\log \gamma_{\pm} = -z_+z_-A\sqrt{I}/(1+4.5B\sqrt{I})$
Bjerrum	0.7623	0.6526	0.5900	0.5498	0.5012	0.4731	0.4630	0.4418	0.4249	$\log \gamma_{\pm} = -z_+z_-A\sqrt{I}/(1+Ba_B\sqrt{I})$ takes into account ion pairing if ion diameter is less than $a_B$ .

**Table 6.1:** Theoretical mean activity coefficients at 25°C and 0.1M Ionic Strength <sup>692</sup>

$$a_A = \left( \frac{2\pi N}{1000} \right)^{1/2} \frac{e}{\ln 10 \cdot K^{3/2}} \frac{1}{T^{3/2} \epsilon^{3/2}} = 0.5116 \text{ dm}^{3/2} \text{ mol}^{-1/2} \text{ at } 25^\circ$$

$$b_B = \left( \frac{8\pi N}{1000} \right)^{1/2} \frac{e}{k^{1/2}} \frac{1}{T^{1/2} \epsilon^{1/2}} = 0.3292 \times 10^{-8} \text{ dm}^{3/2} \text{ cm mol}^{-1/2} \text{ at } 25^\circ$$

$$c_{a_B} = \frac{z_+ z_- e^2}{2 \epsilon kT} = 3.58 \times 10^{-8} \text{ cm at } 25^\circ$$

Table 6.1: Theoretical mean activity coefficients at 25°C and 0.1M Ionic Strength.<sup>692</sup>  
(cont.)

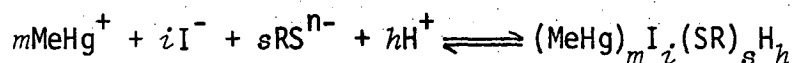
indicated by Bates,<sup>693</sup> that  $K^m$  has the disadvantage that it reflects small changes in ionic environment via  $\{H\}$  but neglects interionic effect on ions other than  $H^+$ .

The third form of equilibrium constant is used in this work and tabulated extensively elsewhere.<sup>393, 694</sup> The concentration or stoichiometric constant,  $K^c$ , is defined as

$$K^c = \frac{[H^+][L^-]}{[HL]}$$

In this case, it is necessary to evaluate hydrogen ion concentration,  $[H^+]$ , instead of activity, e.g. using a glass-electrode calibrated in terms of proton concentration by the methods described in Section 6. The concentrations of ligand species can be measured as for  $K^m$  (rarely) or calculated by least-squares procedures. Stoichiometric constants are used throughout this work unless otherwise stated, and can be written for more complex metal-ligand-proton equilibria in an identical fashion to those above.

For example, the formation equilibrium of the complex  $(MeHg)_m I_i (SR)_s H_h$  would be written in terms of components  $MeHg^+$ ,  $I^-$ ,  $RS^{n-}$  and  $H^+$ :



with an overall stoichiometric equilibrium constant,

$$\beta_{mish} = \frac{[(MeHg)_m I_i (SR)_s H_h]}{[MeHg^+]^m [I^-]^i [RS^{n-}]^s [H^+]^h}$$

It has been found that mixed iodide-thiolate species are not formed in this study (page 97), and so the iodide subscript has been omitted from the  $MeHg(II)$ -thiolate constants recorded in Chapter 3. (However, for

data input to the computer program MINQUAD 81, all component subscripts are required).

In addition, hydroxo complexes will be described with  $h < 0$ , e.g.

$$(\text{MeHg})_2\text{OH}^+ \text{ will have } \beta_{20-1} = \frac{[(\text{MeHg})_2\text{OH}^+]}{[\text{MeHg}^+]^2[\text{H}^+]^{-2}}$$

It should therefore be emphasised that  $\beta$ 's of complexes involving hydroxide, are not *formal* formation constants, but can be related to these by the autoprotolysis constant of water,  $K_w^C$ , since, for example:

$$\beta(\text{actual formation})_{(\text{MeHg})_2\text{OH}^+} = \beta_{20-1} (K_w^C)^{-1}$$

This practice is widely used in the stability constant literature, and is used here for consistency. Equilibrium constants, such as  $\beta_{20-1}$ , can be evaluated from pH titration data in acid solution, without recourse to experimental values of  $K_w^C$  whereas the corresponding actual formation constant requires accurate values for  $K_w^C$  in order to evaluate  $[\text{OH}^-]$ , contributing additional uncertainty.

### 6.2.2 Calibration of glass-electrodes as $[\text{H}^+]$ probes

When a glass-electrode assembly is calibrated using a primary standard buffer,  $\text{pH}(s)$ , and then transferred to a measurement solution, the pH reading corresponding to  $[\text{H}^+]'$  is related to  $[\text{H}]_s$  of the buffer by the defined relationship<sup>695</sup>

$$(6.1) \quad -\log[\text{H}^+]' = \text{pH}_S - \frac{(E_s - E') + (E_j' - E_{js})}{2.303 \text{ RT/F}} + \log \gamma_{\text{H}^+}'$$

The measured pH can be related to  $[\text{H}]$  only if (i) liquid junction potentials for the buffer,  $E_{js}$ , and test solution,  $E_j'$ , are either negligible or identical, and (ii) the activity coefficient  $\gamma_{\text{H}^+}'$  can

be accurately calculated or measured in both solutions. Since the test solution and primary buffers are of totally different ionic composition, e.g. the NBS standard buffers commonly used for calibration, 0.05M potassium hydrogen phthalate and 0.01M sodium tetraborate, have ionic strengths 0.053M and 0.02M respectively, it is most unlikely that either condition can be fulfilled.

It is therefore necessary to calibrate the glass-electrode assembly as a  $H^+$ -concentration probe, in the ionic medium to be used as measurement solution.<sup>696</sup> This is done by noting that the emf of the electrode varies linearly with  $\log[H^+]$  in acidic solutions as follows:

$$(6.2A) \quad E_{\text{meter}} = E_{\text{H}}^{\circ'} + (RTF^{-1} \ln 10) \log[H^+] + j_{\text{H}}[H^+]$$

where the term  $E_{\text{H}}^{\circ'}$  includes the standard potentials of reference and glass half-cells, the asymmetry potential of the glass electrode, and activity coefficient terms which are assumed to remain constant during an experimental titration. The term  $j_{\text{H}}[H^+]$  accounts for the fact that the liquid junction potential varies with  $[H^+]$  at low pH (i.e. the glass-electrode becomes 'non-linear' at low pH).

A similar expression can be written to calibrate the glass-electrode in alkaline conditions.

$$(6.2B) \quad E_{\text{meter}} = E_{\text{OH}}^{\circ'} + RTF^{-1} \ln [H^+] + j_{\text{OH}} K_{\text{w}}^{\text{C}}/[H^+]$$

where  $E_{\text{OH}}^{\circ'}$  accounts for the glass-electrode asymmetry potential (which is observed to differ in acid and alkaline solutions by up to 2 mV) and  $j_{\text{OH}}$  accounts for non-linearity at high pH (assuming the electrode has negligible 'sodium error', which is true for modern high resistance glass-electrodes).

Since the emf of the electrode assembly can usually be determined with a precision of 0.1 mV using commercially available pH-meters, the

pH range with which  $j_H$  and  $j_{OH}$  are negligible (i.e. the electrode response is linear) can be calculated. In titrations of the highest precision, additional small corrections to the liquid junction potential of the form  $[HL^-]j_{HL^-}$ ,  $[L^{2-}]j_{L^{2-}}$  have been used.<sup>697</sup> Typical values for  $j_H$  are shown in Table 6.2. Less information is available for  $j_{OH}$ , but it is generally considered to be smaller in magnitude than  $j_H$ , and of opposite sign.

$x/M$	$(j_H/[H^+])/mV$	pH at which $j_H[H^+] = 0.1 \text{ mV}$	ref.
3.0	16.5	2.2	698
1.0	63	2.8	698
0.1	440	3.6	699

Table 6.2: Acid region non-linear corrections,  $j_H$  for cells of the type  $Na^+ (x-h,M), H^+ (h,M), ClO_4^- (xM) | NaClO_4 (xM)$

It can be seen from this table that even in the least linear case (0.1M  $NaClO_4$ ), the glass-electrode behaves linearly (within 0.1 mV or 0.002 pH) as a concentration probe above pH 3.6 and since the effect is smaller in alkaline solution, below pH 10.4. From preliminary titrations of 0.1M  $KNO_3$  (or 0.1M  $KOH$ ) with 0.1M  $HNO_3$  in this study, it has been found that the value of  $j_H[H^+]$  is approximately 200 mV, giving electrode linearity in the range  $3.3 < pH < 10.7$ .

At the concentrations of metal and ligand solutions used in this work, it has rarely been necessary to use pH values below 3.0, and so non-linearity corrections are not needed. However, several ligands of interest, especially vicinal dithiols, have thiol acid dissociation constants  $pK_A > 10$ , necessitating titration to pH 11, where some non-linearity correction is necessary. This will be treated in Section 6.



The calibration parameters  $E_{\text{H}}^{\circ'}$ ,  $j_{\text{H}}$  and  $E_{\text{OH}}^{\circ'}$ ,  $j_{\text{OH}}K_{\text{W}}^{\text{C}}$  are usually obtained from preliminary titrations of either standardised strong acid with strong base, or ionic medium with acid or base, and fitting the emf versus  $[\text{H}^+]$  data manually or by non-linear least-squares procedures.<sup>700</sup> The non-linearity terms  $j_{\text{H}}$ ,  $j_{\text{OH}}K_{\text{W}}^{\text{C}}$  seem to be dependent only on ionic medium, whereas  $E_{\text{H}}^{\circ'}$ ,  $E_{\text{OH}}^{\circ'}$  vary somewhat day-to-day. Trends in these latter values may be used to monitor the condition of the glass-electrode assembly. In addition, it should be noted that values of  $K_{\text{W}}^{\text{C}}$  in the ionic medium of interest can be evaluated since  $2.303RTF^{-1} = \text{p}K_{\text{W}}^{\text{C}}$ . In this work,  $\text{p}K_{\text{W}}^{\text{C}}$  has been determined at 25° (0.1  $\text{KNO}_3$ ) to be  $13.74 \pm 0.02$  from eight such titrations, using a variety of glass and reference electrode systems.

Measurements of  $K_{\text{W}}^{\oplus}$  and the quotient of activity coefficients and water activity,  $\gamma_{\text{H}}\gamma_{\text{OH}}/[\text{H}_2\text{O}]$ , can be used to calculate values of the concentration ionic product of water,  $K_{\text{W}}^{\text{C}}$ . Such values have been tabulated by Sweeton, Mesmer and Baes<sup>701</sup> ( $K_{\text{W}}^{\text{C}}$  is  $Q_{\text{W}}$  in their terminology) using the activity quotient obtained from Harned and Owen in alkali metal halide solutions.<sup>702</sup> The quotient does not seem to have been reported for  $\text{KNO}_3$  solutions. Assuming identical behaviour in  $\text{MCl}$  and  $\text{KNO}_3$  solutions, at 25°,  $\text{p}K_{\text{W}}^{\text{C}} = 13.781 \pm 0.006$  <sup>701</sup> and the density of water  $997.048 \text{ kg m}^{-3}$  at this temperature,<sup>703</sup> on the molar scale used in this work

$$\text{p}K_{\text{W}}^{\text{C}} = 13.784 \pm 0.006$$

which is in good agreement with the value found in this study.

An alternative procedure which avoids preliminary titrations, considers the terms  $E_{\text{H}}^{\circ'}$ ,  $E_{\text{OH}}^{\circ'}$ ,  $j_{\text{H}}$  and  $j_{\text{OH}}$  as parameters to be refined simultaneously with the equilibrium constants, etc., in the ligand hydrolysis constant determination. The extra parameters of course

necessitate the accumulation of additional titration data, but this approach has been used successfully for high precision potentiometric evaluation of acid dissociation constants of multiprotic acids and bases.<sup>704-6</sup> The implementation of this method by the program TITRAT derived for such purposes in this work will be described in Section 6.2.5.

The TITRAT program assumes a glass-electrode-reference electrode response of the type <sup>695,707-9</sup>

$$(6.3) \quad -\log[H^+] = \text{pH}_{\text{meter}} + \text{correction}$$

If activity coefficients are considered to be invariant, as in this work in 0.1 M KNO<sub>3</sub> ionic background, this can be written

$$(6.4) \quad -\log[H^+] = \text{pH meter} + \text{pH}_{\text{cal}}$$

where  $\text{pH}_{\text{cal}}$  incorporates terms for standard electrode potentials of glass and reference half-cells, glass-electrode asymmetry potential and proton activity. It can be seen to be analogous to the expression used previously (equation 6.1) for calibration in terms of  $[H^+]$  using electrode emf readings

$$(6.5) \quad -\log[H^+] = \frac{E_{\text{meter}}}{RTF^{-1} \ln 10} - \frac{E^{\circ'} + j_H[H^+]}{RTF^{-1} \ln 10}$$

The first term is exactly  $\text{pH}_{\text{meter}}$ . The correction term in this case accounts for non-linearity of the electrode system in acid solution (page 292), which normally can be neglected in the range  $3 < \text{pH} < 10$ . It is of interest that this relationship is identical to that used by VanUitert and Haas <sup>710</sup> and Agrawal<sup>711</sup> to calibrate glass-electrodes in

mixed-solvents, so that TITRAT can be used under these conditions. It should be noted that neglect of non-linearity is not essential, and an  $[H^+]$  dependent term could be included on the right hand side of equation 6. and the coefficient treated as a titration parameter, accessible from low pH titration data.

The term  $pH_{cal}$  simply calibrates a  $pH_{meter}$  in terms of hydrogen ion concentration, and can be refined from titration data at  $pH < 4$  using TITRAT. In this work, the pH meter was standardised daily (at least) with three NBS primary buffers<sup>†</sup> in order to monitor the linearity of the electrode, and to make values of  $pH_{cal}$  comparable on a day-to-day basis, although this is not strictly necessary. Values for  $pH_{cal}$  evaluated by TITRAT from many titrations fall within the range -0.04 to -0.08 pH units. This is in excellent agreement with similar values<sup>695,707-9</sup> found elsewhere using electrodes standardised in a similar manner, and the uncertainty in  $pH_{cal}$ ,  $\pm 0.02$  units, is of the same order as the uncertainty in NBS buffers.

Hydroxide concentration is calculated in TITRAT by defining  $K_W^C = [H^+][OH^-]$ . Values of  $K_W^C$  in the titration medium can be evaluated from  $E_{H}^{\circ}$  and  $E_{OH}^{\circ}$  terms as described previously (page 294), but it is convenient to treat  $K_W^C$  as a titration parameter accessible from titration data at high pH.

It has been found in this work that titration regions above pH 10 cannot be fitted satisfactorily with TITRAT using the value  $pK_W^C = 13.74(2)$  found by prior experiment (page 294). This is due to non-linearity of the glass-electrode system described by  $j_{OH} K_W^C/[H^+]$  term (page 293) above pH 10.7, which has not been taken into account in the pH calibration

---

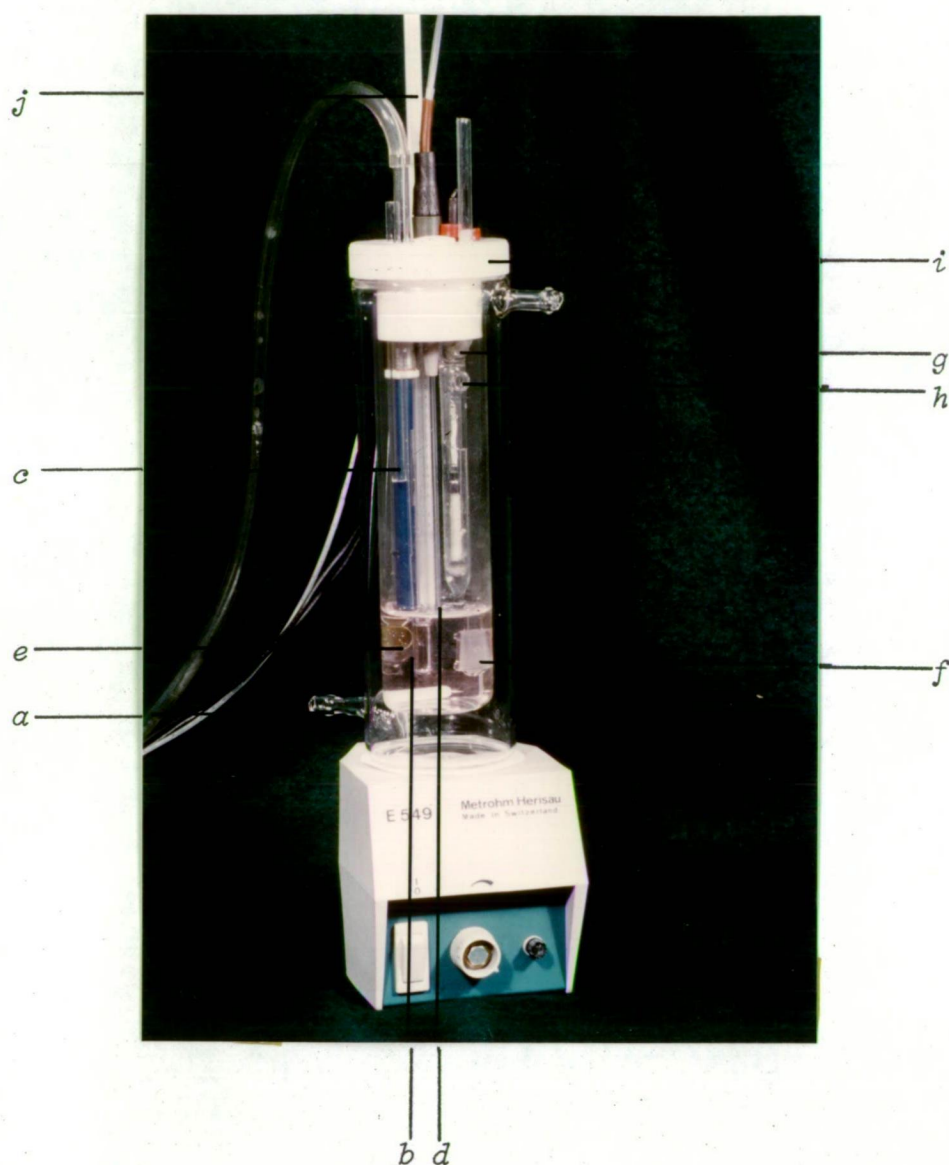
<sup>†</sup>0.025 equimolal phosphate pH(s) 6.865, 0.01M phthalate, pH(s) 4.008 and 0.01M carbonate/bicarbonate, pH(s) 10.012, page 305.

equation 6. . It has been found however, that refinement of  $K_W^C$  satisfactorily fits titration data in this region, with refined values of  $pK_W^C$  lying in the range  $13.82 < pK_W^C < 13.90$  for many titrations.

Refinement of  $K_W^C$  is tantamount to inclusion of an alkaline non-linearity coefficient similar to  $j_{OH}$ . Since the absolute value of  $pK_W^C$  is not of intrinsic value for this work, this calibration procedure was considered to be totally satisfactory, and has been used to determine values of  $pK_a > 10$  for thiols, in good agreement with previously reported values (Section 3.3.2). It should be noted however, that the value for  $j_{OH}$  could be treated as a TITRAT parameter (similar to  $j_H$  mentioned previously) if the value of  $pK_W^C$  has been determined independently. (Attempted simultaneous evaluation of  $j_{OH}$  and  $K_W^C$  as parameters would be unwise since these variables are perfectly correlated

### 6.2.3 Titration assembly

The titration cell used in this work is based on the water-jacketed cell described by Perrin,<sup>712</sup> in which the glass and reference electrodes are thermostatted for their entire lengths to avoid thermal gradients which cause pH drifts. The double-walled vessel, shown in Figure 6.1, was maintained at a constant temperature of  $25.00 \pm 0.02^\circ$  by circulation of water through the jacket from a large water bath, which also contained buffer solutions and volumetric glassware kept at this temperature. (The water bath Beckman thermometer was calibrated against a second thermometer which in turn had been calibrated to within  $\pm 0.005^\circ$  using a Pt-resistance thermometer). The cell could be hermetically sealed by a Teflon stopper holding the glass and reference electrodes, thermometer, nitrogen-inlet and outlet tubes, two titrant delivery tubes, and which had provision for an additional two electrodes. The vessel was mounted atop a magnetic stirrer and thermally insulated from it by



**Figure 6.1:** Magnetically stirred double-wall titration cell with capacity 30-100 mL.

*a* circulating water for temperature control ( $\pm 0.02^\circ$ ), *b* nitrogen inlet capillary and *c* outlet tube, titrant delivery capillary, *e* Philips GAT130 (or GA110) glass electrode, *f* Philips R44 glass-sleeve double-junction calomel reference electrode, *g* polyethylene tubing connecting the inner half cell of *h* (saturated KCl) to outside the cell, *h* filling hole for the outer half-cell of *f* (1M  $\text{KNO}_3$ ), *i* tight fitting Teflon stopper which contains capped holes for additional electrodes and *j* thermometer ( $0.01^\circ$ ).

a ceramic tile and the water jacket of the cell. High purity nitrogen which had been passed through a column containing Carbasorb<sup>®</sup> (to remove CO<sub>2</sub>) and 4 Å molecular sieves, was presaturated by bubbling through 200 cm<sup>3</sup> of 0.1M KNO<sub>3</sub> held in the circulating water bath, before passage through the cell. A drawn-out piece of glass tubing (0.5 mm i.d.) was found to be more suitable than a glass frit for this purpose because the latter, although more dispersive, invariably caused a coating of fine bubbles on the glass-electrode bulb, causing pH instability.

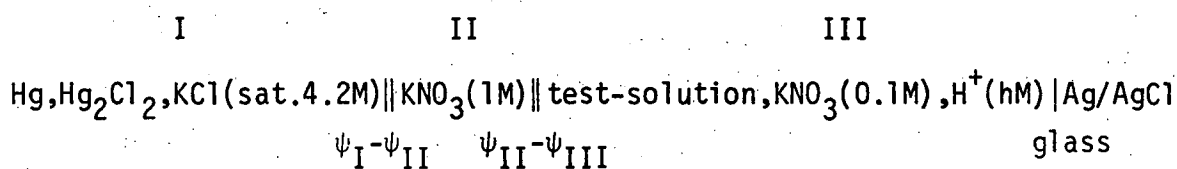
Preliminary work was done using combination glass-Ag/AgCl electrodes, primarily as a space-saving device, however, these were found to be unsatisfactory in solutions containing both methylmercuric ion and some dithiols (particularly DMSH<sub>4</sub>). Erratic behaviour, characterised by large drifts (>1 pH unit) from calibration during a titration lasting several hours, could not be ascribed solely to MeHgCl formation at the glass-sinter liquid junction, since methylmercuric solutions alone (up to 0.01M) behaved satisfactorily under similar titration conditions (e.g. for evaluation of MeHg(II) hydrolysis constants). Some evidence for chloride complexation was found in more dilute solutions due to leakage of the saturated KCl filling solution.

The reason for erratic behaviour in the presence of DMSH<sub>4</sub> is not completely understood. It was considered that perhaps H<sub>2</sub>S, known to be formed as a decomposition product of DMSH<sub>4</sub> in alkaline solutions, might be responsible by diffusion through the reference half-cell filling hole, thereby altering the Ag/AgCl reference potential. Venting this filling hole outside the cell by insertion of tightly fitting Teflon tubing was not successful in eliminating the effect, however it was considered that this precaution was advantageous in protecting the long term stability of the reference half-cell, particularly in titrations

involving volatile thiols, and was maintained throughout all subsequent titrations (including the eventual use of separate calomel reference electrodes). The use of separate glass (or Ag/AgCl) reference electrodes eliminated hysteresis problems, which may have been due to the close proximity of the combination electrode glass-bulb and liquid junction frit. A double junction (glass-sleeve) calomel reference electrode, with saturated KCl in the inner cell, and 1M KNO<sub>3</sub> in the outer junction, was finally used to prevent chloride diffusion into the titration solution.

An important consideration when using potentiometric methods is the stability of liquid junction potentials in the electrode chain. Potentiometric cells of highest stability must incorporate no liquid junction, e.g. use of Ag/AgCl reference electrodes, or incorporate a liquid junction whose magnitude is small (for high precision) and remains constant.

The magnitude of the diffusion potential due to the double liquid junction for the cell, C, below.



can be evaluated from potentials  $\psi_I - \psi_{II}$  and  $\psi_{II} - \psi_{III}$  using Henderson's solution to the Nernst-Planck equation,<sup>7,13</sup> if mobilities,  $\mu_i$ , of the species with charge  $z_i$  and concentration  $c_{i,I}$  and  $c_{i,II}$ , in the two solutions, are known. For example, the diffusion potential of the liquid junction  $\psi_I - \psi_{II}$  is given approximately by

$$\psi_I - \psi_{II} = \frac{RT}{F} \frac{\sum_i (c_{i,II} - c_{i,I}) \mu_i / z_i}{\sum_i (c_{i,II} - c_{i,I}) \mu_i} \cdot \ln \left( \frac{\sum_i c_{i,II} \mu_i}{\sum_i c_{i,I} \mu_i} \right)$$

The mobilities of background electrolyte species  $K^+$ ,  $NO_3^-$  and highly mobile  $H^+$ ,  $OH^-$  will dominate in this expression.

Ionic mobilities can be derived from transport numbers and used to calculate estimates of liquid junction potentials  $\psi_I - \psi_{II}$  and  $\psi_{II} - \psi_{III}$  for varying test-solution pH. These are given in Table 6.3.

pH	$\psi_I - \psi_{II} / \text{mV}^a$	$\psi_{II} - \psi_{III} / \text{mV}^b$	$\psi_I - \psi_{III} / \text{mV}$
1.5	2.50	7.88	10.38
2	2.50	1.57	4.07
3	2.50	-1.58	0.92
4	2.50	-1.92	0.58
5	2.50	-1.96	0.54
6	2.50	-1.96	0.54

Table 6.3: Estimated liquid junction potentials at various pH values for cell C employing a double-junction calomel reference electrode.

<sup>a</sup>Calculated using  ${}^{702}\mu_{Cl^-} = 1.0383\mu_{K^+}, \mu_{NO_3^-} = 0.9716\mu_{K^+}$ , independent of pH.

<sup>b</sup>Calculated using  ${}^{702}\mu_{H^+} = 4.882\mu_{NO_3^-}$ ,  $\mu_{K^+} = 1.0292\mu_{NO_3^-}$ .

It can clearly be seen that high proton mobility contributes dominantly to high liquid junction potentials at pH values below 3-4. A similar effect can be shown to be due to high hydroxide mobility, above pH 10-11. Together with high and moderate resistance glass-electrodes (Philips GA110 (200-300M $\Omega$ ) and GAT130 (15-40M $\Omega$ )) the double-junction reference electrode reliably provided rapid pH response, and good pH stability (e.g. pH(s) 6.865 NBS buffer is stable to within 0.005 units over periods of 48 hours) The major cause of pH drift seemed to be



loss of 1M  $\text{KNO}_3$  junction solution from the glass-sleeve double-junction reference electrode (capacity  $\sim 3\text{mL}$ ).

The stability of the double-junction electrode assembly is presumably due to the constancy of the glass-sleeve junction<sup>714</sup> and low liquid junction potential, and is quite adequate for potentiometric work of this nature. The use of unwieldy Wilhelm salt-bridges and massive calomel electrodes can only be justified when high precision emf measurements (e.g.  $0.01\text{ mV}$ )<sup>715</sup> are required over long titration periods. No differences in stability could be unambiguously attributed to the use of moderate resistance ( $15\text{--}40\text{M}\Omega$ ) instead of high resistance ( $200\text{--}300\text{M}\Omega$ ) glass electrodes.

#### Titrant solutions

Titration were performed with potassium hydroxide solutions prepared from commercially available ampoules (Merck Titrisol<sup>®</sup>) and diluted to nominally 0.1M using freshly deionised water. These solutions were stored in one litre KOH-leached amber borosilicate glass vessels connected directly to the automatic dispensing valve of a Dosimat Model E535 autoburette and protected from atmospheric  $\text{CO}_2$  with Carbasorb<sup>®</sup>. A second titrant solution of 0.1M  $\text{HNO}_3$  prepared from AR (conc.)  $\text{HNO}_3$  was prepared and stored similarly, but without  $\text{CO}_2$  protection. Preliminary work using KOH solutions prepared by the tedious ion exchange method of Albert and Serjeant<sup>716</sup> showed that solutions prepared from commercial ampoules were of identical quality. The presence of weakly acidic impurities (mainly carbonate) was periodically monitored when the solutions were standardised against potassium hydrogen phthalate (dried  $120^\circ$ , nominally  $100.0 \pm 0.2\%$ ).

#### Titration procedure

Prior to each titration, the asymmetry-potential control of the

pH-meter was set using the NBS pH 6.865 phosphate buffer previously maintained at 25.00°. (The iso-potential point of the meter was pre-set to 6.865). When the pH of this buffer was constant for at least 15 minutes the 'slope' of the electrode assembly was set by standardisation in the pH 4.00 phthalate buffer. Finally, as an additional check on buffer conditions and electrode linearity, the pH 10.012 carbonate buffer was tested. The measured pH of this buffer was always within the range 10.002-10.012. (The three buffers described above are not perfectly internally consistent, in particular, the carbonate buffer is reported to give an operational pH of 10.002<sup>693</sup>).

The electrode assembly was finally rinsed several times with deionised water (kept at 25.00° to reduce thermal shock) and blotted dry with clean tissue (not wiped, to avoid static electricity transfer to the high resistance bulb which takes some time to dissipate<sup>717</sup>). The titration vessel was quickly dried with clean tissue, the appropriate mass of twice recrystallised  $\text{KNO}_3$  added together with magnetic stirrer bar, the titration solution added using calibrated glassware, and electrodes replaced. Nitrogen purging and magnetic stirring were maintained for at least 15 minutes for the electrodes to reattain thermal equilibrium and for removal of dissolved oxygen.

The delivery capillary of the automatic burette was inserted to well below the surface of the titration solution. The tip of the glass capillary (0.1 mm i.d.) was not inverted to minimise titration diffusion, as reported elsewhere.<sup>718</sup> The hydrostatic head of titrant (from titrant reservoir to delivery tip) was 5-10 cm, and titrant diffusion was estimated to be less than 0.001 mL/10 minutes by monitoring the pH at the unbuffered endpoint of a strong acid/strong base titration. This diffusion rate produces no detectable change of pH in moderately buffered titration regions.

Small volumes of titrant were added using the automatic burette in the 0.01 mL 'step' mode while the solution was stirred magnetically and with nitrogen. Stirring was then stopped and nitrogen passed over the solution surface until the pH showed less than 0.001 units change per minute. Maintenance of pH equilibrium was at first monitored with the output of the pH meter connected to a chart recorder (10 mV full scale) and subsequently with the device described in Appendix 6.1.

Some confusion appears in the literature over the decision to record equilibrium pH values in stirred or unstirred solutions, even in work covering high precision pH measurements. In cells containing liquid junctions the liquid junction potential can show significant stirring effects.<sup>717</sup> In order to maintain a constant liquid junction potential throughout a long titration, it is necessary in these cases to ensure a constant stirring speed. In this work, it was felt that a 'zero' stirring speed could be maintained most precisely, even though attainment of equilibrium may be slightly slower in this case.

Titration data in this region invariably required inordinately long equilibrium times (>30 minutes) even when the titrant delivery capillary was removed (to eliminate titrant diffusion) and the vessel maintained under a static nitrogen atmosphere. In addition, it is to be expected that the pH of this region is determined by the presence of minor amounts of weakly acidic and basic impurities, e.g. dissolved CO<sub>2</sub>, boron and aluminium-containing anions leached from the glass vessel etc. Ciavatta has shown that very small amounts (<1  $\mu$ mole) of these products are inevitably present, even under the most rigorous titration conditions.<sup>719</sup> We have found in this work, by refinement of the total proton concentration,  $H_{tot}$ , in these titrations, that  $H_{tot}$  is always 1-4  $\mu$ mole greater than expected from analytical  $H^+$  concentrations. This behaviour is reflected by 0.001-0.004 mL equivalent point systematic

errors, consistent with the above impurities (page 302). For these reasons data in this region, unless buffered by the system under investigation (rarely), have not been included for refinement of equilibrium constants.

#### pH(s) buffers

The choice of pH(s) values for standard buffers varies on a nation-wide basis, according to national definitions of the pH scale. Compositions of buffer solutions are not universal,<sup>693,720</sup> e.g. potassium hydrogen phthalate studies are prepared as 0.05 molal (10.12 g per 1000 mL solution at 25°) with pH(s) at 25° 4.004 (U.S.A.), 4.01 (Hungary), 4.01 (Poland), 4.008 (U.S.S.R.), or 0.05 molar (10.21 g/1000 mL at 25°) with pH(s) at 25° 4.008 (Germany), 4.01 (Japan), 4.005 (U.K., defines pH scale).

Although variations between scales are small, they are not immeasurable in the pH-meters capable of 0.001 pH resolution. The recently recommended IUPAC values for standard pH buffers at 25°C have been used in this work. They are pH(s) 4.008 for 0.05 molal potassium hydrogen phthalate (10.12 g/1000 mL at 25°), pH(s) 6.865 for 0.025 equimolal potassium dihydrogen orthophosphate (3.39 g) and disodium hydrogen orthophosphate (3.53 g/1000 mL at 25°).

To extend the calibrated pH range of the glass electrode to high pH, the NBS 0.01 equimolal sodium carbonate (2.640 g  $\text{Na}_2\text{CO}_3$  and 2.092 g  $\text{NaCO}_3$ /1000 mL at 25°) was used. The highest pH buffer recommended by IUPAC i.e. 0.01 molal sodium tetraborate decahydrate, pH(S)=9.180<sup>721</sup>. Preliminary work with  $\text{Na}_2\text{B}_4\text{O}_7 \cdot 10\text{H}_2\text{O}$  as an acidimetric standard indicated that our product was partially dehydrated. Although the dilution effect of this buffer is small,<sup>693</sup> it was found to be more convenient to use the carbonate-bicarbonate buffer for which high purity reagents were available.

#### 6.2.4 Available computer programs for evaluation of ligand-hydrolysis equilibria

Acid dissociation constants for mono- or diprotic ligands of known purity can be obtained from potentiometric data by manual calculation, e.g. using well-established methods, even under circumstances where two acidic groups dissociate simultaneously.<sup>716</sup> For more complex multiprotic ligands, the deprotonation equilibria are best evaluated using least-squares data fitting, and many simple computer programs are available for this task of calculating *only* the acid-dissociation constants from potentiometric data. Such programs require that the concentrations of ligands and titrant be known precisely, electrode calibration factors (e.g.  $E^\circ$ ,  $j_H$ ,  $pH_{cal}$ , etc., page 291) be determined before the titration and assumed to remain applicable during the titration, and for weakly basic ligands the value of  $K_W^C$  be known for the appropriate conditions under study. It is often inconvenient or impossible to satisfy all of these requirements simultaneously, particularly for high precision titrations. Electrode calibrations may change on transfer from calibrant solution (e.g. standard buffers or strong acid/base titration, page 292) to measuring solution, the purity of readily oxidisable ligands (e.g. thiols used in this work) is often not 100% and the ligands may decompose significantly if kept in solution, even for short periods before titration etc. An acidic ligand solution may be dilute or may involve overlapping buffer regions so that equivalent points cannot readily be detected by the usual means. In these circumstances it is convenient to use least-squares procedures to obtain values for electrode-calibration constants, concentration of ligand, etc., from the same data used to evaluate the ligand hydrolysis constants, albeit at necessarily reduced precision since extra parameters are being extracted from the data. Situations may also arise where mixtures of

multiprotic ligands with similar acidity constants are titrated, e.g.  $H_nL$  in the presence of  $CO_3^{2-}$  impurity. Least-squares procedures have been used to treat such multi-protolyte equilibria. The few published multiparametric curve-fitting programs which achieve some or all of these ends, have been reviewed elsewhere.<sup>690,722-5</sup>

Although multiparametric curve-fitting procedures are widely used in chemistry and other fields, the use of correct weighting of data is often overlooked, giving rise to incorrect estimates of fitted-model parameters.<sup>726-8</sup>

Similarly, conventional least-squares curve-fitting approaches almost invariably assume that random errors reside with only one of the experimental variables. In a two variable case, e.g. titration curves consisting of pairs of (titrant volume, pH) data, the values of titrant volume are usually considered to be totally reliable whereas the measured pH values incorporate some random error. In many modern titration systems, including the system used in this work, this is not the case. Specifically, the automatic syringe type burette used in this work of capacity 5 mL is reproducible to within 0.001 mL, hence titres of 0.5 and 5.0 mL incorporate uncertainties of 0.2 and 0.02% respectively. The measured pH can often be recorded to a precision, in buffered regions, of 0.001 pH units over the entire pH range, corresponding to a constant relative error of 0.1% in  $[H^+]$  (or, if pH is considered to be a variable, rather than  $[H^+]$ , 0.05% and 0.01% at pH 2 and 10 respectively).

Extremely high precision titrations can be performed with precision of 0.01 mV in glass electrode emf<sup>715</sup> (0.0002 pH units) and  $10^{-4}$  mL in 0.5 mL titres.<sup>729</sup> It can clearly be seen that both experimental variables carry comparable uncertainties, and hence normal least-squares methods should not be applied. The use of 'rigorous' least-squares techniques are therefore necessary, and these have been described generally elsewhere,

but seem to have been used infrequently in the potentiometric field. The rigorous least-squares approach has been applied to straight-line fitting of variables with correction errors, and used to obtain formation constants of diprotic acids and mononuclear metal-ligand complexes  $ML$  and  $ML_2$ .<sup>700</sup> A computer program using this approach, RIGREG, has been written by this author and used to calculate diprotic acid dissociation constants for evaluation of the general acid-base titration program TITRAT, described below.

The only computer program for treatment of ligand hydrolysis constants using rigorous least-squares approach, of which this author is aware, is TITRA, described by Schwartz and Gelb.<sup>706</sup> A copy of this program was kindly made available by one of the authors (LMS) and was used in the initial stages of this study.

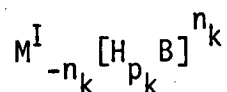
The original interactive program has been made more efficient in terms of convergence properties and running time, and generalised to treat the titration of any number of multiprotic acids or bases, and to extract any titration parameter by rigorous least-squares curve-fitting.

#### 6.2.5 TITRAT and related programs for treatment of titrations of mixtures of multiprotic acids and bases

TITRAT is an interactive computer program which has been written in OS/8 Basic for implementation on a Digital PDP8E minicomputer with 12K available core memory for array storage etc. The program uses an iterative non-linear least-squares algorithm to fit experimental data from an aqueous titration of a mixture of Brønsted acids or bases by a strong monofunctional acid or base, and refine simultaneously any number of titration parameters described in the model below. The procedure is statistically rigorous, using a weighting scheme which accounts for statistical uncertainties in both pH and titrant volume. The statistical procedure is based on that in the program TITRA<sup>706</sup> but the

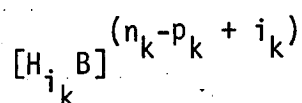
refinement algorithm has been generalised to cope with (theoretically) any number of acids or bases and has much more efficient convergence properties than TITRA.

The aqueous solution model considers that a number of  $N$  protolytic bases, the  $k^{\text{th}}$  of which is

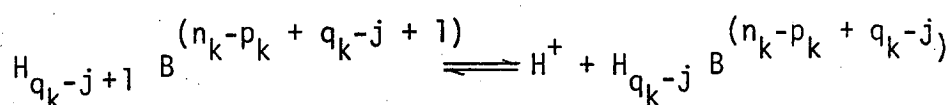


have been added to an initial solution volume,  $V_0$  mL and the mixture titrated with strong monofunctional acid or base, of molarity,  $F$ . In the above generalised species, the charge,  $n$ , of the ionic species involved in protonation or deprotonation which was initially added to the titration system, may be negative, e.g.  $K^+[H_2PO_4]^-$  or positive, e.g.  $[NH_4]^+Cl^-$  or zero, e.g.  $[H_2 \text{ succinate}]^0$ . The number of displaceable protons of the general ampholyte is  $p$ . It is assumed further that the ampholyte can accept a maximum number of protons,  $q$ , described as its functionality.

The concentration of the  $i^{\text{th}}$ -protonated form of the  $k^{\text{th}}$  base is



For the  $j^{\text{th}}$  dissociation of the  $k^{\text{th}}$  base:



the stepwise thermodynamic equilibrium constant can be written

$$K_{j_k}^\ominus = \frac{[H_{q_k - j} B^{n_k - p_k + q_k - j}][H^+] \gamma_H}{[H_{q_k - j + 1} B^{n_k - p_k + q_k - j + 1}]} \cdot \frac{\gamma_{\pm}^{(n_k - p_k + q_k - j)^2}}{\gamma_{\pm}^{(n_k - p_k + q_k - j + 1)^2}}$$

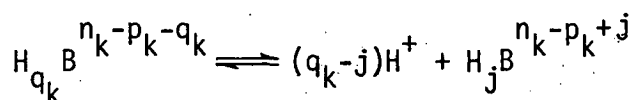


The mean activity coefficient term simplifies so that

$$K_{j_k}^{\ominus} = (K_{j_k}^c \gamma_{H^+}) \cdot \gamma_{\pm}^{-2(n_k - p_k + q_k - j) - 1}$$

$$\text{or } K_{j_k}^{\ominus} = K_{j_k}' \cdot \gamma_{\pm}^{-2(n_k - p_k + q_k - j) - 1}$$

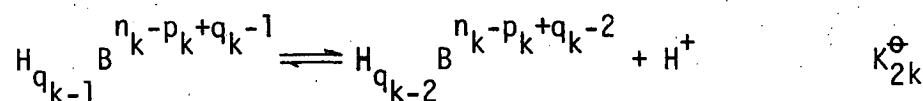
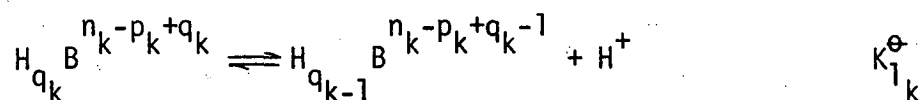
The  $(q_k - j)^{\text{th}}$  overall dissociation of the fully protonated form of  $k^{\text{th}}$  base



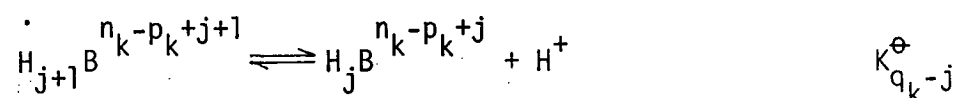
has the overall *thermodynamic* equilibrium constant

$$\beta_{q_k - j}^{\ominus} = \frac{\{H_j B^{n_k - p_k + j}\} \{H^+\}^{(q_k - j)}}{\{H_{q_k} B^{n_k - p_k - q_k}\}}$$

The  $(q_k - j)^{\text{th}}$  overall dissociation can be expressed as a sum of  $(q_k - j)$  consecutive stepwise dissociations, with thermodynamic stepwise equilibria constants as shown



⋮



Hence  $\beta_{q_k-j}^{\ominus} = K_{1_k}^{\ominus} K_{2_k}^{\ominus} \dots K_{q_k-j}^{\ominus}$ , with analogous relationships holding for mixed constants  $\beta_{q_k-j}'$ :

$$\begin{aligned}\beta_{q_k-j}' &= K_{1_k}' K_{2_k}' \dots K_{q_k-j}' \\ &= \frac{[H_j B_{k-p_k+j}^{n_k-p_k+j}][H^+]^{(q_k-j)}}{[H_{q_k} B_{k-p_k+q_k}^{n_k-p_k+q_k}]}\end{aligned}$$

so that the concentration of the general  $j^{\text{th}}$ -protonated form of the  $k^{\text{th}}$  base can be written in terms of the fully  $(q_k^{\text{th}})$  protonated form:

$$[H_j B_{k-p_k+j}^{n_k-p_k+j}] = \frac{(K_{1_k}' K_{2_k}' \dots K_{q_k-j}')}{\{H^+\}^{(q_k-j)}} \cdot [H_{q_k} B_{k-p_k+q_k}^{n_k-p_k+q_k}]$$

We can now consider the  $N$  mass-balance equations for the  $N$  bases in the mixture. Consider that  $N_k$  mmoles of  $k^{\text{th}}$  base was added initially to the  $V_0$  mL titration solution, i.e. the  $k^{\text{th}}$  analytical concentration is  $N_k/V_0$ . After the addition of  $v_i$  ml strong monofunctional titrant (completely dissociated) of normality  $F$ , we have  $N$  equations of the form:

$$\begin{aligned}N_k &= (V_0 + v_i) \sum_{j=0}^{q_k} [H_j B_{k-p_k+j}^{n_k-p_k+j}] \quad k=1, \dots, N \\ &= (V_0 + v_i) [H_{q_k} B_{k-p_k+q_k}^{n_k-p_k+q_k}] \sum_{j=0}^{q_k} \frac{(K_{1_k}' K_{2_k}' \dots K_{q_k-j}')}{\{H^+\}^{(q_k-j)}}\end{aligned}$$

Similarly, we have the electroneutrality expression at the  $i^{\text{th}}$  titration point:

$$[H^+]_i - [OH^-]_i + (U^+ - U^-) + \sum_{k=1}^N \sum_{j=0}^{q_k} (n_k - p_k + j) [H_j B^{n_k - p_k + j}] = 0$$

where the terms  $U^+$  and  $U^-$  represent concentration sums of all singly charged counteranions and counteranions, other than  $H^+$  and  $OH^-$ , respectively. These compounds come from titrant  $K^+(OH^-)$  or  $H^+(NO_3^-)$  and initial forms of base  $M_{-n_k}^+(H_{p_k} B^{n_k})$ .

$$\text{If the titrant is strong base, } U^+ - U^- = \frac{v_i F - \sum_{k=1}^N n_k N_k}{V_0 + v_i}$$

$$\text{If the titrant is strong acid, } U^+ - U^- = \frac{-v_i F - \sum_{k=1}^N n_k N_k}{V_0 + v_i}$$

By analogy with Schwartz and Gelb, we write

$$P_{1k} = \sum_{j=0}^{q_k} \frac{K'_0 K'_1 \dots K'_{q_k-j}}{\{H^+\}^{q_k-j}}$$

$$\text{and } P_{2k} = \sum_{j=0}^{q_k} \frac{(n_k - p_k + j) K'_0 K'_1 \dots K'_{q_k-j}}{\{H^+\}^{q_k-j}}$$

It should be noted in passing that a minor error seems to have appeared in the paper by these authors.<sup>706</sup> On p.1574 of their paper, they write (in the nomenclature used here)

$$P_1 = 1 + \frac{K_1^\ominus}{G_1 \{H^+\}} + \frac{K_1^\ominus K_2^\ominus}{G_1 G_2 \{H^+\}^2}$$

$$\text{and } P_2 = \frac{K_1^\ominus}{G_1 \{H^+\}} + \frac{2K_1^\ominus K_2^\ominus}{G_1 G_2 \{H^+\}^2} \text{ where } G_1 = \gamma_{H^+} \gamma_{HR^-} \text{ with } \gamma_{H_2R} = 1$$

$$\text{and } G_2 = \gamma_{H^+} \gamma_{R^{2-}} / \gamma_{HR^-}$$

The term  $\gamma_{H^+}$  should not appear in the expressions for  $G_1$  and  $G_2$ .

The  $N$  mass-balance equations of the  $i^{\text{th}}$  titration point become:

$$N_k = (V_o + v_i) [H_{q_k} B^{n_k - p_k + q_k}] P_{1_k}$$

and the electroneutrality expression becomes

$$[H^+]_i - [OH^-]_i + \sum_{k=1}^N [H_{q_k} B^{n_k - p_k + q_k}] P_{2_k} + U^+ - U^- = 0$$

Therefore the electroneutrality expression can be written:

$$[H^+]_i - [OH^-]_i + \sum_{k=1}^N \frac{N_k}{(V_o + v_i)} \frac{P_{1_k}}{P_{2_k}} + \left[ \frac{\pm v_i F - \sum_{k=1}^N n_k N_k}{V_o + v_i} \right] = 0$$

Thus the volume of titrant can be simply expressed in terms of pH

$$v_i = \frac{\sum_{k=1}^N \left( \frac{P_{k2}}{P_{1_k}} - n_k \right) N_k + V_o ([H^+]_i - [OH^-]_i)}{\pm F - ([H^+]_i - [OH^-]_i)}$$

This surprisingly simple relationship is exact, requires no assumptions and can be used to calculate the titration curve for complex mixtures of bases. The volume of titrant is calculated for a given pH rather than the classical treatment which would calculate  $[H^+]$  for a given titrant volume by solution of a high order polynomial in  $[H^+]$ . This approach has been used to calculate complex titration curves with hand-held calculators.

The expression of  $N_i$  is a generalised version of that given by Schwartz and Gelb for the rhodizonic acid ( $H_2B$ ) system.<sup>706</sup> We define the 'condition function',  $F_i$ , similar to that used by Deming<sup>730</sup>

$$F_i = \frac{\sum_{k=1}^N \left[ \frac{P_{2k}}{P_{k2}} - n_k \right] N_k + v_0 ([H^+]_i - [OH^-]_i)}{\pm F - ([H^+]_i - [OH^-]_i)} - v_i$$

For rigorous least-squares curve-fitting, we are required to minimise the weighted sum-of-squares,  $S$ , over all  $N$  titration points:

$$S = \sum_{i=1}^N [W_{x_i} (pH_{calc} - pH_i)^2 + W_{y_i} (v_{calc} - v_i)^2]$$

where the weighting factors  $W_{x_i}$ ,  $W_{y_i}$  are inversely proportion to *a priori* variance estimates of the  $pH_i$  and  $v_i$  measurements.

Since  $F_i$  is a non-linear function of most of the titration parameters  $K_{j_k}$ ,  $F$ ,  $N_k$  etc., the calculation procedure requires an iterative approach. We have used a Gauss-Newton procedure, which requires values of the partial derivatives of  $F_i$  with respect to each parameter, and those with respect to  $pH_i$  and  $v_i$ . Although the algebra for derivation of these derivatives is tedious, the use of analytical expressions, rather than numerical estimates of the partial derivatives, results in much faster program operation (a comparison between TITRAT and TITRA showed speed improvements of an order of magnitude in some systems).

Expressions for derivatives used in TITRAT are given below for completion:

$$\frac{\partial F_i}{\partial F} = \pm \frac{\sum_{k=1}^N \left[ \frac{P_{2k}}{P_{1k}} - n_k \right] N_k + v_0 ([H^+]_i - [OH^-]_i)}{[\pm F - ([H^+]_i - [OH^-]_i)]^2}$$

$$\frac{\partial F_i}{\partial v_i} = -1$$

$$\frac{\partial F_i}{\partial N_k} = \left( \frac{P_{2k}}{P_{1k}} - n_k \right) / [\pm F - ([H^+]_i - [OH^-]_i)] \quad k=1, \dots, N$$

$$\frac{\partial F_i}{\partial K_w^\ominus} = \frac{-1}{\pm F - ([H^+]_i - [OH^-]_i)} \cdot \frac{[OH^-]}{K_w^\ominus} \cdot [V_0 + (F_i + v_i)]$$

$$\frac{\partial F_i}{\partial K_{j_k}^\ominus} = \frac{N_k}{\pm F - ([H^+]_i - [OH^-]_i)} \cdot \frac{1}{P_{1k}^2} \cdot \left\{ P_{1k} \frac{\partial P_{2k}}{\partial K_{j_k}^\ominus} - P_{2k} \frac{\partial P_{1k}}{\partial K_{j_k}^\ominus} \right\}$$

where  $\frac{\partial P_{2k}}{\partial K_{j_k}^\ominus} = \frac{1}{K_{j_k}^\ominus} \sum_{\ell=0}^{q_k-j_k} \frac{h_k - p_k + \ell}{\{H^+\}^{q_k-\ell}} (K'_{1k} K'_{2k} \dots K'_{q_k-1})$

and  $\frac{\partial P_{1k}}{\partial K_{j_k}^\ominus} = \frac{1}{K_{j_k}^\ominus} \sum_{\ell=0}^{q_k-j_k} \frac{1}{\{H^+\}^{q_k-\ell}} (K'_{1k} K'_{2k} \dots K'_{q_k-1})$

$$\frac{\partial F_i}{\partial pH_i} = \frac{\partial F_i}{\partial pH_{cal}}$$

$$= \frac{-1 \ln 10}{\pm F - ([H^+]_i - [OH^-]_i)} \{ (V_0 + v_i)([H^+] + [OH^-]) + \{H^+\} \sum_{k=1}^N N_k \frac{P_{1k} \frac{\partial P_{2k}}{\partial \{H\}} - P_{2k} \frac{\partial P_{1k}}{\partial \{H\}}}{P_{1k}^2} \}$$

where  $\frac{\partial P_{2k}}{\partial \{H\}} = - \frac{1}{\{H\}} \sum_{j=0}^{q_k} \frac{(q_k-j)(n_k-p_k+j)}{\{H^+\}^{q_k-j}} \cdot K'_{1k} K'_{2k} \dots K'_{q_k-j}$

$$\text{and } \frac{\partial^2 p}{\partial \{H\}^2} = \frac{-1}{\{H\}} \sum_{j=0}^{q_k} \frac{(q_k - j)}{\{H^+\}^{q_k - j}} \cdot K'_1 K'_2 \dots K'_{q_k - j}$$

The values of  $[H^+]_j$  used in the equations above must be obtained by choosing an appropriate glass-electrode calibration expression.

In this case, the operational definition of pH becomes

$$pH_{\text{meas}} + pH_{\text{cal}} = -\log\{H^+\} = -\log[H^+]_{Y_H^+}$$

The proton activity coefficient can be evaluated by empirical relationships, e.g. Debye-Huckel etc. as discussed previously (page 287) and is the method used by Schwartz and Gelb.<sup>706</sup> Activity coefficients of all other species can be evaluated similarly for titrations at low ionic strength where the component activities are expected to change during the titration. Under these conditions, TITRAT equilibrium constants are *thermodynamic* constants. The original version TITRA, has been shown to generate highly accurate values for  $K^\ominus$  using this method. TITRAT has the facility to calculate activity coefficients at each titration point, by evaluating ionic strength and using the Debye-Huckel expression for  $\gamma_{\pm}$ , or to fix activity coefficients to unity, in cases where constant ionic strength titrations are performed. The latter case is applicable to this study, in which all titrations were carried out in 0.1M  $\text{KNO}_3$  or 0.1M KI media. Under these conditions, the operational definition of pH becomes

$$pH_{\text{meas}} + pH_{\text{cal}} = -\log[H^+]$$

which has been shown previously (page 293) to apply in the range  $3 < \text{pH} < 11$ , and TITRAT equilibrium constants are consequently *stoichiometric* constants. The variable  $pH_{\text{cal}}$  can be determined by prior experiment

(page 296) or can be treated as a parameter by TITRAT. The latter alternative is used in this work, since small daily variations in electrode calibration are conveniently taken into account. Values of  $\text{pH}_{\text{cal}}$  in 0.1M KI or  $\text{KNO}_3$  at  $25^\circ$  using the Philips GAl10 glass-electrode/R44 (sat. KCl, 1M  $\text{KNO}_3$ ) double junction reference electrode, invariably lie in the range -0.04 to -0.08 units when refined by TITRAT from data below pH 4, in good agreement with directly determined values.

To evaluate  $[\text{OH}^-]$ , the expression  $K_W^\ominus = \{\text{H}^+\}\{\text{OH}^-\} = [\text{H}^+][\text{OH}^-]\gamma_{\text{H}^+}\gamma_{\text{OH}^-}$  is used. For fixed activity coefficients, this simplifies to  $K_W^C = [\text{H}^+][\text{OH}^-]$ . Values for  $K_W^C$  can be determined by prior experiment or treated as a titration parameter at high pH (page 294). Since the operational definition of pH involves no non-linearity terms, and since many titrations in this study are performed up to pH 11, where non-linearity becomes measurable (page 293), the value of ' $K_W^C$ ' is always treated as a parameter in these titrations. This has been shown to be equivalent to 'calibrating' the electrode at high pH, by evaluation of a non-linearity term such as  $j_{\text{OH}} K_W^C / [\text{H}^+] = 'K_W^C' / [\text{H}^+]$  (page 292).

It should be noted that, in principle, any glass-electrode calibration expression e.g. for using electrode emf rather than pH, could be incorporated into TITRAT, and the appropriate calibration 'constants' treated as parameters. Calibration expressions of the form  $E = E^\circ + \log[\text{H}^+] - j_{\text{OH}} K_W^C / [\text{H}^+]$  have been treated by other multiparametric curve-fitting programs (non-rigorous) in this way, and reliable values of the parameters obtained. 704-5

### 6.3 Evaluation of formation constants of stable complexes

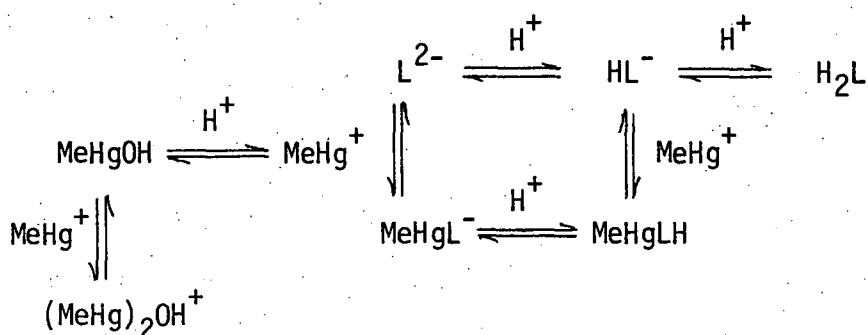
#### 6.3.1 $\text{H}^+$ - competition method for obtaining aqueous stability constants

In this section potentiometric methods for evaluation of equilibrium constants in a system containing hydrolysable methylmercuric ion and



and basic ligand,  $L^{n-}$ , will be considered. Measurement of  $[H^+]$  under different equilibrium conditions can be used to evaluate the concentrations of the equilibrium components, usually using *a priori* assumptions about the existence of various MeHgL species (however see page 319 for recent methods which are model independent). Such an experiment can be carried out in several ways. The change in pH (hence in  $[H^+]$  if the electrode is calibrated correctly, page 295) can be measured as a function of total ligand concentration, or alternatively the pH can be monitored as a solution containing constant total MeHg(II) and ligand concentrations is titrated with acid or alkali.

The latter method, used in this work and widely elsewhere, relies on the existence of competition between protons and methylmercuric ions for basic ligands, e.g. the following equilibria should co-exist between  $MeHg^+$  and  $L^{2-}$  (considering only 1:1 MeHgL complexes).



The concentrations of components  $MeHg^+$ ,  $L^{2-}$  (and hence all complex species incorporating these components) will be changed to new (unknown) values if protons are added (e.g. by HL or  $HNO_3$ ) or removed (e.g. by KOH) from this system. The new  $[H^+]$  can be measured and the procedure repeated to give a set of (volume of titrant,  $[H^+]$ ) data pairs which can be treated by least-squares methods to be described in Section 6. to obtain the equilibrium constants for the system described above.

This  $H^+$ - competition method can be used for many equilibrium systems, and has been used in this work to evaluate equilibrium constants for

multiprotic thiol dissociation (Section 3.3.2), MeHg(II) hydrolysis (Section 3.2.1), and MeHg(II) association with chloride and iodide (Section 3.2.1).

A powerful series of variations of a general method for evaluating equilibrium constants by potentiometric titration has received some attention in recent literature.<sup>731-9</sup> The general method, originating from the work of Österberg, Sarkar and Kruck, exploits the differential properties of component mass balance equations, derived from the Gibbs-Duhem equation, to enable calculation of free metal and ligand concentrations from measurement of  $[H^+]$  only. Values of  $[H^+]$  are usually measured in a series of solutions of constant metal, or ligand concentration ( $C_M, C_L$ ). Values of  $[L]$  can be obtained via differential relationships such as

$$\log \frac{[L]}{[L]_0} = - \left\{ \frac{\partial}{\partial C_L} \left| \int \frac{\log[H^+]}{\log[H^+]} C_H d \log[H^+] \right|_{C_M, C_L} \right\}_{C_M, [H^+]}$$

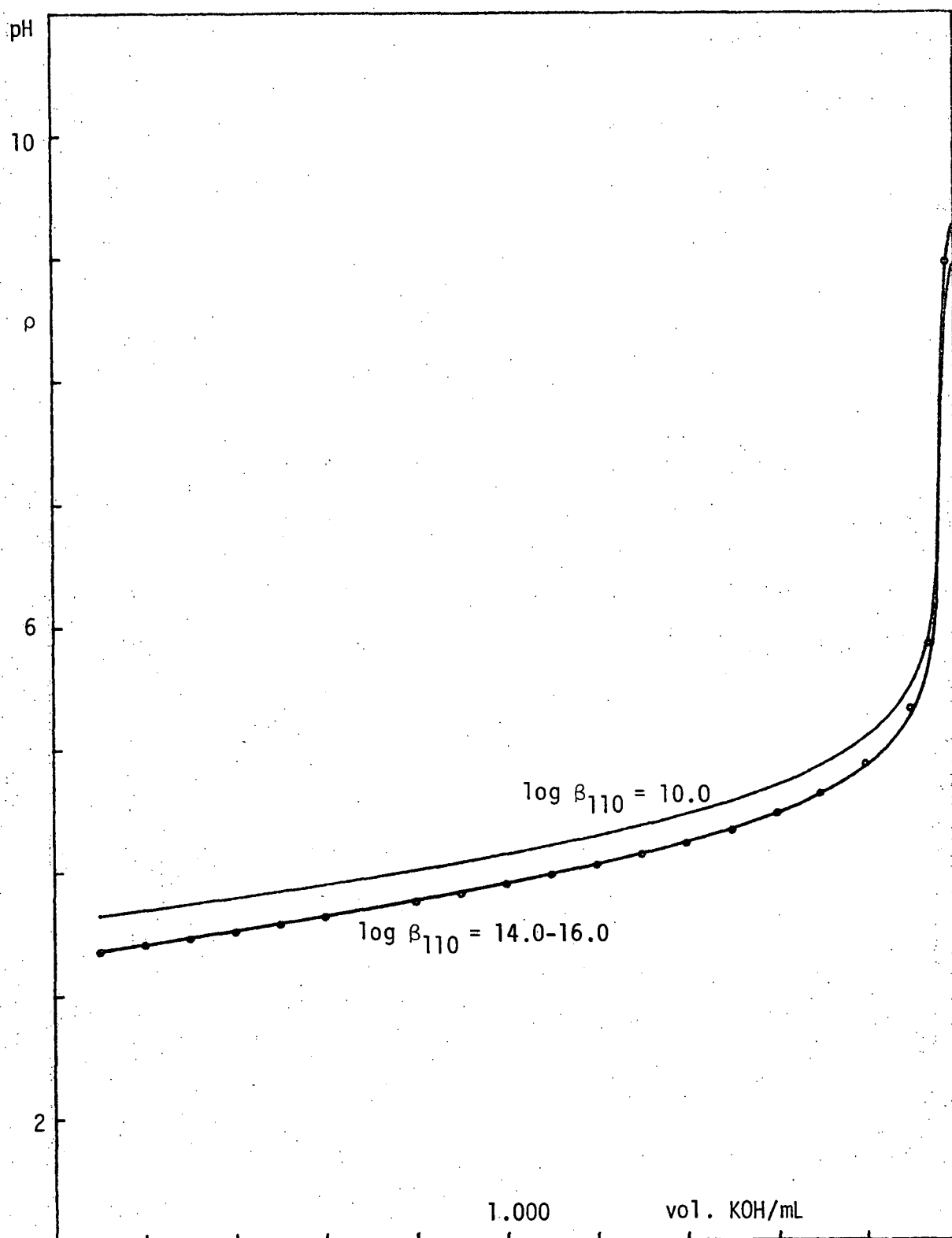
A similar relationship holds for  $[M]$ . The integration and differentiation requirements of constant  $C_M, C_L, [H^+]$  etc. require data of utmost precision,<sup>731-5</sup> which seems to have limited the technique to date.

Despite the stringent requirements of the technique, it has been successfully applied to the study of several ternary (M-L-H)<sup>735-6</sup> and quaternary (M-L-L'-H)<sup>732</sup> systems. A very simple recent theoretical approach involves repeated dilution of an initial metal-ligand-proton system with pure solvent, but does not seem to have been applied to practical systems.<sup>739</sup>

A singular advantage of these methods lies in the fact that free component concentrations can be evaluated without *a priori* knowledge of equilibria involved, i.e. they are model independent.

For routine application of this general method, automated gravimetric titration techniques seem to be necessary to obtain data of adequate precision. For this reason the method was not used in this study, although it would seem to be applicable to the study of MeHg-thiolate-iodide-proton equilibria (Section 3.3.1).

An inherent limitation for evaluation of metal-ligand equilibrium constants by the  $H^+$ -competition method lies in the assumption that changing  $[H^+]$  can significantly alter the position of metal-ligand equilibria. The method cannot be used to evaluate systems in which neither metal or ligand is hydrolysable or, more important in this study, in which metal-ligand complexation is so strong that the changing  $[H^+]$  does not affect complex dissociation. The latter situation occurs for methylmercury(II)-thiolate complexation. Proton nmr studies have shown that MeHg(II)-monothiolate complexes do not detectably dissociate in the range  $1 < pH < 13$ , i.e. protons (even at  $[H^+] = 0.1M$ ) cannot compete with thiolate for  $MeHg^+$ , and hydroxide (even at  $[OH^-] = 0.1M$ ) cannot compete with thiolate for  $MeHg^+$ . When such stable systems are titrated with acid or base, the pH only reflects changes in protonation of ligand sites not involved in MeHg-binding. An example of this effect is shown in Figure 6.2 for the methylmercury(II)-mercaptoacetate system. The solid curves have been calculated using the assumptions that only the species shown in Table 6.4 exist in solution (see also page 103 for discussion of this system). Values for stability constants of hydrolysed MeHg(II) and protonated ligand species were determined independently. The titration data shown in Figure 6.2 can be treated as a simple monoprotic acid HL, due to the carboxylate group of the complex, with acid dissociation constant  $pK_a^C = 3.757(6)$ , reflecting the lack of MeHg-thiolate dissociation. The data are seen to be very insensitive to changes in the stability



**Figure 6.2:** Calculated<sup>*α*</sup> and experimental titration curves for the methylmercury(II)-mercaptoacetate system in the absence of iodide.

<sup>*α*</sup> Using COMIXH with species formation constants shown in Table 6.4.

constant for MeHg-thiolate interaction.

Species	<u>log (formation constants) used for calculated curves</u>		
	A	B	C
MeHgOH <sup>a</sup>	-4.607	-4.607	-4.607
(MeHg) <sub>2</sub> OH <sup>+a</sup>	-2.234	-2.234	-2.234
HSCH <sub>2</sub> CO <sub>2</sub> <sup>-b</sup>	10.157	10.157	10.157
HSCH <sub>2</sub> CO <sub>2</sub> H <sup>b</sup>	13.710	13.710	13.710
MeHgSCH <sub>2</sub> CO <sub>2</sub> <sup>-</sup>	10.000	14.000	16.000
MeHgSCH <sub>2</sub> CO <sub>2</sub> H <sup>c</sup>	13.757	17.757	19.757

**Table 6.4:** Equilibrium data used by COMIXH to calculate solid curves in Figure 6.2.

<sup>a</sup>log  $\beta_{10-1}$  = -4.607 and log  $\beta_{20-1}$  = -2.234 are not true formation constants (page 64).

<sup>b</sup>Table 3.6 (page 90).

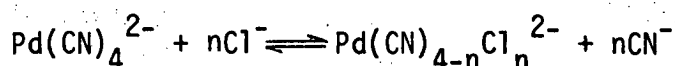
<sup>c</sup>this complex has  $\text{pK}_a^C = 3.757$  for carboxylate deprotonation (Table 3.8, page 98).

Attempts to extract log  $\beta_{110}$  (for formation of MeHgSCH<sub>2</sub>CO<sub>2</sub><sup>-</sup>) from the titration data would be fruitless, since any value between 14 and 16 will fit the experimental data satisfactorily. Unfortunately, the indiscrete use of sophisticated least-squares programs such as those described in Section 6.3.3 will generate values of log  $\beta_{110}$  etc. for high stability constants to which no useful meaning can be ascribed. Although it should be possible to calculate model-independent values of 'secondary' variables such as the average number of ligands  $L^{2-}$  bound to MeHg(II),  $\bar{Z}$ , and thereby use only data for which  $\bar{Z} < 1$  to obtain  $\beta_{110}$  for example, this approach does not seem to have been widely used for ternary [MLH] systems. For the situation of inadequate H<sup>+</sup>-competition,

values of  $\bar{Z}$  would not deviate significantly from 1 (i.e. complex MeHgL is undissociated) within the accessible range  $2 < \text{pH} < 12$ .

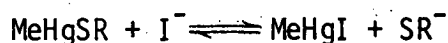
### 6.3.2 Evaluation of high stability constants for MeHg-thiolate complexes

In the situations where  $\text{H}^+$ - competition is ineffective, stability constants for high stability complexes can be obtained indirectly. By analogy to  $\text{H}^+$ - competition, addition of a second metal ion which competes with MeHg(II) for ligand could be used. This approach has been used to investigate transition-metal complexation with EDTA, using  $\text{Hg}^{2+}$  as competing metal.<sup>740</sup> An alternative approach, used here, is to use a second ligand, which competes with thiolate for protons and MeHg(II). Chloride, for example, has been used to obtain  $\log \beta_4 = 63$  for  $\text{Pd}(\text{CN})_4^{2-}$  formation, by competition with cyanide<sup>741</sup> in the equilibria:

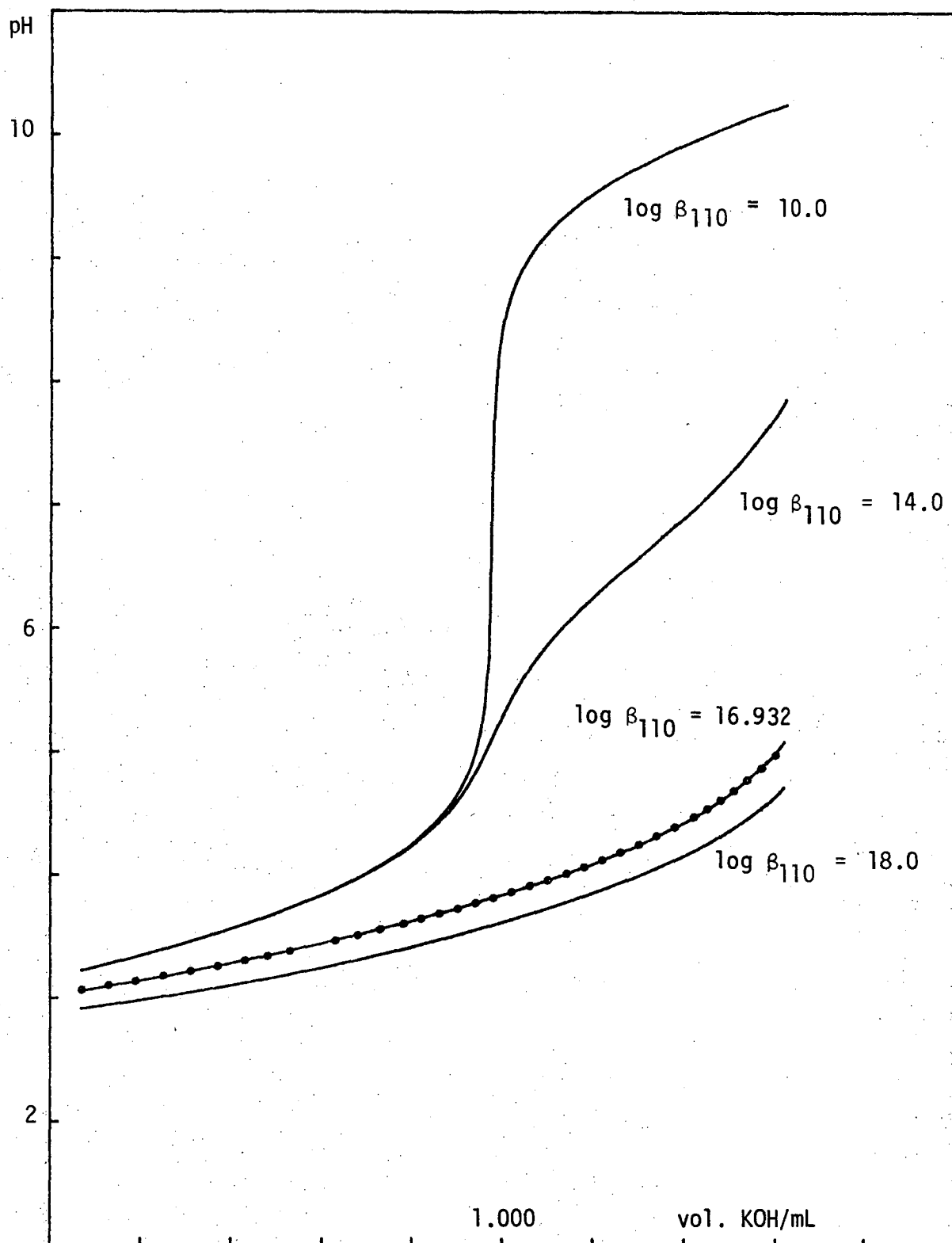


Since the formation constants of  $\text{Pd}(\text{Cl})_n^{(n-2)-}$  complexes can be determined using  $\text{H}^+$ - competition, these can be used, together with values of the competition equilibrium constants, to evaluate  $\beta_4$  for the formation of  $\text{Pd}(\text{CN})_4^{2-}$ .

Schwarzenbach and Schellenberg<sup>305</sup> have used iodide competition to obtain values of formation constants for MeHg(II) with glutathione and mercaptoethanol. This work has extended their method to other monothiols by evaluating the equilibrium constants for the competition:



The effectiveness of this approach can perhaps best be seen by re-appraisal of the MeHg(II)-mercaptoacetate system (Figure 6.3) in the presence of 0.1M KI. The calculated titration curves assume the same



**Figure 6.3:** Calculated<sup>a</sup> and experimental titration curves for the methylmercury(II)-mercaptoacetate system in the presence of 0.1M KI. <sup>a</sup>Using COMIXH with species formation constants shown in Table 6.4 and  $\log \beta(\text{MeHgI}) = 8.500$ . The complex  $\text{MeHgSCH}_2\text{CO}_2\text{H}$  has  $\text{pK}_a^C = 3.757$  for carboxylate deprotonation (Table 3.8, page 90).

species as those in Figure 6.2, but in addition, include  $\log \beta(\text{MeHgI}) = 8.500$ . It can be seen that the titration data are best fitted using  $\log \beta_{110} = 16.932$  and are much more sensitive to values of  $\log \beta_{110}$  than the titration performed in absence of iodine. Methylmercury(II)-monothiolate stability constants obtained by this method, are discussed in Section 3.3.

It has been found in this work that the complexes formed between  $\text{MeHg(II)}$  and the vicinal dithiols  $\text{BALH}_2$  and Unithiol are too stable even for iodide competition to be used effectively to determine the formation constants for 1:1 interaction (page 138). Treatment of these systems, using mercaptoethanol as a competing ligand, has been discussed previously (page 139).



### 6.3.3. Computer programs for the evaluation of metal-ligand stability constants

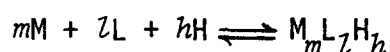
Except for the simplest mononuclear systems of metal-ligand complexes, evaluation of species formation constants is almost exclusively performed nowadays by computer programs using multiparametric curve fitting techniques. Several such programs have been described to date, and their advantages and idiosyncracies reviewed. Four of these have achieved dominant use, due to their wide areas of applicability and ready availability. Sillén's LETAGROP<sup>742</sup> was the original in the field and is still the most comprehensive (versions are available for treatment of heterogeneous systems, with spectrophotometric, potentiometric, coulometric data), but is not widely used outside Scandinavian circles. The program SCOGS<sup>743</sup> by Perrin and Sayce is still widely used, and has been used to refine the formation constants of some MeHg(II)-thiol-iodide systems in this study. The main competitor with SCOGS is Vacca and Gans' MINQUAD.<sup>744-6</sup> Several versions of this program have evolved since its inception (1974) and it is now widely used. It has been found elsewhere, and in this work, that MINQUAD is much faster than SCOGS in refinement of many equilibrium systems and has in consequence been used nearly exclusively in this study. The most recent program of which this author is aware is DALSFEK, which is unique in being able to simultaneously treat spectrophotometric and potentiometric data.<sup>746</sup> Copies of DALSFEK were only recently available,<sup>690</sup> and so this program has not been used in this study.

All current programs refine initial estimates of complex species formation constants, by iteratively solving the appropriate system of component mass-balance equations described below. It must be emphasised that these procedures require an *a priori* description of the equilibrium species which are expected to be sufficient to describe

<sup>†</sup>The version used here was kindly provided by Dr. R.N. Sylva (Australian Atomic Energy Commission).<sup>747</sup>

the relevant equilibrium system under study. The programs, as yet, are not able to determine the *nature* of the species present, or even their number. The decision remains with the chemist, who must subjectively consider the relative chemical and statistical virtues of the computer generated fits to his experimental data, calculated with different proposed equilibrium models.

We write the overall formation equilibrium of the complex species  $M_m L_z H_h$  from its components M,L,H as follows:



with overall stoichiometric formation constant

$$\beta_{mzh} = \frac{[M_m L_z H_h]}{[M]^m [L]^z [H]^h}$$

The three mass balance equations for conservation of M,L,H can be written in terms of all  $N$  supposed species

$$M_T = [M] + \sum_{i=1}^N m_i \beta_{mzh} [M]^{m_i} [L]^{z_i} [H]^{h_i}$$

$$L_T = [L] + \sum_{i=1}^N z_i \beta_{mzh} [M]^{m_i} [L]^{z_i} [H]^{h_i}$$

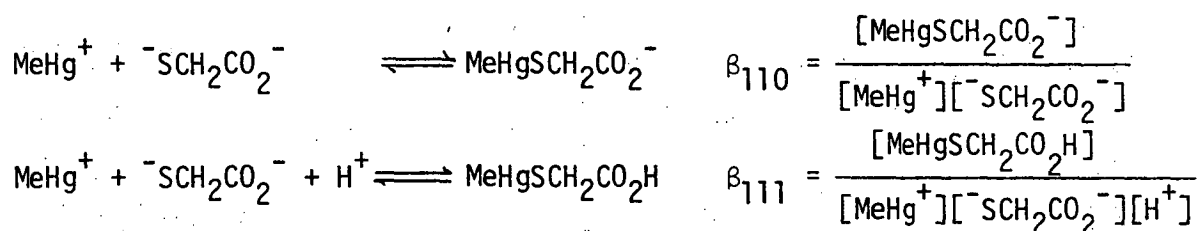
$$H_T = [H] + \sum_{i=1}^N h_i \beta_{mzh} [M]^{m_i} [L]^{z_i} [H]^{h_i}$$

These equations can of course be generalised to any number of components, e.g. in this study it has been necessary to consider four components simultaneously:  $\text{MeHg}^+$ ,  $\text{I}^-$ , thiolate and  $\text{H}^+$ ; or  $\text{MeHg}^+$ , dithiolate, thiolate and  $\text{H}^+$ .

It may be informative to mention that it has been shown that it

is not compulsory to consider the 'free' or uncomplexed species M,L,H as components.<sup>748</sup> All equilibria could equally well be written in terms of formation from the complex species MLH for example, in which case MLH may be considered as a component and  $\beta$ 's changed accordingly. This technique has been used in this study to evaluate equilibrium constants for the addition of a second MeHg(II) group to the 1:1 MeHg(II) complex of L-cysteine (page 111). In this case, the complex  $\text{MeHgSCH}_2\text{CH}(\text{NH}_2)\text{CO}_2^-$  was considered as a component or 'ligand' which could be further protonated or coordinated to  $\text{MeHg}^+$ .

A significant weakness of MINIQAD, and of all similar currently available programs of which this author is aware, becomes evident with the relatively simple MeHg(II)-thiolate systems studied here. Such programs refine values of *overall* formation constants, e.g. for the simple MeHg(II)-mercaptoacetate system described previously (page 320), these are  $\beta_{110}$  and  $\beta_{111}$ :



The first constant indicates the affinity of  $\text{MeHg}^+$  for the deprotonated sulfhydryl group of the ligand. The second reflects not only protonation of the carboxylate group of the MeHg(II)-thiolate complex, but also the affinity of  $\text{MeHg}^+$  for the deprotonated sulfhydryl group. Thus the two constants are highly correlated and simultaneous refinement of them by SCOGS or by several versions of MINIQAD, has been found here to be slow. In several of the other MeHg(II)-thiolate systems, described in Chapter 3, which have two or three acidic groups involved in proton association in addition to the sulfhydryl group involved in MeHg(II) complexation,

correlation between overall formation constants has been found to be extreme. Simultaneous refinement of these constants, using data over a wide pH-range, often fails (except with very good initial estimates) or at best is very slow.

In a chemical sense, a set of overall constants, e.g.  $\beta_{110}$  and  $\beta_{111}$  above, contains redundant information, i.e.  $\beta_{111}$  excludes a component due to MeHg(II)-thiolate association, namely  $\beta_{110}$ :

$$\log \beta_{111} = \log \beta_{110} + pK'_a(\text{CO}_2\text{H})$$

The proton dissociation constant,  $pK'_a$ , for the carboxylate group of the MeHg(II)-thiolate complex can be obtained from highly correlated  $\beta_{110}$  and  $\beta_{111}$  (Table 3.8)

$$\text{thus: } pK'_a(\text{CO}_2\text{H}) = 20.689(11) - 16.932(12) = 3.757(6)^\dagger$$

An identical value 3.78(2) has been found by titrating the solid protonated complex in the absence of iodide and treating the complex as a simple monoprotic acid (page 98 ).

The problem of correlation would be alleviated if refinement of *stepwise* stability constants, e.g.  $\beta_{110}$  and  $pK'_a$ , could be achieved. Surprisingly however, general programs do not seem to be available for this purpose. The major programming problem would seem to be the difficulty of defining a general system of equilibrium equations such as those described on page 327 in terms of stepwise constants. Although the

---

<sup>†</sup>As  $\beta_{110}$  and  $\beta_{111}$  are correlated, the standard deviations,  $\sigma$ , (in parentheses) are correlated. The standard deviations of  $pK'_a$  must be determined using the general relationship for correlated variables a,b: <sup>749</sup>

$$\sigma_{a \pm b}^2 = \sigma_a^2 + \sigma_b^2 - 2\rho_{ab}\sigma_a\sigma_b$$

The correlation coefficient,  $\rho_{ab}$ , is obtained from the non-linear least-squares procedure.

term 'stepwise' has been used here to describe successive protonation equilibria, it could equally well apply to successive metal or ligand association, requiring a different set of equilibrium equations. Thus it would appear that programs would need to be specific to the equilibrium system at hand, and as such, would have limited general appeal. Specific programs have been written elsewhere when high correlations between overall constants is a problem<sup>750</sup> and the mathematical treatment of highly correlated multiparametric functions has been elucidated by Sillén.<sup>751</sup>

#### 6.4 Display of titration data and species distributions

As described in the previous section, the component mass-balance equations in complex equilibrium systems can be used to evaluate equilibrium constants by treating them as unknowns in a multiparametric least-squares refinement. In this situation, it is necessary to measure at least one of the component concentrations in order to solve the set of non-linear equations. (Concentrations of components, other than those measured, are also treated as unknowns and iteratively refined.)

In order to efficiently display the contents of such an equilibrium system it is usual to draw the concentrations of the participating species as a function of an experimental variable, e.g. volume of base added or pH etc. so long as the equilibrium constants have been established. To this author's knowledge there are two generally published computer programs for this purpose: COMIC (Concentrations in Mixtures of Metal Ions and Complexing Species) by Perrin and Sayce<sup>752</sup> and HALTAFALL by Sillén's group.<sup>753</sup>

The latter program is very comprehensive and can account for heterogeneous as well as homogeneous systems in the gas, liquid and solid phases. Its main drawback is due to its generality inasmuch as data input is extremely tedious and the program is large and is therefore necessarily implemented

on large computers. COMICS on the other hand is much smaller (and thus less general) and can only handle homogeneous equilibria, but was admirably suited to implementation on the departmental Digital PDP8/e minicomputer.

Experience with the original COMICS indicated that it was abysmally slow to solve the non-linear mass-balance equations (for a given pH value) for many of the more complex MeHg(II)-thiolate equilibria described in Chapter 3. Since the production of a species distribution diagram may require the solution of these equations at 50-200 pH values in succession, a more efficient algorithm was devised and incorporated into the new program COMIX.

#### 6.4.1 COMIX

The major problem with COMICS seems to be due to the use of numerical differentiation in the Gauss-Newton iterative procedure. The mass-balance equation can, however, be analytically differentiated with respect to the component concentrations. It has been found here that the use of analytical expressions for these derivatives, increased the efficiency of COMICS by an order of magnitude, at least.

The advantages of analytical derivatives in equilibrium calculations was noted independently elsewhere<sup>754</sup> and the program MINQUAD (and earlier versions) uses analytical derivatives to refine overall formation constants.

A further difficulty encountered with COMICS was that the iteratively calculated values of some component concentrations occasionally converged to negative values. To prevent against this occurrence, component concentrations were restrained to be positive by rewriting the mass-balance equations in terms of  $\ln[M]$  etc., rather than  $[M]$  as shown below for the simple system containing metal, ligand and protons:

$$M_{\text{tot}} - [M] - \sum_{i=1}^N m_i \beta_i [M]^{m_i} [L]^{z_i} [H]^{h_i} = 0$$

To solve the system of two non-linear equations (one in  $[M]$  above, and the analogous one in  $[L]$ ) by the Gauss-Newton iterative method, it is necessary to write the left-hand side of this equation as the function  $F$ , and obtain the derivatives  $\partial F/\partial[M]$  and  $\partial F/\partial[L]$ .

If the mass-balance equation in  $[M]$  is logarithmically transformed, it becomes

$$F = M_{\text{tot}} - \exp(\ln[M]) - \sum_{i=1}^N m_i \beta_i \exp(m_i \ln[M] + z_i \ln[L] + h_i \ln[H]) = 0$$

The transformed ligand mass-balance equation is analogous and both equations are readily differentiated with respect to  $\ln[M]$  and  $\ln[L]$ .

The program COMIX using this new logarithm (analytical derivatives and logarithmic variables) has been used to efficiently calculate all the species distributions shown in this thesis, and draw them on a Hewlett-Packard HP7221A plotter.

#### 6.4.2 COMIXH

A closely similar procedure can be applied to the calculation of a hypothetical 'titration' curve, given the total concentrations of all components and all equilibrium constants which define the system.<sup>748</sup> However, this situation differs from that described above for the calculation of species distributions, in that  $[M^+]$  is now no longer known, but needs to be treated as an unknown in the mass-balance equations (now three: in  $\ln[M]$ ,  $\ln[L]$  and  $\ln[H]$ ).

A computer program, COMIXH, has been written as a modified version of COMIX, in order to calculate and draw the titration curves shown in Chapter 3. A listing of COMIXH, which contains all the essential

features of the COMIX algorithm, has been included as Appendix 2.

#### 6.5 Appendix. A simple device for monitoring attainment of pH-equilibrium

Some modern pH-meters incorporate a facility to indicate when a pH (or mV) reading is 'stable' according to the manufacturer's criteria. The Model 701A Orion pH-meter used in this study does not have this facility, and the use of a chart-recorder connected to the 10 mV analog output of the pH-meter, is one means of monitoring attainment of equilibrium.

Figure 6.4 describes a simple electronic device which can be attached to the  $3\frac{1}{2}$  digit BCD output of the Model 701A meter, and which generates a visible or audible alarm when the digital display remains unchanged for a predetermined length of time. The device was designed to detect stability of the least significant digit (lsd) for periods of 30s to 5 minutes, by monitoring the two least significant bits (lsb's) of the lsd. The particular time period can be varied by the operator to suit titration conditions. The device ignores one digit oscillations of the lsd (digital 'noise') by logically combining the lsb of the second least significant digit with the lsd input.

In principle, most devices with continuous BCD output could be monitored for stability with this circuit. The audible/visible alarms could easily be replaced by triggers for automatic pH-printout or activation of an automatic burette etc.. allowing inclusion of the device in a fully automated potentiometric data acquisition system.



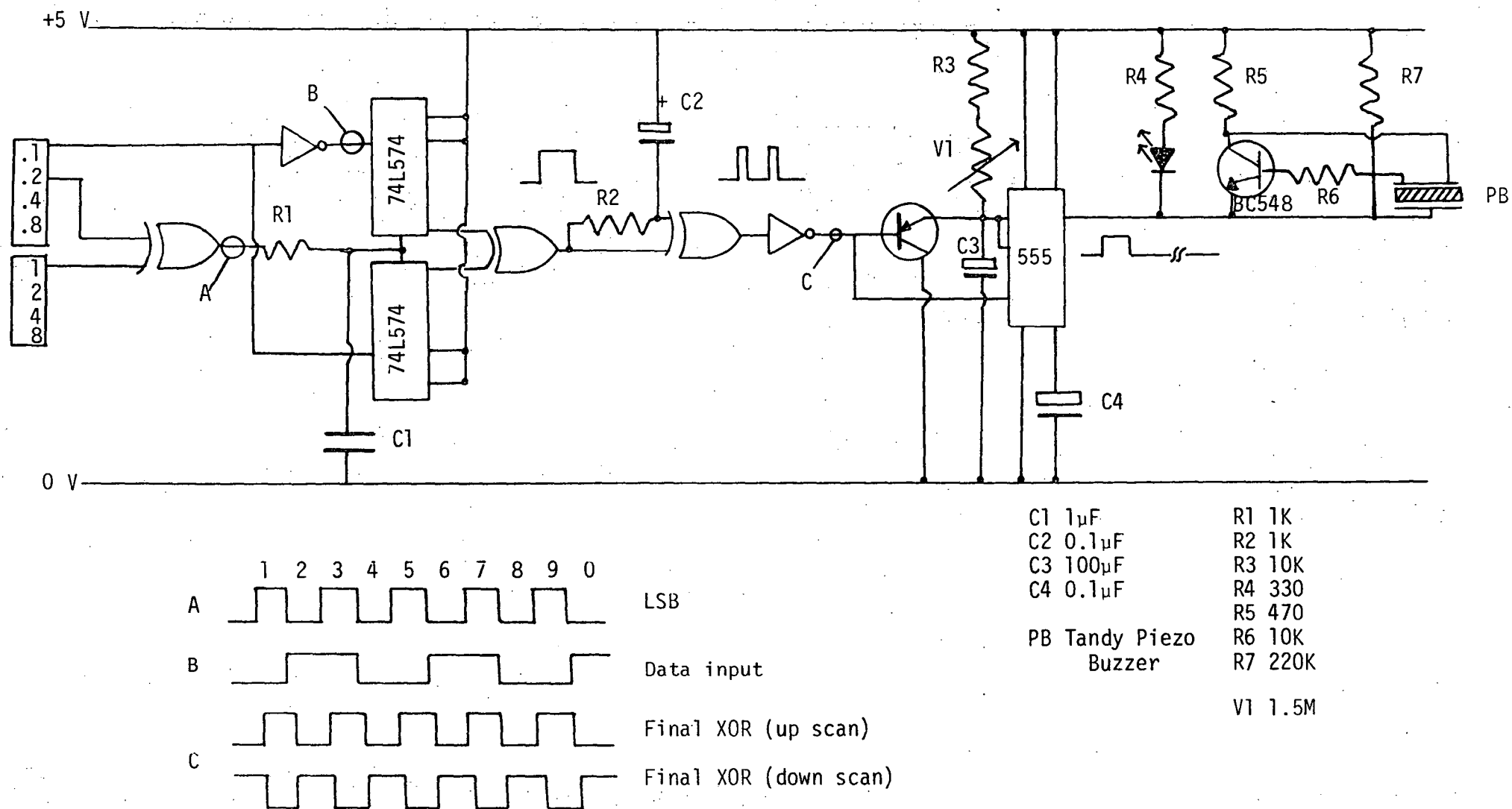


Figure 6.4: Circuit diagram for a device for testing for pH-stability.

## CHAPTER SEVEN

### EXPERIMENTAL

Microanalyses were carried out by the Australian Microanalytical Service, Melbourne, on samples dried over  $P_2O_5$  at room temperature unless otherwise stated. Melting points were determined with a Reichart Thermo apparatus and stereomicroscope, and are uncorrected.

The 100 MHz proton magnetic resonance ( $^1H$  nmr) spectra were recorded with a JEOL-JNM-4H-100 spectrometer by Mr. R.R. Thomas in this Department. Tetramethylsilane (TMS) was used as an internal standard. Chemical shifts ( $\delta$ ) are given in parts per million relative to TMS, coupling constants were measured directly from spectra recorded with a sweep width of 900 Hz and are reliable to  $\pm 1$  Hz unless otherwise stated. Resonances are described as singlets(s), doublets(d), triplets(t), quartets(q), or as multiplets(m). Spectra were obtained at a temperature of  $15^\circ$

Infrared spectra ( $4000-400\text{ cm}^{-1}$ ) were recorded in Nujol or hexachlorobutadiene mulls (unless otherwise stated) between KBr plates with a Perkin-Elmer 577 spectrometer. Far infrared spectra were recorded with a Perkin-Elmer 577 spectrometer ( $600-200\text{ cm}^{-1}$ ) or Perkin-Elmer 180 spectrometer ( $500-100\text{ cm}^{-1}$ , Monash University, Melbourne) as Nujol mulls between polyethylene plates. Unless otherwise stated, spectra were obtained at room temperature.

Raman spectra were obtained from samples in sealed capillaries with a Cary 82 Laser Raman spectrometer using  $Ar^+$  514.5 nm radiation (60-100 mW at sample) unless otherwise stated. For some samples, particularly those containing selenium, it was necessary to use a Coherent Radiation Model 190 dye laser (Rhodamine 6G) as the exciting source to prevent

sample decomposition or minimise sample fluorescence. For some samples, it was further necessary to defocus the incident laser beam by sample spinning, and for  $\text{Hg}(\text{SeCH}_2\text{CO}_2\text{H})_2$  it was necessary to cool the sample to 10 K with a Cryodyne Model 21 cryostat.

Maximum errors are considered to be  $\pm 4 \text{ cm}^{-1}$  for both i.r. and Raman spectra. The ultraviolet absorption spectra were obtained on a Cary 17 spectrophotometer, using 1 cm quartz cells.

Mass spectra were obtained with a Vacuum General Micromass 7070F spectrometer using the direct insertion technique, with electron beam energy 70 ev. Peaks of more than 10% base-peak intensity are reported in descending m/e order. High resolution accurate mass measurements were obtained on this instrument using electron impact ionisation unless otherwise stated.

Debye-Scherrer X-ray powder diffraction patterns were recorded photographically from finely ground samples contained in sealed Lindemann capillaries using Ni-filtered  $\text{CuK}_\alpha$  ( $\lambda = 1.5418 \text{ \AA}$ ) or Mn-filtered  $\text{FeK}_\alpha$  ( $\lambda = 1.9373 \text{ \AA}$ ) radiation. Automatically recorded powder diffraction patterns were obtained from some samples using a Philips diffractometer and ratemeter with Ni-filtered  $\text{CuK}_\alpha$  radiation. These patterns were calibrated with the  $2\theta = 56.12^\circ$  line of silicon.

### 7.1 General reagents

Ethanol (95%) was used with no further purification. Benzene, chloroform and acetone (AR grade) were used as received.

Pyridine and 4-methylpyridine were refluxed and distilled from potassium hydroxide before use.

Methylmercuric nitrate for synthetic studies was prepared by metathesis of silver nitrate and a slight excess of methylmercuric iodide (Alfa-Ventron) in water. The filtrate was evaporated to give a

colorless crystalline product which was stored over  $P_2O_5$ .

Solutions of methylmercuric nitrate, free of mercuric ion, were prepared for potentiometric studies. Preparation and analysis of these solutions for  $MeHg(II)$  and  $H^+$  content are recorded on page 92.

Mercuric salts  $HgCl_2$  (B.D.H. Ltd.),  $Hg(O_2CMe)_2$  (Ajax Chemicals Ltd.), and  $Hg(CN)_2$  (May and Baker Ltd.) were used as received.

Crystalline thiols were used as received and stored under nitrogen over  $P_2O_5$ : meso-2,3-dimercaptosuccinic acid and 2-mercaptosuccinic acid (Aldrich Chemical Co., Inc.), 2,3-dimercapto-1-propanesulfonate, sodium salt (Heyl and Co. Chem.-Pharm. Fabrik.), reduced glutathione (Sigma Chemical Co.), L-cysteine, DL-homocysteine, N-Acetyl-DL-penicillamine (Koch-Light Laboratories Ltd.) and DL-penicillamine (Ega-Chemie). Thiocholine perchlorate was a gift from P. Guerney, University of New South Wales.

Liquid thiols: 2-mercaptoethanol (Koch-Light), 1,3-dimercapto-2-propanol, 2,3-dimercapto-1-propanol (Aldrich) were fractionally distilled under reduced nitrogen pressure and stored under nitrogen at  $-20^\circ$ . Mercaptoacetic acid (Aldrich) was treated similarly after azeotropic distillation from benzene.

The purity of the thiols used in potentiometric titration studies was determined alkalimetrically prior to each titration, and are recorded in Chapter 3. Melting and boiling points are recorded in that chapter together with proton dissociation constants of the thiols.

## 7.2 General procedures used in organoselenium preparations

The offensive odours of many organoselenium reagents are legend, and all selenium chemistry was performed in an efficient fumehood. Much of the problem is due to relatively small amounts of volatile

impurities which may be formed during the preparative reactions, especially hydrogen selenide. All reactions were performed under a slow stream of nitrogen after rigorous nitrogen purging of apparatus to remove oxygen. The effluent nitrogen was passed through at least one trap containing 50% aqueous sodium hydroxide (to form NaSeH) and then into a lead acetate solution. All glassware, used gloves, etc. were decontaminated by soaking in 10% aqueous sodium hypochlorite solution which converts offensive selenols etc. into odourless, non-volatile, oxidised products.

Many of the organoselenium preparations make use of an ethanolic solution of sodium hydrogenselenide, NaSeH. This reagent is very conveniently produced using the method of Klayman and Griffin<sup>487</sup> by reacting finely ground grey selenium, which had been stored over P<sub>2</sub>O<sub>5</sub>, with sodium borohydride in 95% ethanol until a nearly colourless solution is obtained. These authors describe the addition of ethanol to the mixture of solid selenium and NaBH<sub>4</sub>. This reaction was found to be extremely vigorous on a moderate scale with the rapid evolution of considerable quantities of hydrogen, and required careful cooling in ice to moderate the reaction. Some H<sub>2</sub>Se is produced, especially in the initial stages of ethanol addition. It was subsequently found that addition of an ethanolic sodium borohydride solution to a vigorously stirred slurry of grey selenium in ethanol, contained in a 3-necked flask equipped with nitrogen inlet, double surface reflux condenser and pressure-equalised dropping funnel, was a much more controllable and cleaner, if slightly longer, procedure. The purity of sodium borohydride used in this work was found to be quite variable, despite storage in tightly closed containers. This seemed to be due to some decomposition to sodium carbonate, which was difficult to dissolve in ethanol. As a consequence, it was invariably necessary to add small quantities of solid NaBH<sub>4</sub> to

the final NaSeH solution to achieve total reduction of red diselenide,  $\text{Se}_2^{2-}$ , to colorless  $\text{HSe}^-$ .

The use of 95% ethanol in this procedure produces some  $\text{H}_2\text{Se}$  due to the reaction of selenium and sodium borohydride with water impurity, however this was a minor inconvenience since efficient traps were used and substitution with absolute ethanol was not considered warranted.

After reaction (e.g. alkylation) with the ethanolic NaSeH solution the reactant mixture was often acidified with glacial acetic acid to pH 4 (tested with indicating paper) in order to ensure that any derived selenol product was fully protonated, and to facilitate subsequent ether extraction. This procedure also protonates any anionic selenide impurity and excess NaSeH to  $\text{H}_2\text{Se}$ , and decomposes excess sodium borohydride to hydrogen. Dissolved  $\text{H}_2\text{Se}$  was removed before further workup by vigorously bubbling nitrogen through the reactant mixture. Simultaneously reducing the pressure inside the apparatus by slight water-pump aspiration aided  $\text{H}_2\text{Se}$  removal. Absence of hydrogen selenide was confirmed by testing the effluent nitrogen with lead-acetate paper until no darkening ( $\text{PbSe}$ ) occurred. The resultant mixture, often containing small amounts of undissolved grey selenium, was most conveniently filtered in a static nitrogen atmosphere through a pressure-equalised sinter containing a bed of acid-washed sand.

Subsequent reduction of solvent volume was performed on a Büchi evaporator under water-pump vacuum, with nitrogen purging to restore atmospheric pressure. Solvent extraction was performed using peroxide-free ether in nitrogen purged separating funnels to avoid spurious oxidation of products.

These experimental details are not repeated in specific preparations, except where significant deviations were required.

### 7.3 Preparation of complexes [MeHg(II) and Hg<sup>2+</sup>] of dithiols and model thiols

#### (meso-2,3-dimercaptobutanedioato)bis[methylmercury(II)], (MeHg)<sub>2</sub>DMSH<sub>2</sub>

A filtered solution of MeHgNO<sub>3</sub> (0.445 g, 1-60 mmol) in 15 mL EtOH was rinsed into 20 mL ethanolic solution of meso-2,3-dimercaptosuccinic acid, with 5 ml EtOH. Evaporation of the clear solution deposits (MeHg)<sub>2</sub>DMSH<sub>2</sub> as very small needles which were collected by filtration at low volume and dried *in vacuo*. The analysis of this product is shown in Table 2.2, page 38.

Infrared absorption: 3070w,sh, 2980m,br, 1677vs, 1422s, 1311s and 1290w,sh, 1219vw, 1188 and 1176s, 950m, 785m, 686m, 632m, 530w,sh, 537m, 433m, 352s, 279m, 226w.

Raman bands: (below 1200 cm<sup>-1</sup>, sample decomposes): 1195m, 1075vw, 974vw, 822s, 782vw, 708vw,sh and 675s, 550s and 535vw,sh, 391w, 358m, 320vw,sh and 309m.

<sup>1</sup>H nmr (D<sub>2</sub>O, pH = 7-8) δ(CH<sub>3</sub>Hg) -3.00 (dioxane = 10.0), |<sup>2</sup>J(<sup>1</sup>H-<sup>199</sup>Hg)| = 172.0 Hz.

#### poly-(meso-2,3-dimercaptobutanedioato)mercury(II) dihydrate, Hg(DMSH<sub>2</sub>)·2H<sub>2</sub>O

An ethanolic (20 mL) solution of meso-2,3-dimercaptosuccinic acid (0.092 g, 0.50 mmol) was added with stirring to mercuric chloride (0.272 g, 1.0 mmol) in 10 ml EtOH. The slightly cloudy solution was filtered and evaporated to give a white powder at low volume. The product was collected, washed with acetone and dried *in vacuo*. Yield 0.13 g (68%).

The analysis shown in Table 2.4, page 49 is consistent with a dihydrate.

Infrared absorption: 3200-3600m,vbr, 2900w, 1710s,br, 1565w, 1360m,br, 1290w,br, 1220w,br, 1170vw,sh, 800vw, 389m, 306vw, 216w, 180vw.

This sample gives an unusable Raman spectrum.

(2,3-dimercapto-1-propanesulfonato)bis[methylmercury(II)], sodium salt,  
MeHgSCH<sub>2</sub>CH(SHgMe)CH<sub>2</sub>SO<sub>3</sub>Na, Na[(MeHg)<sub>2</sub>UT]

A solution of MeHgNO<sub>3</sub> (1.36 g, 4.91 mmol) in methanol (10 mL) was filtered into a stirred methanolic solution of Unithiol (0.545 g, 2.46 mmol) containing 2.5 mL 2M NaOH. When approximately one-third of the MeHgNO<sub>3</sub> was added, cloudiness persisted. The slightly cloudy solution was filtered and the filtrate evaporated to low volume. Fine microcrystals were collected by filtration and dried over P<sub>2</sub>O<sub>5</sub> (the product seems to be hygroscopic).

The analysis of anhydrous Na[(MeHg)<sub>2</sub>UT] is shown in Table 2.2, page 38. Infrared absorption: 3200-3650w,br, 1632w, 1187m,br, 1054vs, 967w, 892w, 854vw, 838m, 783s.br. 724m, 660w, 586m, 526m, 4552, 412vw, 333w,br. Raman bands (below 1200 cm<sup>-1</sup> only): 1184m, 1057w, 780w, 713w, 655vw, 585vw, 531s, 329m,br. <sup>1</sup>H nmr (D<sub>2</sub>O, pH = 6.2) δ(CH<sub>3</sub>Hg) -2.80 (dioxane = 10.0), |<sup>2</sup>J(<sup>1</sup>H-<sup>199</sup>Hg)| = 171.0 Hz.

poly-(2,3-dimercapto-1-propanesulfonato)mercurate(1-), sodium salt,  
Na[Hg(UT)]

Unithiol (1.30 g, 5.68 mmol) was dissolved in water (10 mL) and partially neutralised with NaOH (5.16 mL 2M, 110.3 mmol). To this solution was added 10 ml aqueous solution of mercuric acetate (1.65 g, 5.16 mmol) in portions with stirring, waiting for the white precipitate to dissolve before the next addition. The slightly brown solution was filtered and evaporated to low volume but no crystallisation occurred. A very small amount of residue was removed by filtration, and ethanol added to precipitate a white powder which was filtered with difficulty. Drying *in vacuo* over P<sub>2</sub>O<sub>5</sub> yielded a slightly sticky product which appeared



somewhat heterogeneous and consequently was not analysed. The product is probably hygroscopic like the bis(methylmercury) complex and the free ligand.

Infrared absorption: 3100-3600m,vbr, 1675m, 1283vw.sh, 1265vw.sh, 1200s,vbr and 1130w,sh, 1050s and 1028w,sh, 970w, 892vw, 853vw, 785vw, 580w and 540vw, 360w,sh.

Raman bands (below 1200  $\text{cm}^{-1}$  only, poor quality spectrum): 1063w, 790w, 700vw,br, 632vw, 578vw, 510vw,br, 316s,br.

2-mercaptoputanedioato(methyl)mercury(II),  $\text{MeHg}[\text{SCH}(\text{CO}_2\text{H})\text{CH}_2(\text{CO}_2\text{H})]$

A solution of  $\text{MeHgNO}_3$  (0.91 g, 3.26 mmol) in 5 mL acetone was filtered into an acetone (5 mL) solution of 2-mercaptopuccinic acid (0.488 g, 3.25 mmol) and 1 mL water. The clear solution was evaporated under nitrogen and colorless needles were collected by filtration at low volume, washed with acetone and dried *in vacuo*. The filtrate deposited more crystals on further evaporation. Total yield 0.97 g (82%).

The analysis of this product is shown in Table 2.2, page 38.

Infrared absorption: 1705w,sh and 1680vs, 1410w, 1310m,br and 1260vw,sh, 1218vw, 1192m, 1178m and 1160vw,sh, 1054vw, 962m and 945w,sh, 780m, 673m, 617m, 539m and 524vw,sh, 448m,br, 377vw,sh and 361m, 296s,br.

Raman bands: 2985w,br, 2915s, 1635w, 14302, 1265vw, 1193s, 955w, 782w, 710vw, 677w, 620w, 550vs and 526 vw,sh, 420vw, 362m, 298s, 215w, 147m,sh and 147m,

( $\text{D}_2\text{O}$ , pH = 5.2) 2988m, 2927s, 2874m, 1415w, 1318vw, 1191s, 1025vw, 950 vw,br, 547vs, 365m.

$^1\text{H}$  nmr ( $\text{D}_2\text{O}$ , pH = 5.2)  $\delta(\text{CH}_3\text{Hg})$  -2.99 (dioxane = 10.0),  $|^2J(^1\text{H}-^{199}\text{H})| = 173.4$  Hz.

Attempted preparation of bis(2-mercaptobutanedioato)mercury(II)

Addition of mercuric acetate (3.28 g, 10.3 mmol) in 15 mL water to a solution of 2-mercaptosuccinic acid (3.09 g, 20.6 mmol) gave a clear solution which deposited white microcrystals at very low volume but which rapidly turned black and obviously decomposed.

(1-methyl-3,4-dimercapto)bis[methylmercury(II)]

An aqueous (5 mL) solution of  $\text{MeHgNO}_3$  (1.30 g, 4.70 mmol) was added with stirring to toluene-3,4-dithiol (0.442 g, 2.83 mmol) in 5 ml warm water containing NaOH (0.266 g, 6.6 mmol). (The dithiol melts at room temperature, making weighing difficult). The resultant oily mixture was stirred with ethanol (5 mL) and separated into a gum and white precipitate which was collected by filtration after 2 hr. The crude product was dissolved in 30 mL hot toluene and the solution filtered to remove some yellow residue. The filtrate deposited a white powder overnight which was collected and dried in air.

The analysis of this product is shown in Table 2.2, page 38.

Infrared absorption: 1594w, 1308vw, 1256w, 1210w, 1175vw,br, 1105w, 1029m, 871 and 858m, 808s, 770m, 685w, 549w, 528w, 354w, 335w, 273m,br.  
Raman bands: 3042w, 2913m, 1608m, 1575w, 1472w, 1397w, 1290 and 1275w, 1229m, 1200m, 1126s, 1050m, 887w, 689w, 650vw,br, 526vs, 470w, 447w, 415w, 370 and 357m, 337w, 300vw, 263m.

[N,N,N-trimethylaminoethylmercapto(methyl)mercury(II)] perchlorate

Methylmercuric nitrate (0.66 g, 2.38 mmol) in 1 ml water was added to thiocholine perchlorate dissolved in hot water (5 mL). Within two minutes, on cooling, the solution deposits colorless crystals which were collected by careful Buchner filtration on a small paper and dried

over  $P_2O_5$ . (CAUTION - perchlorate salts of sulfur-containing compounds are potentially explosive. The crystals were collected using a polyethylene 'spatula' to prevent scratching.)

Yield 0.73 g (71%), mp. 163-5°.

The analysis of this product is shown in Table 2.2, page 38.

Infrared absorption: 3040w, 2000w, 1492w and 1475m, 1418m, 1343w, 1186m, 1085vs,br, 1008m, 966m, 942w, 892m, 774 and 764m, 727w, 621vs, 542m, 454w, 381vw, 359m, 329s, 287w.

Raman bands: 3040m, 2985m and 2940w, 2909m, 1452w, 1405vw, 1181s, 1090w,br, 970w, 943vw,sh and 931vs, 908w, 894w, 772m, 725w, 621w, 542vs, 500vw, 478w, 331s.

$^1H$  nmr ( $D_2O$ ):  $\delta(CH_3Hg)$  -2.97 (dioxane = 10.0),  $|^2J(^1H-^{199}Hg)| = 169.6$  Hz.

#### 4,4'-dimercapto-N-methylpiperidine hydrate

This intermediate was prepared according to the method of Barrera and Lyle<sup>406</sup> for subsequent reduction to 4-mercapto-N-methylpiperidine.

N-methyl-4-piperidone (14.2 g, 125 mmol, bp. 56-8°/10 mm) was dissolved in 100 mL isopropanol. Hydrogen sulfide<sup>†</sup> (CAUTION) was passed from a Kipp's generator at 2 bubbles/sec through the  $Pr^iOH$  solution cooled in ice which deposited white crystals of the product after 3½ hrs. The crystalline product was collected after 8 hours by filtration and washed with cold  $Pr^iOH$  (3 x 5 mL). On standing at -20° for 48 hrs, the filtrate deposited a second crop of product which was combined with the first. Total yield 20.32 g (90%), mp. ~54° (dec.) [lit.<sup>406</sup> 48-50°].

---

<sup>†</sup>Effluent  $H_2S$  was trapped in 10%  $CuSO_4$  in 0.3N  $HCl$ . The  $H_2S$  has a distinct tendency to suck back into the reaction vessel.

4-mercapto-N-methylpiperidine

4,4'-Dimercapto-N-methylpiperidine hydrate (10.7 g, 59 mmol) was suspended in 27 mL isopropanol and added in small portions to a stirred suspension of sodium borohydride (3.55 g, 94 mmol) in 27 mL  $\text{Pr}^i\text{OH}$  under nitrogen. The mixture was cooled in ice to moderate the exothermic reaction (evolution of  $\text{H}_2\text{S}^\dagger$ ). After 30 min additional stirring, more  $\text{Pr}^i\text{OH}$  was added (20 mL) and the stirred pale yellow mixture heated on a water bath at  $58^\circ$  for 2 hrs. The solution was then acidified (Congo Red) by dropwise addition of ethanolic HCl (12.7M, CAUTION  $\text{H}_2$  evolution) to decompose excess borohydride, and diluted with water (20 mL) to dissolve inorganic salts. After the addition of solid KOH to pH 12, the aqueous solution was extracted with ether (4 x 35 mL).

The combined ether extracts were dried over magnesium sulfate then evaporated by flash rotary distillation under nitrogen to yield a slightly cloudy colorless oil which was fractionally distilled, bp.  $31.5\text{--}2^\circ/1\text{ mm}$  [lit.<sup>406</sup>  $62^\circ/0.8\text{ mm}$ ]. The oil freezes to a colorless crystalline solid, mp.  $7\text{--}9^\circ$ .

Mass spectrum:  $M^{+\cdot} = 130.0684$ ; calc. for  $\text{C}_6\text{H}_{13}\text{NS} = 130.0690$ .

The acid dissociation constants of the N-protonated form of this thiol are recorded in Table 3.6, page 91.

[4-mercapto-N-methylpiperidinium(methyl)mercury(II)] nitrate

4-Mercapto-N-methylpiperidine (0.207 g, 1.59 mmol) was added by syringe to a stirred aqueous (5 mL) solution of  $\text{MeHgNO}_3$  (0.445 g, 1.60 mmol). The clear, colorless solution was evaporated to low volume and the resulting colorless crystals collected on a sinter, washed with

---

<sup>†</sup>Effluent  $\text{H}_2\text{S}$  was trapped in 10%  $\text{CuSO}_4$  in 0.3N HCl. The  $\text{H}_2\text{S}$  has a distinct tendency to suck back into the reaction vessel.

ethanol and dried *in vacuo* over  $P_2O_5$ . A second crop of crystals was

recovered from the filtrate, total yield 0.334 g (51%), mp. 176-8°.

The analysis of this product is shown in Table 2.2, page 38.

Infrared absorption: 3025m, 2945w,br, 2900w, 2700w,br, 1715w,br,

1480m, 1450w, 1385s,br and 1300s, 1250m, 1216m, 1170w, 1150m, 1127w,

1110w, 1085m, 1067w, 1040m, 1021w, 979s and 968m,sh, 832s, 808w,

760m,br, 748w, 719w, 549w,sh and 535m, 484w, 458w, 423w, 371m, 348m,

3212, 269w.

Raman bands (below 1500  $cm^{-1}$  only): 1482w, 1430w, 1262w, 1218m, 1175m,

1081w, 1043s and 1024m, 882w, 803w, 750s, 718w, 539vs, 487w, 459w,

425vw, 373m, 353m, 323m, 195s.

$^1H$  nmr ( $D_2O$ )  $\delta(CH_3Hg)$  = -2.97 (dioxane = 10.0),  $|^2J(^1H-^{199}Hg)|$  =

169.6 Hz.

#### 7.4 Preparation of selenium compounds and complexes (and S-analogs)

##### Diselenides $R_2Se_2$ ( $R=Me, Et$ )

The diselenides  $R_2Se_2$  ( $R=Me, Et$ ) were prepared by the alkylation of  $Na_2Se_2$  in liquid ammonia by the alkyl iodides.<sup>755-6</sup> Preparation of dimethyl diselenide will be described in detail.

Thinly sliced metallic sodium (3.26g, 140 mmol) was dissolved in approx. 150 mL liquid ammonia which had been previously dried over sodium and distilled into the 500 mL 3-necked reaction vessel via an acetone-dry ice condenser. Addition of small quantities of grey selenium (total 11.5g, 140 mmol) produced a color change from deep blue, through red brown to dark green. Methyl iodide (25g, 180 mmol) was added dropwise at a rate sufficient to dissolve the yellow  $Me_3SeI$  which formed. Water (50 ml) was added after evaporation of the ammonia at room temperature, and the deep crimson oil extracted with ether (4 x 50 ml). The combined yellow extracts were dried ( $CaCl_2$ ), evaporated and fractionally distilled *in vacuo* to give  $Me_2Se_2$  as a putrid orange oil, bp. 42-44°/8-9 mm. [lit.<sup>757</sup> 43-4°/15mm].

Diethyl diselenide was prepared similarly (using ethyl iodide) as a putrid orange oil, bp. 68-70°/9-10 mm [lit.<sup>757</sup> 74-5°/14 mm].

##### catena-Bis( $\mu$ -methaneselenolato)mercury(II), $Hg(SeMe)_2$

Excess metallic mercury was stirred with  $Me_2Se_2$  (2.81g, 15 mmol) in pyridine (50 mL) for 2 days. The resulting black suspension was extracted with hot pyridine until the extract was colorless (200 mL). The black mercuric selenide and finely divided metallic mercury were removed by filtration through cellulose powder and a fine sinter under slight positive pressure (CAUTION).

Yellow leaflets of  $\text{Hg}(\text{SeMe})_2$  formed on cooling (5.28g, 90%), mp.  $119^\circ(\text{dec.})$ . Infrared absorption: 2925vw, 2915vw, 1414m, 1253s, 900w,sh, 890s, 578 and 570w, 161vs,b, 151vs,b, 134vs,b, 103m. Raman bands (spinning cup): 2995 and 2988m, 2927m, 2913s, 1415w, 1262m, 898 and 890w, 576w,sh and 570s, 182vw,sh, 158m, 131vs, 112w.

The analysis of  $\text{Hg}(\text{SeMe})_2$  is shown in Table 4.1, page 174.

#### Bis(ethaneselenolato)mercury(II), $\text{Hg}(\text{SeEt})_2$

Excess metallic mercury was stirred with  $\text{Et}_2\text{Se}_2$  ( $\sim 2$  mL, unweighed because of stench) in chloroform (50 mL) for 1 day. The yellow powder which formed was dissolved by addition of hot chloroform (100 mL), and metallic mercury removed by decantation and filtration through a fine sinter under slight positive pressure (CAUTION). Chloroform was removed under vacuum, and the yellow powder recrystallised from pyridine to form yellow crystalline or glassy  $\text{Hg}(\text{SeEt})_2$ , mp.  $72^\circ(\text{dec.})$ . Infrared absorption: 2945m, 2905m, 2865m, 1441s and 1425sh, 1372s, 1221vs, 1041m, 750m, 570w,sh, 555m, 291w, 198w, 175vs,b, 150vs,vb, 130 vs, 110vs,b. Raman bands: (red excitation, spinning capillary) 2950 and 2933w, 2913m, 2857w, 1442 and 1424w, 1370vw, 1217s, 1041w, 991w, 963w, 745vw, 550m, 298w, 131vs.

The analysis of  $\text{Hg}(\text{SeEt})_2$  is shown in Table 4.1, page 174.

#### cyclo-Tetrakis-[chloro- $\mu$ -ethaneselenolato-pyridine]mercury(II)], $[\text{EtSeHgCl}(\text{py})]_4$

Mercuric chloride (0.59g, 2.18 mmol) in 5 mL pyridine was added to bis(ethaneselenolato)mercury(II) (0.91g, 2.18 mmol) dissolved in 10 mL warm pyridine, and the mixture filtered to remove a small amount of unreacted  $\text{Hg}(\text{SeEt})_2$  after 10 minutes.

Addition of 15 ml EtOH and evaporation overnight yields small, colorless prisms (1.18g, 64% as EtSeHgCl.py).

Small colorless prismatic crystals, suitable for crystallographic investigation (page 202) were deposited after 1 hour which were collected by filtration. The crystals showed negligible weight loss at room temperature over 36 hrs.

EtSeHgCl.py ( $C_7H_{10}ClNSeHg$ ) requires: C 19.9, H 2.38, N 3.31, Hg 47.4%; found C 20.2, H 2.46, N 3.50, Hg 47.4%.

Infrared absorption: 3080vw, 3055w, 3025w, 2990vw, 2950w, 2915w, 2860w, 1592m, 1428m, 1449s and 1449s, 1420w,sh, 1325m, 1232, 1222 w,sh and 1222m, 1207m, 1070w, 1062 and 1059m, 1081m, 1004s, 961w, 763s, 710s, 621m, 565vw,sh and 544m, 408m, 212s(br), 179s(br), 156m.

The compound rapidly loses pyridine and decomposes in the Raman laser-beam.

### tert-Butyl selenol

An ethereal solution of  $Bu^tSeH$  was prepared by the Grignard route to  $Bu^tSH$ .<sup>452</sup>

A Grignard solution of tert-butylmagnesium chloride was prepared by the dropwise addition of  $tBuCl$  (8.98g, 97 mmol, distilled, bp.50.5-51° and stored over  $K_2CO_3$  at -20°) to activated magnesium<sup>†</sup> (3.62g, 149 mmol). The reaction was initiated by adding approx. 3 mL  $tBuCl$  to the magnesium under 15 ml sodium-dried diethyl ether after warming the magnesium with a single iodine crystal in the oven-dried 250 mL three-

---

<sup>†</sup>A large portion of magnesium turnings was rinsed successively with four portions of 0.5% HCl, freshly deionised water (until pH ~5) ethanol and acetone, then dried over  $CaCl_2$  under nitrogen. The turnings were stored in a tightly stoppered container containing a few crystals of iodine.



necked flask. The subsequent rate of addition of  $t\text{BuCl}$  (dissolved in 50 ml ether) was sufficient to maintain gentle ether reflux.

Powdered grey selenium (3.83g, 49 mmol) was added slowly to the grey suspension over 30 min. with vigorous mechanical stirring and after a further 30 min., ether (50 mL) was added. After standing for 12 hr under nitrogen, the solution was cooled in ice, and ice-cold water (50 mL) then sulfuric acid (150 mL, 2.5M) were added slowly over a period of two hours. Only a small amount of unreacted selenium remained undissolved. The ether layer was separated and combined with an ether extract (50 mL) of the aqueous layer. The combined colorless extracts (100 mL) were dried over sodium sulfate and stored at  $-20^\circ$  until use. This solution remained colorless (free of  $\text{Bu}^t_2\text{Se}_2$ ) under these conditions for 30 months.

Bis(tert-butaneseelenolato)mercury(II),  $\text{Hg}(\text{SeBu}^t)_2$

A portion of the ether extract from the preparation of  $\text{Bu}^t\text{SeH}$  (~80 mL) was distilled into a stirred solution of mercuric cyanide (6.12g, 24 mmol) in methanol (50 mL). The slightly brown precipitate was collected (Whatman No.1), dissolved in boiling chloroform (250 mL), and on cooling, white, hairlike needles of  $\text{Hg}(\text{SeBu}^t)_2$  were collected on a coarse sinter, mp.  $145^\circ(\text{dec.})$ .

Infrared absorption: 2965m, 2925w, 2880w, 2815vw,sh, 1458sh and 1450m, 1389w, 1365s, 1148s, 1023m, 514m, 397m, 296w, 270w, 135vs.

Raman bands: (yellow excitation, below  $1200\text{ cm}^{-1}$  only) 1147m, 1027w, 805w, 519s, 299m, 272w, 139vs,b.

The analysis of  $\text{Hg}(\text{SeBu}^t)_2$  is shown in Table 4.1, page 174.

1,3;1,3-Di- $\mu$ -chloro-2,4-dichloro-1,2;1,4;2,3;3,4-tetrakis-  
 $\mu$ -1,1'-di-methylethaneselenolato-2,4-bis(pyridine)-  
quadro-tetramercury(II),  $[\text{Bu}^t\text{SeHgCl}(\text{py})_{0.5}]_4$

Mercuric chloride (0.106g, 0.39 mmol) dissolved in 1 ml pyridine was added to a stirred solution of bis(tert-butylselenolato)mercury(II) (0.185g, 0.39 mmol) suspended in 14 mL pyridine. Stirring for three minutes resulted in a clear, colorless solution which deposits a grey crystalline product at low volume. This product was redissolved in pyridine (10 mL), 10 ml EtOH added, and the solution filtered to remove a small amount of grey material. Evaporation deposits small prismatic crystals which rapidly darken if kept exposed to the atmosphere. A single crystal of this product was suitable for crystallographic investigation (page 195) and was mounted in a Lindemann capillary while still wet with pyridine.

Insufficient sample was available for spectral characterisation.

tert-Butaneselenolato(methyl)mercury(II),  $\text{MeHgSeBu}^t$

A portion of the ether extract from the preparation of  $\text{Bu}^t\text{SeH}$  (~20 mL, page 348) was distilled into an ice-cold solution of  $\text{MeHgOH}$  [prepared from  $\text{MeHgNO}_3$  (0.927g, 3.34 mmol) and  $\text{NaOH}$  (3mL 2M, 6 mmol)] in 40 mL methanol. Water (10 mL) was added, and after standing for 12 hr, the solution was filtered through a sinter containing cellulose powder. The sinter was rinsed with 20 mL MeOH and the combined aqueous MeOH solutions extracted with hexane (2 x 25ml). Additional  $\text{NaOH}$  (3 mL 2M) and water (10 mL) were added to the aqueous layer which was extracted again with hexane (3 x 25 mL). The hexane extracts were taken to dryness under low vacuum (~25 mm) at 0°C. The crude white solid was purified by sublimation (50-60°/15 mm), mp. 57-8.5° (sealed capillary).  $\text{MeHgSeBu}^t$  ( $\text{C}_5\text{H}_{12}\text{HgSe}$ ) requires: C 17.1, H 3.44, Hg 57.0%; found: C 17.0, H 3.50, Hg 57.0%.

Infrared absorption: 2970 and 2950vw, 2930w, 2885w, 2855w, 1465s,sh and 1450w, 1361m, 1172w, 1148s, 1020w, 756m, 521m, 290w, 194s.

Raman bands: (below  $600\text{ cm}^{-1}$  only) 526m, 302m, 200s, 142 and 127m.

$^1\text{H}$  nmr ( $\text{CDCl}_3$ ):  $\delta$  0.85 [3H,  $\text{CH}_3\text{Hg(II)}$ ], 1.65 [9H,  $\text{C}(\text{CH}_3)_3$ ],  $|^2J(^1\text{H}-^{199}\text{Hg})|$  146.8 Hz (see Figure 3.34, page 168).

tert-Butanethiolato(methyl)mercury(II),  $\text{MeHgSBu}^t$

$\text{MeHgSBu}^t$  was prepared in a similar manner to the selenium analog but using  $\text{Bu}^t\text{SH}$ , and pentane as the extractant. mp.  $40-2^\circ$  (sealed capillary, sublimes  $40^\circ/25\text{ mm}$ ) [lit.<sup>250b</sup>  $41-2^\circ$  (sublimes  $28^\circ/40\text{ mm}$ )].

Infrared absorption: 2970 and 2960vw, 2937 and 2920vw, 2890w, 2857w, 1470w and 1454m, 1363s, 1152s, 821vw, 766m,br, 581w, 532m, 428m, 383m, 352m, 305w, 234m, 130m.

Raman bands: 2972m, 2958 and 2950m, 2932w, 2910vs, 2888s, 2795vw, 2769w, 2707w, 1456 and 1438m, 1212m, 1180vs, 1150w, 1028vw, 932vw, 822s, 586s, 536ys, 432m, 390s, 368m, 228s, 147m,br.

$^1\text{H}$  nmr ( $\text{CDCl}_3$ ):  $\delta$  0.78 [3H,  $\text{CH}_3\text{Hg(II)}$ ], 1.51 [9H,  $\text{C}(\text{CH}_3)_3$ ],  $|^2J(^1\text{H}-^{199}\text{Hg})|$  150.1 Hz, [lit.<sup>250b</sup> ( $\text{CDCl}_3$ ) 0.77, 1.48, 150.2].

Bis(phenylmethyl)diselenide,  $(\text{PhCH}_2\text{Se})_2$  [Dibenzyldiselenide]

Dibenzyldiselenide was prepared by the selenation of benzaldehyde in the presence of morpholine hydrochloride<sup>†</sup>. Morpholine hydrochloride (6.20 g, 50 mmol) was added in one portion to a nearly colourless ethanolic solution of  $\text{NaHSe}$  (prepared from 4.74 g, 60 mmol Se, page 338).

Benzaldehyde (5.00 g, 47 mmol) was added in one portion to the resultant

---

<sup>†</sup>Morpholine hydrochloride was obtained by protonation of morpholine (100 g, 1.15 mole) dissolved in 100 mL ethanol, by ethanolic  $\text{HCl}$  (12.7M, prepared by the addition of  $\text{HCl}$  to conc.  $\text{H}_2\text{SO}_4$ ).<sup>758</sup>

white suspension, and the mixture heated to reflux on a water bath for 1 hr then cooled in ice. Red polyselenide impurities were reduced with small portions of solid  $\text{NaBH}_4$  to produce a yellow solution. Addition of ice-cold water (100 mL) precipitated the yellow product which was collected by filtration and rapidly washed with water to remove easily oxidised selenol impurities which otherwise rapidly decompose in air to red Se. The yellow powder ( $\sim 10$  g crude) was recrystallised from ethanol.

The product was used as a source of benzylselenolate anion, but subsequent preparation of benzylselenol was more convenient for this purpose.

#### Phenylmethaneselenol, $\text{PhCH}_2\text{SeH}$ [Benzylselenol]

Benzylselenol was prepared by Painter's Grignard method<sup>501</sup> from benzylmagnesium chloride (prepared from 24.3 g Mg, 1 mole and freshly distilled benzylchloride, 115 g, 1 mole, bp.  $61.0\text{--}61.5^\circ/8\text{mm}$ ) and selenium (78.98 g, 1 mole) by the same method as for  $^t\text{BuSeMgCl}$  (page 349).

Gaseous  $\text{HCl}$  (prepared from 53.5 g  $\text{NH}_4\text{Cl}$  and conc.  $\text{H}_2\text{SO}_4$ <sup>758</sup>) was passed over the ether solution with vigorous stirring. An appreciable quantity of  $\text{H}_2\text{Se}$  evolved and trapped in 50% sodium hypochlorite solution. Water (250 ml) was slowly added (CAUTION - vigorous decomposition) followed by an additional 80 ml conc.  $\text{HCl}$  in 250 ml water. The combined aqueous/ether layers (1000 mL) were filtered (gravity only) into a 1L separating funnel and separated. The ether layer was dried over sodium sulfate, filtered, and evaporated to yield 120 mL yellow oil. Fractional distillation under nitrogen yielded  $\sim 50$  mL colorless oil, bp.  $67\text{--}8^\circ/2\text{ mm}$  [lit.<sup>501</sup>  $100\text{--}5^\circ/20\text{ mm}$ ].

Bis(phenylmethylselenolato)mercury(II),  $\text{Hg}(\text{SeCH}_2\text{Ph})_2$

Benzylselenol (5.96 g, 35 mmol) was added with magnetic stirring to mercuric cyanide (4.95 g, 19 mmol) in 25 ml methanol, under nitrogen. The immediately precipitated yellow product was collected by filtration and washed with MeOH (5 x 5 mL). Portions of the crude product were recrystallised from benzene or chloroform to yield bright yellow, crystalline  $\text{Hg}(\text{SeCH}_2\text{Ph})_2$ , mp. 111°(dec.).

Infrared absorption: 3020vw, 1598vw, 1492m, 1175m, 1062w, 1028w, 907w, 827s, 757s, 694s, 598s, 549m, 449m, 328vw, 236w, 158s, br.

Raman bands: (spinning cup below 1700  $\text{cm}^{-1}$  only) 1603m, 1219m, 1177m, 1002m, 605m, 232w, 149s.

The analysis of  $\text{Hg}(\text{SeCH}_2\text{ph})_2$  is shown in Table 4.1, page 174.

Bis(phenylmethylthiolato)mercury(II),  $\text{Hg}(\text{SCH}_2\text{Ph})_2$

This compound was prepared in quantitative yield in an identical manner to  $\text{Hg}(\text{SeCH}_2\text{Ph})_2$  as a white microcrystalline product, mp. 115-7°.

Infrared absorption: 3050 and 3020vw, 1490m, 1460m, 1442m, 1229m, 1195vw, 1151vw, 1065w, 1028m, 910vw, 760w, 690vs, 620w, 565m, 472m, 381s, 352vw, 325vw, 246w.

Raman bands: 3050s, 2936m, 1602s, 1230s, 1430vw, 1230s, 1202w, 1160w, 1021w, 1004s, 810w, 767m, 688m, 627w, 566w, 476vw, 385vw, sh, 356s, 327vw, sh, 244m, 107s.

Phenylmethanethiolato(methyl)mercury(II),  $\text{MeHgSCH}_2\text{Ph}$

Benzylthiol (0.25 g, 2.2 mmol) was added by syringe, under nitrogen, to  $\text{MeHgNO}_3$  (0.60 g, 2.2 mmol) in 5 ml MeOH. After one minute, a transitory cloudiness disappeared to give two clear phases.

Water (5 mL) was added and the cloudy mixture extracted with pentane (4 x 10 mL). The pentane extracts were dried by passage through

a microcolumn of silica<sup>†</sup>, then evaporated to dryness under nitrogen to yield 0.25 g (34%) of colorless oil. The product smells of BzSH impurity confirmed by the Raman spectrum.

Infrared absorption: 3090vw, 3065w, 3030m, 3000vw,sh, 2915m, 2860vw, 2400vw, 1738vw, 1601w, 1494m, 1453m, 1382s,br, 1233m, 1202w, 1183w, 1157w, 1069m, 1029w, 912w, 828m, 767s, 700s, 680m, 566m, 538m, 476w, 346m.

Raman bands: 2055s, 2925w,sh, 2913s,(2580w) , 1601m, 1233s, 1203m, 1179s, 1030m, 1004vs, 804m, 770m, 702vs,sh and 684m, 621w, 565vw,sh and 540vs, 477w, 365vw,sh and 342s, 277w.

#### Phenylmethaneselenolato(methyl)mercury(II), MeHgSeCH<sub>2</sub>Ph

This compound was prepared in a similar manner to MeHgSCH<sub>2</sub>Ph, using benzylselenol (0.30 g, 1.7 mmol) and extracting with carbon tetrachloride. The silica microcolumn drying step was omitted as significant losses of sulfur analog appeared to be due to this procedure.

Infrared absorption: 3085vw, 3065w, 3038m, 3000w,sh, 2940w,sh and 2910m, 2400w, 1600m, 1495s, 1464m, 1385vs, 1174m, 1030w, 913w, 829m, 760s, 699s, 600m, 551w, 528m, 447w.

The complex decomposes in the Raman laser-beam.

The crude product (0.58 g, 88%) was pumped under high vacuum (21 mm) to remove solvents, excess selenol and water, but still smelled of Bu<sup>t</sup>SeH, and was consequently not analysed.

#### Diselenodiacetic acid, (SeCH<sub>2</sub>CO<sub>2</sub>H)<sub>2</sub>

Selenocyanatoacetic acid, NCSeCH<sub>2</sub>CO<sub>2</sub>H,<sup>759</sup> was prepared by displacement

---

<sup>†</sup>previously dried at 250°.

of bromide from bromoacetic acid (9.57 g, 69 mmol) dissolved in 50 mL dry acetone. Potassium selenocyanate (9.95 g, 69 mmol) dissolved in 100 mL dry acetone was added dropwise with magnetic stirring to this solution cooled in ice. The precipitated KBr (light purple due to Se impurities) was removed by filtration under slight positive pressure (CAUTION). Acetone was removed by rotary evaporation of the nearly colorless filtrate, to leave a pale yellow oil. Acid hydrolysis of the oil by refluxing  $2\frac{1}{2}$  hrs with 100 mL 1M HCl produced a deep yellow-orange solution which was allowed to stand overnight, exposed to the atmosphere, but in the dark. This solution was extracted with ether (5 x 50 mL) then with ethyl acetate (2 x 50 mL). The combined extracts were evaporated and the yellow residue dissolved in 50 mL ethyl acetate. Addition of 100 mL benzene and cooling produced  $(\text{SeCH}_2\text{CO}_2\text{H})_2$  as light yellow crystals (7.72 g, 53%), mp.  $93-5^\circ$  [lit.<sup>759</sup>  $101^\circ$ ].

Bis(selenoacetato)mercury(II),  $\text{Hg}(\text{SeCH}_2\text{CO}_2\text{H})_2$

Diselenodiacetic acid (0.64 g, 2.3 mmol) was dissolved in 20 mL water and the pH lowered to 1.5 with 2.5 M  $\text{H}_2\text{SO}_4$ . Excess metallic mercury was added and the yellow mixture immediately turned brown, changing to yellow on stirring overnight. The metallic mercury was removed by dissolving the yellow precipitate with saturated  $\text{NaHCO}_3$  solution followed by rapid filtration into 2.5M  $\text{H}_2\text{SO}_4$  (the dianion is unstable in alkaline solution). This procedure was repeated until the filtrate was clear yellow (twice), and the reprecipitated yellow powder filtered with some difficulty.

Infrared absorption: 2700-3300s,br, 2525w, 2515w, 1692s, 1612w, 1452s and 1394vw,sh, 1301vw,sh and 1275ys, 1172m, 930m and 911w,sh, 854vw, 713vw, 649m, 521vw, 446m and 433w,sh, 241s and 222m.

Raman bands (orange excitation at 10K, below  $350\text{ cm}^{-1}$  only because of sloping background): 313m, 284s, 224m, 192s, 172m.

Bis(mercaptoacetato)mercury(II),  $\text{Hg}(\text{SCH}_2\text{CO}_2\text{H})_2$

Mercuric chloride (0.272 g, 1.00 mmol) in 5 ml EtOH was added with stirring to mercaptoacetic acid (0.187 g, 2.03 mmol) in 25 mL water containing 1 mL 5M  $\text{HNO}_3$ . Glistening, white plates were precipitated and were collected by filtration and dried *in vacuo*. Yield 0.255 g (67%).

The analysis of  $\text{Hg}(\text{SCH}_2\text{CO}_2\text{H})_2$  is shown in Table 2.4, page 49.

Infrared absorption: 2800-3300m,vbr, 2960w, 2915w, 1713s, 1688s, 1418m, 1382w, 1305s, 1238vw, 1202s, 1170w, 898m, 862w,br, 787m, 677m, 552m, 464w,sh, 446s,br, 379s, 351w, 226s, 155m.

Raman bands (below  $1700\text{ cm}^{-1}$  only): 1650vw, 1395w, 1215w, 920w and 900vw,sh, 795m, 670vw, 435w, 370w,sh and 347s, 235m, 177w, 142vw.

[bis(mercaptoacetato)mercurate(2-1)], dipotassium salt,  $\text{K}_2[\text{Hg}(\text{SCH}_2\text{CO}_2)]$

Bis(mercaptoacetato)mercury(II) (3.65 g, 9.5 mmol) was suspended in 50 mL  $\text{N}_2$ -bubbled water and dissolved by the addition of KOH (1.06 g, 19.0 mmol). The solution was filtered and evaporated in a nitrogen-filled  $\text{CaCl}_2$  dessicator to give a grey powder. The powder was dissolved in 70 mL hot water containing a small amount of activated charcoal, filtered and cooled. The resulting white microcrystalline precipitate was filtered off, washed with ethanol and dried *in vacuo* over  $\text{CaCl}_2$ .

The analysis of this product is shown in Table 2.4 page 49.

Infrared absorption: 2900-3600vs,vbr, 2895vw, 1572s, 1382s, 1228m, 1216m, 1160vw, 919w, 894m, 769m, 678 and 670w, 550m, 431s, 355s, 321w, 235w.

Raman bands (yellow excitation, below  $800\text{ cm}^{-1}$  only): 710m, 437w, 417w,



360w, 328vs, 241w (in H<sub>2</sub>O, pH 6.3, below 400 cm<sup>-1</sup> only) 336vs,p.

Acetato(methaneselenolato)mercury(II), MeSeHgO<sub>2</sub>CMe

Bis(methaneselenolato)mercury(II) (0.120 g, 0.34 mmol) was added to a solution of mercuric acetate (0.107 g, 0.34 mmol) in 5 mL water containing 3 mL EtOH. After 15 min the colorless solution was filtered to remove a small amount of unreacted Hg(SeMe)<sub>2</sub>. The filtrate deposited colorless crystals on slow evaporation which were collected (0.193 g, 81%) and dried over P<sub>2</sub>O<sub>5</sub>.

MeSeHgO<sub>2</sub>CMe (C<sub>3</sub>H<sub>6</sub>O<sub>2</sub>SeHg) requires C 10.2, H 1.71, Hg 56.7%; found: C 10.2, H 1.75, Hg 56.5%.

Infrared absorption: 2995vw, 2955w,sh, 2925w, 2857w, 1535s, 1410m,sh and 1392s, 1339m, 1282m, 1040w, 1008m, 931 and 923m, 661s, 611m, 474m, 218s, 182m, 134s and 114m,sh.

Raman bands (below 2200 cm<sup>-1</sup> only): 1535vw,br, 1400vw, 1334vw, 1279vw, 923w, 663vw, 613vw, 574m, 480w, 230vw,sh, 197 and 182s, 143s.

Selenoacetato(methyl)mercury(II), MeHgSeCH<sub>2</sub>CO<sub>2</sub>H

Diselenodiacetic acid (0.388 g, 1.40 mmol) was dissolved in ammonium hydroxide solution (10 mL 2M) under nitrogen. Rongalite<sup>†</sup> (0.237 g, 1.54 mmol) was added in one portion with magnetic stirring, and very small additional portions added until the initial yellow solution remained colorless for 5 min.

Methylmercuric nitrate (0.78 g, 2.81 mmol) dissolved in 5 mL deaerated water was added, followed by immediate acidification (Congo Red) with 5M HNO<sub>3</sub>. The deposited white shiny leaflets were collected

---

<sup>†</sup>Rongalite = 'sodium formaldehyde hydrosulfite', HOCH<sub>2</sub>SO<sub>2</sub>Na.2H<sub>2</sub>O, was obtained from Fluka AG, Buchs.

on a sinter (#4) and briefly washed with dilute  $\text{HNO}_3$ , then a few drops of ethanol and dried *in vacuo*. Yield 0.65 g (67%). Attempted recrystallisation from ethanol resulted in deposition of grey Se.

The product is photosensitive and was stored at  $-20^\circ$ .

$\text{MeHgSeCH}_2\text{CO}_2\text{H}$  ( $\text{C}_3\text{H}_6\text{O}_2\text{SeHg}$ ) requires : C 10.2, H 1.68, Hg 56.7, Se 22.3%; found: C 9.9, H 1.68, Hg 56.7, Se 22.1%.

Infrared absorption: 2995vw, 2955w,sh, 2925w, 2857vw, 1530s,br, 1410w,sh and 1395s, 1339m, 1282m, 1040w, 1008m, 931 and 923m, 661s, 611w, 474w, 218s,br, 182m, 134s,br, 114w,sh.

Raman bands (below 1600 only): 1535vw,br, 1402vw,br, 1334vw, 1279vw, 1006vw, 923w, 663vw, 613vw, 574m, 480w, 230vw,sh, 197s,sh, 182m, 143s.

#### Mercaptoacetato(methyl)mercury(II), $\text{MeHgSCH}_2\text{CO}_2\text{H}$

Mercaptoacetic acid (0.172 g, 1.86 mmol) was added to methylmercuric nitrate (0.517 g, 1.86 mmol) in 15 mL water with stirring. An additional 5 ml water was added to clarify the slightly cloudy mixture which was filtered and allowed to evaporate. Fine colorless needles were collected after 20 hr. The analysis of this product is given in Table 2.2, page 38.

Infrared absorption: 2985w, 2940vw, 2910m, 1702s, 1440m, 1412w,sh, 1390 and 1375m, 1282m, 1185 and 1179s, 900 and 870m, 778 and 769 m, 722w,sh, 654 and 627m, 550 and 529w, 477m, 426m, 334 and 318m, 243w.

Raman bands: 2991m, 2932m, 2916vs, 1188m, 910vw, 793w, 676m, 580w, 538vs, 329s, 265vw, 180w, 153m, 138m.

(in  $\text{D}_2\text{O}$ , pH = 5.6): 2983m, 2921s, 2870m, 1450w, 1392w, 1334w, 1189s, 1017w, 932w, 831m, 779w, 546vs, 500vw, 351m.

$^1\text{H}$  nmr ( $\text{D}_2\text{O}$ , pH = 5.6)  $\delta$  -2.98 relative to dioxane = 10.0,  $|^2J(^1\text{H}-^{199}\text{Hg})|$  = 170.5 Hz.

Bis(2-hydroxyethyl)diselenide,  $(\text{HOCH}_2\text{CH}_2\text{Se})_2$

Rongalite (19.7 g, 128 mmol) and sodium hydroxide (12.6 g, 315 mmol) were dissolved in 250 mL water under nitrogen. This solution was added in one portion to grey selenium (25.2 g, 319 mmol) in a 1L 3-necked flask and the mixture stirred and heated on a boiling water bath to dissolve Se (3 hrs). Freshly distilled 2-chloroethanol, bp. 176-7° (26.3 g, 327 mmol) was added dropwise with stirring to the deep red  $\text{Na}_2\text{Se}_2$  solution. When ~95% of the halide was added, an orange oil separated which was decanted and dissolved in acetone after cooling to room temperature. The aqueous phase was extracted with chloroform until the extracts were light yellow. The combined acetone and chloroform extracts were evaporated to dryness, then pumped at high vacuum (0.1 mm) to remove water. Yield of crude oil 26.2 g (83%) which was fractionally distilled, bp. 152-60°/0.05-0.2 mm [lit.<sup>755</sup> 169-79°/1.6-4 mm]. Surprisingly, the diselenide is odorless.

Attempted isolation of 2-hydroxyethaneselenol,  $\text{HOCH}_2\text{CH}_2\text{SeH}$

Bis(2-hydroxyethyl)diselenide (8.78 g, 35 mmol) was dissolved in 30 mL sodium-dried ether, and cooled to -30° with dry ice/acetone. Sodium-dried liquid ammonia was condensed into this solution (~130 mL) under a slight flow of nitrogen. Metallic sodium was added as a solution in liquid ammonia (using a refluxing condenser-thimble arrangement described in reference 756) until a blue color persisted for 5 min.

At this stage the mixture turned white and cloudy. The ammonia was evaporated under nitrogen and 10 mL deaerated water added dropwise to the residue followed by conc. HCl (CAUTION - vigorous) until pH 3-4. The white oily residue ( $\text{NH}_4\text{Cl}$ ) was pumped (~4 mm) in warm water (<55°) to remove water, HCl, etc., then at higher vacuum (0.1-0.2 mm) with

warming to 60°. A colorless oil was condensed in a cold trap (-15°). Addition of freshly dried 5Å molecular sieves to the oil under nitrogen resulted in gas evolution and complete decomposition overnight.

(2-phenylmethylseleno)butanedioic acid

Bis(phenylmethyl)diselenide (0.655 g, 1.93 mmol) was dissolved in 20 mL EtOH and just reduced with small additions of solid NaBH<sub>4</sub> under nitrogen. A solution of cis-2-butenedioic acid (maleic acid, 0.456 g, 3.93 mmol) in 20 mL EtOH containing NaOH (0.3 g, 7.5 mmol) was added by syringe to the solution of selenolate. The nearly colorless solution was stirred for 2 hr at 50° and separated into two phases. The bottom layer was separated and acidified with conc. HCl (5 mL). The resultant white precipitate was collected by filtration and washed with 10% HCl. Yield 0.54 g (48%), mp. 169-71°.

PhCH<sub>2</sub>SeCH(CO<sub>2</sub>H)CH<sub>2</sub>CO<sub>2</sub>H (C<sub>11</sub>H<sub>12</sub>O<sub>4</sub>Se): requires C 46.0, H 4.21, Se 27.5%; found C 46.0, H 4.39, Se 27.2%.

Infrared absorption: 2600-3300s,br, 1690vs, 1494m, 1415s, 1319m, 1235m, 1198m, 1065m, 918m,br, 854w, 811w, 758s, 699s.

<sup>1</sup>H nmr (acetone-d<sub>6</sub>; Figure 5.3 page 259)

7.35 (m, 5H, C<sub>6</sub>H<sub>5</sub>), 4.7 (br, 2H, CO<sub>2</sub>H), 4.15 (s, 2H, CH<sub>2</sub>Se), 3.75 (q, 1H, CHCO<sub>2</sub>H), 2.85 (m, 2H, CH<sub>2</sub>CO<sub>2</sub>H). See Table 5.7, page 261 for coupling constants.

Mass spectrum: M<sup>+</sup> = 287.9904; calc. 287.9898

(2-phenylmethylmercapto)butanedioic acid

This compound was prepared by base-catalysed addition of benzylthiol (2.22 g, 17.9 mmol) to the sodium salt of maleic acid (2.08 g, 17.9 mmol) in an identical manner to the selenium analog, mp. 173-5°.

Infrared absorption: 2600-3300 m,vbr, 1710 and 1692s, 1495w, 1434m, 1410m, 1352vw, 1321m, 1240s, 1206 and 1198m, 1177w, 1081m, 999w, 921m and 7w,sh, 853w, 837vw, 771w, 718 and 710m, 672w.

$^1\text{H}$  nmr (acetone- $\text{d}_6$ ; Figure 5.2 page 258):

$\delta$  7.39 (m, 5H,  $\text{C}_6\text{H}_5$ ), 4.2 (br, 2H,  $\text{CO}_2\text{H}$ ), 4.03 (s, 2H,  $\text{CH}_2\text{Se}$ ), 3.17 (q, 1H,  $\text{CHCO}_2\text{H}$ ), 2.80 (m, 2H,  $\text{CH}_2\text{CO}_2\text{H}$ ). See Table 5.7, page 261, for coupling constants.

Mass spectrum:  $\text{M}^{+\bullet} = 240.0420$ ; ca;c. 240.0456.

#### trans-(2-phenylmethylseleno)butenedioic acid

Acetylenedicarboxylic acid<sup>†</sup> (0.99 g, 8.7 mmol) was dissolved in 15 mL 1M NaOH, the pH of this solution adjusted with HCl until just alkaline (pH  $\sim$ 8) and solid sodium carbonate (1.84 g, 17 mmol) added. This solution was deaerated by nitrogen bubbling for 15 min then added by syringe to neat benzylselenol (1.49 g, 8.7 mmol) under nitrogen. After stirring for 40 hr, the mixture was extracted with ether (25 mL) and the aqueous phase acidified with conc. HCl (Congo REd). The bright yellow precipitate was collected by filtration, and recrystallised from ethanol as bright yellow needles. Yield 2.09 g (84%), mp. 180-3° (dec.).  $\text{PhCH}_2\text{SeC}(\text{CO}_2\text{H})\text{:CHCO}_2\text{H}$  ( $\text{C}_{11}\text{H}_{10}\text{O}_4\text{Se}$ ) requires: C 46.7, H 3.53, Se 27.7%; found: C 46.6, H 3.59, Se 27.8%.

Infrared absorption: 2600-3400s,vbr, 1695w,sh, 1670s, 1557m, 1493m, 1453w, 1414s, 1312m, 1266s, 1231s, 1173w, 1060w, 1028w, 952w, 916w, 888 and 875m, 861m, 778w, 764m, 743w, 695s, 656w, 617w.

$^1\text{H}$  nmr (acetone- $\text{d}_6$ ):  $\delta$  7.38 (m, 5H,  $\text{C}_6\text{H}_5$ ), 6.45 (s, 1H,  $\text{CH}=\text{C}$ ), 5.1 (br,

---

<sup>†</sup>Acetylenedicarboxylic acid was prepared from the dipotassium salt by acidification with sulfuric acid and extraction with ether.<sup>761</sup>

2H, CO<sub>2</sub>H), 4.25 (s, 2H, CH<sub>2</sub>).

Mass spectrum:  $M^{+} = 285.9794$ ; calc. 285.9744.

trans-(2-phenylmethylmercapto)butenedioic acid

This compound was prepared in 78% yield by the base-catalysed addition of benzylthiolate to acetylenedicarboxylic acid in an identical manner to the selenium analog.

The product was recrystallised as pale yellow crystals from EtOH, mp. 151-2°.

Infrared absorption: 2500-3300m,vbr, 1706 and 1674vs, 1560m, 1497w, 1416m, 1326 m and 1313w, sh, 1270m, 1238 and 1232s, 1070w, 1048m, 1028w, 957w, 920w, 890m,br, 857m, 783m, 752m, 729m, 710w and 699m.

<sup>1</sup>H nmr (acetone-d<sub>6</sub>) = δ 7.39 (m, 5H, C<sub>6</sub>H<sub>5</sub>), 6.69 (s, 1H, CH=C), 5.3 (br, 2H, CO<sub>2</sub>H), 4.21 (s, 2H, CH<sub>2</sub>).

Mass spectrum:  $M^{+} = 238.0306$ , calc. 238.0300.

### Attempted preparations of 1,3-diseleno-2-propanol (SeDMPH<sub>2</sub>)

1,3-dibromo-2-propanol was prepared for these reactions by hydrobromination of epibromohydrin.<sup>762</sup> Hydrobromic acid (38 mL 46-48% w/v, 0.342 mole) was added dropwise over a period of 30 minutes to epibromohydrin (Fluka, 41.55 g, 0.303 mole) in 40 mL ethanol at 70-75°, with magnetic stirring. After stirring for a further 30 minutes at 60-70°, the solution was cooled to room temperature and ethanol removed under reduced pressure. The yellow oily residue was stirred with ether (300 mL) and washed successively with H<sub>2</sub>O (3 x 100 mL), 1% w/v sodium bicarbonate solution (3 x 80 mL), then H<sub>2</sub>O (3 x 100 mL). The dried (MgSO<sub>4</sub>) ether extract was evaporated and vacuum distilled to give the product as a colourless oil (51-55%) bp. 77-80°/4mm (lit.<sup>762</sup> 82°/6 mm). The product darkens in amber glass at room temperature and was redistilled before use.

#### (i) Selenocyanation of 1,3-dibromo-2-propanol

Potassium selenocyanate (1.715 g, 119 mmole) dissolved in 10 mL dry methanol was added to 1,3-dibromo-2-propanol (1.270 g, 58.3 mmole) under nitrogen and the resulting red solution refluxed for 30 minutes.

Silica TLC showed no change in product distribution after this time. The reaction mixture was diluted with water (20 mL) and extracted with ether (3 x 30 mL) under nitrogen. The dried (Na<sub>2</sub>SO<sub>4</sub>) ether extracts were evaporated under nitrogen to yield a dark yellow oil (1.14 g) having intense infrared absorption (2135 cm<sup>-1</sup>) due to selenocyanate. This oil could be separated by Kugel-Rohr distillation, giving two fractions. The first, bp. 50-53°/0.01 mm, showed no absorption due to C≡N in the infrared spectrum, and was discarded. The second, bp. 60-75°/0.01 mm, has  $\nu$  C≡N 2135 cm<sup>-1</sup> and was identified as 1-bromo-3-selenocyanato-2-propanol.

Infrared absorption:

3390 vs(br,OH), 3010 vw, 2955 w, 2880 w, 2135 s( $\nu\text{C}\equiv\text{N}$ ), 1694 m(br), 1610 w, br, 1418 s and 1400 sh, 1300 vw, 1274 w, 1232 m, 1210 m, 1170 w, 1147 w, 1074 m, 1046 m, 1020 s, 966 w, 926 vw, 905 vw, 855 sh and 836 w, 697 w, sh and 670 m, 582 w, 520 w and 498 w.

 $^1\text{H}$  nmr ( $\delta\text{CDCl}_3$ ) - see page

2.9(br, 1H,  $\text{CO}_2\text{H}$ ); 3.28, 3.38(d, 1H,  $\text{H}_a$ ); 3.35(s, 1H,  $\text{H}_b$ ); 3.56, 3.62(d, 2H,  $2\text{H}_d$ ); 4.23(m, 1H,  $\text{H}_c$ ).

Mass spectrum - see page

$\text{M}^+$  accurate mass 242.8814,  $\text{C}_4\text{H}_6\text{BrNOSe}$  requires 242.8796.

(ii) Alkylation of NaSeH with 1,3-dibromo-2-propanol

A solution of 1,3-dibromo-2-propanol (38.35 g, 176 mmole) in ethanol (20 mL) was added dropwise to a light grey ethanolic solution of NaSeH (300 mL containing 25.3 g, 320 mmole Se). After 1 hour, small portions of solid sodium borohydride were added to produce an orange solution (which could be decolourised in subsequent preparations by addition of further small amounts of solid  $\text{NaBH}_4$ ) and a white precipitate ( $\text{NaBr}$ ,  $\text{H}_3\text{BO}_3$ ). The solution was cooled in ice, and glacial acetic acid (26 mL) added with vigorous nitrogen bubbling to expel  $\text{H}_2\text{Se}$  after warming to room temperature. (A prior attempt to steam-distil the reaction products at this stage produced large quantities of red selenium and much  $\text{H}_2\text{Se}$ ). The mixture was filtered, evaporated to low volume, and the resultant orange slurry shaken with ether and refiltered. Evaporation of the ether extract produced an orange oil which could be distilled under reduced pressure to give an orange oil, bp. 79-85°/3.5 mm (11.49 g), containing some unreacted 1,3-dibromo-2-propanol (nmr).



The crude oil was fractionally distilled (Kügel-Rohr) to give two fractions. The first (bath temp. 60-3/4 mm) was mainly selenetan-3-ol. Infrared absorption: 3100-3800vs,vbr, 3005w, 2948m, 1655w,sh and 1610s, 1635w, 1445s and 1418m, 1322m, 1270w,br, 1165m, 1124m, 1050s,br, 980w,sh, 898m, 869m, 813w, 710w,sh, 680w,sh and 655m.

$^1\text{H}$  nmr ( $\text{CDCl}_3$ ):  $\delta$  4.85 (q, 1H,  $\text{CHOH}$ ), 4.23 (br, 1H,  $\text{OH}$ ), 3.38 and 3.15 (d.t., 4H,  $\text{SeCH}_2$ ). See Figure 5.6, page 270.

Mass spectrum: (Figure 5.5a, page 267)  $M^{++} = 137.9603$ ; calc. 137.9603).

The higher boiling fraction gave a less well resolved nmr spectrum. The mass spectrum of the major component in this fraction is shown in Figure 5.5b, page 268.

# REFERENCES

1. "Minamata Disease: Methylmercury poisoning in Minamata and Niigata, Japan", T. Tsubaki and K. Irukayama (Eds.), Elsevier, Amsterdam (1977).
2. W.E. Smith and A.M. Smith, "Minamata", Holt, Rinehart and Winston, New York. (1975).
3. T.B. Eyl, J. Am. Med. Assoc., 215 287 (1971).
4. a) R.D. Snyder, New Eng. J. Med. 284 1014 (1971);  
b) Arch. Neurol. 26 379 (1972);  
c) "Environmental Mercury Contamination", R. Hartung and B.D. Dinman (Eds.), Ann Arbor Science, Michigan (1972).
5. F. Bakir, S.F. Damluji, L. Amin-Zaki, M. Murtadha, A. Khalidi, N.Y. Al-Rani, S. Tikriti, H.I. Dhakir, T.W. Clarkson, J.C. Smith and R.A. Doherty, Science 181 239 (1973).
6. K. Al-Takriti and A.W. Al-Mufti, Bull. W.H.O. 53 (Suppl) 15 (1976) and S.B. Skerfving and J.F. Copplestone, Bull. W.H.O. 54 101 (1976).
7. A.R. Greco, Riv. Neurol. 3 515 (1930) and references therein.
8. J.R. Wood, Environ. Sci. Res. 17 223 (1980).
9. J.M. Wood, F.S. Kennedy and C.G. Rosen, Nature (London) 220 173 (1968).
10. L. Landner, Nature (London) 230 452 (1971).
11. T.W. Clarkson, Ann. Rev. Pharmacol. 12 375 (1972).
12. a) "Mercury, Mercurials and Mercaptans", M.W. Miller and T.W. Clarkson (Eds.), C.C. Thomas Publ., Springfield, Illinois (1973);  
b) J.T. MacGregor and T.W. Clarkson in Adv. In Expt. Med. Biol. M. Friedman ed. 48 463 (1974).
13. "Mercury in the Environment: An Epidemiological and Toxicological Appraisal", L. Friberg and J. Vostal (Eds.), C.R.C. Press, Cleveland, Ohio (1972).
14. H.B. Gerstner and J.E. Huff, J. Toxicol. Environ. Health 2 491 (1977).
15. A. Gilman, R.P. Allen, F.S. Philips and E. St. John, J. Clin. Invest. 25 549 (1946).
16. M. Berlin, L.-G. Jerksell and H. Von Ubisch, Arch. Environ. Health 12 33 (1966).
17. F.A. Cotton and G. Wilkinson, "Advanced Inorganic Chemistry: a Comprehensive Text" (4th ed.) John Wiley and Sons, New York (1980).

18. J.J. Chisholm, Jr., Pediatr. Clinics Nth. Am. 17 591 (1970).
19. J.H.R. Kagi and B.L. Vallee, J. Biol. Chem. 236 2435 (1961).
20. S. Jensen and A. Jernelöv, Nature (London) 223 753 (1969).
21. L. Magos and W.H. Butler, Arch. Toxicol. 35 25 (1976).
22. T. Norseth and T.W. Clarkson, Arch. Environ. Health 21 717 (1970).
23. R. Klein *et al.*, Arch. Pathol. 96 83 (1973).
24. J.M. Wood, A. Cheh, L.J. Dizikes, W.P. Ridley, S. Rakow and J.R. Lakowicz, Fed. Proc. Fed. Am. Soc. Exp. Biol. 37 16 (1978).
25. M. Berlin and S. Ullberg, Arch. Environ. Health 6 589 (1963).
26. Å. Swensson and U. Ulfvarson, Acta Pharmacol. Toxicol. 26 273 (1968) and references therein.
27. P.J. Gallagher and R.L. Lee, Toxicology 15 129 (1980).
28. J.M. Wood, Adv. Environ. Sci. Technol. 2 39 (1971).
29. F.L. Hoch and B.L. Vallee, Arch. Biochem. Biophys. 91 1 (1960).
30. T. Norseth and M. Brendeford, Biochem.-Pharmacol. 20 1101 (1971).
31. N. Sone, M.K. Larsstuvold, Y. Kagawa, J. Biochem. 82 859 (1977).
32. J.H. Southard, P. Nitisewojo, Biochem. Biophys. Res. Comm. 52 921 (1973).
33. J.H. Southard, P. Nitisewojo and D.E. Green, Fed. Proc. Fed. Am. Soc. Exp. Biol. 33 2147 (1973).
34. R.H.S. Thompson and V.P. Whittaker, Biochem. J. 41 346 (1947).
35. E.S. Barron and G. Kalintsky, Biochem. J. 41 351 (1947).
36. L.R. Roberts, L.K. Steinrauf and R.T. Blickenstaff, J. Pharm. Sci. 69 964 (1980).
37. S. Nakada, K. Inoue, S. Nojima and N. Imura, Chem.-Biol. Interact. 22 15 (1978).
38. R. Magnaval, J. Thiessard, R. Batti and R. Bittel, Rev. Int. Oceanogr. Med. 49 111 (1978) CA89:1226c.
39. S. Omata, K. Sakimura, T. Ishii and H. Sugano, Biochem. Pharmacol. 27 1700 (1978).
40. K.R. Olson, K.S. Squibb, R.J. Cousins, J. Fish. Res. Board Can. 35 381 (1978).
41. D.L. Rabenstein, Acc. Chem. Res. 11 100 (1978).

42. M. Ohsawa and L. Magos, Biochem. Pharmacol. **23** 1903 (1974).
43. J.W. Daniel, J.C. Gage and P.A. LeFevre, Biochem. J. **121** 411 (1971).
44. I.U. Haq, Br. Med. J. **1** 1579 (1963).
45. A.J. Canty and R. Kishimoto, Aust. J. Chem. **30** 669 (1977).
46. F. Matsamura, Y. Gotch and G.M. Boush, Science **173** 49 (1971).
47. K. Tonomura, K. Furukawa and M. Yamada in "Environmental Toxicology of Pesticides", F. Matsamura *et al.* (Eds.) Academic Press, New York (1972).
48. J.D. Nelson, W. Blair, F.E. Brinckman, R.R. Colwell and W.P. Iverson, Appl. Microbiol. **26** 321 (1973).
49. M.M. Jones and T.H. Pratt, J. Chem. Ed. **53** 342 (1976).
50. P.M. May, D.R. Williams and P.W. Linder in "Metal Ions in Biological Systems", H. Sigel (Ed.) Volume 7, Marcel Dekker, New York (1978).
51. S. Ahrland, J. Chatt and N.R. Davies, Quart. Rev. Chem. Soc. **12** 265 (1958).
52. a) R.G. Pearson, J. Am. Chem. Soc. **85** 3533 (1963);  
b) R.G. Pearson, "Hard and Soft Acids and Bases", Dowden, Hutchinson & Ross, Pennsylvania (1973).
53. L.L. Waters and C. Stock, Science **102** 601 (1945).
54. F.W. Oehme, Clin. Toxicol. **5** 215 (1972).
55. a) G.W. King, Ariz. Med. **11** 335 (1954);  
b) F.T. Matthes, R. Kirschner, M.D. Yow and J.C. Brennan, Pediatrics **22** 675 (1958).
56. W.J. Burke and J.M. Quagliana, J. Occup. Med. **5** 157 (1963).
57. H.C. Brugsh, J. Occup. Med. **7** 394 (1965).
58. G. Baldi, Med. Lavoro **41** 10 (1950).
59. K.R. Adam, Br. J. Pharmacol. **6** 483 (1951).
60. R.F. Bell, J.C. Gilliland and W.S. Dunn, Arch. Indust. Health **11** 231 (1955).
61. L. Magos, Brit. J. Indust. Med. **24** 152 (1968).
62. M. Berlin and T. Lewander, Acta Pharmacol. Toxicol. **22** 1 (1965).
63. J.R. Fitzsimons and F.L. Kozelka, J. Pharmacol. Exp. Ther. **98** 8 (1950).
64. J.E. Wynn, B. Van't-Reit and J. Borzelleca, Toxicol. Appl. Pharmacol. **16** 1807 (1970).

65. T. Norseth, Acta Pharmacol. Toxicol. 32 1 (1973).
66. Å. Swensson and U. Ulfvarson, Intern. Arch. Gewerbepath. Gewerbehyg. 24 12 (1967).
67. M. Berlin, L.-G. Jerksell and G. Nordberg, Acta Pharmacol. Toxicol. 23 312 (1965).
68. A.K.M. Anisuzzaman and L.N. Owen, J. Chem. Soc. (C) 1021 (1967).
69. W.T. Longcope and A. Luetscher, Ann. Int. Med. 31 545 (1949).
70. L.S. Goodman and A. Gillman, "The Pharmacological Basis of Therapeutics", 5th ed., McMillan, New York (1975), p.912.
71. P. Zvirbilis and R.I. Ellin, Toxicol. Appl. Pharmacol. 36 297 (1976).
72. H. Eagle, H.J. Magnuson and R. Fleischman, J. Clin. Invest. 25 451 (1946).
73. L. Friedrich and F. Zimmermann, Arzneim.-Forsch. 25 162 (1975).
74. a) H.V. Aposhian and M.M. Aposhian, J. Pharm. Exp. Ther. 131 139 (1959);  
b) H.V. Aposhian, Ann. N.Y. Acad. Sci. 179 481 (1971).
75. "The Merck Index", 9th ed. Merck and Co. Inc., Rahway, New Jersey (1976).
76. I.G. Mizyukova and D.S. Lokantsev, Farmakol. i Tokikol. 23 355 (1960); CA 55:12660.
77. Y-I. Liang, Ch.-Ch. Chu, Y-L. Tsen and K-Sh. Ting, Acta Physiol. Sinica 21 24 (1957) CA51:14982g
78. E. Friedheim and C. Corvi, J. Pharm. Pharmacol. 27 624 (1975).
79. A.Y. Hadengue, P. Fabiani and A. Queuille, Arch. Mal. Prof. 11 45 (1950).
80. J.M. Walshe, Am. J. Med. 21 487 (1956)
81. a) G. Kazantzis, K.F.R. Schiller, A.W. Asscher and R.G. Drew, Quart. J. Med. 31 403 (1962);  
b) J. Teisinger and J. Srbova, Prac. Lek. 16 433 (1964);  
c) S.N. Javett and G. Kaplan, Am. J. Dis. Child. 115 71 (1968).
82. J. Aaseth, Acta Pharmacol. Toxicol. 39 289 (1976).
83. L. Magos, T.W. Clarkson and J. Allen, Biochem. Pharmacol. 27 2203 (1978).
84. K. Hirota, Clin. Neurol. 9 592 (1969).
85. N.S. Ishihara, S. Shiojima and T. Suzuki, Brit. J. Ind. Med. 31 245 (1974).

86. J. Aaseth, A. Wannag and T. Norseth, Acta Pharmacol. Toxicol. 39 302 (1976).
87. H. Matsumoto, A. Suzuki, C. Morita, K. Nakamura and S. Saeki, Life Sciences 6 2321 (1967).
88. J. Aaseth, Acta Pharmacol. Toxicol. 36 193 (1975).
89. J. Aaseth, Acta Pharmacol. Toxicol. 39 289 (1976).
90. N.S. Johary and L.N. Owen, J. Chem. Soc. 1307 (1955).
91. V.E. Petrun'kin, Ukrain. Khim. Zh. 22 603 (1956); CA51:5629h, 14537i and CA54:24378f, CA57:16374d.
92. F. Planas-Bohne, B. Gabard and E.H. Schäffer, Arzneim.-Forsch. 30 1291 (1980).
93. B. Gabard, F. Planas-Bohne and G. Regula, Toxicology 12 281 (1979).
94. G.A. Belonozhko, Farmakol. Tokikol. 21 69 (1958) CA52:20677i.
95. E. Ogara, S. Suzuki, N. Tsuzuki, M. Tabe, K. Kobayshi and M. Hojo in "Proc. Int. Symp. on Thiola" Osaka, Japan, p.238 (1970).
96. F. Planas-Bohne, Arzneim.-Forsch. 22 1426 (1972).
97. L.K. Klimova, Farmakol. Tokikol. 21 53 (1958) CA52:20677d.
98. Sh. A. Galoyan and T.M. Turpaev, Dokl. Akad. Nauk. Armyan. S.S.R. 27 59 (1958); CA53:12465f.
99. B. Gabard, Acta Pharmacol. Toxicol. 39 250 (1976).
100. J. Aaseth and E.A.H. Friedheim, Acta Pharmacol. Toxicol. 42 248 (1978).
101. L.K. Klimova in "Tiiovyie soyedineniya v meditsine", N.N. Luganskiy, V.E. Petrun'kin, P.V. Rodionov and A.J. Cherkas (Eds.), Gos. Med. Izd. Ukrain S.S.R., Kiev 135 (1959).
102. M.G. Cherian, Nature (London) 287 871 (1980).
103. J.H. Graziano, D. Cuccia and E. Friedheim, J. Pharm. Exp. Ther. 207 1051 (1978).
104. E.A.H. Friedheim, J.R. Da Silva and A.V. Martins, Am. J. Trop. Med. Hyg. 3 714 (1954).
105. E.A.H. Friedheim, R.T. De Jongh, Trans. Roy. Soc. Trop. Med. Hyg. 53 262 (1959).
106. J.H. Graziano, J.K. Leong and E. Friedheim, J. Pharmacol. Exp. Ther. 206 696 (1978).
107. E. Ogawa, Igaku To Seibutsugaku 94 357 (1977).

108. J. Aaseth, E. Jellum and E. Munthe, Scand. J. Rheumatol. 9 157 (1980).
109. I.E. Okoshnikova, Prom. Toksikol. Klin-Prof. Zabolevanii Khim. Etiol. Sbornik. 205 (1962) CA62:12357h
110. L. Magos, Brit. J. Pharmacol. 56 479 (1976).
111. E. Friedheim, C. Corvi and C.H. Wakker, J. Pharm. Pharmacol. 28 711 (1976).
112. E. Ogawa, Igaku To Seibutsugaku 91 295 (1975) CA84:145614x.
113. L. Magos, G.C. Peristianis and R.T. Snowden, Toxicol. Appl. Pharmacol. 45 403 (1978).
114. J.A. Hughes and S.B. Sparber, Res. Comm. Chem. Path. Pharmacol. 22 357 (1978).
115. J. Aaseth and T. Norseth, Acta Pharmacol. Toxicol. 35 23 (1974).
116. T. Norseth, Acta Pharmacol. Toxicol. 34 76 (1974).
117. K. Shirakawa, K. Hirota, T. Katagiri, T. Tsubaki and H. Saito, Niigata Igakkai Zasshi 90 495 (1976) CA89:17979m.
118. M.M. Jones and R.D. Harbison, Res. Comm. Chem. Pathol. Pharmacol. 7 389 (1974).
119. R.T. Blickenstaff, B. Cox, E. Foster, L. Roberts and L.K. Steinrauf, J. Pharm. Sci. 69 556 (1980).
120. V. Ebyl, J. Sykora and F. Mertl, I.R.C.S. Libr. Compend. 2 1169 (1974) CA82:26370p.
121. V. Eybl, J. Sykora, M. Koutenska, J. Koutensky and F. Mertl, Arzneim.-Forsch. 23 867 (1973).
122. T.W. Clarkson, H. Small and T. Norseth, Fed. Proc. 30 543 (1971) and Arch. Environ. Health 26 173 (1973).
123. J. Schubert and S.K. Derr, Nature (London) 275 311 (1978) and 278 581 (1978).
124. J. Schubert and R.A. Bulman, F.E.H. Crawley and D.A. Geden, Nature (London) 281 406 (1979). (correspondence).
125. P.M. May and D.R. Williams, FEBS. Lett. 78 134 (1977).
126. G.E. Jackson, P.M. May and D.R. Williams, FEBS. Lett. 90 173 (1978).
127. P.J. Kostyniak, T.W. Clarkson, R.V. Cestero, R.B. Freeman and A.H. Abbasi, J. Pharmacol. Exp. Ther. 192 260 (1975).
128. P.J. Kostyniak, T.W. Clarkson and A.H. Abbasi, J. Pharmacol. Exp. Ther. 203 253 (1977).
129. a) J.F. Maher and G.E. Schreiner, Clin. Res. 7 298 (1959);  
b) L. Sanchez-Sicilia, D.S. Seto, S. Nakamoto and W.J. Kolff, Ann. Intern. Med. 59 692 (1963).

130. S. Margel, J. Med. Chem. **24** 1263 (1981).
131. M.M. Jones, T.H. Pratt, W.G. Mitchell, R.D. Harbison and J.S. MacDonald, J. Inorg. Nucl. Chem. **38** 613 (1976).
132. T. Norseth and T. Clarkson, Arch. Environ. Health **22** 568 (1971).
133. H. Takahashi and K. Hirayama, Nature (London) **232** 201 (1971).
134. M.J. Benes, J. Stamberg, J. Peska, M. Tichy and M. Cikrt, Angew. Makromol. Chem. **44** 67 (1975).
135. R.D. Harbison, M.M. Jones, J.S. MacDonald, T.H. Pratt and R.L. Coates, Toxicol. Appl. Pharmacol. **42** 445 (1977).
136. M.M. Jones, H.D. Coble, T.H. Pratt and R.D. Harbison, J. Inorg. Nucl. Chem. **37** 2409 (1975).
137. D.E. Trimmell, E.I. Stout, W.M. Doane and C.R. Russell, J. Appl. Polym. Sci. **21** 655 (1977).
138. L. Magos and T.W. Clarkson, Chem.-Biol. Interact. **14** 325 (1976).
139. K. Schwarz and C.M. Foltz, J. Am. Chem. Soc. **79** 3292 (1957).
140. "Selenium", R.A. Zingaro and W.C. Cooper (Eds.), Van Nostrand Rheinhold, New York (1974).
141. "Organic Selenium Compounds: their Chemistry and Biology", D.L. Klayman and W.H.H. Gunther (Eds.), Wiley-Interscience, New York (1973).
142. a) H.E. Ganther, Biochemistry **7** 2898 (1968).  
b) H.E. Ganther and C. Corcoran, Biochemistry **8** 2557 (1969).
143. E.P. Painter, Chem. Rev. **28** 179 (1941).
144. C.C. Tsen and A.L. Tappel, J. Biol. Chem. **233** 1230 (1958).
145. K.J. Jenkins and M. Hidirolou, Can. J. Physiol. Pharmacol. **50** 927 (1972).
146. M. Sandholm and P. Sipponen, Arch. Biochem. Biophys. **155** 120 (1975).
147. T.A. Gasiewicz and J.C. Smith, Chem.-Biol. Interact. **23** 171 (1978).
148. T.A. Gasiewicz and J.C. Smith, Biochim. Biophys. Acta **428** 113 (1976).
149. R.F. Burk, K.A. Foster, P.M. Greenfield and K.W. Kiker, Fed. Proc. **145** 782 (1974).
150. M. Sandholm, Acta Pharmacol. Toxicol. **33** 1 (1973).
151. a) A.B. Kar and R.P. Das, Acta Biol. Med. Ger. **5** 153 (1960).  
b) A.B. Kar, R.P. Das and B. Mukerji, Proc. Nat. Inst. Sci. India, Part B (Suppl) **26** 40 (1960).



152. a) J. Parizek and I. Ostadalová, Experientia **23** 142 (1967).  
 b) J. Parizek, I. Ostadalová, J. Kalouskova, A. Babicky and J. Benes, Chapter 6 in "Newer Trace Elements in Nutrition", W. Mertz and W.E. Cornatzer (Eds.), Marcel Dekker, New York (1971).
153. D.V. Frost and P.M. Lish, Ann. Rev. Pharmacol. **259** (1975).
154. J.M. Tobias, C.C. Lushbaugh, H.M. Patt, S. Postel, M.N. Swift and R.W. Gerard, J. Pharmacol. Exp. Ther. Suppl. **87** 102 (1946).
155. Z.M. Holl6 and S. Zlatarov, Naturwissenschaften **47** 87 (1960).
156. W. Rusiecki and J. Brzezinski, Acta Polon. Pharm. **23** 69 (1966).
157. O.A. Levander and L.C. Argrett, Toxicol. Appl. Pharmacol. **14** 308 (1969).
158. D.V. Frost, C.R.C. Crit. Rev. Toxicol. **1** 467 (1972).
159. a) J. Parizek, J. Kalouskova, A. Babicky, J. Benes and L. Pavilik in "Trace Element Metabolism in Man and Animals", W.G. Hoekstra, J.W. Suttie, H.E. Ganther and W. Mertz (Eds.), University Park Press, Baltimore (1974).  
 b) J. Parizek, I. Benes, I.O. Ostadalová, A. Babický, J. Benes and J. Pitha, Chapter 8 in "Mineral Metabolism in Pediatrics", D. Barltrop and W.L. Barland (Eds.), Blackwell Scientific Publications, Oxford (1969).
160. L. Magos and M. Webb, C.R.C. Crit. Rev. Toxicol. **8** 1 (1980).
161. J. Parizek, J. Kalouskova, J. Benes and L. Pavlik, Ann. N.Y. Acad. Sci. **355** 347 (1980).
162. The Task Group on Metal Interaction, Environ. Health Perspect. **25** 3 (1978).
163. D.L. Dilworth and R.S. Bandurski, Biochem. J. **163** 521 (1977).
164. H.E. Ganther, Biochemistry, **10** 4089 (1971).
165. T.A. Gasiewicz and J.C. Smith, Chem. Biol. Interact. **21** 299 (1978).
166. H.S. Hsieh and H.E. Ganther, Biochemistry **14** 1632 (1975).
167. H.E. Ganther and H.S. Hsieh in ref. 159a.
168. M. Sandholm, Acta Pharmacol. Toxicol. **36** 321 (1975).
169. A.T. Diplock, C.R.C. Crit. Rev. Toxicol. **4** 271 (1976).
170. K. Nakomuro, Y. Sayato and Y. Ose, Toxicol. App. Pharmacol. **39** 521 (1977).
171. I.S. Palmer, R.P. Gunsalus, A.W. Halverson and O.E. Olson, Biochim. Biophys. Acta **208** 260 (1970).

172. J.L. Byard, Arch. Biochem. Biophys. **130** 556 (1969).
173. a) J.T. Rotruck, W.G. Hoekstra and A.L. Pope, Nature New Biol. **231** 223 (1971).  
b) J.T. Rotruck, A.L. Pope, H.E. Ganther, A.B. Swanson, D.G. Hafeman and W.G. Hoekstra, Science **179** 588 (1973).
174. D.G. Hafeman, R.A. Sunde and W.G. Hoekstra, J. Nutr. **104** 580 (1974).
175. S.H. Oh, H.E. Ganther and W.G. Hoekstra, Biochemistry **13** 1825 (1974).
176. J.W. Forstrom, J.J. Zakowski and A.L. Tappel, Biochemistry **17** 2639 (1978).
177. H.E. Ganther, Chem. Scr. **8A** 79 (1975).
178. A. Wendel, W. Pitz, R. Ladenstein, G. Sawatzki and U. Weser, Biochim. Biophys. Acta **377** 211 (1975).
179. a) J.E. Cone, R. Martín del Río and T.C. Stadtman, J. Biol. Chem. **252** 5337 (1977).
180. H.G. Enoch and R.L. Lester, J. Biol. Chem. **250** 6693 (1975).
181. a) P.D. Whanger, Fed. Proc. **31** 691 (1972).  
b) P.D. Whanger, N.D. Pedersen and P.H. Weswig, p571 in ref.
182. M. Berlin, Environ. Health Perspect. **25** 67 (1978).
183. D.A. Levander, Fed. Proc. **36** 1683 (1977).
184. S.P. Nygaard and J.C. Hansen, Bull. Environ. Contam. Toxicol. **20** 20 (1978).
185. a) S.D. Potter, G. Matrone, Fed. Proc. **32** 929 (1973) and  
b) J. Nutr. **104** 638 (1974).
186. D.H. Groth, L. Stettler and G. Machey in "Effects and Dose-Response Relationships of Toxic Metals", G.F. Nordberg (Ed.), Elsevier, Amsterdam (1976), p.527.
187. N.G. Carmichael and B.A. Fowler, J. Environ. Pathol. Toxicol. **3** 339 (1980).
188. a) V. Eybl, J. Sykora and F. Mertl, Experientia **25** 504 (1969) and  
b) Arch. Toxicol. **25** 296 (1969).
189. A.E. Moffitt and J.J. Clary, Res. Commun. Chem. Pathol. Pharmacol. **7** 593 (1974).
190. B.R. Stillings, H. Lagally, P. Bauersfeld and J. Soares, Toxicol. Appl. Pharmacol. **30** 243 (1974).
191. P. Kristensen and J.C. Hansen, Toxicology **16** 39 (1980).
192. J. Parizek, I. Ostadalova, I. Benés, A. Babický and J. Benés, Cs. Fysiol. **16** 41 (1967).

193. L. Magos and M. Webb, Arch. Toxicol. **36** 63 (1976).
194. a) Y. Yamane, H. Fukino, Y. Aida and M. Imagawa, Chem. Pharm. Bull. **26** 703 (1977) and  
b) Yakugaku Zasshi **97** 667 (1977).
195. a) O. Wada, N. Yamaguchi, T. Ono, M. Nagahashi and T. Morimura, Environ. Res. **12** 75 (1976).  
b) D.H. Groth *et al.* in ref.
196. R.W. Chen, V.L. Lacy and P.D. Whanger, Res. Commun. Chem. Pathol. Pharmacol. **12** 297 (1975).
197. E. Komsta-Szumaska, J. Chmielnicka and J.K. Piotrowski, Biochem. Pharmacol. **25** 2539 (1976).
198. J.K. Piotrowski and J.A. Szymanska, Toxicol. Environ. Health **1** 991 (1976).
199. a) J.M. Wisniewska, B. Trojanowska, J.K. Piotrowski and M. Jakubowski, Toxicol. Appl. Pharmacol. **16** 754 (1970).  
b) J.K. Piotrowski, B. Trojanowska, J.M. Wisniewska-Knypl and W. Bolanowska, Toxicol. Appl. Pharmacol. **27** 11 (1974).  
c) J.K. Piotrowski, B. Trojanowska and A. Sapota, Arch. Toxicol. **32** 351 (1974).
200. E. Komsta-Szumaska and J. Chmielnicka, Arch. Toxicol. **38** 217 (1977).
201. J. Chmielnicka, E. Komsta-Szumaska and B. Sulkowska, Bioinorg. Chem. **8** 291 (1978).
202. O.A. Levander, V.C. Morris and D.J. Higgs, Biochemistry **12** 4586 (1973).
203. R.W. Chen, P.D. Whanger and S.C. Fang, Pharmacol. Res. Commun. **6** 571 (1974).
204. A. Naganuma, S.-K. Pan and N. Imura, Res. Comm. Chem. Pathol. Pharmacol. **20** 139 (1978).
205. H. Mengel and O. Karlog, Acta Pharmacol. Toxicol. **46** 25 (1980).
206. R.F. Burk, H.E. Jordan Jr., K.W. Kiker, Appl. Pharmacol. **40** 71 (1977).
207. J.H. Koeman, W.H.M. Peeters, C.H.M. Koudstaal-Hol, P.S. Tijoe and J.J.M. de Goeij, Nature (London) **245** 385 (1973).
208. R. Martoja and D. Viale, Compt. Rend. Acad. Sci. Paris **285D** 109 (1977).
209. J.H. Koeman, W.S.M. Van de Ven, J.J.M. De Goeij, P.S. Tjioe, J.L. Van Haaften, Sci. Total Environ. **3** 279 (1975).
210. L. Kosta, A.R. Byrne and V. Zelenko, Nature (London) **254** 238 (1975).
211. L.C. Rossi, G.F. Clementeand and G. Santaroni, Arch. Environ. Health **31** 160 (1976).

212. J. Parizek, I. Benes, A. Babický, V. Procházková and J. Lener, Physiol. Bohemoslov. **18** 105 (1969).
213. A. Hellesberg and N. Gyrd-Hansen, Acta Pharmacol. Toxicol. **38** 284 (1976).
214. J. Chmielnicka and E.A. Brzeznicka, Bull. Environ. Contam. Toxicol. **19** 183 (1978).
215. S. Skerfving, Environ. Health Perspect. **25** 57 (1978).
216. Y. Hirota, S. Yamaguchi, N. Shimojoh and K. Sano, Toxicol. Appl. Pharmacol. **53** 174 (1980).
217. a) H.E. Ganther and M.L. Sunde, J. Food Sci. **39** 1 (1974).  
b) H.E. Ganther, C. Goudie, M.L. Sunde, M.J. Kopecky, P. Wagner, S.-H. Oh, and W.G. Hoekstra, Science **175** 1122 (1975).  
c) H.E. Ganther, Environ. Health Perspect. **25** 71 (1978).
218. G.S. Stoewsand, C.A. Bache and D.J. Lisk, Bull. Environ. Contam. Toxicol. **11** 152 (1974).
219. S.O. Welsh and J.H. Soares, Nutr. Rep. Int. **13** 43 (1976).
220. J.L. Sell and F.G. Horani, Nutr. Rep. Int. **14** 439 (1976).
221. a) G. Ohi, S. Nishigaki, H. Seki, Y. Tamura, T. Maki, K. Minowa, Y. Shimamura, I. Mizoguchi, T. Inaba *et al.* Food Cosmet. Toxicol. **18** 139 (1980).  
b) G. Ohi, S. Nishigaki, H. Seki, Y. Tamura, T. Maki, H. Kanno, S. Ochiai, H. Yamada, I. Mizoguchi and H. Yagyu, Environ. Res. **12** 49 (1976).
222. H. Iwata, H. Okamoto and Y. Ohsawa, Res. Comm. Chem. Pathol. Pharmacol. **5** 673 (1973).
223. L. Magos and M. Webb, Arch. Toxicol. **38** 201 (1977).
224. H.E. Ganther, P.A. Wagner, M.L. Sunde and W.G. Hoekstra in "Trace Substances in Environmental Health", D.D. Hemphill (Ed.), Univ. Missouri Press, Columbia (1973).
225. M.M. El-Begearmi, M.L. Sunde and H.E. Ganther, Poultry Sci. **56** 313 (1977).
226. J.A. Froseth, R.C. Piper and J.R. Carlson, Fed. Proc. **33** 660 (1974).
227. S.L. Johnson and W.G. Pond, Nutr. Rep. Int. **9** 135 (1974).
228. S.C. Fang, Res. Comm. Chem. Path. Pharmacol. **9** 579 (1974).
229. K. Sumino, R. Yamamoto and S. Kitamura, Nature (London) **268** 73 (1977).
230. N.W. Alcock, P.A. Lampe and P. Moore, J. Chem. Soc., Dalton Trans. 1471 (1980).
231. A.J. Canty, R. Kishimoto, G.B. Deacon and G.J. Farquarson, Inorg. Chim. Acta **20** 161 (1976).

232. a) R.L. Coates and M.M. Jones, J. Inorg. Nucl. Chem. 39 677 (1976).  
b) J.S. Casas and M.M. Jones, J. Inorg. Nucl. Chem. 42 99 (1980).
233. A. Albert "Selective Toxicity" 6th ed. Chapman & Hall (1979).
234. I.M. Weiner, R.I. Levy and G.H. Mudge, J. Pharmacol. Exp. Ther. 138 96 (1962).
235. B.D. Hilton, M. Man, E. Hsi and R.G. Bryant, J. Inorg. Nucl. Chem. 37 1073 (1975).
236. N.J. Taylor, Y.S. Wong, P.C. Chieh and A.J. Carty, J. Chem. Soc., Dalton Trans. 438 (1975).
237. Y.S. Wong, A.J. Carty and P.C. Chieh, J. Chem. Soc., Dalton Trans. 1801 (1977).
238. A.J. Carty and R. Kishimoto, Inorg. Chim. Acta. 24 109 (1977).
239. A.T. Hutton, H.M.N.H. Irving, L.R. Nassimbeni and G. Gafner, Acta Crystallogr. 36B 2064 (1980).
240. R.D. Bach, A.T. Weibel, W. Schmonsees and M.D. Glick, J. Chem. Soc., Chem. Comm. 961 (1974).
241. L.G. Kuz'mina, N.G. Bokii, Yu. T. Struchkov, D.N. Kravtsov and E.M. Rokhlina, J. Struct. Chem. 15 419 (1974).
242. L. Pauling, "The Nature of the Chemical Bond", 3rd ed., Cornell University Press, Ithaca, New York (1960) p.225.
243. D. Grdenić, Quart. Rev. Chem. Soc. 19 303 (1965).
244. C. Chieh, Can. J. Chem. 56 560 (1978).
245. D.A. Stuart, L.R. Nassimbeni, A.T. Hutton and K.R. Koch, Acta Crystallogr. 36B 2227 (1980).
246. A.J. Carty, Chapter 21 in "Organometals and Organometalloids: Occurrence and Fate in the Environment", F.E. Brinckman & J.M. Bellama (eds), A.C.S. Symposium Series 82 (1978).
247. Y.S. Wong, P.C. Chieh and A.J. Carty, J. Chem. Soc., Chem. Comm. 741 (1973).
248. Y.S. Wong, P.C. Chieh and A.J. Carty, Can. J. Chem. 51 2597 (1973).
249. A.J. Carty, N. Chaichit, B.M. Gatehouse, E.E. George and G. Hayhurst, Inorg. Chem. 20 2414 (1981) and references therein.
250. a) R.D. Bach and A.T. Weibel, J. Am. Chem. Soc. 97 2575 (1975)  
b) R.D. Bach and A.T. Weibel, J. Am. Chem. Soc. 98 6241 (1976).
251. R.A. Nyquist and J.R. Mann, Spectrochim. Acta 28A 511 (1972).
252. N. Iwasaki, J. Tomooka and K. Toyoda, Bull. Chem. Soc. Jap. 47 1323 (1974).

253. J. Devereux, B.Sc. Hons. thesis, University of Tasmania (1979).
254. Y.S. Wong, A.J. Carty and C. Chieh, J. Chem. Soc., Dalton Trans. 1801 (1977).
255. H.S. Gutowsky, J. Chem. Phys. 17 128 (1949).
256. D. Breitinger, A. Zober and M. Neubauer, J. Organomet. Chem. 30 C49 (1971).
257. J.H.S. Breen, Spectrochim. Acta 24A 863 (1968).
258. Z. Meić and M. Randić, J. Mol. Spectrosc. 39 39 (1971).
259. Z. Meić and M. Randić, J. Chem. Soc., Faraday Trans. II 68 444 (1972).
260. Z. Meić, J. Mol. Struct. 23 131 (1974).
261. P.L. Goggin and L.A. Woodward, Trans. Faraday Soc. 62 1423 (1966).
262. P.L. Goggin, G. Kemeny and J. Mink, J. Chem. Soc., Faraday Trans. II 72 1025 (1976).
263. P.L. Goggin, R.J. Goodfellow and N.W. Hurst, J. Chem. Soc., Dalton Trans. 561 (1978).
264. Z. Meić and M. Randić, Trans. Faraday Soc. 64 1438 (1968).
265. F. Glockling, N.S. Hosmane, V.B. Mahale, J.J. Swindall, L. Magos and T.J. King, J. Chem. Res. (S.) 116 (1977).
266. J.R. Hall and J.C. Mills, J. Organomet. Chem. 6 445 (1966).
267. R.P.J. Cooney and J.R. Hall, Aust. J. Chem. 22 2117 (1969).
268. J. Relf, R.P. Cooney and H.F. Henneike, J. Organomet. Chem. 39 75 (1972).
269. N. Iwasaki, Bull. Chem. Soc. Jap. 49 2735 (1976).
270. A.F. Wells, Z. Kristallogr. 96 435 (1937).
271. a) D.C. Bradley and N.R. Kunchur, J. Chem. Phys. 40 2258 (1964).  
b) D.C. Bradley and N.R. Kunchur, Chem. Ind. (London) 1240 (1962).
272. P. Biscarini, L. Fusina and G. Nivellini, J. Chem. Soc., Dalton Trans. 2140 (1974).
273. N.R. Kunchur, Nature (London) 204 468 (1964).
274. D.C. Bradley and N.R. Kunchur, Can. J. Chem. 43 2786 (1965).
275. A.Ozola, J. Ozols and A. Ievins, Latv. PSR. Zinat. Akad. Vestis, Kim. Ser. 361 (1972); CA77: 80694.
276. P. Lavertue, J. Hubert and A.L. Beauchamp, Inorg. Chem. 15 322 (1976).
277. N.J. Taylor and A.J. Carty, J. Am. Chem. Soc. 99 6143 (1977).

278. A.J. Carty and N.J. Taylor, J. Chem. Soc., Chem. Comm. 214 (1976).
279. C.N. Myers, J. Lab. Clin. Med. 6 359 (1921); CA15: 2274.
280. A.H. Freidheim, Brit. Patent 716,647 (1954) CA:49 12530d.
281. V.E. Petrun'kin, Ukr. Khim. Zh. 22 787 (1956); CA51: ;4537h.
282. M.B. Mishra and H.L. Nigam, Ind. J. Chem. 9 601 (1971).
283. S.K. Srivastava and H.L. Nigam, Current Science 41 601 (1972).
284. P.R. Patil and V. Krishnan, J. Inorg. Nucl. Chem. 40 1255 (1978).
285. G.E. Coates and D. Ridley, J. Chem. Soc. 166 (1964).
286. G.B. Deacon, J.H.S. Green and W. Kynaston, Aust. J. Chem. 19 603 (1966).
287. M.A. Hooper and D.W. James, Aust. J. Chem. 24 1331 (1971).
288. D.H. Roxenblatt and G.N. Jean, J. Phys. Chem. 59 626 (1955).
289. W.H. Mills and R.E.D. Clark, J. Chem. Soc. 175 (1935).
290. A.J. Downs, E.A.V. Ebsworth and H.J. Emeléus, J. Chem. Soc. 3187 (1961).
291. A.J. Carty and R.K. TYson, Inorg. Chim. Acta 29 227 (1978).
292. A.J. Carty and R.K. TYson, Inorg. Chim. Acta 24 L77 (1977).
293. A.J. Carty, C.L. Raston and A.H. White, Aust. J. Chem. 31 677 (1978).
294. H. Puff, R. Sievers and G. Elsner, Z. Anorg. Allg. Chem. 413 37 (1975).
295. A.J. Carty, C.L. Raston and A.H. White, Aust. J. Chem. 32 311 (1979).
296. A.J. Carty, C.L. Raston and A.H. White, Aust. J. Chem. 32 1165 (1979).
297. A.J. Carty, Spectrochim. Acta 37A 283 (1981).
298. a) A. Terzis, J.B. Faught and G. Pouskoullelis, Inorg. Chem. 19 1060 (1980).  
b) G. Pouskoullelis, P. Kourounakis and T. Theophanides, Inorg. Chim. Acta 24 45 (1977).
299. P. Biscarini, L. Fusina and G. Nivellini, Spectrochim. Acta 36A 593 (1980).
300. a) Y. Mikawa, R.J. Jakobsen and J.W. Brasch, J. Chem. Phys. 45 4528 (1966).  
b) H. Poulet and J.P. Mathien, J. Chem. Phys. Phys.-Chim. Biol. 60 442 (1963).
301. A.J. Carty, R. Kishimoto and R.K. TYson, Aust. J. Chem. 31 671 (1978).
302. R.S. Reid and D.L. Rabenstein, Can. J. Chem. 59 1505 (1981).

303. R.S. Reid and D.L. Rabenstein (unpublished) ref. [25] in ref. 337.
304. a) A.J. Canty, N. Chaichit, B.M. Gatehouse and E.E. George, Inorg. Chem. 20 in press (1981) and references therein.  
b) A.J. Canty and C.V. Lee, Inorg. Chim. Acta 54 L205 (1981) and references therein.
305. G. Schwarzenbach and M. Schellenberg, Helv. Chim. Acta 48 28 (1965).
306. D.L. Rabenstein, C.A. Evans, M.C. Tourangeau and M.T. Fairhurst, Anal. Chem. 47 338 (1975).
307. J.H.R. Clarke and L.A. Woodward, Trans. Faraday Soc. 62 3022 (1966).
308. P.L. Goggin and L.A. Woodward, Trans. Faraday Soc. 56 1591 (1960) and 58 1495 (1962).
309. S. Libich and D.L. Rabenstein, Anal. Chem. 45 118 (1973).
310. D. Grdenic, B. Kamenar and S. Pocev, Acta Crystallogr. 34A S127 (1978).
311. M. Bruvo, D. Grdenic, B. Kamenar and S. Pocev, Izc. Jug. Cent. Krist., Ser. A. 11 24 (1976).
312. G. Anderegg, Helv. Chim. Acta 57 1340 (1974).
313. M. Jawaid, F. Ingman and D.H. Liem, Acta Chem. Scand. 32A 333 (1978).
314. P. Zanella, G. Plazzogna and G. Tagliavini, Inorg. Chim. Acta 2 340 (1968).
315. T.D. Waugh, H.F. Watton and J.A. Laswick, J. Phys. Chem. 59 395 (1955).
316. F. Ingman and D.H. Liem, Acta Chem. Scand. 28A 947 (1974).
317. J.L. Sudneier, R.R. Birge and T.G. Perkins, J. Magn. Reson. 30 491 (1978).
318. C.W. Davies, J. Chem. Soc. 2093 (1938).
319. I.W. Erni, Ph.D. Dissertation ETH, Zurich (1977).
320. R.P. Bell, "The Proton in Chemistry", Chapman and Hall, London (1973).
321. J. Lorberth and F. Weller, J. Organomet. Chem. 32 145 (1971) see L.A. Fedorov, J. Struct. Chem. 216 (1976).
322. J.V. Hatton, W.G. Schneider and W. Siebrand, J. Chem. Phys. 39 1330 (1963).
323. D.L. Rabenstein, M.C. Tourangeau and C.A. Evans, Can. J. Chem. 54 2517 (1976).
324. R.B. Simpson, J. Am. Chem. Soc. 83 4711 (1961).
325. R. Scheffold, Helv. Chim. Acta 52 56 (1969).
326. R. Scheffold, Helv. Chim. Acta 50 1419 (1967).



327. L.F. Sytsma and R.J. Kline, J. Organomet. Chem. **54** 15 (1973).
328. R.J. Maguire, S. Anand, H. Chew and W.A. Adams, J. Inorg. Nucl. Chem. **38** 1659 (1976).
329. G.C. Hood, O. Redlich, C.A. Reilly, J. Chem. Phys. **23** 2229 (1955).
330. P.R. Wells and W. Kitching, Tetrahedron Lett. 1531 (1963).
331. D.L. Rabenstein, R. Ozubko, S. Libich, C.A. Evans, M.T. Fairhurst and C. Suvanprakorn, J. Coord. Chem. **3** 263 (1974).
332. A.J. Canty and A. Marker, Inorg. Chem. **15** 425 (1976).
333. M. Jawaid, Talanta **25** 215 (1978).
334. R.B. Simpson, J. Am. Chem. Soc. **86** 2059 (1964).
335. P. Svejda, A.H. Maki and R.R. Anderson, J. Am. Chem. Soc. **100** 7138 (1978).
336. P.A. Lampe and P. Moore, Inorg. Chim. Acta **36** 27 (1979).
337. M.V. Hershberger and A.H. Maki, J. Inorg. Biochem. **13** 273 (1980).
338. M.T. Fairhurst and D.L. Rabenstein, Inorg. Chem. **14** 1413 (1975).
339. G. Geier, I. Erni and R. Skiner, Helv. Chim. Acta **60** 9 (1977).
340. M.D. Rausch and J.R. Van Wazer, Inorg. Chem. **3** 761 (1964).
341. A.J. Brown, O.W. Howarth and P. Moore, J. Chem. Soc., Dalton Trans. 1589 (1976).
342. M. Jawaid, F. Ingman, D.H. Liem and T. Wallin, Acta Chem. Scand. **32A** 7 (1978).
343. Y. Kawasaki, M. Aritomi and J. Iyoda, Bull. Chem. Soc. Jpn. **49** 3478 (1976).
344. R.A. Jones and A.R. Katritzky, J. Chem. Soc. 3610 (1958).
345. L. Ciavatta, M. Grimaldi and R. Palombari, J. Inorg. Nucl. Chem. **37** 1685 (1975).
346. N.G. Carmichael and B.A. Fowler, J. Environ. Pathol. Toxicol. **3** 399 (1980).
347. V.S. Petroxian and O.A. Reutov, J. Organomet. Chem. **76** 123 (1974).
348. R.R. Dean and W. McFarlane, Mol. Phys. **13** 343 (1967).
349. J.M.T. Raycheba and G. Geier, Inorg. Chem. **18** 2486 (1979).
350. M. Eigen, Angew. Chem. Int. Ed. Engl. **3** 1 (1964).
351. M. Eigen, G. Ilgenfritz and W. Kruse, Chem. Ber. **98** 1623 (1965).

352. G. Schwarzenbach and E. Felder, Helv. Chim. Acta **27** 1701 (1944).
353. "Stability Constants of Metal-Ion Complexes", L.G. Sillen and A.E. Martell (eds), The Chemical Society (London), Spec. Publ. 17 (1964) and Supplement 1, Spec. Pub. 25 (1971).
354. D.L. Rabenstein, J. Chem. Ed. **55** 292 (1978).
355. H.F. Henneike, J. Am. Chem. Soc. **94** 5945 (1972).
356. R.B. Simpson, J. Chem. Phys. **46** 4775 (1967).
357. L.L. Murrell and T.L. Brown, J. Organomet. Chem. **13** 301 (1968).
358. P.R. Wells, W. Kitching and R.F. Henzell, Tetrahedron Lett. 1029 (1964).
359. D.L. Rabenstein and C.A. Evans, Bioinorg. Chem. **8** 107 (1978).
360. D.L. Rabenstein and M.T. Fairhurst, J. Am. Chem. Soc. **97** 2086 (1975).
361. S. Arakawa, R.D. Bach and T. Kimura, J. Am. Chem. Soc. **102** 6847 (1980).
362. G. Schwarzenbach and U. Karlen (unpublished) ref [49] in ref. 361.
363. Y. Hojo, Y. Sugiura and H. Tanaka, J. Inorg. Nucl. Chem. **38** 641 (1976).
364. H. Gross (unpublished) ref [136] in ref. 361.
365. G. Geier and I.W. Erni, Chimia **27** 635 (1973).
366. O Bud evsky, F. Ingman and D.H. Liem, Acta Chem. Scand. **27** 1277 (1973).
367. W.L. Hughes, Ann. N.Y. Acad. Sci. **65** 454 (1957).
368. W.L. Hughes, Jr., Cold Spring Harbour Symp. Quant. Biol. **14** 79 (1950).
369. D.L. Rabenstein, J. Am. Chem. Soc. **95** 2797 (1973).
370. N.C. Li and R.A. Manning, J. Am. Chem. Soc. **77** 5225 (1955).
371. D.L. Leussing and L. Newman, J. Am. Chem. Soc. **78** 552 (1956).
372. D.L. Leussing and I.M. Kolthoff, J. Am. Chem. Soc. **75** 3904 (1953).
373. D.L. Leussing, J. Am. Chem. Soc. **80** 4180 (1958).
374. J.L. Kurz and J.C. Harris, J. Org. Chem. **35** 3086 (1970).
375. G.R. Lenz and A.E. Martell, Inorg. Chem. **4** 378 (1965).
376. G.E. Cheney, Q. Fernando and H. Freiser, J. Phys. Chem. **63** 2055 (1959).
377. L.J. Porter and D.D. Perrin, Aust. J. Chem. **22** 267 (1969).

378. S.J. Backs and D.L. Rabenstein, Inorg. Chem. **20** 410 (1981).
379. P.J. Antikainen and K. Tevanen, Suomen Kemi. **35B** 224 (1962).
380. R.J. Irving, L. Nelander and I Wadsö, Acta Chem. Scand. **18** 769 (1964).
381. J.H. Ritsma and F. Jellinek, Recl. Trav. Chim. Pays-Bas **91** 923 (1972).
382. L. Pillai, R.D. Boss and M.S. Greenberg, J. Solution Chem. **8** 635 (1979).
383. G.R. Lenz and A.E. Martell, Biochemistry **3** 745 (1969).
384. K. Wallenfels and C. Streffer, Biochem. Z. **346** 119 (1966).
385. E.J. Kuchinskas and Y. Rosen, Arch. Biochem. Biophys. **97** 370 (1962).
386. E.W. Wilson and R.B. Martin, Arch. Biochim. Biophys. **142** 445 (1971).
387. N. Kojima, Y. Sugiura and H. Tanaka, Bull. Chem. Soc. Jpn. **49** 1294 (1976).
388. D.A. Doornbos, Pharm. Weekblad. **102** 269 (1967).
389. R.B. Martin and J.T. Edsall, Bull. Soc. Chim. (Biol). **40** 1763 (1958).
390. N.C. Li, O. Gawron and G. Bascuas, J. Am. Chem. Soc. **76** 225 (1954).
391. Ya. L. Kostyukovskii, Yu. A. Bruk, A.V. Kokushkina, B.S. Mirkin, N.M. Slavachevskaya, L.V. Pavlova and I.A. Belen'kaya, Zh. Obshch. Khim. **42** 2104 (1972); CA78: 42615v.
392. L. Larsson and B. Hansen, Svensk. Kem. Tidskr. **68** 521 (1956).
393. a) G. Gran, Acta Chem. Scand. **4** 559 (1950).  
b) A. Johansson and G. Gran, Analyst **105** 802 (1980).  
c) G. Gran and A. Johansson, Analyst **106** 231 (1981).
394. a) G. Gran, Analyst **77** 661 (1952).  
b) L. Pehrsson, F. Ingman and A. Johansson, Talanta **23** 769 (1976).
395. F.J.C. Rossotti and H. Rossotti, J. Chem. Ed. **42** 375 (1965).
396. K. Matsunaga, T. Ishida and T. Oda, Anal. Chem. **48** 1421 (1976).
397. F. Ingman, Talanta **18** 744 (1971).
398. R.B. Simpson and H.A. Saroff, J. Am. Chem. Soc. **80** 2129 (1958).
399. A.I. Vogel, "A Textbook of Quantitative Inorganic Analysis", 3rd ed., Longmans, London (1972), p.349.
400. D.D. Perrin, W.L.F. Armarego and D.R. Perrin, "Purification of Laboratory Chemicals", Pergamon Press, London (1966).

401. D.L. Leussing and I.M. Kolthoff, J. Electrochem. Soc. **100** 334 (1953).
402. Aldrich Chemical Co. Ltd., Catalog Handbook of Fine Chemicals (1981-2).
403. P.G. Simpson, T.E. Hopkins and R. Hague, J. Phys. Chem. **77** 2282 (1973).
404. Y. Sugiura, Y. Tamai and H. Tanaka, Bioinorg. Chem. **9** 167 (1978).
405. Y. Sugiura, Y. Hojo, Y. Tamai and H. Tanaka, J. Am. Chem. Soc. **98** 2339 (1976).
406. H. Barrera and R.E. Lyle, J. Org. Chem. **27** 641 (1962).
407. R.E. Benesch and R. Benesch, J. Am. Chem. Soc. **77** 5877 (1955).
408. D.L. Leussing, J. Am. Chem. Soc. **81** 4208 (1959).
409. D.L. Leussing and J.P. Mislan, J. Phys. Chem. **64** 1908 (1960).
410. I.E. Okonishnikova, L.G. Egorva, V.L. Nironberg and I.Ya. Postovskii, Khim.-Farm. Zh. **4** 21 (1970).
411. A. Agren and G. Schwarzenbach, Helv. Chim. Acta **38** 1920 (1955).
412. A.T. Pilipenko and O.P. Ryabushko, Ukrain. Khim. Zh. **32** 622 (1966); CA65: 114126.
413. P.J. Antikainen and V.M.K. Rosi, Suomen Kemi. **36B** T32 (1963).
414. A.T. Pilipenko and A.P. Kostyshina, Isv. Vysshikh. Uchebn. Zavedanii Khim. i Khim. Tekhnol. **5** 502 (1962); CA57: 14482c.
415. M.-O. Hedblom, Arkiv Kemi. **31** 489 (1969).
416. M. Gerecke, E.A.H. Friedheim and A. Brossi, Helv. Chim. Acta **44** 955 (1961).
417. E. Bittar, "Cell pH" Butterworths (Washington D.C.) (1964).
418. see, for example, W. Derbyshire, in "Nuclear Magnetic Resonance", The Chemical Society (London). Specialist Periodical Reports, Vol. 9, Chapter 12.
419. G. Berthon, P.M. May and D.R. Williams, J. Chem. Soc., Dalton Trans. 1433 (1978).
420. O. Siggaard-Andersen, R.A. Durst and A.H.J. Maas, Pure Appl. Chem. **53** 1605 (1981).
421. H. Sakurai and S. Takeshima, Inorg. Chim. Acta **56** L29 (1981).
422. J.T. MacGregor and T.W. Clarkson, Adv. Exp. Med. Biol. **48** 463 (1974).
423. E.M. Kosower, Chapter 1 in "Glutathione: Metabolism and Function", I.M. Arias and W.B. Jakoby (eds) Raven Press, New York (1976).
424. M.C. Lim and R.B. Martin, J. Inorg. Nucl. Chem. **38** 1911 (1976).

425. W.H.H. Günther and H.G. Mautner, J. Med. Chem. **8** 845 (1965).
426. G. Zdansky, Chapter XIIA in ref. 195.
427. G. Zdansky, Arkiv. Kemi. **17** 519 (1961), **29** 443 (1968), **26** 213 (1966).
428. a) C.-G. Späre and A.I. Virtanen, Acta Chem. Scand. **18** 280 (1964).  
b) S.N. Nigam and W.B. McConnell, Biochim. Biophys. Acta **192** 185 (1969), and S.N. Nigam, J.I. Tu and W.B. McConnell, Phytochemistry **8** 1161 (1969).
429. C. Drăguet and M. Penson, Bull. Soc.Chem. Belg. **81** 303 (1972).
430. N.N. Yarovenko, M.A. Raksha and V.N. Shemanina, Zh. Obshch. Khim. **30** 4069 (1960): CA55:20542f.
431. D. Theodoropolous, I.L. Schwartz and R. walter, Tetrahedron Lett. **2411** (1967) and Biochemistry **6** 3927 (1967).
432. B. Nygård, Arkiv. Kemi. **27** 341 (1967), and Chem. Zvesti **16** 320 (1962); CA58 7609a.
433. S.F. Malone, M.Sc. thesis, University of Waterloo (1979).
434. A.J. Carty, S.F. Malone and N.J. Taylor, J. Organomet. Chem. **172** 201 (1979).
435. D. Breitinger and W. Morell, Inorg. Nucl. Chem. Lett. **10** 409 (1974).
436. C. Siemens, Annalen der Chemie und Pharmacie **61** 360 (1847).
437. E. Wertheim, J. Am. Chem. Soc. **51** 3661 (1929).
438. P. Claesson, Justus Liebig's Ann. Chem. **187** 113 (1877).
439. A. Baroni, Atti. Accad. Naz. Lincei Mem., Classe Sci., Fis., Mat. Nat. **12** 234 (1930).
440. A. Fredga, "Studien über Selen-di-karbonsäuren under diselen-di-karbonsäure" Uppsala (1935).
441. L. Tschugaeff, Chem. Ber. **42** 49 (1909).
442. D.S. Margolis and R.W. Pittman, J. Chem. Soc. 799 (1957).
443. A. Fredga, Svensk. Kem. Tidskr. **48** 91 (1936).
444. A. Fredga, Arkiv. Kemi., Mineral. Geol. **11B** no.44 (1934) (see also 217).
445. Y. Okamoto and T. Yano, J. Organomet. Chem. **29** 99 (1971).
446. D. Spinelli and C. Dell'Erba, Ann. Chim. (Rome) **51** 45 (1961).
447. J.W. Dale, H.J. Emeléus and R.N. Haszeldine, J. Chem. Soc. 2939 (1958).
448. H.J. Clase and E.A.V. Ebsworth, J. Chem. Soc. 940 (1965).
449. M.L.N. Reddy, M.R. Wiles and A.G. Massey, Nature (London) **217** 740 (1968).

- 449b. H.J. Antweiler, Dissertation, Bonn (1935), see 'Beilsteins Handbuch der Organischen Chemie', 4th ed., Vol.6, Supplement III, p1650.
450. E. Kostlner, M.L.N. Reddy, D.S. Urch and A.G. Massey, J. Organomet. Chem. **15** 383 (1968).
451. N.C. Vyazankin, V.T. Bushkov, I.A. Vostokov and O.V. Pinzina, Zh. Obshch. Khim. **38** 663 (1965).
452. H. Rheinboldt, F. Mott and E. Motzkus, J. Prakt. Chem. **134** 17 (1932).
453. R. Kishimoto, Ph.D. thesis, University of Tasmania (1977).
454. D.T. Cromer and J.B. Mann, Acta Cryst. Allogr. **24A** 321 (1968).
455. D.T. Cromer and D. Liberman, J. Chem. Phys. **53** 1891 (1970).
456. R.F. Stewart, E.R. Davidson and W.T. Simpson, J. Chem. Phys. **42** 3175 (1965).
457. 'The X-RAY system, Version of March 1976', Technical Report TR-446, J.M. Stewart (ed), Computer Science Centre, University of Maryland.
458. L.S. Dent Glasser, L. Ingram, M.G. King and G.P. McQuillan, J. Chem. Soc. (A) 2501 (1969).
459. P. Coppens, Y.W. Yang, R.H. Blessing, W.F. Cooper and F.K. Larsen, J. Am. Chem. Soc. **99** 760 (1977).
460. O. Foss and V. Janickis, J. Chem. Soc., Chem. Comm. 834 (1977).
461. P. Böttcher, Z. Anorg. Aus. Chem. **432** 167 (1977).
462. A. Cisar and J.D. Corbett, Inorg. Chem. **16** 632 (1977).
463. O. Foss, K. Johnsen and T. Reistad, Acta Chem. Scand. **18** 2345 (1964).
464. A. Whitaker, Z. Kristallogr., Kristallgeom., Kristallphys., Kristallchem. **148** 45 (1979); CA90:144574w.
465. O. Foss and V. Janickis, J. Chem. Soc., Chem. Comm. 833 (1977).
466. C.M. Woodard, D.S. Brown, J.D. Lee and A.G. Massey, J. Organomet. Chem. **121** 333 (1976).
467. M. Sacerdoti, G. Gilli and P. Domiano, Acta Crystallogr. **31B** 327 (1975).
468. M.R. Spirlet, G. Van den Bossche, O. Dideberg and L. Dupont, Acta Crystallogr. **35B** 203 (1979).
469. F.H. Kruse, R.E. Marsh and J.D. McCullough, Acta Crystallogr. **10** 201 (1957).
470. A.C. Villa, A.G. Manfredotti, M. Nardelli and M.E. Vidoni Tani, Acta Crystallogr. **28B** 356 (1972).

471. J.E. Fergusson and K.S. Loh, Aust. J. Chem. **26** 2615 (1973).
472. R.J.H. Clark, Spectrochim. Acta **21** 955 (1965).
473. R.M. Silverstein and G.C. Bassler, 'Spectrometric identification of Organic Compounds', 2nd ed, Wiley, New York, (1967).
474. J. Liesk and G. Klar, Z. Anorg. Allg. Chem. **435** 103 (1977).
475. N.S. Gill, R.H. Nuttall, D.E. Scaife and D.W.A. Sharp, J. Inorg. Nucl. Chem. **18** 79 (1961).
476. S. Akyüz, A.B. Dempster, R.L. Moorehouse and S. Suzuki, J. Mol. Struct. **17** 105 (1973).
477. see for example, p.151 of reference 141.
478. M.V. Lakshmikantham, M.P. Cava and A.F. Garito, J. Chem. Soc., Chem. Comm. 383 (1975).
479. A. Baroni, Atti. Accad. Lincei, Classe Sci. Fis., Mat. Nat. **26** 460 (1937).
480. W. Levason, C.A. McAuliffe and S.G. Murray, J. Chem. Soc., Dalton Trans. 269 (1976).
481. A. Davison and E.T. Shawl, J. Chem. Soc., Chem. Comm. 670 (1967) and Inorg. Chem. **9** 1820 (1970).
482. B. Nygård, Acta Chem. Scand. **15** ;039 (1961).
483. A. Fredga, Ann. N.Y. Acad. Sci. **192** 1 (1972).
484. A. Fredga, Arkw. Kemi., Mineral., Geol. **11B** (15) (1933); CA27:5079
485. D.L. Klayman, Chapter 4 in reference 141.
486. K.J. Irgolic and M.V. Kudchadker, Chapter 8 in ref. 194.
487. D.L. Klayman and T.S. Griffin, J. Am. Chem. Soc. **95** 197 (1973).
488. L. Zervas, I. Photaki and N. Ghelis, J. Am. Chem. Soc. **85** 1337 (1963).
489. A. Schöberl and A. Wagner, Vol. **9**, Chapter 1 in ref. 193.
490. L.A. Stocken, J. Chem. Soc. 592 (1947).
491. H.R. Ing, J. Chem. Soc. 1393 (1948).
492. R.M. Evans, J.B. Fraser and L.N. Owen, J. Chem. Soc. 248 (1949).
493. A. Rosenheim and W. Stadler, Chem. Ber. **38** 2687 (1905).
494. A.A. Pavlic, W.A. Lazier and F.K. Signaigo, J. Org. Chem. **14** 59 (1949).

495. B.G. Garrilov and V.E. Tischenko, J. Gen. Chem. (USSR) **18** 1687 (1948) and **17** 967 (1947).
496. L.N. Owen, Chapter 19 in reference 566.
497. E.P. Adams, F.P. Doyle, D.L. Hatt, D.O. Holland, W.H. Hunter, K.R.L. Mansford, J.H.C. Nayler and A. Queen, J. Chem. Soc. 2649 (1960).
498. R.G. Hisckey, V.R. Rao and W.G. Rhodes, 'Protective groups in Organic Chemistry', J.F.W. McOmie (ed), Plenum Press, London (1973).
499. E. Wunsch, Vol.15(1) in 'Methoden der Organischen Chemie (Houben-Weyl)', Georg Thieme Verlag, Stuttgart.
500. A. Fredga, Svensk, Kem. Tidskr. (a) **48** 160 (1936) and (b) **49** 124 (1937).
501. E.P. Painter, J. Am. Chem. Soc. **69** 229 (1947).
502. J. Janicki, J. Skupin and B. Zagalak, Rocz. Chem. **36** 353 (1962).
503. W. Frank, Hoppe-Seyler's Z. Physiol. Chem. **339** 202 (1964).
504. L.R. Williams and A. Ravve, J. Am. Chem. Soc. **70** 1244 (1948).
505. G. Zdansky (a) Arkiv. Kemi. **17** 273 (1961), and (b) **29** 443 (1968).
506. S.-H. Chu, W.H.H. Günther and H.G. Mautner, Biochem. Prepn. **10** 153 (1963).
507. J. Roy, W. Gordon, I.L. Schwartz and R. Walter, J. Org. Chem. **35** 510 (1970).
508. H.J. Klosterman and E.P. Painter, J. Am. Chem. Soc. **69** 2009 (1947).
509. E.P. Painter, J. Am. Chem. Soc. **69** 232 (1947).
510. H.-D. Jakubke, J. Fischer, K. Jost and J. Rudinger, Collect. Czech. Chem. Commun. **33** 3910 (1968).
511. C.S. Pande, J. Rudick and R. Walter, J. Org. Chem. **35** 1440 (1970).
512. G. Zdandky, Arkiv. Kemi. **19** 559 (1962).
513. G. Zdansky, Arkiv. Kemi. **21** 211 (1963).
514. F. Pan, Y. Natori and H. Tarver, Biochim. Biophys. Acta **93** 521 (1964).
515. F. Pan and H.T. Tarver, Arch. Biochem. Biophys. **119** 429 (1967).
516. G. Zdansky, Arkiv. Kemi. **29** 47 (1968) and **21** 211 (1963) and **19** 559 (1962).
517. G. Zdansky, Arkiv. Kemi. **27** 447 (1967).



518. H. Plieninger, Chem. Ber. **83** 265 (1950).
519. F. Kerdel-Vegas, F. Wagner, P.B. Russel, N.H. Grant, H.E. Alburn, D.E. Clark and J.A. Miller, Nature (London) **205** 1186 (1965).
520. A. Shrift and T.K. Virupaksha, Biochim. Biophys. Acta **100** 65 (1965).
521. M.J. Horn and D.B. Jones, J. Biol. Chem. **139** 649 (1941).
522. G. Zdansky, Arkiv. Kemi. **26** 213 (1966).
523. G. Zdansky, Arkiv. Kemi. **29** 449 (1968).
524. W. Frank Hoppe-Seyler's Z. Physiol. Chem. **339** 214 (1964).
525. R. Walter and W.Y. Chan, J. Am. Chem. Soc. **89** 3892 (1967).
526. R. Walter and V. du Vigneaud, J. Am. Chem. Soc. **87** 4192 (1965).
527. C.C. Chiu, R. Walter and I.L. Schwartz, Science **163** 925 (1969).
528. R. Walter, in 'Peptides: Chemistry and Biochemistry', B. Weinstein (ed), Marcel Dekker, New York (1970) p467.
529. W. Frank Hoppe-Seyler's Z. Physiol. Chem. **339** 222 (1964).
530. R. Walter and V. du Vigneaud, J. Am. Chem. Soc. **88** 1331 (1966).
531. W.H.H. Günther and H.G. Mautner, J. Am. Chem. Soc. **82** 2762 (1960).
532. W.H.H. Günther and H.G. Mautner, J. Am. Chem. Soc. **87** 2708 (1965).
533. H. Yajima, N. Fujii, H. Ogawa and H. Kawatani, J. Chem. Soc., Chem. Comm. 107 (1974).
534. L. Chierici and R. Passerini, Ric. Sci. **25** 2316 (1955).
535. J. Gosselck, Chem. Ber. **91** 2345 (1958).
536. G. Wagner and G. Lehmann, Pharm. Zentralhalle **100** 160 (1961).
537. G. Wagner and P. Nuhn, Arch. Pharm. **296** 374 (1973).
538. N. Marziano and R. Passerini, Gass. Chim. Ital. **94** 1137 (1964).
539. H. Rheinboldt and E. Giesbrecht, Chem. Ber. **88** 666 (1955).
540. B. Kamber, Helv. Chim. Acta **54** 398 (1971).
541. I. Photaki, J. Taylor-Papadimitriou, C. Sakarellos, P. Mazarakis and L. Zervas, J. Chem. Soc. (C) 2683 (1970).
542. H. Zahn, W. Danho, H. Klostermeyer, H.G. Gattner and J. Repin, Z. Naturforsch., Teil B **24** 1127 (1969).
543. J.J. Pastuszak and A. Chimiak, J. Org. Chem. **46** 1868 (1981).

544. S. Yurugi, J. Pharm. Soc. Japan **74** 502 (1954).
545. U. Weber and P. Harttner, Z. Physiol. Chem. **351** 1384 (1970);  
CA74:13398p
546. A. Schöberl, Angew. Chem. **69** 478 (1957).
547. P. Harttner and U. Weber, Z. Physiol. Chem. **354** 365 (1973);  
CA79:32281q
548. D.F. Veber, J.D. Milkowski, S.L. Varga, R.G. Denkwalter and  
R. Hirschmann, J. Am. Chem. Soc. **94** 5456 (1972).
549. L. Schotte, Arkiv. Kemi. **9** 377 (1956).
550. L.N. Owen and M.U.S. Sultanbawa, J. Chem. Soc. 3109 (1949).
551. B. Sjöberg, Chem. Ber. **75** 13 (1942).
552. P. Bladon and L.N. Owen, J. Chem. Soc. 598 (1950).
553. L.W.C. Miles and L.N. Owey, J. Chem. Soc. 817 (1952).
554. P.S. Fitt and L.N. Owen, J. Chem. Soc. 2240 (1957).
555. L.W.C. Miles and L.N. Owey, J. Chem. Soc. 2943 (1950).
556. Q. Mingoa, Gazz. Chim. Ital. **58** 667 (1928) CA23:3439 (1929).
557. M.T. Bogert and Y.G. Chen, J. Am. Chem. Soc. **44** 2354 (1922).
558. K.A. Jensen, L. Bøje and L. Henriksen, Acta Chem. Scand. **26**  
1467 (1972).
559. F. Mendlik and J.P. Wibaut, Recl. Trav. Chim. Pays-Bas. **50** 91  
(1931).
560. 'Organic Compounds of Sulphur, Selenium and Tellurium', The  
Chemical Society(London), Specialist Periodical Reports.
561. E. Fromm and K. Martin, Justus Liebig's Ann. Chem. **401** 177 (1913).
562. E.E. Aynsley, N.N. Greenwood and J.B. Leach, Chem. Ind. (London)  
379 (1966).
563. A.D. Westland and L. Westland, Can. J. Chem. **43** 426 (1965).
564. I.E. Fritzmann, Z. Anorg. Allg. Chem. **73** 239 (1912) and **133** 119  
(1924).
565. A.A. Pavlic, U.S. Pat. 2408094 (1946); CA41:775g.
566. A.A. Oswald and K. Griesbaum, Chapter 9 in 'The Chemistry of Organic  
Sulfur Compounds' Vol.2, N. Kharasch and C.Y. Meyers (eds)  
Pergamon Press, Oxford (1966).
567. W.E. Truce, Chapter 12, Vol.1, in reference 566.

568. J.G. Hendrickson and L.F. Match, J. Org. Chem. **25** 1747 (1960).
569. A.L. Guy, L.T. Burka, M.M. Jones and M.A. Basinger, J. Inorg. Nucl. Chem. **43** 1099 (1981).
570. L.B. Agenäs, Arkiv. Kemi. **23** 463 (1964).
571. G. Bergson and A. Biezaïs, Arkiv. Kemi. **18** 143 (1961).
572. G. Zdansky, Arkiv. Kemi. **29** 437 (1968).
573. R. Walter and W.Y. Chan, J. Am. Chem. Soc. **89** 3892 (1967).
574. E.G. Kataev and F.G. Gabdrakhmanov, J. Gen. Chem. USSR **37** 725 (1967).
575. L.M. Kataeva, E.G. Kataev, Z.S. Titova and N.A. Aleksandrova, J. Struct. Chem. **7** 668 (1966).
576. S.R. Buzilova, I.D. Sadekov, T.V. Lipovich, T.M. Filippova and L.I. Vereschagin, Zh. Obshch. Khim. **47** 1999 (1977).
577. L. Chierici and F. Montanari, Bull. Sci. Fac. Chim. Ind. Bologna **14** 78 (1956).
578. I.N. Azerbaev, A.V. Asmanova, L.A. Tsoi and M.K. Dzhamaletdinova, Izv. Akad. Nauk. Kaz. SSR, Ser. Khim. **20** 75 (1970); CA74:12766v
579. H. Ishihara, S. Sato, and Y. Hirabayashi, Bull. Chem. Soc. Jpn. **50** 3007 (1977).
580. E.G. Kataev and V.N. Petrov, J. Gen. Chem. (USSR) **32** 3626 (1962).
581. D.H. Wadsworth and M.R. Detty, J. Org. Chem. **45** 4611 (1980).
582. J. Gosselck and W. Wolters, Chem. Ber. **95** 1237 (1962).
583. J. Gosselck, Angew. Chem. **75** 831 (1963).
584. H. Volger and J.F. Arens, Recl. Trav. Chim. Pays-Bas **77** 170 (1958).
585. D. Liotta, U. Sunay, H. Santiesteban and W. Markiewica, J. Org. Chem. **46** 2605 (1981) and references therein.
586. D.S. Tarbell and P.D. Bartlett, J. Am. Chem. Soc. **59** 407 (1937).
587. B. Hoomberg, J. Prakt. Chem. **88** 553 (1913); (b) Arkiv. Kemi. Mineral., Geol. **6** (1916); Chem. Ber. **60** 2194 (1927).
588. O.L. Chapman, P.W. Wojtkowski, W. Adam, O. Rodriguez and R. Rucktäschel, J. Am. Chem. Soc. **94** 1365 (1972).
589. R. Wheland and P.D. Bartlett, J. Am. Chem. Soc. **92** 6057 (1970).
590. W. Adam, J.-C. Liu and O. Rodriguez, J. Org. Chem. **38** 2269 (1973).
591. A. Fredga, Uppsala Univ. Arsskrift **5** (1935); CA29:7281

592. N.N. Yarovenko and M.A. Raksha, Zh. Obshch. Khim. 30 4064 (1960).
593. W.H.H. Günther, J. Org. Chem. 31 1202 (1966).
594. L.A. Khatzemova and V.M. Al'bitskaya, Zh. Org. Khim. 5 1926 (1969) and 6 935 (1970).
595. D.L. MacPeck and W.H. Rauscher, U.S. Pat. 2,729,676 (1956) CA50 12102 (1956).
596. L.B. Agenäs and B. Persson, Acta Chem. Scand. 21 837 (1967).
597. W.H.H. Günther, J. Org. Chem. 32 3929 (1967).
598. L.B. Agenas, Arkiv. Kemi. 24 415 (1965) and 573.
599. L.-B. Agenäs and B. Persson, Acta Chem. Scand. 21 835 (1967).
600. M. Tazaki and M. Takagi, Chem. Lett. 767 (1979).
601. see for example Beilstein 18:EIV 4424, EII 283a, EI 446c, H 318d.
602. see for example 'Rodd's Chemistry of Carbon Compounds' Vol. IE p39.
603. E.G. Kataev, E.M. Faizullin, G.A. Chmutova and V.A. Kuzina, Zh. Org. Chem. 10 722 (1974); CA77:87862n
604. F.P. Doyle and J.H.C. Nayler, Chem. Ind. (London) 714 (1955).
605. N.S. Johary and L.N. Owen, J. Chem. Soc. 1302 (1955).
606. E. Larsson, Bull. Soc. Chim. Belg. 84 697 (1975).
607. e.g. L.K. Mustikato and D.I. Sheiko, Zh. Obshch. Khim. 33 157 (1903).
608. L-B. Agenas, Acta Chem. Scand. 17 268 (1963), Arkiv. Kemi. 28 145 (1967); 30 417 (1969); 37 159 (1969).
609. J. Gosselck, Chem. Ber. 91 2345 (1958).
610. E. Sekido, Q. Fernando and H. Freiser, Anal. Chem. 36 1768 (1964).
611. a) L.C.F. Blackman, M.J.S. Dewar, J. Chem. Soc. 171 (1957);  
b) R. Paetzola and D. Lienig, Z. Anorg. Allg. Chem. 335 289 (1965).
612. E. Rebane, Acta Chem. Scand. 21 652 (1967).
613. D.C. Goodall, J. Inorg. Nucl. Chem. 30 1269 (1968).
614. L. Hagelberg, Chem. Ber. 23 1083 (1890).
615. T. Van Es, J. Sth. Afr. Chem. Inst. 21 82 (1968) and Carbohydr. Res. 5 282 (1967).
616. R. Bonnett, R.G. Guy and D. Lanigan, Tetrahedron 32 2439 (1976).

617. R.G. Guy and J.J. Thompson, Tetrahedron **34** 541 (1978).
618. R.G. Guy, S. Cousins, D.M. Farmer, A.D. Henderson and C.L. Wilson, Tetrahedron **36** 1839 (1980).
619. see for example H. Rheinboldt, p.934 in ref. 17b.
620. F. Wille, A. Ascherl, G. Kaupp and L. Capeller, Angew. Chem. **74** 753 (1962).
621. C.C.J. Culvenor, W. Davies and K.H. Pausacker, J. Chem. Soc. 1050 (1946).
622. S.M. Iqbal and L.N. Owen, J. Chem. Soc. 1030 (1960).
623. T. Taguchi, Y. Kiyoshima, O. Komori and M. Mori, Tetrahedron Lett. **41** 3631 (1969).
624. G. Gattow and M. Draeger, Z. Anorg. Allg. Chem. **348** 229 (1966).
625. D.J.G. Ives, R.W. Pittman and W. Wardlaw, J. Chem. Soc. 1080 (1947).
626. L. Henriksen, Acta Chem. Scand. **21** 1981 (1967).
627. A. Rosenbaum, H. Kirchberg and E. Leibnitz, J. Prakt. Chem. **19** 1 (1962).
628. K.A. Jensen and V. Krishnan, Acta Chem. Scand. **21** 2904 (1967).
629. a) J.H. Chapman and L.N. Owen, J. Chem. Soc. 579 (1950);  
b) P. Bladon and L.N. Owen, J. Chem. Soc. 585 (1950);  
c) N.S. Johary and L.N. Owen, J. Chem. Soc. 1299 (1955).
630. J.M. Lalanecette and M. Laliberte, Tetrahedron Lett. 1401 (1973).
631. J.M. Lalanecette and J.M. Arnac, Can. J. Chem. **47** 3695 (1969).
632. T.H. Chan and J.R. Finkenbine, Tetrahedron Lett. 2091 (1974).
633. F.G. Bordwell and H.M. Andersen, J. Am. Chem. Soc. **75** 4959 (1953).
634. L.M. Katayeva, E.G. Katayev and D.Ya. Idiyatullina, J. Struct. Chem. **7** 361 (1966).
635. H. Hauptmann and W.F. Walter, Chem. Rev. **62** 347 (1962).
636. J.W. Lewicki, W.H.H. Günther and J.Y.C. Chu, J. Org. Chem. **43** 2672 (1978).
637. E. Larsson, J. Prakt. Chem. **318** 761 (1976).
638. E. Larsson, J. Prakt. Chem. **319** 857 (1977).
639. M.G. Voronkov, A.N. Pereferkovich and V.A. Pestinovich, J. Struct. Chem. **9** 545 (1968).
640. U. Svanholm, Chapter 15 in ref. 141.

641. C. Rodger, N. Sheppard, C. McFarlane and W. McFarlane, Chapter 12 in 'NMR and the Periodic Table', R.K. Harris and B.E. Mann (eds), Academic Press, London (1978).
642. A.T. Nielsen, J. Org. Chem. **22** 1539 (1957).
643. A.I. Scott, 'Interpretations of the Ultraviolet Spectra of Natural Products', Pergamon Press, Oxford (1964) p61.
644. a) A. Smakula, Angew. Chem. **47** 657 (1934).  
b) H. Ley and H. Wingchen, Chem. Ber. **67** 501 (1934).
645. H.G. Mautner and W.D. Kumler, J. Am. Chem. Soc. **78** 97 (1956).
646. H.G. Mautner and E.M. Clayton, J. Am. Chem. Soc. **81** 6270 (1959).
647. H.G. Mautner, S-H. Chu and C.M. Lee, J. Org. Chem. **27** 3671 (1962).
648. E. Larsson, Kgl. Fysiograph Sallskap. Lund, Forh. **21** 17 (1962); CA58:445 (1963).
649. E.W. Garbisch (Jr.), J. Chem. Ed. **45** 402 (1968).
650. D.H. Williams and I. Fleming, 'Spectroscopic Methods in Organic Chemistry' 3rd ed., McGraw-Hill, London (1980) p100-104.
651. E.I. Snyder, J. Am. Chem. Soc. **88** 1165 (1966).
652. A. Geens, G. Swaelens and M. Anteunis, J. Chem. Soc., Chem. Comm. 439 (1969).
653. W.H. Green and A.B. Harvey, J. Chem. Phys. **49** 3586 (1968), and S.G. Frankiss, J. Mol. Struct. **3** 89 (1969).
654. K.G. Allum, J.A. Creighton, J.H.S. Green, G.J. Minkoff and L.J.S. Prince, Spectrochim. Acta, Part A **24** 927 (1968).
655. R. Gaufrès, A. Perez, and J-L. Bribes, Bull Soc. Chim. Fr. 2898 (1971).
656. G.T. Morgan and F.H. Burstall, J. Chem. Soc. 1497 (1930).
657. H.J. Backer and H.J. Winter, Recl. Trav. Chim. Pays-Bas. **56** 492 (1937).
658. D.A. Ashurov, Zh. Obshch. Khim. **50** 953 (1980); CA93:56821f
659. G.T. Morgan and F.H. Burstall, J. Chem. Soc. 1096 (1929).
660. J.D. McCullough and A. Lefohn, Inorg. Chem. **5** 150 (1966).
661. A. Fredga, J. Prakt. Chem. **127** 103 (1930) and **130** 180 (1931).
662. K-Y. Yu, J. Gen. Chem. USSR **16** 851 (1946).
663. A. Toshimitsu, S. Uemura and M. Okana, J. Chem. Soc., Perkin Trans. I 1206 (1979).

664. G.T. Morgan and F.H. Burstall, J. Chem. Soc. 2197 (1929).
665. W. Haensel and R. Haller, Naturwissenschaften 55 83 (1968).
666. A. Fredga and K. Styrman, Arkiv. Kemi. 14 461 (1959).
667. I. Lalezari, A. Ghanbarpour, F. Ghaigharan, M. Niazi and R. Jafari-Namin, J. Heterocycl. Chem. 11 469 (1974).
668. C.H. Chen, G.A. Reynolds, N. Zumbulyadis and J.A. Van Allan, J. Heterocycl. Chem. 15 289 (1978).
669. P. Nanjappan, K. Ramalingam, M.D. Herd, P. Arjunan and K.D. Berlin, J. Org. Chem. 45 4622 (1980).
670. G. Bergson and G. Claeson, Acta Chem. Scand. 11 911 (1957).
671. H.J. Backer and H.J. Winter, Recl. Trav. Chim. Pays-Bas. 56 691 (1937).
672. G. Bergson, Arkiv. Kemi. 19 195 (1962).
673. G. Bergson, Arkiv. Kemi. 13 11 (1958).
674. J.H. Brown, G.P. Gillman and M.H. George, J. Polymer Sci. Part A-1 5 903 (1967).
675. L-B. Agenas in Chapter 15 in ref. 26.
676. H. Remane and R. Herzs Schuh, Org. Mass. Spectrom. 15 380 (1980).
677. W.B. Moniz, J. Phys. Chem. 73 1124 (1969).
678. B.A. Arbuzov, Yu.Yu. Samitov, A.N. Yereshehagin, O.N. Nuretdinova and T.A. Kostyleva, Vop. Stereokhim. 1 14 (1971): CA78:3577q
679. W.O. Siegl and C.R. Johnson, Tetrahedron 27 341 (1971).
680. W.D. Keller, T.R. Lusebrink and C.H. Sederholm, J. Chem. Phys. 44 782 (1966).
681. Y. Etienne, R. Soulas and H. Lumbroso, Chapter 5 in 'Heterocyclic Compounds with Three- and Four-Membered Rings', A. Weisberger (ed), Interscience Publishers, London (1964).
682. E. Lippert and H. Prigge, Ber. Bunsenges. Phys. Chem. 67 554 (1963).
683. D.W. Scott, H.L. Finke, W.N. Hubbard, J.P. McCullough, C. Katz, M.E. Gross, J.F. Messerly, R.E. Pennington and G. Waddington, J. Am. Chem. Soc. 75 2795 (1953).
684. J.R. Durig, R.C. Lord, J. Chem. Phys. 45 61 (1966).
685. D.O. Harris, H.W. Harrington, A.C. Luntz and W.D. Gwinn, J. Chem. Phys. 44 3467 (1966).
686. A.B. Harvey, J.R. Durig and A.C. Morrissey, J. Chem. Phys. 50 4949 (1969).

687. J.A. Moore, D.L. Dalrymple, 'Experimental Methods in Organic Chemistry' 2nd ed., W.B. Saunders, Philadelphia (1976) p45.
688. S. Uemura, A. Toshimitsu, M. Okana and K. Ichikawa, Bull. Chem. Soc. Jpn. 48 1925 (1975).
689. H. Bader, L.C. Cross, I. Heilbron and E.R.H. Jones, J. Chem. Soc. 619 (1949).
690. F.R. Hartley, C. Burgess and R. Alcock, 'Solution Equilibria', Ellis Horwood, Chichester (1980).
691. F.J.C. Rossotti and H.S. Rossotti, 'The Determination of Stability Constants', McGraw-Hill, New York (1961).
692. W.J. Hamer, 'Theoretical Mean-activity Coefficients of Strong Electrolytes in Aqueous Solution from 0 - 100°C', U.S. Dept. Commerce, Nat. Bureau Standards NS RDS-NBS.24 (1968).
693. R.G. Bates, 'Determination of pH: Theory and Practice', 2nd ed., Wiley-Interscience, New York (1972).
694. G. Kortüm, W. Vogel and K. Andrusson, 'Dissociation Constants of Organic Acids in Aqueous Solution', Butterworths, London (1961).
695. G.R. Hedwig and H.K.J. Powell, Anal. Chem. 43 1206 (1971).
696. H.S. Rossotti, Talanta 21 809 (1974).
697. Å. Ölin and P. Svanström, Acta Chem. Scand. 32A 283 (1978).
698. F.J.C. Rossotti and H. Rossotti, Acta Chem. Scand. 10 957 (1956).
699. D. Dyrssen, Svensk. Kem. Tidskr. 64 213 (1952).
700. G.L. Cumming, J.S. Rollett, F.J.C. Rossotti and R.J. Whewell, J. Chem. Soc., Dalton Trans. 2652 (1972).
701. F.H. Sweeton, R.E. Mesmer and C.F. Baes, Jr., J. Solution Chem. 3 191 (1974).
702. H.S. Harned and B.B. Owen, 'The Physical Chemistry of Electrolytic Solutions' A.C.S. Monograph Series, 2nd ed., Reinhold (1950).
703. I. Brown and J.E. Lane, Pure Appl. Chem. 45 1 (1976).
704. G. Arena, E. Rizzarelli, S. Sammartano and C. Rigano, Talanta 26 1(1979).
705. G. Nowogrocki, J. Canonne and M. Woznicał., Bull. Soc. Chim. Fr., 1 5 (1976) and 1369 (1976).
706. L.M. Schwartz and R.I. Gelb, Anal. Chem. 50 1571 (1978).
707. W.A.E. McBryde, Analyst (London) 94 337 (1969) and 96 739 (1971).
708. H.M.N.H. Irving, M.G. Miles and L.D. Pettit, Anal. Chim. Acta 38 475 (1967).



709. C.W. Childs and D.D. Perrin, J. Chem. Soc. (A) 1039 (1969).
710. L.G. Van Uitert and C.G. Haas, J. Am. Chem. Soc. 75 451 (1953).
711. Y.K. Agrawal, Talanta 20 1354 (1973); 26 599 (1979); and J. Electroanal. Chem. 108 369 (1980).
712. D.D. Perrin and I.G. Sayce, Chem. Ind. (London) 661 (1966).
713. J.O'M. Bockris and R.A. Fredlein, 'A Workbook of Electrochemistry' Plenum Press, New York, (1973) p39.
714. K. Cammann, 'Working with Ion-selective Electrodes: Chemical Laboratory Practice', translated from German by A.H. Schroeder, Springer-Verlag, Berlin (1979) p41.
715. R.P. Henry, J.E. Prue, F.J.C. Rossotti and R.J. Whewell, J. Chem. Soc., Chem. Comm. 868 (1971).
716. A. Albert and E.P. Serjeant, 'The Determination of Ionisation Constants - A Laboratory Manual', Chapman & Hall, London (1971) p13.
717. C.C. Westcott, 'pH Measurements', Academic Press, New York (1978) p61.
718. L.C. Gruen and J.P.F. Human, Mikrochim. Acta 2 431 (1975).
719. L. Ciacatta, Arkiv. Kemi. 20 417 (1963).
720. R.A. Durst and J.P. Cali, Pure Appl. Chem. 50 1485 (1978).
721. I.U.P.A.C. 'Manual of Symbols and Terminology for Physicochemical Quantities and Units' 2nd revision Pure Appl. Chem. 51 1 (1979).
722. F.J.C. Rossotti, J. Inorg. Nucl. Chem. 33 2051 (1971).
723. P. Gans, Coord. Chem. Rev. 19 99 (1976).
724. F. Gaizer, Coord. Chem. Rev. 27 195 (1979).
725. P. Gans, Adv. Mol. Relax. Inter. Proc. 18 139 (1980).
726. W.E. Wentworth, J. Chem. Ed. 42 96 and 162 (1965).
727. E.R. Still, Talanta 27 573 (1980).
728. K. Tettamanti, R. Stomfai, S. Kemény and J. Manczinger, Periodia Polytech. 21 333 (1977).
729. G. Nowogrocki, J. Canonne and M Wozniak, Bull. Soc. Chim. Fr., 1 371 (1978).
730. W.E. Deming, 'Statistical Adjustment of Data', Dover Publications, New York (1964).

731. A. Avdeef and K.N. Raymond, Inorg. Chem. **18** 1605 (1979).
732. R. Guevremont and D.L. Rabenstein, Can. J. Chem. **55** 4211 (1977) and **57** 466 (1979).
733. T.B. Field and W.A.E. McBryde, Can. J. Chem. **56** 1202 (1978).
734. T.P.A. Kruck and B. Sarkar, Can. J. Chem. **51** 3549 and 3555 (1973).
735. B. Sarkar and T.P.A. Kruck, Can. J. Chem. **51** 3541 (1973).
736. A. Avdeef, Inorg. Chem. **19** 3081 (1980).
737. R. Österberg, Acta Chem. Scand. **14** 471 (1960).
738. W.A.E. McBryde, Can. J. Chem. **51** 3572 (1973).
739. L.C. Van Poucke, J. Yperman and J.P. François, Inorg. Chem. **19** 3078 (1980).
740. K.W. Schnid and C.N. Reilly, J. Am. Chem. Soc. **78** 5513 (1956).
741. R.D. Hancock and A. Evers, Inorg. Chem. **15** 995 (1976).
742. N. Ingri and L.G. Sillén, Acta Chem. Scand. **16** 173 (1962) and subsequent papers in this series.
743. I.G. Sayce, Talanta **15** 1397 (1968), **18** 653 (1971) and **19** 831 (1972).
744. A. Sabatini, A. Vacca and P. Gans, Talanta **21** 53 (1974).
745. P. Gans, A. Sabatini and A. Vacca, Inorg. Chim. Acta **18** 237 (1976).
746. M. Alcock, F.R. Hartley and D.E. Rogers, J. Chem. Soc., Dalton Trans. 115 (1978).
747. R.N. Sylva and M.R. Davidson, J. Chem. Soc., Dalton Trans. 465 (1979).
748. I. Nagypál, Acta Chim. Acad. Sci. Hung. **82** 29 (1974).
749. M. Micheloni, A. Sabatini and A. Vacca, Inorg. Chim. Acta **25** 41 (1977).
750. A. Avdeef, S.R. Sofen, T.L. Bregante and K.N. Raymond, J. Am. Chem. Soc. **100** 5362 (1978).
751. L.G. Sillén, Acta Chem. Scand. **18** 1085 (1964).
752. D.D. Perrin and I.G. Sayce, Talanta **14** 833 (1967).
753. N. Ingri, W. Kakolowicz, L.G. Sillén and B. Warnqvist, Talanta **14** 1261 (1967).
754. I. Nagypál, I. Páka and L. Zékany, Talanta **25** 549 (1978).
755. B. Lindgren, Acta Chem. Scand. **31B** 1 (1977).

756. L. Brandsma and H.E. Wijers, Recl. Trav. Chim. Pays-Bas **82** 68 (1963).
757. G.M. Bogolybov, Yu.N. Shtyk and N.A. Petrov, Zh. Obshch. Khim. **39** 1804 (1969).
758. R. Paetzold, H.-D. Schumann and A. Simon, Z. Anorg. Allg. Chem. **305** 96 (1960).
759. O. Behagel and M. Rollmann, Chem. Ber. **62** 2696 (1929).
760. B.S. Furniss, A.J. Hannaford, V. Rogers, P.W.G. Smith and A.R. Tatchell, "Vogel's Textbook of Practical Organic Chemistry including Qualitative Organic Analysis", 4th ed., Longman, London (1978) p279.
761. T.W. Abbott, R.T. Arnold and R.B. Thompson, 'Organic Syntheses' Collective vol.2, p10.
762. J.R. Piper, L.M. Rose and T.P.J. Johnston, J. Med. Chem. **18** 803 (1975).

APPENDIX 1

Conference poster-paper PI-1, presented at the 10th annual meeting of the RACI Division of Coordination and Metal-Organic Chemistry (COMO-10), Queenstown, New Zealand, May 11-14, 1981.

# AQUEOUS SOLUTION EQUILIBRIA FOR $\text{MeHg}^{\text{II}}$ WITH ANTIDOTES FOR MERCURY POISONING

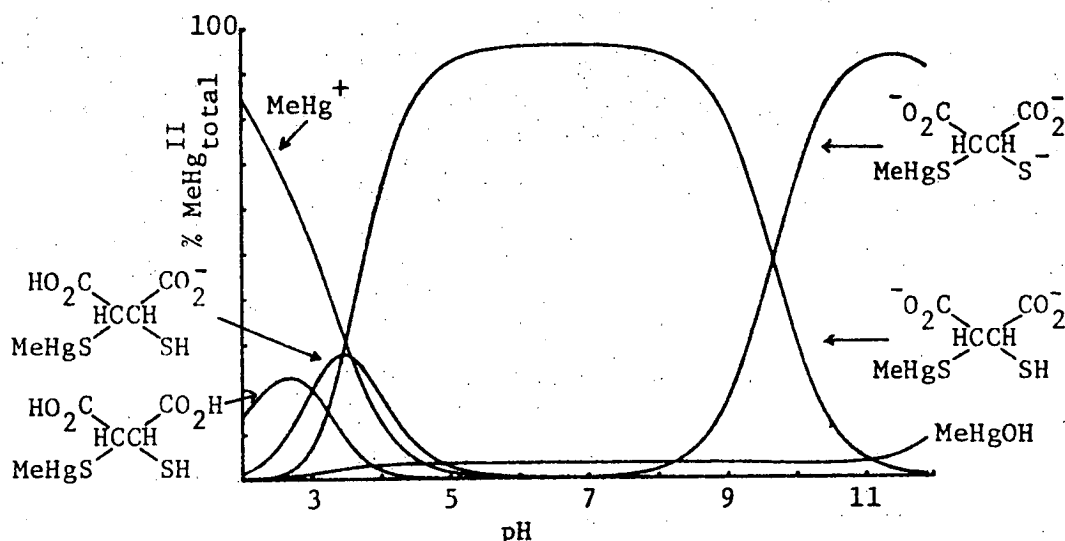
A.P. Arnold and A.J. Canty, Chemistry Department, University of Tasmania, Hobart, Australia.

The classical antidote for heavy metal poisoning, British Anti-Lewisite (I, 2,3-dimercapto-1-propanol) is ineffective for  $\text{MeHg}^{\text{II}}$  poisoning in mammals. Administration of I increases the amount of mercury in the brain, contrary to the requirements of an effective antidote. In vitro formation of complexes such as  $(\text{MeHg})_2\text{BAL}^1$ , which are soluble in pyridine but insoluble in aqueous systems, may be relevant to the suggested lipid solubility of such species in vivo. A successful  $\text{MeHg}^{\text{II}}$  antidote (animal testing only) is meso-2,3-dimercaptosuccinic acid (II, DMSA) which is far less toxic than I and may be administered orally.

In view of the close structural relationships between I and II, we have investigated the aqueous solution equilibria in systems containing  $\text{MeHg}^{\text{II}}$  with these dithiols, as well as with thiol ligands such as 2,3-dimercapto-1-propane sulfonate $^-\text{Na}^+\cdot\text{H}_2\text{O}$  (III, Unithiol), 2-mercaptosuccinic acid (IV) and mercaptoacetic acid (V). Thiols II-V are expected to form  $\text{MeHg}^{\text{II}}$  complexes which are deprotonated at physiological pH, thus minimising lipid solubility and enhancing the possibility of renal excretion.

Solid  $\text{MeHg}^{\text{II}}$  complexes have been obtained with I-V. IR and Raman evidence support the expected unifunctional  $\text{MeHg}^{\text{II}}$  with linear Me-Hg-S coordination, e.g.  $(\text{HO}_2\text{C})(\text{MeHgS})\text{CHCH}(\text{SHgMe})(\text{CO}_2\text{H})$  for II.

Potentiometric titration studies using a modified version of MINIQUAD,<sup>4</sup> show high formation constants, as expected for 'soft'  $\text{MeHg}^{\text{II}}$  with 'soft' thiol donors. Under conditions used in animal studies of II with  $\text{MeHg}^{\text{II}}$  poisoning, ( $[\text{DMSA}] > 100 [\text{MeHg}^{\text{II}}]$ )<sup>2,5</sup>, the predominant species at pH  $\sim 7$  is likely to be  $(^-\text{O}_2\text{C})(\text{MeHgS})\text{CHCH}(\text{SH})(\text{CO}_2^-)$  as shown in the species distribution diagram. This is consistent with efficient elimination of  $\text{MeHg}^{\text{II}}$  as a water soluble complex via the kidneys after administration of II.



1. A.J. Canty and R. Kishimoto, *Inorg. Chim. Acta*, **24**, 109 (1977).
2. M. Berlin, L.-G. Jerksell and G. Nordberg, *Acta Pharmacol. Toxicol.*, **23**, 312 (1965).
3. See, for example, J. Aaseth and E.A.H. Friedheim, *Acta Pharmacol. Toxicol.*, **42**, 248 (1978).
4. R.N. Sylva and M.R. Davidson, *J.C.S. (Dalton)*, 465 (1979) and ref. therein.
5. Using model conditions of  $10^{-7}$  mole  $\text{MeHg}^{\text{II}}$  and  $5 \times 10^{-6}$  mole DMSA in 10 ml aqueous volume. Species with two  $\text{MeHg}^{\text{II}}$  per dithiol ligand are unimportant under these conditions (less than 1% total  $\text{MeHg}^{\text{II}}$ ).

APPENDIX 2

Computer program COMIXH.

Written in Algol/8 (a compact implementation of Algol 60 for the Chemistry Department's PDP8/e computer) and incorporating plotting routines to suit the Chemistry Department's HP7221A plotter.

The data input formed is described in the initial comments to the program.

```

'BEGIN 'COMMENT' PROGRAM COMIXH SIMULATES TITRATION CURVE, GIVEN EXPTL.
DATA AND APPROPRIATE FORMATION CONSTANTS.
THIS VERSION INCORPORATES A GAUSS-NEWTON PROCEDURE
FOR ITERATIVE SOLUTION OF THE NON-LINEAR EQUATIONS FOR
FREE-LIGAND, METAL AND PROTON CONCENTRATIONS.
FREE COMPONENT CONCENTRATIONS HAVE BEEN CONSTRAINED
TO BE POSITIVE BY LOGARITHMIC TRANSFORMATION.

```

THE PROGRAM WAS WRITTEN IN ALGOL/B BY ALAN ARNOLD  
FOR USE ON THE CHEMISTRY DEPARTMENT'S PDP8  
COMPUTER. PLOTTING ROUTINES ARE DESIGNED FOR USE  
WITH THE HP221A PLOTTER.;

```

'COMMENT' INPUT DATA IN THE FOLLOWING FORMAT:

```

1. TITLE OF EXPT., BETWEEN QUOTATION MARKS (")
2. NUMBER OF COMPONENTS (MAX. 4)
3. NUMBER OF COMPLEXES (MAX. 20)
4. DATA FOR EACH COMPLEX SPECIES:
  - NO. MOLECULES EACH COMPONENT
  - LOG. OF CUMULATIVE STOICHIOMETRIC ASSOCIATION CONSTANT
5. DATA FOR EACH COMPONENT (SAME ORDER AS 2)
  - INITIAL MMOL
  - CONCENTRATION IN TITRANT (M)
  - ESTIMATE OF INITIAL CONCENTRATION (M)
6. INITIAL VOLUME (ML.)
7. NUMBER OF TITRATION POINTS (MAX. 80)
8. PHCAL SUCH THAT  $-\log[H^+] = PH(EXPTL.) + PHCAL$
9. TITRATION DATA IN PAIRS OF VOL(ML.), PH(EXPTL.);

```

'REAL' 'ARRAY' VOL, PHC(80), BETAC(1:20),
TITCONC, TOT, MMOL, LNFREE, INITCONC(1:4), HC(1:80, 0:10);
'REAL' HX, V, VINC, MAXX, MAXY, MINX, MINY, VINIT, VTOT,
L, R, T, R, PHCAL;
'INTEGER' NC, NDATA, N, IPT, I, J, K, INDEX, MAXIT, PEN, ITY, COMP1, COMP2;
'BOOLEAN' SINGUL, SUFLAG;
'INTEGER' 'ARRAY' Q(1:4, 1:20);

```

```

'PROCEDURE' SIMUL(N, X0, A, EPS); 'VALUE' N, EPS;
'COMMENT' GAUSS-JORDAN SOLUTION OF N EQUATIONS OF AUGMENTED MATRIX, A
USING MAXIMUM-PIVOT STRATEGY.
REF. 'APPLIED NUMERICAL METHODS', CARNAHAN ET AL., P289;
'INTEGER' N; 'REAL' 'ARRAY' X0, A; 'REAL' EPS;
'BEGIN'

```

```

'REAL' PIVOT, AIJCK;
'INTEGER' I, J, K, ISCAN, JSCAN, IROWK, JCOLK, IROWI, JCOLI;
'INTEGER' 'ARRAY' IROW, JCOL(0:NC);
'FOR' K:=1 'STEP' 1 'UNTIL' N 'DO'
'COMMENT' BEGIN ELIMINATION;
'BEGIN' PIVOT:=0.0;
'FOR' I:=1 'STEP' 1 'UNTIL' N 'DO'
'FOR' J:=1 'STEP' 1 'UNTIL' N 'DO'
'BEGIN'
'COMMENT' SCAN FOR INVALID PIVOT-ROW SUBSCRIPTS;
'IF' K#1 'THEN'
'FOR' ISCAN:=1 'STEP' 1 'UNTIL' K-1 'DO'
'FOR' JSCAN:=1 'STEP' 1 'UNTIL' K-1 'DO'
'IF' I=IROW[ISCAN] 'OR' J=JCOL[JSCAN] 'THEN'
'GOTO' LOOP;
'IF' ABS(A(I, J)) > ABS(PIVOT) 'THEN'
'BEGIN' PIVOT:=A(I, J);
IROWK:=I; JCOLK:=J;
'END';
'END';

```

LOOP:

```

'END';
'IF' ABS(PIVOT) < EPS 'THEN'
'BEGIN'
SINGUL:= 'TRUE'; IPT:=1;
'GOTO' EXIT;
'END';
IROWK:=IROWK; JCOLK:=JCOLK;
'COMMENT' NORMALISE PIVOT-ROW ELEMENTS;
'FOR' J:=1 'STEP' 1 'UNTIL' N+1 'DO'
ACIROWK, JJ:=ACIROWK, JJ/PIVOT;
ACIROWK, JCOLK:=1.0/PIVOT;
'COMMENT' CARRY OUT ELIMINATION;
'FOR' I:=1 'STEP' 1 'UNTIL' N 'DO'
'BEGIN' AIJCK:=A(I, JCOLK);
'IF' I#IROWK 'THEN'
'BEGIN' ACI, JCOLK:=-AIJCK/PIVOT;
'FOR' J:=1 'STEP' 1 'UNTIL' N+1 'DO'
'IF' J#JCOLK 'THEN'
ACI, JJ:=ACI, JJ-AIJCK*ACIROWK, JJ;
'END';
'END';

```

```

'END';
'COMMENT' ORDER SOLUTION ARRAY;
'FOR' I:=1 'STEP' 1 'UNTIL' N 'DO'
'BEGIN' IROWI:=IROWK;
JCOLI:=JCOLK;
X0(JCOLI):=ACIROWI, N+1;
'END';
'COMMENT' ARRAY X0 CONTAINS THE SOLUTION VALUES;
'END' OF SIMUL;
EXIT:

```

```

'PROCEDURE' LABEL;
'COMMENT' TRANSFERS 'LABELS' FROM VDU OR DECWRITER TO PLOTTER;
'BEGIN' 'IF' 'NOT' SUPLAB 'THEN'
  'BEGIN'
    REPEAT: TEXT(7, '*SYS:LABELS.DA/2 OPEN FOR O/P');
    TEXT(TTY, 'PLOT LABEL'); TITLE(TTY, 3);
    FILE(3);
    'COMMENT' CLOSES LABELS.DA FOR O/P AND REOPENS FOR I/P;
    TEXT(4, ' PLOTTER GET ENTRY PRINT ');
    TITLE(3, 4);
    CHOUT(4, 129); TEXT(4, ' VDU ');
    TEXT(TTY, 'ANOTHER LABEL? (Y/N)');
    'IF' CHIN(TTY)=217 'THEN' GOTO REPEAT;
  'END';
'END' OF LABEL;

'PROCEDURE' TITLE(DEVIN, DEVOUT); 'VALUE' DEVIN, DEVOUT;
'COMMENT' READS LABELS BETWEEN QUOTATION MARKS FROM DEVICE IN,
AND TRANSFERS THEM TO DEVICE OUT;
'INTEGER' DEVIN, DEVOUT;
'BEGIN' 'REAL' CHAR; 'INTEGER' CASE;
CASE:=1; 'IF' DEVOUT=4 'THEN' CHOUT(4, 146);
'IF' DEVOUT=3 'THEN' CHOUT(DEVOUT, 162);
L: CHAR:=CHIN(DEVIN); 'IF' CHAR#162 'THEN' GOTO L;
'FOR' CHAR:=CHIN(DEVIN) 'WHILE' CHAR#162 'DO'
  'BEGIN'
    'IF' CHAR#163 'THEN' CHOUT(DEVOUT, CHAR)
    'ELSE'
      'BEGIN' CASE:=-CASE;
      'IF' DEVOUT=4 'THEN' CHOUT(4, 147-CASE);
      'ELSE' CHOUT(DEVOUT, CHAR);
    'END';
  'IF' DEVOUT=3 'THEN' CHOUT(DEVOUT, 162);
'END' OF TITLE;

'PROCEDURE' PAIR(X, Y);
'COMMENT' OUTPUTS PAIR OF CO-ORDINATES TO PLOTTER;
'VALUE' X, Y; 'REAL' X, Y;
'BEGIN' PRINT(4, 5, 1, X); TEXT(4, ' ');
PRINT(4, 5, 1, Y); TEXT(4, ' ');
'END' OF PAIR;

'REAL' 'PROCEDURE' SCALE(X, OFFSET, VAR, MAXVAR, MINVAR);
'COMMENT' SCALES X FOR PLOTTER;
'VALUE' X, OFFSET, VAR, MAXVAR, MINVAR;
'REAL' X, OFFSET, VAR, MAXVAR, MINVAR;
'BEGIN'
  SCALE:=OFFSET+(VAR-2.0*OFFSET)*(X-MINVAR)/(MAXVAR-MINVAR);
'END' OF SCALE;

```

```

'PROCEDURE' ITERATE;
'COMMENT' GAUSS-NEWTON ITERATIVE ROUTINE FOR PARAMETER SHIFTS WITH
CONCENTRATIONS RESTRAINED TO BE POSITIVE BY LOGARITHMIC
TRANSFORMATION I.E. THE UNKNOWN'S ARE LN(FREECII)
*** A HIGHLY MODIFIED VERSION OF COGS ***
'BEGIN'
  'REAL' 'ARRAY' AOC(1:NC, 1:NC+1); XOC(1:NC); CC(1:NC);
  'INTEGER' NIT, I, J, K;

  NIT:=0;
  'COMMENT' CALCULATE SPECIES CONCENTRATIONS;
  'FOR' J:=1 'STEP' 1 'UNTIL' N 'DO'
    'BEGIN'
      CC(J):=BETAC(J);
      'FOR' I:=1 'STEP' 1 'UNTIL' NC 'DO'
        CC(J):=CC(J)+Q(I, J)*LN(FREEC(I));
        CC(J):=EXP(CC(J));
      'END';
      NIT:=NIT+1;
      'IF' NIT<MAXIT 'THEN'
        'BEGIN'
          'COMMENT' CALCULATE ELEMENTS OF FIRST NC COLUMNS OF A,
          WHICH IS THE AUGMENTED JACOBIAN (SYMMETRICAL);
          'FOR' I:=1 'STEP' 1 'UNTIL' NC 'DO'
            'BEGIN'
              AOC(I, NC+1):=EXP(LN(FREEC(I))-TOTC(I));
              'FOR' J:=1 'STEP' 1 'UNTIL' NC 'DO' AOC(I, J):=0.0;
              XOC(I):=0.0;
              'FOR' J:=1 'STEP' 1 'UNTIL' I 'DO'
                'BEGIN'
                  'FOR' K:=1 'STEP' 1 'UNTIL' N 'DO'
                    AOC(I, J):=AOC(I, J)+Q(I, K)*Q(J, K)*CC(K);
                    AOC(I, J):=
                      'IF' I=J 'THEN' -EXP(LN(FREEC(J)))-AOC(I, J)
                      'ELSE' -AOC(I, J);
                'END';
              'COMMENT' CALCULATE ELEMENTS OF LAST COLUMN OF A0;
              'FOR' K:=1 'STEP' 1 'UNTIL' N 'DO'
                AOC(I, NC+1):=AOC(I, NC+1)+Q(I, K)*CC(K);
            'END';
            'FOR' I:=1 'STEP' 1 'UNTIL' NC 'DO'
              'FOR' J:=I+1 'STEP' 1 'UNTIL' NC 'DO' AOC(I, J):=AOC(J, I);

            SINGUL:='FALSE';

            SIMUL(NC, X0, A0, 1.0E-600);
            'IF' 'NOT' SINGUL 'THEN'
              'BEGIN' 'COMMENT' UPDATE LN(FREEC(I)) UNTIL CONVERGENT;
                'FOR' I:=1 'STEP' 1 'UNTIL' NC 'DO'
                  LN(FREEC(I)):=XOC(I)+LN(FREEC(I));
                  'FOR' I:=1 'STEP' 1 'UNTIL' NC 'DO'
                    'IF' ABS(XOC(I))>0.002 'THEN' GOTO LOOP;
                    IPT:=IPT+1;
                'END';
                'COMMENT' IPT NOT RESET IF NOT CONVERGENT;

                WRITE(TTY, NIT); TEXT(TTY, ' ');
                'IF' NIT=MAXIT 'THEN'
                  TEXT(TTY, 'ITERATION DID NOT CONVERGE');
                'IF' SINGUL 'THEN' TEXT(TTY, 'MATRIX SINGULAR');
              'END' OF PROCEDURE ITERATE;
            'END';
          'END';
        'END';
      'END';
    'END';
  'END';

```



```

'PROCEDURE' PRINT(DEV,N,M,X);
'VALUE' DEV,N,M,X: 'INTEGER' DEV,N,M; 'REAL' X;
'BEGIN' 'COMMENT' PRINTS <X> IN FORMAT (-) NNN.MMM;
      'INTEGER' V,R,I,Y; 'REAL' Z;

      'PROCEDURE' S;
      'BEGIN' Z:=Z*10; Y:=ENTIER(Z);
            CHOUT(DEV,176+Y); Z:=Z-Y;
      'END';

      I:=0; Z:=10*ABS(X)+5/10^M; V:=0;
      'FOR' Z:=0.1*Z 'WHILE' Z>=1 'DO' V:=V+1;
      'IF' V>N+M 'THEN' RWRITE(DEV,X) 'ELSE'
      'BEGIN' 'IF' V>N 'THEN'
            'BEGIN' Z:=Z-0.5/10^(V+M);
                  M:=N+M-V; N:=V; I:=1;
                  Z:=Z+0.5/10^(V+M);
                  'IF' Z>=1 'THEN'
                        'BEGIN' V:=V+1; N:=N+1;
                              M:=M-1; Z:=0.1*Z;
                        'END' FIXING ROUNDING;
                  'END' FIXING OVERFLOW;
            'FOR' K:=V+1 'STEP' 1 'UNTIL' N 'DO' CHOUT(DEV,160);
            CHOUT(DEV,'IF' X<0 'THEN' 173 'ELSE' 160);
            'FOR' K:=1 'STEP' 1 'UNTIL' V 'DO' S;
            'IF' M>0 'OR' I=1 'THEN' CHOUT(DEV,174);
            'FOR' K:=1 'STEP' 1 'UNTIL' M 'DO' S;
      'END' FORMATTED OUTPUT;
'END' PRINT;

'PROCEDURE' PLOT;
'COMMENT' PLOTS AXES AND EXPERIMENTAL TITRATION POINTS (CIRCLED);
'BEGIN' 'REAL' X,Y,YSTEP,XSTEP;
'INTEGER' I,P,PEN;
SKIP(TTY);
TEXT(TTY,*** LOAD NEW PLOTTER PAPER...);SKIP(TTY);
TEXT(TTY,PEN NUMBER FOR AXES= );PEN:=READ(TTY);SKIP(TTY);
TEXT(TTY,PLOTTING SPEED (CM/SEC)= );P:=READ(TTY);SKIP(TTY);
TEXT(TTY,SUPPRESS AXES LABELS (Y/N));
SUPLAB:='IF' CHIN(TTY)=217 'THEN' 'TRUE' 'ELSE' 'FALSE';
SKIP(TTY);
TEXT(TTY,MAXX:);MAXX:=READ(TTY);SKIP(TTY);
TEXT(TTY,MINX:);MINX:=READ(TTY);SKIP(TTY);
TEXT(TTY,MAXY:);MAXY:=READ(TTY);SKIP(TTY);
TEXT(TTY,MINY:);MINY:=READ(TTY);SKIP(TTY);
TEXT(TTY,NO.VOLUME STEPS FOR PLOTTER =);
VINC:=READ(TTY);SKIP(TTY);
TEXT(TTY,MAXIMUM NO.ITERATIONS= );MAXIT:=READ(TTY);
SKIP(TTY);
TEXT(TTY,INPUT GRID LIMITS: LEFT:);L:=READ(TTY);SKIP(TTY);
TEXT(TTY,BOTTOM:);B:=READ(TTY);SKIP(TTY);
TEXT(TTY,RIGHT:);R:=READ(TTY);SKIP(TTY);
TEXT(TTY,TOP:);T:=READ(TTY);SKIP(TTY);

```

```

TEXT(4,PLOTTER INITIALISE DEFINE VELOCITY );WRITE(4,P);
TEXT(4,DEFINE LIMITS );PAIR(L,B);PAIR(R,T);
'COMMENT' SETS UP 0.025MM GRID;
TEXT(4,DEFINE GRID );PAIR(R-L,T-B);
TEXT(4,LABEL TERMINATOR );CHOUT(4,129);'COMMENT' CNTL/A;
TEXT(4,LABEL LCASE );CHOUT(4,148);'COMMENT' CNTL/T;
TEXT(4,LABEL UCASE );CHOUT(4,146);'COMMENT' CNTL/R;
TEXT(4,LABEL SIZE 100,300);
TEXT(4,PEN );WRITE(4,PEN);TEXT(4,MOVE );
PAIR(500,T-B-500);PAIR(500,500);PAIR(R-L-500,500);
PAIR(R-L-500,T-B-500);PAIR(500,T-B-500);
XSTEP:=(MAXX-MINX)/10.;
'FOR' X:=MINX+XSTEP 'STEP' XSTEP 'UNTIL' MAXX-XSTEP 'DO'
'BEGIN' TEXT(4,MOVE );
      PAIR(SCALE(X,500,R-L,MAXX,MINX),500);
      TEXT(4,IDRAW 0,50 IMOVE 0,-250);
      'IF' NOT SUPLAB 'THEN' 'BEGIN'
            TEXT(4,PRINT );
            CHOUT(4,136);CHOUT(4,136);CHOUT(4,136);
            PRINT(4,1,2,X);CHOUT(4,129);
      'END';
      YSTEP:=(MAXY-MINX)/10.;
      'FOR' Y:=MINY+YSTEP 'STEP' YSTEP 'UNTIL' MAXY-YSTEP 'DO'
      'BEGIN' TEXT(4,MOVE );
            PAIR(500,SCALE(Y,500,T-B,MAXY,MINY));
            TEXT(4,IDRAW 50,0);
            TEXT(4,IMOVE -100,0 ROTATE 90 NOP);
            'IF' NOT SUPLAB 'THEN' 'BEGIN'
                  TEXT(4,PRINT );
                  CHOUT(4,136);CHOUT(4,136);CHOUT(4,136);
                  PRINT(4,1,2,Y);CHOUT(4,129);
            'END';
            TEXT(4,ROTATE);
      'END';
      TEXT(4,GET SIZE VDU );
      SKIP(TTY);
      TEXT(TTY,PEN NUMBER FOR DATA =);PEN:=READ(TTY);
      SKIP(TTY);
      TEXT(4,PLOTTER PEN );WRITE(4,PEN);
      'FOR' I:=1 'STEP' 1 'UNTIL' NDATA 'DO'
      'BEGIN' TEXT(4,MOVE );
            PAIR(SCALE((MMOLES[COMP1]+VOL[I])*TITCONC[COMP1])/
                    (MMOLES[COMP2]+VOL[I])*TITCONC[COMP2]),
                  500,R-L,MAXX,MINX);
            SCALE(PHEN,500,T-B,MAXY,MINY);
      'COMMENT' DRAW CIRCLES 0.02 PH UNITS IN RADIUS;
      TEXT(4,IMOVE );
      PAIR(0.02*(T-B)/(MAXY-MINY),0);
      TEXT(4,TURN );
      PRINT(4,5,1,0.02*(T-B)/(MAXY-MINY));
      'END';
      TEXT(4,NOP VDU );
      LABEL;
'END' OF PLOT;

```



## PUBLICATIONS

1. Synthesis, Structure and Spectroscopic Studies of Mercury (II) Selenolates and  $\text{MeHgSeBu}^t$ ,  
A.P. Arnold and A.J. Canty, Inorg. Chim Acta, **55** 171 (1981)
2. Mercury (II) Selenolates. Crystal structures of Polymeric  $\text{Hg}(\text{SeMe})_2$  and the Tetrameric Pyridinates  $[\{\text{HgCl}(\text{py})(\text{SeEt})\}_4]$  and  $[\{\text{HgCl}(\text{py})_{0.5}(\text{SeBu}^t)\}_4]$ ,  
A.P. Arnold, A.J. Canty, B.W. Skelton and A.H. White, J. Chem. Soc., Dalton Trans., (1982) in press.

The articles listed above have been removed for copyright or proprietary reasons.